
**Hydrogeology of the Kalahari in north-eastern
Namibia**

**with special emphasis on
groundwater recharge, flow modelling and
hydrochemistry**

Doctorate Thesis
submitted at the
Julius-Maximilians-University of Würzburg

by

Heike Klock

from

Pinneberg/Schleswig-Holstein

Würzburg 2001

**Die Hydrogeologie der Kalahari im Nordosten
Namibias**

**unter besonderer Berücksichtigung der
Grundwasserneubildung,
Strömungsmodellierung und Hydrochemie**

Dissertation zur Erlangung des
naturwissenschaftlichen Doktorgrades
der Bayerischen Julius-Maximilians-Universität Würzburg

vorgelegt von

Heike Klock

aus

Pinneberg/Schleswig-Holstein

Würzburg 2001

Acknowledgements

I would like to thank Prof. Dr. Peter Udluft for giving me the opportunity to research within the field of large hydrogeological dryland systems. With his open minded continuous support he enabled me to work through all stages of this work. I am very thankful for his liberal co-operation and for his assistance whenever it was needed. Many thanks go also to PD Dr. Barbara Sponholz for the final suggestions to the manuscript and her motivating thoughts.

The co-operation with the Department of Water Affairs in Windhoek is gratefully acknowledged. Without allowing me to use all their data, this thesis would never have been possible. Therefore special thanks go to Greg Christelis, Ingo Bardenhagen, Hartmut Strub and Antje Eggers for their generous support. Additional data have been made available by the Weather Bureau in Windhoek which added up the climatic data used in this thesis. Many thanks go to Adolf Heilos and Mrs Li who always analysed reliably and promptly the hydrochemical samples for this project.

I am very grateful to Dr. Stephen White and Dr. Ansgar Wanke who spend some good time with me in the Kalahari. Both have patiently, open minded and fruitfully discussed tectonic and sedimentological problems with me in the field and during office work.

Many people supported me during my stays in Namibia and did not only make it logistically easier but also an amicable, great time: Heike, Christian, Kaja & Erik Rubbert, Arnold & Katharina Bittner, Hartmut & Marita Strub, Karl & Freeda Steiner (Windhoek), Herma & Karl Mayer (Farm Rheinpfalz), Christian of the Omatako Camp, Reverend Jako and his wife Ina-Marie (Mangetti Dune), Mr. & Mrs Tölken (Farm Strumfeld), Mr. Chipango (Tsumkwe), Nigel Berriman and his successor in the Department of Nature Conservation in Tsumkwe.

Thanks also go to the DFG who provided a scholarship and research funding which paved the way for this project from the financial point of view. The idea of the interdisciplinary graduate school "Geosciences in Africa" is also very much appreciated as this allowed many aspects to be considered and discussed not only with lecturers and professors during the weekly seminar but also in great detail with many of the PhD colleagues as there are: Holger Mainardy, Christoph Külls, Matthias Kukulus, Carmen Krapf, Frank Holzförster, Ulrike Beyer and Silke Bertram.

For proof reading many thanks are owed to Dr. Stephen White, Dr. Ansgar Wanke, Matthias Kukulus and Matthias Fleckenstein.

And many thanks to everybody inside and outside the department who made the last years a convenient time.

Abstract

This study has focused on hydrogeological and hydrochemical settings of the Northern Namibian Kalahari Catchment which is the Namibian part of the Makgadikgadi-Kalahari-Catchment. Recharge has been the subject of process-understanding, quantification and regionalisation. Within the semiarid study area a bimodal surface constitution is prominent: hardrocks areas allow for fast infiltration along karsts and joints, whereas areas covered by unconsolidated sediments receive minor diffuse recharge and locally some preferred flow path recharge develops along shrinkage cracks and rootlets. Five substratum classes have been soil physically studied: Pans and vleis, brown to red soils, dune sand, soil with an aeolian influence, and calcrete. Aeolian sands are most promising for the development of direct diffuse recharge. Recharge by preferred flow might occur in all soil classes either due to joints in calcrete or structures and rootlets in soils. All soil classes contribute to indirect recharge because even the dune sand allows, albeit very locally, the generation of runoff. The occurrences of recharge through the unconsolidated soil and the hardrocks have been confirmed by hydrograph interpretation and by a study of hydrochemical data which identified groundwater of flood water and flood water after soil passage composition. Other prominent hydrochemical processes in the Kalahari are associated with the carbonate-equilibrium-system, mixing with highly mineralised water that is either SO_4^{2-} - (central area) or Cl^- -dominated (fringe area) and development of Na^+ - HCO_3^- -water types. The latter is mostly generated by feldspar weathering. Variations of the hydrochemical compositions were observed for shallow groundwaters. They do not only reflect the recharge amount but also the recharge conditions, e.g. a wetter year is allowing more vegetation which increases the HCO_3^- -content because of an increased CO_2 partial pressure in the root zone. Inverse determination of recharge by the chloride mass balance method gives recharge amounts between 0.2 and locally more than 100 mm/a. The least favoured recharge conditions are found for Kalahari covered areas, the largest amount occurs in the Otavi area. The distribution of recharge areas within the catchment is rather complex and regionalisation of recharge for the entire catchment was done by a forward approach using satellite images and by an inverse approach using hydrochemical data. From the inverse hydrochemical approach a basin-wide balanced recharge amount of 1.39 mm/a is achieved. The forward approach gave a basin-wide figure of 0.88 (minimum assumption) to 4.53 mm/a (maximum assumption). A simplistic groundwater flow model confirmed the results from the minimum recharge regionalisation by satellite images and the result from the hydrochemical approach. Altogether a mutually verified basin-wide recharge figure of ca. 1 mm/a turns out.

Acknowledgements	1
Abstract	2
Table of contents	3
1 Introduction	6
1.1 The problem.....	6
1.2 Aim.....	7
1.3 Overview of applied methods.....	7
1.4 Overview of the research area.....	8
1.4.1 Location.....	8
1.4.2 Climate.....	8
1.4.3 Morphology and vegetation.....	9
2 General methods for the research project	12
2.1 Data sources and pre-processing.....	12
2.2 Regionalisation.....	13
2.3 Basics of a geographic information system and required data pre-processing.....	17
2.3.1 Geographic information systems.....	17
2.3.2 Digitising and georeferencing.....	18
2.4 Scale problems.....	18
3 Geological settings of north-eastern Namibia	21
3.1 Lithology and distribution of the stratigraphic units.....	22
3.1.1 Pre-Damara.....	23
3.1.2 Damara.....	23
3.1.3 Karoo.....	26
3.1.4 Kalahari.....	29
3.2 Thickness and structure of the sedimentary basins.....	45
3.2.1 Thickness of the Karoo deposits in northeastern Namibia.....	45
3.2.2 Thickness and structure of the Kalahari basin.....	48
3.3 Tectonic settings in the Eiseb Block.....	55
3.3.1 Interpretation of Landsat TM imagery.....	55
3.3.2 Time of the faulting.....	58
3.3.3 Regional correlation and interpretation.....	58
4 Hydrogeological settings	61
4.1 Groundwater levels and definition of catchments.....	61
4.1.1 Method.....	61
4.1.2 Results.....	61

4.2 Distribution of groundwater strikes and definition of the topmost aquifers.....	66
4.2.1 Method.....	61
4.2.2 Results.....	61
4.3 Distribution of well yield.....	68
4.3.1 Method.....	68
4.3.2 Results.....	69
4.4 Hydraulic conductivity.....	71
4.4.1 Method.....	72
4.4.2 Hydraulic conductivity for the pre-Kalahari aquifers.....	73
4.4.3 Hydraulic conductivity for the Kalahari aquifers.....	75
4.5 Porosity.....	79
5 Groundwater recharge.....	81
5.1 Summary of previous recharge research in the Kalahari.....	81
5.2 Surface Properties.....	84
5.2.1 Methods.....	84
5.2.2 Resulting description of the four soil groups and calcrete.....	88
5.2.3 Discussion of results from infiltration tests.....	94
5.2.4 Interpretation of recharge properties for surface groups and their regional aspects.....	96
5.3 Climatic data.....	97
5.3.1 Rain amount.....	98
5.3.2 Pan Evaporation.....	106
5.4 Hydrograph interpretation.....	110
5.4.1 Method.....	110
5.4.2 Results.....	110
5.4.3 Summary and conclusion from hydrograph interpretation.....	114
5.5 Soil water balance model.....	114
5.5.1 Method.....	115
5.5.2 Results and conclusion.....	115
5.6 Estimation of recharge rates by use of the chloride mass balance method.....	119
5.6.1 Wet chloride deposition.....	120
5.6.2 Chloride mass balance in the unsaturated zone.....	121
5.6.3 Chloride mass balance in the saturated zone.....	123
5.6.4 Interpretation of the results from chloride mass balance method.....	125
5.7 Regionalisation of recharge by inverse hydrochemical approach.....	129
5.7.1 Method.....	129
5.7.2 Results and interpretation.....	132
5.8 Regionalisation of recharge and evapotranspiration by the use of satellite images.....	135
5.8.1 Regionalisation of hardrock recharge by the use of satellite images.....	136

5.8.2 Regionalisation of recharge through unconsolidated sediments and soils.....	151
5.8.3 Regionalisation of evaporation and transpiration by use of groundwater level distance and satellite images.....	153
5.8.4 Combined recharge for the research area from hardrock recharge, soil recharge, evaporation and transpiration.....	158
5.9 Summary and methodological recommendation.....	162
5.9.1 Summary of the recharge results.....	162
5.9.2 Methodological recommendations.....	165
6 Groundwater flow model.....	166
6.1 Method.....	166
6.1.1 Pre- and post-processing.....	166
6.1.2 Model set-up.....	167
6.1.3 Modelling execution and calibration.....	171
6.2 Results.....	171
6.3 Sensitivity analysis.....	174
6.4 Interpretation and recommendation for further water resource planning.....	175
7 Hydrochemistry.....	177
7.1 Methodological aspects.....	177
7.2 Spatial distribution of hydrochemical parameters in the study area.....	182
7.2.1 The northern hydrochemical study area (NHSA).....	186
7.2.2 The southern hydrochemical study area (SHSA).....	195
7.2.3 The central hydrochemical study area (CHSA).....	204
7.2.4 Implication for the entire catchment.....	207
7.3 Temporal variations of the hydrochemical parameters.....	208
7.4 Conclusions.....	213
8 Summary.....	216
9 Zusammenfassung (German summary).....	219
10 References.....	225
Appendices	
Appendix A: Piezometer test data (4 pages)	
Appendix B: Soil physical data (21 pages)	
Appendix C: Hydrographs (5 pages)	
Appendix D: Hydrochemical data (79 pages)	

1 Introduction

1.1 Problem

Arid areas cover between 26 and 36 % of the world's land surface depending on the climate index used (AGNEW & ANDERSON, 1992). In these areas the population relies on groundwater as the almost exclusive source of drinking water. There the over-exploitation of the groundwater resource will result in survival-threatening lack of water.

For sustainable groundwater management it is essential to understand groundwater recharge mechanisms and quantify its amount reliably. Groundwater catchments in arid areas are very large compared to central European humid groundwater catchments due to a lack of discharging streams. Surface properties vary remarkably in these large catchments. It is thus inadvisable to assume mean values of point data to represent a large arid catchment.

The definition of catchment wide recharge is often achieved by areal water balance calculations:

$$D = P - (R + ET + \Delta S) \quad (1.1)$$

With deep percolation or recharge D , precipitation P , runoff R , evapotranspiration ET and change in soil moisture storage ΔS . If the recharge amount is in the order of magnitude of the uncertainty of precipitation and evaporation, the calculated recharge will have an uncertainty as large as its value which is inadequate for meaningful sustainable water resource planning. Therefore more reliable methods need to be applied.

Unconsolidated Kalahari sands, covering an area of approximately 2.5 Mio km² between Gabon and the Republic of South Africa, still embrace many geoscientific unknowns. Climatic conditions in the Kalahari of Namibia range from arid in the south to semiarid in the north and thus the use of limited hydrogeological point data cannot reflect the large catchment. Therefore, most hydrogeological research projects that have focused on small research areas give consistent results within the project but inconsistencies between different research projects are common.

The increasing population in Namibia is highly demanding of further water resource development. In the eastern part of the research area in north-eastern Namibia especially, it is planned to develop new grazing areas with the aim of repatriating Herero cattle farmers from Botswana (DWA, 1993e). It has to be assessed if the Kalahari catchment can still provide the expected 4 000 people and about 50 000 cattle with a long-term potable water supply. Springs within this catchment have stopped flowing, e.g. Rietfontein, Grootfontein, Gam and Otjombindi

which might indicate some changes in the groundwater dynamics. Furthermore, it appears that new expensive drillings have often resulted in water not good for human consumption due to a high amount of total dissolved solids or single specific concentrations.

1.2 Aim

The aim of this research project is to understand groundwater dynamics in the Kalahari catchment of north-eastern Namibia with respect to recharge and discharge areas, and the related processes. This requires that the catchment scale be respected by studying the major recharge and discharge processes and projecting them meaningfully to the entire catchment.

This project focuses on the development of regionalisation methods that should be mutually verifiable and thus lead to a more reliable recharge figure than previous studies. The regional approach should also help to understand the distribution of recharge and discharge zones within the catchment which might point out areas that would need protection to guarantee a qualitatively and quantitatively reliable groundwater resource.

1.3 Overview of applied methods

A variety of methods had been employed to address the problems, questions and aim outlined above:

- study of geological setting of the research area with special emphasis on the Kalahari geology by the use of literature review, interpretation of borehole data and a field campaign
- literature review for hydrogeological settings, evaluation of pumping test data and regionalisation of available data
- examination of soil physical properties during field work and by laboratory testing
- interpretation of climatic data
- definition of recharge occurrences from hydrograph observation
- application of the chloride mass balance method in the unsaturated zone and in the saturated zone (limited to areas without lateral inflow) to develop a data set of point recharge data
- use of a water balance model to point out favourable recharge conditions
- regionalisation of recharge and discharge by an inverse hydrochemical approach
- regionalisation of recharge and discharge by a forward remote sensing approach
- development of a groundwater flow model
- interpretation of the spatial distribution of hydrochemical properties and processes
- temporal variations of hydrochemical parameters for shallow groundwater

1.4 Overview of the research area

1.4.1 Location

The research area is situated in north-eastern Namibia, southern Africa, between Latitude S 22.25° and S 17.75° and Longitude E 16.25° and E 21° as indicated in Fig. 1.4-1. In the north it is bordered by the Okavango that also defines the national border towards Angola. The research area is limited to the east by the national border with Botswana. The western and southern limits of the research area are selected according to the hydrogeological catchments (Chapter 4.1).

The research area comprises the administrative regions Okavango, Otjozondjupa and Omaheke with the districts Rundu (eastern part only), Tsumkwe,

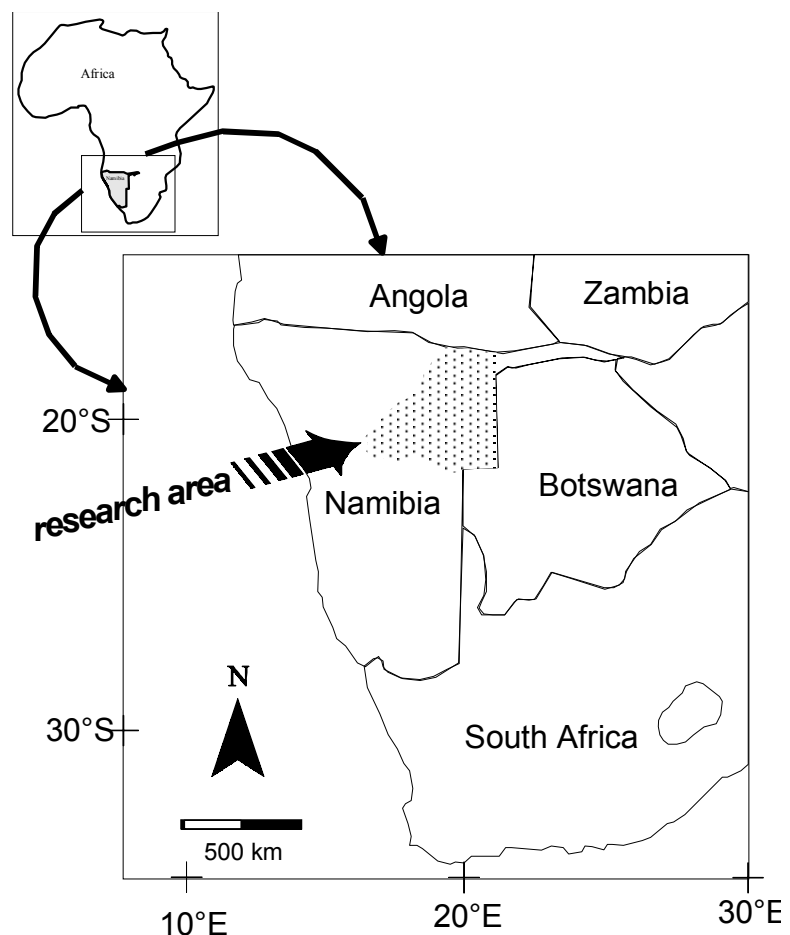


Fig. 1.4-1: Location of the research area in southern Africa.

Okakarara, Grootfontein (northern and eastern part), Otjiwarongo (eastern part), Okahandja (northern part), Otjinene and Gobabis (northern part). The most prominent towns situated within the research area are Rundu, Grootfontein, Tsumkwe, Gam, Okakarara, Hochfeld, Otjinene and Talismanis-Rietfontein.

1.4.2 Climate

According to the climate classification of the UNESCO (1979) the research area is classified as a arid to semiarid zone (mean annual precipitation between 350 and 575 mm, mean annual evaporation between 3300 and 2500 mm, with a aridity quotient $P/EV = 0.11$ to 0.23) with warm

winter (mean temperature of the coldest month from 13 - 17 °C), a mean temperature of the warmest month between 25 and 27 °C and dominant winter aridity.

1.4.3 Morphology and vegetation

The research area is characterised by a flat plain that is covered by sand and surrounded by hardrocks outcropping as ridges, hilly areas, flat hardrocks or as inselbergs. Apart from the surrounding hardrock areas the Aha Hills in the Tsumkwe district between Tsumkwe, Gam and the border to Botswana form some prominent hills.

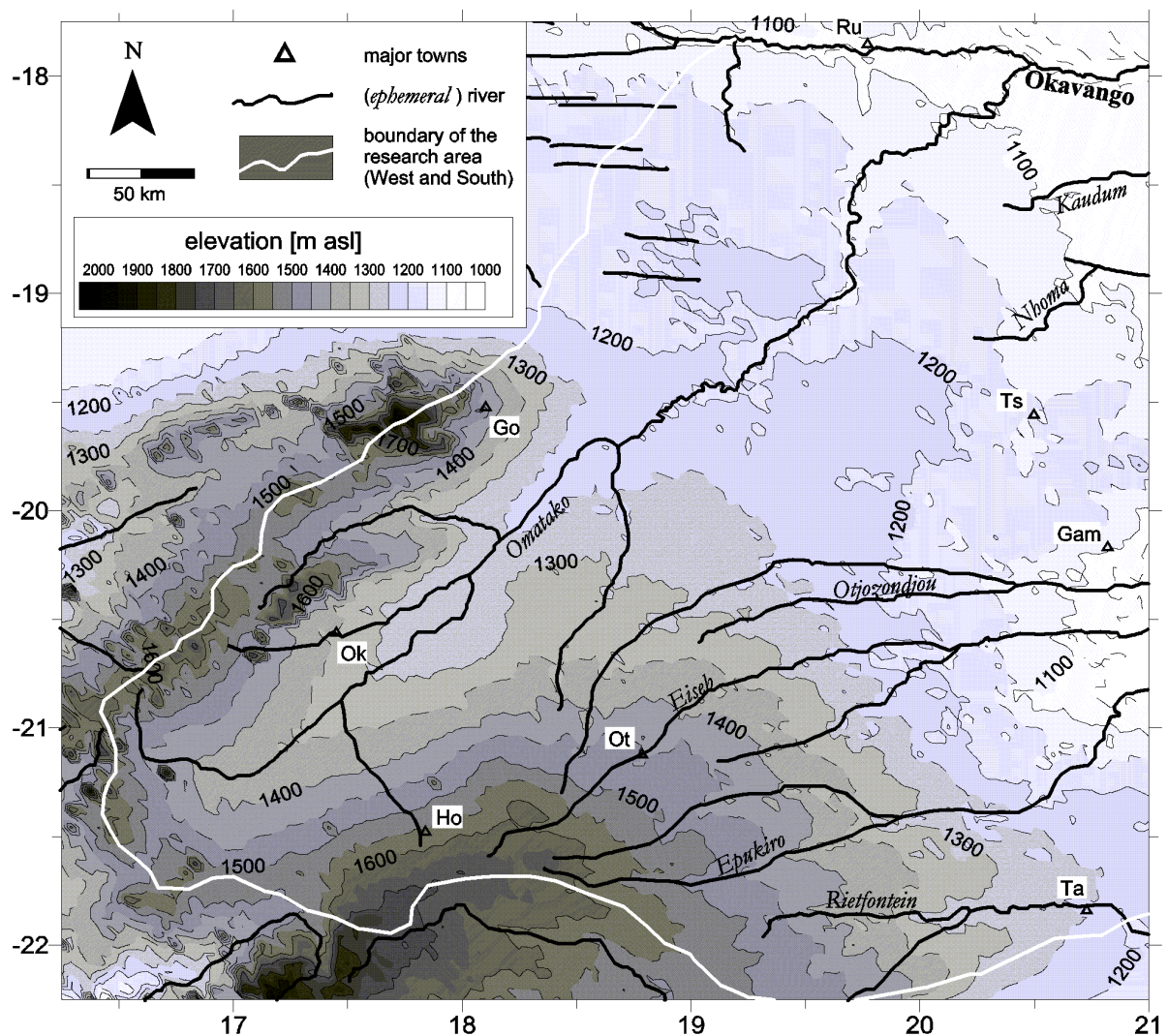


Fig. 1.4-2: Surface topography of the research area with ephemeral rivers and major towns: Go-Grootfontein, Ot-Otjinene, Ru-Rundu, Ts-Tsumkwe, Ta-Talismanis-Rietfontein, Ho-Hochfeld, Ok-Okakarara.

The topographic surface, given in Fig. 1.4-2, slopes gently from the southern and the western highs which attain altitudes of up to 1800 m to the east and the north with approximately 1050 m above mean sea level (m asl).

The sand cover locally forms, often associated with the major ephemeral rivers, inactive longitudinal dunes. Predominantly in the eastern part of the research areas the east-west striking dunes and interdunes alternate frequently. Those dunes are relicts of drier periods and they are now stabilised by vegetation, but in some overstocked areas reactivation of the dune tops has been observed.

The only permanent surface water is the Okavango in the north which originates in the humid Angolan highlands. An endorheic drainage system with ephemeral rivers represents further but only very temporary open waters. The ephemeral rivers in the research areas are named "Omuramba" (plural Omiramba) from the Otjiherero word for "small river", "flat area" or "river that you can't find". The Omuramba Omatako and its major tributaries Ohakane, Ombatjipuro, Klein Omatako, Omambonde, Gunib and Ngcasawa drain towards the Okavango. While in the upper catchment of the Omatako some surface runoff has been reported, the lower part is only fed by back-flow from the Okavango during very high water stands. For the central part of this Omuramba only very local and very short runoff events are reported by the local people.

The ephemeral rivers that drain towards the east (Okavango Delta and Makgadikgadi System in Botswana) are from south to north Omuramba Rietfontein with tributary Amasib, Omuramba Grootlaagte, Omuramba Epukiro with tributaries Alexest, Otjourundu, Gemsboklaagte, Steenboklaagte, Elandslaagte and Rooiboklaagte, Omuramba Eiseb with tributaries Ozondjou and Otjinoko, Omuramba Otjozondjou with tributaries Daneib and Karakapi, Omuramba Nhoma and Omuramba Kaudum with tributary Tclabasche.

This drainage system was produced during more humid times by interaction of surface water and groundwater. In some parts the drainage paths are directed by the dune shape, and in other parts the flood courses follow neotectonic lineaments. The Omiramba valleys show mostly very gentle slopes and only when the country rock is of a consolidated nature steep river beds are developed and expose several metres of geological sections.

Ephemeral open water bodies are also appearing as pans, which are also named "vlei" according to the Afrikaans name. They are formed in shallow depressions where surface runoff is collected. Some larger pans in the Tsumkwe district are also expected to receive some interflow that feeds ephemeral springs there, e.g. Gura Pan and Dobe Pan.

The vegetation border from Zambezian dry deciduous forest and shrub forest to Kalahari acacia deciduous bushlands and wooded grassland cuts across the research area in the Kavango district

in a east-western direction (WHITE, 1983). CORREIRA & BREDENKAMP (1987) indicate the vegetation gradient in the research area from the south to the north to be very long and incomplete from Zambezian dry deciduous forest and shrub forest to Kalahari acacia deciduous bushlands and wooded grassland with *Colophospermum mopane* missing. It develops from *Acacia erioloba* and *Acacia mellifera* (southern Namibia) via *Burkea africana* (north of the Omuramba Rietfontein), *Ricinodendron rautanenii* (north of Omuramba Epukiro), *Pterocarpus angolensis* (north of the Omuramba Eiseb), *Baikiaea plurijuga* and *Guibourtia coleosperma* (northern Bushmanland) and *Baikiaea plurijuga* (northern Kavango) to *Brachystegia spp.* (Angola). In the northern part of the research area the vegetation gradient from the east to the west is short and incomplete and develops directly from *Colophospermum mopane* to *Baikiaea plurijuga*.

The natural vegetation is used for cattle and sheep farming in the southern part of the research area (Gobabis district) and for cattle farming in the rest of the research area. Farming is in general of an extensive nature with a grazing capacity of 1 large stock unit per 8-12 ha. While in the farmland these values are quite representative, land-use differs significantly in the communal areas due to water availability. The vicinity of wells is often overstocked whereas not yet accessed areas are not used for farming. Throughout the research area only minor crop farming occurs exclusively for home use. Game parks and nature conservation areas are constrained to the Waterberg Plateau Park in the west, Eden Nature Reserve east of Grootfontein, Nyae-Nyae Conservancy in the Tsumkwe area, Kaudum National Park in the south-eastern Kavango district and Embo Game Park east of Eiseb Post 10.

2 General methods for the research project

2.1 Data sources and pre-processing

As this project depends highly on existing data some aspects of data availability and how the data were obtained, examined and filtered will be described here in general. If more detailed information is necessary it follows in the corresponding chapters.

Topographic information of the entire catchment have been available by a digital elevation model from the USGS (approximate resolution 1*1 km) which has been checked for confidentiality by comparing it with the topographic sheets (1:250 000 and 1:50 000) from the Surveyor General Windhoek. This elevation model with reference to mean sea level presents the basis for further topographic models produced during this study, e.g. the elevation of the pre-Kalahari surface.

Data from the Department of Water Affairs in Windhoek (DWA) were available in form of internal reports and public reports as which they will be cited when used in the following chapters. The most extensive source of data is represented by the digital database at the DWA. Wells in Namibia are catalogued according to the topographic sheets with borehole numbers (also named WW-numbers), drilling date, level below collar, elevation of collar above mean sea level, yield, strike, diameter and coordinates. All these data have been available in ASCII format and were transformed into a Microsoft-Excel-datasheet for the entire catchment. Hydrochemical data for some wells are existing in the DWA database, which is further discussed in Chapter 7.

AA	AB	BA	BB
A		B	
AC	AD	BC	BD
2120			
CA	CB	DA	DB
C		D	
CC	CD	DC	DD

Fig. 2.1-1: Specification of topographic sheets in Namibia.

Some of the original borehole logs (hardcopies) have been available at the DWA which have been used to develop a database that combines the locations from the DWA digital database with the geological sections.

All data were carefully examined as coordinates were sometimes found to be unreliable. It was checked if the locations by latitude and longitude coordinates are inside the according topographic sheet, e.g. 2120AC1 lies in the according quadrant. Maps in Namibia are labelled as indicated in Fig. 2.1.-1. The number of the topographic sheet is there referring to

the latitude and longitude of the upper left corner. Each of the 1:50 000 sheets, e.g. 2120DD, covers an area of 15' in latitude by 15' in longitude.

Plausibility of level and strike was checked by comparing them to the depth of the borehole. If the original borehole logs were available (it occurred very seldom) it was also reconciled with this information. Elevation of the borehole was checked with the according topographic sheet. If data were insufficient, they were either excluded from the new database or corrected according to best knowledge from all available resources.

2.2 Regionalisation

When focusing on a large groundwater catchment one of the basic demands is a meaningful spatial approach. Therefore one cannot use point data only but needs to consider the groundwater catchment as a spatially variable system. For some purposes detailed regionalisation processes are required (e.g. groundwater recharge zone identification by satellite images) which will be described in the corresponding chapters (5.7 and 5.8). For other purposes already available statistic models such as *kriging* or *(weighted) average interpolation* provide established tools to regionalise data. In order to obtain a regularly scattered data set from irregularly scattered data one needs to use the procedure of gridding, which has to be subdivided into two main steps:

- 1) Define the search modus for the data that will be used to calculate the new grid data.
- 2) Calculate the value of the new grid point from the measured data points by a certain mathematical function.

The available data have to be carefully examined before using one of the gridding methods. Tools for this are histograms and variograms.

Histograms reflect the distribution of the data without concerning the spatial distance between data points. For visualisation of data distribution by histograms the data set is subdivided into consecutive intervals (classes) and the frequency of each class is given either numerically or as a diagram.

Variogram

Variograms reflect the scale of fluctuation of the variable $z(x)$ by plotting the square differences $1/2[z(x_i)-z(x'_i)]^2$ against the separation distance $\|x_i-x'_i\|$ for all measurement pairs (where $\| \ \|$ means the length of a vector). For n measurements one receives $\frac{n(n-1)}{2}$ such pairs that make up a raw variogram. In order to receive an experimental variogram, which is a smooth line through the scatter plot, one has to group the measurement pairs by dividing the axis of separation

distance in consecutive intervals. For every interval an experimental square difference will be calculated for the k -th interval is $[h_k^l, h_k^u]$ and contains N_k pairs of measurements $[z(x_i), z(x'_i)]$ as:

$$\hat{\gamma}(h_k) = \frac{1}{2N_k} \sum_{i=1}^{N_k} [z(x_i) - z(x'_i)]^2 \quad (2.1)$$

where the index i refers to each pair of measurements $z(x_i)$ and $z(x'_i)$ for which

$$h_{lk} \leq \|x_i - x'_i\| < h_{uk} . \quad (2.2)$$

Each interval is represented by a single point h_k that is equal to the average value:

$$h_k = \frac{1}{N_k} \sum_{i=1}^{N_k} \|x_i - x'_i\| . \quad (2.3)$$

The connecting line of the data pairs, which is named experimental variogram or semivariogram, expresses the spatial correlation of the regionalised variable independent of orientation (KITANIDIS, 1997). Parabolic forms indicate excellent continuity of the regionalised variable, a linear form indicates moderate continuity and a horizontal form of $\gamma(h) = \sigma^2$ is produced by a random variable having no spatial auto-correlation. A nugget effect, which is an apparent failure of the semivariogram to go through the origin, indicates a regionalised variable that is having measuring mistakes or a high micro-variability over distances less than the sampling interval (HEINRICH, 1992). Idealised semivariograms of the described types are given in Fig. 2.2-1.

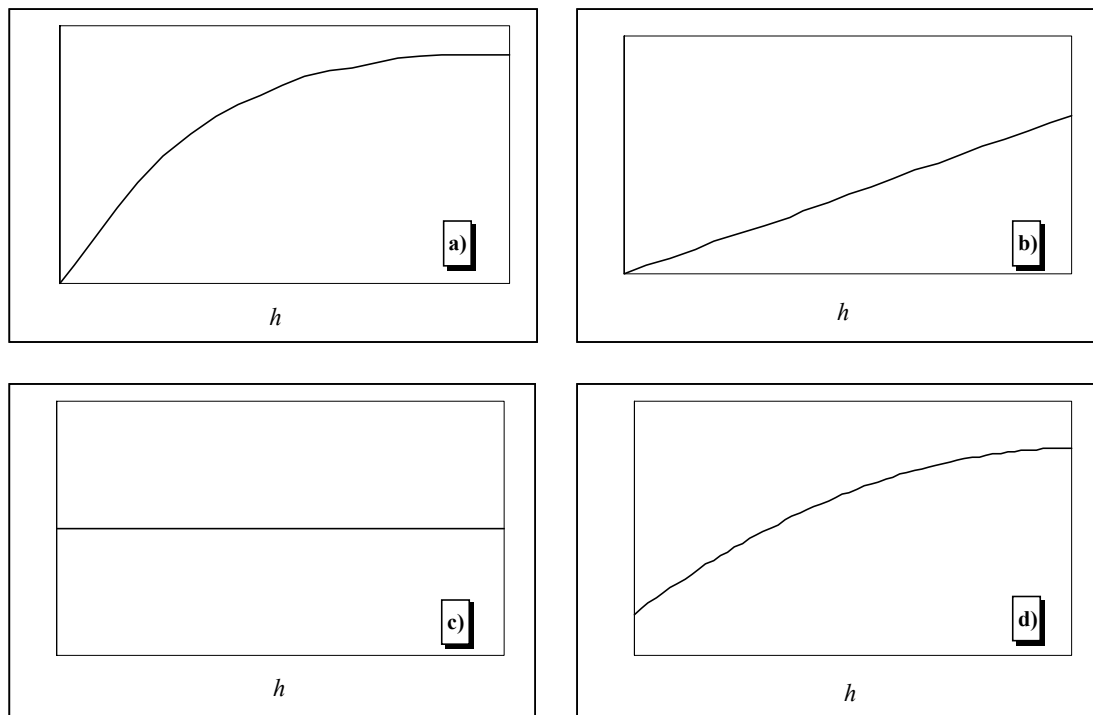


Fig. 2.2-1: Idealised semivariograms showing (a) parabolic form, (b) linear form, (c) horizontal form at the level of σ^2 and (d) nugget effect. Modified from DAVIS (1986).

Search modus for gridding procedure

For every gridding procedure one has to decide if the applied mathematical method to calculate the new grid point should consider all available data points or if a limitation is reasonable. When using large data sets a limitation will decrease computation time significantly. For the limitation different search criteria may be specified such as using a certain amount of nearest neighbours only or specification about the amount of how many nearest points from every sector should be used and into how many sectors the search circle should be subdivided. Examples are given in Fig. 2.2-2. Under some circumstances it is also sensible to define a special search ellipsoid if e.g. parameters are stronger depending on the strike direction than on the perpendicular direction.

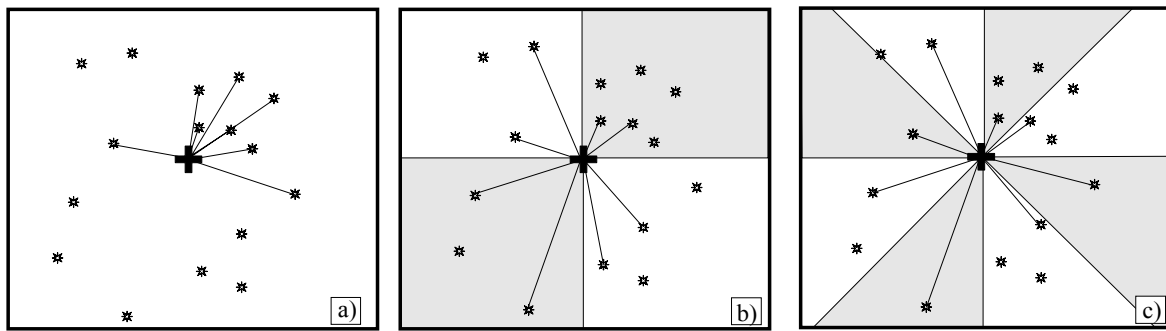


Fig. 2.2-2: Search techniques: (a) nearest neighbour, (b) quadrant search pattern and (c) octant search pattern. Modified from DAVIS (1986).

Average Interpolation

Subsequent to data selection, a model that appropriately calculates the grid values must be chosen. Average interpolation projects the surrounding measured data $z(x_i)$ to the regionalised grid coordinate and calculates the average in dependence of the distance from the original data point to the regionalised data point. The grid node elevation $\hat{z}(x)$ will be calculated as:

$$\hat{z}(x_k) = \frac{\sum_{i=1}^n \frac{z(x_i)}{D_{ik}}}{\sum_{i=1}^n \frac{1}{D_{ik}}} \quad (2.4)$$

with the distance D_{ik} from observation point i to grid node k :

$$D_{ik} = \sqrt{(x_{1k} - x_{1i})^2 + (x_{2k} - x_{2i})^2} \quad (2.5)$$

A widespread case of the average interpolation is the inverse distance to a power method. With this method control points are weighted according to their distance by a weighting power parameter β as given in the following equation:

$$\hat{z}(x_k) = \frac{\sum_{i=1}^n \frac{z(x_i)}{D_{ik}^\beta}}{\sum_{i=1}^n \frac{1}{D_{ik}^\beta}} \quad (2.6)$$

A main characteristic of maps produced by this procedure is that the calculated grid nodes all lie within the range of the original data and that it sometimes produces "bull's-eyes" surrounding the position of observation points within the grid. The clear advantage of this procedure is its fastness and the exact reproduction of the data value at each measuring point.

Kriging

The procedure of kriging is used to estimate grid values at assumed dimensionless points from measurements that are themselves made at dimensionless points. The main kriging equation defines that the estimated value $\hat{z}(x)$ at point x is a linear combination of the known nearby values $z(x_i)$, with $\delta_i(x)$ being the weight:

$$\hat{z}(x) = \sum_{i=1}^n \delta_i(x) * z(x_i) \quad (2.7)$$

Assumptions for the kriging method are:

- the estimation value $\hat{z}(x)$ is independent of x
- the average error will be zero
- kriging variance will be minimal

It thus follows that the weighted averages in the main kriging equation sum up to 1:

$$\sum_{i=1}^n \delta_i(x) = 1 \quad (2.8)$$

In the case that one wishes to make a kriged estimate of the value $\hat{z}(x)$ at a point x from n observations $z(x_1), z(x_2), \dots, z(x_n)$ the n weights $\delta_1, \delta_2, \dots, \delta_n$ must be found for the kriging equation which requires the solution to a system of n simultaneous equations:

$$\delta_1 \gamma(h_{11}) + \delta_2 \gamma(h_{12}) + \dots + \delta_n \gamma(h_{1n}) = \gamma(h_{1p}) \quad (2.9)$$

$$\delta_1 \gamma(h_{21}) + \delta_2 \gamma(h_{22}) + \dots + \delta_n \gamma(h_{2n}) = \gamma(h_{2p})$$

...

$$\delta_1 \gamma(h_{n1}) + \delta_2 \gamma(h_{n2}) + \dots + \delta_n \gamma(h_{nn}) = \gamma(h_{np})$$

With $\gamma(h_{ij})$ is the semivariance over a distance d corresponding to the separation between control point i and j , and $\gamma(h_{np})$ is the semivariance for a distance equal to that between known point one

and the location p where the estimate is to be made. Values of the semivariance are taken from the semivariogram which must be known or estimated prior to the kriging (DAVIS, 1986).

$(n+1)$ equations with n unknowns are available concerning the additional equation 2.8. That gives an extra degree of freedom, and it will be used to give the solution the minimum possible estimation error by adding a Lagrange multiplier λ . By rearranging into matrix form one receives:

$$\begin{pmatrix} 0 & 1 & \cdots & 1 \\ 1 & \gamma(x_1, x_1) & \cdots & \gamma(x_1, x_n) \\ \vdots & \vdots & \ddots & \vdots \\ 1 & \gamma(x_n, x_1) & \cdots & \gamma(x_n, x_n) \end{pmatrix} \begin{pmatrix} \lambda(x) \\ \delta_1(x) \\ \vdots \\ \delta_n(x) \end{pmatrix} = \begin{pmatrix} 1 \\ \gamma(x, x_1) \\ \vdots \\ \gamma(x, x_n) \end{pmatrix} \quad (2.10)$$

Such equation systems can be solved using common methods (e.g. STOER, 1983) as long as the equation system has an unequivocal solution. In this thesis all geostatistic modelling was performed by the software package Surfer 7.0 (GOLDENSOFTWARE, 1999). Detailed descriptions of kriging origin are given by OLEA (1975) and CRESSIE (1990; 1991).

2.3 Basics of a geographic information system and required data pre-processing

2.3.1 Geographic information system

As the research project focuses on spatial distribution within an entire hydrogeological catchment it is necessary to examine spatial distribution of data and combine them with other data. Established tools for such purpose are geographic information systems (GIS) that support raster formats as well as vector formats. For proper use of a GIS it is necessary to transform all available data into georeferenced digital data. The procedure of digitising and georeferencing as they have been used during the project will be described.

Three GIS software packages have been used during the research period: IDRISI Version 2.007 by CLARK LABS (1997), TNTmips Version 5.4 by MICROIMAGES (1996) and ArcView GIS Version 3.0 by ESRI (1996). IDRISI is the easiest to handle software but has several limitations for vector formats. Although TNTmips appears to be the best organised program it demands advanced familiarising with the software. As TNTmips opens a wide range of tools with digitising, data examinations and geostatistical modelling up to classifications of large satellite images, it is the only package that fully suits the demands of this study.

2.3.2 Digitising and georeferencing

As most of the used data, e.g. geological maps, are only available in paper printouts, they need to be transformed into a digital georeferenced form. First of all, printout cards had to be scanned in with as little distortion as possible. The resulting image files were combined using a picture processing program (e.g. Adobe Photoshop version 4.0LE by ADOBE, 2001). The resulting image file was then imported into the digitising software, e.g. TNTmips. There the spatial data were connected with a georeference that relates the raster or vector to a specific global coordinate system. If available data are distorted (e.g. aerial photographs) they need to undergo a geometric transformation. This process stretches the image differentially by changing its internal geometry and by projecting it from one plan to another. Control points with known geographic coordinates thus needed to be located in the processed image. The required minimum number of control points depends on the model used for the transformation (affine transformation demands a minimum of 3 control points, plan projective and bilinear 4) and increases with the number of orders of polynomial function to be used (second order requests 6 control points, third order 10). When aerial photographs are imported into a GIS, georeferenced and rectified, they can be used directly as raster values in the GIS refer to the intensity of the visible grey in the photography. If geological maps are required in digital form, they mostly need to be "digitally redrawn" which is an extraction of the relevant information. This will either happen by auto-tracing some features or by following the required features on-screen and then transform them into vector or raster format.

For the production of digital thickness models from thickness maps with contour lines, it was found the easiest way to digitise the contour lines and produce a text file with x-, y- and z-coordinates from the vector format by a simple Visual Basic program (DXF_to_XYZ by BARTHEL, private program) and then calculate (see Chapter 2.2) a raster grid from those data.

2.4 Scale problems

Working with spatial data requires a careful verification of the scale that will be used for the transformation of "natural data" into a raster format. By transforming natural areas into raster data the natural areas with curved perimeter will be projected onto raster areas with straight and rectangular perimeters. This will result in nonequivalence of the shape of the natural areas and its projection, and different areal dimensions will also occur. With increasing grid resolution the accuracy will increase as squares can be seen as an asymptotic fill up of a circle. From this perspective it seems to be a major demand to work with high grid resolution, but increasing grid resolutions increase file sizes significantly. Very large data sets require long computing time

when using them in groundwater flow models, and combinations of several large data sets in GIS programs or surface models may destabilise the computer system. A compromise between data accuracy and applicability has to be found.

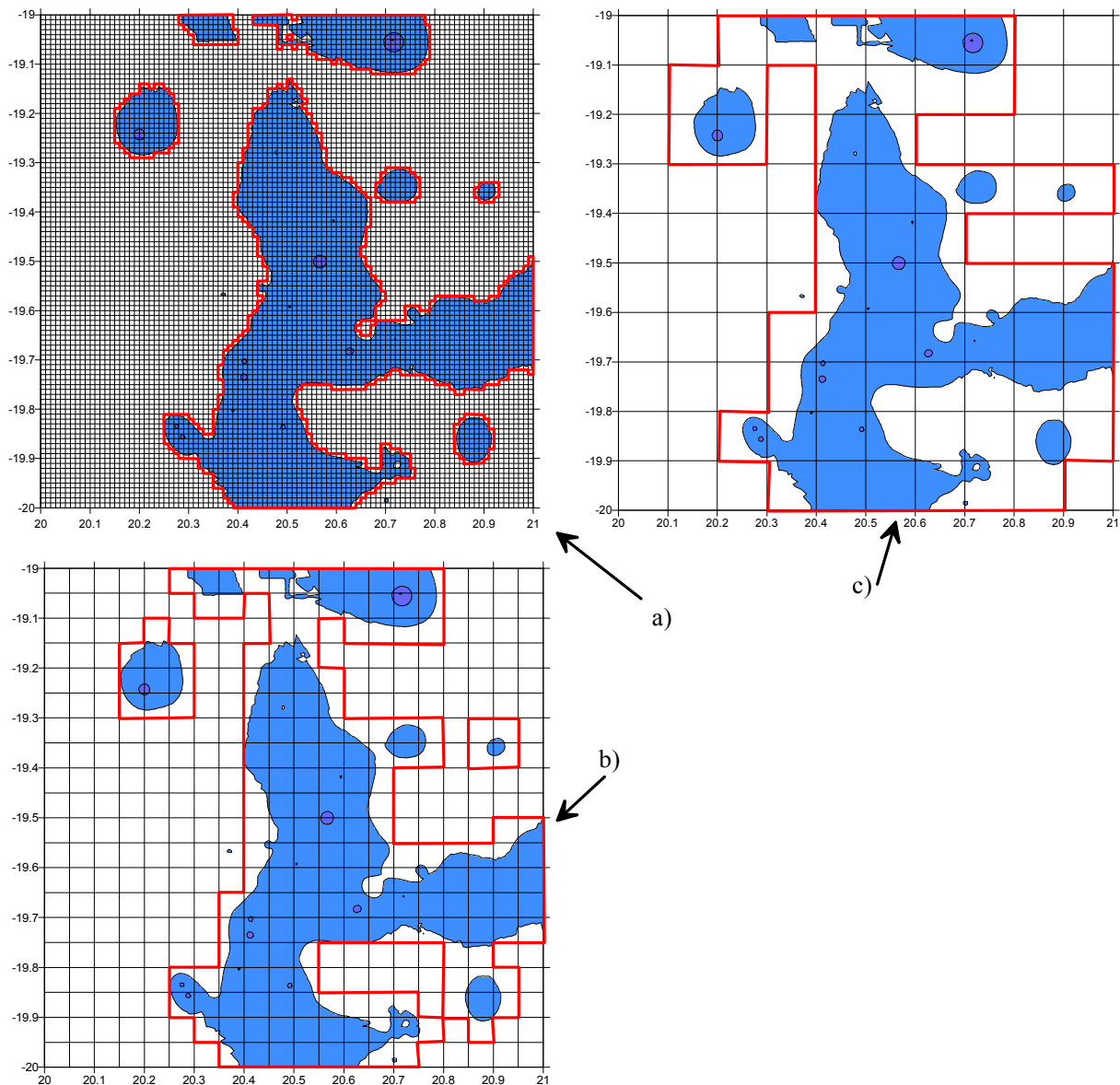


Fig. 2.4-1: Demonstration of effects caused by different raster resolution when classifying areas with groundwater to surface distances less than 20 m. Areas that fall into the criterion with a) 100*100 grid cells, b) 20*20 grid cells and c) 10*10 grid cells are marked by red lines.

The influences of grid resolution on a data set will be demonstrated by one example: all areas with a surface to groundwater depth of less than 20 m should be classified to a group "< 20 m". When using a contour map and projecting grid lines of different scales onto it the resulting area ratios differ significantly (Fig. 2.4-1). For three selected example areas the group "< 20 m" has been quantified with 4 to 5 different grid resolutions. The results of this examination are given in Fig. 2.4-2 with area ratio plotted against the amount of grid cells that the project area is divided

into. The three graphs document that with increasing grid resolution the area ratio decreases asymptotically. From this example it is shown that scale has a significant influence on classified objects. In Fig. 2.4-2a it is shown that a decrease of the grid size from 0.29 km² (950*900 cells) to 0.07 km² (1900*1800 cells) decreases the area ratio "< 20 m" about 1.4 % which is still a tenth. Changes of the grid size from 115.4 km² to 28.9 km² influenced the area ratio more significantly. The conclusion from this observation is, that as long as data are in the pre-classification status, small raster sizes will be used, e.g. 30*30 m for satellite images.

As soon as the binary classified image has been assigned with values, e.g. groundwater recharge rates assigned to areas, the grid resolution can be enlarged without a loss of information accuracy as resolution changes can be made by pixel aggregation that calculated the average of the n surrounding pixels (with n being a factor defined by the user).

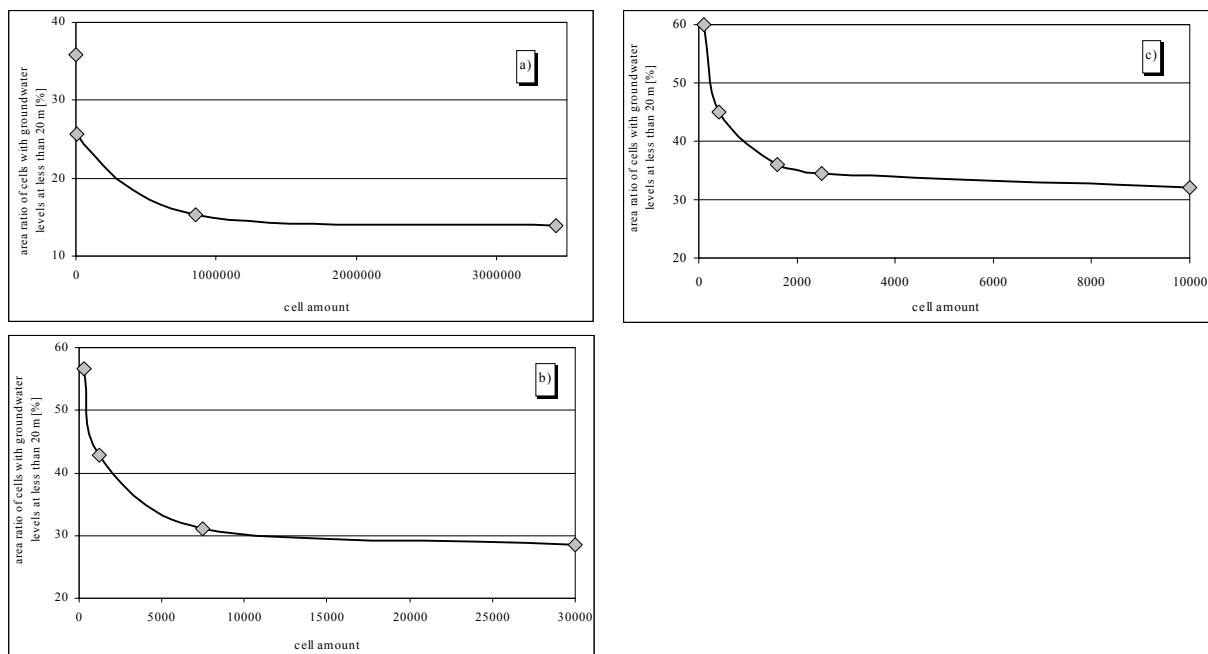


Fig. 2.4-2: Influence of cell amount on classification of areas with groundwater levels at less than 20 m for three example sites: a) northern Kalahari, b) Hochfeld and c) Tsumkwe.

3 Geological settings of north-eastern Namibia

Lithologies of Mokolian to Recent age occur in the research area of north-eastern Namibia (Fig. 3.1-1). The stratigraphic succession can be subdivided into (MILLER & SCHALK, 1980):

- Pre-Damara: the Sinclair Sequences, Grootfontein Complex, Hohenwarte Complex and Abbabis Complex of Mokolian age,
- Damara Sequence of Namibian age,
- Karoo Supergroup of Carboniferous to Jurassic age,
- Kalahari Group of Tertiary (probably Cretaceous) to Recent age.

While rocks of the Pre-Damara units occur only very locally, most of the research area is underlain by the Damara orogenic belt which trends ENE-WSW in north-eastern Namibia. It represents an up to 400 km wide intracontinental branch of the Pan-African orogenic belt that has been dated at 600-535 Ma (HOFFMANN, 1991). These formations were deposited in an intercontinental environment which represents a failed spreading margin (MILLER, 1983). Pelagic and shelf sediments were deformed, metamorphosed and thrust up and over the continental shelf. Pre-Damara basement is included into the thrust belt, as are granites intruded during and after tectonism.

Lower Karoo sediments were deposited during a regional sag while the overlying red beds were deposited during uplift (KEY & AYRES, 2000a). During the Permo-Carboniferous glaciation of Gondwana large glacial deposits of the Dwyka Group were deposited. They are reported from western Namibia and Botswana (MARTIN, 1953; 1981), but not yet from the research area. Isostatic rebound after retraction of the ice shield was accompanied by a south to north directed marine transgression during which the shale-dominated Ecca Group was deposited across large parts of Namibia (MARTIN, 1975). Sediments of the following Beaufort Group document a more continental sedimentation environment with lake deposits, backward setting of the ocean and changing towards a warmer climate. Sediments of wadis, playas and ephemeral rivers were deposited until the lower Jurassic building up the Omingonde Formation (WANKE ET AL., in press). The overlying Etjo Formation reflects a humid sand desert environment that becomes drier (HOLZFÖRSTER ET AL., 1999) and is covered by massive flood basalts of the Kalkrand Formation (MARTIN, 1961a). The flood basalt event heralded the break-up of Gondwana east of Africa as Australia and India separated from the mega-continent at about 161 Ma (GERSCHÜTZ, 1996; HARLAND ET AL., 1990).

While there is no further sedimentation reported from eastern Namibia during the Cretaceous, western Namibia received aeolian deposits of the Etendeka Group which interlayer with basalts that represent the volcanism associated with the break-up of Westgondwana between Africa and

South America, and the subsequent formation of the South Atlantic (MILLNER ET AL., 1994; 1995).

Subsequent to the break-up of Gondwana the massive, intracontinental Kalahari basin was formed by the isostatic lifting of the continental margin leading to the deposition of mainly clastic terrestrial sediments in a fault controlled endorheic drainage system (e.g. THOMAS, 1988).

3.1 Lithology and distribution of the stratigraphic units

The descriptions of the lithostratigraphic units in the research area presented here are combined from literature studies and field observation. The distribution of pre-Kalahari units is mainly based on the Geological Map of Namibia 1:1 000 000 (MILLER & SCHALK, 1980), some 1:250 000 geological sheets and on some own mapping in the field. Fig. 3.1-1 gives an overview of the distribution of the pre-Kalahari units. The distribution of the Kalahari lithologies is mainly based on field work and on descriptions by some other workers, e.g. ALBAT (1978). Results will be presented in Chapters 3.1.4 and 3.2.2. Most of the previous geological research carried out in north-eastern Namibia has focused on pre-Kalahari lithostratigraphic units but not much work has been done on the Kalahari Group. Therefore this chapter will give some results for the Kalahari Group of a more general interest and not only a brief description as required for the characterisation of an aquifer. For all locations referred to in Chapter 3 see Fig. 3.1-11 (page 44).

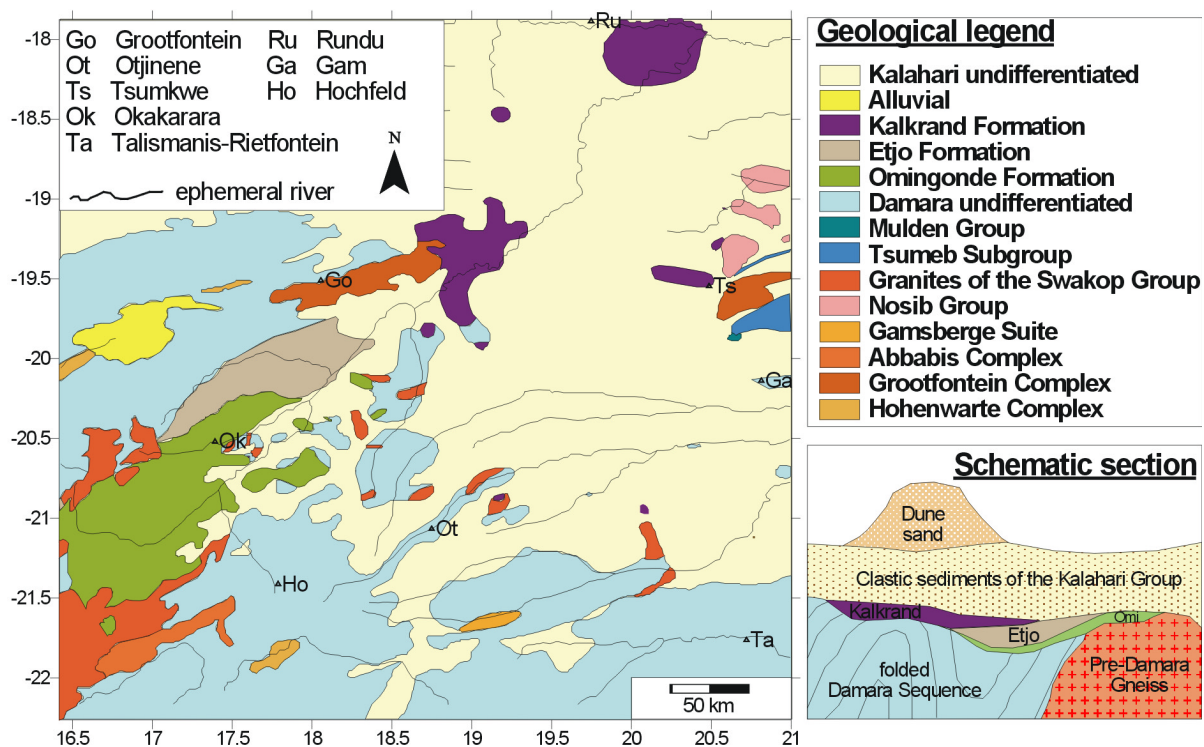


Fig. 3.1-1: Geological overview map of the research area. Map is produced mainly on the basis of the Geological Map of Namibia (MILLER & SCHALK, 1980) and HEGENBERGER (1982). A schematic section is given at the lower right insert.

3.1.1 Pre-Damara

The Grootfontein Complex is built up mainly by paragneisses which are described as coarse grained pink to grey porphyritic gneisses with minor metalavas and quartzites (MILLER & SCHALK, 1980). Exposures of those rocks can be found in the vicinity of Grootfontein and south-east of Tsumkwe (Fig. 3.1-1), e.g. at the Gamsa Pan and Gautscha Pan. The occurrence at Makuri Vlei (Fig. 3.1-2a) comprises coarse grained pinkish gneisses with large alkali feldspar phenocrysts, that HEGENBERGER (1982) interprets as metagranites. The Abbabis Complex comprises mainly paragneisses and other metasedimentary rocks. Paragneisses of this formation outcrop along the road between Okahandja and Hochfeld. Quartz porphyries of the Nuckopf Formation/Sinclair Sequence occur near surface in the south-eastern part of the Kalahari catchment at the Omuramba Otjourundu. The associated granites of this formation (Gamsberg Suite) occur around the Epukiro Mission Station and outcrop on the eastern part of farm 286 Epukiro. Metagranites of the Gamsberg Suite are also mapped in the lower catchment of the Epukiro. In the field they were observed as a deeply weathered greenish metamorphic rock containing much weathered mica but no further distinction was possible.

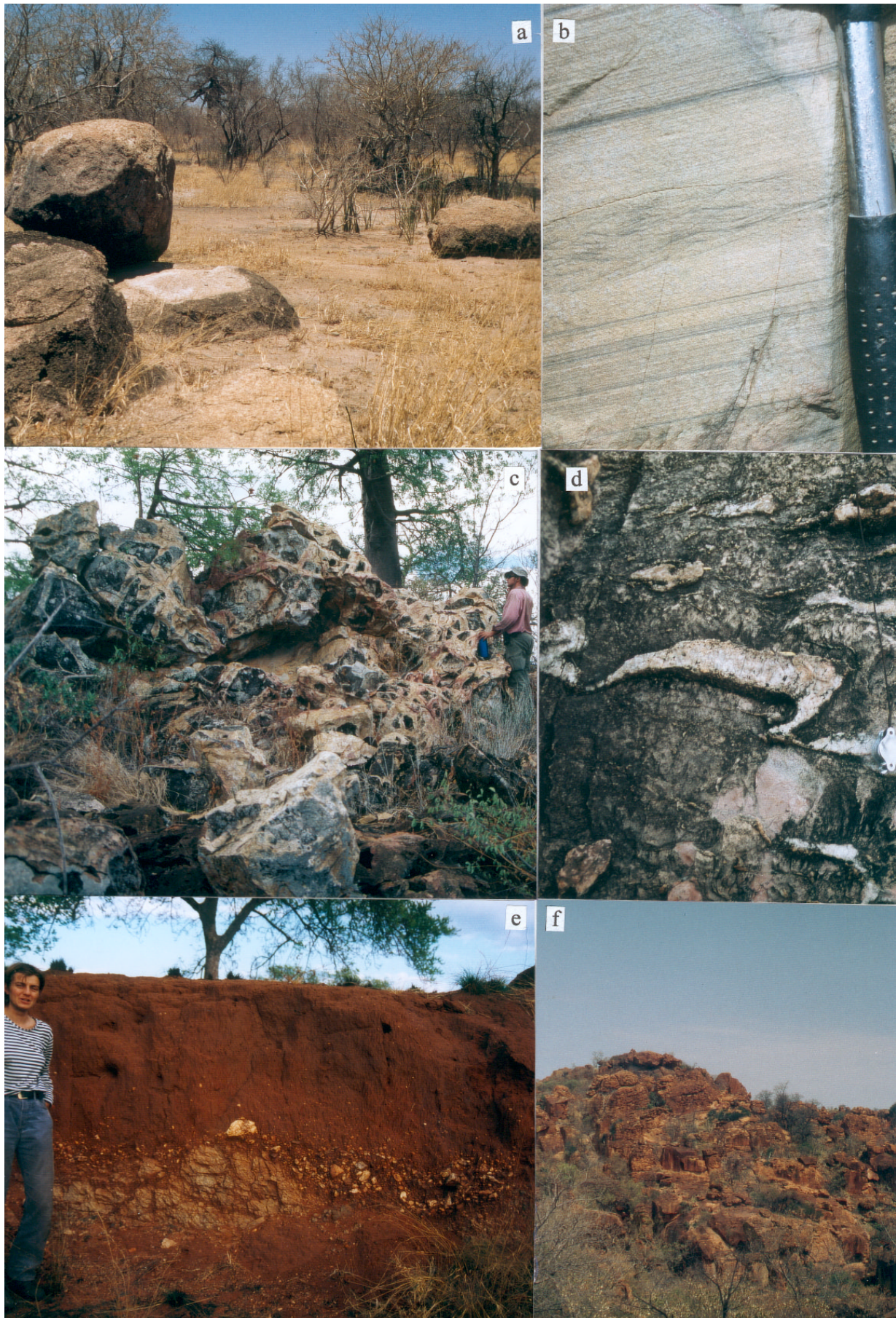
The visited pre-Damara rocks do not show well developed fractures and infiltration tests in the weathering products of the Grootfontein Complex at Makuri Vlei had to be abandoned due to the very low infiltration rate.

3.1.2 Damara

Strongly metamorphosed quartzites, limestones and schists of central Namibia were first grouped under the name “Damara System” by GEVERS (1932). Since then, detailed work has been carried out in the Damara Orogen and it has been subdivided in several tectonostratigraphic units (e.g. MILLER, 1979). The southern foreland and platform zone, the central zone and the northern platform zone occur in the research area (MILLER, 1983). The central zone has undergone regional folding and metamorphism (HAUGHTON, 1963). The northern zone is represented by a similar succession but is less metamorphosed. It is considered as the platform facies of the Damara Sequence that developed on the southern margin of the Congo Craton. It is characterised by shallow water deposits and only minor tectonic deformation (MILLER, 1983). The boundary between the northern and central facies crosses the research area in an approximate SW-NE direction from near Otjiwarongo to the Botswana-Namibia border at 20°S (MILLER & GROTE, 1983).

The north-western part of the research area, the Aha Hills and outcrops north-east of Tsumkwe, belong to the northern platform zone of the Damara Orogen. Dolomites, limestones and shales

Fig. 3.1-2



dominate in the Otavi area. The carbonate rocks show well developed joints and karstification. The limestones and dolomites at the Aha Hills (Fig. 3.1-2c), and in the small NE trending strip north-east of Tsumkwe, are both interpreted as Otavi Group (HEGENBERGER, 1982). Light grey to pink, sometimes folded limestones (Fig. 3.1-2d) were observed to form most of the Aha Hills. At some places carbonate was replaced by silica, mainly in well fractured parts. Greyish phyllites and quartz-phyllites of the Mulden Group have been drilled at the Nama Pan. The Nosib Group north of Tsumkwe consists mainly of quartzites with only minor shale, some mica schists and marble. Near the Dobe Pan and in the Kaudum National Park, quartzites and quartzitic conglomerates have been drilled. GEORGE ET AL. (1993) assume from a study of approximately 400 boreholes that the Damara units underlying the northern Tsumkwe district and the eastern Rundu district consist almost exclusively of quartzites.

Quartzites of the Nosib Group form the cataracts at the Popa Falls in the north-eastern Kavango district just outside the research area. HEGENBERGER (1987) describes them as light grey to green, fine to medium grained quartzites with a maximum thickness of single layers of 5 cm, occasionally containing quartzite pebbles. They are interpreted as fluvial deposits since clay pebbles are rare, and cross-bedding and wave ripples have also been observed.

Outcrops in the Talismanis-Rietfontein Block show only slightly metamorphosed quartzites that still preserve sedimentary structures (Fig. 3.1-2b). They are assigned to the Kamtsas Formation of the southern platform facies. In the north-western and northern part of the Talismanis-Rietfontein Block, greenish to grey phyllites, sericitic quartzites, some mica schists and thin marble were drilled. MARTIN & PORADA (1977) interpreted this as a transition from the Kamtsas to the Duruchaus Formation which was associated with rifting during Nosib Group time. The outcrops at Gam, in the Omuramba Epukiro east of Omaouzonjanda and in the Thereonsvallei (Omuramba Eiseb) are interpreted as a transition between the Swakop Group and the Otavi

◀ **Fig. 3.1-2:** Photo documentation of pre-Kalahari lithologies. **a)** Metagranite of the Grootfontein Complex. Coarse grained pinkish gneisses with large alkali feldspar phenocrysts occur at Makuri Vlei, south-east of Tsumkwe. **b)** Quartzites of the Nosib Group. Sedimentary structures are well preserved in the outcrops of the Talismanis-Rietfontein Block. Cross-bedding is alternating with finely laminated material here. **c)** Dolomite and limestone form the top of the Baobab hill (west of Kremetartkoop). They are interpreted as lower Otavi Group (HEGENBERGER, 1982). **d)** Folded limestone at the Bee Hill (part of the Aha Hills at the Botswana-Namibia border). The thinly laminated white to pink limestone is partly transformed into silica. Silicification occurred preferentially at joints and fractures. The fold axis plunges SSE at approximately 45°. **e)** A strongly weathered basalt (probably Karoo) is exposed in a pit at the Botswana-Namibia border. The basalt is overlain by a unconsolidated conglomerate. **f)** The sandstones of the Etjo formation are well exposed at the Waterberg. Jointing is well developed here. The upper part of the Waterberg is dominated by consolidated dune sand.

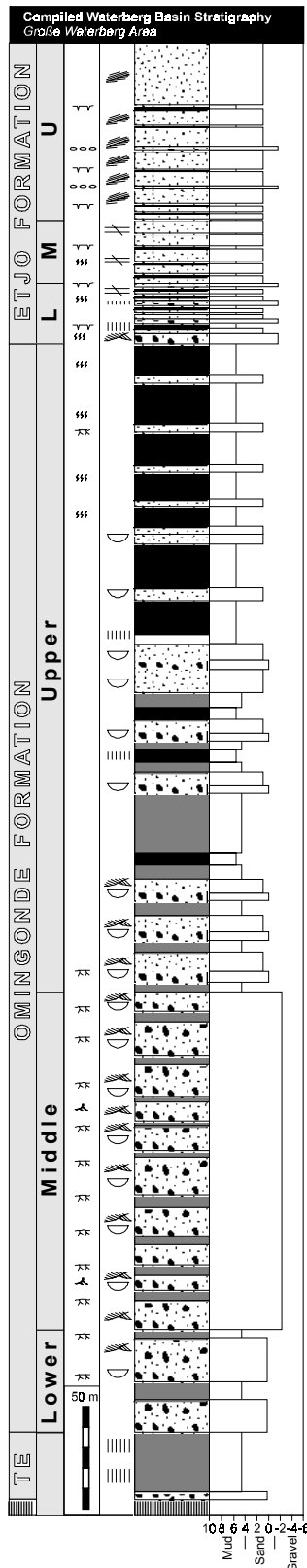


Fig. 3.1-3: Overview section of the Omingonde and Etjo Formation in the Waterberg area (WANKE, 2001; modified from HOLZFÖRSTER ET AL., 1999). For legend see page 29.

Group of the central zone (BAILLIEULE, 1973; REEVES, 1978a; HEGENBERGER, 1982).

Marbles have been described outcropping in the vicinity of Gam. Phyllites, red to dark grey siltstones and cherts, and some marbles were observed in the Thereonsvallei. They show tectonic strain and steep foliation. Mainly dark schists outcrop in the Omuramba Epukiro. In the area between Hochfeld and Okahandja and farther to the north mica schists and ortho-amphibolites of the Kuiseb Formation (Nk) occur with the associated syn- and post-tectonic granites. They are also widespread in drillings in the southern central part of the research area.

Fault planes in the Damara lithologies were reactivated during the break-up of Gondwana. This fracture pattern is clearly developed in the Kamtsas quartzites exposed along the Ghanzi Ridge (HEGENBERGER, 1982). Joints are also well developed in the Talismanis-Rietfontein Block but are often filled with calcrete.

3.1.3 Karoo

The lowermost unit of Karoo age (Permo-Carboniferous to Jurassic) in the working area is the Ecca Group. One small outcrop of Prince Albert Formation/Lower Ecca Group has been reported at farm 433 & 434 Wiums Rus west of the Omuramba Gemsboklaagte. It consists of shale, with subordinate mudstone and sandstone (WITHERS, 1982). The Omingonde and Etjo formations are widespread in the western part of the study area and have been studied in detail by HOLZFÖRSTER (2000) and WANKE (2001). An

overview section for the Waterberg area is given in Fig. 3.1-3.

The Omingonde Formation consists of red to white clastic material. The Lower and Middle Omingonde Formation is dominated by gravely sandstone interlayered with siltstone. Trough cross-bedding is documented for the sandstone units, together with palaeosol development and occurrences of fossil rootlets. The Upper Omingonde Formation is showing a development from trough cross-bedded, gravely sandstones to a mudstone dominated unit with some sandstones. The mudstones are laminated in the middle Upper Omingonde Formation, while they show some bioturbation in the upper part.

The thickness and style of the Omingonde Formation varies laterally due to the synsedimentary activity of the Waterberg Fault (WANKE, 2001). Massive and coarser grained varieties are constrained to positions very proximal to the Waterberg fault, e.g. at the Kleine Waterberg. An Omingonde section visited at farm 179 Matador showed a distal facies which is mudstone dominated.

The base of the Etjo Formation is marked by trough cross-bedded gravely sandstone. The entire Etjo succession is dominated by several upwardly thickening sandstone units which interlayer with gravely sandstones and minor mudstones. Mudcracks are developed in the clayey units. Sandstones of the Upper Etjo Formation show large scale planar cross-bedding. They are well exposed at the upper cliff of the Große Waterberg (Fig. 3.1-2f). The aeolian dune deposits form a homogenous sandstone which consists of well sorted, well rounded, medium size quartz grains.

Basalts of the Karoo Supergroup occur only very locally in the western part of the study area but they build some very distinctive features like the Omatako Hills (farm 189 and 256 Omatako View). In the northern part of the study area small outcrops of basalts were described by HEGENBERGER (1982) at Dobe Pan and 10 km north of it. More extensive occurrences of flood basalts intercalating with sandstones have been drilled in north-eastern Namibia. This lithostratigraphic unit is named Rundu Formation which is assumed to be equivalent to the Kalkrand Formation of southern Namibia (MILLER, 1997), but the flood basalts of northern Namibia have not yet been dated.

A section of interlayered basalts and sandstones has been drilled at Kano Vlei under a 259 m thick cover of Kalahari Group (Fig. 3.1-4). The Rundu Formation is here 215 m thick. It rests on Cave Sandstone (drilled thickness is 29 m) of the Etjo Formation. The upper 10 m of the Rundu Formation showed weathered basalts. Sandstones up to approximately 17 m thick in the Rundu formation are all fritted and grey. The basalt layers are reported to be mostly between 1 and 3 m, seldom up to 7 m, thick. WANKE (2001) assumes for the intersected profile of the Rundu Formation that the basaltic lava was poured out onto a desert environment that is characterised

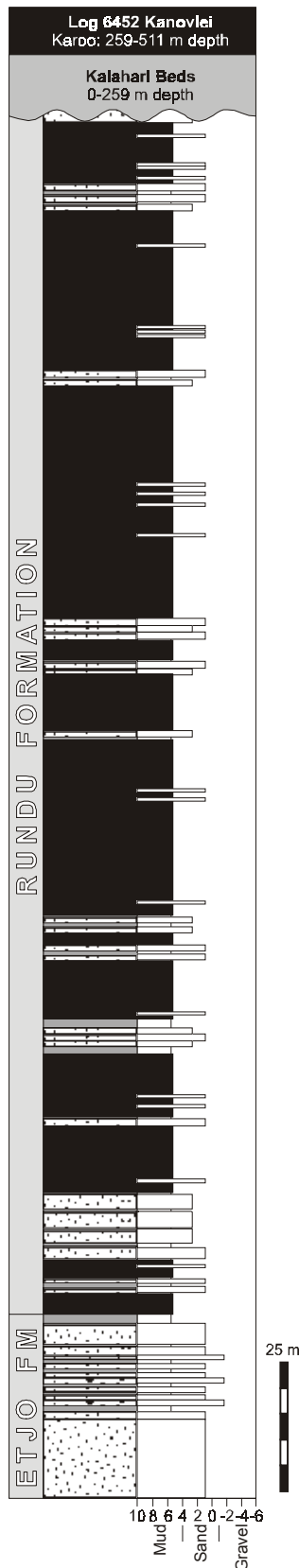




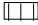
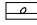
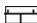
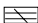



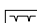


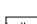







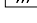
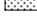

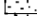


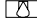




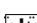





Fig. 3.1-4: Drilled profile of the Rundu Formation at the Kano Vlei (WANKE, 2001), legend on page 29.

by fluvial and aeolian deposition. The underlying Etjo Formation consists of a red, very well rounded medium grained sandstone here.

A small outcrop of basalt was found in a pit on the Botswana-Namibia border at 19.6732°S (Fig. 3.1-2e). It is not clear if this basalt belongs to a local relict of flood basalts or to a dyke swarm crossing the research area in a WNW direction (REEVES, 1978b; MUBU, 1995; REEVES, 2000). This dyke swarm is younger than the Karoo flood basalts (CROCKETT, 1968, STANSFIELD, 1973; LITHERLAND, 1975; PAYA, 1996) which have been dated at 182 ± 2 Ma in Botswana (ENCARNACIÓN ET AL., 1996). REEVES (2000) gives an age for the dyke swarm of 150 - 140 Ma.

A conglomeratic mudstone (Sikereti Mudstone) is described in the vicinity of Sikereti by BALFOUR ET AL. (1985). As this mudstone was observed to be fritted by late Karoo dykes in some pits (MEDLEYCOTT, 1980) it must be older than late Karoo. It is most likely to be equivalent to the Omingonde Formation (BALFOUR ET AL., 1985). Similar occurrences of "deep red clay containing a variety of angular and subangular clasts" were described by LEO HATZ CONSULTING (1993) to be intersected in boreholes in the Omuramba Elandsplaagte and along the red line fence in former Hereroland East. For these occurrences it has not been determined if they represent either weathered Karoo sediments or the Lower Kalahari Formation, or even a distal equivalent of the Middle Kalahari Formation.

LEGEND FOR SECTIONS		
Rocks	Structures, fossils etc.	
 Basalt (Lava)	 Lamination	 Normal grading
 Damara Basement	 Parallel planar bedding	 Pebble imbrication
 Limestone/ marl	 Massive, no apparent bedding	 Intraclasts
 Calcareous sandstone	 Large-scale planar cross-beds	 Mud cracks
 Claystone	 Trough cross-beds	 Syneresis-/ shrinkage cracks
 Siltstone	 Lag (channel lag deposit)	 Palaeosol
 Mudstone with sand and pebble-component	 Channelized units	 Bioturbation
 Sandstone		 Rootlets
 Sandstone (coarse grained)		 Ichnofossils
 Gravelly sandstone		 Bivalves
 Conglomerate		 Ferruginous concretions
 Breccia		 Calcareous concretions
 Matrix supported Breccia		 <i>In situ</i> Breccia
 Chert		 Karst
 Ferruginous		
 Silica precipitation		

3.1.4 Kalahari

The Kalahari Group in the research area consists of a wide variety of terrestrial sediments. The age of the sediments is not very clear but most authors assume an onset of sedimentation during the upper Cretaceous (THOMAS, 1988; THOMAS & SHAW, 1990; 1991; DU PLESSIS & LE ROUX, 1995) by correlation with fission track data as an indicator for the isostatic uplift of the coastal escarpments in Namibia and South Africa and the evolution of an intracontinental hinterland basin. As terrestrial sediments tend to vary significantly between stratigraphically equal units, the following descriptions mainly focus on outcrop observations of lithotypes (basal conglomerates and breccias; carbonate deposits; pebbly sandstones and immature sandstones; pipe sandstone) rather than assigning stratigraphic units. Some aspects of correlation with published data is proposed in a final subchapter.

Basal conglomerates and breccias

The Kalahari Group rests with a pronounced unconformity on Precambrian (Damara Sequence, Grootfontein Complex) and Karoo rocks. This conspicuous unconformity is well exposed in the Tsumkwe district north of the Gura Pan and at several localities in the Omiramba Eiseb and Epukiro. In the Tsumkwe district the top of the country rocks immediately below the unconformity is compact and unweathered, whereas it shows incipient saprolite formation in the outcrops in the Omiramba Eiseb and Epukiro. Additionally, the lithologies of the basal Kalahari rocks differ between the three regions. In the Tsumkwe district the basal Kalahari Group rocks

comprise exclusively matrix rich, carbonate-cemented conglomeratic sandstones, whereas in the Omuramba Eiseb both matrix and clast supported breccias and angular conglomerates occur. The Omuramba Epukiro exhibits a spectrum of rock types including immature pebbly sandstones, matrix-supported conglomerates and clast-supported, highly angular mega-breccias. According to their spatial lithological variations, two facies types are distinguished here: Gautscha facies and Epukiro facies.

Gautscha facies

This facies is exposed at the pan-grounds of small pans north of the Gura Pan (outcrops 6, 7, 20, see Fig. 3.1-11), in shallow outcrops south-east of the Gautscha Pan (9 - 13), at the southern bank of the Gautscha Pan (8) and north of the Bee Hill (19). The Gautscha facies is up to 2 m thick and sits on the slightly deformed Otavi Group. The unconformity to the Kalahari Group is represented by a relatively plane bounding surface with shallow depressions and several metre-wide, slightly incised shallow channels.

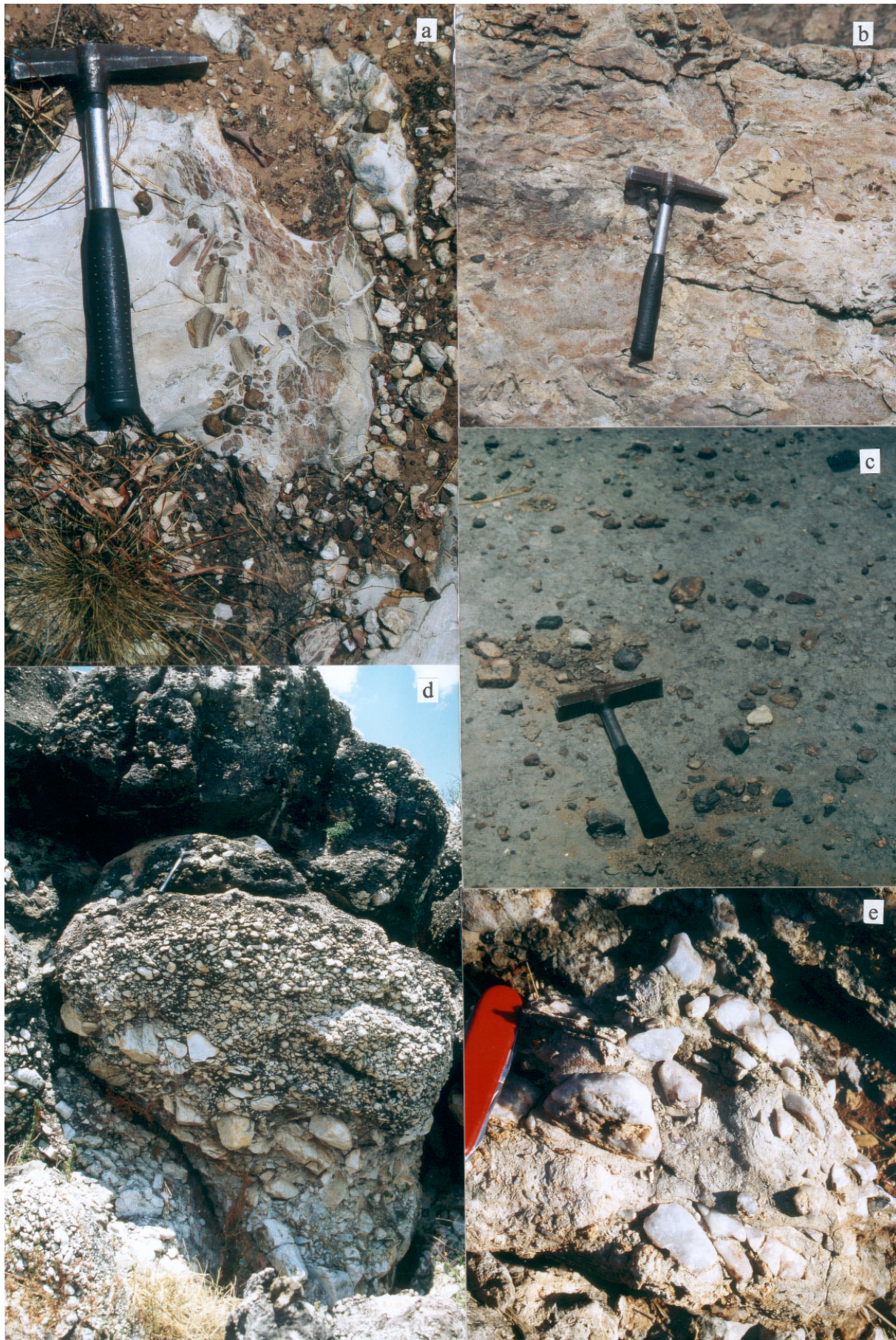
Pebbly sandstones and matrix-supported conglomerates with widely varying clast-sizes and clast-contents (< 40 %) are present. The matrix consists of lime with varying contents of medium to coarse grained silicic sands. The sand concentration is always too low for a grain-supported texture. Locally the matrix is indurated by weak silica precipitation and a transition to concretionary chert formation has been observed rather rarely.

Clast components are grey and black chert, quartzite, white vein quartz, grey sandstone (medium sorted and angular), red conglomeratic sandstones and subordinate laminated mudstone (Fig. 3.1-5a - c). The clasts are subangular and vary in diameter from 2 - 18 cm with the majority between 5 - 12 cm. Clast concentrations in bands (Fig. 3.1-5b) and in very shallow depressions above the unconformity occur.

Angular to subangular chert-intraclasts have been occasionally observed immediately above the unconformity. There the clasts have mosaic-like arrangements, which points to an autochtoneous *in situ* breccia of a locally developed chert-layer (Fig. 3.1-5a).

An unconsolidated conglomerate (Fig. 3.1-2e), up to 35 cm thick, comprising subangular clasts sitting in a red loamy matrix was observed overlaying strongly weathered basalt at the Botswana-Namibia border (outcrop 19).

Fig. 3.1-5



Epukiro facies

This facies is exposed in the Omuramba Eiseb particularly in the vicinity of farm Otjoni, Thereonsvallei and Thereons Vlei (25, 53-55, 57a). More exposures are found in the Omuramba Epukiro (outcrops 78,79).

The bedrock below the Kalahari Group consists of schists of the Damara Sequence at most of the exposures of this facies, e.g. at the Donkey-Car Locality and at Thereonsvallei. The unconformity is uneven with dip-inclinations of up to 40°. The Damara rocks beneath the unconformity are characterised by incipient saprolite formation and in places by large (30 cm - 2 m) disassembled plates and blocks of Damara schist. These deposits are laterally discontinuous with maximum thickness of 1 m for platy parts and 2 m for blocky parts. Clast imbrication is a common phenomenon. Therefore these deposits are interpreted as proximal debris- and mass flow deposits. Loosened Damara bedrock, as well as the succeeding Damara saprolite and debris, have been partly infiltrated by sandy calcrete or calcite-cemented, matrix-supported sandstone. Matrix-supported conglomerates and pebbly sandstones follow up-section. There the matrix comprises sandy calcrete or carbonate-cemented sandstone. Silica precipitation associated with this facies has only been observed at farm Otjoni. Locally, incipient karst formation in carbonate-cemented parts occur. The clasts are highly angular to subrounded, with angular clast prevailing clearly (Fig. 3.1-5d & e). The clast spectrum includes vein quartz (< 8 cm in diameter), platy Damara schist (< 25 cm), Damara quartzite (< 25 cm) and chert (< 4 cm). Clast abundance is rather variable, and lateral and vertical transitions from conglomerates, with up to 40 % clast content, to pebbly sandstones are common.

◀ **Fig. 3.1-5:** Photo documentation of the basal conglomerates and breccias of the Kalahari Group. **a)** Clast concentration in a shallow depression above the basal unconformity at outcrop 13. The mosaic-like orientation of some chert clasts in the carbonate-cemented matrix shows the *in situ* brecciation of a locally developed chert layer. **b)** Conglomeratic band at the southern edge of the Gautscha Pan (outcrop 8). This band is traceable for several 10s of metres in the entire outcrop. A pattern of red spots in a white matrix, both consisting of the same material, is displayed here. **c)** The pan floor at outcrop 7 (north of Gura Pan) exposes subangular clasts with diameters up to 10 cm swimming in a lime-cemented matrix. **d)** A mega-breccia of the Epukiro facies outcrops at Donkey-car Locality at the northern bank of the Omuramba Epukiro (outcrop 79). Angular quartzite clasts (up to 60 cm in diameter) are seen to overlay heavily weathered basement. A fining-upward trend of the clast population is documented here. The mega-breccia is topped by several units of matrix supported breccias and clast-rich sandstones. **e)** Exposure of a breccia east of farm Otjoni (outcrop 54). The angular clasts consist exclusively of Damara quartzites.

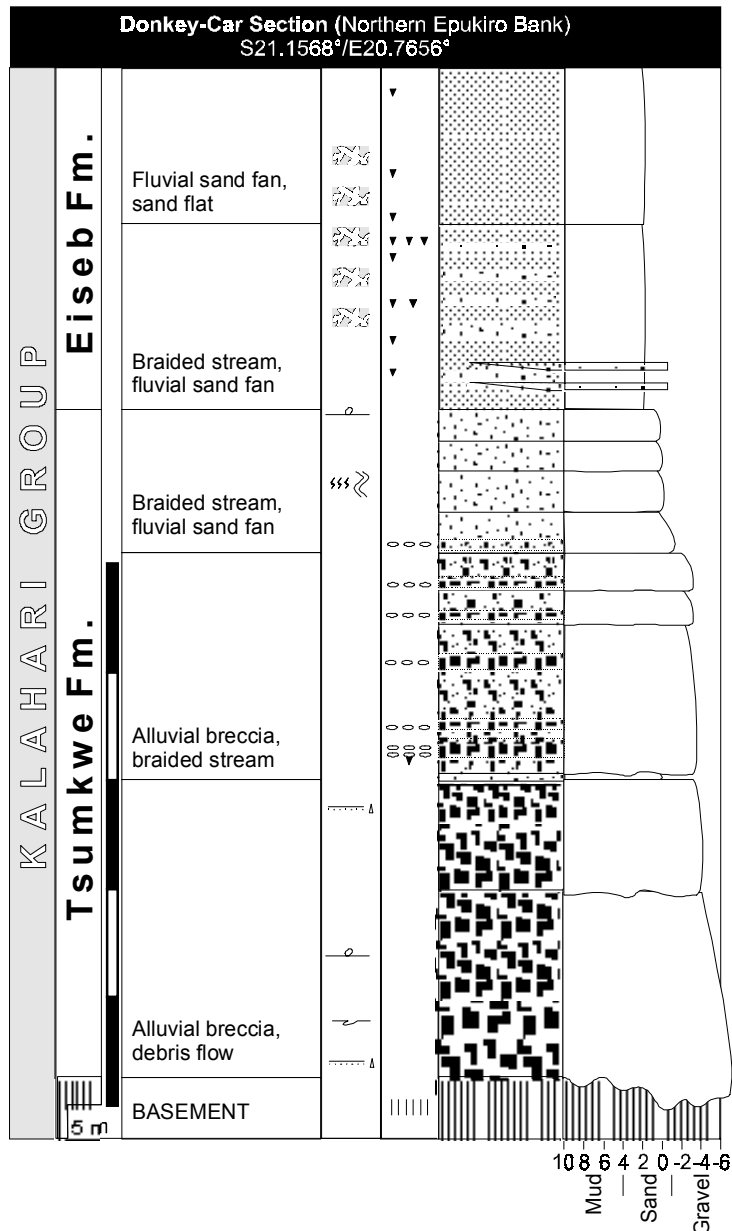


Fig. 3.1-6: Section of the sedimentary strata at the Donkey-car Locality with facies interpretation. Legend on page 29.

An ultra-proximal type of the Epukiro facies has been exclusively observed in the Omuramba Epukiro at the Donkey-car Locality (Fig 3.1-6 and outcrop 78 in Fig 3.1-11). Due to its extraordinary appearance and good exposure it is described separately here. An 8 m thick sequence of breccia and clast-enriched sandstones outcrop here (Fig. 3.1-5d). At this section, the bedrock consists of dark grey-green saprolite, which has probably been a mafic metamorphic or igneous rock due to its feldspar and chlorite content. The lowermost 2 m of the basal Kalahari Group consist of a clast-supported mega-breccia. The clasts consist exclusively of vein- or metamorphic quartz. They are highly angular with diameters ranging from 20 - 60 cm. Sand and gravel of weathered bedrock form the matrix of the lowermost 0.5 m of the section. Up-section the matrix composition changes into grey to reddish grain-supported sandstone. A unit of moderately-sorted, clast-supported breccia of Damara quartzites forms the third metre of the section. The majority of the clasts are 5 - 8 cm in size. The upper part of this unit shows normal grading and clast imbrication. Several units of matrix supported breccias and clast-rich sandstones follow up-section. A fining-upward trend of the clast-population and an upward-decrease in clast abundance are observed. Normal and inverse grading, and concentration of clasts in bands and lenses are found in individual horizons. Besides the upward-fining trend, a bimodal distribution

in clast sizes has been observed: The majority of clasts are 3 cm in diameter while a second clast population ranges from 7-15 cm in diameter. In all matrix-supported horizons the clasts are highly angular. The matrix consists of carbonate-cemented, moderately to poorly sorted, grain-supported quartz sand.

Carbonate deposits

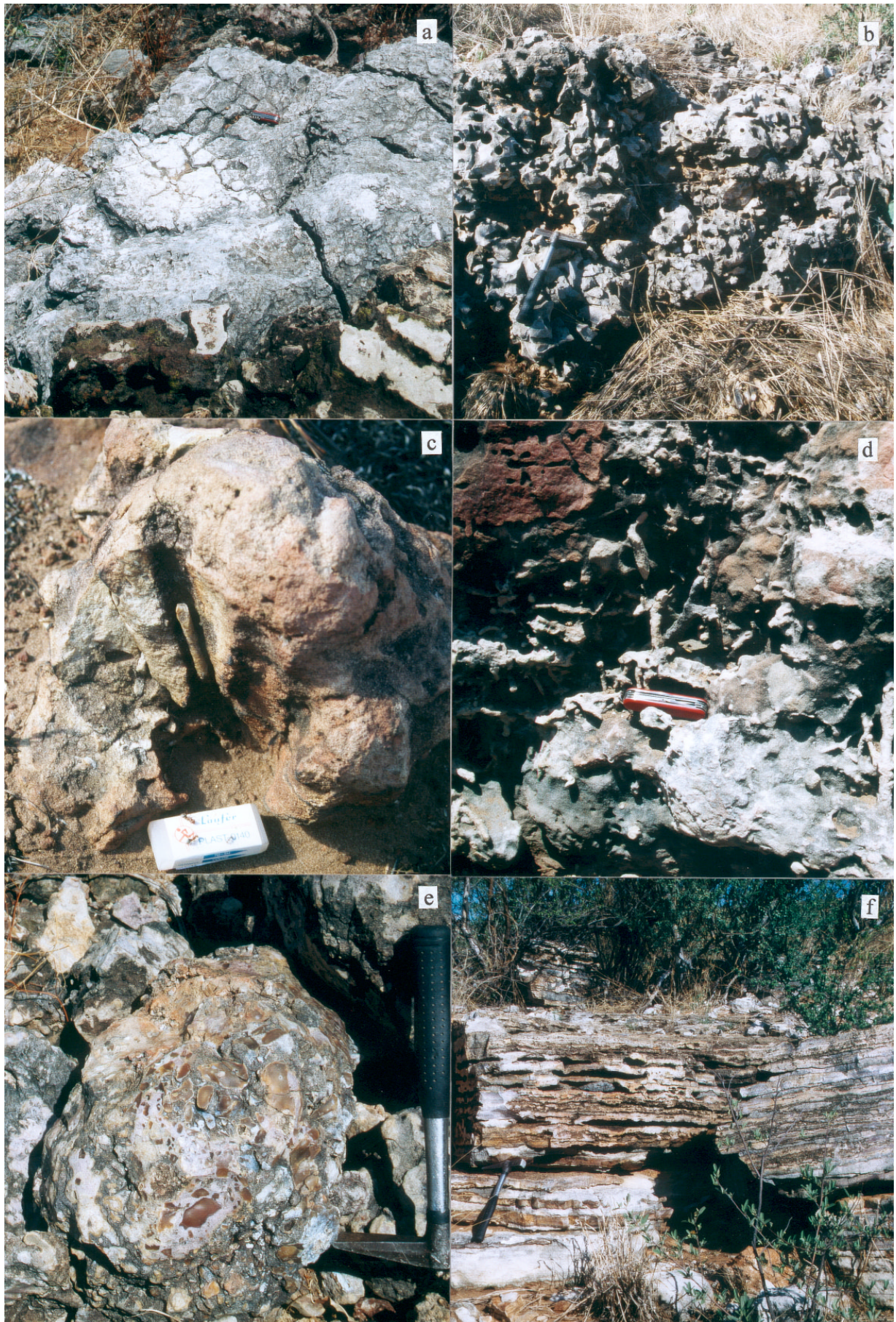
Carbonate deposits, comprising massive limestones, laminated limestones and limestones with a silici-clastic component, occur at numerous localities (outcrops 3, 31, 34, 41, 59a, 59, 60, 63, 46, 72, 74, 75). The limestones are white to cream coloured and show light grey weathering surfaces. The majority of the limestones are interpreted as calcretes, but some bear definitely a clastic carbonate component.

In the Tsumkwe district and the Omiramba Rooiboklaagte and Eiseb, they are relatively restricted and usually show vertical transitions to silici-clastic deposits. The limestone units are up to 3 m thick and bear a quartz-sand component of less than 5 %. This sand is usually of medium sand grain-size, moderately sorted and subangular to moderately rounded. Laterally discontinuous concentrations of chert, quartzite and red sandstone pebbles occur in bands and lenses. The pebbles are subangular and less than 3 cm in diameter. Except for the pebble bearing bands, only subtle sedimentary structures, such as a faint sub-horizontal layering and slightly nodular limestone forming within some thicker (20 cm) limestone horizons, occur.

In the Omuramba Eiseb (outcrops 31, 33 in Fig. 3.1-11) a unit up to 2 m thick of almost pure limestone with a quartz-sand content well below 1 % is exposed. This unit consists of several up to 35 cm thick, limestone layers. The majority appears massive, but lamination and an internal planar and low-angle cross-stratification has been observed. The basal parts of individual horizons are commonly massive, the upper parts tend to become porous. Occasionally fossil gastropods occur (outcrop 41).

The most massive and continuous carbonate deposits have been found in the Omuramba Epukiro, where laterally continuous carbonate units are up to 12 m thick. The banks of the Omuramba expose a carbonate sequence with a thickening-upward cycle (outcrops 63, 65). The lowermost metre of the section comprises an alternation of 1 - 4 cm thick horizons of laminated limestones or marls with a minor quartz-sand component, which alternate with carbonate-cemented sandstone layers of a similar thickness. Up-section the limestone and marl horizons become successively thicker with the three top horizons being approximately 30 cm thick. The limestones still alternate with up to 1 cm thick carbonate-cemented sandstones which do not exhibit the upward-thickening architecture of the limestones.

Fig. 3.1-7



The limestone horizons are characterised by their wavy to irregular surfaces intersected by shrinkage cracks (Fig. 3.1-7a). These cracks reach up to 3 cm from the surface into the horizons and are infiltrated by carbonate-cemented quartz sandstone. Another characteristic of the upper carbonate horizons are subvertical tubes of 1 mm in diameter. They are open or filled with calcite and are interpreted as grass-rootlets and grass blades.

The uppermost limestone/marl horizon is mostly followed by carbonate-cemented sandstone which grades rapidly in silicified pipe sandstone.

Pebbly sandstones and immature sandstones

White to cream coloured quartz sandstones, weathering in greyish to reddish yellow colours, are exposed in the central part of Omuramba Eiseb (outcrops 23, 24). This unit is up to 10 m thick and rarely exhibits a stratification by layering or banding. The sandstones consists of poorly sorted, angular to sub-rounded quartz grains, mostly clear quartz. Sub-rounded pebbles of clear quartz (magmatic?) of up to 1.5 cm diameter are abundant. Occasionally white milky quartz pebbles (metamorphic) up to 3 cm in diameter occur. The sandstones are grain-supported and thought to be often primarily carbonate-cemented, commonly but not always silicified. The degree of silicification generally increases up-section.

Pipe sandstone

The pipe sandstone unit is widespread and an often observed feature of this unit is a ventilating network by interconnected pipes (Fig. 3.1-7b). The pipe sandstone often forms the upper bank of the Omuramba Nhoma (outcrops 1- 3) and the upper cliffs in the Omiramba Eiseb (outcrops 28, 30, 32, 34, 37, 38) and Epukiro (outcrops 41- 45, 47- 49, 56, 58a, 58, 61, 62, 64, 66, 67, 69, 73, 75, 77, 78, 80 - 82, 84, 86 in Fig. 3.1-11).

◀ **Fig. 3.1-7:** Photo documentation of the Kalahari Group. **a)** The carbonate units show sometimes shrinkage cracks at the surface (outcrop 64). **b)** The pipe sandstone (outcrop 56) shows a interconnecting network of air passages that developed by karstification of the silicified sandstone. **c)** Tube like structures were observed in the upper part of outcrops along the Omuramba Nhoma (outcrop 3). The homogenous tube fillings weathers here out as a pens like structures. **d)** Y shaped tube like structures where observed along the Omuramba Epukiro (outcrop 77). They are interpreted as burrows of *Thalasinoides* isp. on a purely morphological basis. **e)** Outcrop 64 in the Omuramba Epukiro: *In situ* reworking of highly intersected chert-layers formed an autochthonous chert-breccia with yellow to orange chert clasts in a pink pebbly sandstone matrix. The colour spectrum of cherts clasts in the entire research area includes red-brown, varieties of yellow, grey-blue and black varieties. **f)** Alternation of thin silcretes layers (1 - 8 cm) with laminated carbonates was observed in the Omuramba Eiseb (outcrop 50).

Outcrops in the Omuramba Nhoma

The pipe sandstone unit is up to 3 m thick in the Omuramba Nhoma and it is light-grey or cream coloured, weathering in greyish to red-brown colours. The unit comprises immature and sometimes pebbly, dominantly silica-cemented, sandstones which are transitional between grain- and matrix supported. The sand component includes fine to coarse subrounded quartz grains. Discontinuous, massive pebble bands occur sporadically. They are either dominated by reddish subangular quartz-sandstone clasts or angular chert-clasts. Intense silicification occurs around cavities and lens-shaped chert-clast accumulations. However, most cavities are partly or completely filled with red, bluish or yellow-brownish chalcedony. Carbonate-cement dominates in zones with low or no silicification. These zones are restricted to the lower parts of the unit, where joint-fissures are often also filled with calcite. Open cavities of a few cm diameter become a significant feature up-section and form a network of complete air-passage interconnecting in the uppermost metre.

Subvertical tube-like structures (Fig. 3.1-7c) are concentrated in a 60 cm thick horizontal zone below the cavity network zone. The tubes are mostly filled with the same material as the host-sandstone, but are sometimes open. The tube structures are subvertical, in average 10 cm long and up to 1 cm in diameter. The majority of the tubes are 6-8 mm in diameter. The tube surfaces do not show any ornamentation and the fillings appear to be homogeneous.

Outcrops in the Omiramba Eiseb and Epukiro

This unit attains more than 10 m thickness in the Omiramba Eiseb and Epukiro where the maturity of the pipe-sandstone unit varies from moderately sorted sandstones to pebbly sandstones with concentrations of pebbles in bands and lenses. However, homogenous, more mature sandstones with no or a subordinate pebble population clearly dominate. Compared to outcrops in the Omuramba Nhoma, a reddish to brownish weathering colour is more common, but light-grey and cream colours are still frequent. Fresh rocks show light-grey to cream colours, although rare greenish colours were also found.

Only at one outcrop (77) it was observed that the red, grain supported sandstone consists most likely of reassorted well to very well sorted aeolian sand with rounded quartz grains. This occurrence is approximately 8 m thick, showing tube like structure in the topmost part.

Silicification features are rather diverse. In general it seems that a primary carbonate-cement is partly replaced and/or impregnated by silica. The silification often increases progressively up-section, but abrupt changes in the intensity of silification are also common. Sometimes silica is concentrated in irregular laminae or thin wavy layers. 1-3 cm thick chert layers have been

observed at numerous localities. The colour spectrum of such layers includes red-brown, yellow, grey-blue and black. Often the chert-layers are intersected by shrinkage cracks. At places where the intersection is intense, the primary layering is disturbed, but still visible. Small scale tepee structures in such layers have been observed rarely. Sometimes an *in situ* reworking of highly intersected chert-layers formed an autochthonous chert-breccia (Fig. 3.1-7e).

Tube structures often appear in the outcrops of the Omiramba Eiseb and Epukiro, too. But the preferred vertical orientation described for the outcrops in the Omuramba Nhoma occurs only sporadically here. Y-shaped and partly interconnected tube-structures are frequent (Fig. 3.1-7d), and they are interpreted as burrows of *Thalasinoides* isp. on a purely morphological basis.

Karstification of the silicified parts of the pipe-sandstone unit is a common and widespread phenomenon. Intense karstification occurs in well silicified parts, usually in the upper 5 m of the exposed unit only. The karst cavities have the shape of irregular tubes with 1-15 cm in diameter. Usually the tubes and hollows form a slightly to completely interconnected network without a preferred orientation (Fig. 3.1-7b). A preferred vertical or horizontal orientation of tube- or fissure-shaped cavities has only been observed at a few places. Real caves of more than 1 m in diameter occur in parts where the volume of the karstification exceeds the volume of the remaining solid rock.

Silcretes

Silcretes occur, as described above, usually in the upper parts of the pipe-sandstone. There they very commonly exhibit an internal lamination which follows the shape of the silcrete bodies. The silcretes in the pipe-sandstones either form discontinuous layers or irregular nodules of a few cm in size. At places it is not clear whether these nodules fill cavities or replace the host rock. The possibility of the latter case is proven where sand-grains are still visible in the centre of silica-nodules. Furthermore, silcretes are sometimes associated with laminated carbonates, in which silica is concentrated in disc-shaped nodules or in layers up to 5 cm thick. Even a perfect alternation of thin (1-8 cm) calcrete-silcrete layers has been observed (Fig. 3.1-7f, outcrop 56).

Sedimentary successions from outcrop observations

Three example profiles of the sedimentary successions that have been observed in the Omiramba Nhoma and Epukiro are given in Fig. 3.1-8. It is clear that carbonate and fluvial sands, interpreted as sand flats, interlayer extensively with each other. Sheet flood deposits are mostly observed in the sandstone units while in the lower laminated limestone unit only minor sheet flood deposits were observed. Silcrete precipitation occurs throughout the succession without

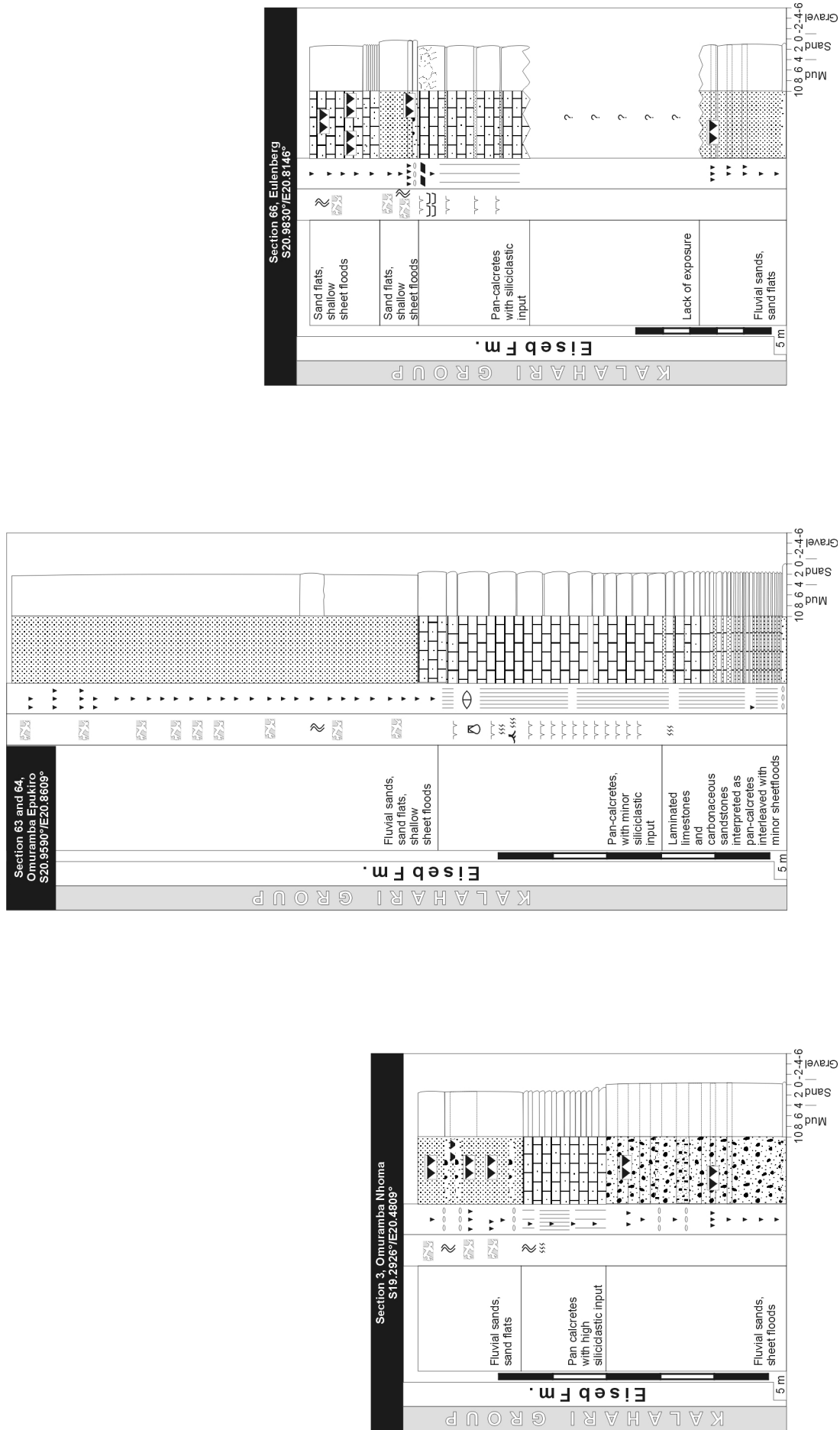


Fig. 3.1-8: Three profiles observed in the Omiramba Nhoma and Epukiro giving rock type, bedding and structures. Facies interpretation is given in the left column of each section. The successions show intense interlayering of limestones with varying siliclastic input and silica-cemented sandstones interpreted as sand flats. For legend see page 29.

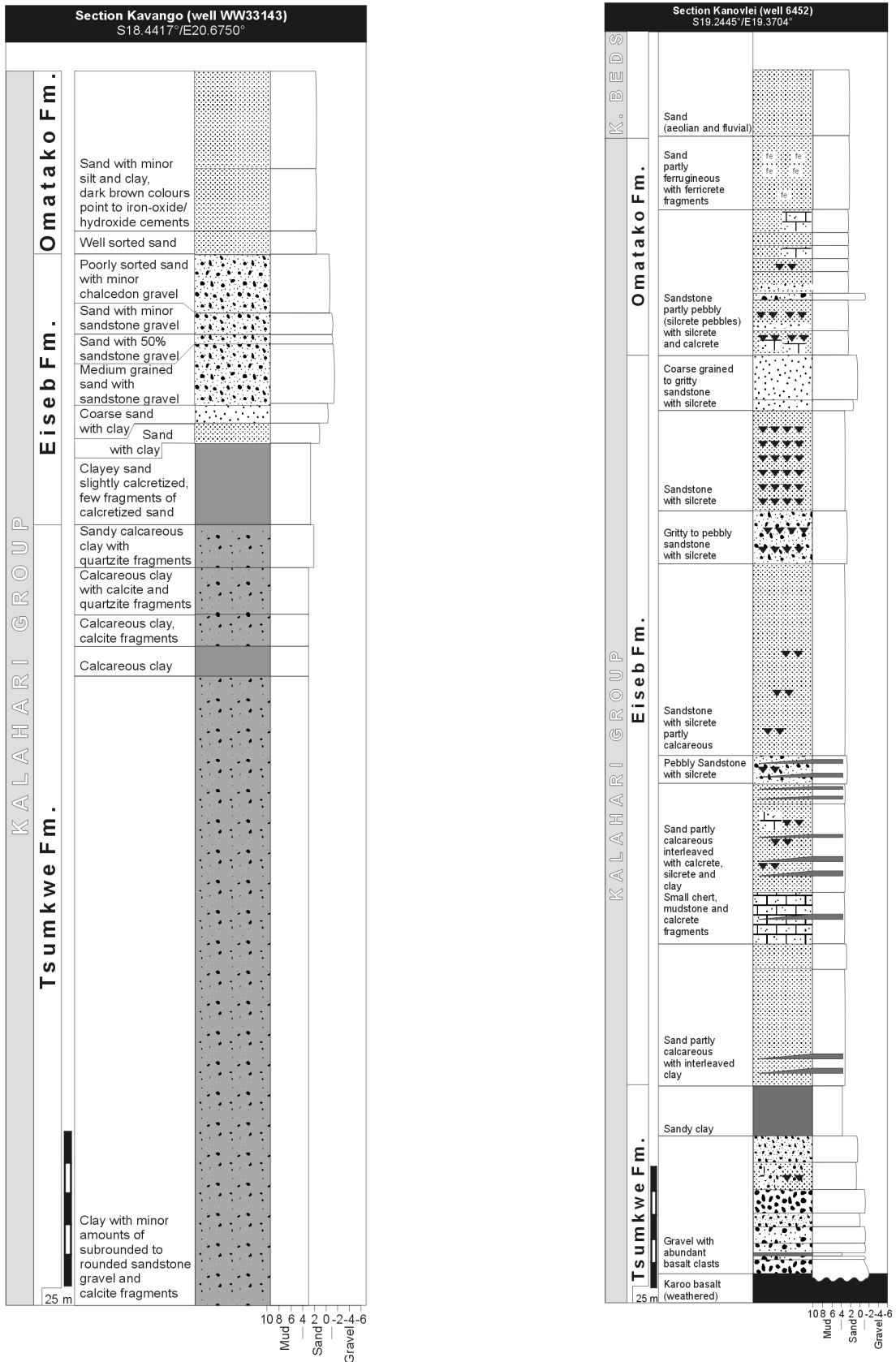


Fig. 3.1-9: Two example sections with lithological interpretation of the Kalahari Group at Kano Vlei and in the eastern Kavango district compiled with descriptions from the DWA borehole catalogue. For legend see page 29.

respect to silica-cemented sandstones or laminated carbonates. Karstification features were always observed in the topmost unit of the outcrops. This indicates that it is a morphologic feature and not of primary origin. The thickening upward trend is very well exposed at the outcrops 63 and 64 (middle profile in Fig. 3.1-8). Such trends are in general interpreted as increased pan deposition.

From all observed profiles it is concluded that silicified sandstones mostly overlie the unit of conglomerates and breccias. Up-section an alternating sequence of carbonate deposits and sandstones, including the pipe sandstone unit and the immature and pebbly sandstones, follows. Silcrete occurrences were observed throughout all parts of the succession, but they favour the upper part of the succession.

Sedimentary succession from drillings

Besides the observation of outcrops, available data from the DWA borehole catalogue were examined. Two example profiles are given in Fig. 3.1-9. The profile at the Kano Vlei showed a succession from pre-Kalahari basalt up to the Omatako Formation. A basal gravel layer is followed by a sandy clay layer. The sequence of alternating sandstones includes pebbly and gritty to pebbly sandstone units. In Fig. 3.1-9 this sequence is subdivided into 9 lithological sub-units which might reflect 3 to 4 sedimentary cycles. The top of the succession comprises ferruginous sand and ferricrete.

The profile in the eastern Kavango district shows a succession that develops from clay with minor rounded gravel towards a calcareous clay. In an upper part medium-grained sand with sandstone gravel are described. The uppermost part consists of dark-brown sand with minor silt and clay content. The occurrence of a sandstone gravel components could either reflect reworked pre-Kalahari lithologies (Omingonde, Etjo or Rundu formation) or intra-formational reworking within the Kalahari Group.

The division into formations within the Kalahari Group in the two boreholes given in Fig. 3.1-9 is adopted from the drilling report. A possible alternative interpretation for the borehole of the Kavango region (WW33143) it is that strata that have been interpreted as Tsumkwe Formation and the lower part of the Eiseb Formation are indeed Omingonde Formation and the medium grained sand with sandstone gravel might represent the basal Kalahari while the assigned Omatako Formation could be the Eiseb Formation. Red clays similar to those in the lower part of the Kavango borehole were interpreted by BALFOUR ET AL. (1985) as Omingonde, as they are intruded by a late Karoo dyke near Sikereti.

Correlation and summary

The interpretation of strata observed in the field as Tsumkwe and Eiseb formations has been made according to the lithological descriptions given by ALBAT (1978). He describes a threefold Kalahari Group subdivided into Tsumkwe, Kalahari and Omatako formations. This subdivision was adopted by SACS (1980) who renamed ALBAT'S (1978) Kalahari Formation into Eiseb Formation. In this study the formation names according to SACS (1980) have been used. The Tsumkwe Formation is described as conglomerates of poorly sorted clasts in a sandy matrix cemented by calcium carbonate. The clasts are irregularly scattered. By clasts of conglomeratic sandstones ALBAT (1978) also recognised at least two erosional cycles, for the Eiseb Formation a subdivision into six conformable units that show alternating silica and carbonate-cementation was proposed. He described interlocking networks of air passages for the three silica-cemented units. The Omatako Formation is dominated by ferruginous sandstones, ferricrete and pebble horizons cemented by clastic free iron-hydroxide.

No gypsum relicts or pseudomorphoses have been found during the field work although DU PLESSIS & LE ROUX (1995) recognised gypsum in the lower Kalahari Group of northern Botswana.

It is not clear how transferable the lithotypes are on a basin-wide scale but from the descriptions by MILLER (1997) it seems likely that the Beseib Formation of the Ovambo Basin is equivalent to the Tsumkwe Formation as he proposed. It is assumed that the Beseib Formation is deposited at a distal position (Gautscha Facies).

A summarising profile of a generalised Kalahari succession is given in Fig. 3.1-10. The Tsumkwe Formation overlies the pre-Kalahari unit with an unconformity and consists either of breccias in proximity to source areas (Epukiro facies), or it begins with sheet flow deposits in shallow depressions in distal settings (Gautsch Facies). The Eiseb Formation is dominated by alternating fluvial sands, carbonate deposits and locally with pebble bearing horizons. The drilled profile at the Kano Vlei (Fig. 3.1-8) showed the entire Kalahari succession. The number of depositional cycles observed locally cannot be correlated basin-wide. Furthermore, the silica-cementation of some sandstones is secondary, replacing original carbonate-cement. Same phenomena have been described by SMALE (1973) and by JONES (1982) who assume the percolation of alkaline waters from pans to cause silica precipitation. Therefore it is assumed that the Eiseb Formation might consist of any number of alternating silicate- and carbonate-cemented units. Karstification features are not dependent on primary conditions but on the exposure of the succession and on the groundwater regime.

The Omatako Formation that was only observed in boreholes overlies the Eiseb Formation with fluvial sand and ferruginous soils. Its distribution is probably limited to the Omuramba Omatako.

For the Kalahari Group it was found that in general the grain size fines towards the basin centre. This has also been proposed by SACS (1980) for the entire southern African Kalahari basin, by MILLER (1997) for the Ovambo Basin and by ALBAT (1978) from outcrops in north-eastern Namibia.

The three Kalahari formations are overlain by aeolian sand interfingering with interdune deposits that form both the Kalahari Beds. The mechanism for reassorting of Kalahari Beds and their origin is in discussion and for further information the reader is referred to MOORE & DINGLE (1998), THOMAS & SHAW (1990; 1991) and THOMAS (1987; 1988). Some physical properties of this topmost unit are given in Chapter 5.2.

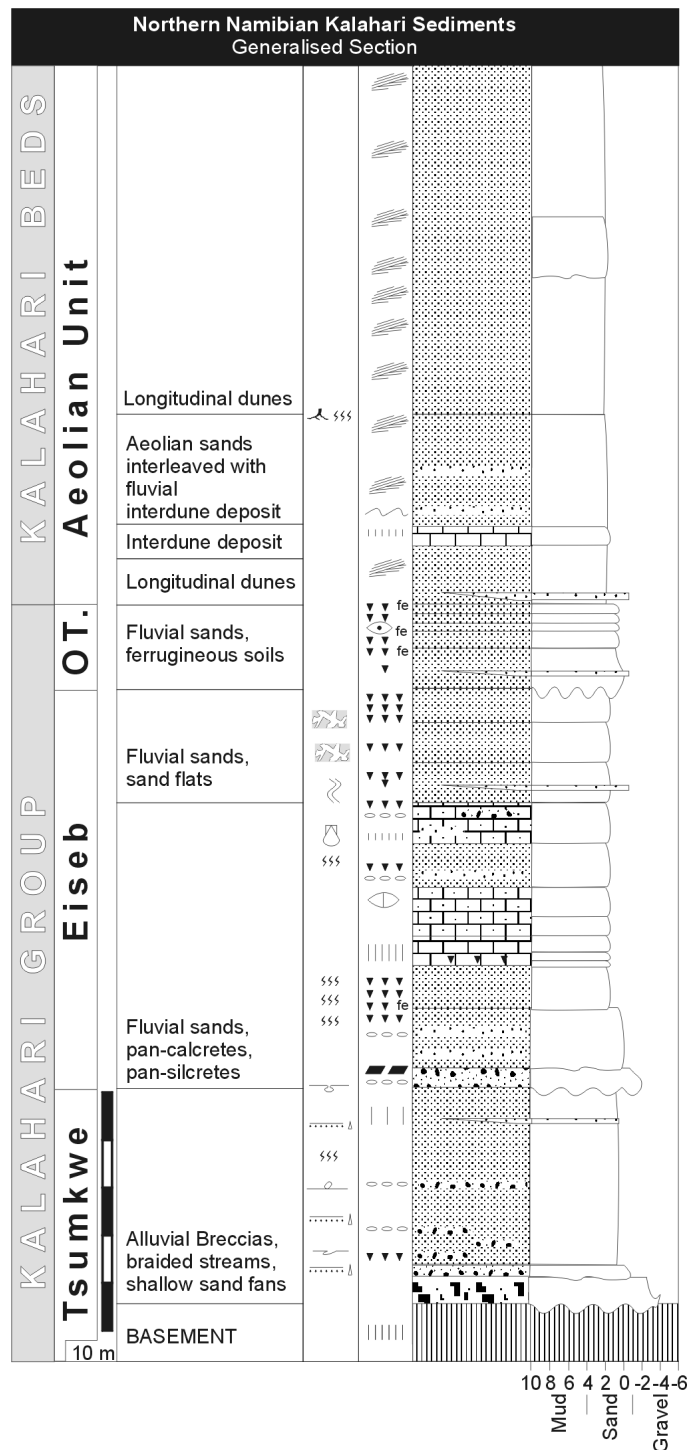
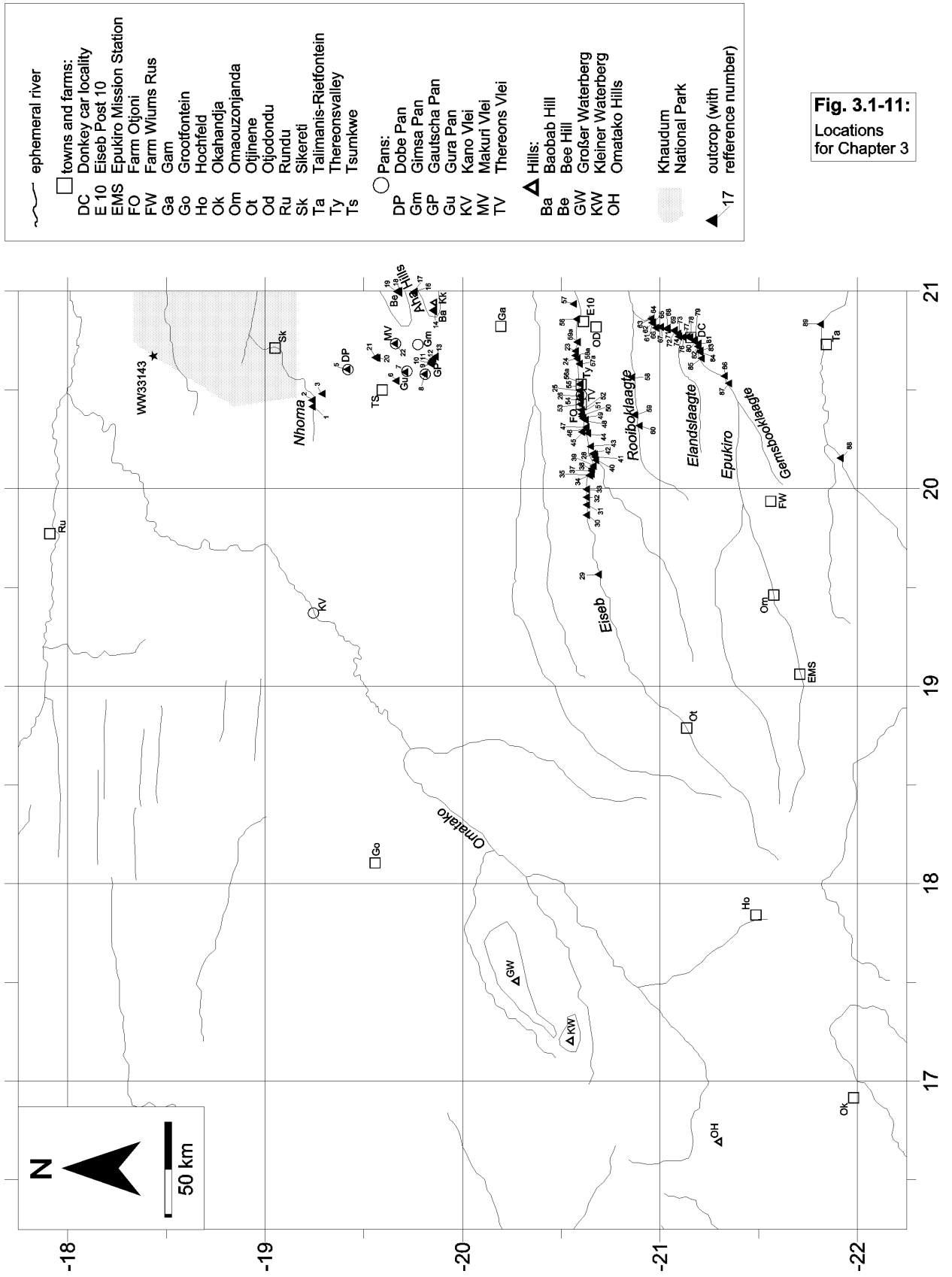


Fig. 3.1-10: Generalised profile of the Kalahari Group in north-eastern Namibia compiled from outcrop observations, study of borehole information at the DWA and descriptions by ALBAT (1978). Legend on page 29.



3.2 Thickness and structure of the sedimentary basins in the study area

3.2.1 Thickness of the Karoo deposits in north-eastern Namibia

Karoo deposits are fairly well known from the western part of the research area e.g. from the Waterberg region, but less well known in the eastern part of the study area. A summary map is given in Fig. 3.2-1. Drilling results from the DWA borehole catalogues are also included in this map. In the Geological Map of Namibia (MILLER & SCHALK, 1980) Karoo deposits in the northern and eastern part of the research area are marked as isolated occurrences only. They are mainly represented by basalts e.g. near Rundu or in the Tsumkwe district (Fig. 3.1-1, previous Chapter). More extensive Karoo occurrences that are identified by drilling and gravimetric survey have been suggested by HEGENBERGER (1982;1987) for the Kavango district and the Tsumkwe district. He assumes that this region is entirely underlain by Karoo basalts. Only the eastern most portion is excluded. MILLER (1997) suggests that basalts of the Kalkrand Formation occur in the eastern part of the Ovambo Basin. The Etjo Formation is limited to an inselberg structure which was identified in the western most part of the Ovambo Basin while most of the Ovambo Basin hosts only the Dwyka Formation and Ecce Group.

In the Otjinene district two local occurrences of basalt have been reported by MILLER & SCHALK (1980). HEGENBERGER (1982) assumes from gravimetric evidence that the occurrence between the Omiramba Rooiboklaagte and Epukiro is only a tongue. Further basalts were drilled south of the Epukiro at the Botswana-Namibia-border. KEY & AYRES (2000b) show a north-east trending depocentre of Lebung strata (equivalent to Omingonde and Etjo formations) to underlie the area between the Eiseb Block/Namibia and Lake Ngami/Botswana. A subparallel occurrence of Lebung Formation and Karoo flood basalts is also indicated further south. The basalt occurrence here is most probably associated with the basalts drilled on the Namibian side.

Thickness of the Karoo stratigraphic units in the Waterberg area have been examined by HOLZFÖRSTER (2000). Omingonde sediments reach a thickness of up to 500 m near the Waterberg Fault. The thickness of the Etjo sandstone increases towards the Waterberg Fault, where it reaches up to 200 m, and towards the north-east following the axis of the Waterberg depocentre. Basalt thicknesses from drillings in northern Namibia range from 3 m to more than 200 m. Karoo basalts in Botswana are reported to reach locally a thickness of up to 1000 m (COATES ET AL., 1979). KEY & AYRES (2000a) give cumulative thickness of the entire Karoo Supergroup in Botswana, if well preserved, of up to 3000 m. From this information an isopach

map of the Omingonde Formation in the research area was produced by digitising the available data (Fig. 3.2-2).

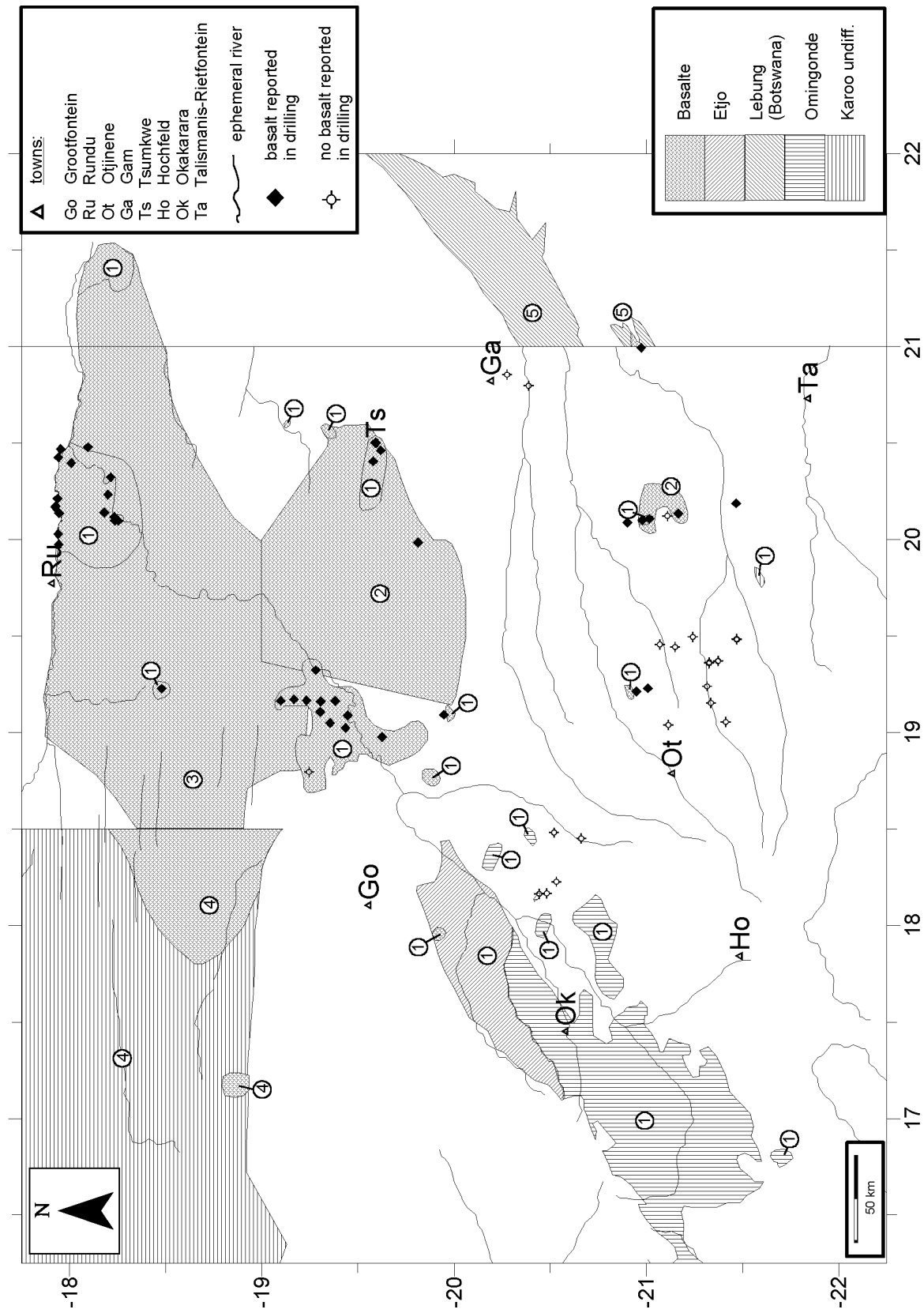


Fig. 3.2-1: Reported occurrences of Karoo deposits in north-eastern Namibia and north-western Botswana from 1) MILLER & SCHALK (1980), 2) HEGENBERGER (1982), 3) HEGENBERGER (1987), 4) HUGO (1969) and HEDBERG (1979) [presented in MILLER (1997)] and 5) KEY & AYRES (2000b).

Drilling at the Kano Vlei (Fig. 3.1-4) has shown that sandstones and basalts interlayer intensively in the Rundu Formation. Therefore Etjo and Rundu formations have been combined to digitise a map of their thickness from the study of literature and drillings (Fig. 3.2-3).

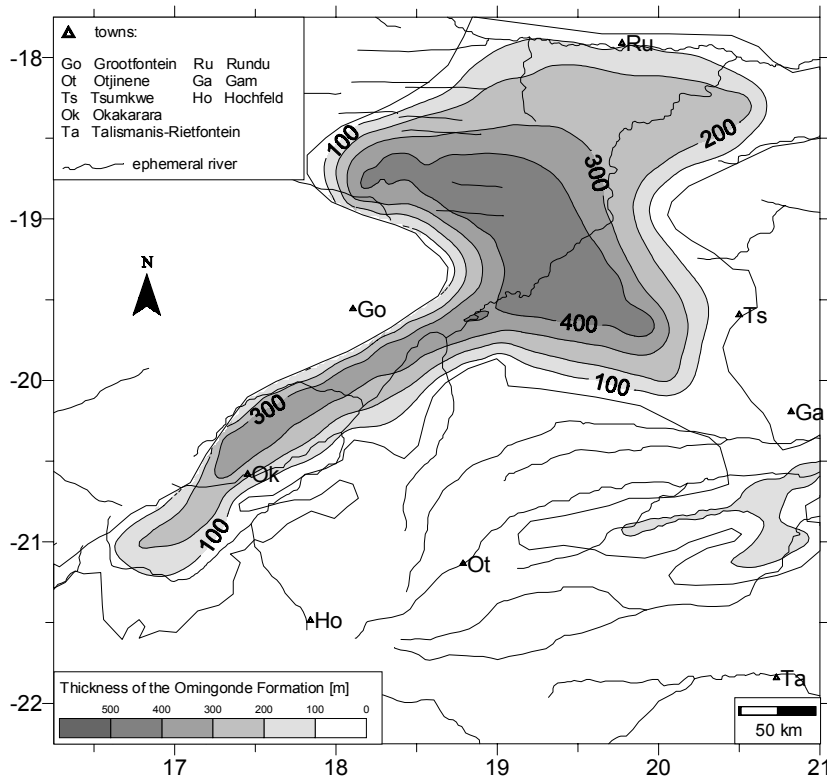


Fig. 3.2-2: Distribution of the thickness of the Omingonde Formation in the research area.

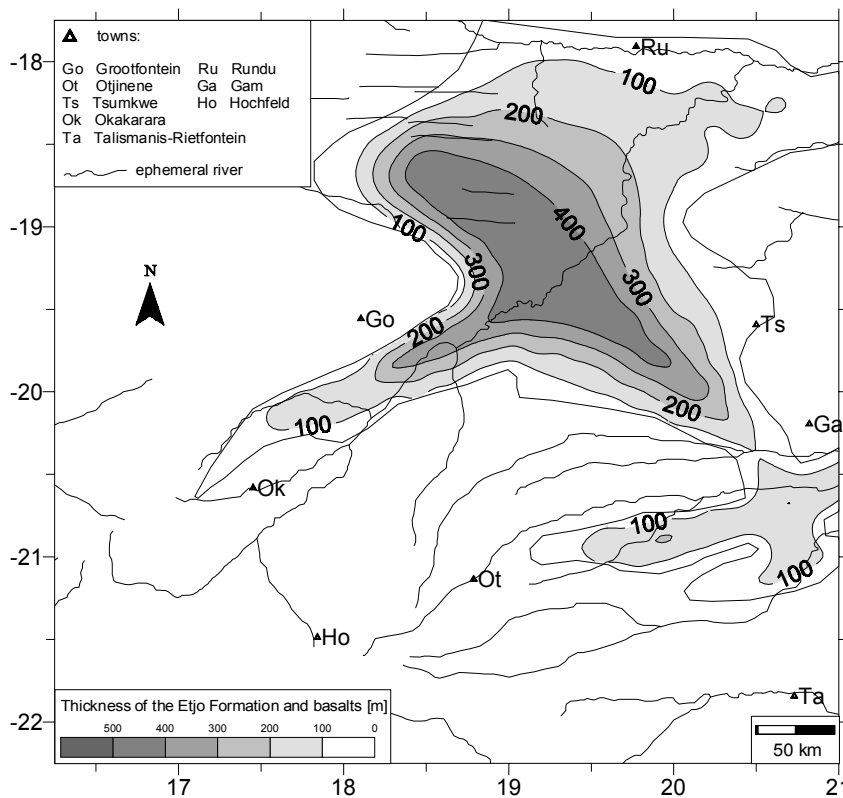


Fig. 3.2-3: Distribution of the combined thickness of the Etjo and Rundu formations in the research area.

3.2.2 Thickness and structure of the Kalahari basin

The distribution of the thickness of sediments belonging to the Kalahari Group is available from the Geological Map of Namibia (MILLER & SCHALK, 1980). Since 1980 further drillings and geophysical exploration has been conducted in the research area. Therefore the information from the Geological Map from 1980 was found to be insufficient. The borehole catalogue of the DWA contains about 1400 drillings in the research area with descriptions sufficient to distinguish between Kalahari and pre-Kalahari lithologies. Many of these have already been classified by the driller and by geologist from the Geological Survey of Namibia. From this information a data base was developed containing boreholes that penetrated the entire Kalahari (absolute thickness) and boreholes that were abandoned before reaching the pre-Kalahari lithologies (drilled Kalahari thickness is the least Kalahari thickness).

A distribution map of the thickness of the Kalahari Group was developed in several steps: Firstly a variogram of the data set with absolute thickness of the Kalahari has been produced and checked. Automatic fitting to exponential and linear models assumed an anisotropy trend of 162° . But it is known from the tectonic settings of the Kalahari and mapping of lineaments by satellite images that, for example in the Eiseb Block, the major tectonic directions are $40 - 50^\circ$ and $140 - 160^\circ$ (Chapter 3.3). The $140 - 160^\circ$ tectonic trend is dominant in the Eiseb Block but in the western part of the research area the $40 - 50^\circ$ direction is more significant. Therefore kriging with anisotropy could not be applied to regionalise the thickness of the Kalahari for the entire research area. Average interpolation with inverse distance to a power function has been chosen to produce a preliminary distribution map of the Kalahari thickness from the 807 data points of absolute Kalahari thickness. In a next step, the drilled least thickness of the Kalahari have been compared with the calculated thickness of the regionalised map for those data points. If the minimum measured thickness at a location was larger than the calculated thickness, the data point was added to the data set. If the calculated thickness was greater than the drilled thickness, the point was not further considered.

Additional data points from the observation of satellite images, giving a thickness of 0 m where pre-Kalahari hardrocks outcrop, have been added to the data set. Some geophysical data are available for the Eiseb Graben, where a Kalahari thickness of more than 750 m is indicated (CSIR, 1982; DWA, 1996b). Those results are doubtful, however, as it is not yet understood if the geophysical results might also represent Karoo lithologies (FILITZ, 1999 in BITTNER, 1999). In the Botswana counterpart of the Eiseb Graben, the thickness of the Kalahari Group is assumed by KEY & AYRES (2000a; 2000b) to be 90 to 120 m, but they have not taken into account the results from drilling and geophysical data from the Namibian side. Drillings in the Eiseb Block

exceeded 250 m without reaching the basal formation of the Kalahari and a drill-site at Otjodundu (visited during field work in 2000), near Eiseb Post 10, penetrated sandstones and pebbly sandstones for at least 150 m. Therefore, the thickness of the Kalahari Group in Botswana is probably underestimated and extrapolation of this assumed thickness into Namibia does not improve the data set. Given the uncertainties associated with the geophysical data, a compromise solution between borehole and geophysical data was reached by assuming a thickness of 400 m for the Kalahari Group within the Eiseb Graben.

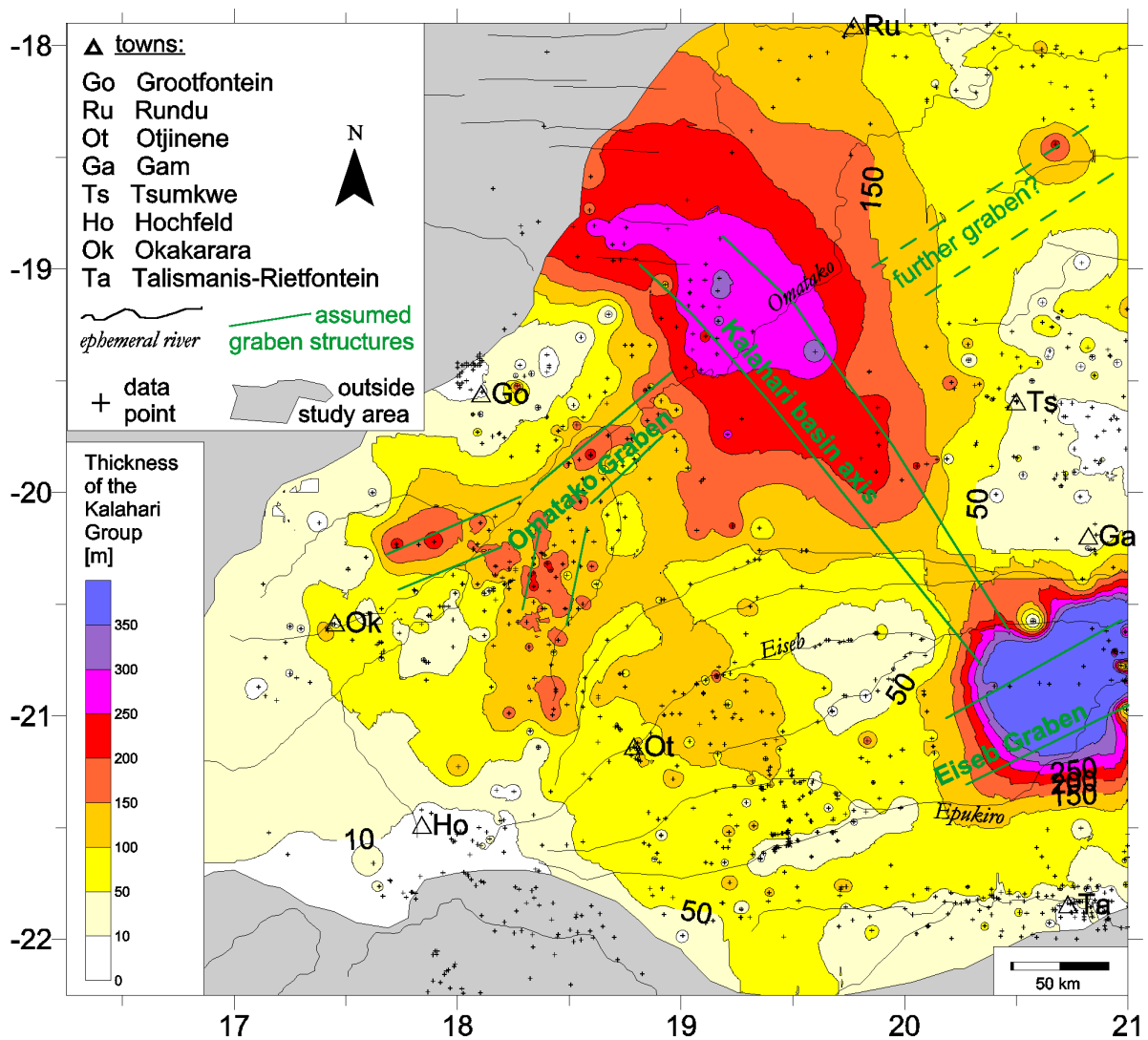


Fig. 3.2-4: Distribution of regionalised thickness of the Kalahari Group in the research area of north-eastern Namibia. Proposed graben structures are indicated in green.

The above procedure resulted in 1080 data points from which useful estimates of Kalahari thickness could be obtained. A final map of the distribution of the thickness of the Kalahari Group was produced by average interpolation with inverse distance to a power function. The resulting map is given in Fig. 3.2-4. Since geophysical distinction between Kalahari and Karoo is uncertain, further subdivision of the Kalahari into Lower, Middle and Upper formations, as done in the western part of the research area (WORTHINGTON, 1979; DWA, 1993f), cannot be meaningfully applied to the whole research area. Furthermore, correlation between formations of the Kalahari Group in the Tsumkwe and Rundu district with those in the Eiseb area or Omatako catchment may result from lateral facies variations rather than stratigraphic nonequivalence (Chapter 3.1.4). So this implies that regional subdivision into formations is unreliable on this basis also.

The thickness of the Kalahari sediments reaches locally up to 350 m in the western part of the research area underneath the Omuramba Omatako, thickness is up to 400 m in the Eiseb Graben and in the northern part of the study area. The above described regionalisation revealed three major trough structures in the research area (Fig. 3.2-4). Two of them trend NE-SW; the Omatako Graben is located underneath the course of the upper Omatako and the Eiseb Graben appears in the eastern part of the study area. Both structures have already been described (e.g. WORTHINGTON, 1979; HEGENBERG, 1982; HUTTON, 1996). The third structure trends perpendicular to them in a NW-SE direction. This structure has been referred to as the Kalahari basin axis (DWA, 1991). Only limited data are available for the north-eastern part of the research area, but the occurrence of thick Kalahari sediments at approximately 20.7°E/18.4°S might be traceable south-westward up to the proposed Kalahari basin axis along the trace of the Omuramba Omatako. This may represent an extension of the Waterberg Fault. The proposed graben might represent the continuation of the Omatako Graben, which does not continue north-west of the Kalahari basin axis. The intersections of two perpendicular graben structures (Omatako Graben & Kalahari basin axis; Eiseb Graben & Kalahari basin axis) shows the largest thicknesses of the Kalahari Group.

Implication for palaeo-drainage during (early) Kalahari deposition

A palaeo-drainage map was produced from the obtained thickness of the Kalahari map, assuming that the thickest deposits are associated with flood courses and that the sediments have been shed from palaeo-highs. The resulting map is given in Fig. 3.2-5. The palaeo-drainage system in the research area is bimodal. In the south-eastern part, the system drained east towards a palaeo-Okavango-Makgadikgadi-system. Maximum thickness of the Kalahari sediments in Botswana,

belonging to this endorheic system, is reported to be mostly less than 120 m and only locally more than 210 m at Bushman's Pit/Makgadikgadi Pan (KEY & AYRES, 2000a; 2000b). In the western and northern part of the research area, drainage flowed northward towards the Ovambo Basin where Kalahari sediments reach thicknesses of more than 600 m (MILLER 1997; 1992).

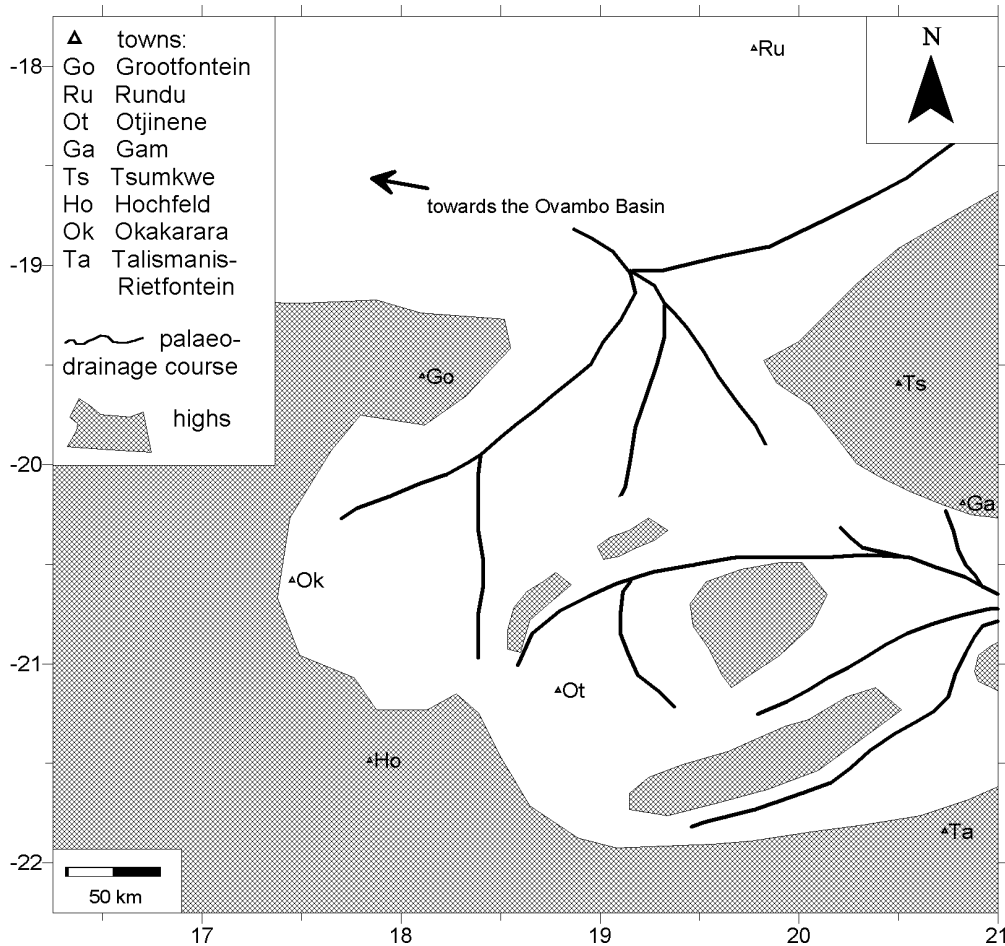


Fig. 3.2-5: Palaeo-drainage pattern during the deposition of the Kalahari Group derived from thickness variations in north-eastern Namibia.

The eastern part of the today's endorheic drainage system in the research area has not changed much since the evolution of the Kalahari drainage system. At present, the ephemeral rivers show the same direction, only slightly meandering compared to the old system. It has been noted that the recent system looks more diverse which most likely results from the scale and resolution of the available data. The northern part of the research area has experienced a major change in flow direction, changing from north-western to north-eastern flow direction. This could have resulted either from relative downward movement in the eastern part (interior of the continent) or uplift of the western (exterior) part, or both. It is worth mentioning that the assumed palaeo-Omatako course is now covered by a large dune field (THOMAS ET AL., 2000) west of the present day's flood course.

Regional context

The research area is located in the southern part of the Northern Mega-Kalahari Basin which is divided from the Southern Kalahari Basin by the Ghanzi ridge (THOMAS, 1986). The thickness of the Kalahari sediments in the research area is greater than the thickness in the Southern Kalahari Basin, as well as in most parts of Botswana belonging to the northern Kalahari basin. For the deposition of up to 400 m sediments, accommodation space had to be created. Two mechanisms are proposed for the evolution of the Kalahari depocenter: uplift of the African continental margin after the break-up of Gondwana (KING, 1962; DE SWARDT & BENNET, 1974; SUMMERFIELD 1985; THOMAS 1988; THOMAS & SHAW 1990; 1991; DU PLESSIS & LE ROUX, 1995) and incipient rifting in the Makgadikgadi Depression (BAILLIEUL, 1979) and Okavango Delta (REEVES, 1972; SCHOLZ ET AL. 1976; MALLICK ET AL. 1981; DINGLE ET AL. 1983; MCCARTHY, 1993; MODISI, 2000; MODISI ET AL., 2000). These two suggestions appear to be contradictory. Uplift of the continental margin should produce compression in the hinterland while rifting is an expression of extensional tectonics (Fig. 3.2.6), although it is also possible to generate accommodation space in compressive graben structures (BEANLAND & BERRYMAN, 1989).

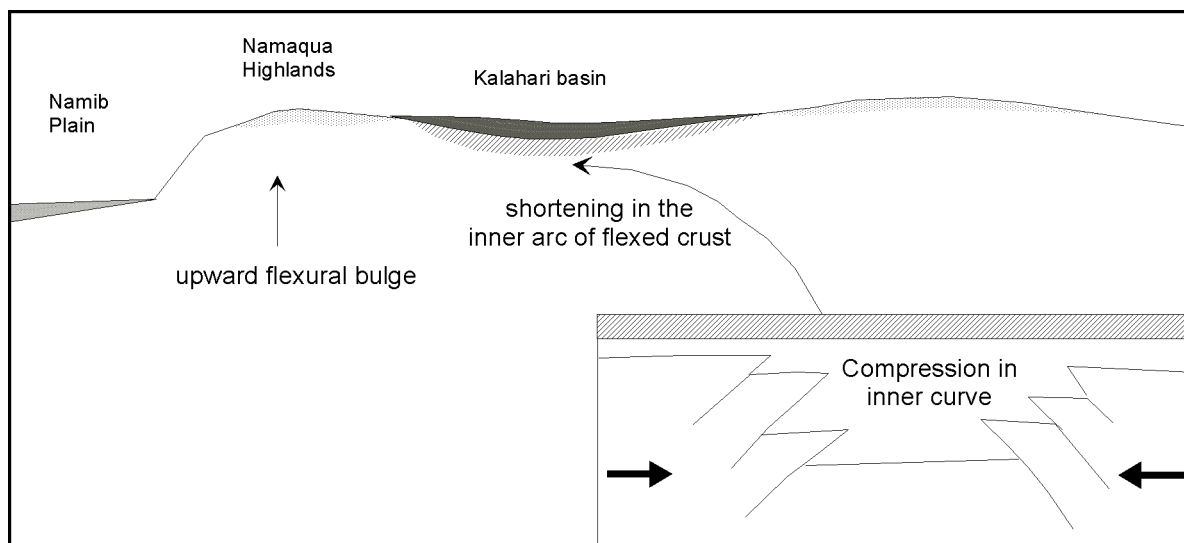


Fig. 3.2-6: Schematic cross-section of southern Africa after the split-up of Gondwana (modified from THOMAS & SHAW, 1991) with respect to compressing structures. Uplift at the African continental margin leads to compression in the interior of the continent allowing the development of a sedimentary basins. Sketches are exaggerated.

POULIMENOS & DOUSOS (1997) explain back basins that border landwards the flanks of uplifted rifts as flexurally controlled hinterland basins giving accommodation space. In this example, a depocentre developed at a distance of 30 km to the continental margin only, but this distance

depends strongly of the physical properties of the model, especially the elastic thickness of the flexing crust.

TEN BRINK & STERN (1992) have modelled the development of the hinterland basin for the south-western African margin by the uplift of a continuous elastic plate. They concluded that an elastic thickness of 100 - 120 km (consistent with the low geotherm under southern Africa [JONES, 1988]) would lead to a maximum thickness of Kalahari sediments at 500 - 700 km inland from the continental margin. The model also predicts the lowest point in the Kalahari basin would lie 800 - 1000 km inland which is appropriate. This model explains well the location of the Kalahari basin axis (for location see Fig. 3.2-4) which is 500 km inland from the present coastline trending NW-SE subparallel to the continental margin, while the surface slopes gently further to the north-east up to the Okavango Delta.

The NE-SW trending structures cannot be explained by the uplift of the continental margin as they are perpendicular to the coast line and they are associated with extensional structures e.g. incipient rifting in the Okavango Delta (MODISI ET AL., 2000). The still active tectonic settings are thought to represent an extension of the East African Rift System which started in Oligocene (e.g. SCHOLZ ET AL., 1987; SCHLÜTER, 1997). Similar rift structures have been proposed from post-Karoo to pre-Kalahari time for the Okavango and Makgadikgadi area by VIAL (1967).

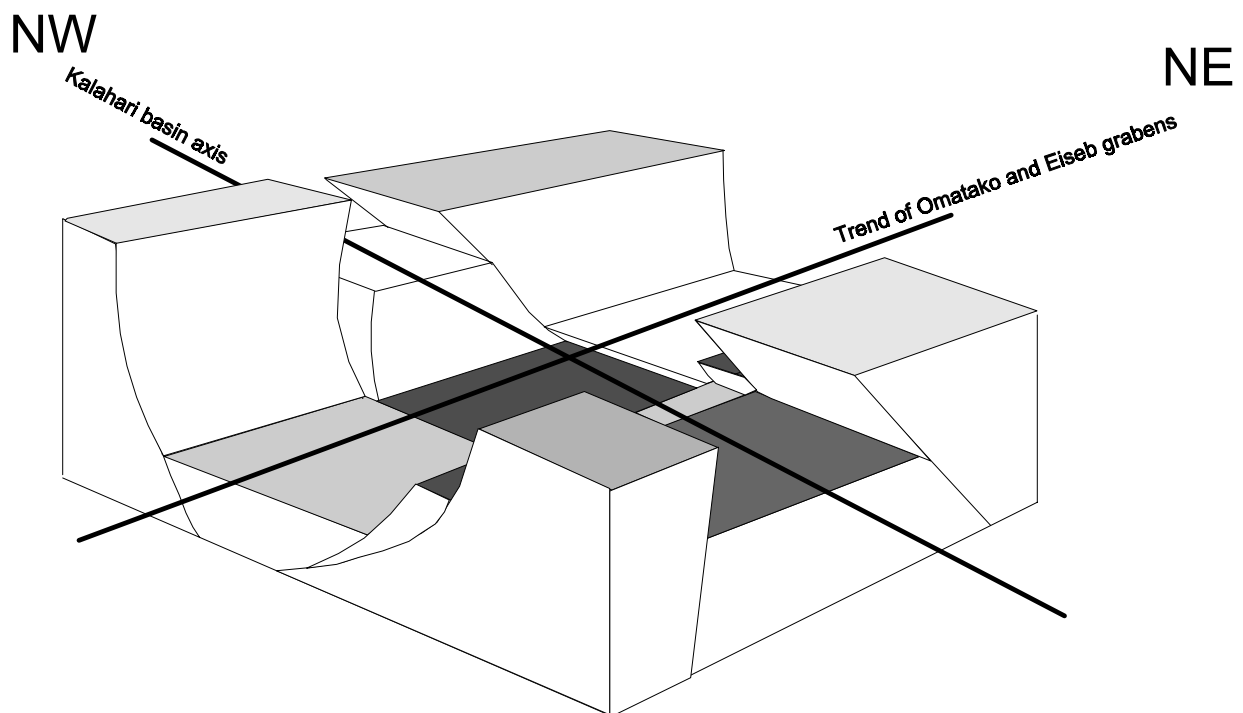


Fig. 3.2-7: Schematic block profile of the Kalahari depocentre in north-eastern Namibia concerning extensional NE-SW trending and compressive NW-SE trending structures.

From this observations it is concluded that the NW-SE and the NE-SW trending structures are independent of each other. The NW-SE structure was initiated by uplift of the African Atlantic continental margin, while the NE-SW structures are extensional structures that have been developed after Karoo deposition prior to the uplift of the continental margin along Damara pre-weakened structures and they are also recently reactivated. It is not clear if this long-lived structures have also been activated during the Kalahari time as transform faults. A summary schematic picture is provided in Fig. 3.2-7.

The picture of a compressive graben, originating from a flexural uplift, with only little displacement at reverse faults is consistent with the facies observation in the Tsumkwe district (Chapter 3.1.4). Better rounded conglomerates have developed here while very angular breccia are exposed along the Omiramba Eiseb and Epukiro, interpreted as fault screens developed at steep scarps, associated with the NE-SW trending extensional graben or half-graben structures.

The structure of the Kalahari basin explains fairly well why Karoo deposits are preserved in the resulting traps of the Omatako and Eiseb grabens (Fig. 3.2-2 and 3.2-3). TEN BRINK & STERN (1992) modelled that deposition is dominant in the hinterland between 500 and 1000 km inland from the coast, while erosion is prominent in the outer 500 km. This correlates well with the ideas of HEGENBERGER (1982; 1987) that Karoo lithologies are still preserved in the north-eastern-most part of Namibia (Fig. 3.2-1).

Detailed mapping in the Makgadikgadi area indicated a WNW trending graben with displacement in the order of tens of meters, which was interpreted as an extensional structure (DU PLESSIS & LE ROUX, 1995). This graben structure trends parallel to the late Karoo (REEVES, 1978) dolerite dyke swarm which was also included in their sections. It is therefore more likely that this structure is related to early Cretaceous extension (REEVES, 2000) or later reactivation of Cretaceous structures by any of the mentioned mechanisms, rather than uplift of the African continental margin as proposed by DU PLESSIS & LE ROUX (1995). As this dyke swarm is also present in the northern part of the research area, WNW trending graben structures might occur here as well, but no variations in sediment thickness related to these could be resolved within the limits of the available data.

3.3 Tectonic settings in the Eiseb Block

HEGENBERGER (1982) interpreted dunes in the lower Eiseb and Epukiro drainage basin (Eiseb Block) of Namibia to be structurally displaced due to tectonic adjustment along south-westerly trending faults. Those faults are marked in the Geological Map of Namibia (MILLER & SCHALK, 1980) as four subparallel faults. HUTTON (1996) describes these faults as marked scarps 30-40 m high of dislocated and truncated dunes. From north to south the four faults are named Eiseb Lineament, Police Camp Fault, Third Fault and Epukiro Fault (Fig. 3.3-4).

The Eiseb Lineament is easily recognisable in the topographic sheets of the area. In the field the fault-line scarp was found to separate a flat plain to the south from rising dunes towards the north. The fault-line scarp is partly accompanied by small ridges at calcrete outcrops (e.g. near Otjinanguruwe S20°39.92/E20°42.915).

Vertical displacement has been observed between the two banks of the Epukiro where a sandstone unit is displaced about 15 m down to the south (vicinity of S20°57.54/E20°51.65).

A NW-SE trending fault was found in the southern cliff of the Omuramba Epukiro showing displacements of 1-2 m down to the West (S20°58.20/E20°48.87).

A small outcrop on the northern bank of the Omuramba Epukiro (S21°12.4'/E20°41.6') showed a slight relative movement down to east where Kalahari silcrete layers are cut. This outcrop is located at the south-western border of a NW-SE trending lineament (indicated by a black arrow in Fig. 3.3-4).

Associated with a basalt outcrop at the Botswana-Namibia-border, north of the Eiseb Block, a small extensional fault observed cutting through the basalt and the overlaying conglomerate, is still visible in the covering red soil (Fig. 3.1-2e). These relationships indicate young extensional faulting.

3.3.1 Interpretation of Landsat TM imagery

Two scenes of Landsat TM 5 (for more details on satellite images see Chapter 5.8) have been used for the mapping of lineaments in the Eiseb Block: LTM 176-74 and LTM 176-75, date of acquisition 1984-07-02. After georeferencing the scenes, lineaments have been mapped with channel combination 3-2-1 (true colour composite), 7-4-1, 7-5-4 and 7-3-1 on the blue, green and red channel of the processing software (TNTmips by MICROIMAGES, 1996). Straight river courses (Fig. 3.3-1 and 3.3-2) and the abrupt termination of dunes (Fig. 3.3-3) are the most obvious features for the interpretation of lineaments. Well developed linear vegetation trends along lineaments, most likely resulting from groundwater flow lines which follow joints in the

partly consolidated sediments of the Kalahari Group have also been used. Joints that are used as groundwater routings are also seen in wetter soil. Very distinctive features defining lineaments are meanders that have been cut off and calcretes forming distinct elongated features.

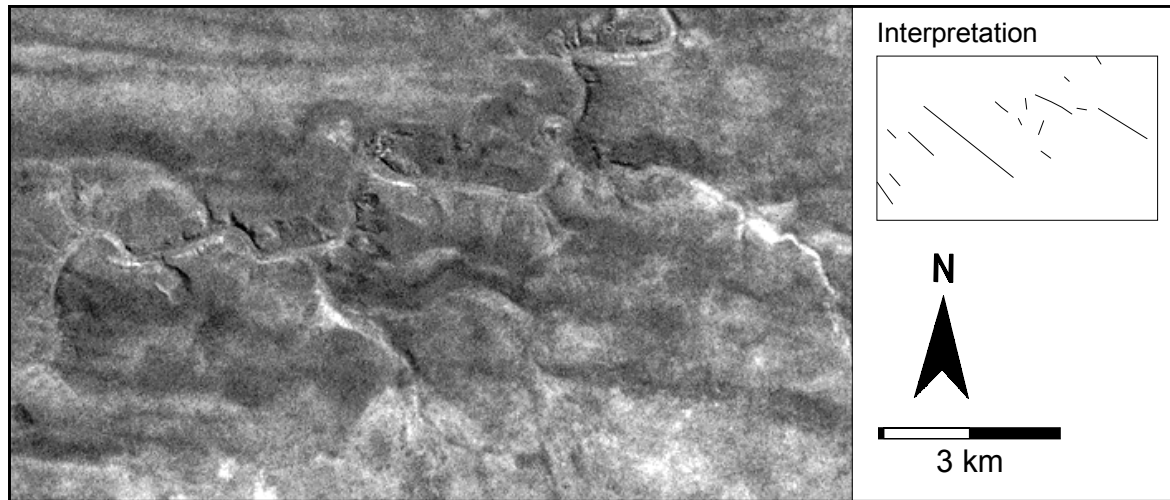


Fig. 3.3-1: Selection of the Epukiro catchment in channel 1, LTM 176-75, date of acquisition 1984/07/02 with interpretation of lineaments. The tributaries of the Omuramba Epukiro are here mostly orientated along NW-SE trending lineaments while some NNE-SSW trends are also apparent.

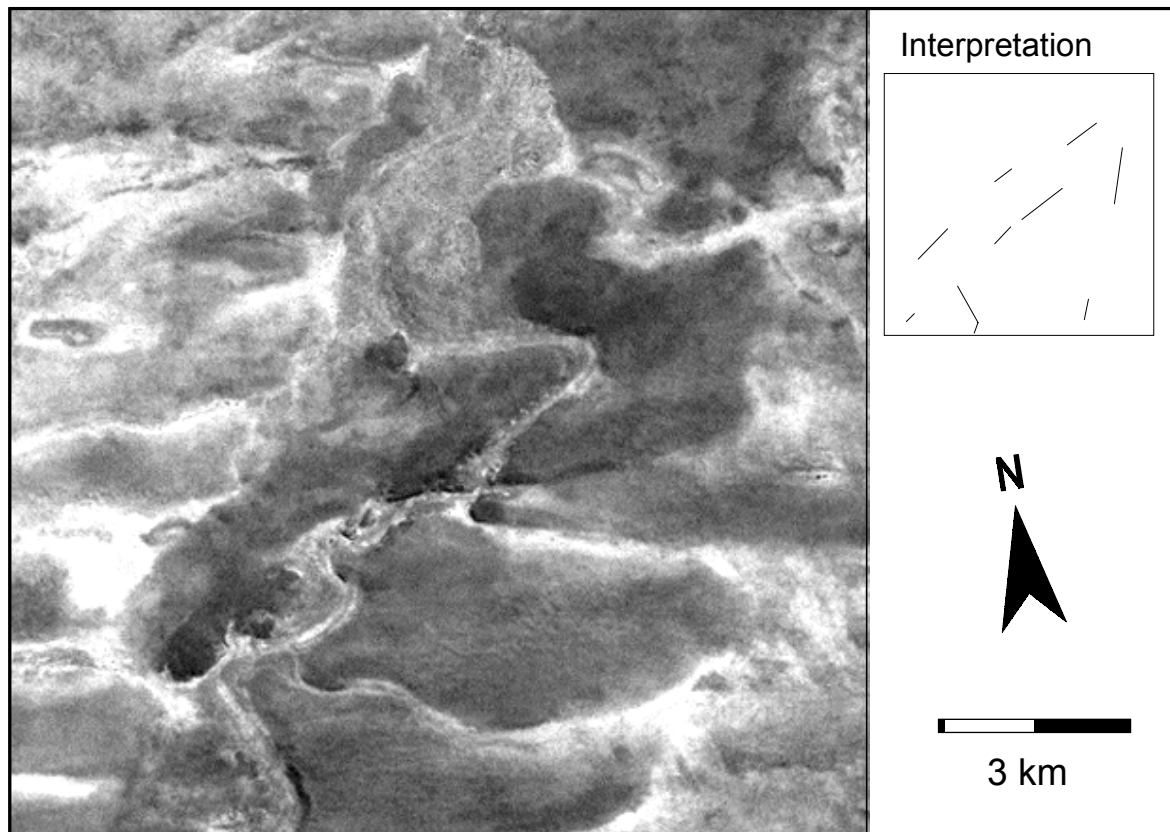


Fig. 3.3-2: Selection of the Epukiro catchment in channel 1, LTM 176-75, date of acquisition 1984/07/02 with interpretation of lineaments. The Omuramba Epukiro is principally orientated along NE-SW trending lineaments here.

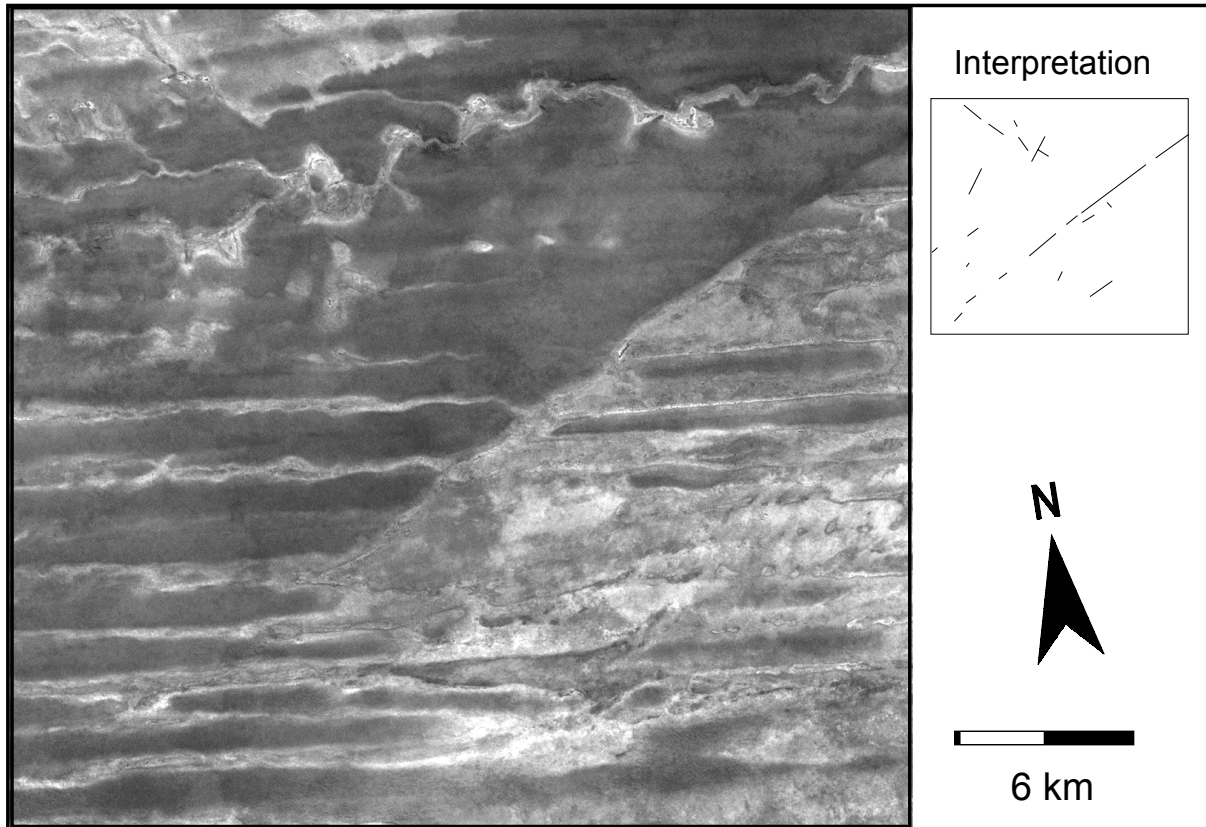
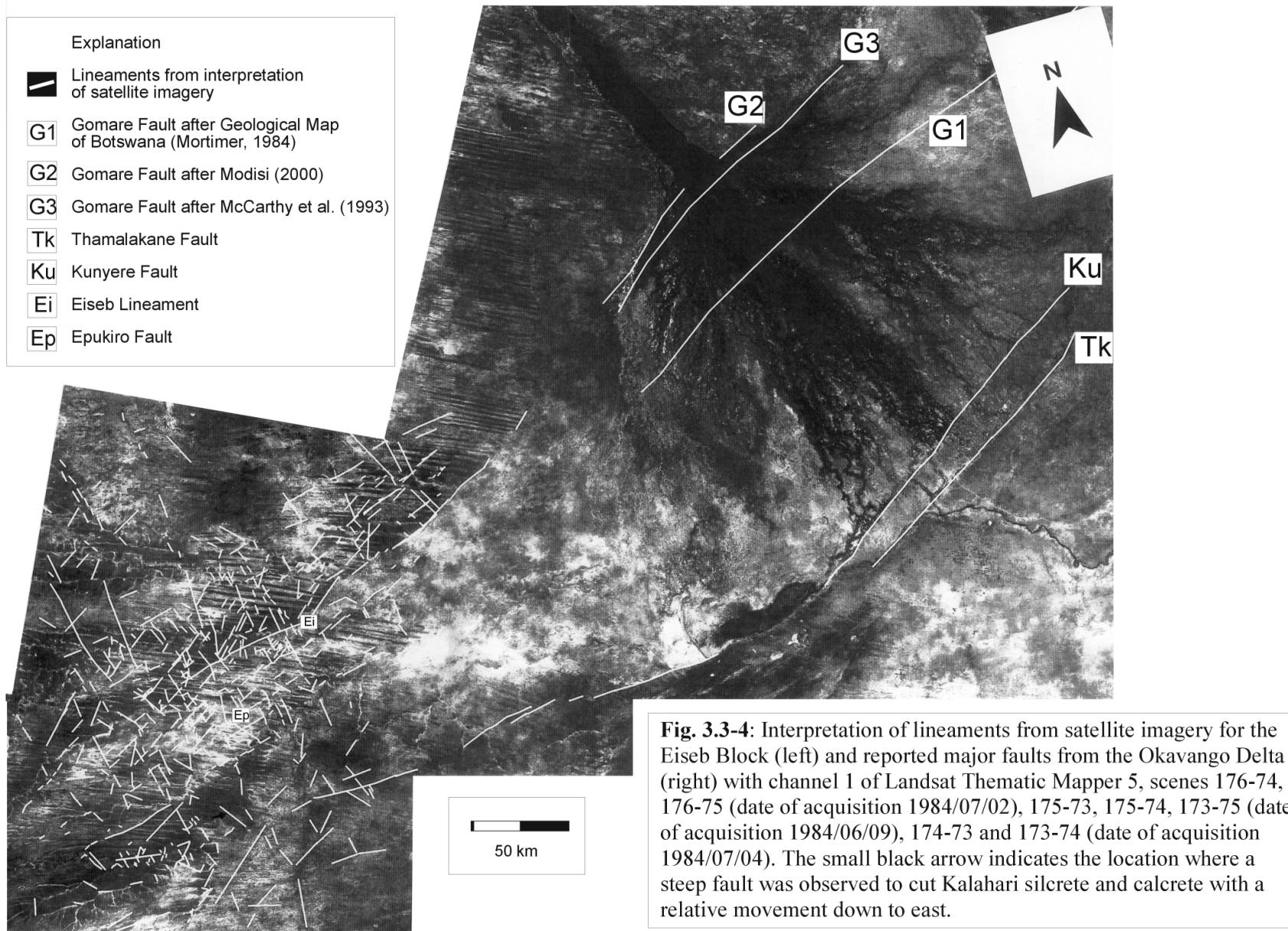


Fig. 3.3-3: Selection of the lower Eiseb catchment in channel 1, LTM 176-75, date of acquisition 1984/07/02 with interpretation of lineaments. Dunes are cut along NE-SW trending lineaments while the tributaries to the Omuramba in the upper left corner of the image follow NW-SE trending lineaments.

The mapped lineaments are given in Fig. 3.3-4 together with Landsat TM channel 1. Two major lineament orientations can be observed: NW-SE and NE-SW. While the NE-SW trend is clearly visualised by dune termination, the NW-SE south east trend is best defined by the orientation of rivers e.g. the Omuramba Daneib and tributaries to the Rooiboklaagte. The two systems intersect in the central part of the study area.

The frequency distribution of lineaments in the Namibian Eiseb Block has been illustrated in a rose diagram (Fig. 3.3-5). Lineaments have been weighted according to the length of traceability in the Landsat TM imagery. The peaks of the weighted lineament trends are at NE-SW (41° to 50°) and NW-SE to NNW-SSE (141° to 160°) with 88 % of the measured lineaments lying between 21° to 70° and between 131° to 170° .

In the satellite images it was observed that the dunes south-east of the Eiseb Lineament are not as high as the dunes north-west of the Eiseb Lineament, which indicates a relative movement downward at the south-eastern side. Thickness variations as presented in Chapter 3.2.2 confirm this observation.



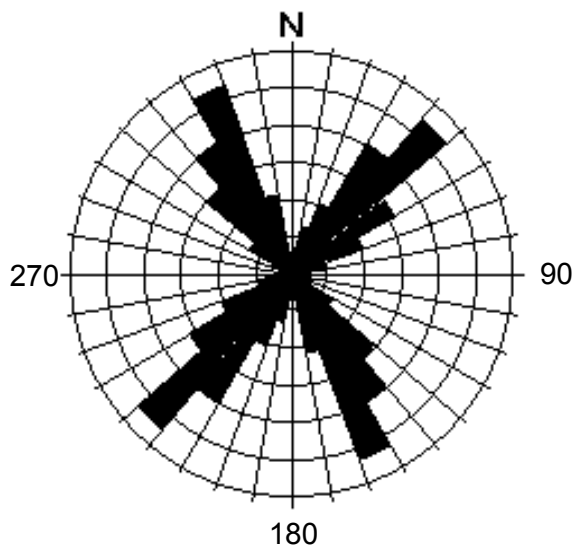


Fig. 3.3-5: Frequency distribution of lineament trends for the Eiseb Block observed from satellite imagery interpretation.

3.3.2 Time of the faulting

The faulting must be younger than the last activity of dunes in the study area as dunes are cut across. The dunes in the lower Eiseb and Epukiro catchment are situated between the dune fields of Zambia, of Zimbabwe, of the southern Kalahari (southern Botswana, Namibia and South Africa) and a dune field west of the Omatako as described by THOMAS ET AL. (2000). Last determined activities of the longitudinal dunes range from 43-21 ka for the Omatako dune field (THOMAS ET AL. 2000), 16-9 ka for Zimbabwe (SINGHVI & WINTLE, 1999), and 5-4 ka for western Zambia (O'CONNOR & THOMAS, 1999). Although every dune field has

its own history, the Eiseb-Epukiro dune field is situated mid-way between the Omatako and western Zimbabwe dune fields and a last time of activity between 21 - 4 ka is most likely. Latest fault activity is therefore constrained to be post-21 ka and possibly as young as post-4 ka.

3.3.3 Regional correlation and Interpretation

Major faults from the Okavango Delta also shown in Fig. 3.3-4 are the Thamalakane Fault, the Kunyere Fault and the Gomare Fault. The first two faults are clearly identified as they follow the rivers they are named after. The assignment of faults to the name Gomare Fault shows some confusion in the literature. Three different faults in the northern part of the delta are named Gomare Fault after the location at the delta's border Gomare (or Gumare in some maps). The south-eastern most of the three faults (G1 in Fig. 3.3-4) is adopted from MORTIMER (1984), the north-western most (G3 in Fig. 3.3-4) was named Gomare Fault by MCCARTHY ET AL. (1993) and the fault G2 (Fig. 3.3-4) was named Gomare Fault by MODISI (2000) and MODISI ET AL. (2000). From the mapped pattern it was observed that the Gomare Faults G2 and G3 could be traced into Namibia towards the lineament that has already been named Gomare Fault-Eiseb Lineament by HEGENBERGER (1982) and HUTTON (1996). The Gomare Fault G1 is more likely to be traced into Namibia's Epukiro Fault. While the Kunyere Fault is traceable into Namibia, the Thamalakane Fault is not found east of Lake Ngamis Longitude. The NE-SW trending Kunyere Fault bends towards ENE-WSW directions west of Lake Ngami.

The dominant lineament trends in Fig. 3.3-5 are consistent with observations from HUTCHINS ET AL. (1976) who found principal orientations of lineaments in the Okavango Delta, mapped by the use of Landsat imagery, between 140° to 160° (with 140° to 150° being the more frequent direction) and a second peak at 40 to 50° . The Kunyere and Thamalakane faults also follow the direction of approximately 40° . MCCARTHY ET AL. (1993) obtained slightly different results from the interpretation of SPOT images. The most dominant direction from their interpretation is ESE (100 - 110°) which they interpreted as traces of dune orientation and a Karoo dyke swarm and are thus not of primary tectonic origin. Apart from these features, their observed main directions are 60 - 70° , 120 - 140° and 150 - 160° . The 60 - 70° peak is as well observed in the Namibian study area, but it is less significant than the 40 - 50° and the 140 - 160° peaks.

REEVES (1972) proposed incipient rifting in the Kalahari, and the Okavango Delta has been seen as the south-western extension of the East African Graben System due to its seismic activities and similar sense of crustal extension (SCHOLZ ET AL., 1976; FAIRHEAD & HENDERSON, 1977; MCCARTHY ET AL., 1993). East-west extension of the African continent is believed to have reactivated ancient, north-easterly-trending basement structures and the Okavango Delta is interpreted as a large half-graben structure formed by this mechanism (MCCARTHY ET AL., 1993). MODISI (2000) indicates continuation of the rift further to the north into the Caprivi Strip of Namibia and it is most likely that it can be traced further into Zambia and Lake Kariba (MALLICK ET AL., 1981; SCHOLZ ET AL., 1976). It seems likely from the observation of satellite imagery, thickness variations and geophysical research by CSIR (1982) that the continuation of the half-graben structure from the Okavango Delta can be traced into the Namibian Eiseb Graben. It is proposed that this structure follows a deep (lithospheric?) zone of weakness, also named conductor, which was observed by DE BEER & VAN ZIJL (1975) and DE BEER ET AL. (1976) with a magnetovariational study, and interpreted as a south-westward extension of the African Rift System. This structure is indicated to reach the Namibian border between 20 and 21° latitude with a NE-SW trend and then bends into east-west direction and further to the west at a longitude of about $E17^{\circ}$ to NE-SW direction. The bending of the conductor cannot be seen in the Gomare Fault (or Gomare fault system), but the southern edge (Kunyere Fault) of the postulated rift follows this trend.

Although cutting off of dunes indicates very young movements, the Eiseb Graben and associated lineaments seem to be a long-lived, often reactivated structure that follows the established structures of the Damara inland branch, Karoo trough and basin structures of the Kalahari (see Chapters 3.1 and 3.2).

4 Hydrogeological Settings

4.1 Groundwater levels and definition of catchments

The spatial distribution of the hydraulic heads indicates groundwater flow directions at a regional scale. They are essentially required for catchment definition and identification of groundwater flow direction, which are used for further purpose, e.g. recharge regionalisation (Chapter 5.6).

4.1.1 Method

Data of groundwater levels below collar are available from the DWA database as well as surface elevation of the borehole collar. Piezometric heads above mean sea level were calculated from this data set. Data were carefully checked for reliability e.g. level must be above borehole bottom and below the topographic surface. It has to be remarked here that the reported levels in the DWA database are all from temporally inconsistent observations. The groundwater level is only reported directly after each borehole was drilled, thus ranging from early last century to present. Monthly observations are only available for wells in state water schemes, but this number is limited to reflect the groundwater levels at a regional scale. It has to be further remarked that groundwater levels are not adjoinable to any specific aquifer as mostly no screening reports of the boreholes exist. Nevertheless 7003 data points were used to produce a raster map by kriging after reliable level observations were filtered for duplicates. A linear model was fitted to the variogram (yellow insert in Fig. 4.1-1) and then used for the calculation with a slope of 16910, and an anisotropy of 1.476 at 13.89°. The search modulus for this large data set was set to 8 search radiant, with a maximum of 8 data points to be used from each sector.

4.1.2 Results

The result of the regionalisation of the hydraulic heads is given in Fig. 4.1-1. Groundwater levels range from 1650 m asl in the southern part of the research area to 900 m asl at the Botswana border between 20.5 and 21° S in the Eiseb Graben. Sub-catchments (Fig. 4.1-2) have been defined from the groundwater level distribution map. The Eiseb-Epukiro-Catchment is the largest sub-catchment of the research area. It is named after the most prominent Omiramba Epukiro and Eiseb which show the same flow direction as the groundwater in this catchment. North-easterly flow direction are observed in the western part of the catchment, bending towards easterly directions in the eastern part. While in the upper Omatoko catchment (upstream of the Omatoko dam) surface runoff is reported during every wet year, surface runoff occurs rather

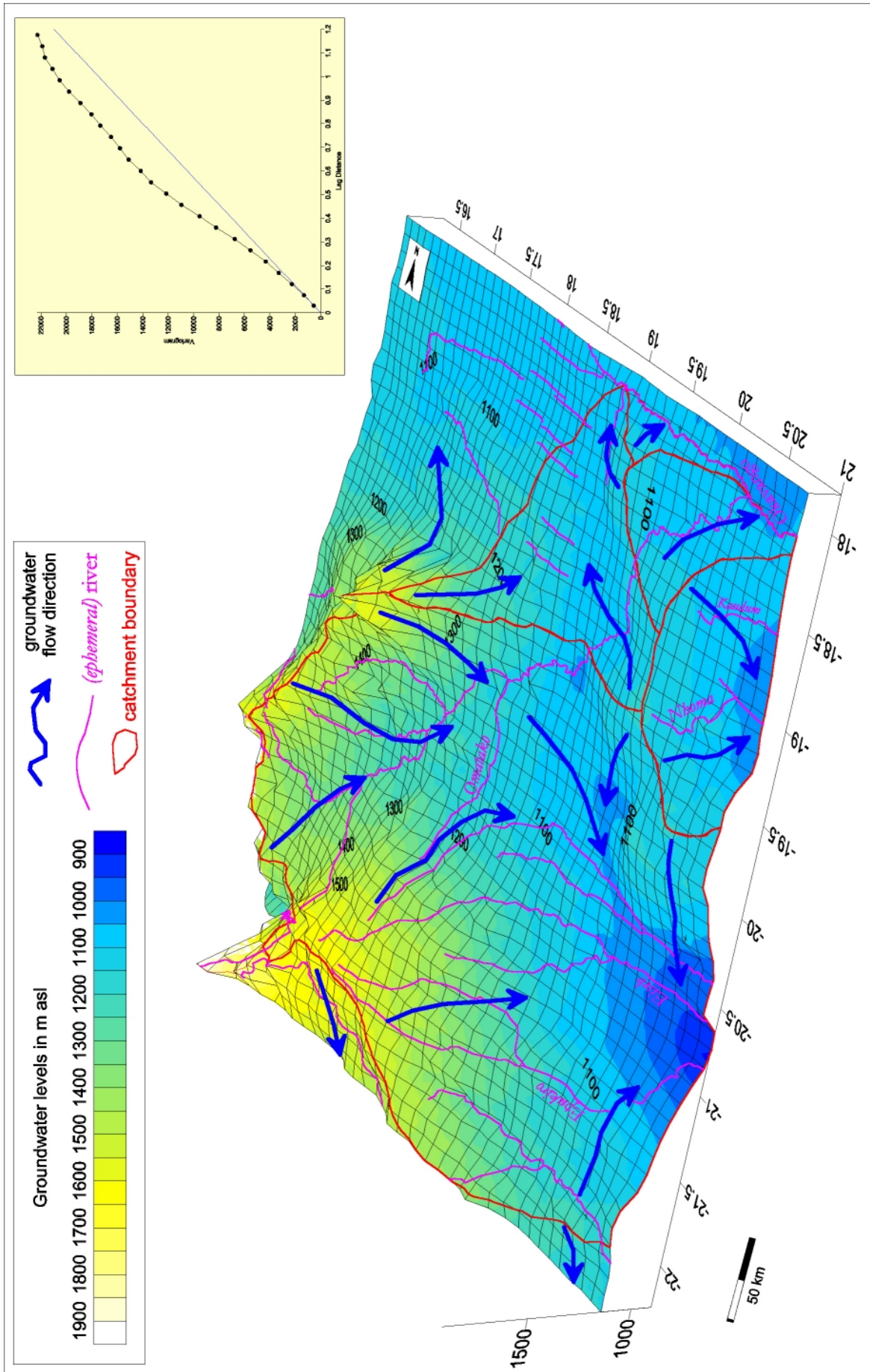


Fig. 4.1-1: 3-D perspective plot of the distribution of groundwater levels and flow directions (blue arrows). Distribution has been obtained from 7003 point data from DWA database (see yellow insert for variogram). Borders of the groundwater catchments are indicated by red lines, (ephemeral) rivers are given in pink.

locally in the eastern part of the Eiseb-Epukiro-Catchment. This limitation is mainly induced by the sandy surface and by dunes blocking the flood courses. In this catchment groundwater flows towards the Eiseb Graben with a hydraulic base level of approximately 900 m asl. From there it is assumed to flow further east towards the Makgadikgadi Pan in central Botswana where evaporation is dominating the groundwater discharge zone.

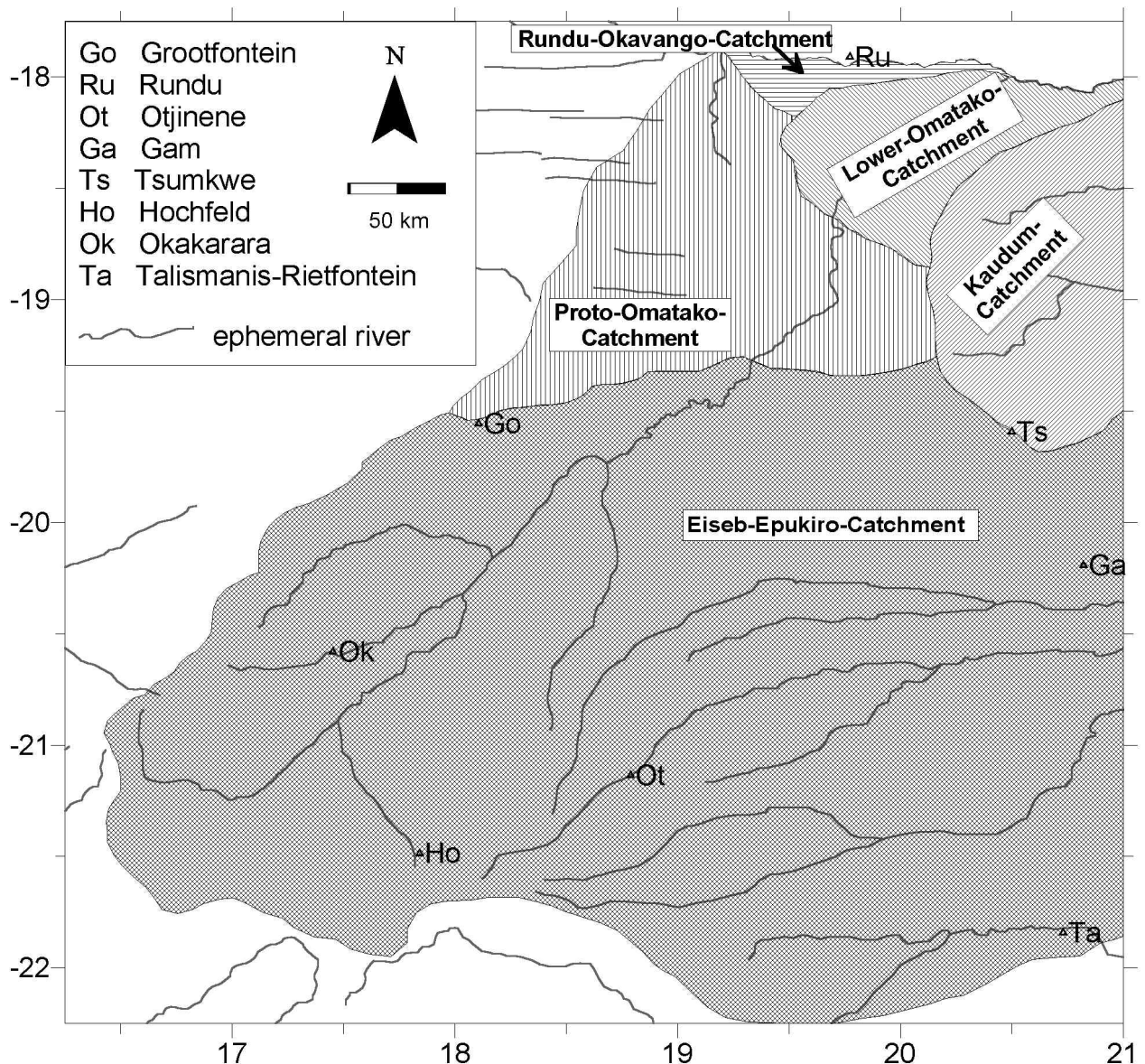


Fig. 4.1-2: Definition of the research area and its subdivision into 5 groundwater sub-catchments from groundwater level distribution.

As groundwater flow directions are not very clear in the area where the Omatako crosses from the Eiseb-Epukiro-Catchment into the Proto-Omatako-Catchment, this region is shown in detail in Fig. 4.1-3. A hydrogeological trough structure is calculated trending NW-SE and draining towards the Eiseb Graben. This structure is not appearing further to the north-west than

approximately S19.8°/E19.6°, but a small area with groundwater levels below 1050 m asl is observed in the elongation of this feature in the area around farm Horabe (~S19.4°/E19.2°). From the surface drainage pattern it seems likely that this low levels would drain north towards the Okavango, but no lower levels occur north of this area. Additionally, the hydraulic base level at the outlet of the Omatako to the Okavango (1050 m asl) lies above the levels measured around farm Horabe. All data in the Horabe area are consistent and thus measuring appears reliable. Consequently it is concluded, that groundwater in the concerned area drains east towards the Eiseb Graben. The lack of date between the trough structure and the Horabe area and the fact that the groundwater divide here is very shallow are most likely to produce the unapparent flow direction. As the groundwater surface is very gently dipping towards the Eiseb Graben it is concluded, that transmissivity must be rather large which will be further discussed in Chapter 6 during the set-up of a groundwater flow model.

At approximately S19.8°/E20.3° a groundwater mound is observed (Fig. 4.1-3), which most probably results from increased groundwater recharge due to a large pan field and hardrock outcrops in this specific area.

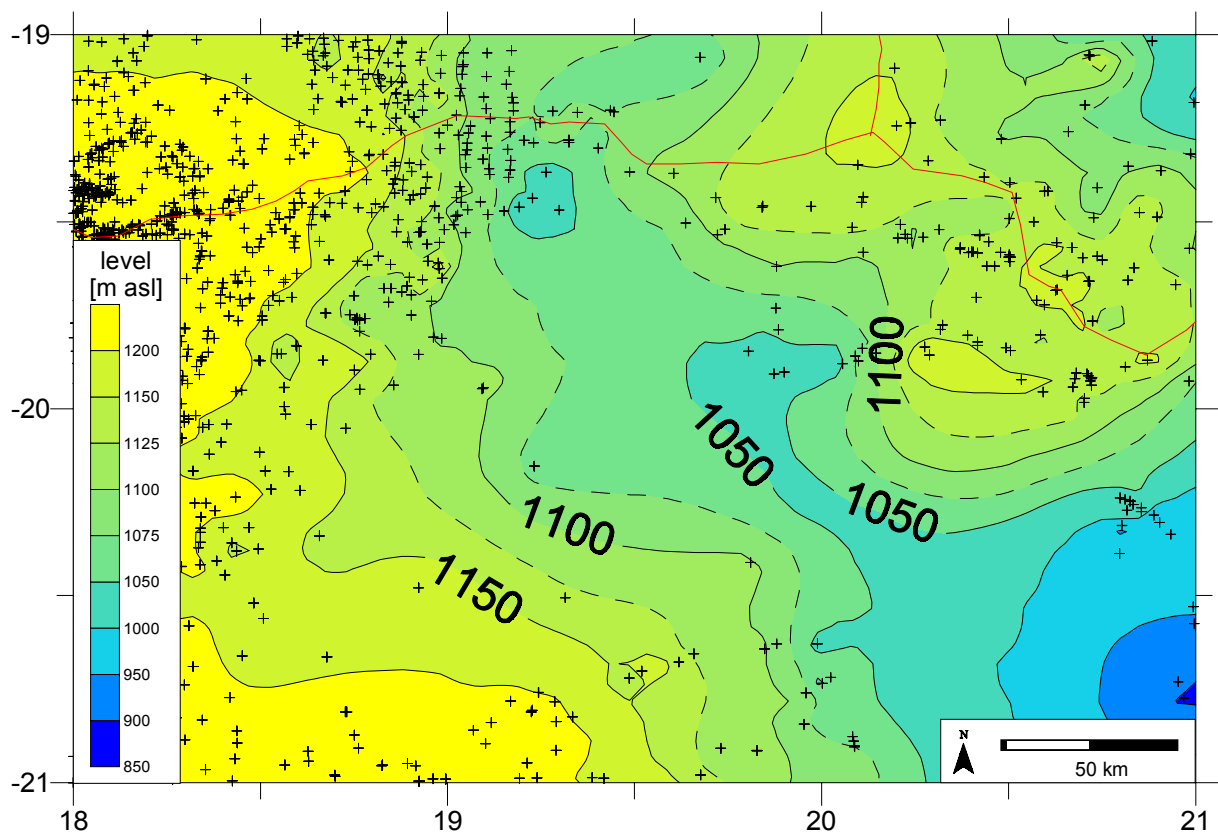


Fig. 4.1-3: Calculated groundwater levels in the area between S19°/E18° and S21°/E21 with observation points (black crosses) and defined catchment boundaries (red line).

Groundwater flows with easterly directions in the Kaudum-Catchment (Fig. 4.1-2) which most likely drains towards the Okavango Delta. The lowest point of this catchment is at 1025 m asl on the Namibian side. Surface runoff occurs fairly seldom at a regional scale but in the Omuramba Nhoma (southern part of the catchment) at least local drainage marks have been observed and both Dobe Pan and Klein Dobe are episodically water filled.

In the Rundu-Okavango-Catchment groundwater and surface water flow directions are northerly towards the Okavango. The lowest point of the Rundu-Okavango-Catchment is at 1050 m asl.

In the Lower-Omatako-Catchment groundwater flow directions is confluent towards the Omatako. The hydraulic base level is situated at the outlet of the Omatako to the Okavango with approximately 1050 m. The groundwater follows roughly the direction of the surface slope in this area. Surface runoff from precipitation occurs very seldom here. The mostly observed surface water flow occurs during relatively high water levels in the Okavango that presses water into the Omatako. This opposes the observed groundwater flow direction and the assumed surface flow direction indicated from the topography.

While most of the ephemeral rivers in the research area follow the groundwater flow directions or vice versa, the Omatako does not show this correlation. It parallels the groundwater flow direction only in its upper part approximately up to the confluence with the Omuramba Gunib. In contrast groundwater flow direction and the river course do not reflect each other in the Omatako river catchment between the confluence with the Omiramba Gunib (Eiseb-Epukiro-Catchment) and Nushe (Proto-Omatako-Catchment). A Proto-Omatako is thought to have roughly followed the upper part of the Omatako course but bent at approximately 19°S/19.25°E towards north-westerly directions to contribute to the Proto-Kunene (see Fig. 3.2-5). Groundwater flow directions in the Proto-Omatako-Catchment follow approximately the direction of the assumed Proto-Omatako. The hydraulic base level (1065 m) of this catchment is situated at the outlet of the ephemeral river Namungundu towards the Okavango.

The three sub-catchments Proto-Omatako-, Lower-Omatako- and Rundu-Okavango-Catchment all drain towards the Okavango where groundwater most probably unites with surface water that originates from the Angolan highlands. The Okavango then transports the water towards the more than 10 000 km² large Okavango Delta (SHAW, 1986) where it is likely to be combined with groundwater from the Kaudum-Catchment. At the very shallow Okavango Delta most of the surface water evaporates. Only very small amounts of water are conducted during water high stands towards the Makgadikgadi depression. At the pan area surface water evaporates together with groundwater that originates from the Eiseb-Epukiro-Catchment and groundwater that flows

towards the salt pan from southern, northern and western directions to make up an inland discharge area of approximately 3000 km² with a distance to groundwater at less than 5 m.

All precipitation that either produces groundwater recharge or surface runoff in the Namibian research area is supposed to arrive finally at the Makgadikgadi depression if it is not evaporated on one of its detours. Therefore the research area for this study has been limited to the five defined sub-catchments that make up the northern Namibian part of the very large endorheic Makgadikgadi-Kalahari-Catchment. The sum of the 5 defined sub-catchments is named "Northern Namibian Kalahari Catchment" and as an abbreviation in this thesis the term "Kalahari catchment" is mostly used.

4.2 Distribution of groundwater strikes and definition of the uppermost aquifers

4.2.1 Method

The concept of aquifer definition is not easily transferable to a large area with very limited data availability. During a regional approach the observed groundwaters have to be characterised by the aquifer material they struck in. The strike that was observed when the borehole was drilled will be used for this purpose and these data are mostly available from the DWA database. Therefore all strike reports for the research area were extracted from the DWA database and plausibility of strikes was checked with the depth of the borehole. 4480 data points remained for the research area after checking the data for duplicates. The variogram of this data set shows a parabolic form and kriging was processed with a linear equation (slope = 2400, nugget effect = 520).

The lithology that the strike was observed in is used to further characterise the aquifers. By subtracting the distance of strike to the surface from the thickness of the Kalahari sediments, a distribution map of the saturated Kalahari thickness is obtained. The saturated thickness indicates the thickness that water strikes in and not the thickness that water levels up to. A negative saturated thickness indicates the Kalahari to be dry and a pre-Kalahari formation serves as the topmost aquifer. The pre-Kalahari aquifers Etjo and basalts, Omingonde or Pre-Karoo are assigned according to the distribution of the lithological units presented in Chapter 3.2.

4.2.2 Results

The resulting distribution of strikes below surface is given in Fig. 4.2-1. Strikes are deepest in the central part of the research area where they reach up to 180 m below surface. The distribution

map of the uppermost water bearing lithologies obtained from strike is given in Fig. 4.2-2. The Kalahari Group is the dominant aquifer in the northern part of the research area, whereas the western part is dominated by Karoo and pre-Karoo aquifers. As the pre-Kalahari unconformity often serves as a good aquifer, strike in it is labelled separately. It has been assumed that areas with strike at ± 5 m to the boundary Kalahari - pre-Kalahari lithology are dominated by the strike in the unconformity. This areas are mostly constrained to the passage from Kalahari to pre-Kalahari aquifers, but the unconformity seams to represent a more regional aquifer in the vicinity of Gam, between the Omuramba Omatako and Hochfeld and near the Omuramba Nhoma north of Tsumkwe. In the Omuramba Nhoma conglomeratic deposits immediately above the unconformity have been described by ALBAT (1978) and field observation showed outcrops of the pipe sandstone here (Chapter 3.1.4). These lithologies represent units that have well defined water routings.

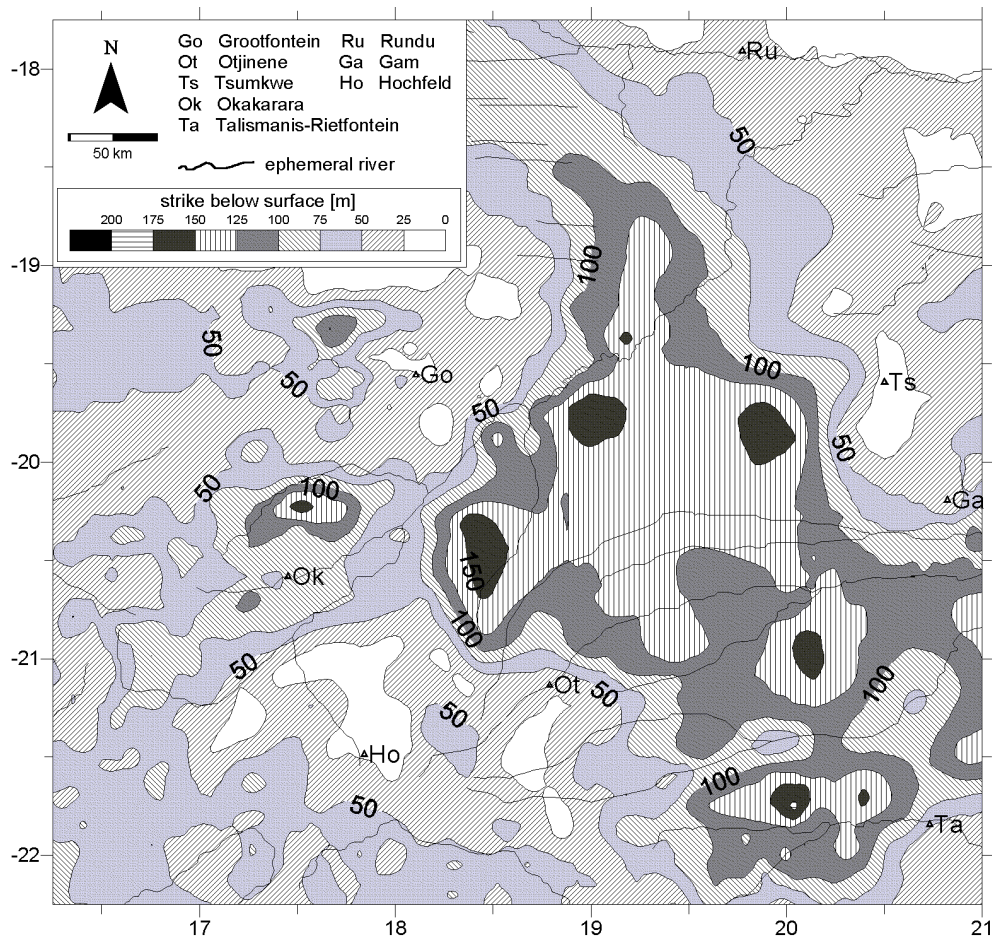


Fig. 4.2-1: Distribution of groundwater strikes (distance from surface [m]) in the research area.

The pre-Kalahari aquifers Etjo and basalts, Omingonde or Pre-Karoo are fractured aquifers, whereas the only partly consolidated Kalahari sediments have to be interpreted mostly as a porous to fractured aquifer.

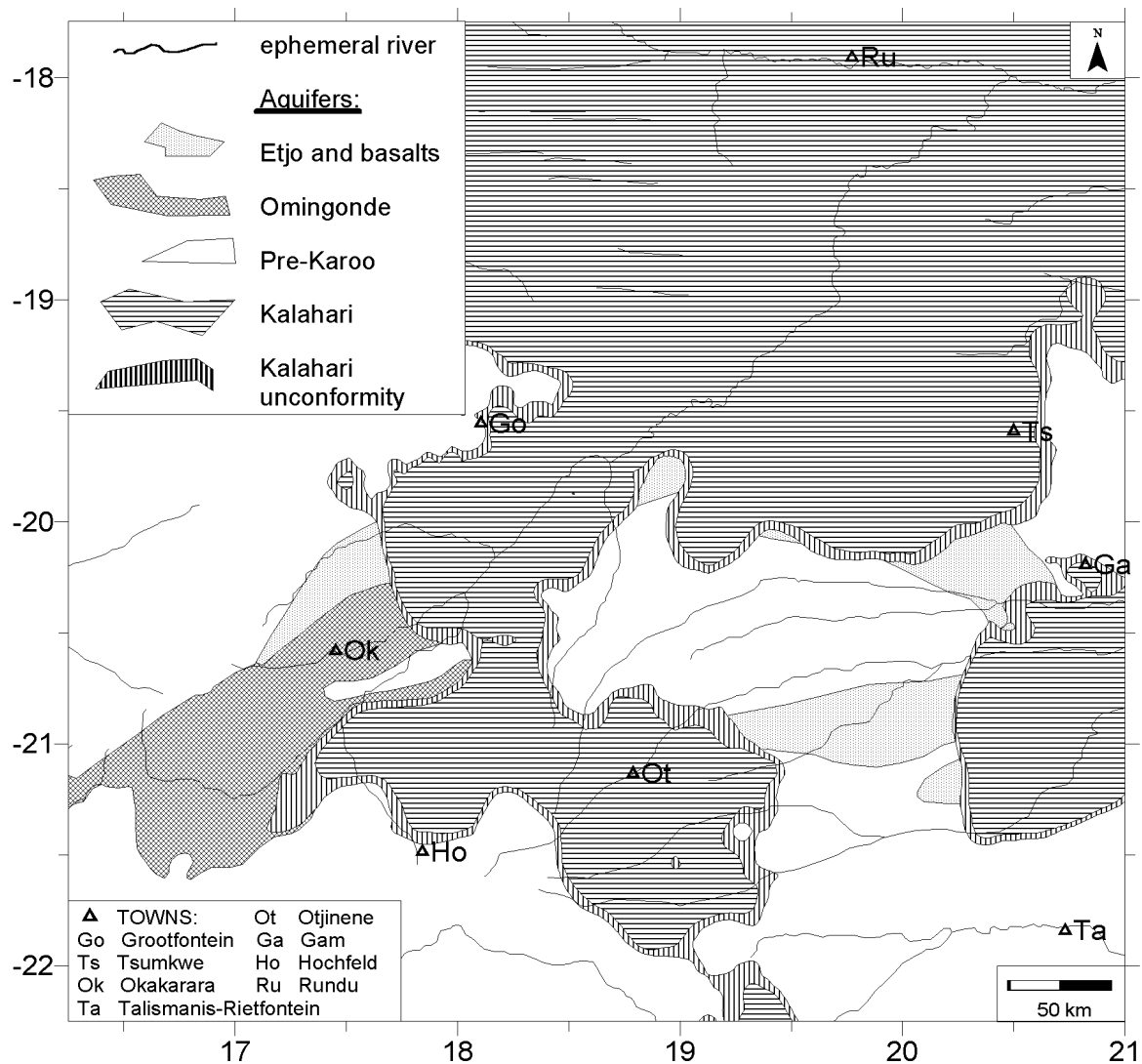


Fig. 4.2-2: Distribution of uppermost lithologies serving as aquifers in the research area.

4.3 Distribution of well yield

4.3.1 Method

Well yield is defined as the maximum pumping rate that can be supplied by a well without lowering the water level in the well below the pump intake (FREEZE & CHERRY, 1979). Well yield is here not referring to the German "spezifische Brunneneigebigkeit" which describes the relation between the extracted water amount and the lowering of the water level. The amount of lowering of a water level by pumping at a set pumping rate in a well of a defined effective radius is a function of transmissivity and storativity (e.g. THEIS, 1935; COOPER & JACOB, 1946). The safe yield for most of the Namibian wells is estimated somehow by pumping directly after the borehole was drilled. But as no additional information, e.g. the pump intake, are given, the well yield in the database reflects the transmissivity in some way, but no calculations are possible.

In the DWA database 5239 data points with yield data are available. The variogram (Fig. 4.3-1) of this data set indicates that the spatially closest data are not the most similar ones. This is not very surprising for highly inhomogeneous and anisotropic, fractured aquifers and therefore boreholes that are further away but situated on the same fault structure should be more similar as wells that are located closer to each other but are not in the same fault. Regionalisation of the well yield by mathematical function is thus not reasonable.

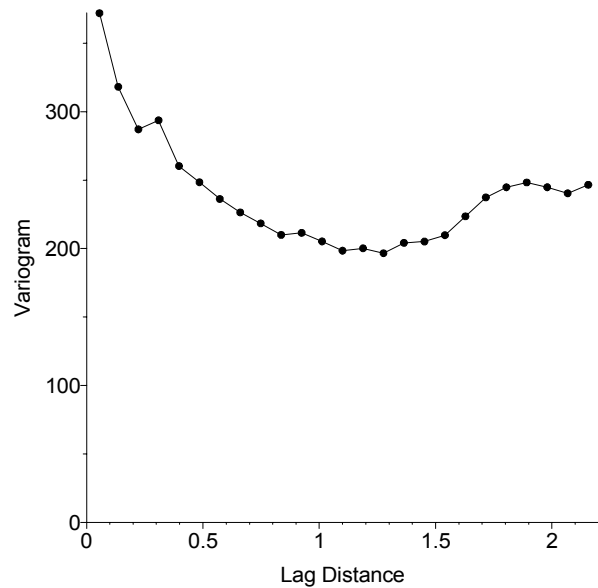


Fig. 4.3-1: Variogram of the well yield for the research area.

Yield values have been plotted at the measured points together with the aquifer (only uppermost) and the major lineaments (Fig. 4.3-2). The lineaments have been digitised from the Aeromagnetic Interpretation Map of Namibia (WACKERLE, 1996), the Geological Map of Namibia (MILLER & SCHALK, 1980) and from the observation of satellite images in the eastern part of the research area (Chapter 3.3).

4.3.2 Results

The highest reported yield is 273 m³/h at a spring at Rietfontein/Grootfontein area. Mean yield of all available borehole data is 7.4 m³/h with a standard deviation of 13.5 m³/h. Most of the boreholes that yield more than 50 m³/h are limited to the karst area west of Grootfontein. Such high yielding boreholes were also found in the vicinity of Goblenz (c.f. KÜLLS, 2000) with water striking in the Kalahari aquifer. The high yielding boreholes between Okahandja and Otjiwarongo are constrained to the unconformity of the Kalahari with the underlying Damara rocks. Boreholes in the Kalahari are mostly yielding between 1 and 10 m³/h. The only high yielding well (> 50 m³/h, dark blue square in Fig. 4.3-2) in the Eiseb Block from the DWA database is located at the junction of the continuation of two major faults mapped in satellite images at approximately S 21.15°/E 20.75°. At least the NE-SW striking fault is quite young as it sets off dunes farther to the north (Chapter 3.3).

The boreholes in the Damara units in the southern part of the research area are mostly not yielding more than 5 m³/h and quite often yield is lower than 1 m³/h. The wells in the vicinity of

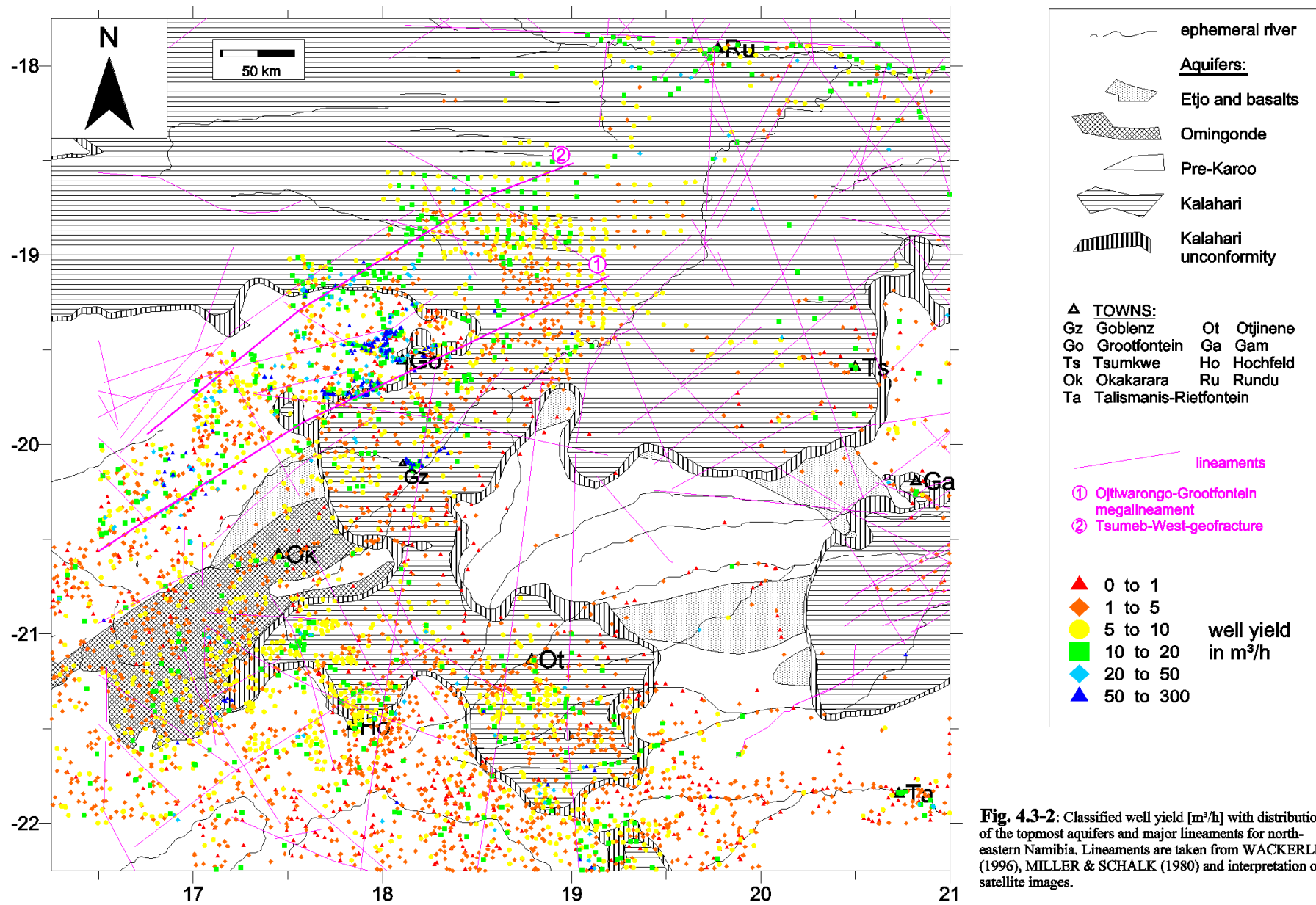


Fig. 4.3-2: Classified well yield [m³/h] with distribution of the topmost aquifers and major lineaments for north-eastern Namibia. Lineaments are taken from WACKERLE (1996), MILLER & SCHALK (1980) and interpretation of satellite images.

Gam that yield more than 5 m³/h are constrained to the junction of the NW-SE trending Gam lineament with a NE-SW trending structure.

As most of the major faults are not very constrained to the high yielding boreholes, apart from the Otjiwarongo-Grootfontein-Mega-lineament and the Tsumeb-West-geofracture, it is concluded that not the geological significant fractures are associated with well water bearing structures. Most probably the recent reactivation or origin of the faults, e.g. in the Eiseb Block, are very promising hydrogeological structures.

A detailed map of the Eiseb Block is provided in Fig. 4.3-3. The boreholes constrained to the Eiseb Lineament and the Police Camp Fault show higher yields than the wells situated along the NW-SE and NNE-SSW trending structures. The borehole situated at the crossing of the Eiseb

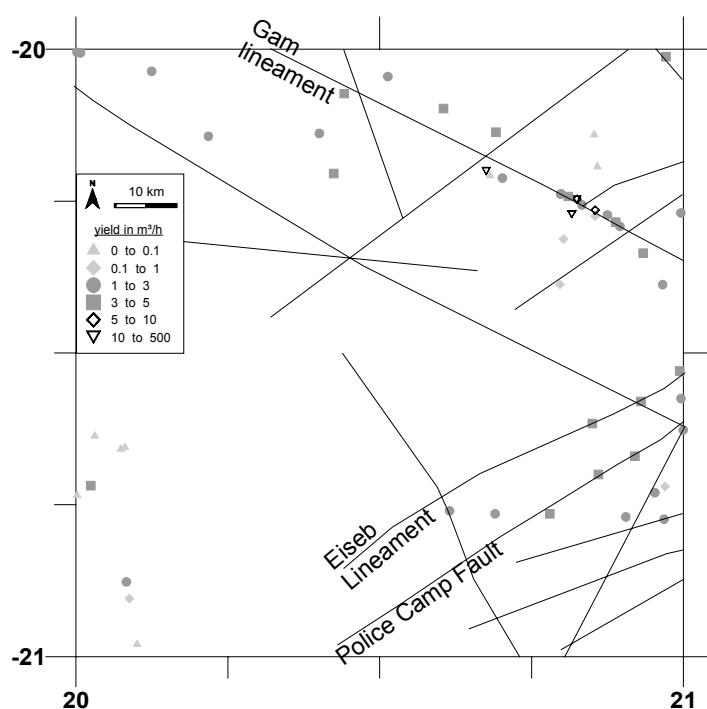


Fig. 4.3-3: Well yield in the Eiseb Block and Gam area (E 20 - 21°, S 20 - 21°) with reference to lineaments. The lineaments result from the examination of satellite images and available data from HUTTON (1996).

fault with the easternmost NW-SE trending lineament shows a yield of 4 m³/h which is not higher than the other boreholes along this lineament with 3.5 and 4.8 m³/h. It is concluded that the NE-SW trending structures, which are also assumed to be of very young origin and are best identifiable in satellite imagery, have the highest potential of providing further high yielding boreholes.

The cumulative well yield for all boreholes in the Northern Namibian Kalahari Catchment that are documented in the DWA database gives a figure of 220 Mio m³/a.

4.4 Hydraulic conductivity

Hydraulic conductivity is the usual translation of DARCY'S (1856) "coefficient dependant de la permeabilité de la couch". It is often used as synonym for specific or intrinsic permeability, but in fact the hydraulic conductivity (k_f) is a function of the porous medium and the fluid, whereas permeability (k) is a function of the porous medium. Both parameters are related as:

$$k_f = \frac{k^* p^* g}{\mu} \quad (4.1)$$

With density p , gravity g and dynamic viscosity μ . Permeability is mostly used in the petroleum geology. For the description of the hydraulic properties of an aquifer the term transmissivity (T) is also often used which is the product of hydraulic conductivity and layer thickness.

From the description of the geological units that form the aquifers in the research area it is clear, that all pre-Kalahari units have to be treated as fractured aquifers. The rock permeability is several orders of magnitude smaller than the permeability of ground for these aquifers. The Kalahari lithologies compromise units that act as fractured aquifers and in the less consolidated parts, the aquifer is of a porous nature. Additionally karstification plays an important role for the development of water routings.

4.4.1 Method

Data for the hydraulic conductivity are available from some reports by the DWA, from MAINARDY (1999) and the BGR (1998). Data from single well pumping tests that are available from the DWA have been used with the THEIS recovery method (THEIS, 1935) to obtain additional hydraulic conductivity data. The distribution of the hydraulic conductivity for the Kalahari aquifer was achieved by a complex GIS-based classification.

Analysis of piezometer test data

The piezometer test data that are available from the DWA (Appendix A) can be evaluated by the THEIS recovery method (THEIS, 1935). After turning off of a pump the water level in a borehole rises until it reaches a final recovered level. The rising water level conducts a residual draw-down s'' which is the difference between the initial water level before pumping and the water level at time t'' after turning off of the pump.

The THEIS (1935) assumption is: instationary flow (no equilibrium reached) occurs in a confined homogenous, isotropic aquifer of infinitive extension towards a well with a very small diameter with the water level assumed as almost horizontal. If the observed aquifer fits into this assumption within some natural exaggeration the residual draw-down is given as:

$$s'' = \frac{Q}{4\pi T} \left(\ln \frac{4Tt}{r^2 S} - \ln \frac{4Tt''}{r^2 S''} \right) \quad (4.2)$$

with the residual draw-down s'' , the diameter of the well r , storage coefficient during pumping S and recovery S'' , time since start of pumping t and end of pumping t'' , transmissivity T and the inflow Q . If the storage coefficient during pumping S and recovery S'' is constant and the term

$u = \frac{r^2 S}{4kDt''}$ is very small it writes as:

$$s'' = \frac{2.30Q}{4\pi T} \log \frac{t}{t''} \quad (4.3)$$

Processing the s'' values against t/t'' in a semi-logarithmic scale reveals a best-fit-line with the slope:

$$\Delta s'' = \frac{2.30Q}{4\pi T} \quad (4.4a)$$

which is also expressed by:

$$T = \frac{2.30Q}{4\pi \Delta s''} \quad (4.4b)$$

The graphically obtained values for the transmissivity T need to be divided by the aquifer thickness to receive the hydraulic conductivity.

4.4.2 Hydraulic conductivity for the pre-Kalahari aquifers

Two piezometer test are available for the Omingonde aquifer at farm 340 Ringklip (WW27474) and at farm 304 Otjahewita (W27473). They have been evaluated by the THEIS recovery method (THEIS, 1935) as presented. Results are given in Table 4.4-1 together with literature data. DWA data are based on pumping test evaluation, whereas MAINARDY (1999) used fracturing measurements. The assumed mean hydraulic conductivities result from all observed data and consider that only a small amount of random sample is available and that subjective expert knowledge has to influence the assumed mean value respecting the regional scale.

Table 4.4-1: Summary of available hydraulic conductivity data for the pre-Kalahari units (1) from piezometer test, (2) DWA 1992, (3) DWA 1993a, (4) DWA 1993b, (5) MAINARDY 1999 and (6) BGR (1998). Assumed mean values for the aquifers in a regional scale are underlain in grey

Unit	Borehole-number or lithology	Hydraulic conductivity	Quadrant	Location	Source
Etjo	WW35851	2.1*10 ⁻⁵ m/s	2018		2
	WW35852	2.6*10 ⁻⁵ m/s	2018		2
	WW35853	2.6*10 ⁻⁵ m/s	2018		2
	WW35854	1.9*10 ⁻⁵ m/s	2018		2
	WW35930	3.8*10 ⁻⁶ m/s	2018		2
	WW35932	1.3*10 ⁻⁵ m/s	2018		2
	WW35933	4.4*10 ⁻⁶ m/s	2018		2
	WW35934	7.4*10 ⁻⁵ m/s	2018		2
	WW35935	5.1*10 ⁻⁵ m/s	2018		2

Etjo	WW35936	$7.2 \cdot 10^{-6}$ m/s	2018		2
	WW35937	$6.4 \cdot 10^{-5}$ m/s	1918		2
	WW35938	$5.9 \cdot 10^{-6}$ m/s	1918		2
		$1 \cdot 10^{-6}$ m/s		Waterberg Camp	5
		$1 \cdot 10^{-6}$ m/s		Neudorf	5
		$1 \cdot 10^{-6}$ m/s		Ravenna	5
Basalt		$5 \cdot 10^{-8}$ m/s		Omatako Hills	5
		$1 \cdot 10^{-7}$ m/s		North of Okahandja	5
Assumed hydraulic conductivity for the Etjo aquifers and Rundu Formation in a regional scale: $1 \cdot 10^{-5}$ m/s					
Omingonde	WW27474	$1.6 \cdot 10^{-7}$ m/s	2017		1
	WW27473	$1.1 \cdot 10^{-7}$ m/s	2017		1
		$5 \cdot 10^{-8}$ m/s		Otjikona	5
		$1 \cdot 10^{-7}$ m/s		Otjiahevita	5
		$1 \cdot 10^{-9}$ m/s		Otjiuku	5
		$1 \cdot 10^{-7}$ m/s		Upper Omatako	5
Assumed hydraulic conductivity for Omingonde aquifers in a regional scale: $1 \cdot 10^{-7}$ m/s					
Damara	WW3716	$1.9 \cdot 10^{-6}$ m/s	2120		3
	WW24974	$1.7 \cdot 10^{-5}$ m/s	2120		3
	WW25439	$5.2 \cdot 10^{-6}$ m/s	2120		3
	WW26673	$6.1 \cdot 10^{-6}$ m/s	2120		3
	WW25763	$2 \cdot 10^{-6}$ m/s	2120		3
	WW25762	$3.6 \cdot 10^{-6}$ m/s	2120		3
	WW33554	$7.3 \cdot 10^{-7}$ m/s	2119		4
	WW33858	$5.8 \cdot 10^{-7}$ m/s	2119		4
	Marble	$5 \cdot 10^{-6}$ m/s		Ozondjache	5
	Marble	$5 \cdot 10^{-7}$ m/s		Warlencourt	5
	Marble	$5 \cdot 10^{-8}$ m/s		Jan Helpman	5
	Marble	$5 \cdot 10^{-6}$ m/s		Salzbrunnen	5
	Meta-conglomerate	$1 \cdot 10^{-7}$ m/s		Salzbrunnen	5
	Granite	$5 \cdot 10^{-8}$ m/s		Pinnacles	5
	Granite	$5 \cdot 10^{-7}$ m/s		Hohenfels	5
	Quartzite	$1 \cdot 10^{-6}$ m/s		Okuwiruru	5
	Quartzite	$1 \cdot 10^{-7}$ m/s		Voigtskirch	5
	Quartzite	$5 \cdot 10^{-7}$ m/s		Otjivero-Damm	5
	Quartzite	$1 \cdot 10^{-7}$ m/s		Gobabis	5
	Quartzite	$1 \cdot 10^{-6}$ m/s		Pepperkorel	5
	Pegmatite	$1 \cdot 10^{-6}$ m/s		Swakoprevier	5
Pegmatite	$1 \cdot 10^{-7}$ m/s		North of Okahandja	5	
Granodiorite	$5 \cdot 10^{-8}$ m/s		North of Okahandja	5	
Granodiorite	$1 \cdot 10^{-6}$ m/s		Kalkfeld	5	

Damara	Gneiss	$5 \cdot 10^{-8}$ m/s		Weißer Nossob	5
	Mica schist	$5 \cdot 10^{-8}$ m/s		Herbothos	5
	Mica schist	$5 \cdot 10^{-8}$ m/s		Windhoek	5
	Mica schist	$5 \cdot 10^{-8}$ m/s		Pepperkorel	5
	Amphibolite	$1 \cdot 10^{-8}$ m/s		Groß Okuje	5
	Amphibolite	$1 \cdot 10^{-7}$ m/s		Swakoprevier	5
	aquifers	2.3 to $5.8 \cdot 10^{-6}$ m/s		Otavi mountain region	6
	aquitards	2.7 to $5.8 \cdot 10^{-7}$ m/s		Otavi mountain region	6
	aquicluds	up to $2.3 \cdot 10^{-8}$ m/s		Otavi mountain region	6

**Assumed hydraulic conductivity for the Damara aquifers in a regional scale:
 $1 \cdot 10^{-7}$ m/s in general and $5 \cdot 10^{-6}$ m/s when well fractured or karstified**

4.4.3 Hydraulic conductivity for the Kalahari aquifers

Hydraulic conductivity data for the Kalahari aquifers are available from some reports by the DWA. This data were added up by the results from the evaluation of single well pumping test data by the THEIS recovery method (THEIS, 1935) for available records from the Kavango district (DWA, 1991). A summary of the results is given in Table 4.4-2.

Table 4.4-2: Summary of available hydraulic conductivity data for the Kalahari units (1) from piezometer test, (2) DWA (1996a), (3) DWA (1993c) and (4) DE BEER & BLUME (1985)

Borehole-number	Hydraulic conductivity	Quadrant	Location	Source
WW25902	$1.8 \cdot 10^{-5}$ m/s	2118		2
WW25903	$1.2 \cdot 10^{-5}$ m/s	2118		2
WW25904	$1.2 \cdot 10^{-5}$ m/s	2118		2
2120BB002	$1 \cdot 10^{-7}$ m/s	2120		3
2120BA005	$1 \cdot 10^{-7}$ m/s	2120		3
	4.6 to $5.2 \cdot 10^{-6}$ m/s	2018	NW-Herero	4
1819DD9	$5.3 \cdot 10^{-6}$ m/s	1819	Kavango district	1
1820CB8	$5.9 \cdot 10^{-8}$ m/s	1820	Kavango district	1
1820BC7	$7.1 \cdot 10^{-7}$ m/s	1820	Kavango district	1
1820AC9	$4.2 \cdot 10^{-8}$ m/s	1820	Kavango district	1
1820BC9	$1.5 \cdot 10^{-5}$ m/s	1820	Kavango district	1
1819BA9	$2.6 \cdot 10^{-5}$ m/s	1819	Kavango district	1
1820AA10	$6 \cdot 10^{-8}$ m/s	1820	Kavango district	1

Hydraulic conductivity for the Kalahari units in the research area varies more than three orders of magnitude, ranging from $2.6 \cdot 10^{-5}$ m/s to $4.2 \cdot 10^{-8}$ m/s. This is reflecting the various lithologies described in Chapter 3.1.4, ranging from extraordinary well developed water routing

for the pipe sandstones to red clays in the Kavango district that are not likely to be very conductive. Therefore it seems not meaningful to use a single value to represent the entire Kalahari aquifer.

Regionalisation

A regionalisation of the primary hydraulic conductivity for the Kalahari aquifer has been made by a GIS-based classification. The factors that influence the hydraulic conductivity of the Kalahari aquifer are the distribution of the primary porosity and the development of secondary porosity by fracturing. As the primary porosity of the Kalahari reflects the grain size distribution, the hydraulic conductivity is also a function of the grain size distribution influencing factors: distance from the source area and slope of the pre-Kalahari surface. The sorting and rounding of the sediments increases with the distance from the source area, while the mean grain size decreases. Therefore the closer a deposit is to the source area, the larger primary hydraulic conductivity is expected. As areas with high dip angles received mostly very coarse sediments, but in the gently dipping areas often fine grained materials were deposited, it is assumed that the hydraulic conductivity is also influenced by the slope of the pre-Kalahari surface.

The pre-Kalahari surface is calculated by subtracting the raster image "thickness of the Kalahari" (Fig. 3.2-4) from "recent topography" (Fig. 1.4-2) in IDRISI. The highest slope for every grid cell was calculated from the obtained pre-Kalahari surface using IDRISI.

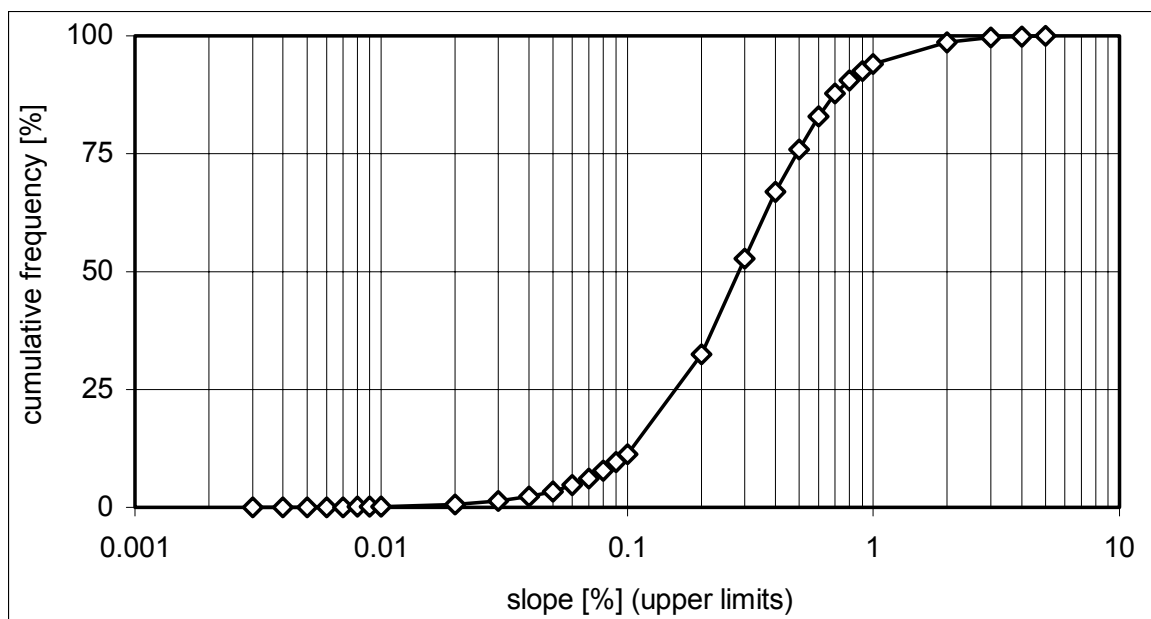


Fig. 4.4-1: Frequency distribution of the slopes of the assumed pre-Kalahari surface (Kalahari thickness distribution subtracted from recent topography).

Calculated slopes range from less than 0.003 % to more than 4 %. The frequency distribution of the resulting slopes is given in Fig. 4.4-1. 95 % of the grid cells show slopes between 0.01 and 1 %. The resulting raster image was classified with slopes less than 0.18 % (which represents 25 % of the area) as class 1 "low hydraulic conductivity expected", slopes from more than 0.18 to 0.5 % (representing 50 % of the area) to class 2 "intermediate hydraulic conductivity expected" and slopes of more than 0.5 % (representing 25 % of the area) to class 3 "higher hydraulic conductivity expected".

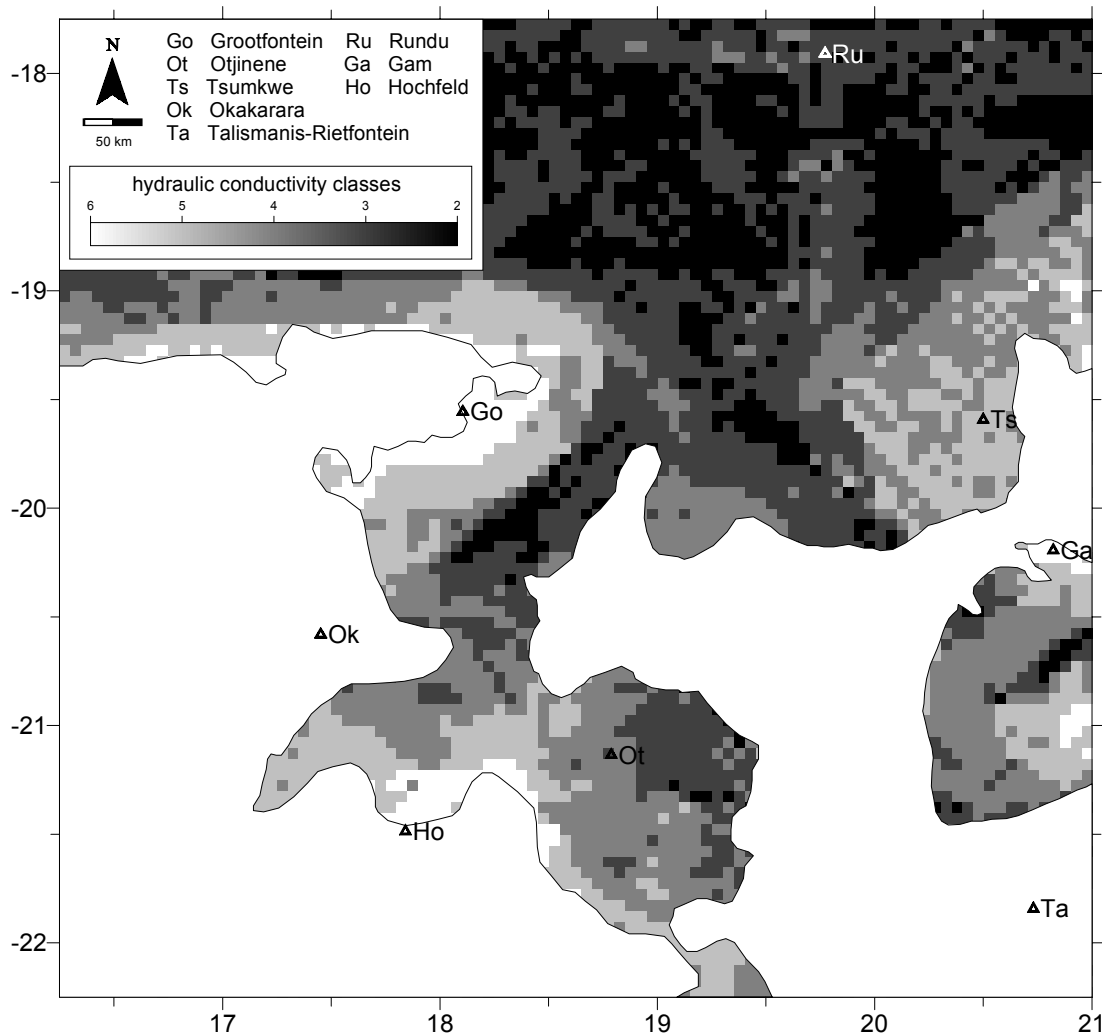


Fig. 4.4-2: Distribution of the expected primary hydraulic conductivity for the Kalahari aquifers in five classes ranging from 2 to 6 (very low to very good) resulting from the parameters "distance to the source area" and "slope of the pre-Kalahari surface" (influencing rounding, sorting and mean grain size).

A classified image of the distance from the source area was obtained by digitising three different features from the palaeo-drainage map (Fig. 3.2-5):

- a) the source areas (assigned to class 3 "higher hydraulic conductivity expected")

- b) a strip in which intermediate sorting and rounding is expected (assigned to class 2 "intermediate hydraulic conductivity expected")
- c) the remaining areas (assigned to class 1 "low hydraulic conductivity is expected").

Both classed raster images were then added and a resulting image was obtained that shows the distribution of the expected primary hydraulic conductivity for the Kalahari aquifer in five classes ranging from 2 to 6 (Fig. 4.4-2).

Besides the primary hydraulic conductivity the secondary conductivity, which is a function of fracturing and karstification, has to be considered for the quantification of the regional hydraulic conductivity. It is somehow reflected by the borehole yield but factors such as the thickness of the aquifer, the primary conductivity and the well performance interfere this phenomenon so that the well yield cannot be used as a classification basis.

Additionally the primary conductivity is drastically influenced by the degree of consolidation and cementation of the aquifer material. From the description in Chapter 3.1.4 it is clear that mostly the outcropping parts are well cemented (that's why they are not yet eroded), e.g. in the Eiseb and Epukiro area, but from many drillings in the northern part of the research area it is reported that the Kalahari sediments are unconsolidated. Fractures of a very young origin are present in the southeastern part of the Kalahari aquifers (named Eiseb-Graben Aquifer by BITTNER, 1999). Therefore higher hydraulic conductivity values, that show higher variations, have been assigned here compared to the northern and western part of the research area. The assumed values are summarised in Table 4.4-3.

Table 4.4-3: Values of hydraulic conductivity k_f that have been assigned to the obtained classes from Fig. 4.4-2 considering that the Eiseb Graben Aquifer received more intensive fracturing and that the hydraulic conductivity in the northern and western part of the research area is dominated by the primary hydraulic conductivity

Class		Assigned hydraulic conductivity	
Value	name	western and northern part of the research area	Eiseb-Graben Aquifer
2	very low k_f expected	$1 \cdot 10^{-7}$ m/s	$1 \cdot 10^{-8}$ m/s
3	low k_f expected	$5 \cdot 10^{-6}$ m/s	$1 \cdot 10^{-7}$ m/s
4	intermediate k_f expected	$1 \cdot 10^{-6}$ m/s	$1 \cdot 10^{-6}$ m/s
5	high k_f expected	$5 \cdot 10^{-5}$ m/s	$1 \cdot 10^{-5}$ m/s
6	very high k_f expected	$1 \cdot 10^{-5}$ m/s	$1 \cdot 10^{-4}$ m/s

4.5 Porosity

Porosity (n) is defined as the ratio of void space per unit volume of porous medium. In natural rocks the porosity is a factor of grain size distribution, grain shape, packing, cementation, dissolution, compaction and fracturing. Effective porosity (n_{eff}) is the ratio of the void space that is available for groundwater flow, thus excluding void spaces used by adhesive and capillary water. The eff. porosity is significant smaller for clayey to silty sediments than for coarser grained material although the total porosity is larger. A further parameter to describe void spaces in an unconfined aquifer is the specific yield. This parameter is defined as the volume of water released from an unit area of the aquifer for an unit decline in the water table. It represents a significant portion of the eff. porosity.

Eff. porosity data for the Kalahari aquifer given in DWA reports range from 0.20 to 0.25. DE BEER & BLUME (1985) assume $n_{eff} = 0.23$ for the Middle Kalahari aquifer. DE VRIES ET AL. (2000) assume a specific yield of 0.15 for Kalahari sand aquifers of Botswana.

For loose dune sand an eff. porosity of 0.345 is given by BROWN & NEWCOMB (1963). With respect to a porosity reduction of up to 0.25 due to mechanic processes during subsidence (MATTHEB & UBELL, 1983) $n_{eff} = 0.259$ is revealed.

WORTHINGTON (1979) gives detailed information for the exploration drilling in Okangema (Fig. 4.5-1). After drilling of 44 m calcrete, red sand becoming coarser and more compact with depth (44 - 75 m below collar) were drilled that showed eff.

porosities of about 0.19. After some 13 m of hard limestone (75 - 88 m below collar) a pink sandstone unit (calcareous sandstone becoming increasingly argillaceous with depth) was drilled for another 167 m. Eff. porosity ranges from 0.19 to 0.30 for these units. From the reviewed data a mean eff. porosity of 0.25 for the Kalahari aquifer at the regional scale is assumed.

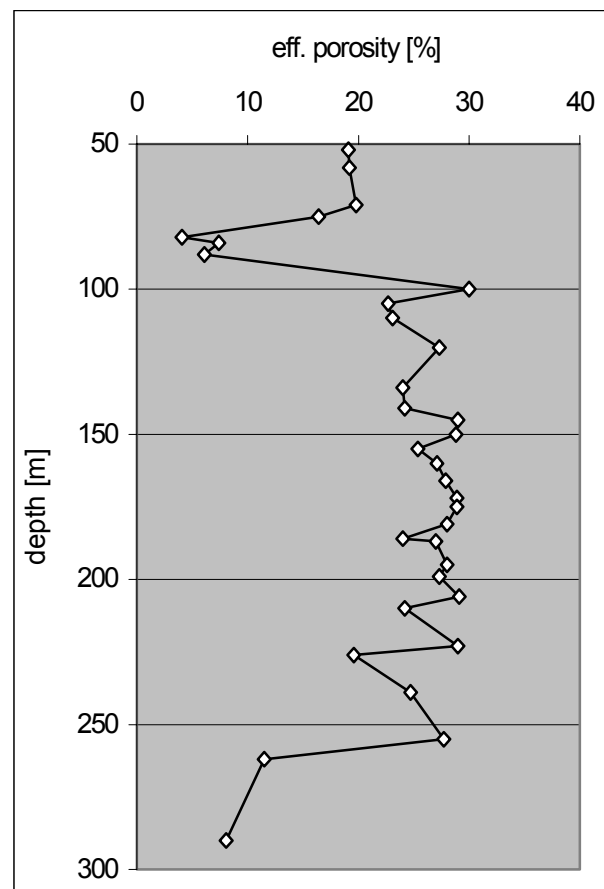


Fig. 4.5-1: Distribution of the effective porosity with depth at the exploration drilling at Okangema. Produced with data from WORTHINGTON (1979).

Eff. porosities for the Etjo sandstone units are given with 0.13 to 0.21 (carbon tetrachloride method) and 0.11 to 0.12 (Darcy's apparatus) by MAINARDY (1999) and total porosity as 0.13 to 0.30. SELAOLO (1998) assumes $n_{eff} = 0.10$ for an aquifer of the Ecca Group (lower Karoo). No further porosity data are available for the aquifers in the research area. Thus data from similar lithologies were reviewed (Table 4.5-1) and eff. porosities for the research area were estimated on this basis. Results are given in Table 4.5-2.

Table 4.5-1: Review of porosities n for lithologies comparable with the aquifers in the research area

n	Lithology	Source
0.05 - 0.30	sandstone aquifers in general	DAVIS & DEWIEST (1998)
0.05 - 0.25	Buntsandstein aquifers in central Europe	PRETSCHOLD (1977)
Up to 0.085	well fractured secondary porosity in Buntsandstein	HIMMELSBACH & WENDLAND (1999)
Up to 0.4	coarse grained Keuper sandstones	RIETZLER (1979) DÜMMER (1982)
Up to 0.05	secondary porosity in sandstones	MATTHEß & UBELL (1983)
Up to 0.05	lavas	MATTHEß & UBELL (1983)
Up to 0.2	contact zone between basalts and sediments	FREEZE & CHERRY (1979)
0.084 - 0.124	pelitic rocks of the Lower Buntsandstein	HATZSCH (1978)
0.096 to 0.268	pelitic rocks of the Zechstein	HATZSCH (1978)
0.133	pelitic rocks of the Rotliegendes	HATZSCH (1978)
0.15 - 0.24	mudstone from Kansas	MANGER (1963)
0.01-0.03	fresh igneous and metamorphic rocks	MATTHEß & UBELL (1983)
Up to 0.5	weathered schist	MATTHEß & UBELL (1983)
Up to 0.25	saprolite in Georgia /USA	STEWART (1962)

Table 4.5-2: Summary of the effective porosities assumed for the aquifers (regional scale) in the research area from reviewed data

Aquifer	effective porosity
Kalahari	0.25
Etjo and Rundu	0.15
Omingonde	0.10
Damara and pre-Damara	0.08
Karstified Damara	0.12

5 Groundwater recharge

In this chapter an introduction to previous recharge research carried out in the Kalahari and the surrounding hardrock areas in southern Africa is presented. It is then followed by the methods and results of this study. The surface properties of the Kalahari (Chapter 5.2) and the recharge influencing climatic factors (Chapter 5.3) are examined and described as they are the basic factors that influence recharge. Hydrographs are interpreted to define precipitation conditions that allow recharge under recent Kalahari conditions in a further chapter (5.4). A water balance model (Chapter 5.5) with daily climatic data is used to define favoured conditions for recharge generation. Point recharge rates are determined by the chloride mass balance method (Chapter 5.6). Recharge has been regionalised by hydrochemical data in an inverse approach (Chapter 5.7) and by the use of satellite images in a forward approach (Chapter 5.8). A final chapter (5.9) summarises the results and compares them with previous results.

5.1 Summary of previous recharge research in the Kalahari

Early studies, such as by PASSARGE (1906), led to the belief that recent climatic conditions in the Kalahari combined with a thick sand cover meant that groundwater recharge is not possible. Later work by FROMMURZE (1953), VAN STRATEN (1954; 1961), BOOCOCK & VAN STRATEN (1961; 1962), MARTIN (1961b), HYDE (1971) and BAILLIEULE (1975) confirmed this view. However MAZOR ET AL. (1974) reported 16 wells in the Kalahari for which tritium data clearly indicate recharge during the past few decades. Pore waters of the central Kweneng area (Botswana) were analysed by FOSTER ET AL. (1982) and these also clearly indicated active recharge by their tritium values. Groundwater recharge has also been identified by groundwater level fluctuation observation in Botswana (MAZOR, 1982). Following research projects have obtained recharge values which are summarised in Table 5.1-1. For the central Kalahari recharge is determined to be less than 0.5 mm/a to 3.8 mm/a and at the Kalahari's fringe it is in the range of 1 to 50 mm/a. The table also contains recharge values from projects in southern Africa outside the Kalahari to compare them with data from similar climatic conditions. By this summary the wide range of recharge values is clearly documented. It indicates that a major task of any new research project must be to focus strongly on recharge distribution within in a large catchment and that point data can only represent regional features in a limited way.

From previous research (e.g. KÜLLS (2000), MAINARDY (1999), SELAULO (1998)) different sources for groundwater recharge in the Kalahari are apparent; such as direct recharge through jointed or karstified hard rocks, recharge along preferred flow path in structured soils or rootlets,

and direct diffuse infiltration through sand cover. Indirect recharge from ephemeral rivers or from ponded water bodies is also identified.

Table 5.1-1: Summary of previous recharge estimations conducted in southern Africa in the Kalahari and hardrock areas

Country	Regional K= Kalahari entirely KF= Kalahari fringe CK=central Kalahari	Method U= unsaturated Zone S = saturated Zone	Mean annual precipitation [mm]	Annual recharge [% of precipitation]	Source
Namibia	KF	Chloride mass balance	270 - 417	0.65 - 4.2	DACHROTH & SONNTAG (1983)
	KF: Karst Aquifer		550	6 - 8	SEEGER (1990)
	KF (unconsolidated substratum)	Chloride mass balance (U) Chloride mass balance (S)	400	0.6 - 1.1 0.3 - 10.3*	WRABEL (1999)
	KF (hardrocks)	Chloride mass balance (U) GW flow model	400 - 500	0.8 - 7 0.6 - 10	MAINARDY (1999)
	CK (Stampriet)	hydrographs	150 - 250	3 -10 (irrigated?)	JICA (2000)
	Entire Namibia			1	HEYNES (1992)
Botswana		Chloride mass balance	550	9.6	DE VRIES & HOYER (1988)
	KF: Pitsanyane Molepolole Kanye	Chloride mass balance and well level fluctuation	561 492 529	2 - 2.9 2 4.7 - 5.7	GIESKE (1992)
	KF	Groundwater flow model	500	3.6	GIESKE (1992)
		Chloride mass balance	450	1.8 - 3.3	VERHAGEN (1995)
	KF Hardrocks		550	2 - 4	KELLER & VON HOYER (1992)
	KF Molepolole	Chloride mass balance (S) Chloride mass balance (U)	492	1.2 1.7 - 2.5	SLOTS & WIJEN (1990)
	KF Kanye	Chloride mass balance (S) Chloride mass balance (U) Water balance	529	4.3 - 6.2 4.2 - 5.9 4.5 - 7	GEHRELS & VAN DER LEE (1990)
	KF, Kanye	Chloride mass balance	529	3.8	BRGM (1988)

* The maximum value is questionable due to an inappropriate use of the chloride mass balance method in the saturated zone without concerning the lateral inflow

Country	Regional K= Kalahari entirely KF= Kalahari fringe CK=central Kalahari	Method U= unsaturated Zone S = saturated Zone	Mean annual precipitation [mm]	Annual recharge [% of precipitation]	Source
Botswana	KF Letlhakeng- Botlhapatlou.	Chloride mass balance (U) Tritium Chloride mass balance (S) GW-flow-model Hydochem.-isotop-model ⁴ He method	350 - 450	0.3 - 2.2 0.4 - 3 0.9 -3.1 0.9 - 1.6 0.3 0.6 - 0.7	SELAOLO (1998)
	CK	Chloride mass balance (U) and Tritium	350 - 400	< 0.25	SELAOLO (1998)
	KF	Chloride mass balance (U) and Tritium	350 - 450	< 1.1	FOSTER ET AL. (1982)
	CK	Chloride mass balance (U) and Tritium	400	0.15 - 0.95	BEEKMAN ET AL. (1996)
	K	GW flow model transect	400 - 550	< 0.1	DE VRIES (1984)
	KF	¹⁴ C exponential model	450	0.7 - 1.8	VERHAGEN (1988)
	KF Ghanzi	Chloride mass balance	400	0.75 - 2	MOROSINI (1996)
Republic of South Africa	Karoo Aquifer	Soil water balance, zero flux methode, soil water flow, GW flow model, isotope techniques	287 - 584	3 - 5	VAN TONDER & KIRCHNER (1990)
	Dolomite	Water balance	346 - 1250	3.2 - 23	BREDEKAMP (1988)
	Fractured aquifer	Chloride mass balance	483	0.6 - 1.7	SAMI & HUGHES (1996)
	Dolomite	¹⁴ C, Tritium		17 mm	BREDEKAMP & VOGEL (1970)
	Dolomite	Tritium		30 mm	BREDEKAMP ET AL. (1974)
Zambia		Water balance	937	8.5 (natural forest) 30 (agriculture)	HOUSTON (1982)
Zimbabwe		Water balance	500	2	HOUSTON (1988)

5.2 Surface properties

Physical properties of the unsaturated zone of the Kalahari catchment influence the recharge distribution besides the meteorological features. The most important physical parameters controlling the water movement in the unsaturated zone are the hydraulic conductivity and the water retention.

For the surface properties a major subdivision has to be made between soft sediments and soils, hardrock outcrops and calcrete. The hardrocks have already been characterised in Chapter 4. Therefore this chapter focus on calcrete and soft sediments to soils. "Soil" as used refers only to the material of the uppermost metres and does not consider any pedogenic process.

During three field trips (Sep to Nov 1999; Apr to May 2000; Nov to Dec 2001) four groups of surface constitutions have been classified and soil samples have been grouped as:

- 1) pan and vlei,
- 2) brown to red soils,
- 3) dune sands and
- 4) soils with an aeolian influence.

The classification has been made according to the topography and occurrence in the field. The four soil classes were tested in field and laboratory experiments. Calcrete cannot be examined with the same physical methods as the other soils due to its non-grainy nature. Therefore it is described from field observation only.

In this chapter the methods that have been used to characterise the soil groups are presented (Chapter 5.2.1) and the description of each group follows with the inclusion of field observations (Chapter 5.2.2). The full soil physical data set is provided in Appendix B. The relevance of the soil groups from the point of view of groundwater recharge development is given with some aspects of the regional distribution (Chapter 5.2.4). The results from infiltration test are of special interest as they represent short-time natural infiltration (Chapter 5.2.3).

5.2.1 Methods

Infiltration test

Infiltration test with a falling head infiltrometer have been conducted during the field trips to all surface classes in order to obtain values of hydraulic conductivity. The model of GREEN & AMPT (1911), modified by MOREL-SEYTOUX & KHANJI (1974) has been used to analyse the infiltration test. It is referred to in this study as the GA-model. The GA-model can be directly developed from Richard's equation. It assumes a piston-like vertical flux and a sharp wetting front of

infinite steepness. In porous media a sharp wetting front develops with the diffusivity as a delta function.

PHILIP (1992) gives an implicit relationship between time and infiltration rate by integration of the GA-model equation with:

$$t = \frac{I}{K_{rw}} - \frac{(H + h_e)(\theta - \theta_i)}{K_{rw}} \ln \left[1 + \frac{I}{(\theta - \theta_i)(H + h_e)} \right] \quad (5.1)$$

The input parameters are depth of ponded water applied during the infiltration test H , the measured parameters time t and cumulative infiltration I . The re-wetted hydraulic conductivity K_{rw} , suction head at the wetting front h_e , and residual water content $(\theta - \theta_i)$ are properties of the soil and can be determined by fitting calculated t and I data to the measured data. Fitting has been done by a trial-and-error procedure.

Soil sampling

About 90 undisturbed soil samples have been collected as core samples in the Kalahari research area to be used for the following laboratory experiments: water content at field situation (for further use to estimate recharge rates by chloride mass balance method as presented in Chapter 5.6), estimation of porosity (= water content at saturation), and estimation of the hydraulic conductivity by falling head permeameter. The cores have been covered with plastic lids and wrapped with adhesive tape to avoid moisture loss or uptake. The wrapped samples have been weighed directly in the field to allow correction of possible moisture content changes. In addition, for every core sample, a corresponding disturbed samples has been collected for analysing the grain size distribution and the ignition loss.

Estimation of hydraulic conductivity with falling head permeameter

After fully saturating the core samples, they have been tested for hydraulic conductivity using a falling head permeameter (for detailed description see HABETHA, 1969). Core samples have therefore been covered at the ends either with filter paper and plastic sieve lids or water inlet. 5 to 10 permeameter tests have been conducted to each sample. In this test a hydraulic head, measured in a plastic tube of diameter a , is allowed to fall from Δp_0 to Δp_t during time t with the soil core having a diameter A and a length L . The hydraulic conductivity k_f is then given as:

$$k_f = \frac{a * L}{A * t} \ln \left(\frac{\Delta p_0}{\Delta p_t} \right) \quad (5.2)$$

Equation (5.2) can be derived from the simple boundary-value problem that describes one-dimensional transient flow across the soil sample (TODD, 1959).

Water content at saturation and at field situation

Water content at field situation θ_F (not to be mistaken for field capacity!) and at saturation θ_S have been determined gravitatively. Therefore undisturbed core samples have been dried at 105 °C until weight constancy was achieved. After weighing them, the dry samples have been saturated in a water bath while slowly raising the water level to allow air to escape. Samples were left in the water bath for up to 5 days in order to allow full saturation.

Water content at field situation θ_F and at saturation θ_S was calculated from mass of field-wet sample M_F , mass of dry sample M_D , mass of saturated sample M_S , d_w density of the water and the volume of the saturated sample V_S as:

$$\theta_F = \frac{(M_F - M_D)}{V_S * d_w} \quad (5.3)$$

$$\theta_S = \frac{(M_S - M_D)}{V_S * d_w} \quad (5.4)$$

Grain size analyses

Grain size distribution has been analysed by dry sieving samples of 100 - 200 g that have been dried at 105° until weight constancy was achieved. Sieves with mesh sizes of 2 mm, 1 mm, 0.63 mm, 0.4 mm, 0.2 mm, 0.1 mm and 0.063 mm have been used with a sieving time of 15 min. The characterising values d_{10} (grain diameter at 10 % cumulative sieve passage), d_{60} (grain diameter at 60 % cumulative sieve passage) and u (non-uniformity) have been read off the resulting grain size distribution curve. Non-uniformity u is given as:

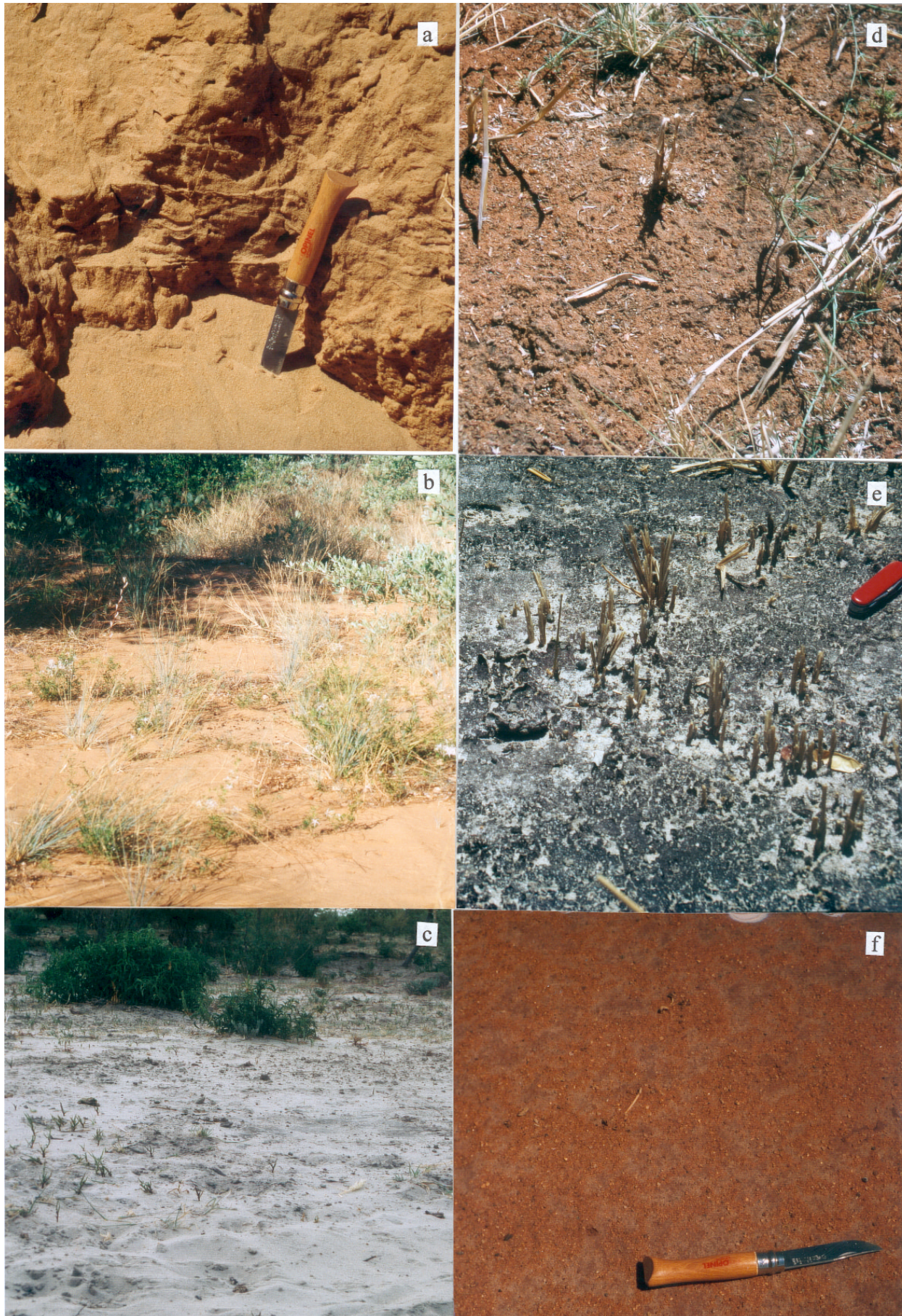
$$u = \frac{d_{60}}{d_{10}} \quad (5.5)$$

Grain size nomenclature in this thesis follows DIN 18 123 (1996) with max. grain diameter for clay is 0.002 mm, for silt it is 0.063 mm and for sand it is 2 mm.

Ignition loss

Ignition loss has been determined by glowing dry (dried at 105° until weight constancy) and ground (1 minute in a porcelain mortar) soil samples of 5 to 20 g (according to the expected carbon content from soil colour) at 500 °C for 2 hours. They have been allowed to cool in a desiccator and weighed. Ignition loss has been determined by weighing cups, dry samples and glowed samples and calculating the weight difference.

Fig. 5.2-1



5.2.2 Resulting description of the four soil groups and calcrete

Vleis and pans

Vleis and pans are found throughout the research area. South of Tsumkwe pans occur in a half moon shaped pan field. They are also often arranged along flood courses of ephemeral rivers or they form in small depressions in flat areas. 16 samples representing the group of vleis and pans have been taken in the field. In general all these samples showed large shrinkage cracks and display dark brown, dark grey or black colours in the field.

The mean hydraulic conductivity is $k_f = 3.76 \cdot 10^{-6}$ m/s (permeameter) with a standard deviation of $2.82 \cdot 10^{-6}$ m/s. The largest standard deviation for a single sample for the hydraulic conductivity was observed for the two samples (4-a and 5-a) which show the largest shrinkage cracks. The results of other laboratory experiments are given in Table 5.2-1. All samples show an ignition loss higher than 1.3 % and up to 8 %. The highest observed fine grain fraction (< 0.063 mm) is 16 %.

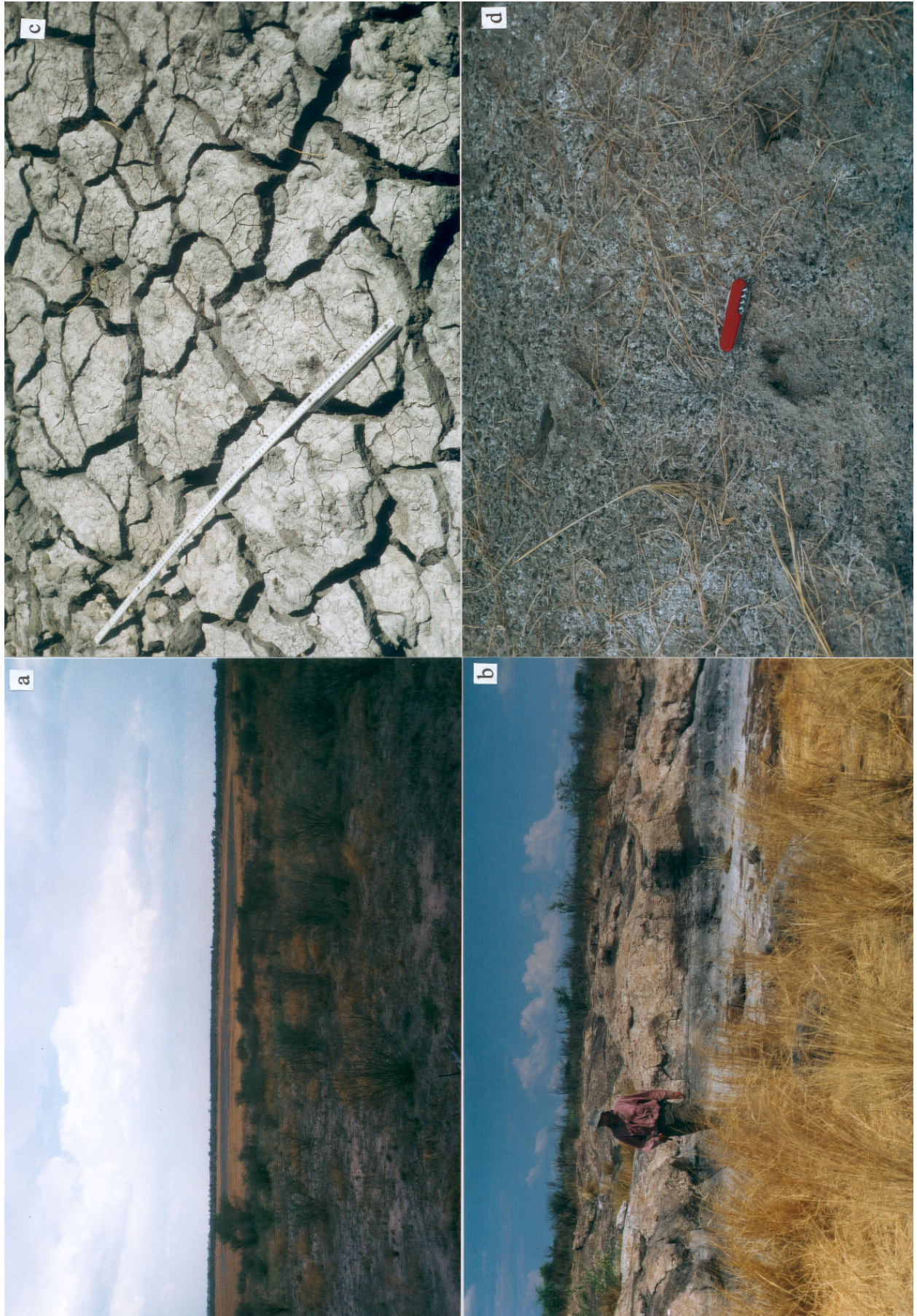
Table 5.2-1: Summary of the soil physical properties of the group vleis and pans (16 samples)

	k_f [m/s]	d_{10}	d_{60}	u	$< 63 \mu\text{m}$ fraction [%]	ign. loss	θ_s	k_{rw} [m/s]
Mean	$3.76 \cdot 10^{-6}$	0.089	0.34	3.91	6.03	4.24	0.58	$4.62 \cdot 10^{-5}$
Standard deviation	$2.82 \cdot 10^{-6}$	0.024	0.16	1.36	4.38	2.41	0.13	$2.88 \cdot 10^{-5}$

The observed values from laboratory experiments for ignition loss, θ_s and fine grain fraction correspond well with the idea of pan sediments being influenced by surface runoff that brings into these depressions organic material and water transported clay and silt material washed out

◀ **Fig. 5.2-1:** Photo documentation of the surface classes in the research area. **a)** Dune sand east of Tsumkwe. The fine grained, well sorted, red aeolian sands display sedimentary structures while they are very dry before the rainy season starts. **b)** Dune sand between the Omiramba Eiseb and Otjozondjou. The red dunes are no longer active as they are covered by vegetation. **c)** Aeolian sand in an interdune at the Namibia-Botswana-border. The light greyish coloured sands have similar grain size distribution as the red variety but the surface of the grains is not covered by iron oxide. **d)** Dark red soil in the vicinity of Steinhausen. These soils are sometimes densely packed and the development of aggregates was observed. Thin surface crusts develop from fine grain fraction and organic material. Micro-organisms produce additional crusting. **e)** Pan surface at the Kano Vlei, Omuramba Omatako. Surface crusts of mainly organic material develop in pans where surface runoff containing washout from the surrounding soils accumulates. Slow settling of the fine grain fraction from a ponded water body allows a normally graded sorting with the fine clay fraction on top. Shrinking clay particles produce rolling up clay-curls. **f)** Red soil near the Makuri Vlei, east of Tsumkwe. A fairly fine grained sandy soil is thinly covered by coarse sands (weathering produces of paragneisses from the Grootfontein Complex).

Fig. 5.2-2



from the surrounding soils. This material was frequently observed to form thin, dark grey to black crusts (Fig. 5.2-1e).

The desiccation cracks that have been observed in the field (Fig. 5.2-2c) represent a network of macro pores which allow fast infiltration along these preferred flow paths. Shrinkage cracks occur in different dimensions ranging from small ratios of mm to 4 cm. Large fissures were observed to be open to depths of more than 30 cm.

It was often observed that pans contain a remarkable thickness of calcrete. Halite was only found as very small local occurrences in the pan Klein Dobe (Fig. 5.2-2d), and nowhere in the research areas were salt crusts identified. Proper salt crusts would indicate evaporation of groundwater and pans would then act as groundwater discharge zones. Proper salt crusts would not develop if water from surface runoff only is evaporated at the pans, due to seasonal flushing and transport into the saturated zone.

Some pans in the pan field around Tsumkwe were seen to keep filled with water after a good rainy season until the next rainy season starts, e.g. Gura Pan was still partly filled in Nov 2000 from the previous rainy season. Water marks up to 50 cm high were observed at the beach of the Gautscha Pan (Fig. 5.2-2b).

Red to brown soils

The red to brown soils have been observed to cover large parts of the Steinhausen (Fig. 5.2-1d), Hochfeld and Otjasondu area. Examples have also been found south of Tsumkwe where they are associated with weathering products of paragneisses of the Grootfontein Complex (Fig. 5.2-1f). These soils show dense packing and single grains are often sticking together; in few locations they build small aggregates. 10 core samples were taken to represent this group. Results of field and laboratory experiments are given in Table 5.2-2. Mean hydraulic conductivity $k_f = 1.32 \cdot 10^{-5}$ m/s with a standard deviation of $1.25 \cdot 10^{-5}$ m/s. An extraordinary low hydraulic conductivity was observed for a sample from the vicinity of Otjasondu (34-a) with

◀ **Fig. 5.2-2:** Photo documentation of pans in the research area. **a)** Dobe Pan north of Tsumkwe. The pan is situated in a small depression in a fairly flat area. Beaches of the pan are gently sloping. Most of the larger pans are surrounded by large trees and green vegetation while the pan itself is unvegetated and only grass occurs at the slopes and beach. **b)** Northern bank of the Gautscha Pan south of Tsumkwe. Pondered water has left marks implying water high stand of more than 0.5 m. In Nov 2000 some surface water was still left over from the rainy season 1999/2000. **c)** Pan surface near Summerdown. Large shrinkage cracks have developed here. The top opening widths are up to 4 cm. **d)** Pan surface at Klein Dobe. Some local occurrences of salt secretion have been observed here. The salt originates from the evaporation of precipitation and the surface runoff that accumulated in this depression.

$k_f = 9.7 \cdot 10^{-8}$ m/s. This sample represents the densest and stickiest example for this group and it has a well developed surface crust. Those crusts have been found to be a product of ponded water where the fine grain fraction is gradually settling and occasional organic mats develop (Fig. 5.2-1d). These crusts swelled when wetted in the laboratory and in the field. Swelling of surface crusts decreases hydraulic conductivity. It was observed in the field that surface runoff developed here while no runoff occurred under similar conditions only a few metres away where no crusts were observed. The crusts are not very stable against mechanical deformation, e.g. cow steps, but rain of low intensity (simulated by a water can with a finely perforated rose) does not infect the stability. It was also observed for this soil group that rootlets of grass increase hydraulic conductivity (infiltration tests at farm 252 Sturmfeld: $k_{rw} = 4.6 \cdot 10^{-5}$ m/s without grass, $k_{rw} = 9.2 \cdot 10^{-5}$ m/s with rootlets).

Table 5.2-2: Summary of the soil physical properties of the group red to brown soils (10 samples)

	k_f [m/s]	d_{10}	d_{60}	u	< 63 μm fraction [%]	ign. loss	θ_s	k_{rw} [m/s]
Mean	$1.32 \cdot 10^{-5}$	0.083	0.32	3.87	5.76	1.66	0.50	$1.02 \cdot 10^{-4}$
Standard deviation	$1.25 \cdot 10^{-5}$	0.009	0.08	1.09	1.51	0.36	0.07	$6.26 \cdot 10^{-5}$

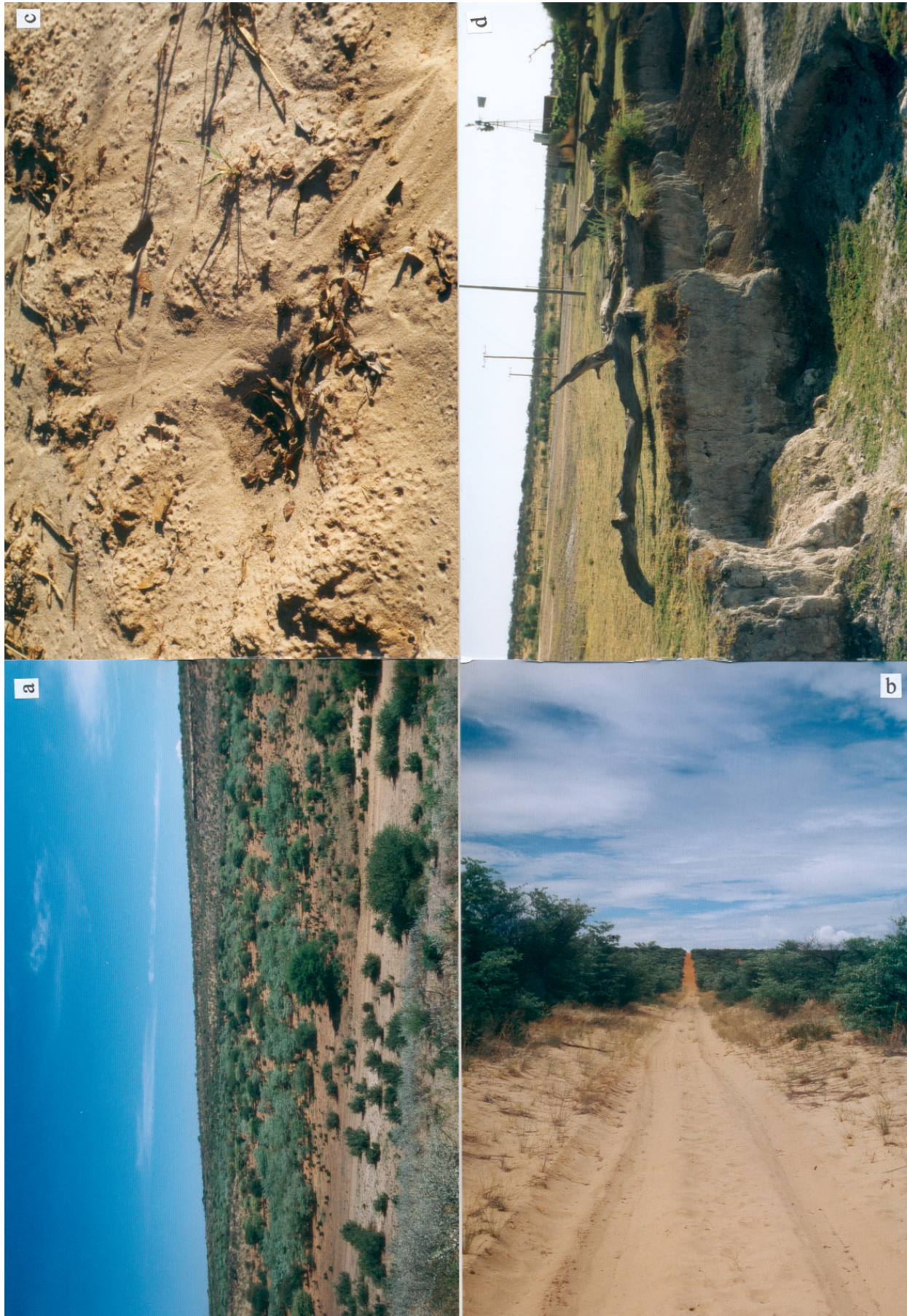
Brownish soils with aeolian influence

The brownish soils with aeolian influence, mostly only a few centimetres in thickness, have been found in the field as soils in flat areas with a component of wind-blown sand. Results of field and laboratory tests are given in Table 5.2-3. This group shows a hydraulic conductivity lower than the aeolian unit and higher than the soil unit with mean $k_f = 3.53 \cdot 10^{-5}$ m/s and a standard deviation of $2.29 \cdot 10^{-5}$ m/s. The high absolute standard deviation might arise from the variable composition of samples in this group as it includes samples with only very little aeolian input and samples with significant proportions of aeolian material. But a further subdivision of the 45 samples for this group was not possible because there is a continuum of compositional variations. The fine grain fraction and the ignition loss is low, and the value for saturated porosity $\theta_s = 0.46$ lies between the range given by the group of aeolian sand and by the red to brown soils.

Table 5.2-3: Summary of soil physical properties of the group brownish soils with influence of aeolian sand (45 samples)

	k_f [m/s]	d_{10}	d_{60}	u	< 63 μm fraction [%]	ign. loss	θ_s	k_{rw} [m/s]
Mean	$3.53 \cdot 10^{-5}$	0.102	0.30	3.03	3.33	1.26	0.46	$1.78 \cdot 10^{-4}$
Standard deviation	$2.29 \cdot 10^{-5}$	0.016	0.06	0.62	1.86	0.66	0.09	$9.86 \cdot 10^{-5}$

Fig. 5.2-3



Aeolian sands

Aeolian sands cover a large part of the Kalahari catchment and are well developed in the eastern part of the research area. These sands have mostly accumulated in longitudinal dunes (Fig. 5.2-3b) which are no longer active. Only due to overgrazing some dune tops are reactivated, especially in the vicinity of Gam. Very few occurrences of aeolian sands have been recognised in flat areas. Dunes of the red sand were also found in the Omiramba Eiseb and Epukiro where they block the flood course (Fig. 5.2-3a).

Flooding marks (Fig. 5.2-3c) have been observed on dunes after a rainfall which also left drop marks. The very round drop marks with a sharp perimeter document a rain event with drops of low intensity (WASMUND, 1930) falling vertically (REINECK & SINGH, 1980; REINECK, 1984) on an already wetted sand (REINECK, 1956).

The aeolian sands of the Kalahari mostly display beautiful red colours when forming dunes (Fig. 5.2-1a and 5.2-1b). Only very rarely do they show very light colours of greyish-orange. Sand of the interdunes mostly has greyish-white colours (Fig. 5.2-1c). The red colour of the aeolian sand is caused by thin covers of red dust (iron oxide) on the grain surfaces. In some cases this iron oxide sticks the grains together to form small clusters. Less than 0.1 % of dark minerals have been found in the red and the white samples. The matrix consists nearly exclusively of quartz which shows many percussion marks.

22 samples of this soil group have been examined in the laboratory. They are well sorted with a mean non-uniformity of 2.62 and a standard deviation of 0.4. Ignition loss is fairly low (Table 5.2-4) and water content at saturation shows a typical value for well sorted sand with a mean value of $\theta_s = 0.42$ and a standard deviation of 0.07.

It was observed on farm 511 Aurora (Fig. 5.2-3b) that the white sand in the interdunes has a slightly higher hydraulic conductivity ($k_{rw} = 3.3 \cdot 10^{-4}$ m/s) than the red variety at the dune tops ($k_{rw} = 3.1 \cdot 10^{-4}$ m/s). Sometimes the inter-dunes showed a slightly higher ignition loss and poorer sorting, but these differences are not statistically significant.

◀ **Fig. 5.2-3:** Photo documentation of the aeolian sands and calcrete. **a)** A small dune of red sand was found in the Omuramba Epukiro where it blocks the flood course. **b)** Red and white aeolian sands on farm 511 Aurora. While red sands form longitudinal dunes that are now stabilised by dense vegetation, the white variety dominates in the interdunes. The hydraulic conductivity was found to be slightly lower for the red variety. **c)** Pale red sand on a dune at the Namibia-Botswana border (real picture size is approximately 20 * 30 cm). Runoff generation was documented here. Rainfall has also left drop marks on the surface. **d)** Occurrence of calcrete at the Epukiro Mission Station. Calcrete is often observed to underlie the river bed of the Omuramba Epukiro. The flood course has eroded some of the calcrete that now displays a thick outcrop of calcrete with many cracks.

Table 5.2-4: Summary of soil physical properties of the group aeolian sand (22 samples)

	k_f [m/s]	d_{10}	d_{60}	u	< 63 μm fraction [%]	ign. loss	θ_s	k_{rw} [m/s]
Mean	$5.30 \cdot 10^{-5}$	0.111	0.29	2.62	2.09	0.78	0.42	$2.63 \cdot 10^{-4}$
Standard deviation	$3.17 \cdot 10^{-5}$	0.014	0.05	0.40	0.93	0.23	0.07	$1.71 \cdot 10^{-4}$

Calcrete

Occurrences of calcrete with light grey to white or cream colours have been found throughout the research area. It occurs in variable thickness ranging from a few centimeters to several metres. Calcrete can be either hard and massive or of a softer and porous nature. It contains a variable amount of mostly sandy to rarely conglomeratic clastic material that is lime-cemented. Cracks of preferred vertical orientation were often observed. Calcrete very often underlies pans or is associated with flood courses where the river sometimes eroded its bed into massive calcrete (Fig. 5.2-3d). Very thick occurrences of calcrete were found in the Omatako Valley between Maroelaboom and Tsumkwe. These occurrences are associated with karstification, e.g. small caves. Calcrete has also been observed to underlay all types of soil cover. Calcretes that have developed in pans are found to contain creatures (often gastropods) or flash flood sediments. On farm 252 Sturmfeld a calcrete occurrence associated with a remarkable amount of bones and teeth was observed. At this location several generations of calcrete development and erosion were exposed. This calcrete occurrence was associated with a spring in historical times. In the Eiseb Block calcrete was observed forming small, flat ridges for which an association with the young fault system is assumed (Chapter 3.3).

5.2.3 Discussion of the results from infiltration tests

The values for hydraulic conductivity that have been obtained by infiltration test interpretation with the GA-model differ significantly from the laboratory results. All soil types show higher hydraulic conductivity in the field tests than in the laboratory tests (Fig. 5.2-4). This contradicts the assumption that fully saturated soil reach the highest hydraulic conductivity because of to the saturation of large pores only near saturation (HARTGE & HORN, 1991). This classical assumption does not respect two reported behaviours of soils:

- 1) Natural structured soils display bimodal pore size distribution which causes preferred flow in shrinkage cracks and rootlets in the partly wetted soils (DURNER & FLÜHLER, 1993).
- 2) Dynamic disequilibria occurs during infiltration (STONESTROM & AKSTIN, 1994).

When a natural soil is wetted in an infiltration test, the water first wets the preferred flow paths. The surrounding soil will be wetted at any later time. If a soil is slowly wetted in the laboratory

test, first of all the smallest pores will be saturated. The large pores will only fill up if the matrix potential pF is approaching 0 (saturation in classical assumption, e.g. VAN GENUCHTEN, 1980; BROOKS & COREY, 1964). If the laboratory soil is wetted, the entire fine grain matrix shows swelling by take up of water in the clay-interlayers (CHAMLEY, 1989). This increases the ratio of medium size pores which is accompanied by decreasing hydraulic conductivity (ZAUSIG & HORN, 1992). In the field experiment such swelling is not induced and therefore large pores are not transformed into medium size pores. The soil in the preferred flow paths in the field experiment is thus looser packed than the soil in the laboratory experiment. Lower bulk density allows faster hydraulic conductivity (HARTGE & HORN, 1991). Therefore it is concluded that the higher hydraulic conductivity of the field experiment is caused by a flow along looser packed preferred flow paths.

If natural infiltration occurs due to a ponded water body, the very short-time infiltration could be represented by k_{rw} (rewetted hydraulic conductivity in the infiltration test). But after some time full saturation occurs inducing swelling and transforming k_{rw} into k_f (saturated hydraulic conductivity from the laboratory tests). Therefore k_f is assumed to represent long time infiltration. The preferred flow path hydraulic conductivity k_{rw} can nevertheless show that under natural circumstances infiltration (eventually becoming groundwater recharge) might occur faster than long time saturated hydraulic conductivity predicts.

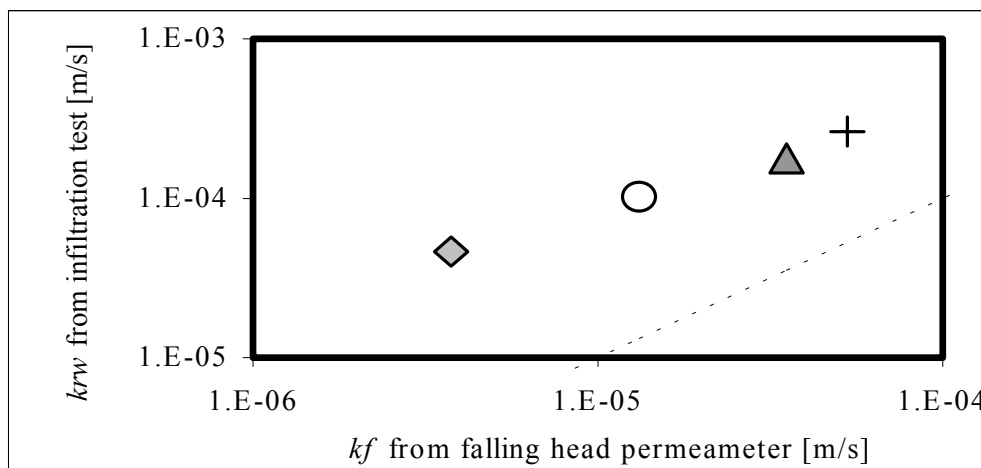


Fig. 5.2-4: Relationship of k_f values from falling head permeameter and k_{rw} from infiltration test for the 4 soil classes: pans and vlees (\diamond), red and brown soils (o), soils with aeolian influence (Δ) and aeolian sands (+). The dotted line indicates the function $k_f = k_{rw}$.

One might question at this point if the infiltration tests in the field might have had some experimental mistakes such as water loss during infiltration or preferred flow path along the core fringe. But as the discrepancy has been observed prior to the third field trip, every experiment

during this third field trip was always checked very carefully for water loss and ring like infiltration structures, neither of which occurred. Therefore malfunctioning of the infiltration tests is excluded.

Although the hydraulic conductivity from the two methods differ, they show the same trends with the hydraulic conductivity being lowest for pans and vleis and highest for aeolian sand. Red to brown soils and brownish soils with aeolian influence are situated in between (Fig. 5.2-4).

5.2.4 Interpretation of recharge properties for surface groups and their regional aspects

The hydraulic conductivity data indicate that the aeolian sand probably allows the largest amount of direct recharge. Pans are not likely to permit a large amount of direct deep percolation because their hydraulic conductivity is relatively low, and decreased even further by swelling surface crusts. Detailed calculation for direct recharge are presented in Chapter 5.5.

Pans (e.g. Klein Dobe, Fig. 5.2-2a) do, however, seem to be a major source for indirect groundwater recharge as surface runoff and interflow is collected here. A seasonal water body allows infiltration and prohibits evaporation from the groundwater and soil water as it is then covered by the water body.

Assuming the mean hydraulic conductivity for pans given in Table 5.2-1, a ponded water body could allow an infiltration depth of 90 cm/month (assuming a hydraulic gradient of 1 and that

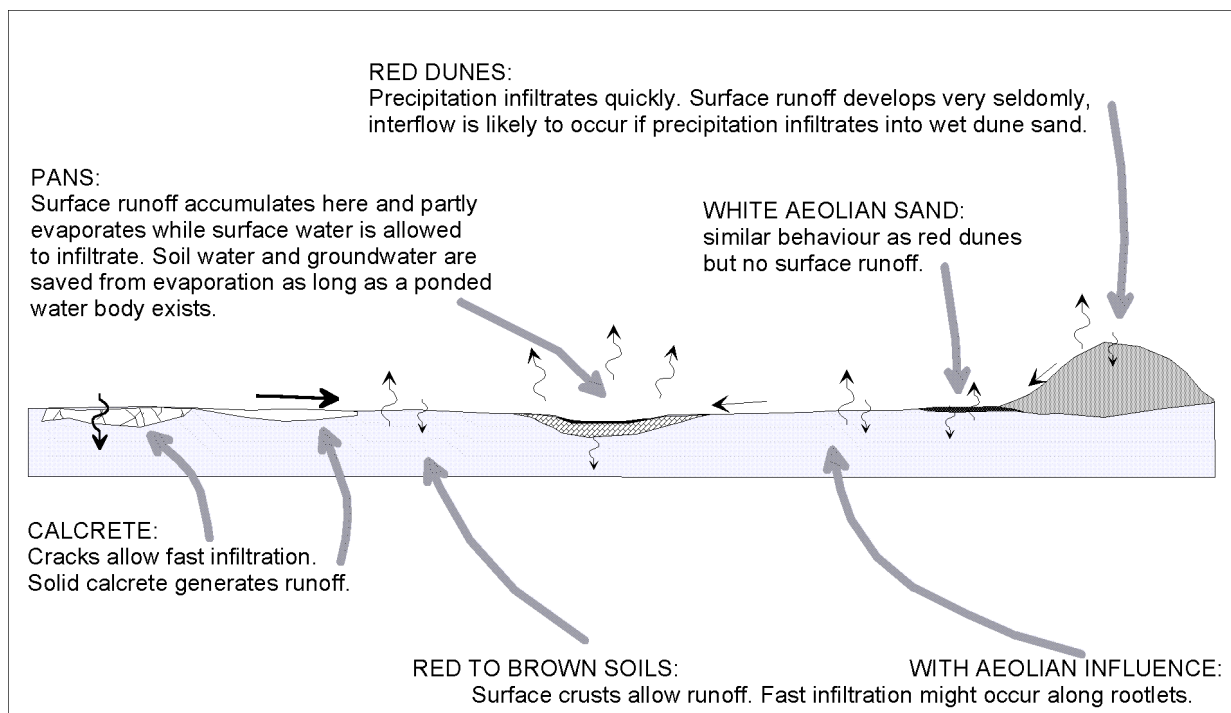


Fig. 5.2-5: Summary of the water infiltration conditions for each of the four soil classes and calcrete. A situation comparable to this schematic profile has been observed at farm 947 Blystroom.

saturation is reached and that swelling of organic crusts decreases the hydraulic conductivity by one order of magnitude) which is equal to a ponded high of 0.52 m (with $\theta_s = 0.58$). With this simplified assumption it appears likely that infiltration from a ponded water body in the pan field allows to arrive at depth of 2 m during the rainy season. From there groundwater recharge probably occurs as evaporation is very significantly lower at depth exceeding 2 m (GIESKE, 1992). Consequently it appears that groundwater recharge is very likely to occur associated with the large pans in the Tsumkwe pan-fields. Transpiration is negligible here at depths more than 0.5 m as only grass vegetation occurs in the pans (Fig. 5.2-2a). Marks of ponded water bodies were observed at Gura Pan, Gautscha Pan, Klein Dobe, Dobe Pan and have been reported by the Nature Conservation Department in Tsumkwe for the Nyae-Nyae Pan. High stands of the ponded water body at Gautscha Pan was 0.5 m at the beach and at least 1.5 m in the central part. Observations in the Gura Pan indicate a ponded high locally of up to 2 m.

The other three soil groups are not very promising for indirect groundwater recharge under average climatic conditions. But since even the aeolian sand group shows evidence (very locally) for surface runoff, all groups are likely to contribute indirectly to the recharge in pans. A synoptic picture is presented in Fig. 5.2-5.

If calcrete occurs at the surface in a rather massive form and has only very few cracks, it is likely to allow only a limited amount of infiltration and surface runoff might there develop. Calcrete with many cracks is likely to allow fast infiltration along the open flow paths thus provided. If calcrete occurs underneath a soil cover, it mechanically prevents roots from transpiring soil water. Karstification of calcrete develops preferred flow path. Karstification processes in deeper parts of the hydrological system might induce some sinking in the overlaying profile, which is associated with mechanically induced small scale shear zones and preferred flow path development.

Occurrences of calcrete likely to facilitate groundwater recharge have been observed during the field trips in the upper Epukiro catchment, the Otavi foreland, the area between Grootfontein and Otjituuo, parts of the Hochfeld-Summerdown-Otjinene-area and locally the eastern part of the Eiseb Block.

5.3 Climatic data

Precipitation and evaporation are the climatic factor influencing the timing, amount and distribution of recharge. Their influence is basically described in the areal water balance equation (see eq. 1.1, page 6).

Precipitation occurs in the study area almost exclusively in the form of rainfall and in this thesis both terms are used synonymously, as well as rain amount.

Evaporation is defined as the rate of liquid water transformation to vapour from open water bodies or soil. The potential evaporation is the maximum evaporation at the given meteorological conditions whereas the actual evaporation is limited by the momentary water supply. Significant differences might occur between measured maximum evaporation (pan evaporation) at meteorological stations (*Oasis effect*, e.g. MAIDMENT, 1993) and the potential evaporation, and thus both words are not used synonymously here. The process of transformation from liquid water into vapour by plants is called transpiration. Often both processes are treated in a combined form as the evapotranspiration.

5.3.1 Rain amount

While, for a more general approach, annual time series of precipitation are required, e.g. in humid catchment, water balance models for arid areas rely strongly on daily data. Daily data are also the minimum demand for a study of rain intensities which strongly influences runoff generation and thus recharge amount. From this background it was concluded that a study of different time series of precipitation (annual, monthly and daily) is the basic demand for an understanding of recharge development in the study area.

Further more, daily rain data are required as input data for a soil water balance model (Chapter 5.5), monthly data are required for the interpretation of hydrographs which are recorded once per month (Chapter 5.4) and annual data are required for recharge estimation by chloride mass balance method in unsaturated (Chapter 5.6.2) and saturated (Chapter 5.6.3) zone.

Daily rain data for 36 stations, and monthly rain data for 162 stations, in the area of interest were provide by the DWA.

Annual data: selected examples

Five stations, Rundu, Tsumkwe, Maroelaboom, Epukiro and Hochfeld, were selected to illustrate the variability of annual precipitation (Fig. 5.3-1). For these graphs some data had to be excluded as an unknown part of the precipitation has been lost. For Rundu the data from 1937 until 1997 are reliable with a mean annual precipitation of 572 mm/a and a standard deviation of 180 mm/a. For Tsumkwe data are available from 1963 until 1998, 1974 had to be excluded, mean is 416 mm/a with a standard deviation of 196 mm/a. Maroelaboom reported rain data from 1931 until 1994 but seven years had to be excluded due to missing data. Mean for Maroelaboom is 452 mm/A with a standard deviation of 205 mm/a. The two station further in the south Hochfeld

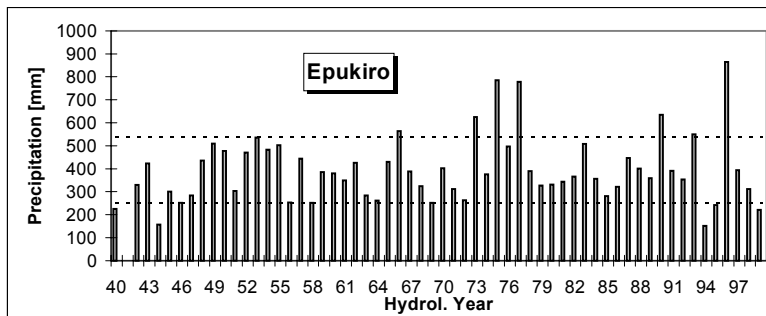
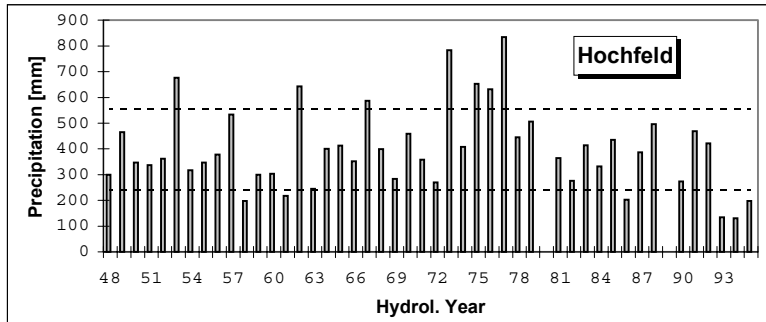
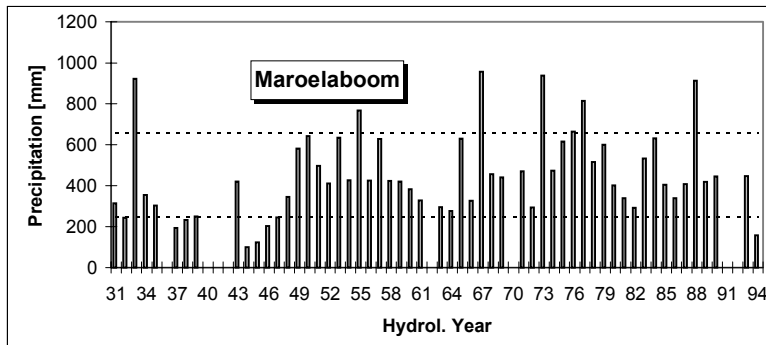
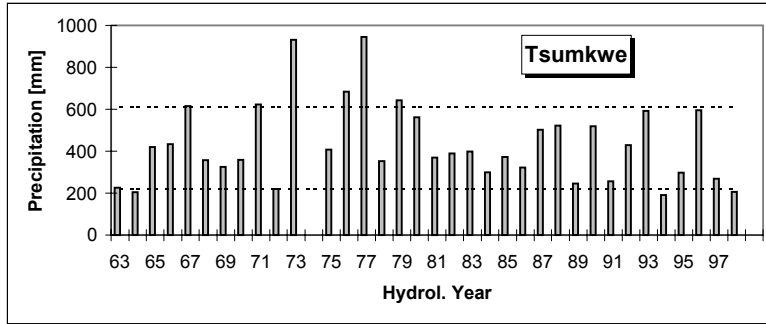
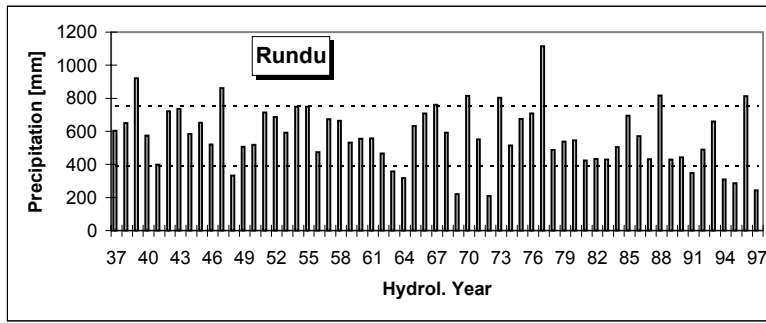


Fig. 5.3-1: Annual precipitation for 5 stations of the research area. Hydrological years are taken from 1st Oct of the given year to 30th Sep of the following year. Mean plus one standard deviation and mean minus one standard deviation are indicated by dotted lines.

and Epukiro receive less precipitation with a mean of 398 mm/a for Hochfeld and 394 mm/a for Epukiro and standard deviations are 158 mm/a and 144 mm/a, respectively.

Table 5.3-1: Transferability of extraordinary rain seasons for 5 rain stations of the research area. Events that are transferable over the entire catchment are shaded grey

Rain station	<u>Rundu</u>	<u>Tsumkwe</u>	<u>Maroelaboom</u>	<u>Hochfeld</u>	<u>Epukiro</u>
Year					
1963/64	EL	L	L	L	L
1964/65	EL	EL	L	M	L
1966/67	H	M	H	L	EH
1967/68	EH	H	EH	EH	M
1969/70	EL	L	M	L	L
1970/71	EH	L	No rep.	H	M
1971/72	M	EH	M	L	L
1972/73	EL	L	L	L	L
1973/74	EH	EH	EH	EH	EH
1975/76	H	M	H	EH	EH
1976/77	H	EH	EH	EH	H
1977/78	EH	EH	EH	EH	EH
1979/80	L	EH	H	H	L
1986/87	M	L	L	EL	L
1988/89	EH	H	EH	H	M
1990/91	L	H	M	L	EH
1991/92	EL	L	No rep.	H	M
1993/94	H	H	M	EL	EH
1994/95	EL	EL	EL	EL	EL

Legend: EH = extraordinary high; EL = extraordinary low; L = lower than mean; H = higher than mean; M = approximately mean; No rep. = no reliable data are available

For the five presented rain stations 11 to 15 % of the reported rainy seasons indicate extraordinarily high rain amounts (higher than mean plus one standard deviation) and during 9 to 15 % of the reported years the stations received extraordinary low rain amounts (less than mean minus one standard deviation).

All raingraphs document the 1970's as a wet period in general. Fig. 5.3-1 and Table 5.2-1 also show that rain data from one location are not readily transferred to the others. For only 3 out of 19 years is the extraordinary rain situation similar for all five stations. For example 1996, was an extraordinarily wet year for Epukiro and Rundu, but Tsumkwe which lies between those two locations received an extraordinarily low rain amount (for location see Fig. 5.3-2).

Mean annual precipitation

For the distribution of mean annual precipitation within the catchment it is necessary to first extract data from the database that satisfy the demand of reliability and a minimum of 15 years needs to be reported for statistical purposes. 126 rain stations have been selected from the 162 rain stations of the study area. The lowest reported rainy season occurred at Otjozonjati in

1941/42 with 30 mm. The highest annual precipitation occurred in 1977/78 at Mashere with 1208 mm. Mean annual precipitation ranges from 322 mm for the station Vrede to 604 mm for station Sambiu.

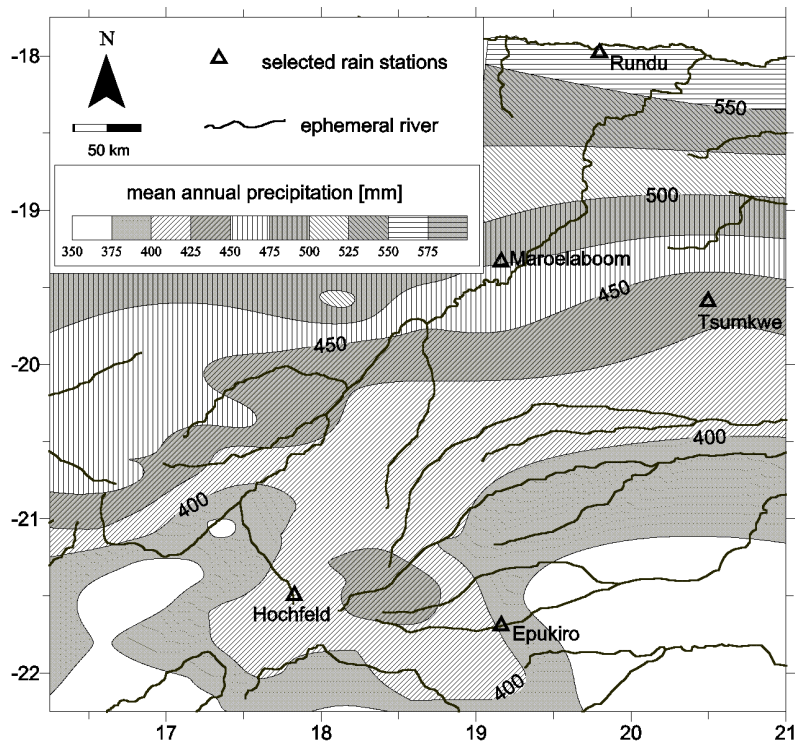


Fig. 5.3-2: Spatial distribution of mean annual precipitation for the north-eastern part of Namibia. Point data are derived from DWA database with 126 rain station.

For further purposes a raster map of mean annual precipitation is required. Therefore the mean annual precipitation has been calculated for each of the 126 usable rain stations. From the mean annual precipitation values a raw variogram has been produced to which a experimental variogram of the linear type with nugget effect has been fitted using a least squares model. The grid has then been produced by using point kriging with a slope of 650.7, a nugget effect of 378.9 and an anisotropy factor of two by 169° . A contour map of the produced grid is given in Fig. 5.3-2 that shows mean annual rain amount to increase towards the North.

Monthly rain data

Monthly data are mainly required for the interpretation of hydrographs to identify months of extraordinary high rainfall. Extraordinary is here defined as mean precipitation plus/minus one standard deviation or more. For the required rain stations, mean and standard deviation of all available and reliable data were calculated on a monthly basis and then the extraordinary month were extracted for the hydrograph interpretation (Chapter 5.4).

A summary of the calculated means and standard deviations for the 8 rain stations that are further used is given in Table 5.3-2. As almost no rain was reported from May to August, those months are not considered and rain data are missing very often for September so that this month is also left out of the interpretation.

Table 5.3-2: Summary of monthly rain [mm] for 8 selected rain stations of the research area. For location see Fig. 5.2-2 and 5.2-3

Station		Epukiro Reserve	Epukiro	Du-Plessis	Hennep	Frisge-waagd	Owingi	Otjinene	Hochfeld	Tsumkwe
October	MEAN	17.8	17.9	18	27.3	30.6	20.6	15.6	17.7	21.1
	STD	15.6	16.2	11.5	42.4	27.6	19.7	15.2	14.4	24.9
November	MEAN	38.6	41.6	27.3	51.4	42.1	48.6	47.2	37.3	49.5
	STD	26.9	28.8	19.9	42.9	20.4	46.3	36.6	28	45.1
December	MEAN	45.8	57.6	60.5	52	49	52.4	50.3	58.9	78.9
	STD	29.5	38.4	48.9	37	44.6	29.2	37	50.6	60.4
January	MEAN	71.6	93.9	137.8	84.7	78.9	89.3	109.4	101.3	121.2
	STD	54.3	80.3	94.4	80.9	63.8	60.9	82.1	76.7	84.9
February	MEAN	74.1	86.6	66.7	84.1	91.2	97.5	96.5	88.7	105.3
	STD	66.7	65.2	48.8	50	67.6	69.5	84.2	65.1	80.3
March	MEAN	63.2	62.8	44.3	71.3	66.2	64.7	63.3	72.3	59.3
	STD	46.9	48.4	37.7	48.1	50.5	43.6	52.5	49.2	50.3
April	MEAN	39.1	40.1	50.7	42.8	32.2	42	42.7	44.1	39.5
	STD	30.8	29.6	58.5	35.5	20.4	41.2	36.8	40.2	26

February is the month with the highest mean for the stations Epukiro reserve, Frisge-waagd and Owingi while it is January for all other stations. The 3 months with greatest rain amount are December to February for DuPlessis and Tsumkwe, for all other stations it is January to March. October is reported to be the month with the lowest rainfall, from the rainy season, for all stations that have been examined.

For the monthly data of the area Epukiro-DuPlessis (Fig. 5.3-3) in the south eastern part of the research area, it was checked how transferable those data are between the stations. Results are presented in Table 5.3-3.

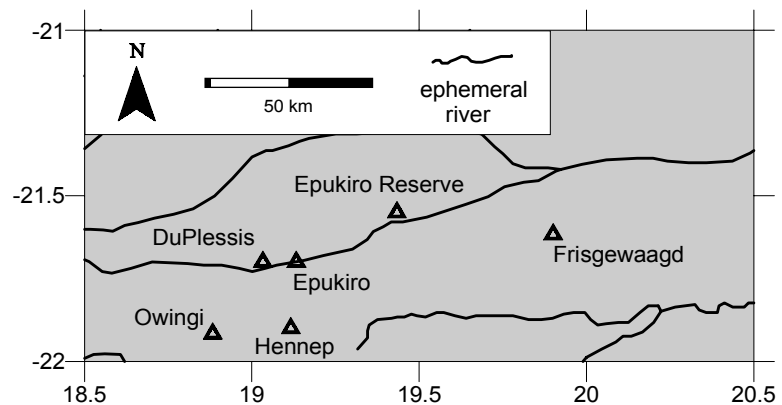


Fig. 5.3-3: Locations of rain stations in the Epukiro-DuPlessis area.

Table 5.3-3: Summary of extraordinary rainy months for the area of Epukiro-DuPlessis. If extraordinary rain is observed the month is given, a means that a normal rain amount was reported and b indicates that no reliable observation is made during this time. Column H gives the amount of rain station that reported an extraordinary rain amount divided by the amount of rain station that reported reliable results for this month. Extraordinary rain events that have been observed in at least 60 % of the stations are underlain in light grey. Years in which observations were made throughout the entire region are marked in dark grey with white letters

Epukiro Reserve	Epukiro	Du-Plessis	Hennep	Frisge-waagd	Owingi	H	Epukiro Reserve	Epukiro	Du-Plessis	Hennep	Frisge-waagd	Owingi	H
a	a	b	Mar 50	b	b	1/3	a	a	b	Jan 72	b	Jan 72	2/4
Nov 50	Nov 50	b	Nov 50	b	b	3/3	a	Mar 72	b	Mar 72	b	Mar 72	3/4
Dec 50	a	b	a	b	b	1/3	a	Oct 73	b	Oct 73	b	Oct 73	3/4
Apr 51	Apr 51	b	a	b	b	2/3	Dec 73	a	b	Dec 73	b	a	2/4
a	a	b	a	b	Dec 51	1/4	Jan 74	Jan 74	b	Jan 74	b	Jan 74	4/4
Oct 52	a	b	a	b	a	1/4	Feb 74	a	b	a	b	a	1/4
Feb 53	Feb 53	b	Feb 53	b	a	3/4	a	Apr 74	b	Apr 74	b	a	2/4
a	a	b	a	b	Apr 53	1/4	Oct 74	a	b	a	b	a	1/4
a	a	b	Dec 53	b	a	1/4	a	Nov 74	b	a	b	Nov 74	2/4
Jan 54	a	b	a	b	a	1/4	a	a	b	Mar 75	b	Mar 75	1/4
a	a	b	Mar 54	b	Mar 54	2/4	Jan 76	Jan 76	b	b	b	Jan 76	3/3
Dec 54	a	b	a	b	Dec 54	2/4	Feb 76	Feb 76	b	b	b	Feb 76	3/3
Feb 55	a	b	Feb 55	b	Feb 55	3/4	a	Apr 76	b	b	b	a	1/3
Mar 55	a	b	a	b	a	1/4	a	a	b	b	b	Apr 77	1/3
a	a	b	a	b	Oct 55	1/4	a	Feb 77	b	b	b	a	1/3
Feb 56	Feb 56	b	a	b	Feb 56	3/4	Dec 77	a	b	b	b	a	1/3
Mar 56	a	b	a	b	Mar 56	2/4	Jan 78	a	b	b	b	Jan 78	2/3
Oct 57	a	b	a	b	a	1/4	Feb 78	Feb 78	b	b	b	Feb 78	3/3
a	Nov 57	b	a	b	Nov 57	2/4	Nov 79	Nov 79	b	b	b	a	2/3
a	Dec 57	b	a	b	Dec 57	2/4	a	Oct 82	a	b	b	Oct 82	2/4
Dec 58	a	b	a	b	a	1/4	a	a	Nov 82	b	b	a	1/4
Feb 60	Feb 60	b	Feb 60	b	Feb 60	4/4	a	a	a	b	a	Dec 82	1/5
Nov 60	a	b	a	b	a	1/4	a	Nov 83	a	b	Nov 83	a	2/5
Apr 61	Apr 61	b	a	b	a	2/4	b	Dec 83	Dec 83	b	a	Dec 83	3/4
a	Nov 61	b	a	b	a	1/4	a	Apr 84	Apr 84	b	Apr 84	Apr 84	4/5
a	Dec 61	b	Dec 61	b	Dec 61	3/4	a	Nov 84	Nov 84	b	a	Nov 84	3/5
Jan 63	Jan 63	b	Jan 63	b	Jan 63	4/4	a	Oct 86	b	b	a	Oct 86	2/4
a	a	b	Mar 63	b	a	1/4	a	a	Feb 88	b	a	a	1/5
a	Nov 63	b	Nov 63	b	Nov 63	3/4	a	Apr 88	Apr 88	b	Apr 88	a	3/5
a	Apr 65	b	a	b	a	1/4	a	Dec 88	Dec 88	b	Dec 88	Dec 88	4/5
Jan 66	a	b	a	b	a	1/4	a	a	a	b	a	Jan 89	1/5
Dec 66	a	b	a	b	a	1/4	b	a	Mar 90	b	Mar 90	a	2/4
a	Jan 67	b	a	b	a	1/4	b	Jan 91	Jan 91	b	Jan 91	Jan 91	4/4
a	a	b	Feb 67	b	a	1/4	b	a	a	b	Feb 91	b	1/3
Apr 67	Apr 67	b	b	b	a	2/3	b	a	a	b	b	Oct 91	1/3
b	Oct 67	b	b	b	a	1/4	b	Nov 91	a	b	b	b	1/2
Mar 68	a	b	b	b	Mar 68	2/4	b	a	a	b	b	Dec 91	1/3
Feb 69	a	b	a	b	a	1/4	b	a	a	b	Nov 92	b	1/3
Nov 69	a	b	a	b	a	1/4	b	Feb 93	Feb 93	b	Feb 93	b	3/3
a	a	b	Feb 70	b	a	1/4	b	Oct 93	Oct 93	b	Oct 93	Oct 93	4/4
a	Dec 70	b	Dec 70	b	Dec 70	3/4	b	Jan 94	Jan 94	b	Jan 94	a	3/4
Feb 71	a	b	a	b	Feb 71	2/4							

Of the 83 observed extraordinary wet months, the month most often extraordinarily wet are December and February with 15 reports each. March showed the fewest extraordinary events with only 9 occurrences. 40 % of the extraordinary events that have been reported throughout all rain stations occur in January and 40 % in February. Extraordinary rain events were reported at all rain stations of the selected area once only for each of the month October and November from 1940 to 1995. None of the other month received an extraordinary rain amount that was widely distributed. Above mean-plus-standard-deviation rainy months were observed in at least 60 % of the rain stations most frequently in December and April with 4 occurrences each.

From these observations it is concluded, that rain events in January and February are more likely to be transferable to a regional scale than during the other months.

Daily rain data

Daily rain records were available for 36 rain stations. Those rain records were taken for a study of rain intensities. Therefore the daily rain amounts have been classed into 6 groups (less than 1 mm/day, 1 to 10 mm/day, 10 to 25 mm/day, 25 to 50 mm/day, 50 to 100 mm/day and more than 100 mm/day). The rain amount of the events that fall in every class have been added and the contribution to the total rain amount during the observed time of every class has been calculated. A summary of the results is given in Table 5.3-4. Some of the stations (underlain in light grey in Table 5.3-4) only provide daily data during the rainy season (October - March) and the station Talismanis-Rietfontein often reported unreliable data (sum of several days). The stations Okanjatu and Okamatapati frequently produced reliable data but were used for only 7 and 6 years, respectively. These data are therefore not statistically reliable (underlain in dark grey with white letters in Table 5.3-4).

Rain events of less than 1 mm influence the cumulative rain amount by less than 1 %. For all rain stations it is observed that rain events of 10 to 20 mm/day contribute most to the cumulative rainfall with 33 - 42 %. Rain events of more than 100 mm/day occur only very seldom. Rundu and Simondeum received 5 times rain amounts of more than 100 mm/day. For Epukiro and Tsumkwe 4 such events were reported, all other rain stations observed 0 to 3 rain events of more than 100 mm/day during observations. But these events contribute with up to 3.5 % to the total observed rain amount. Rain events of more than 100 mm/day have been reported 55 times at the rain stations used in northern Namibia. Only 7 of those reports could be correlated from one station to another. The largest rain amount occurred on 13-January-1978 at Sambiu (171 mm/day). Most of the rain events with more than 100 mm/day occur during January and

Table 5.3-4: Summary of contribution to rain amount with respect to rain classes and number of rainy days during the observation period. Station giving only daily data during the rainy season are underlain in light grey. Okanjatu and Okamatapati produced reliable data only for 6 and 7 years, respectively.

Rain station	Location		Contribution to cumulative rain amount during observation period [%] divided into rain amount classes (rain amount in [mm/day])						Rainy days during observation period
	Long	Lat	< 1	1 - 10	10.1 - 20	20.1 - 50	50.1 - 100	> 100	[%]
Arbeitsgenood	19.9500	-22.1167	0.24	24.26	34.01	26.22	13.04	2.23	7.8
Du Plessis	19.0333	-21.7000	0.10	22.54	38.97	27.27	11.12	0.00	8.1
Epukiro	19.1333	-21.7000	0.46	21.38	40.02	28.00	7.93	2.23	10.3
Epukiro Reserve	19.4333	-21.5500	0.16	23.92	39.81	27.14	8.97	0.00	7.4
Frisgewaagd	19.9000	-21.6167	0.16	26.49	38.39	23.74	11.22	0.00	8.9
Rietfontein-Talismanis	20.7000	-21.8000	0.13	12.04	32.00	36.29	19.54	0.00	6.1
Summerdown	18.5000	-21.3833	0.13	19.79	34.86	29.74	11.96	3.52	8.8
Otjosondjou	18.5333	-21.1167	0.13	28.16	35.89	25.30	10.52	0.00	10.9
Okasondana	18.6833	-21.4333	0.26	24.43	36.14	23.77	13.67	1.73	10.6
Okatombaka	18.8000	-21.1667	0.18	22.27	36.86	27.91	12.78	0.00	7.2
Otjinene	18.8333	-21.1000	0.21	17.93	39.01	28.26	11.67	2.92	4.0
Okanjatu	18.2000	-20.9667	0.03	14.50	30.30	24.15	14.03	16.99	7.9
Okamatapati	18.0500	-20.3333	0.06	11.01	41.67	29.36	12.97	4.91	7.2
Otjituuo	18.5833	-19.6667	0.14	19.34	37.77	30.29	11.90	0.56	8.0
O_Woestney	18.9500	-19.6333	0.04	18.22	33.87	33.83	11.34	2.70	9.9
Simondeum	19.0667	-19.5667	0.08	14.88	36.69	31.10	14.24	3.01	7.2
Tsumkwe	20.5333	-19.5833	0.39	22.44	37.58	28.14	8.58	2.87	10.1
Abendruhe	18.7667	-19.2500	0.24	24.81	34.79	26.82	13.34	0.00	12.8
Maroelaboom	18.8500	-19.2667	0.39	23.87	37.70	28.30	8.44	1.30	9.8
Alpha	19.0333	-19.3833	0.14	13.90	38.72	33.25	13.99	0.00	7.6
Njangana	20.6333	-18.0167	0.73	23.47	34.31	30.10	10.87	0.51	11.3
Rundu	19.7667	-17.9167	0.90	24.29	34.86	27.77	10.55	1.63	11.9
Sambiu	20.0333	-17.9000	0.19	17.64	36.81	30.34	14.03	0.99	12.3
Mashare	20.1500	-17.9000	0.43	25.00	35.70	25.30	13.57	0.00	11.9
Awagobib	17.8667	-19.6500	0.29	21.95	38.75	29.83	7.66	1.52	28.1
Grootfontein	18.1000	-19.5667	1.61	26.21	37.69	20.41	11.28	2.79	18.9
Katateno	18.0167	-21.7000	0.08	22.63	38.21	28.16	9.64	1.28	18.6
Korasiep	17.9833	-21.9500	0.00	26.95	36.80	25.64	10.61	0.00	7.8
Okatana	17.7333	-21.1000	0.71	23.03	34.04	27.83	14.38	0.00	21.1
Otjisoro	18.0500	-21.7833	0.08	20.83	36.80	27.06	11.03	4.19	8.2
Otavi	19.6333	-17.3333	0.24	21.33	34.39	28.40	15.64	0.00	19.9
Steinhausen	18.2500	-21.8167	0.27	20.06	32.80	32.41	9.35	5.11	13.9
Tsintsab	17.9500	-18.7833	0.19	19.65	38.93	29.30	10.26	1.67	17.8
Tsumeb	17.7167	-19.2333	0.44	20.94	36.34	27.05	13.07	2.15	18.1
Uitkomst	17.9833	-19.6667	0.28	24.19	34.69	29.95	9.04	1.85	24.3
Waihoek	17.8167	-21.7833	0.64	25.30	36.62	25.99	11.45	0.00	21.3

February (Fig. 5.3-4). Such rain events were not reported in the study area during May to October. Occurrences in November, December, January and February are rather rare. 11 of the reported 55 very heavy rain events occurred in the rainy season 1977/78. 4 such events were reported in the rainy season 1968/69. All other rainy seasons received more than 100 mm/day of rain on only three days or less.

Rain events with more than 70 mm/day were observed 271 times at the selected rain stations. These events occurred most frequently during February (29.9%) and January (27.7%), followed by March (16.6 %), December (12.2 %) and April (8.9 %). Heavy rain occurs only very rarely during the early months of the rainy season (November 4.1 %; October 0.7 %; September 0.4 %). 39 of the observed 271 heavy rain reports could be correlated between at least two stations.

Very heavy and heavy rains occur mostly during January and February and they are also most transferable during this time. This correlates with the monthly observations, from which it was concluded that extraordinary rainy monthly data are most transferable for the two month with the highest rain amount January and February. During most of the other months either only a negligible amount of rain occurs (May to September) or rain data are not readily transferable from one station to another (October to December, March and April).

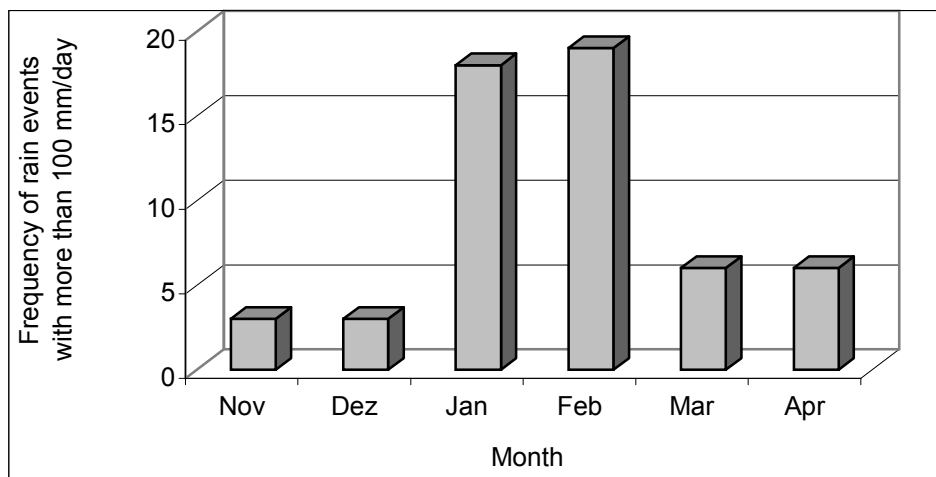


Fig. 5.3-4: Occurrence of very heavy rain (more than 100 mm during one day) during the observation period in the selected 42 rain stations.

5.3.2 Pan Evaporation

Evaporation is one of the factors that influence groundwater recharge heavily in arid and semiarid areas. Measurements of gross pan evaporation are made by the DWA (1988) using standard class-A evaporation pans. These pans (1.22 m in diameter, 0.254 m deep, made from galvanised iron) are filled with water and the depth by which the water level decreases is the pan

evaporation loss (WMO, 1965; 1966). Gross pan evaporation measurements in the research area are limited to Grootfontein. Therefore stations outside the study area were considered: Gobabis, J.G. Strijdom, S. von Bach Dam, Omaruru, Outjo, Sitrusdal, Okuakuejo and Tsumeb in Namibia, Ghanzi and Maun in Botswana.

June is the month with the lowest mean gross pan evaporation for all stations. The lowest cumulative pan evaporation value was reported for Tsumeb during June 1966 with 62 mm only. Mean cumulative pan evaporation values range from 102 mm/month (Tsumeb) to 187 mm/month (S. von Bach Dam) for June. December and October are reported as the months with the highest mean gross pan evaporation. The highest reported value occurred during October 1961 with 506 mm/month in Grootfontein, but such a high value appears energetically questionable. Mean for the month with the highest values range from 249 (Tsumeb) to 397 mm/month (S. von Bach Dam) for October and 235 (Maun) to 397 mm/month (S. von Bach Dam) for December.

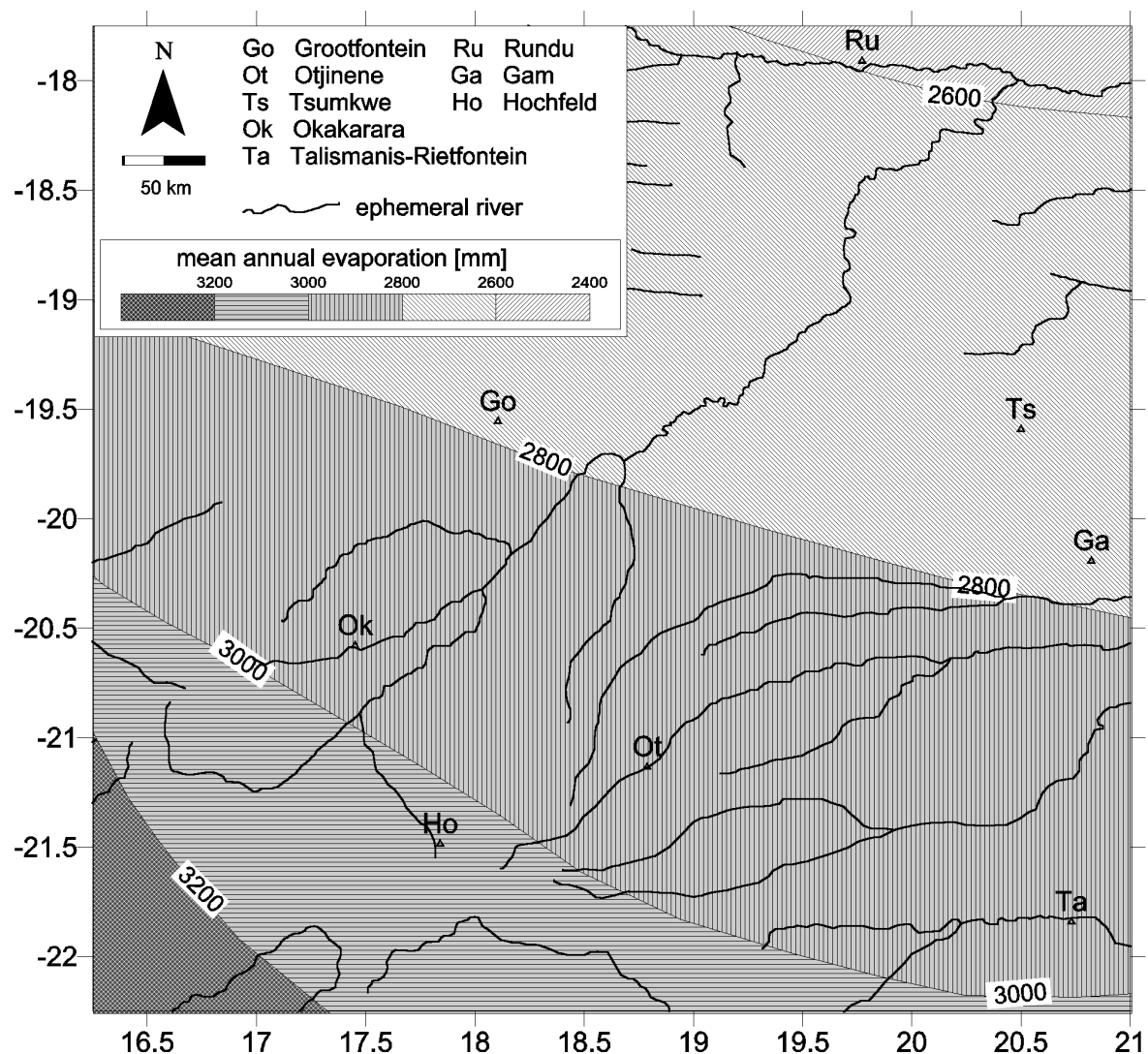


Fig. 5.3-5: Mean annual evaporation for the research area. Modified from DWA (1988).

The distribution of mean annual pan evaporation is given in Fig. 5.3-5. Mean annual pan evaporation decreases from the south-west with more than 3200 mm/a towards the north-east with less than 2600 mm/a. The DWA (1988) reported the north-eastern part of the research area as an area with relative high evaporation loss during winter compared to the central Namibian areas.

The station Tsumeb is left out for the regionalisation by DWA (1988) as it showed a questionable change in its reported values after 1968. For the same reason data for Gobabis were not considered after 1976.

Monthly gross pan evaporation data are available from October 1950 until September 1985 for the station Grootfontein in the research area. A summary of the monthly pan evaporation at this station is given in Table 5.3-5. The table compares the pan evaporation data with the monthly rain fall. May to September is not considered as pan evaporation is clearly higher than rain amount during the dry season.

Pan evaporation is always higher than the rain amount during the months with the highest gross pan evaporation (October and December). Rain amount is most often exceeding the gross pan evaporation loss during February (9 of 35 observed months). Rain fall exceeds pan evaporation less often in March (5 times), January (4 times), April (2 times) and November (one observation). Mostly rain exceeds pan evaporation only during one month in a rainy season (9 observations). In 4 rainy seasons there were 2 months in which rain fall exceeded pan evaporation, while it happened only once that rain amount was larger than pan evaporation loss during 3 out of the 7 rainy months (rainy season 1973/74). From December 1973 until March 1974 the rain amount clearly exceeds the total pan evaporation (889.4 mm rain and 647 mm evaporation only). Such periods are fairly promising for recharge generation.

The described evaporation data are pan evaporation data which are, of course, only applicable to open water bodies with an infinite water supply. Effective evaporation data are required for recharge estimations, and can be calculated by techniques based on Penman-type equations (e.g. HOWARD & LLOYD, 1979; RUSHTON & WARD, 1979). It is also obvious that mean annual data are inadequate for the use in a water balance model for the Kalahari as precipitation and evaporation are highly variable in arid areas, as presented in this chapter.

Table 5.3-5: Comparison of rain amount and gross evaporation for the wet months at the climatic station Grootfontein. Rain data are taken from station Grootfontein 1 until 1968 while the later rain records were reported at Grootfontein 2. Months with rain amount exceeding evaporation are underlain in light grey. Evaporation data are missing for 5 months during 1969 - 72 (marked as n.o.). Evaporation data obtained from DWA (1988)

Season	OCT		NOV		DEC		JAN		FEB		MAR		APR	
	Rain [mm]	Ev. [mm]	Rain [mm]	Ev. [mm]	Rain [mm]	Ev. [mm]	Rain [mm]	Ev. [mm]	Rain [mm]	Ev. [mm]	Rain [mm]	Ev. [mm]	Rain [mm]	Ev. [mm]
1950/51	106.7	358	218.4	324	74.3	301	74.6	325	108.6	198	79.8	259	52.5	193
1951/52	35.8	363	19.8	347	144.3	332	27.7	395	93.1	234	9.4	243	330.1	204
1952/53	35.1	357	58.9	316	39.4	341	142.5	356	209.9	163	32	208	58.6	176
1953/54	35.2	337	68.2	404	89.1	312	184.6	316	260.9	190	273.4	147	42.2	194
1954/55	6.9	365	21.4	349	77.5	322	91.3	303	90	224	115.4	197	56.9	173
1955/56	16.5	367	51.1	423	97.1	336	152.7	298	252.8	230	240.8	166	14.5	177
1956/57	18.7	400	31.3	351	16.5	388	123.1	290	198.9	169	118	168	5.7	215
1957/58	38.4	398	84.9	315	171.2	309	194.6	306	127.2	248	95.6	234	17.2	268
1958/59	27.5	395	23.5	373	99.6	367	108.6	336	147.8	229	36.1	238	25.7	236
1959/60	3.1	430	33.8	382	74.3	443	49.8	425	252.7	201	22.4	292	21.9	242
1960/61	13.1	407	35.5	385	71.9	479	38.1	412	119.6	282	145	200	31.5	182
1961/62	76.3	506*	80	382	71	416	116	373	41.5	275	8	327	36.5	250
1962/63	44.7	356	15	373	33.2	404	155.2	241	31	294	87.8	172	132.5	174
1963/64	14	382	139.5	266	63.7	329	28.7	383	27.7	314	54	250	7.5	251
1964/65	4.5	414	7	427	68.8	394	57.3	359	50.4	241	81.4	240	60	176
1965/66	3.2	389	135.4	356	44.1	416	247.3	230	106.1	296	92.4	230	62	188
1966/67	8.2	319	102.9	357	132	325	121.3	304	59.1	168	42.9	203	1.3	189
1967/68	14.3	373	281.3	193	30.4	215	222.2	272	94.3	266	166.4	145	22.4	166
1968/69	0.3	346	57.2	232	15.9	331	167.7	n.o.	105.1	208	162	184	14.3	179
1969/70	13.5	n.o.	104.1	n.o.	22.7	377	127.3	356	127.5	271	30.9	319	34.2	252
1970/71	0.7	322	37.3	345	143.8	300	148.3	242	167.8	157	37.7	224	17.4	199
1971/72	0.6	n.o.	15.8	386	35.1	409	255.5	259	82	267	330.3	n.o.	28.6	161
1972/73	32.4	384	30.4	419	62.3	398	136.2	378	54.4	259	156.5	205	51.2	178
1973/74	28.5	284	16.7	351	73.7	277	353.5	174	218.8	162	150.5	190	166.6	121
1974/75	14.1	260	33.3	247	26.1	295	47.7	276	56.4	228	159.2	177	61	162
1975/76	3.8	382	50.5	318	59.6	379	258.5	192	155.8	186	110.9	176	78.7	168
1976/77	5.4	336	25.1	327	21.5	347	131.3	308	234.2	173	64.3	203	127.8	170
1977/78	27.2	329	56.4	319	138.9	292	381.3	249	368.1	176	29.1	202	44.3	197
1978/79	26.5	363	48.7	363	23.3	356	106.1	278	148	227	16.1	291	25.2	255
1979/80	25.3	387	62.5	309	33.3	324	58.7	348	192.4	227	223.8	216	58.8	211
1980/81	35.7	424	34.2	37	171.1	337	106.1	271	22.9	225	19.9	243	5.4	214
1981/82	14.3	413	32.7	373	41	356	94.8	325	121.5	223	212.4	197	23.7	183
1982/83	10.7	441	36.4	420	153.4	359	104.2	273	20.7	239	20.9	340	7.2	269
1983/84	10.7	385	98.7	398	222	369	46.5	238	72	269	48.1	263	78.9	229
1984/85	37.4	385	60.8	329	18.2	400	107.5	348	102.7	219	57.3	216	5.7	196

* questionable value

5.4 Hydrograph interpretation

5.4.1 Method

Groundwater levels react to factors such as changes in the relation between inflow to and outflow from the aquifer, evaporation, transpiration, human activities, freezing and barometric effects (OLIN & SVENSSON, 1992). Evaporation is negligible if groundwater surface is at more than 2 to 5 m below the ground surface for comparable climatic and geological conditions as shown by stable isotopes in Botswana (GIESKE, 1992). Transpiration is limited to direct contact of plants with groundwater or capillary fringe, and freezing of groundwater does in generally not occur in Namibia. As barometric effects are limited to confined aquifers, the groundwater level fluctuation in the Kalahari catchment responds to recharge and human activities only. The human activities can be divided into abstraction and irrigation. As hydrographs in the research area are only available at state water schemes, the observed groundwater levels are clearly influenced by pumping. This means that the observed hydrographs can only be interpreted in a qualitative way and a quantitative recharge estimation with methods introduced by OLIN & SVENSSON, (1992), OLSSON (1980) or DAS GUPTA & PAUDYAL (1988) is impossible. Thus the occurrence of recharge in the research area and the associated climatic conditions is identified by the qualitative interpretation of the hydrographs, considering the reaction of the aquifer in cases of extraordinary high monthly rain and extraordinary annual precipitation only. Extraordinary is here defined as more than mean plus one standard deviation. Hydrograph figures are provided in the Appendix C.

5.4.2 Results

Hydrographs in the Epukiro well field

Three hydrographs are available for the period of Aug 1985 to Aug 1992 for the well field Epukiro. One hydrograph report starts two years later in Jun 1987, while data for the fifth well stops in Oct 1988. The hydrographs for well WW28805, WW10173, WW16994 and WW8976 show a general trend of lowering in hydraulic heads, but for well WW7637 a rising trend is observed. Earlier observations in 1964, when this well was drilled, report the initial level at 64 m below collar (m bc). From 1985 until 1992 the level rose from approximately 86 m to 67 m bc. This indicates that the well was less overexploited in 1992 than it was during the 1980s. In Oct 1986 two of the four processing rain stations observed extraordinary rainfall amount. Well WW28805 has no reports for this period. The pumping rate was increased in wells WW10173

and WW8976 from Oct 1986 to Nov 1986 but nevertheless the water level is rising which indicates recharge. For the two wells WW16994 and WW7637 water levels are falling due to increased pumping rates.

In Feb 1988 one of the five processing rain stations observed extraordinary rainfall amount. No groundwater level observations are made after this event at wells WW7637 and WW16994. Wells WW10173 and WW8976 show a lowering in water level resulting from increased pumping rates. Well WW28805 shows a rising water level although pumping rates are increasing, which is likely to result from groundwater recharge.

In Apr 1988 three of the five processing rain stations observed extraordinary rainfall amount. No observations are made in wells WW16994 and WW7637 during that time, wells WW101073 and WW8976 have approximate constant levels and well WW28805 shows lowering groundwater level after this extraordinary rain event.

In Jun 1988 wells WW16994, WW8976 and WW7637 show rising water levels although pumping rates are increased. The same can be observed for wells WW28805 and WW10173 in Jul 1988 which all reflect delayed recharge.

Four of the five proceeding rain stations observed extraordinary rainfall amount in Dec 1988, while the extraordinary rainfall in Jan 1989 is limited to one of five stations. Directly after the widely distributed extraordinary rainfall no rise in water levels has been observed, only well WW7637 shows a slightly rising level which could also result from the lower pumping rate. But for four wells (WW10173 is out of order from Dec 1988 on) rising groundwater levels are observed from Apr 1989 to May 1989. The rises for wells WW28805, WW8976 and WW7673 indicate groundwater recharge as pumping increased during this time, but for well WW16994 it is questionable as pumping is decreased. The rise in groundwater levels during increased abstraction in Apr 1990 for WW7637 might also be induced by an extraordinary rainfall amount in Mar 1990 that has been observed by two of the four processing rain stations.

In general the hydrographs from late 1990 to Jul 1991 do not showing many fluctuations. A slightly rising groundwater level in well WW16994 could be interpreted as recharge following the extraordinary rainfall amount noted at all processing rain stations in Jan 1991 and one of three processing rain stations in Feb 1991.

During Oct 1991 one of three, then in Nov 1991 one of two and in Dec 1991 one of three processing rain stations documented an extraordinary amount of rainfall. The four processing hydrographs all show the same pattern. Groundwater levels fell in Nov 1991 due to increased pumping and rose in Dec 1991 as the pumping rate was lowered. Until Aug 1992 the reported hydrographs do not show rising groundwater levels during increased or constant pumping. The

fluctuation of the hydrographs seems to react only to the pumping rates and no groundwater recharge could be defined during this period.

For each well 2-3 recharge events were identified. In general the hydrographs indicate that groundwater recharge occurs in this area and that it is not limited to good overall rainy seasons but most of the hydrographs already react to a single extraordinary month. The well WW7673 reacts quicker to extraordinary precipitation than the other wells which most probably results from its first strike (68.9 m bc) being shallower than the other wells (strike at 89.2 to 109 m bc).

Hydrographs at DuPlessis

Two hydrographs are available from well WW3858 and WW9095 for the well field of DuPlessis. Both show are a constant level with 28 to 29 m from Aug 1985 compared to Aug 1992. However the level in well WW3858 ha dropped significantly compared with its initial (1953) level of 18 m bc, and the level in well WW9095 had dropped lightly from the initial (1967) level of 27 m bc. Both wells also show a significant drop from May 1990 until Nov 1991, followed by a constant level at 30 m bc. A similar behaviour was also observed in about the same period for wells WW8976, WW7637, WW28805, WW16994 (all at Epukiro). This is more likely to reflect a malfunctioning measuring procedure than hydrological phenomenon in the aquifer, therefore this period is not further interpreted.

The earliest relevant extraordinary rain amount occurs in Oct 1986, but is only mentioned in the surrounding rain stations and not at DuPlessis itself. From Oct 1986 to Nov 1989 there is a clear rise in level which is accompanied by decreasing pumping rates at well WW9095 and therefore recharge is not clearly identifiable. As there has been no pumping at WW3858 during this time, recharge influence is assumed for this well.

During the wet months Feb 1988 and Apr 1988 levels in well WW9095 dropped, but the rising levels need not result from recharge, because pumping in well WW3858 is largely reduced. During Jan 1989 and Feb 1989 (of which only the January event has been observed at DuPlessis rain station itself) a rising level at well WW3858 is observed while pumping is increasing, which indicates groundwater recharge. The rising levels in well WW9095 could result from the decreased pumping rate. Groundwater levels in both wells rise after the three wet months Oct to Dec 1991, but as pumping rate is lowered, no positive correlation with recharge influence is meaningful.

The only definitive recharge for WW3858 occurs during a lower than average rainy season after two months of extraordinary precipitation amount (Jan and Feb 1989). For WW9095 no recharge event could be clearly identified.

Hydrographs at Hochfeld

Two hydrographs were recorded from Aug 1985 until Sep 1992 in the Hochfeld well field. Depth to groundwater is between 6 and 13 m during the observation period. Groundwater level has fallen during increased abstraction rates in the rainy season 1988/89 but it recovered to levels between 7 and 9 m during 1992, which is similar to the observed level of 8.2 m when it was drilled in 1967. Well WW542 shows levels between 6 and 12 m bc and no specific trend is seen. Well WW9117 shows three possible recharge events with rising groundwater level although pumping rate is increased: Jan/Feb 1987, Jun/Jul 1988 and Dec 1991/Jan 1992. While the first event is not associated with a extraordinary rain amount, the second one reacts to the extraordinary rain amount in April 1988 and the last one is positively correlated with the good rainy month in Oct 1991 and the good overall rainy season 1991/1992.

For WW542 rising water levels occur in Sep/Oct 1986, Dec 1987/Jan 1988 and Jun/Jul 1991 although abstraction was increased. It seems difficult to attribute any extraordinary rain event to a particular recharge occurrence, which is most likely to result from a small irrigation scheme at the Farm Eahero.

Hydrograph at Tsumkwe

A hydrograph from the main well at Tsumkwe WW16561 is available from Jan 1986 until Jun 1999 from the Tsumkwe State Water Scheme. Levels in this well are mostly between 5 and 9 m bc which is in the same range as when it was drilled in 1973 when the level was at 6 m bc.

This well shows rising groundwater levels during most rainy seasons. Only during the lower than mean rainy seasons of 1991/92 and 1992/93 is no increasing ground water level reported.

Although some of the rising groundwater levels result from lower pumping rates, at least three recharge events can be identified: groundwater level is rising during Feb to Mar 1989, Mar to May 1990 and Nov to Dec 1990 although pumping is increased. During the rainy seasons of 1993/94 levels are rising almost 3 m between Nov 1993 and Apr 1994 but data are missing for Feb and Mar 1994. This indicates a strong influence of recharge phenomena during this good rainy season with 592 mm (mean 416 mm). The higher than mean rainy season in 1996/97 is followed by a rise in groundwater level of 2.5 m from Jul 1996 until Mar 1997, but as no pumping occurs from Jul 1996 till Feb 1997 the recharge influence could be questioned. Extraordinary rainy months have been reported at Tsumkwe for Oct 1986, Feb 1988, Feb 1989, Dec 1990, Mar 1990, Nov 1993, Jan 1994 and Jan 1997. All of these months are followed by recovering groundwater levels. Only the rain events of Oct 1986, which are not coupled with a better than mean rainy season, do not increase the groundwater level. Therefore one is tempted to

conclude that a good rainy season is more important for recharge than a single extraordinary rainy month in the Tsumkwe area.

Hydrographs at Otjinene

As rain reports are only available until Dec 1986 for Otjinene only one out of seven hydrographs (WW25404) is considered here. The water level shows a general lowering during the observed time falling from around 17 m to about 19.5 m bc. It showed an initial level of 16.3 m bc when it was drilled in 1980.

The only reported extraordinary rainy month is Oct 1986 which is not coupled with an entire wet rainy season. It is followed by a rising level of about 30 cm while pumping increased from Oct 1986 to Nov 1986, which indicates recharge.

5.4.3 Summary and conclusions from the hydrograph interpretation

Indicators for the occurrence of recharge have been found in all five regions. For the Hochfeld area the definition of favourable climatic conditions is limited as an irrigation scheme influences the hydrographs here. For Otjinene and DuPlessis only limited interpretation is possible showing that recharge occurs mainly after a single extraordinary monthly event.

Detailed interpretation of the wells in Epukiro area identified several recharge occurrences after extraordinary rainy months. Wells with shallower strikes react quicker to increased precipitation. The hydrograph in Tsumkwe indicates that this is a region where a good rainy season is required to allow groundwater recharge.

The difference between the Epukiro and Tsumkwe areas most likely results from different surface conditions. In the Tsumkwe area a large pan field allows infiltration from ponded water bodies. Thus the recharge is of an indirect diffuse nature. In the Epukiro area hardrock aquifers are overlain by a calcrete surface and it seems likely that the recharge occurs mainly due to preferred flow path infiltration and thus single events act as recharge sources.

5.5 Soil Water balance

In this study a soil water balance model has been used to identify the timing of direct recharge occurrences. Soil water balance models can only be used for the determination of recharge rates, if those models are calibrated. As no groundwater level reports for wells without abstraction exist in the research area, and runoff reports are only available for the upper Omatako catchment, no calibration of the dynamic system is possible. Results from the soil water balance model are verifiable with results from the chloride mass balance method (Chapter 5.6). But mean annual

recharge rates from the chloride mass balance models are not punctiliously comparable with annual results from the water balance model. 4 years that are modelled in this study are insufficient to estimate a mean value. Nevertheless the soil water balance model is used to demonstrate how strongly dependent recharge is on the soil class and on the field capacity.

5.5.1 Method

The recharge estimation model REGIS used in this study is based on the systematic descriptions of the soil water balance modelling with MODBIL (UDLUFT & ZAGANA, 1994; UDLUFT & KÜLLS, 2000; KÜLLS & UDLUFT, 2000; KÜLLS ET AL., 2000) and has been programmed and described in detail by KÜLLS (2000). Potential evaporation is calculated based in the HAUDE system (1954). The transport in the unsaturated soil is basically influenced by the hydraulic conductivity as a function of saturated hydraulic conductivity and soil moisture content (VAN GENUCHTEN, 1980).

Daily rain data for the station Simondeum have been combined with daily maximum and minimum temperature and relative humidity at 14.00 h from the station Grootfontein. The latter data are exclusively available for Grootfontein and the station Simondeum was selected as it has the least missing daily rain data for the selected period.

Modelling has been processed for the four soil classes as described in Chapter 5.2 and field capacity has been varied by changing the thickness of the root zone thickness. The crucial thing about the field capacity is the assumption of a root depth as the very variable vegetation cover in the study area ranges from the order of tens of cm for grass to several metres where there are large trees and shrubs. Root depths of 0.7, 1, 2 and 5 m have been tested, respectively.

5.5.2 Results and Conclusions

The results of the modelling for the four soil classes with an assumed average root depth of 2 m from 1993 until 1997 are given in Fig. 5.5-1. In all soil classes recharge occurs in the rainy seasons 1993/94 and 1996/97 that both represent wetter than average rainy seasons with 536 mm and 925 mm, respectively. Only for the aeolian sand has very little recharge (0.1 mm) been modelled for 1995/96 which had a cumulative rain amount of 301 mm. For the fairly dry season 1994/95 with only 136 mm cumulative precipitation, no recharge is calculated for any soil class for this station.

Recharge occurs only in the second half of the rainy season, which is consistent with the rain intensity studies in Chapter 5.3.1 where it is pointed out that heavier rains occur mostly in the second half of the rainy season. The calculated recharge amounts are highest for the dune sands

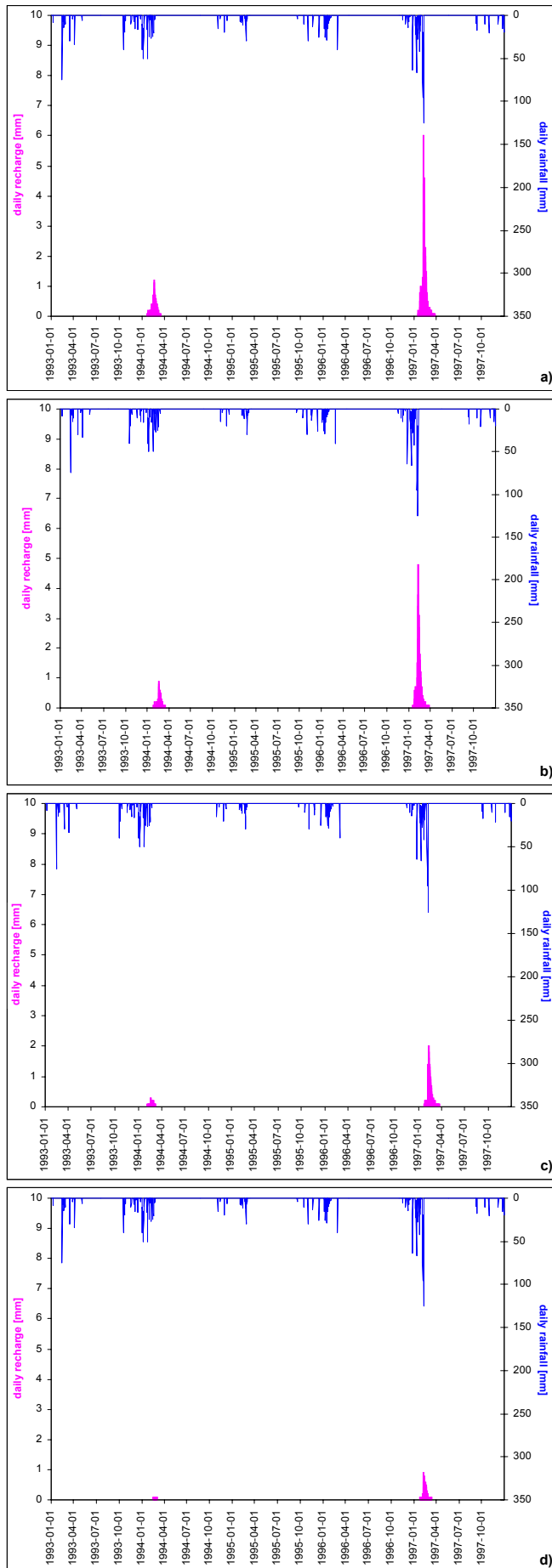


Fig. 5.5.1: Distribution of direct recharge for a time series from 1993 to 1997 for the station Simondeum for the four soil groups presented in Chapter 5.2 with a) aeolian sands, b) soil with aeolian influence, c) red to brown soils and d) pans and vleis.

and lowest for the group of pans and vleis and it was also found, that recharge occurs earlier in the aeolian group than in the other soils.

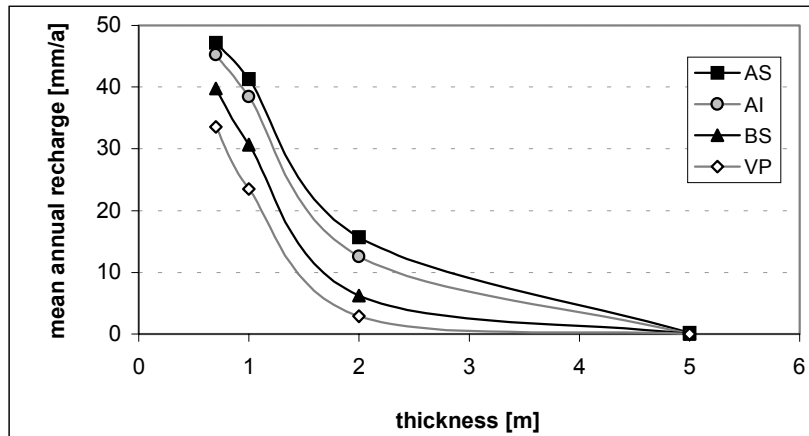


Fig. 5.5-2: Correlation between the assumed thickness of the root zone and the mean annual recharge for the period of 1.1. 1993 until 31.12.1997 for the four soil classes with AS-aeolian sands, AI-aeolian influenced soils, BS- red to brown soil, VP- pans and vleis.

The variation of the modelled mean annual recharge amount with the assumed thickness of the rooting zone is given in Fig. 5.5-2. Calculated mean recharge for the four-year-period varies by more than one order of magnitude for the selected soil groups and root thicknesses. The correlation between thickness of the root zone and annual precipitation is a very steep gradient for the variation of the first two metres but becomes less significant with very large assumed thicknesses. This calculation demonstrates very well the problem with any soil water balance model: with small variations in a highly variable parameter, it is possible to model almost every desired result, if no calibration is obtained. Thus no quantitative recharge estimation is possible for any study area by means of a soil water balance model without careful calibration.

Recharge amount, calculated with a rooting depth of 2 m, is plotted against annual rain amount, for the example locality in Fig. 5.5-3. It is observed that recharge increases with rain amount and that the slope of the function increases, from pans and vleis via red to brown soil towards the aeolian influenced soils and the aeolian sands. The assumption of any correlation when only two data points are available, is quite crucial, but it shows that a threshold for recharge occurrence is likely to lie somewhere below an annual precipitation of 400 mm, if a root zone of 2 m is assumed. This figure also demonstrates that recharge through the soil matrix is not a linear function of the rain amount, but more likely to be an exponential function. A full correlation of recharge amount with rain amount and thickness of the root zone is given for the aeolian sands in Fig. 5.5-4. It shows that an assumed root depth of 5 m does not allow recharge to develop even with a very extreme rainy season (more than 900 mm). This is also indicated by the results from the chloride mass balance method (Fig. 5.6-5) for recharge development with rain amounts

below 500 mm/a. Recharge rates from this method for the aeolian sand (Fig 5.5-4) with root depth between 0.7 and 2 m give the same rang as the chloride mass balance gives for the areas covered by Kalahari sands (Fig. 5.6-5b).

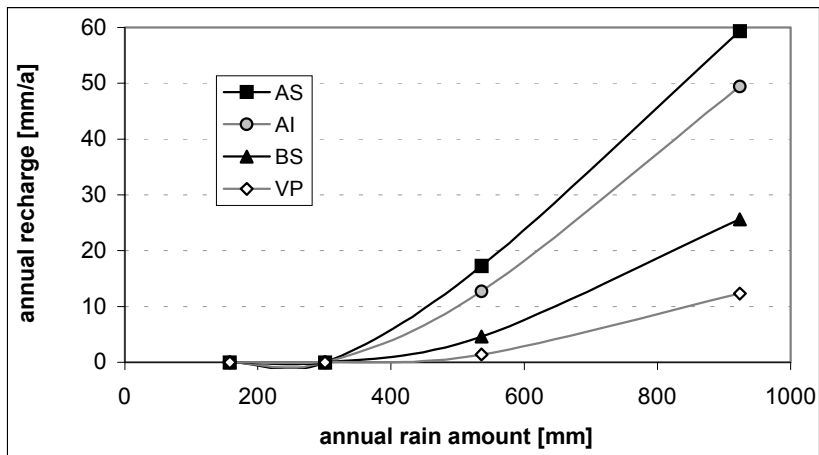


Fig. 5.5-3: Correlation of annual recharge with cumulative annual precipitation for the rainy seasons 1993/94 until 1996/97 with an assumed root thickness of 2 m for the four soil classes: AS-aeolian sands, AI-aeolian influenced soils, BS- red to brown soil, VP- pans and vleis.

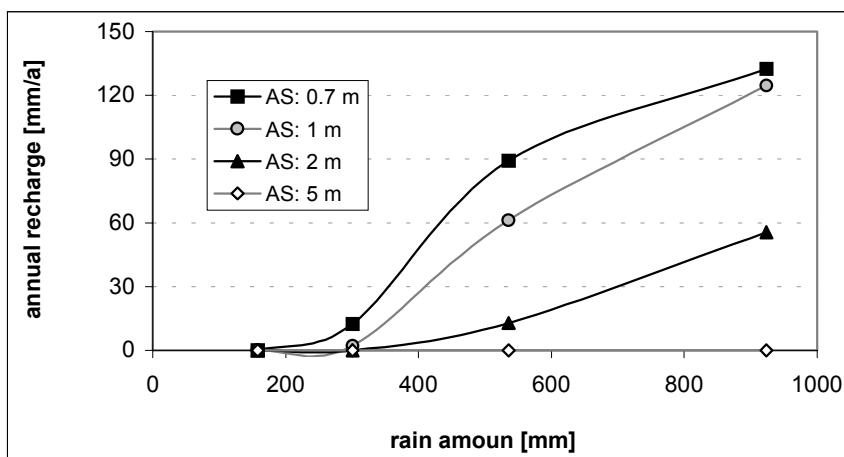


Fig. 5.5-4: Correlation between the annual recharge and the annual precipitation for the rainy seasons 1993/94 until 1996/97 for the aeolian sands for four assumed root depth.

It is concluded from the water balance modelling that the assumption of a recharge value based on the mean annual precipitation without considering the variability of the soil classes and the vegetation is not meaningful. For a forward regional approach it is thus required to develop an integrated approach which considers the soil depth and class, the vegetation and the spatial dimension of any of the occurring surface features. Variation of these parameters are expected to occur within very small areas. Therefore it appears more powerful to use an inverse approach for the determination of point recharge values, that integrates over some area containing different soil and vegetation features and that gives reliable results without calibration, e.g. the chloride mass balance method (next chapter).

5.6 Estimation of recharge rates by use of the chloride mass balance method

When surface water recharges groundwater it has to pass the unsaturated zone. Therefore the chemistry of the recharge water is a result of the interaction of rain water chemistry, input from dry deposition and reactions with the soil matrix. The soil water is also modified due to evaporation and transpiration by plants in the root zone.

As a simple mass balance approach for a given soil water volume one writes (EDMUNDS ET AL., 1988):

$$F_N + F_D = F_S + F_M \quad (5.6)$$

Where F_N , F_D , F_S and F_M are mean mass input by wet deposition (precipitation), mean mass input by dry deposition, mean mass output by seepage water, and mean mass output by adsorption and transformation into the mineral phase.

ALLISON & HUGHES (1978) and GIESKE ET AL. (1995) showed that chloride can be considered as a conservative tracer, therefore the adsorption and transformation term F_M is negligible. In the Kalahari, the dry input is small compared with the wet deposition (GIESKE, 1992) and it is assumed to be negligible for the study area (c.f. KÜLLS, 2000; MAINARDY, 1999; WRABEL, 1998). For areas without geogenic chloride sources equation 5.7 is obtained by balancing the flux of chloride into a soil column with the outflow at the bottom of the root zone and assuming that both surface runoff is not significant and that chloride up-take by plants is negligible:

$$R = \frac{P * Cl_P}{Cl_{SW}} \quad (5.7)$$

Where R , P , Cl_P and Cl_{SW} are groundwater recharge, mean annual precipitation, chloride concentration in precipitation and chloride concentration in the soil water of the unsaturated zone.

PHILLIPS ET AL. (1988) and SCALONE (1992) showed the chloride mass balance approach to be a reliable tool for recharge estimations even with expected recharge less than 1 mm/a. If high recharge rates are observed the factor of anion exclusion has to be considered where anion transport appears to be faster than the infiltration rate (GVIRTZMANN ET AL. 1986; JAMES & RUBIN, 1986;). BACHMAT ET AL. (1989) showed the critical recharge rate to be at about 100 mm/year.

The limits of the chloride mass balance method for the saturated and unsaturated zones is be discussed in the relevant chapters.

5.6.1 Wet chloride deposition

Rain chemistry is limited to chloride content here as it is the only parameter further required for calculation of groundwater recharge using the mass balance approach. Detailed descriptions of rain chemistry for northern Namibia are given by WRABEL (1999) and MAINARDY (1999). Data of chloride concentration are available from WRABEL (1999) and MAINARDY (1999) in Namibia. Data published by GIESKE (1992) and SELAULO ET AL. (1994) for Botswana have been used as well. Additional data were obtained by analysis of rain samples from Windhoek and Tsumkwe. During the third field trip two small rain events have been sampled and tested directly in the field for chloride content only. From all data a raster map has been produced by using point kriging. The resulting chloride distribution in rain is given in Fig. 5.6-1. Chloride content ranges from 0.4 to 1.1 mg/l in the research area and decreases towards the east.

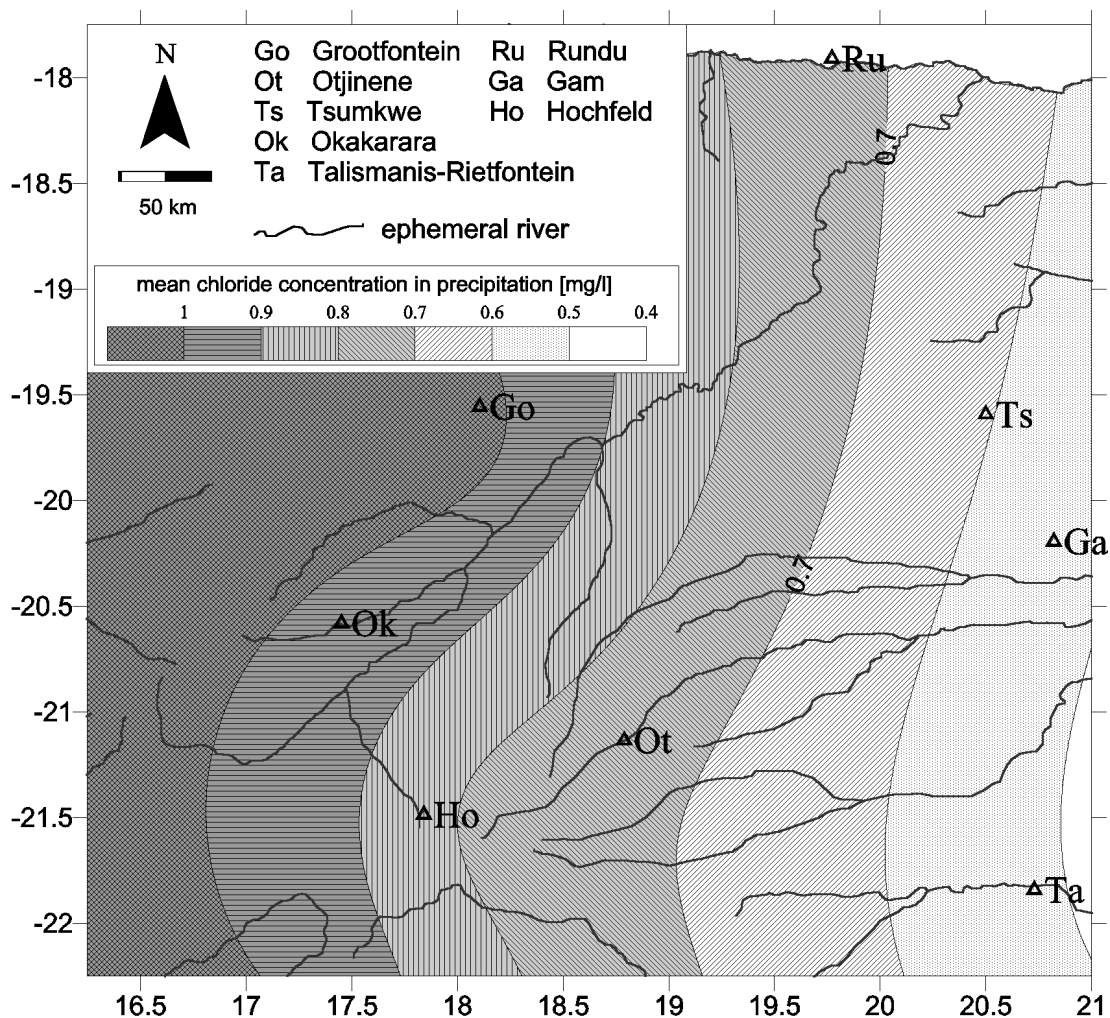


Fig. 5.6-1: Distribution of the chloride concentration in precipitation in northeastern Namibia. Map was derived by using own analyses, data from WRABEL (1999), MAINARDY (1999), GIESKE (1992) and SELAULO ET AL. (1994).

5.6.2 Chloride mass balance in the unsaturated zone

Method

In the upper part of a soil profile a complex trade-off between upward water flux as transpiration and evaporation and downward flux as infiltration takes place. The chloride mass balance method in the unsaturated zone is limited to the parts where upward flux is negligible. This means that the chloride mass balance approach is not applicable in the root zone. The root zone under grassland cover in the Kalahari of Namibia is observed to be less than 75 cm.

As the main subject of this thesis is not to work on point data but on a catchment scale, the appropriate method for recharge estimation cannot focus on detailed work on chloride profiles in the unsaturated zone as others have done (GIESKE, 1992; SELAULO, 1998; WRABEL, 1999) with sampling many deep profiles and several repeating times. As digging of deep profiles would have been time consuming and no help from a mechanical digger is available in the remote areas of the central Namibian Kalahari, sampling was limited to soil profiles in existing pits dug for rubbish disposal. Therefore only two profiles were sampled. As the localities could only be visited once, the results cannot be representative for a long period but for the period after which they were sampled and analysed. After cleaning the profiles for at least 50 cm, soil samples were placed in plastic containers and wrapped by tape to avoid moisture loss or uptake.

100 g of soil was eluated three times with 100 ml of deionised water for 24 h and then centrifuged for analysing the soil water following the descriptions by EDMUNDS & WALTON (1980). The eluats were then analysed for major ions (see Chapter 7.1 for methods).

Water content was obtained by drying a second set of samples at 105°C until weight constancy was achieved (for calculation see Chapter 5.2.1, eq. 5.3).

Recharge is calculated as:

$$R = \frac{P * Cl_P}{(VW_{E1} * Cl_{E1}) + (VW_{E2} * Cl_{E2}) + (VW_{E3} * Cl_{E3})} * MS_E * \theta_F \quad (5.8)$$

Where VW_{E1} , VW_{E2} , and VW_{E3} , are volume of water added at first, second and third elution; Cl_{E1} , Cl_{E2} , and Cl_{E3} , are chloride concentration in eluats after first, second and third elution; MS_E is mass of soil input for elution; θ_F is the water content at field situation; R is mean annual recharge, P is annual precipitation, and Cl_P is chloride content in the rain water.

Description of two sand profiles and results from chloride mass balance method in the unsaturated zone

Sand profile SP-1 is located at S 19.5898° / E 20.541° approximately 4 km east of Tsumkwe close to the road from Tsumkwe to the border. Aeolian sand developing from red-brown to white colours with depth is exposed here. This profile was sampled at 19th October 1998. Sand profile SP-2 is located in the Eiseb Block between the Omuramba Eiseb and Eiseb Post 10 at S 20.6071° / E 20.8573°. Red dune sand is exposed here 160 cm deep and was sampled on 27th May 1999. Both profiles belong to the group of aeolian sands (Chapter 5.2.2)

Precipitation during the rainy seasons 1994 to 1998 has been a lower than average period with a five years mean of 312 mm for Tsumkwe (long-time mean 416 mm) and an average period for Epukiro with 392 mm (long-time mean 394 mm) which are the nearest rain stations for the profiles. The calculation has been made with P = 312 mm for SP-1 and P = 352 mm (mean of Tsumkwe and Epukiro) for SP-2. Chloride concentration in rain has been assumed as 0.6 mg/l (Fig. 5.6-1).

Table 5.6-1: Water content and calculated recharge from chloride mass balance for profile SP-1 near Tsumkwe at S 19.5898° / E 20.541°. Data underneath the observed root zone are marked in bold letters

Depth	20	30	40	50	60	70	80	90	100	110	120	150
Water content [%]	0.24	0.26	0.23	0.21	0.22	0.15	0.26	0.23	0.28	0.25	0.11	0.08
Recharge [mm/a]	0.12	0.15	0.06	0.16	0.13	0.12	0.17	0.12	0.03	0.02	0.04	0.08

Table 5.6-2: Water content and calculated recharge from chloride mass balance for profile SP-2 in the Eiseb Block at S 20.6071° / E 20.3573°. Data underneath the root zone are marked in bold letters

Depth	40	100	160
Water content [%]	0.25	0.24	0.26
Recharge [mm/a]	0.15	0.24	0.27

The water content of both soil profiles is much lower than 1 % (Table 5.6-1 and Table 5.6-2). This slows the water movement significantly as only the smallest pores are saturated (e.g. HARTGE & HORN, 1992). Recharge amounts are fairly low for both entire profiles with 0.02 to 0.3 mm/a. Calculated recharge values for the Tsumkwe profile (SP-1) are lower than for Profile SP-2. As the Tsumkwe profile was sampled after a period of dry years and the Eiseb Block profile after a period of dry to average rain amount, the estimated recharge results represent these conditions only. Furthermore, as the application of the chloride balance method to the unsaturated zone represents only the portion of recharge that arises from direct diffuse recharge, these values do not consider recharge by preferred flow path infiltration.

5.6.3 Chloride mass balance in the saturated zone

Modification of the chloride mass balance method for the saturated zone

The procedure to obtain water samples from the saturated zone is a lot easier and less time consuming than the procedure to obtain soil water samples from the unsaturated zone, therefore the chloride balance method should be applied to the saturated zone. As the lateral inflow contributes to the chloride input into a volume of groundwater as well as the groundwater recharge, this flux and its chloride concentration need to be quantified. This is only possible at the groundwater divide (GWD) where lateral inflow is negligible.

Although the recharge mechanisms in a large semiarid catchment are highly variable, one can assume that in a narrow strip the mechanisms that contributes to groundwater recharge are similar. Therefore the mass balance method is applicable to the saturated zone in a narrow zone along the GWD.

The distribution of groundwater levels is given in Fig. 4.1-1 (page 62) where the groundwater divide is also indicated. Hydrochemical analyses for the Kalahari catchment are available from HUYSER (1982) and from field trips in 1999 and 2000 (Appendix D). Analyses for the wells that are situated in the narrow strip along the groundwater divide have been extracted. For the 239 hydrochemical sampling sites the values for mean annual precipitation and chloride content in precipitation have been read automatically from the raster images given in Fig. 5.3-2 and Fig. 5.6-1 using SURFER'S "RESIDUAL" tool. Mean annual recharge amount for those locations have been calculated using the formula:

$$R = \frac{P * Cl_P}{Cl_{GW}} \quad (5.7a)$$

Where R , P , Cl_P and Cl_{GW} are groundwater recharge, mean annual precipitation, chloride concentration in precipitation and chloride concentration in the groundwater, respectively.

Results from chloride mass balance method at the groundwater divide

Mean annual recharge values calculated for the 239 sampling sites along the narrow strip of the groundwater divide range from 0.2 mm to locally more than 100 mm, with an average rate of 55 mm and a standard deviation of 88 mm. The frequency distribution is given in Fig. 5.6-2. The average values seem very high, but one has to keep in mind that most of the wells are situated in selected areas and cannot reflect the recharge average of a catchment.

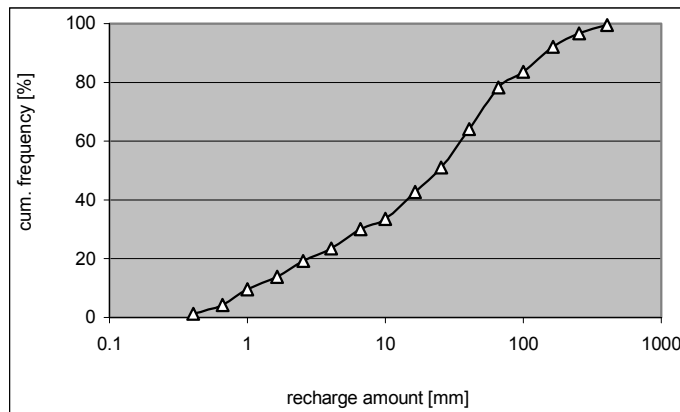


Fig. 5.6-2: Cumulative frequency distribution of recharge values from chloride mass balance approach on the GWD.

The spatial distribution of the calculated recharge amount is given in Fig. 5.6-3. Most of the groundwater divide receives recharge amounts between 1 and 50 mm/a. Most recharge values calculated higher than 60 mm/a are constrained to the western part of the GWD with lithologies of the Otavi Group (karstified carbonate rocks).

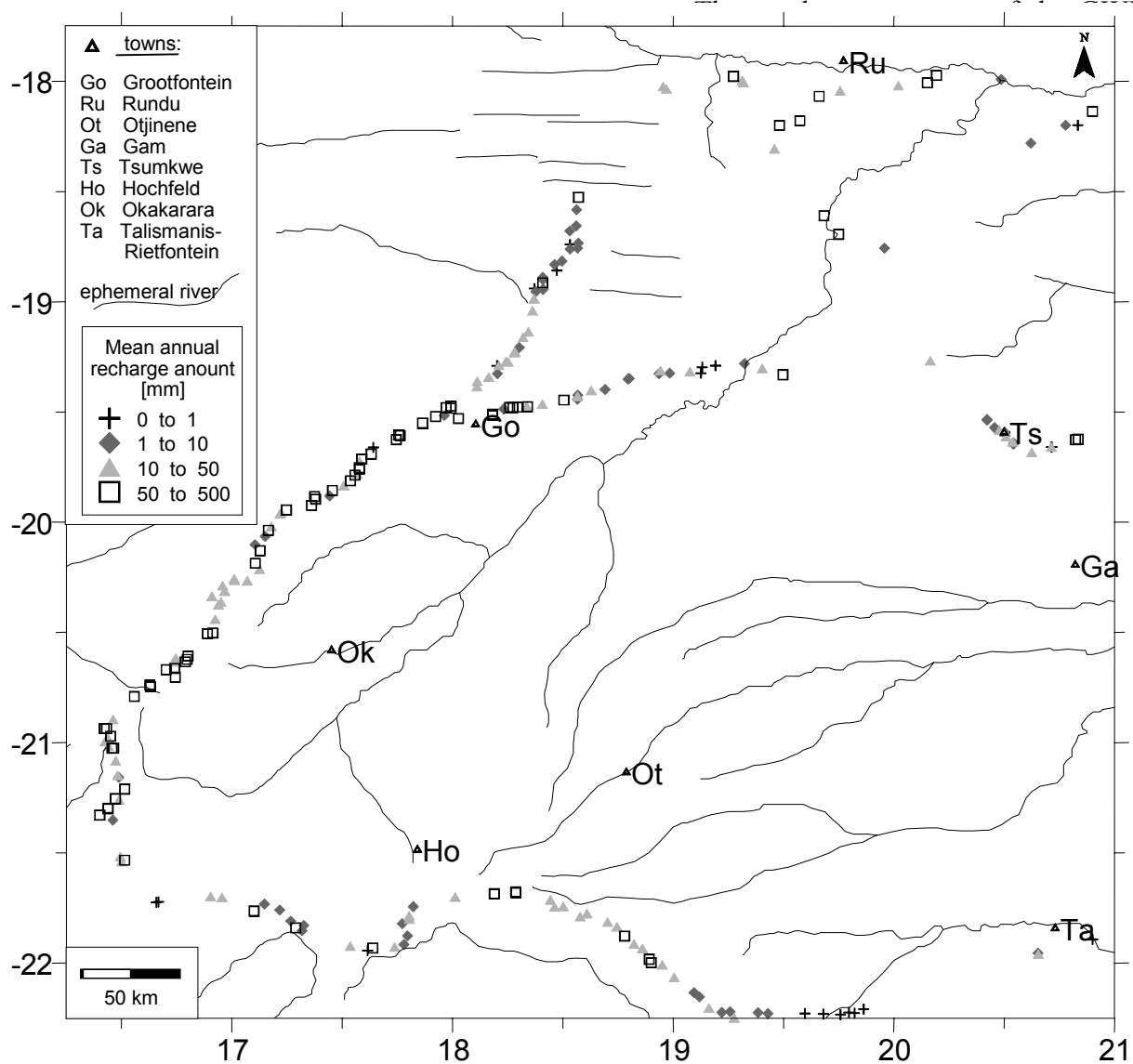


Fig. 5.6-3: Distribution of the recharge amount on the groundwater divide calculated by chloride mass balance approach in the saturated zone.

(Talismanis-Rietfontein Block) receives groundwater recharge of approximately 10 mm/a where quartzites of the Nosib Group crop out. If joints in the quartzites are closed by calcrete, or where a thick cover of sand occurs, the recharge rate is limited to less than 1 mm/a. In the vicinity of Tsumkwe recharge rates less than 20 mm/a are mostly obtained. Most parts of the GWD being covered by Kalahari sand receive a recharge amount of approximately 1 mm/a. Only in the northern most part of the research area do recharge values of locally more than 50 mm occur, although the area is covered by thick Kalahari sediments.

5.6.4 Interpretation of the results from chloride mass balance method

From the presented results of the chloride mass balance method for the research area it is concluded that diffuse recharge under a cover of several metres of soft sediments is very limited. Average rainy years allow recharge amounts in the order of tenths of mm, while during dry years recharge occurs in the range of hundredths of mm.

As the chloride method in the saturated zone reflects the recharge by diffuse flow as well as by preferred flow in the unsaturated zone, it is concluded that the higher recharge values from the saturated zone are mainly induced by preferred flow path recharge.

In Fig. 5.6-4 the relationship of recharge rate and precipitation amount is presented. In Fig. 5.6-4a where all data are plotted without respect to any rock type, no correlation is obvious. In Fig. 5.6-4b the recharge rate is given for areas that are geologically mapped as Kalahari. The upper limit of recharge rates increases more rapidly than the lower limit when rain amount increases. With a mean annual rain amount of less than 400 mm/a the recharge rate from diffuse and preferred flow path is less than 1 mm/a. With rain amounts of 400 to 450 mm/a the recharge rate ranges from 1 to 18 mm/a and if the rain amount is above 550 mm/a recharge rates above 60 mm/a were locally observed.

For recharge in the areas mapped as Damara, increasing recharge is assumed to depend on increasing precipitation (Fig. 5.6-4c), but the results scatter widely around any assumed function. The large variations probably arise from the anisotropic and inhomogenous nature of the jointed and partly karstified rocks.

From these observations it is clear that the recharge rate is not only a function of the geological settings and mean annual precipitation. Rather recharge rates probably also depend on the surface properties. Therefore satellite images (for method see Chapter 5.7.1) have been used to characterise the surface in the vicinity of the sampled wells that fall into Damara and Kalahari geological units. The results are given in Fig. 5.6-5.

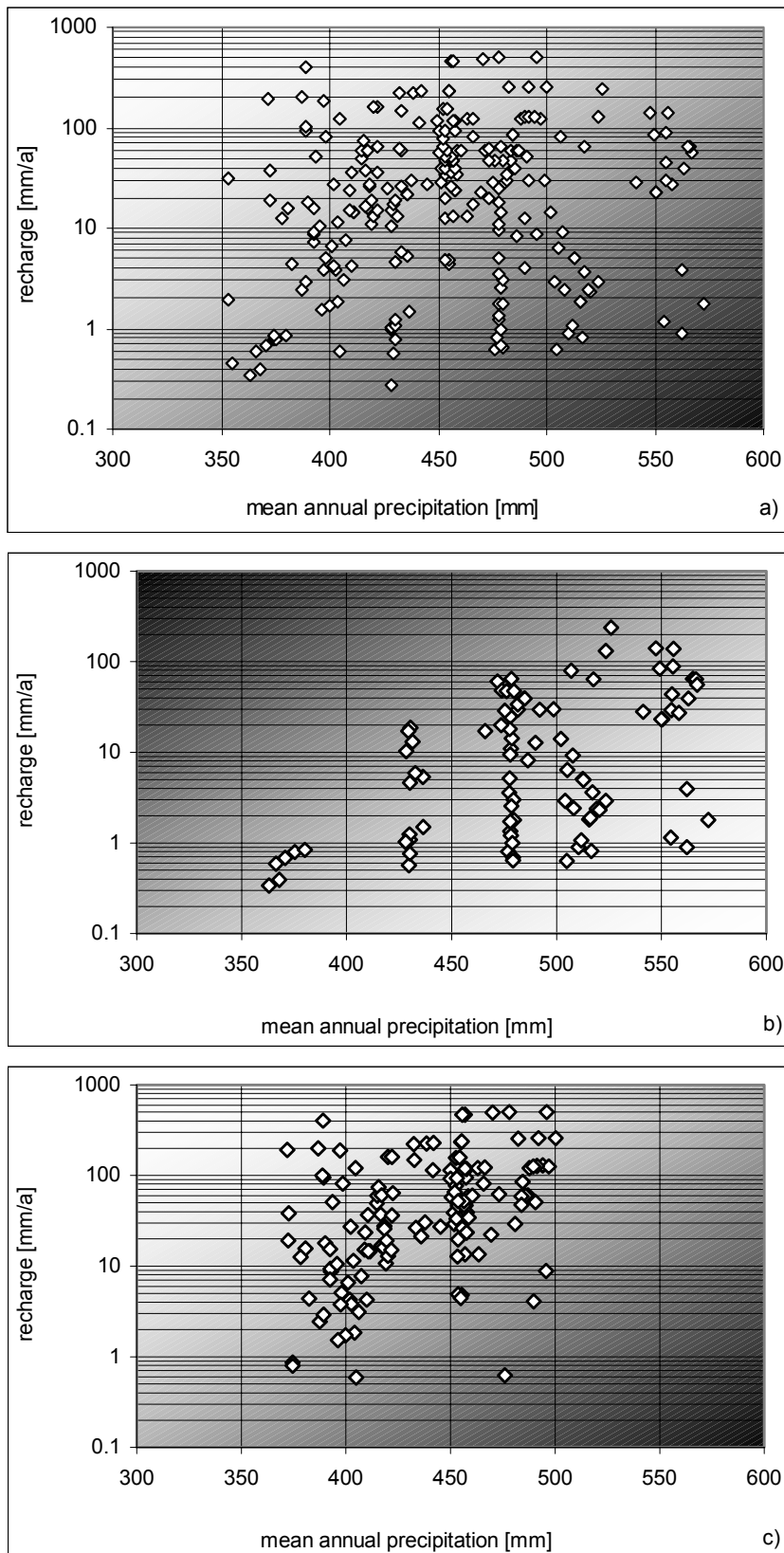


Fig. 5.6-4: Plot of calculated recharge rates with chloride mass balance method against annual precipitation for a) all lithologies at the GWD, b) for boreholes under Kalahari cover and c) boreholes that are in Damara units at the western part of the GWD. Classification is made according to the Geological Map of Namibia (MILLER & SCHALK, 1980).

Enveloping functions for the four presented surface classes are indicated as dashed lines. The recharge rates for Damara rocks outcropping at the surface in hardrock ridges and flat areas are limited by a flat upper limit and a steep lower limit (Fig. 5.6-5a), while for the areas covered by sand the upper limit shows a steeper function than the lower limit (Fig. 5.6-5b).

These observations document fairly well the nature of complex recharge processes in different substrates. Thus, direct recharge has to be divided into three parts: diffuse recharge, recharge along preferred flow paths and very rapid recharge. Diffuse recharge takes place in homogenous porous soils. Preferred flow path recharge takes place in soft, unconsolidated sediments along root channels or shrinkage cracks and in fractured rocks along joints. Very rapid recharge is limited to karstified rocks and sinkholes.

The upper limit of recharge in Damara rocks represents very rapid recharge. This is almost exclusively dependent on the infiltration capacity, which is only affected by the available precipitation at a given time and therefore a flat slope occurs. The upper limit of recharge in the soft sediments represents recharge along preferred flow path. This depends on the infiltration rate as a function of pre-wetting and water availability and therefore increases with an intermediate slope with the amount of precipitation. As recharge in jointed rocks is similar to preferred flow path recharge, the lower limit of the recharge in hard rocks looks similar to the upper limit of the recharge in soft sediments. The lower limit of recharge against precipitation for soft Kalahari sediments shows a relatively flat slope. This function shows the strong influence of the water retention in porous ground that allows evaporation. Recharge occurs only when field capacity is reached, which happens more often as precipitation increases and if precipitation events occur continuously during a limited time period. As the rainy days in the areas with highest average rain (Njangana, Rundu, Sambiu and Mashare) generally occur in a longer period (Table 5.3-4) the function has only a flat slope. The recharge data that lie within the upper and lower limits are combinations of the two described end-member recharge mechanisms.

Recharge in areas with hardrocks overlain by soft sands is given in Fig. 5.6-5c. Recharge in this areas is a mixture of the recharge mechanism described above. The upper part of the unsaturated zone has to be passed by preferred and diffuse flow while the lower part allows preferred and rapid flow into the saturated zone. The very rapid infiltration is therefore slowed and evaporation is limited to the upper part. This results in medium slopes of the upper and lower limits of the recharge dependence on precipitation amount. These recharge rates are, of course, a function of the thickness of the sand cover, with a thicker sand cover resulting in conditions more similar to the phenomena discussed above for sandy areas.

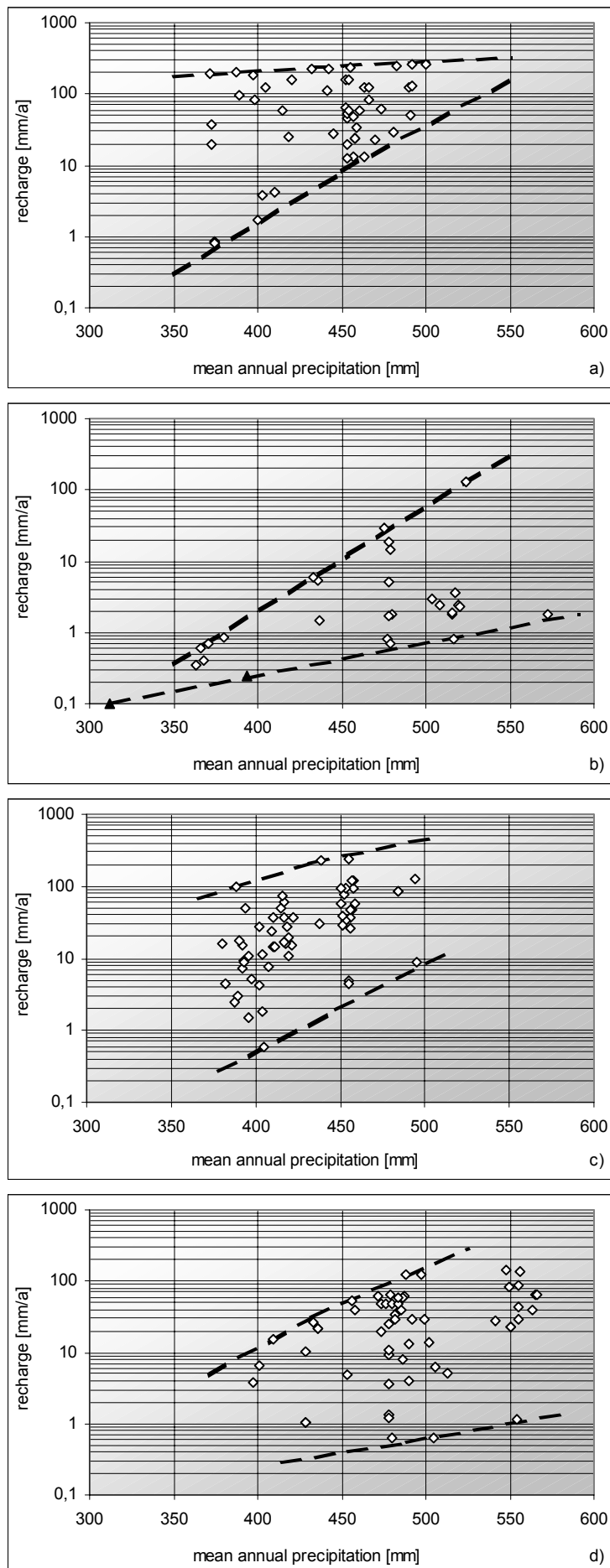


Fig. 5.6-5: Plot of recharge values from chloride balance method at the GWD against mean annual precipitation for four different surface properties a) hardrock of the Damara Sequence, b) Kalahari sand, c) hardrocks covered by sand and d) calcrete near surface. Interpreted enveloping functions are indicated by dashed lines. The filled triangles in b) represent the values from chloride profiles in the unsaturated zone.

Recharge in areas with calcrete near the surface is given in Fig. 5.6-5d. The recharge mechanism that occurs in calcrete is a sort of preferred flow path recharge. Calcrete allows water to infiltrate along joints, cracks or karstified structures. Only seldom calcretes allow very little infiltration (Chapter 5.2). Therefore the medium slope of the plotted recharge values versus precipitation for calcrete is interpreted as preferred flow path infiltration, where most of the samples for the GWD of the research area plot closer to the upper limit than to the lower.

The phenomenon of anion exclusion, that might feign higher recharge rates, has to be discussed here, as locally deep percolation rates of more than 100 mm were observed. But, since anion exclusion is induced by repulsion from the soil matrix, this problem is constrained to diffuse recharge through porous substratum. As the high recharge rates are thought to be induced by preferred flow, joint hard rocks and karst features, no overestimation of recharge rates by anion exclusion is expected in this study.

5.7 Regionalisation of recharge by inverse hydrochemical approach

5.7.1 Method

Chloride has two major advantages that make it useful for the definition of recharge area: it is highly soluble in groundwater and from the geological observation it is confirmed that chloride does not occur from geogenic sources in the research area. In this study it is used to regionalise groundwater recharge by an inverse hydrochemical approach. "Inverse" is here introduced as not the actual process is simulated (forward), but conclusions are made backward: the result (chloride concentration in a water) allows to define the cause (recharge or discharge).

Although in some research projects (e.g. WRABEL, 1999; JACKS & TRAORÉ, 2000) the recharge amount has been calculated by applying the chloride mass balance method to the saturated zone anywhere in a catchment, these applications were not appropriate as the lateral inflow component was not considered there. The observation of the chloride concentration in a single well within a catchment cannot reflect the recharge amount, but the distribution of chloride data of several wells along groundwater flow paths represents the distribution of recharge and discharge. The basic assumptions and decision path of this inverse hydrochemical recharge regionalisation approach are summarised in Fig. 5.7-1. Between two wells along an assumed flow path the chloride content can either decrease, increase or stay constant. If the chloride content decreases it can only result from mixing with water that has a lower chloride content. If mixing with other groundwater is excluded (this might occur in confluent groundwater flow areas) the decrease can only result from inflow of recharge water. If chloride content increases

along a flow path, this can either result from evaporation or transpiration which would be indicated by low groundwater surface distance and/or dense vegetation. Increasing chloride content can also result from decreasing recharge amount along the flow path or from mixing with uprising deep saline groundwater. If the chloride content along a flow path stays constant it can either document the absence of recharge and evapotranspiration, or recharge water has exactly the same chloride concentration as the groundwater.

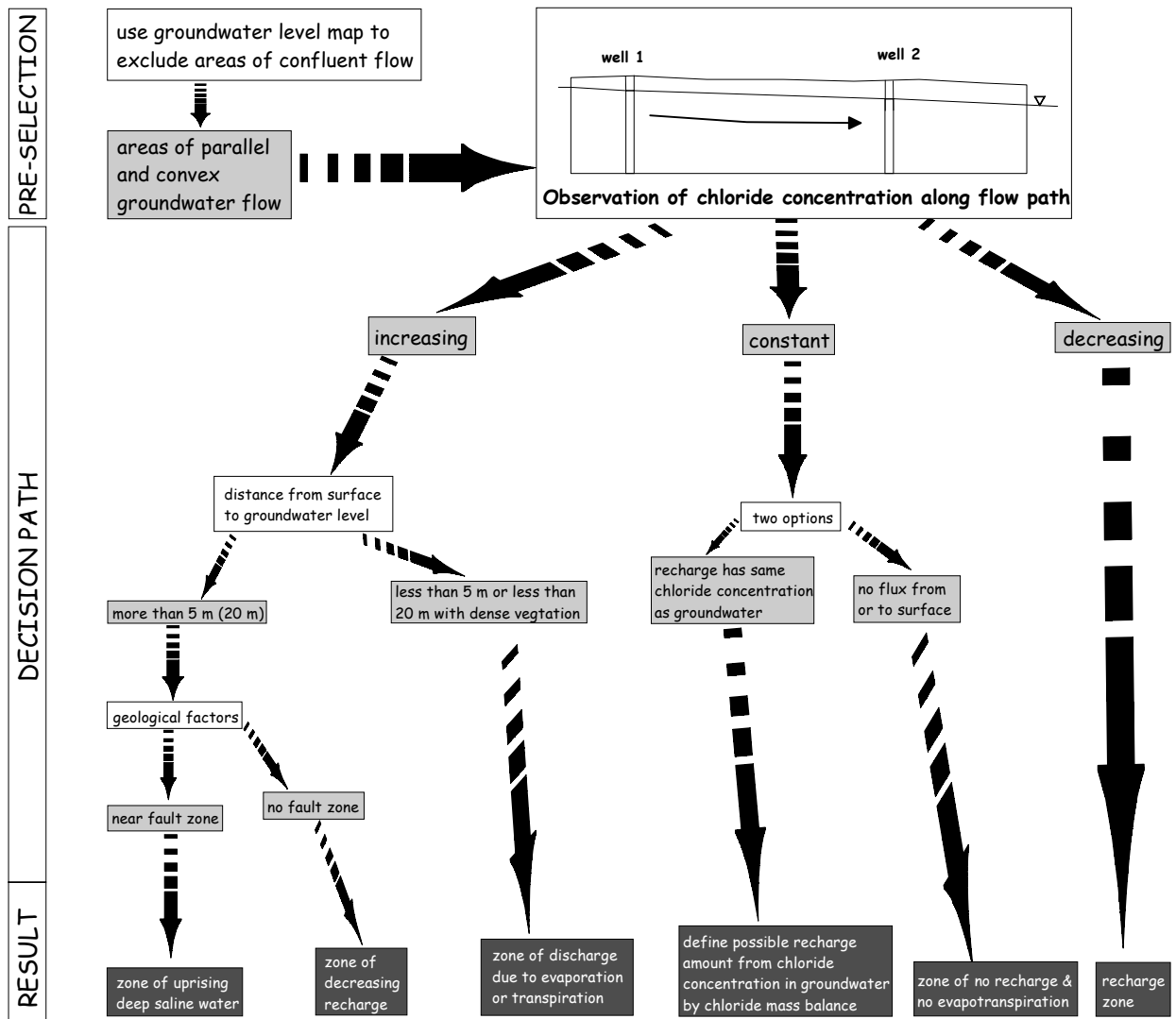


Fig. 5.7-1: Summary of the assumptions and the decision path for inverse hydrochemical recharge and discharge zone definition approach.

First of all, areas of convex flow according to the groundwater level map (Fig. 4.1-1) have to be excluded for this method as the mixing of different groundwater here overprints the recharge and

discharge processes that should be identified. Recharge in these areas is only identifiable, if groundwater with a chloride concentration lower than all upgradient groundwater types occurs. Further areas had to be excluded due to a lack of data. This resulted an excluded area of approximately 43 000 km² ($\approx 25\%$ of the research area). In a next step, chloride concentration of approximately 4100 wells (Appendix D) for the selected part of the research area have been plotted together with groundwater flow directions in a georeferenced frame using SURFER (GOLDENSOFTWARE, 1999). It is not appropriate to use any regionalisation model to achieve a reliable gridded data set of chloride concentration due to the poor variogram (Fig. 5.7-2).

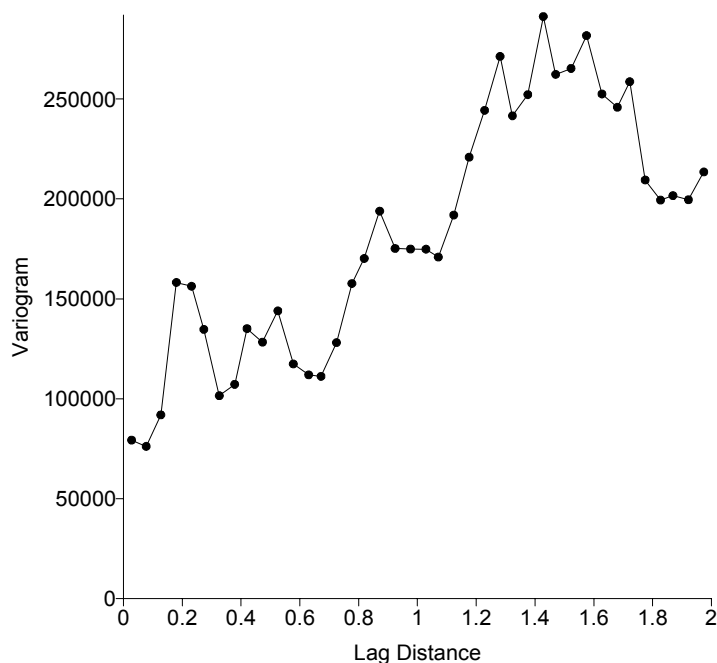


Fig. 5.7-2: Variogram for measured chloride concentration in groundwater samples.

Following the flow direction it was noted (digitally) whether chloride concentration between two wells increases, decreases or stays constant. As no areas in which the chloride concentration stayed constant were found in the research area, this case need not to be further considered. Areas of decreasing chloride concentration along flow paths are assumed to be zones of recharge. In a further step, these zones were characterised by precipitation amount and by geological and surface features, and the appropriate recharge rate as presented in Chapter 5.6 was assigned.

For the zones of increasing chloride concentration the most complex decision path has to be used. For each of these zones the distance from surface to groundwater level was checked and for areas with groundwater levels at less than 5 m it is assumed that those areas represent

discharge areas due to evaporation. For groundwater levels at 5 to 20 m below surface it was further checked by a total vegetation index produced from satellite images if these areas show dense vegetation, e.g. with deep rooting Acacia. If this yielded a high vegetation index, these areas were assumed as zones of transpiration (for more details see Chapter 5.8.3).

As no occurrences of uprising deep saline water associated with fault zones were reported or observed in the research area, it is assumed that the increasing chloride concentration is caused by decreasing recharge rates only. For these zones a gradient of recharge amount was produced by digitising point data of constantly decreasing recharge rates between the wells. From this data set a raster image was produced using the inverse distance to a power function.

The combination of

- (1) the recharge areas from decreasing chloride areas with
- (2) the "background recharge" in the areas of increasing recharge and
- (3) the evapotranspiration

resulted in a recharge image for a large part ($\approx 75\%$) of the research area.

5.7.2 Results and interpretation

The spatial distribution of areas with decreasing and increasing chloride concentration of the research area is in given in Fig. 5.7-3. Approximately 10 % of the area that is appropriate to be examined by the given method have been found to be characterised by decreasing chloride concentration and are thus directly assumed to be recharge zones. 30 of these 259 recharge zones are constrained to hardrock ridges while 80 are only partly characterised by hardrock areas, and 149 are not associated with any hardrocks. 34, mostly small, areas are constrained to the major ephemeral rivers and 14 are partly connected to flood courses.

Any of these recharge areas need not contribute a large amount of recharge to the groundwater system but the amount must be significant enough, compared with the lateral influx to the sampled compartment, to noticeably decrease the chloride content. The contribution to the total recharge amount of the research area from the presented method is summarised in Table 5.7-1. The net recharge inflow to the research area is $1.67 \cdot 10^8 \text{ m}^3/\text{a}$, which is equal to 1.39 mm/a if it were equally distributed across the considered part of the research area. If a recharge of 0.5 mm/a for the southern and 3 mm/a for the northern excluded areas is added, assuming that no further discharge occurs (as groundwater is far from surface in these areas), these areas would contribute approximately $7 \cdot 10^7 \text{ m}^3/\text{a}$ which would result in a entire balanced recharge amount of $2.4 \cdot 10^8 \text{ m}^3/\text{a}$. This equals to 1.5 mm/a assuming an equal distribution across the entire research area. Comparing the received recharge amount with the discharge zone at the Makgadikgadi

depression, where approximately 3000 km² of shallow groundwater allows evapotranspiration in the order of 3 to 6*10⁸ m³/a (assuming discharge amount of 100 - 200 mm/a), suggest that the recharge range calculated for the research area is plausible. 1.04*10⁸ m³/a of the balanced recharge amount are developed within the Eiseb-Epukiro-Catchment.

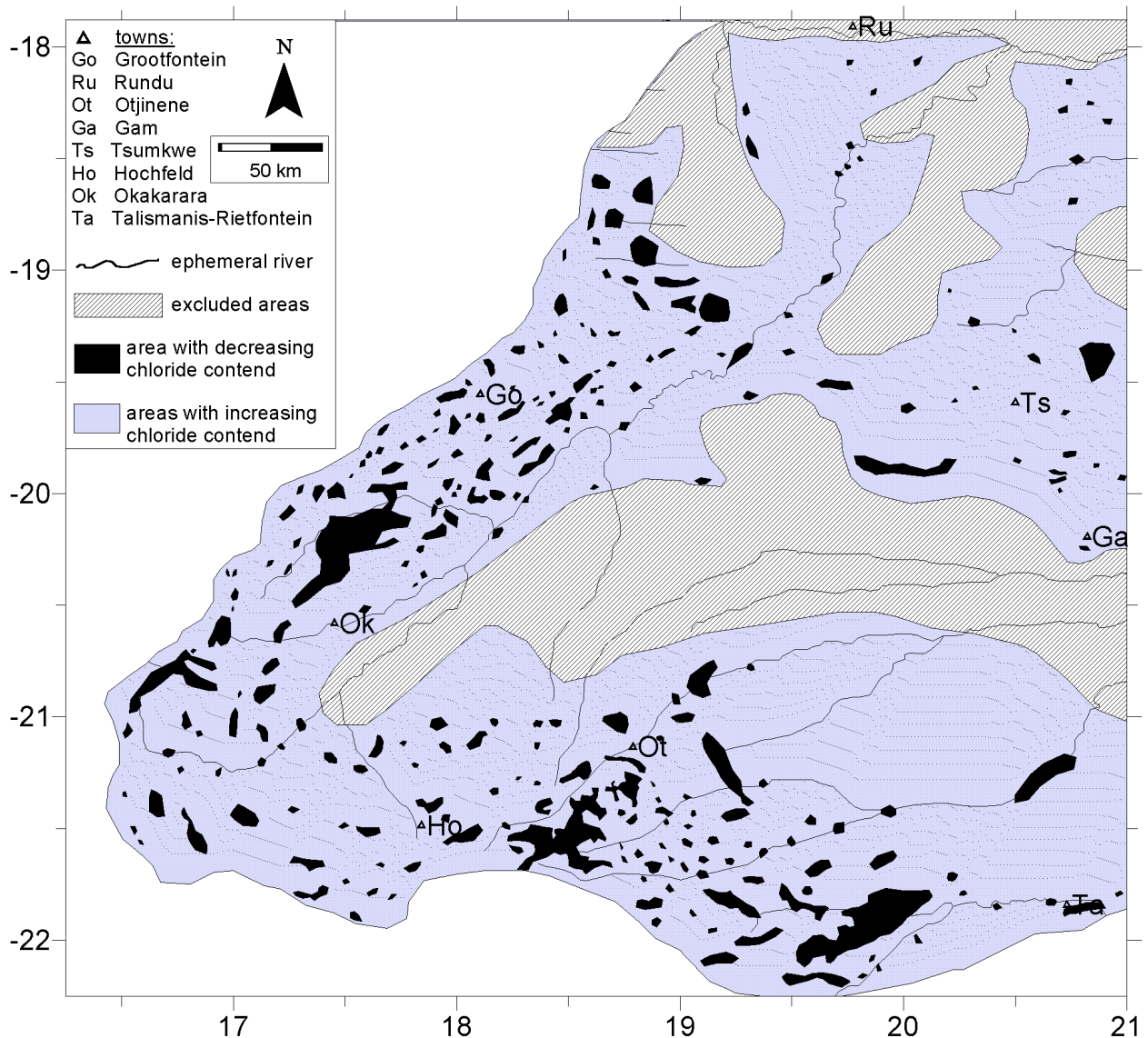


Fig. 5.7-3: Distribution of areas with decreasing and increasing chloride content along regional groundwater flow direction.

The distribution of discharge and recharge zones is given in Fig. 5.7-4. While the areas of evapotranspiration cover only a small portion of the research area, they contribute to a loss of approximately 30 % of the recharge amount. The Otavi area shows the largest contribution to the recharge amount. The Hochfeld area also reflects a major recharge area. In general the recharge decreases from the rim to the centre.

Table 5.7-1: Summary of the results from the recharge regionalisation by inverse hydrochemical approach

	Calculated volume for the considered part of the research area [m³/year] (excluding the hatched areas in Fig. 5.7-4)	Equal to a ponded height [mm/year]
Recharge from areas with decreasing chloride content	$6.66 \cdot 10^7$	0.55
Recharge from areas with increasing chloride content	$2 \cdot 10^8$	1.67
Total recharge amount	$2.67 \cdot 10^8$	2.22
Evapotranspiration from areas with increasing chloride content	$7.91 \cdot 10^7$	0.66
Balanced recharge amount	$1.67 \cdot 10^8$	1.39

In the excluded areas, one area with increasing recharge could be identified, as all the groundwater that might mix the water at this well shows a significant higher chloride content compared with this sample. This well (S20.6613°/E20.7642°) at a small farm near the Embo Game Park showed a low chloride content of 3.2 mg/l only. It indicates that at least very locally the recharge must be higher than 59 mm/a (assuming a mean annual precipitation of 380 mm/a, and a chloride content in the precipitation of 0.5 mg/l). This might reflect recharge along the Eiseb Lineament which is accompanied by calcrete occurrences and thus locally allows very fast preferred infiltration along open cracks.

An important consequence of this regionalisation procedure is that it does not give discrete recharge values for every point in the research area. Rather, it gives integrated values for discrete areas. One of the concepts of regional data (which are data that are not taken at points but over regions and thus have an areal distribution) is that one has to find a satisfactory scale of resolution since every area could be infinitely subdivided: every km² can be subdivided in several m², every m² in several cm², every cm² in several mm², A higher output resolution would not result in an increased accuracy, but an increased amount of input data may. Thus the method presented in this section has to be seen as "pioneer work" for recharge regionalisation by the inverse hydrochemical approach and calls strongly for further research.

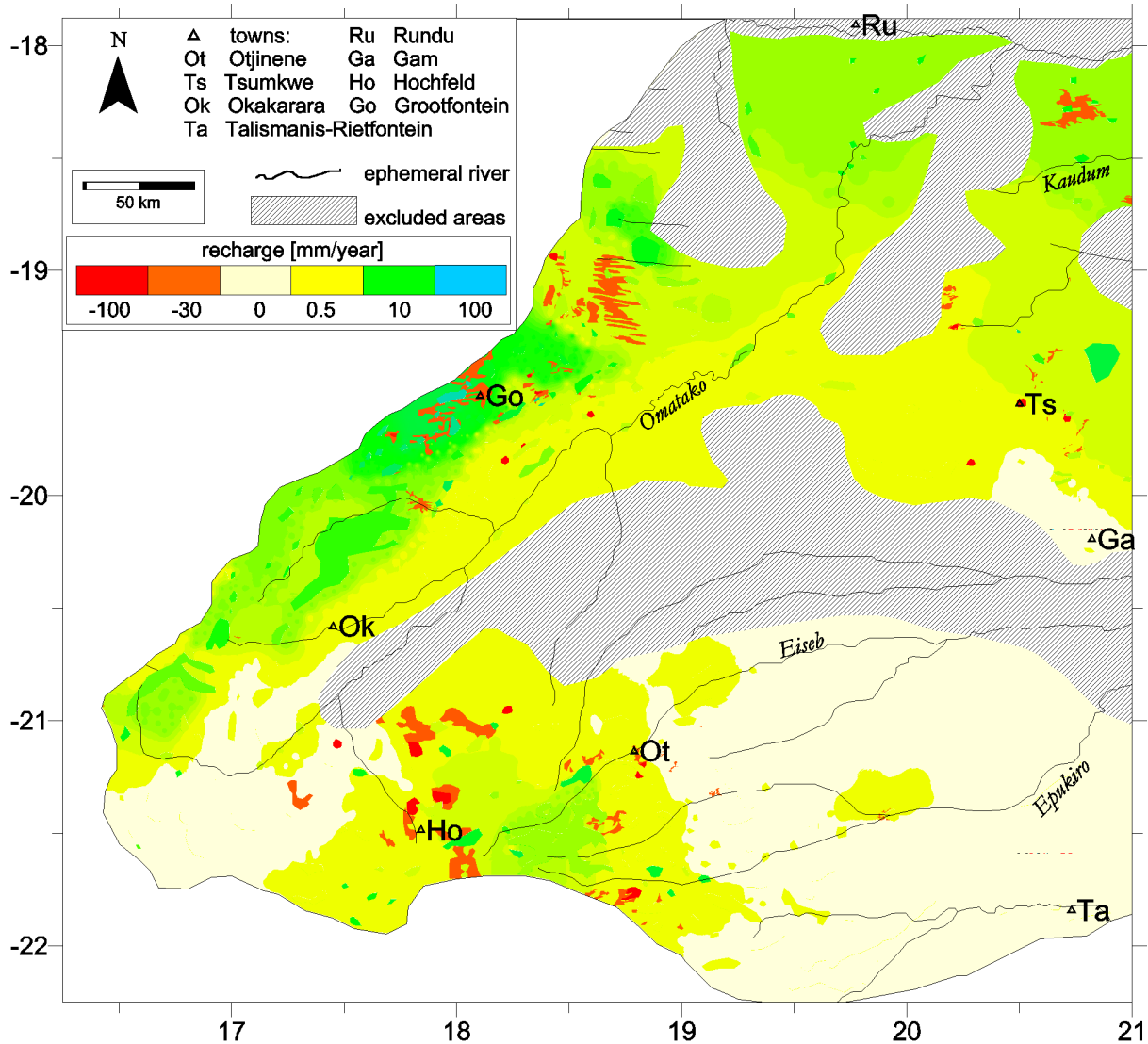


Fig. 5.7-4: Distribution of recharge and discharge zones in the study area. Recharge areas appear in yellowish to greenish colour, while discharge zones are given in orange to red colours. The excluded areas for the inverse hydrochemical recharge regionalisation approach are hatched.

5.8 Regionalisation of recharge and evapotranspiration by the use of satellite images

After the reconnaissance of processes that contribute to recharge and the determination of recharge rates, one of the main purposes of this study is to project those results on the regional scale. MEIJERINKS ET AL. (1999) and BALEK (1988) have proposed satellite images as a powerful tool for regionalisation in hydrology, especially in arid areas. The forward method that has been developed in this study uses satellite images to define major zones of recharge and discharge. This method is subdivided into three basic steps and a final combination of the three sub-results:

- a) Satellite images are used to define hardrock recharge regions to which recharge amounts are assigned.
- b) A mathematical function is used to define the recharge through soils and unconsolidated sediments.
- c) Distance from surface to groundwater in combination with satellite images have been used to define evaporation and transpiration zones.

5.8.1 Regionalisation of hardrock recharge by the use of satellite images

In this chapter the methods for regionalisation of recharge in a forward approach are described in detail as the regionalisation of recharge is not yet a well developed process. "Forward" is used here to describe a regionalisation method that is based on process understanding, namely that the recharge rate in hardrock areas is significantly higher than the recharge rate in soil covered areas (Fig. 5.6-5). Additionally the reason for selecting satellite images as the only appropriate tool for this purpose are presented in the section "Selection of source data" before presenting the results of the regionalisation.

Method

Satellite images were first available from sources in the USA with ERST-1 in 1972. This system was later renamed Landsat and data from Landsat Thematic Mapper 5 (Landsat TM 5) are now widely used. This system is a passive opto-mechanical scanner with a rotation mirror system that rotates along an axis parallel to the flight line. Multispectral data are collected by dividing the reflected ray over a prism to subdivided wavelengths that are then detected by crystal-sensors.

Landsat TM 5 detects 7 different spectral zones (channels or bands). Most of them are at a resolution of 30 x 30 m, only channel 6 (thermal infrared) has a resolution of 120 x 120 m. Spectral zones of Landsat TM 5 are given in Table 5.8-1. The more modern TM 7 scenes have a further panchromatic channel and a higher resolution (20 x 20 m) but TM 5 scenes were expected to be fully satisfactory for the purpose of this study, as well as being affordable.

Remotely sensed data are stretched due to size effects, whereby the marginal parts of the detected area are further from the scanner than the central parts of the area. Additional stretching occurs due to panorama effects and incomplete time and location consistency as the scanner and the scanner's mirror are moving during detection. The de-stretching has already been processed for data available from the USGS that have been used in this study. The Landsat TM 5 scenes are available in digital form on CD-ROM as band sequential raster images in 8-bit format. Besides the raster data a header file is delivered with the data that contains information about the

georeference and the raster image size. With this information the data can be read into the TNTmips system and georeferenced with the available data points as a four point georeferencing where the edge points are given. The georeferencing of the images has been checked for accuracy by comparing known geographic positions of features such as landing strips, farm houses or road intersections with the position given in the satellite image.

Table 5.8-1: Spectral bands of Landsat Thematic Mapper 5 and according wavelength

Band	1	2	3	4	5	6	7
Name	blue-green	green	Red	near infrared	middle infrared	thermal infrared	middle infrared
Wavelength [µm]	0.45-0.52	0.52 - 0.6	0.63 - 0.69	0.76 - 0.9	1.55 - 1.75	10.4 - 12.5	2.08 - 2.35

The major step when using remotely sensed data is to visualise the digital data. This can be done either as grey scale images for every single channel or by producing true colour or false colour composites of three channels on the red, green and blue channel of the processing software, respectively. For a true colour composite the channels of the visible light are assigned to the visualising channel according to the detected wavelengths of the red, blue and green spectral zone. This composition gives a "natural impression" of the surveyed area. However, combination of visible and infrared channels give better results for material-specific distinctions (maximum information amount). Objective best channel combinations can be calculated using the mathematical methods of covariance calculation between rasters and calculation of the Optimum-Index factor (PRINZ, 1996). Best combinations (highest information amount) were often found to be 1-5-7, 1-4-5, 1-3-5, 2-5-7 and 3-5-7-combinations (ZUMSPREZEL & PRINZ, 2000). Correlation values for a test site (south-eastern part of the topographic sheet 1920 Tsumkwe) are given in Table 5.8-2 from which it was concluded that the optimum combination for the research area is 1-4-7.

Table 5.8-2: Correlation values between possible combinations of Landsat TM 5 channels for a test region of the study area. The lowest for correlation values are shaded in light grey

Correlation	channel 1	channel 2	channel 3	channel 4	channel 5	channel 7
channel 1	X	X	X	X	X	X
channel 2	0.928	X	X	X	X	X
channel 3	0.84	0.956	X	X	X	X
channel 4	0.718	0.875	0.932	X	X	X
channel 5	0.719	0.862	0.928	0.875	X	X
channel 7	0.701	0.813	0.861	0.756	0.941	X

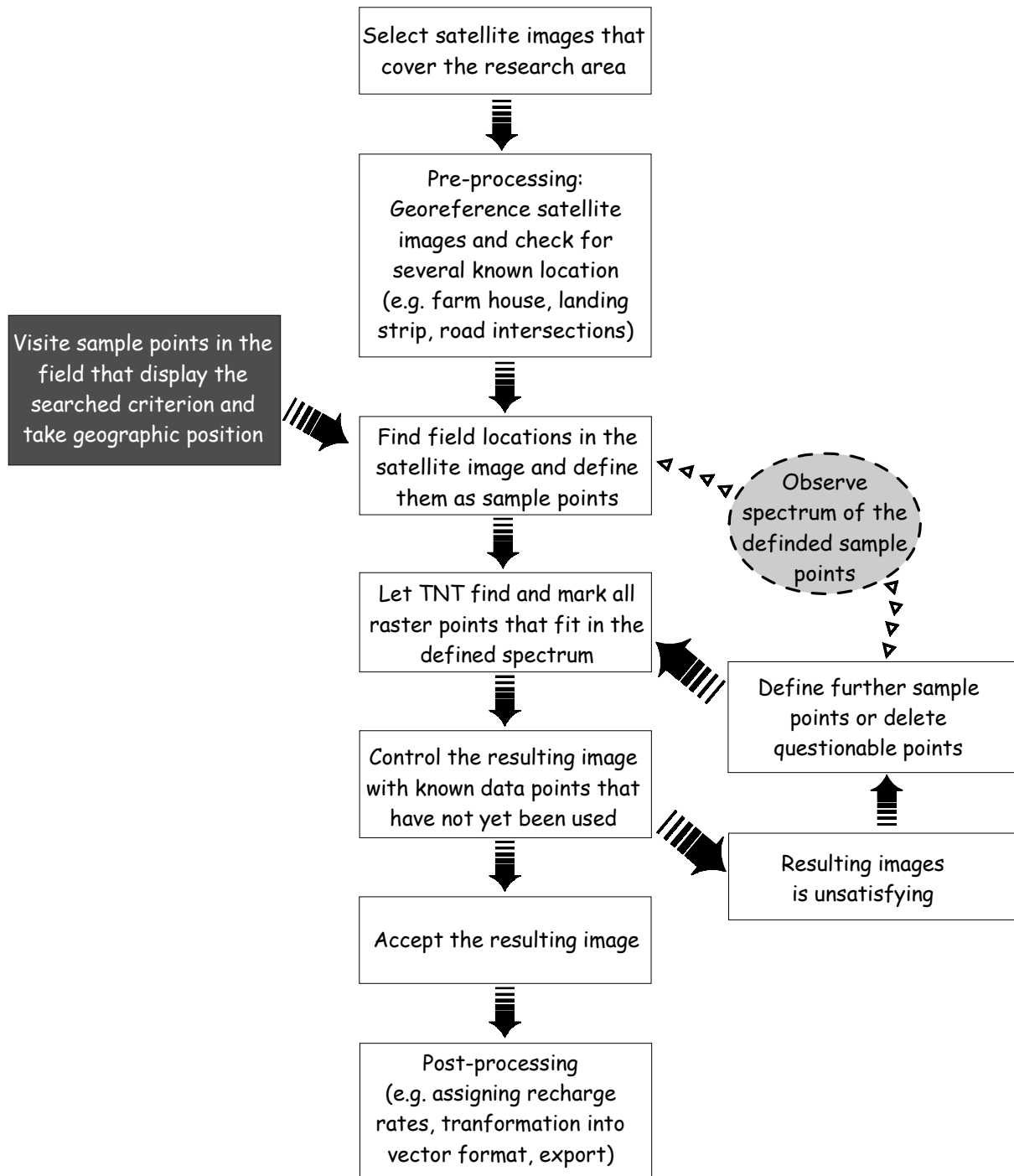


Fig. 5.8-1: The process of feature mapping. In this study TNTmips by MICROIMAGES (1996) is used.

Raster images can also be displayed as histograms that show the frequency distribution of each grey value. To achieve an optimal contrast result for the visualisation of satellite images, the image's colour scale should be stretched according to the observations from the histogram. Colour scale stretching does not change the original data, it only makes them better visible for the construction of our eyes.

Classification of satellite images can be made either by automatic classification, supervised classification or by a feature mapping procedure. Unsupervised classifications mostly lead to unsatisfying results as mixed pixels are more frequent in the images than pure pixels that characterise a certain feature. Supervised classification uses a training side in which features are well known and extrapolates the classified feature spectra to the desired area. These methods are highly demanding of field knowledge, but when processed appropriately they give satisfying results. Feature mapping is a special case of supervised classification. This process is not intended to classify an entire region, but for mapping of a certain feature of interest for a region, which is significantly quicker. Feature mapping is thus the appropriate method for the definition of recharge areas in the research area. The process algorithm for feature mapping is documented in Fig. 5.8-1.

Table 5.8-3: Summary of the Landsat TM 5 scenes that have been used for recharge regionalisation with size and extent

Number	Date of acquisition	Rows	Columns	Upper right corner
178-073 & 178-074	20 th Oct 1984	12826	9233	S17°54'16.5676/E18°49'45.4844
178-075	13 th Dec 1986	7326	7931	S20°41'41.1322/E18°08'44.942
177-073 & 177-074	7 th June 1984	12128	7357	S18°06'01.8006/E20°24'58,1870
177-075	7 th June 1984	7820	7176	S20°45'12.9010/E19°45'56.3017
176-073 & 176-074	2 nd July 1984	12119	7372	S18°06'13.3248/E21°58'22.1728
176-075	2 nd July 1984	7223	7872	S20°44'26.6002/E21°19'11.2239

The basis for any feature mapping is the appropriate location of the sample points. Thus georeferencing of the satellite image has to be checked very carefully for the areas that cover the study area of north-eastern Namibia (Table 5.8-3). If the georeferencing was found to be sufficiently accurate, localities that were visited during field trips in the research area were recognised in the according satellite image by their geographic position. A knowledge of how different features appear in satellite images was thus developed.

As it is concluded from the observation of point recharge values that hardrock areas contribute more significantly to the total recharge amount of the catchment than soft sediment or soil covered areas, it is required to map areas where hardrocks outcrop and in a later step assign recharge rates to these areas. Therefore feature mapping of hardrock areas was selected for the definition of major recharge areas. To reduce the calculation time, not all satellite scenes were used simultaneously but were divided into sub-scenes. For each of these sub-scenes the channels 1,2,3,4,5 and 7 were selected to be the basis of the feature mapping. In a combination of the

channels 7-4-1 the geographic positions of the known hardrock areas were designated as sample points. The range covered by these sample points was selected and TNTmips was used to search for all points that fall within the given limits. The resulting image was checked with known localities of hardrocks that had not been used for the definition of sample points, and by checking that points that are known to be other features were not selected by the process. The resulting image was accepted and transformed into a new raster map "hardrock". After these steps had been processed for all data sub-scenes a single map was combined. A recharge value has been assigned to each of the defined major recharge zones according to the observed surface, geology and mean annual precipitation following the results from the chloride mass balance (Chapter 5.6).

Selection of source data

In a forward method for recharge regionalisation it is aimed to map possible recharge areas and apply recharge amounts to them. In such an approach the accurate selection of source data is of major importance and therefore three different data sources were tested for their reliability for mapping of surface properties. From this, the appropriate data source has been selected for further processing. For the eastern part of sheet 1920 (Tsumkwe area) a geological map (1:250 000), aerial photographs and satellite images were used to define areas where hardrocks outcrop at the surface, while for several other areas satellite images and geological maps only were compared.

The method to define hardrock areas by satellite images is described above in detail. For the geological map the areas that are marked as "pre-Kalahari hardrocks" were transformed from vector files into raster files at a very detailed scale so that scale effects are of minor importance (Chapter 2.4).

For the interpretation of aerial photographs, either a subjective or an objective mapping tool could be used. A subjective tool would assign the property "hardrock" to areas that show darkest grey tones and the form that this feature makes, e.g. hardrock being the most likely interpretation for a ridge. With this process the spatial extent of each feature might differ significantly depending on the user (Fig. 5.8-2).

A more reproducible tool is an automatic objective interpretation according to the grey value and has thus been used in this study. For this, the aerial photography needs to be transformed into digital form by use of a scanner. Importing such images into the TNT raster format assigns a grey value to every cell with 0 representing black and 255 representing white (Fig. 5.8-3).

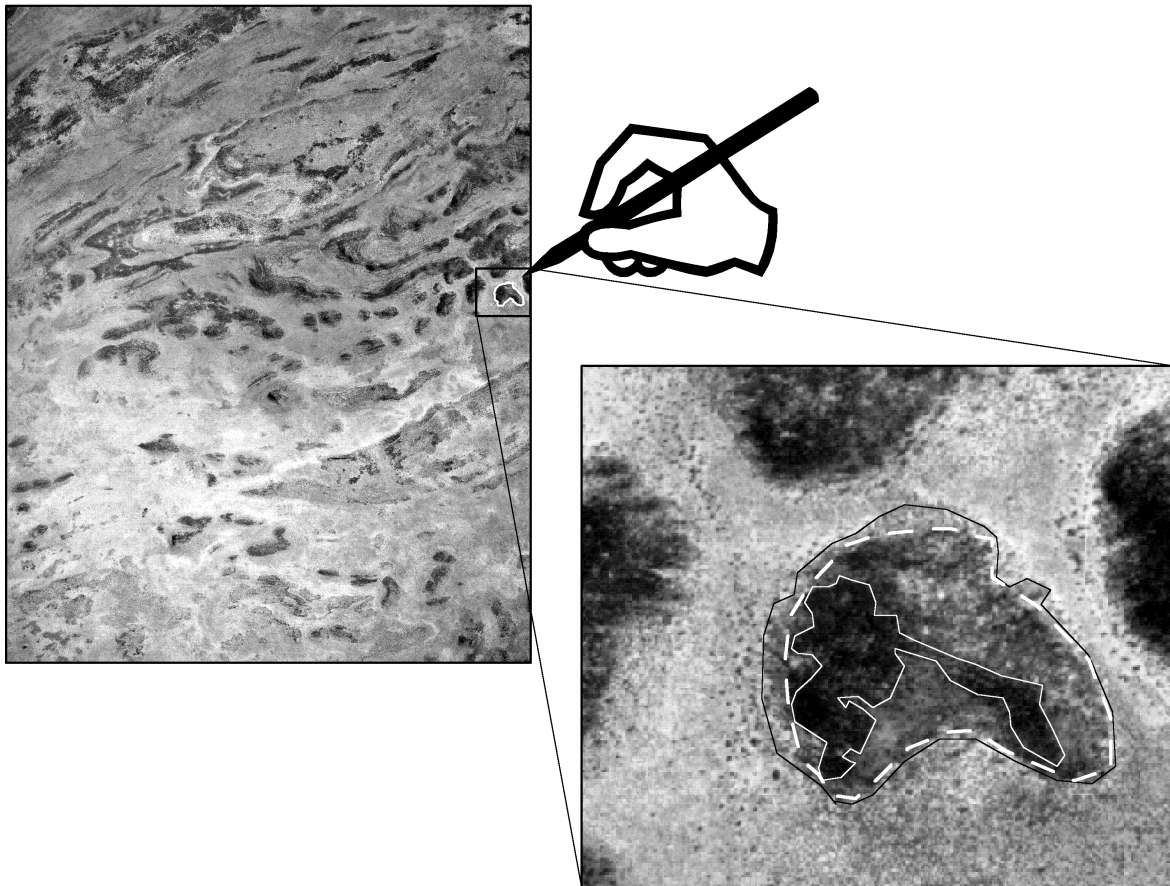


Fig. 5.8-2: Demonstration of subjective mapping of hardrock areas in aerial photograph for an example from the Aha Hills. The zoomed insert shows three different areas that could be mapped by different users as a hardrock region with significant spatial differences (surrounded by black solid line, white solid line and white dashed line).

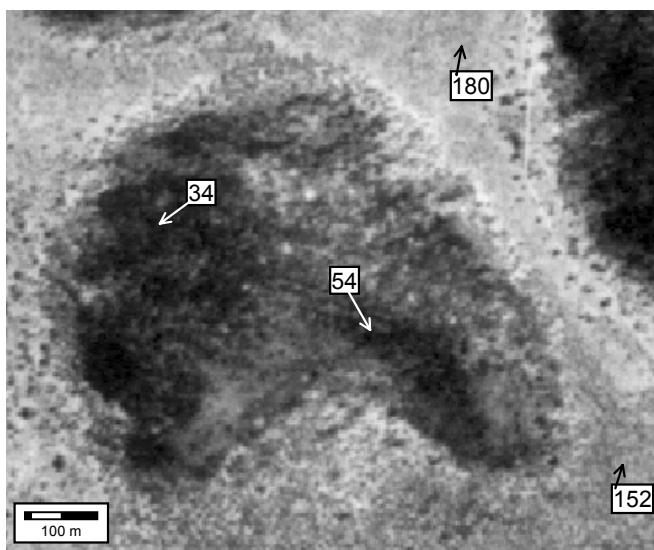


Fig. 5.8-3: Some sample grey values for a scanned, zoomed aerial photograph. Darkest grey tones are represented by low values, light tones by highest values. Threshold values have to be defined for further automatic classification.

For the definition of hardrock areas a threshold value has to be assigned, below which the feature "hardrock" is assumed, since hardrocks produce the darkest grey tones in aerial photographs. From the definition of a threshold value a binary raster is obtained with yes (1) or no (0) allocated to the feature hardrock.

With the described methods, it was found that satellite images always map the smallest amount of the selected area to be hardrock area. The results for three regions in the Tsumkwe district are given in Table 5.8-4. It is concluded, that the geological map is always exaggerating the real hardrock areas as it does not take account of thin covers of soils. For aerial photographs it is concluded that the invariably higher areal proportion classified as hardrocks, compared with satellite images, results from the lack of distinction between dark grey tones due to intense vegetation and not only due to hardrock outcrops.

Table 5.8-4: Result from mapping the feature "hardrock" by three different source data sets

Area	Geology	Extent	Area of hardrocks [%]		
			Aerial photograph	Satellite images	Geological map
Aha	Dolomite	20°41 E – 21° E 19°40 S – 19°54 S	27.79	17.69	33.37
Dobe	Quartzite Basalts	20°40 E – 20°50 E 19°30 S – 19°45 S	11.97	7.67	60.6
Makuri	Gneiss	20°40 E – 20°50 E 19°15 S – 19°30 S	11.18	9.31	83.38

Table 5.8-5: Results from feature mapping by satellite images and from geological map

Area	Geology	Extent	Area of hardrocks [%]	
			Satellite images	Geological map
Tsumkwe	Gneiss, Dolomite	20°30 E – 21° E 19°25 S – 19°55 S	11.51	32.52
Hochfeld	Quartzite, Schists	17°50 E – 18°30 E 21°30 S – 21°45 S	41.82	78.13
Gaikos	Quartzite, Schists, Gneiss	18°20 E – 18°30 E 19°20 S – 19°30 S	31.33	60.39
Hohenstein	Schists, Granite	16°50 E – 17°10 E 20°20 S – 20°40 S	44.39	99.5
Lister	Quartzite, Schists	20°45 E – 21° E 21°45 S – 22° S	7.66	95.54
Gam	Dolomite, Schists	20°45 E – 21° E 20°10 S – 20°20 S	2.26	8.22
Nhoma	Quartzite	20°45 E – 21° E 18°50 S – 19° S	1.9	78.61

In Table 5.8-5 further results of the comparison of hardrock areas from geological map and satellite images are given. For some regions the results differ very significantly, e.g. for the area

of Lister the geological map indicates 99.5 % hardrock surface and in satellite images less than 8 % were mapped for this feature. This is, of course, a result of the purpose for which geological maps are normally made: they should also explain the subsurface where rocks are invisible and covered by soil. Geological maps are often used to regionalise groundwater recharge, but it is clear from these results, that geological maps are an inappropriate tool for regionalisation of recharge in this research area. It is further recommended for any other recharge regionalisation to check the data sources for their reliability.

Results

An example for the reconnaissance of field observations in a true colour composite satellite image is given in Fig. 5.8-4. In this figure the pan field south of Tsumkwe is readily visible as many of the pans, aligned in a half moon shape, occur in very striking white because they reflect strongly in the 3 visible light bands. It is assumed that the high reflection results from the lack of vegetation and from calcrete that is exposed directly at the surface. The road from Grootfontein via Tsumkwe to the border is also easily seen and gives good data for testing the georeferencing that has been applied to the data set. Hardrock ridges, e.g. the Aha Hills, appear in dark colours. They are also well defined by their shape. Small rivers are represented by bluish to white colours due to carbonate accumulation. They are also easily recognisable by their shape. Sandy features like dunes appear in yellowish and reddish colours in the true colour composite with interdunes in more bluish to greenish colours, and they are most easily identified by their longitudinal shape. Experienced satellite image users might criticise the "unsharp" appearance of this image (Fig. 5.8-4), especially in the western part. But it was found during this study, that no common sharpening filter gives good results for the research area. The slight fuzziness is due to a thin sand cover and dry vegetation.

Table 5.8-6 and Fig. 5.8-5 summarise the observed reflection patterns for some selected features of a part of the research area. The south-eastern part of the topographic sheet 1920 Tsumkwe has been selected for this purpose as a large range of features is displayed in a relatively small area. From the given reflection patterns, it is very clear that no single channel can be used to distinguish between features, but only a combination of all channels will be successful. Hardrocks show the lowest reflection in all channels although they overlap with observed values in the valleys between hardrock ridges of the Aha Hills in the channels 1,2 and 4. However, these features are separated from another by the lower reflectance of the hardrock in the visible red and middle infrared wavelength (Fig. 5.8-5).

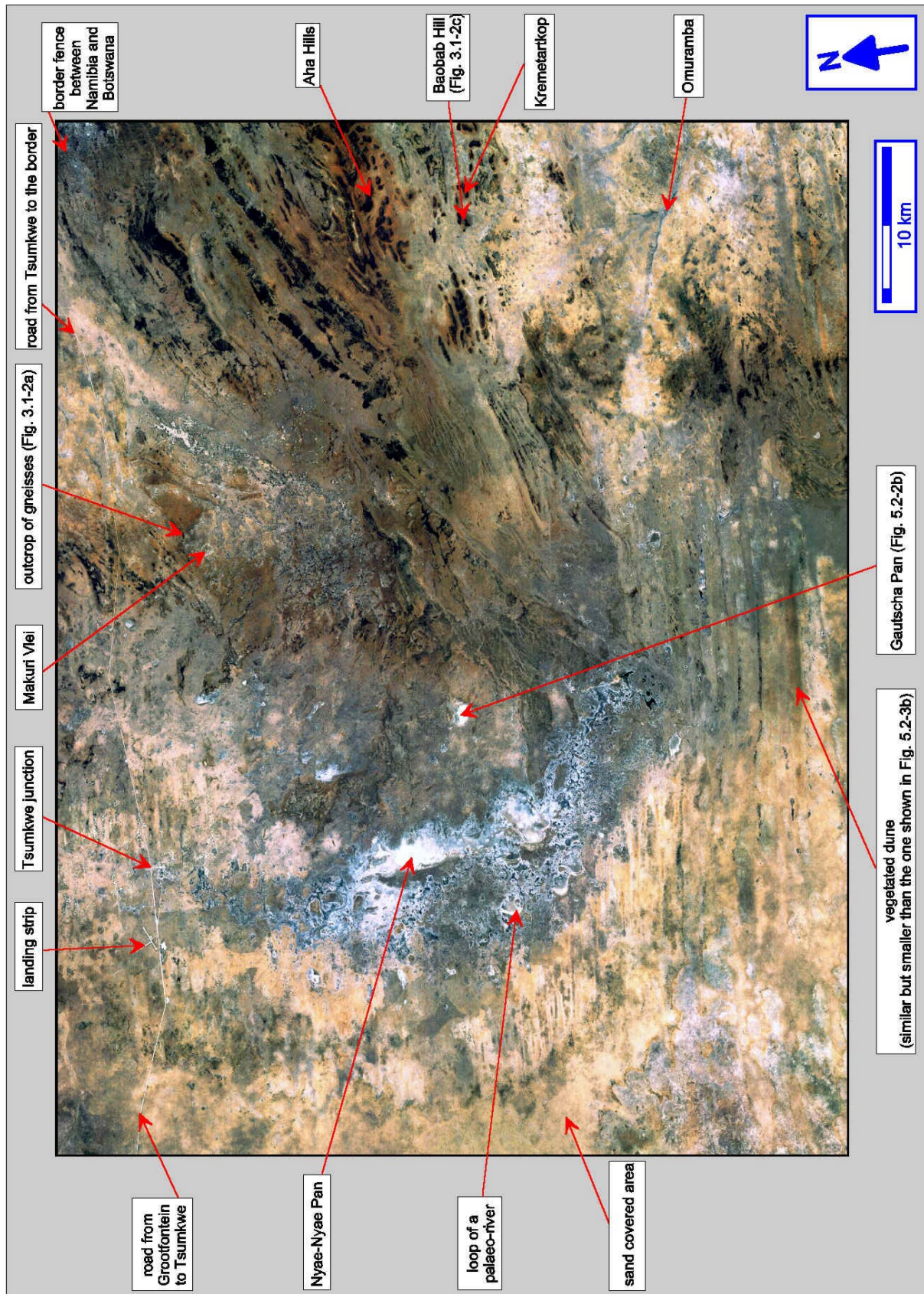


Fig. 5.8-4: True colour composite (3-2-1 RGB) image of the south-eastern part of the topographic sheet 1920 Tsumkwe with pan field and Aha Hills. (Compiled from Landsat TM 5, scenes 176-073 and 176-074, date of acquisition 2nd July 1984).

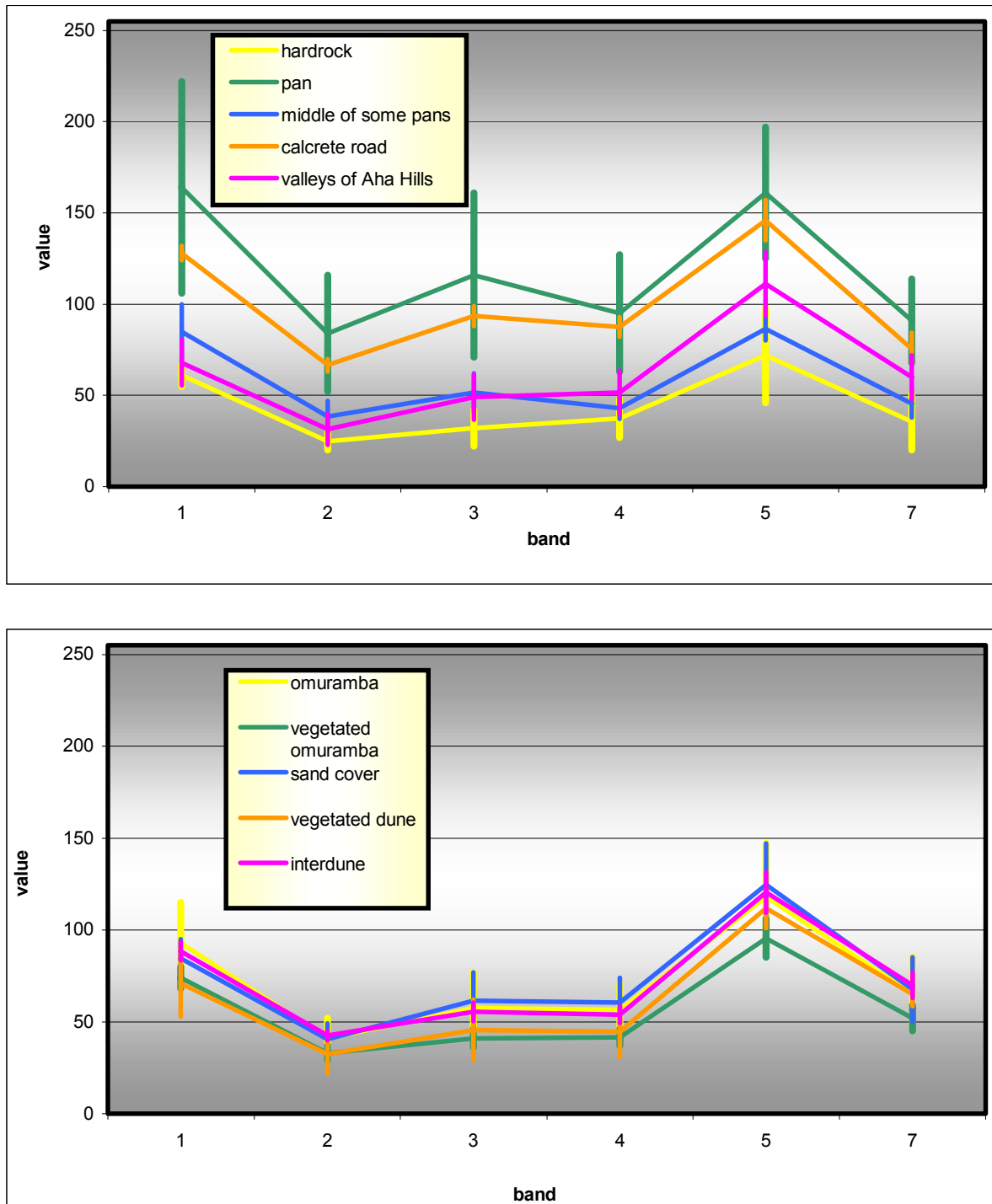


Fig. 5.8-5: Reflection patterns of ten different features in the south-eastern part of topographic sheet 1920 Tsumkwe (same area as displayed in Fig. 5.8-4). The value range of reflecting intensity is given as a line of mean values with observed range indicated as point bars at every band. Values that are used for diagram development are given in Table 5.8-6.

Pans are also clearly distinguishable from other features due to an overall high reflectance. The middle part of some pans (e.g. Dobe Pan, Nama Pan, Namatakwar Pan) occurs with significant lower reflection, which might result from moisture and from some hardrock outcropping flatly

with only a thin or no calcrete cover. This moves the reflection pattern towards the reflection pattern of hardrock ridges.

For comparison, the reflection range of the gravel road from Grootfontein is also indicated in Table 5.8-6 and Fig. 5.8-5 (orange line, upper diagram) as the road is built from calcrete mixed with sand and dirt. It is unvegetated as the pans are. The higher reflectance of the pans is likely to occur from clean calcrete with absence of dirt and sand.

The reflection patterns of the sand covered areas and Omiramba are not very easily distinguished from one-another. But is it still noticeable that the vegetated areas reflect weaker than the less vegetated areas. All features that are indicated in the lower diagram of Fig. 5.8-5 show higher reflections in all channels than the hardrocks.

It is concluded from the reflection pattern analysis that pans and hardrock are distinguishable from the rest of the surface properties in the study area by use of the six Landsat TM channels 1,2,3,4,5 and 7. It would be helpful to use the shape of a special feature for a classification but this additional information is not needed and allows thus a supervised feature mapping on the basis of reflection intensities only.

Table 5.8-6: Summary of observed reflection intensities for some features of the south-eastern part of the topographic sheet 1920 Tsumkwe.

Feature	intensity of reflection for					
	band 1	band 2	band 3	band 4	Band 5	band 6
Hardrock	55 - 67	20 - 30	22 - 42	27 - 48	46 - 98	20 - 51
Pan	106 - 222	52 - 116	71 - 161	63 - 127	125 - 197	68 - 114
Middle of some pans	70 - 100	30 - 47	41 - 62	37 - 49	80 - 93	38 - 53
Calcrete road	110 - 146	56 - 77	77 - 110	74 - 101	135 - 157	69 - 82
Vegetated valleys of Aha Hills	63 - 73	29 - 34	44 - 54	47 - 56	100 - 122	53 - 67
Omuramba	71 - 115	30 - 52	38 - 77	42 - 71	89 - 147	45 - 85
Vegetated Omuramba	68 - 80	29 - 37	36 - 46	37 - 46	85 - 106	45 - 59
Sand cover	74 - 95	32 - 49	46 - 77	47 - 74	102 - 147	50 - 85
Vegetated dune	67 - 75	29 - 36	40 - 51	39 - 50	101 - 123	56 - 74
Interdune	76 - 101	34 - 51	43 - 68	42 - 66	103 - 138	58 - 82

An example of supervised feature mapping of hardrocks in the south-eastern part of topographic sheet 1920 Tsumkwe (true colour composite Fig. 5.8-4) is given in Fig. 5.8-6. The structure of the Aha Hills appears nicely in the north-eastern part of the training site. Minor hardrock

occurrences in the central part and in the south eastern part of the selected areas, that are known from field work, appear as well.

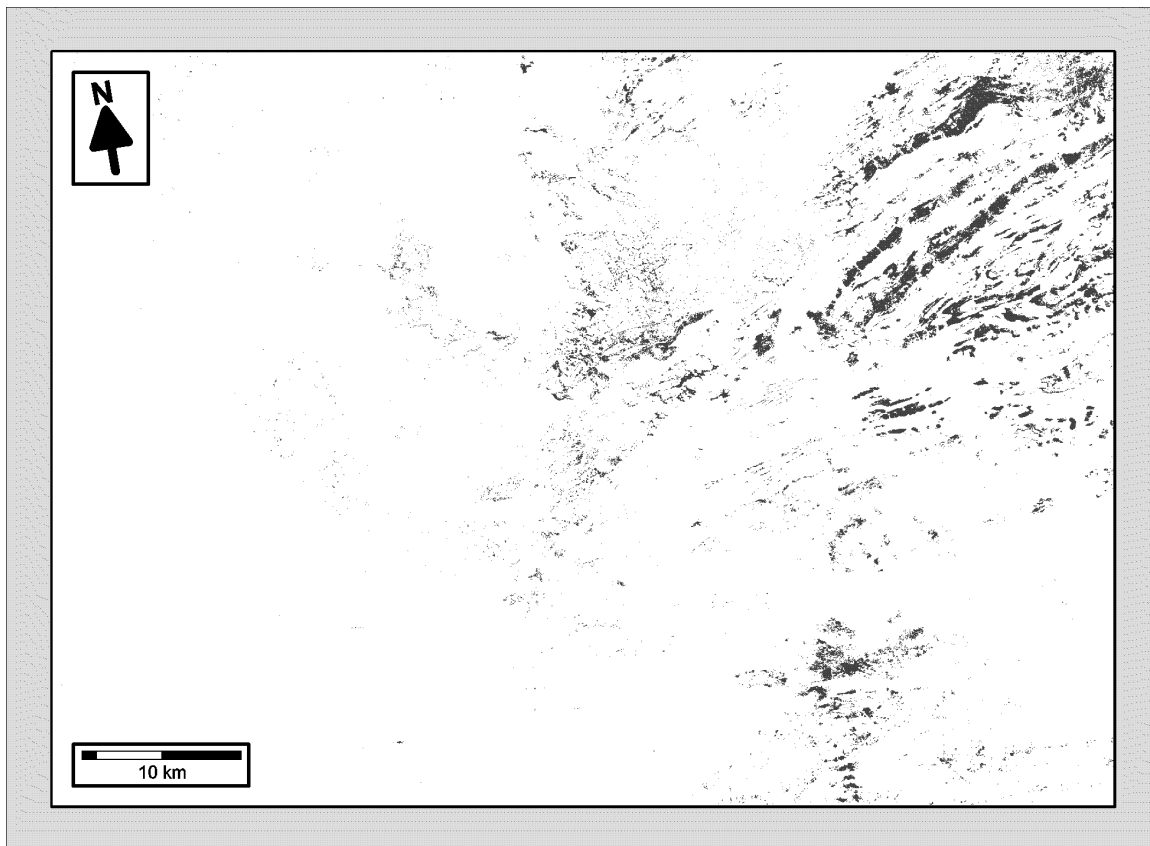


Fig. 5.8-6: Result of a feature mapping "hardrocks" of the area shown as true colour composite in Fig. 5.8-4 with reflection intensities as indicated in Table 5.8-6. Hardrock areas are marked in dark grey.

The results of the feature mapping "hardrocks" for the research area are given in Fig. 5.8-7. Since no hardrocks outcrop directly at the surface in the northern part of the research area, only the southern part (south of Latitude S18.8°) is given here. 6070.7 km² of hardrocks occur in the entire 161 565 km² large research area which is equal to 3.8 %.

The structure of the north-east trending Aha Hills (region 1 in Fig. 5.8-7) appears again very clearly in this classification. Even very small outcrops of Damara schists and limestones are documented in the vicinity of farm Otjoni (region 11 in Fig. 5.8-7). The Omatako Hills (region 13 in Fig. 5.8-7) appear as very distinguishable structures between the two Omingonde areas. In the Omingonde areas (regions 14 and 10 in Fig. 5.8-7) hardrock outcrops are very rare compared to the rest of the western part of the research area. The shape of the Große Waterberg and Kleine Waterberg appear clearly in the Fig. 5.8-7 in the southern part of region 16. Although the Große Waterberg, when observed from the Waterberg Restcamp, appears to be almost exclusively hardrock, the plateau of the Große Waterberg is thickly covered by sand and is appropriately

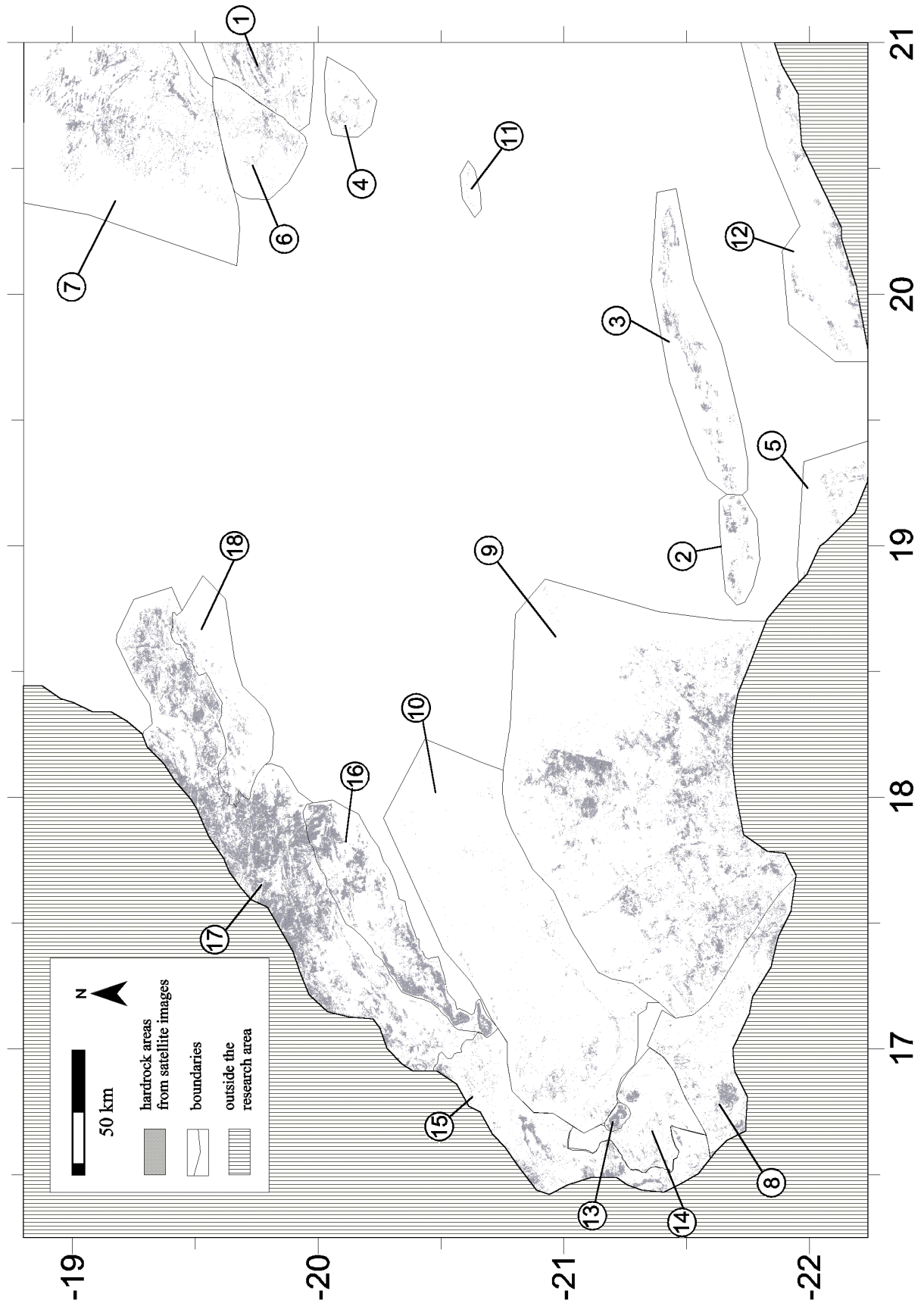


Fig. 5.8-7: Distribution of the hardrock regions in the research area mapped by the use of satellite images. Numbers given here refer to the recharge zone numbers as used in Table 5.8-7 where rain and recharge amount that have been used for the further assignment are documented.

characterised as such by the feature mapping. The largest amount of surface hardrock occurs in the Otavi region (region 17 in Fig. 5.8-7). In the classified image it also appears that the strike of the Damara rocks in the north-east of the research area bends from north-eastern directions in region 1 (Aha Hills) and southern part of region 7 (Nhoma) to north-western direction in the northern part of region 7 (Nhoma).

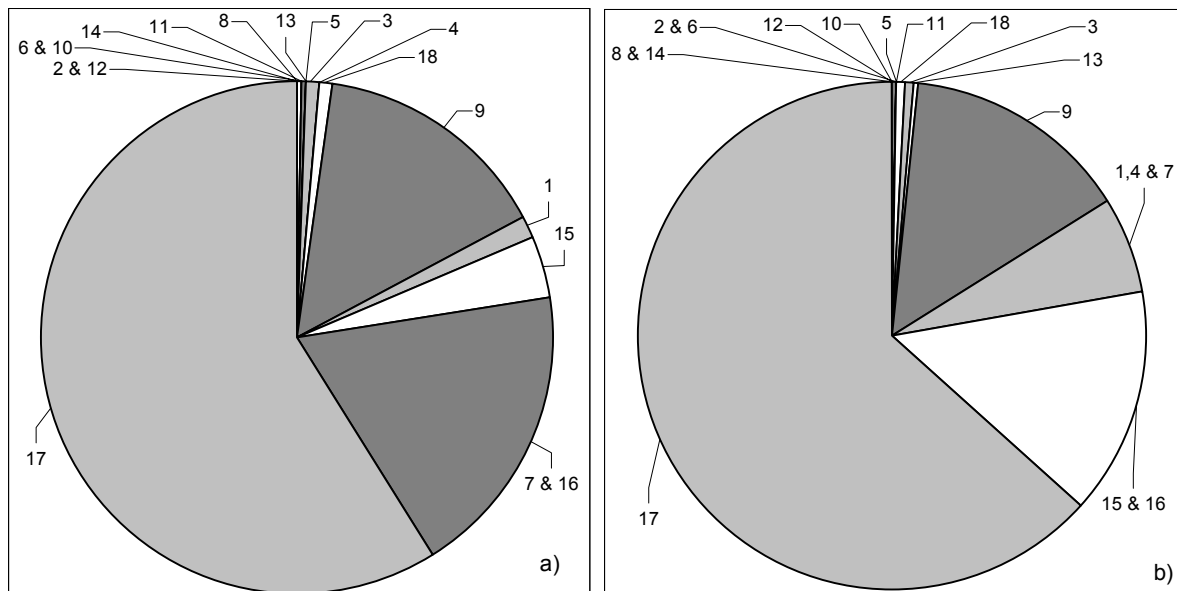


Fig. 5.8-8: Contribution of the recharge regions to the total recharge amount of the research area in hardrock areas with a) highest recharge values and b) lowest recharge values taken from the range given in Table 5.8-7.

The recharge values given in Table 5.8-7 have been assigned to the zones indicated in Fig. 5.8-7 with a resulting recharge volume of $1.82 \cdot 10^8 \text{ m}^3/\text{a}$ to $3.91 \cdot 10^8 \text{ m}^3/\text{a}$ (minimum and maximum values used, respectively). These numbers do not yet allow for recharge through sandy surface and evaporation and transpiration loss in the study areas.

The contribution of the recharge regions to the entire hardrock recharge amount is given in Fig. 5.8-8. The Otavi region (region 17) contributes with the highest percentage to the recharge amount of between 58 and 63 % of the total for the highest (Fig. 5.8-8a) and lowest (Fig. 5.8-8b) assigned recharge amounts, respectively. Regions 1,4,7,15 and 16 together contribute with 23.3 and 20 % towards the total if the highest and lowest recharge amount are assumed, respectively. The contribution of region 9 (Okahandja North) does not change a lot in the percentage of the total with 14.8 to 14.3 %, for the higher and lower assumed recharge amount, respectively. From this observation it is very clear that the Otavi area is the most important source of recharge. The Waterberg area is also a very important source area, as is region 9 (Okahandja North) which

includes the Hochfeld area. But it is also indicated here that the hardrock outcrops in the north-east, region Nhoma, Aha Hills and Gam (regions 1,4 and 7 in Fig. 5.8-7 and Fig. 5.8-8), give also significant contribution to the recharge.

Table 5.8-7: Summary of the recharge values that have been assigned to the hardrock regions in Fig. 5.8-8 according to their mean annual precipitation, surface properties, geology and field observation using the recharge rates obtained at the GWD (Chapter 5.6)

No in Fig. 5.7-8	Name	Mean annual precipitation	Geology	Designated recharge class	Assigned recharge amount (min - max)
1	Aha Hills	400 - 430	Marble	Medium	20 - 50
2	Epukiro West	410 - 420	Gneisses	Low	2 - 3
3	Epukiro East	370 - 400	Schists, quartzites, some marble	Medium	10 - 20
4	Gam	400 - 420	Schists, quartzites, some marble	Medium	20 - 30
5	Gobabis	390 - 410	Schists, quartzites	Low-medium	4 - 7
6	Makuri	410 - 430	Gneisses	Low	2 - 5
7	Nhoma	440 - 500	Quartzites	Low-medium	20 - 70
8	Okahandja South	370 - 400	Granites, gneisses	Low	0.5 - 1.8
9	Okahandja North	380 - 430	Quartzites, schists	Medium	18 - 40
10	Omingonde North	380 - 430	Siltstones	Low	1 - 5
11	Otjoni	390	Schists	Low	1.5 - 4
12	Talismanis	360 - 375	Quartzites, often calcrete cemented joints	Low-medium	0.4 - 3
13	Omatoko Hills	370 - 380	Basalt	Medium	12 - 16
14	Omingonde South	370 - 400	Siltstone	Low	0.5 - 1.5
15	Otjiwarongo	420 - 450	Quartzites, schists	Medium	30 - 60
16	Waterberg	420 - 460	Sandstone	Good	30 - 70
17	Otavi	440 - 500	Dolomites, marble, quartzites,	Good	50 - 100
18	Grootfontein	450 - 500	Gneisses	Low	8 - 35

5.8.2 Regionalisation of recharge through unconsolidated sediments and soils

Although recharge in hardrock areas might be of orders of magnitude higher than the recharge in sand covered areas, the contribution of the latter to the total recharge amount in the research area cannot be neglected as it covers the largest parts of the approximately 160 000 km² research area.

Method

The dependence of the recharge amount on mean annual precipitation in areas with Kalahari soft sediment cover has been documented in Fig. 5.6-5b (repeated here as Fig. 5.8-9). From this graph a maximum and a most likely occurring recharge amount has been read as a function of the mean annual precipitation. The upper enveloping function has not been used, as it represents

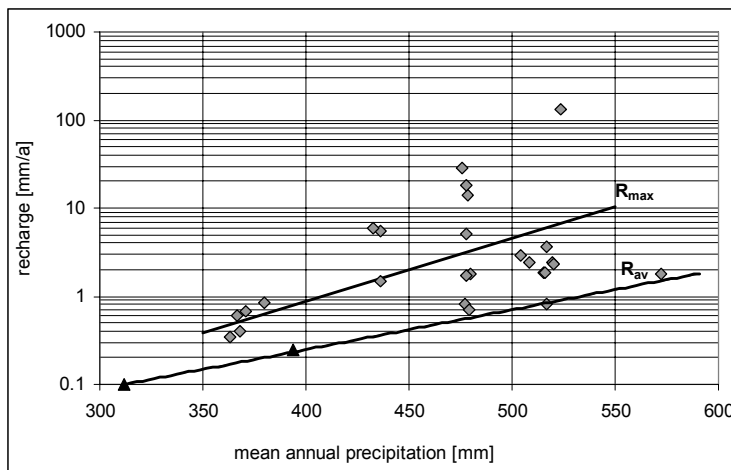


Fig. 5.8-9: Recharge rates from the chloride mass balance method in the saturated zone under Kalahari cover (reproduction of Fig. 5.6-5b) together with recharge-precipitation functions used for regionalisation.

only very favourable conditions which cannot represent the entire region. An average function between the two extremes reflects both the highest and the lowest occurring recharge conditions and assumes that they are in balance. But as the drilled wells are not representing the average study area, having been mostly drilled in favourable areas, the averaging function is more likely to represent a maximum recharge function for the study area (R_{max} in Fig. 5.8-9). It is thus assumed, that the lower enveloping function is an approximation of the average study area conditions and can be used as a most likely or average function (R_{av} in Fig. 5.8-9). Both functions are not produced by regression but by subjective user decision. The map of mean annual precipitation (Fig. 5.3-2) has been processed with the two following functions :

$$R_{max} = 0.0012e^{0.0165P} \quad (5.9)$$

$$R_{av} = 0.0038e^{0.0104P} \quad (5.10)$$

where R_{max} and R_{av} are inferred maximum and average (most likely) recharge, respectively and P is mean annual precipitation. The calculations have been made by the use of SURFER 7 (GOLDENSOFTWARE, 1999) tool "MATH".

Results

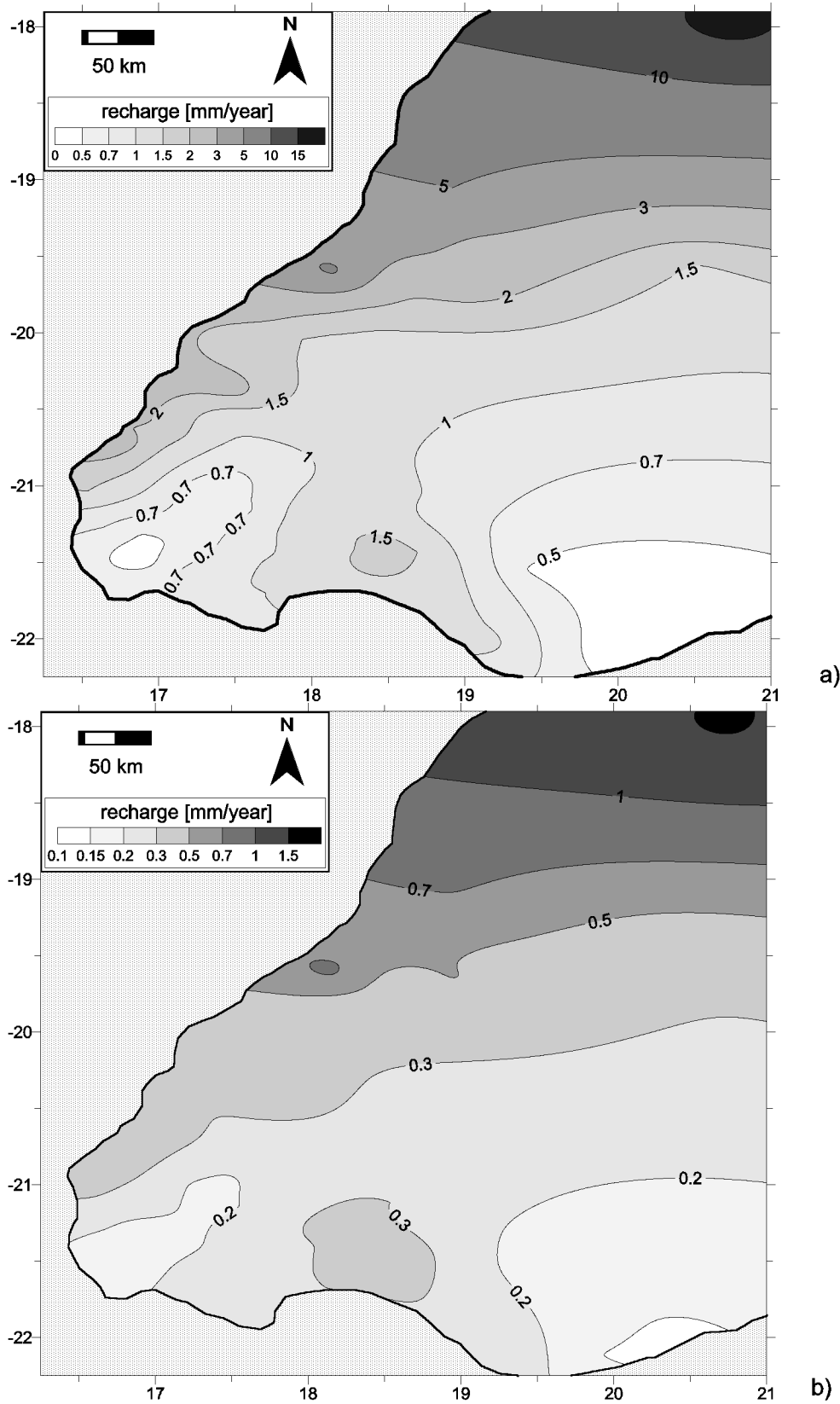


Fig. 5.8-10: Distribution of recharge through soft sediments in the research area without considering recharge through hardrocks. For part a) equation 5.9 and for part b) equation 5.10 has been used to present the inferred maximum and average recharge, respectively.

The results of the mathematical regionalisation are given in Fig. 5.8-10. Here the rain distribution is reflected clearly with recharge increasing towards the north for both cases. The calculation with the average recharge function led to a recharge volume of $7.08 \times 10^7 \text{ m}^3/\text{a}$ which is equal to 0.44 mm/a assuming that it is equally distributed across the entire research area. The calculated recharge rate for the average assumed recharge range from 0.15 to 1.58 mm/a, while the recharge rates for the as maximum assumed recharge function led to values of 0.4 to 17.2 mm/a within the research area. This gives a maximum recharge volume of $4.36 \times 10^8 \text{ m}^3/\text{a}$ which is equal to 2.67 mm/a equally distributed across the entire research area.

5.8.3 Regionalisation of evaporation and transpiration by use of groundwater level to surface distance and satellite images

Method

If groundwater levels are at a shallow depth from the topographic surface, direct evaporation through the soil is possible. While DE VRIES ET AL. (2000) assume a threshold distance of about 20 m with evaporation less than 1 mm/a underneath, GIESKE (1992) indicated that evaporation from depth below 2 m is very unlikely for the Kalahari and KÜLLS (2000) assumes 2.5 m as the critical distance. This reflects the problem when defining a threshold distance for the occurrence of evaporation: evaporation from soil decreases continually with depth. Thus the threshold value indicates the depth from which on only a **negligible** amount of evaporation occurs. "Negligible" makes it thus a subjective threshold. Additionally the topographic surface is not as even as the groundwater surface and level fluctuations occur often in shallow groundwater. Consequently 5 m is used as the *regional threshold* in this study.

Evaporation values are available from the great artesian basin in southern Australia which range from 90 to 280 mm in Lake Eyre (ULLMAN, 1985), 120 to 200 mm in Lake Amadeus (CHENG XIANG YIANG, personnel comm. cited in LLOYD, 1986) and 120 mm/a in Lake Frome (ALLISON & BARNES, 1985). As the climatic data in southern Australia indicate higher evaporation there, it is assumed that the evaporation from groundwater at depths shallower than 5 m in the Namibian Kalahari is at about 80 - 100 mm.

If plants have deep roots, they are able to use groundwater as deep as their roots' range. While very locally Acacia with roots as deep as 50 m were reported (RINGROSE ET AL., 1997 in SELAOLLO, 1998) it is assumed that in general trees transpire groundwater from a maximum depth of 20 m. This might result in local groundwater loss in the order of 20 - 30 mm/a (DE VRIES ET AL., 2000).

For the regionalisation of evaporation and transpiration a two fold method is thus required. Therefore all areas with groundwater levels that fall in the following classes have to be detected:

- a) more than 20 m: Groundwater is saved from evaporation and transpiration,
- b) 5 to 20 m: Groundwater is saved from evaporation, but large trees might transpire groundwater,
- c) less than 5 m: Direct evaporation of the groundwater occurs.

The areas have been defined using a plot of the strike below surface from original DWA data and digitising the areas in which the selected distances were found. Gridded data were only used as background because they might smooth out some areas. For classes a) and c) it is clear that a groundwater loss of 0 mm/a or 80 - 100 mm/a have to be assigned, respectively. For the areas that fall into class b) it has to be further decided if the vegetation in this areas is likely to contribute significantly to a loss of groundwater. This decision has been made based on satellite images. General aspects of satellite images are given in Chapter 5.8.1. Spectral reflection curves are widely used to distinguish between soil and vegetation. Dry soils show a spectral curve that rises constantly with the wavelength from 5.5 % of reflectance at 0.4 μm to about 40 % at 1.3 μm . Vegetation shows a curve with a maximum at about 0.5 μm with 10 % reflectance, a steep rise from a local minima at 0.65 μm with 4 % to a local maximum with about 40 % of reflectance at 1.4 μm (SABINS, 1997). The differences between these spectra are used to define a normalised difference vegetation index (NDVI) by the use of the reflection intensity of the visible red (R) and of the reflected infrared (RIR). It is given as:

$$NDVI = \frac{RIR - R}{RIR + R} \quad (5.11)$$

Values for *NDVI* range from -1 to 1. The higher the value, the higher is the concentration of green vegetation. However it is required for some purposes to have positive values only. Therefore a transformed vegetation index (TVI) is used which calculates as:

$$TVI = 100 * \sqrt{NDVI} \quad (5.12)$$

with $TVI = 0$, if $RIR - R < 0$.

The red band used for this calculation should represent wavelength of 0.6 to 0.7 μm and the reflected infrared from 0.75 to 1 μm . Therefore the Landsat TM bands 3 and 4 have been chosen (for wavelength see Table 5.8-1) for the calculation of TVI for all areas that showed surface to groundwater distances of 5 to 20 m. The areas with dense vegetation with groundwater levels at less than 20 m have been digitised using TNTmips and transpiration values have been assigned to the areas.

The evaporation and the transpiration map were combined to a single grid where the higher z -value of either grid went into the new grid ($z_{\text{new}} = \max(z_{\text{old1}}, z_{\text{old2}})$).

During this procedure the problem occurred that the satellite scenes 177-037, 177-074, 177-075, 176-073, 176-074 and 176-075 are from the dry season while the scenes 178-073 and 178-074 are from the beginning of the wet season and 178-075 are even from the middle of the wet season. Therefore TVI was calculated for the parts in which the satellite scenes overlap and according to the histograms the value that the TVI has to be shifted for a transformation from the beginning or middle of the wet season to the dry season were subtracted.

Results

Within the research area only 16 wells are reported with a distance of groundwater strike to surface less than 5 m. These locations are indicated in Fig. 5.8-11. 50 % of these areas are

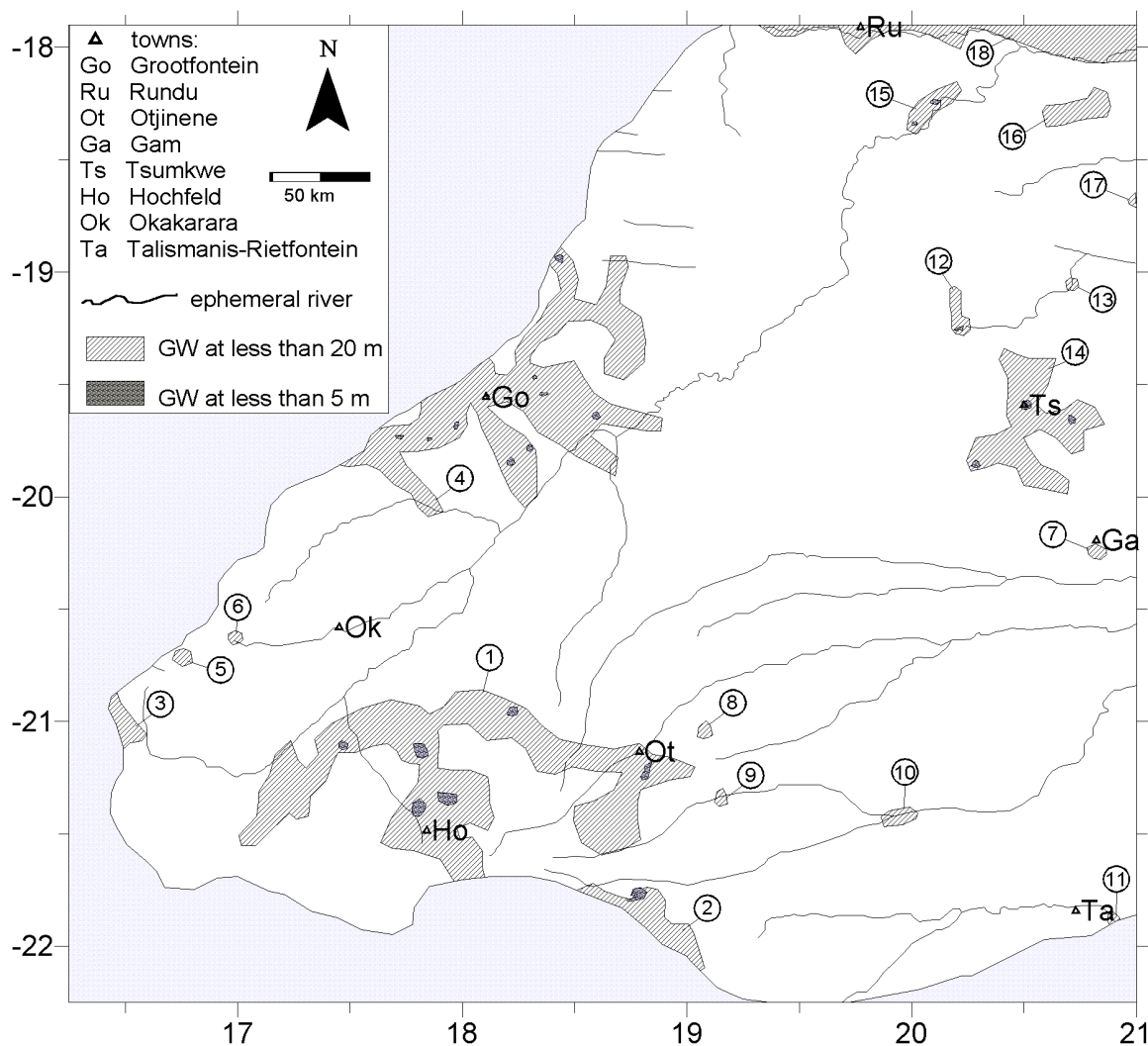


Fig. 5.8-11: Distribution of areas with surface to groundwater distance at less than 5 m (grey dashed pattern) and at 5 to 20 m (hatched area). Numbers indicated here refer to numbers used for region's identification in Table 5.8-8.

restricted to the Grootfontein region, where groundwater is often at a distance less than 20 m from the surface. While only two single occurrences are reported from the Omiramba Nhoma and the Omatako, the area with shallow groundwater in the Hochfeld-Otjinene region reports 3 such occurrences.

The areas where direct evaporation takes place cover only 336 km² of the research area. Assuming the annual evaporation rate from the soil of 80 - 100 mm this leads to an evaporation loss of 2.69 to 3.36*10⁷ m³/a for the entire research area.

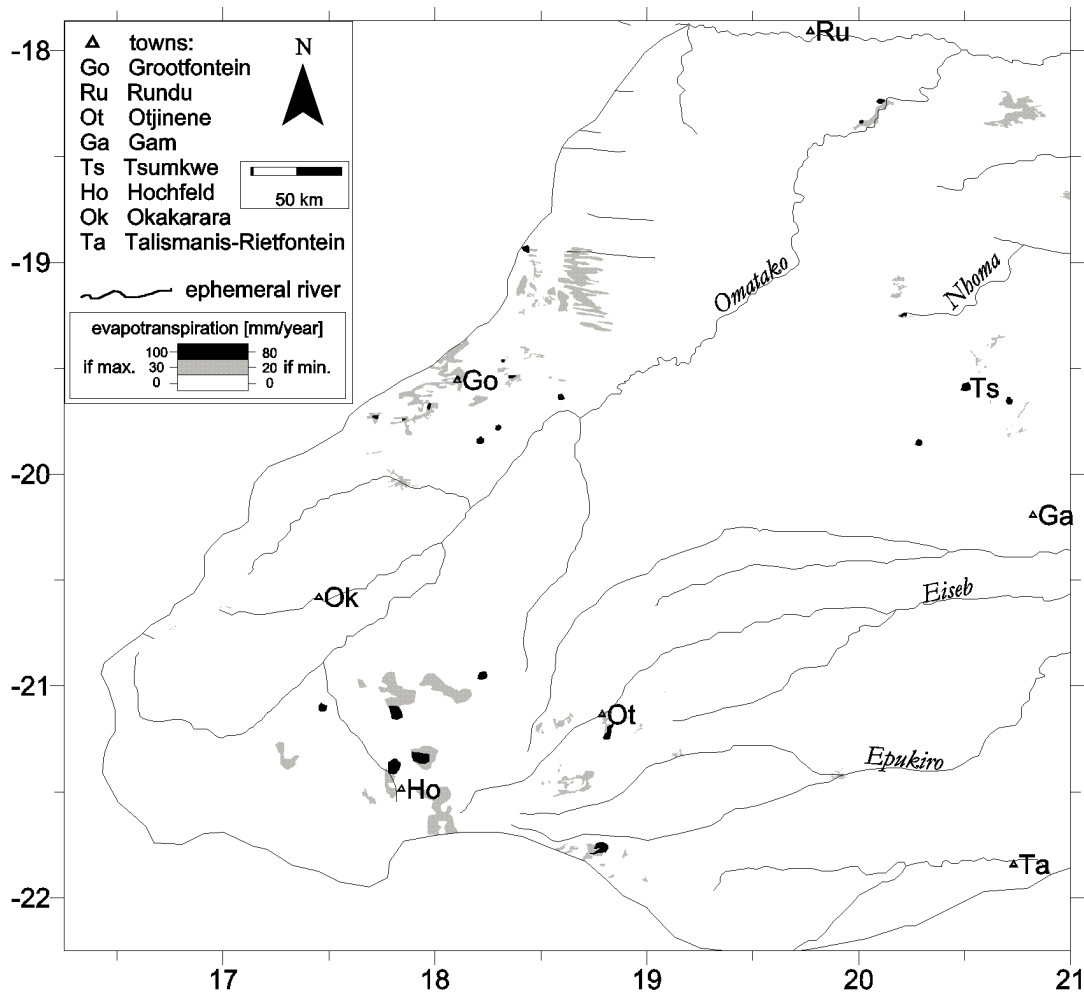


Fig. 5.8-12: Distribution of evaporation and transpiration. The two given scales reflect the ranges of annual evaporation (80 - 100 mm/a) and transpiration (20 - 30 mm/a).

In all, 18 regions have been digitised that show distances from surface to groundwater of less than 20 m. Their size varies significantly from only a few km² to the very large areas near Grootfontein and in the Hochfeld-Otjinene region. A summary of the observed TVI for these areas is given in Table 5.8-8. While the areas 3, 5, 6, 7 and 11 are not significantly vegetated, many areas were found to be at least partly densely vegetated. It was often found that in the areas with very shallow groundwater (less than 5 m) the vegetation was not as dense as in the areas

Table 5.8-8: Summary of TVI observation in processed satellite images for 18 regions (numbered according to Fig. 5.8-11) in the research area where groundwater was found between 5 and 20 m below surface

No	Observation
1	TVI varies in this large area, transpiration is likely in a large part of it
2	Very locally TVI values of more than 60 occur, but mostly between 15 - 30
3	Most part of this area is not significantly vegetated (TVI = 0)
4	TVI varies locally, reaches max. value of 58
5	Most part of this area is not significantly vegetated (TVI = 0)
6	Most part of this area is not significantly vegetated (TVI = 0)
7	Most part of this area is not significantly vegetated (TVI = 0)
8	Only in the central part of this area TVI exceeds 35
9	Within this areas TVI was observed as 0 for the Omuramba Alexest and south of it. North of the Omuramba small areas occur with high TVI values (TVI > 35)
10	TVI shows large values only in its western part north of the two Omiramba
11	Most part of this area is not significantly vegetated (TVI = 0)
12	Directly north of the Omuramba Nhoma TVI above 40 occurs. Large trees were observed here during field trip in 2000. The northern part of this area is also densely vegetated with very large trees in the area of Samagaigai and TVI above 50
13	High TVI values are limited to the Omuramba
14	This area shows high TVI values only in its north-eastern part and locally some "green islands" occur with TVI well below 40
15	Northern part of this area is not significantly vegetated (TVI = 0) but along the southern part of the Omuramba TVI is high
16	Only a very small area in the eastern part of this zones indicated dense vegetation, most of the rest has TVI very low or 0
17	A part from the northern most part this area shows fairly high TVI values (TVI >50)
18	As this region is constrained to the Okavango with its open water TVI is not further observed, as dense vegetation is more likely to occur from this water source rather than from tapping groundwater

with shallow groundwater. The mapped transpiration area covers approximately 2667 km² of the research area which results in a transpiration loss from the groundwater of 5.3 to 8×10^7 m³/a for the research area.

The resulting map of evapotranspiration for the research area is given in Fig. 5.8-12, which also reflects the range of evaporation and transpiration values by a twofold scale. Zones of evaporation are bounded by zones of transpiration, but it was also observed that very shallow groundwater occurs only locally and the surrounding shallow groundwater is not tapped by dense vegetation. The area north-east of Grootfontein marked as a transpiration zone in Fig. 5.8-12 appears in the field to be characterised by Makalani palms. This indicates the water to be saltier than in the areas dominated by Acacia, and confirms the predicted evapotranspiration loss.

Using the maximum assumed transpiration and evaporation values of 30 and 100 mm/a, a total evapotranspiration loss for the research area from shallow groundwater is calculated as 1.12×10^8 m³/a. Using the lower assumed values (20 and 80 mm/a for transpiration and evaporation, respectively) a total evapotranspiration loss for the research area of 7.94×10^7 m³/a is obtained.

5.8.4 Combined recharge balance for the research area respecting hardrock recharge, soil recharge, evaporation and transpiration from shallow groundwater

Method

In the foregoing sub-chapters, results from regionalised recharge and discharge have been presented for the research area. For any further water resource planning it is required to combine these results in a *combined recharge balance*. Therefore recharge from the hardrock areas and recharge through soft sediments have to be added to give the *combined recharge* for the research area. This was obtained by extracting for every cell of the two recharge grids the higher value, and using this value as the new grid value ($Z_{\text{recharge}} = \max(Z_{\text{recharge_hardrock}}, Z_{\text{recharge_soil}})$). The evapotranspiration was then subtracted from the recharge image. As for recharge and evapotranspiration, a maximum and minimum or average result was achieved, here again two cases were considered. The maximum recharge and minimum evapotranspiration were used to calculate the *maximum combined recharge balance*, while the minimum recharge and the maximum evapotranspiration were used to calculate the *minimum combined recharge balance*.

Results

A summary of the recharge and discharge values is given in Table 5.8-9. The combined recharge from hardrock and soft soils gives an overall recharge amount of 2.49 to 8.09×10^8 m³/a which is

equal to 1.53 to 4.99 mm/a. In the minimum assumption, the hardrock recharge plays the most important role for the entire research area as it contributes with 73 % to the combined recharge, while it is only 48 % for the calculation with the assumed maximum values.

Approximately two thirds of the evapotranspiration loss from shallow groundwater in the research area occurs by transpiration and only one third is evaporated directly from the soil under the presented assumptions. In the minimum scenario approximately 45 % of the recharge is lost during the subsequent groundwater flow due to evaporation and transpiration from shallow groundwater which occurs often in the vicinity of Omiramba. In the maximum case it was found that 10 % of the groundwater is lost due to evapotranspiration.

Table 5.8-9: Summary of recharge, evaporation and transpiration values in volumetric and length dimension for the research area that have been calculated with the methods described in this chapter. For the values given as [mm/a] it was assumed that the calculated volume is equally distributed across the entire research area

		Calculated water volume [m ³ /a]	Equally to a ponded highs [mm/a]
Hardrock recharge	Min	1.82*10 ⁸	1.12
	Max	3.91*10 ⁸	2.41
Recharge through soft sediments	Min-Av	7.08*10 ⁷	0.44
	Max	4.36*10 ⁸	2.67
Combined recharge	Min	2.49*10 ⁸	1.53
	Max	8.09*10 ⁸	4.99
Evaporation	Min	2.9*10 ⁷	0.17
	Max	3.36*10 ⁷	0.21
Transpiration	Min	5.33*10 ⁷	0.32
	Max	8*10 ⁷	0.49
Combined evapotranspiration	Min	7.94*10 ⁷	0.49
	Max	1.12*10 ⁸	0.69
Combined recharge balance	Min	1.43*10 ⁸	0.88
	Max	7.34*10 ⁸	4.53

At this point it could be argued, that no indirect recharge has yet been considered. However, as pans cover well below 0.5 % of the research area and if a recharge rate even as high as 30 mm were to be assumed for the Tsumkwe district (as observed under a single pan in Botswana by SELAOLO, 1998), this would in the maximum case lead to an extra recharge amount of the order of 0.1 mm (assuming an equal distribution across the research area) which is not significant compared to the other factors. The influence of flood water on recharge in the Kalahari has been calculated to be 2-5% of the total groundwater flux locally in the western Kalahari fringe by KÜLLS (2000). Since in this areas surface runoff occurs more often than in the rest of the research area, and as this observation was locally very restricted, it is assumed that indirect recharge contributes with less than 1 % to the total recharge value for the research area. This leads to a max. total recharge of $7.34 \cdot 10^8$ to $7.38 \cdot 10^8 \text{ m}^3/\text{a}$ (4.53 to 4.55 mm/a) or a min. total recharge of $1.43 \cdot 10^8$ to $1.44 \cdot 10^8 \text{ m}^3/\text{a}$ (0.88 to 0.89 mm/a).

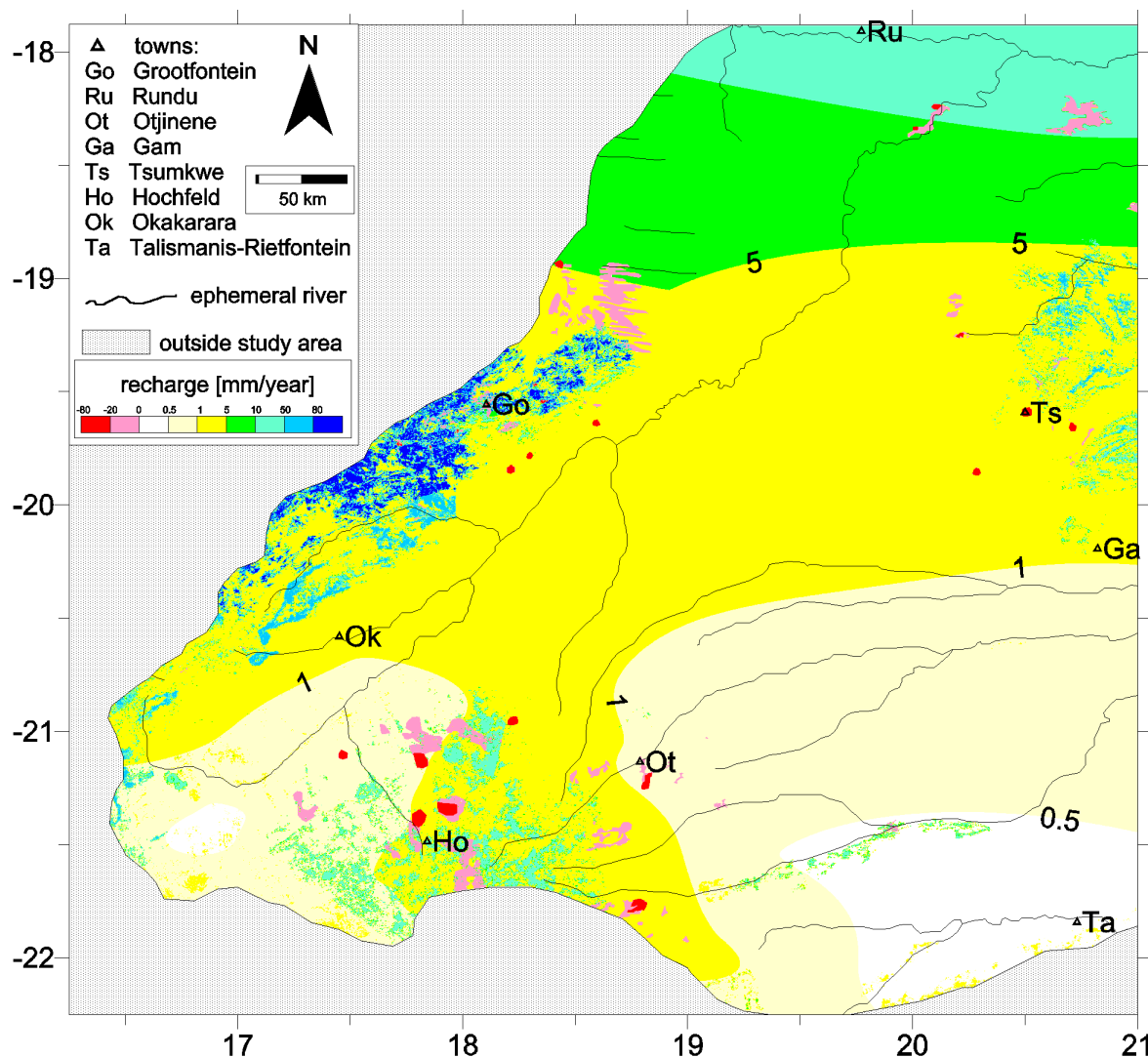


Fig. 5.8-13: Distribution of recharge (minimum values) and discharge (maximum values) zones in the research area by combination of hardrock and soft sediment recharge, evaporation and transpiration from the groundwater. (Discharge is given as negative recharge.)

The balanced recharge amount for the Eiseb-Epukiro-Catchment from the minimum approach gives a volume of $1.13 \cdot 10^8 \text{ m}^3/\text{a}$.

The distribution of recharge and discharge zones is given in Fig. 5.8-13 which considers the minimum recharge and maximum discharge values. Estimates for recharge through soft sediments do not represent proper point recharge values, but more or less an average recharge for a given area with a surface property assemblage as given in Fig. 5.2-5.

Very sharp lines seem to separate the recharge values in the north (e.g. the 0.5 mm line), but this is an artefact of the need to use integer contour values to represent different values in a quality that, in fact, varies very gradually.

Interpretation

From the distribution of recharge and discharge zones it is concluded that a large amount of the recharge in the Hochfeld-Otjinene area is lost by evaporation and transpiration. A smaller but still significant part of the recharge from the Otavi area is lost on its path towards the Omatako Graben, and especially a large part of the recharge water that flows towards the north from the area around Grootfontein is lost due to widespread evaporation and transpiration.

Many of the recharge zones are close to the groundwater divides which reflects the small-scale recharge-discharge systems within a larger catchment following the concept of hierarchical groundwater flow systems (TÓTH, 1962). This conclusion was also reached by observation of the satellite image given in Fig. 5.8-4 where it seems likely that the half moon shaped pan field refers to more humid times when groundwater recharge from the nearby hardrock areas, e.g. Aha Hills, discharged as springs in the pans area.

It cannot be confirmed here that the Omiramba serve as major discharge zone as e.g. DE VRIES ET AL. (2000) have assumed for their study areas in Botswana's Kalahari due to the shorter groundwater to surface distance. The distance from surface to groundwater in the eastern part of the research area is smaller in the Omuramba valleys because they incise the landscape, but with groundwater surface distances at more than 100 m a change of 10 m, or even 50 m, does not induce evapotranspiration.

The estimated balanced recharge amount for the research area is checked against the discharge volume at the assumed discharge zones of the Makgadikgadi depression. In the vicinity of the Makgadikgadi depression an area of approximately 3000 km^2 shows shallow groundwater. This would result in a discharge volume of 3 to $6 \cdot 10^8 \text{ m}^3/\text{a}$ (assuming discharge amount of 100 - 200 mm/a). This volume is smaller than the maximum recharge volume achieved for the Namibian part of the catchment (see above). This either indicates that the assumed maximum

recharge rate is higher than the actual recharge, or that additional discharge zones exist at the Okavango, the Okavango Delta and Lake Ngami, which has not yet been considered. Furthermore, abstraction has not been considered, and this might have lowered the groundwater level and stopped some springs (e.g. springs at Grootfontein, Gam and Otjombindi) that would have added an additional discharge volume for the natural groundwater system. However, the minimum balanced recharge amount is in good overall agreement with the calculated discharge amount.

5.9 Summary and methodological recommendations

5.9.1 Summary of the recharge results

For the study area it is confirmed that indirect recharge occurs as well as direct recharge. Four different soil classes (aeolian sands, soils with aeolian influence, red to brown soils, and pans and vleis) have been examined and it was observed that all four surface classes are relevant for the development of small-scale runoff. Pans and vleis are the areas where the indirect recharge infiltrates. Direct recharge occurs mostly in the sandy areas and depends strongly on the vegetation cover. Calcrete facilitates mainly preferred flow path recharge and mechanically prevents roots from abstracting groundwater.

Estimates of recharge in a basin wide approach requires areal integration of point data because the distribution of at least four soil classes and a very variable vegetation cover cannot be solved at every point of the study area.

Integrated mean values for recharge in the research area are obtained by applying the chloride mass balance method to the saturated zone of the groundwater divide. In general, recharge values for areas covered by Kalahari substratum range from 0.1 to 30 mm/a. It is observed that recharge increases with the mean annual precipitation and that two different recharge mechanisms, diffuse and preferred flow, result in a large variation of recharge rates.

The recharge range for hardrocks varies from 0.8 to more than 100 mm/a and also increases with mean annual precipitation. The factors that cause variations in the recharge rates are mainly preferred infiltration in joints and very fast infiltration in karstified rocks. The highest recharge rates are associated with very favourable conditions and thus cannot represent the basin-wide recharge amount.

From the use of a soil water balance model it is concluded that recharge occurs mainly in the second half of the rainy season (January to March) which is associated with heavier and more catchment-wide transferable rain events.

Recharge areas that are dominated by indirect recharge receive the most significant recharge during entirely good rainy seasons, while direct preferred flow path recharge associated with calcrete and hardrock cover might already react to a single extraordinarily wet rain.

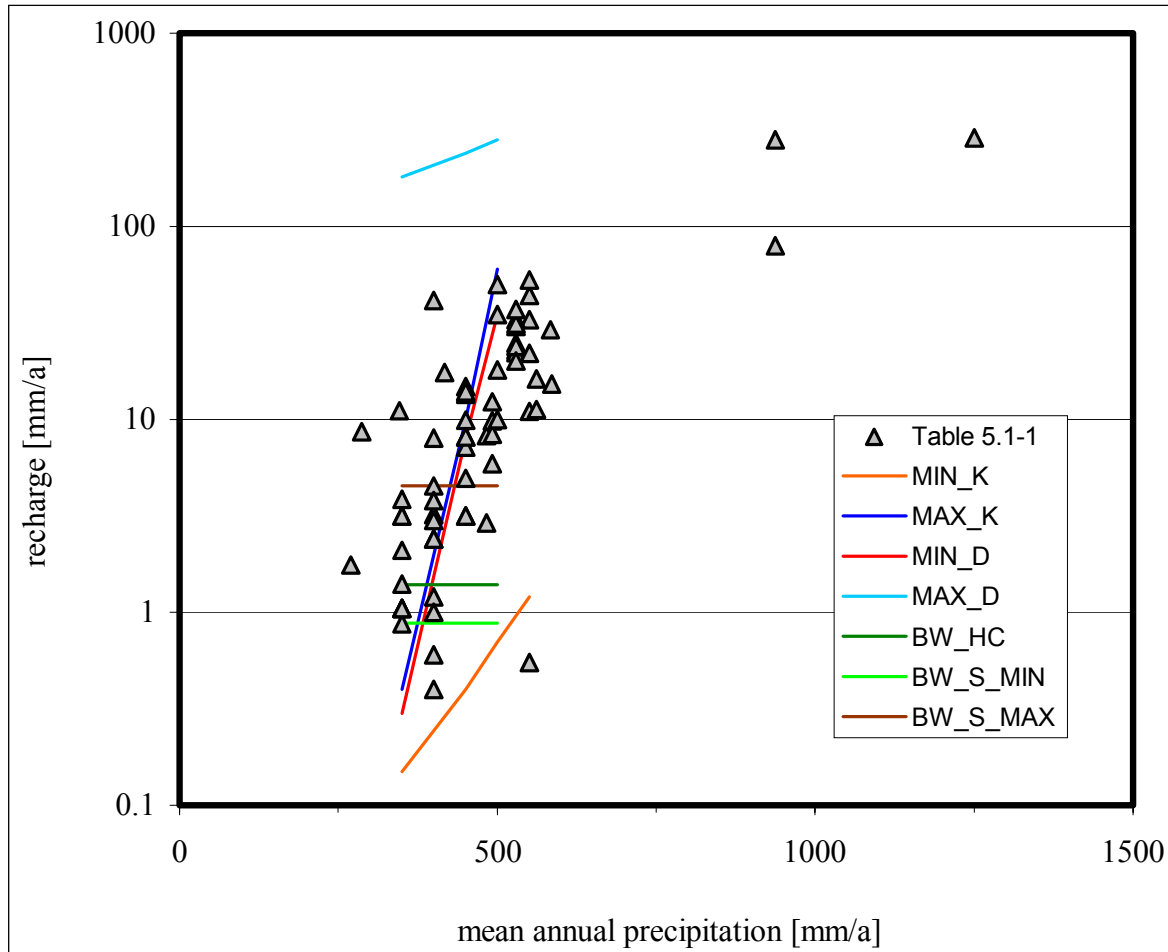


Fig. 5.9-1: Comparison of the recharge results from this study with available data from other studies in southern Africa. Data from the literature are given as grey triangles (values and references are given in Table 5.1-1), results from the chloride mass balance method in the saturated zone are indicated by blue (maximum recharge amount in Kalahari covered areas induced by preferred flow path), light blue (maximum amount induced by very rapid recharge in karstified Damara hardrock areas), red (minimum amount induced by recharge in joint Damara rocks) and orange (minimum recharge amount in Kalahari covered areas induced by diffuse infiltration) lines. The results of the regionalisation are given as light green (assumed minimum basin wide balanced recharge by the use satellite image), bottle green (inverse hydrochemical basin wide approach) and dark brown (assumed maximum basin wide balanced recharge by the use of satellite image) lines. The latter are integrated values over the mean annual precipitation that occurs in the study area and thus having no slope.

The distribution of the recharge and discharge zones in the research area is rather complex and several small scale recharge and discharge zones in the research area are indicated.

The balanced recharge volume from the inverse hydrochemical approach ($1.67 \cdot 10^8 \text{ m}^3/\text{a}$) lies within the limits of the minimum ($1.43 \cdot 10^8 \text{ m}^3/\text{a}$) and maximum ($7.34 \cdot 10^8 \text{ m}^3/\text{a}$) balanced recharge estimated from the forward satellite images regionalisation. It is closer to the assumed minimum amount from the satellite images regionalisation. The two lower values are also consistent with the possible discharge volume of the entire South African Kalahari Catchment at the Makgadikgadi depression ($3 \text{ to } 6 \cdot 10^8 \text{ m}^3/\text{a}$).

The results from this study are given in Fig. 5.9-1 together with the literature data presented in Table 5.1-1. The results fit fairly well with the cluster of available data, but the results of the chloride mass balance in karstified Damara rocks (light blue line in Fig. 5.9-1) are higher than any values in the literature. This reflects the very favourable recharge situation in the Otavi area and underlines strongly that such values are not representative for the entire catchment. The values for the diffuse recharge under Kalahari cover (orange line in Fig. 5.9-1) are lower than most of the compared data and reflect thus the less favourable conditions. As such unfavourable conditions occur in any catchment and are often more prominent than the better conditions, they must be considered in any basin-wide approach. The red and blue lines in Fig. 5.9-1 fit well with the distribution of the reference data, and this is consistent with the previous studies having focused on recharge in joint hardrocks and recharge in Kalahari areas dominated by diffuse and preferred flow path recharge.

The maximum basin wide recharge regionalisation by the use of satellite images (brown line in Fig. 5.9-1) plots in the central part of the reference data cloud and would thus represent the previously assumed regional recharge amount. But from this study it is concluded that the lower basin wide recharge values (bottle green and light green lines in Fig. 5.9-1) are more likely to represent the natural groundwater system in its entirety as they take better account of the least favourable conditions.

From the data plot in Fig. 5.9-1 it is obvious, that the recharge dependence on the annual precipitation is rather complex and that the results from the study area are not transferable to wetter areas with mean annual precipitation of more than 550 mm. This also means that the northern part of the study area (northern Okavango district) might require some further study, that focuses on recharge values for the precipitation conditions (550-600 mm) where the slope of dependence changes from a steep to a smooth gradient.

5.9.2 Methodological recommendations

From the methods used in this recharge study, it is concluded that the application of soil water balance models to determine recharge rates is only meaningful if reliable hydrographs, detailed runoff reports or results from an independent method exist to calibrate the model. Otherwise it is possible to model almost every recharge rate by the change of vegetation cover, which is the least reliable variable in a soil water balance model for a semiarid area with a patchy, highly variable vegetation cover ranging from a few cm (little grass) to several m (large trees) roots' depth. A calibrated soil water balance allows to understand the temporal distribution of recharge process and underlines the dependence on a few heavy rain events in semiarid and arid regions.

The application of the chloride mass balance method in the saturated zone gives reliable recharge values if it is applied appropriately. Therefore the lateral chloride and water inflow has to be determined, which is mostly only possible at the groundwater divide where the lateral inflow component is negligible.

Two methods were introduced to regionalise the recharge in a basin wide scale: an inverse hydrochemical approach and a forward regionalisation mainly based on satellite images. For the hydrochemical approach it is recommended to apply this method only if a large hydrochemical data set is available, otherwise areas have to be excluded. Apart from the available hydrochemical data, a good knowledge of the hydrogeological system is recommended as surface to groundwater distances and flow directions are essential information.

Satellite images are a powerful tool to regionalise recharge in a forward approach. A comparison with geological data and aerial photographs has shown that satellite images are the only tool that allows automatic, reproducible classification of favourable recharge zones. Apart from good georeferencing of the satellite image, field knowledge including accurate geographic positions is recommended for a reliable classification result. The definition of transpiration zones is possible by the use of a total vegetation index calculated from satellite images in combination with distance from groundwater to surface data.

It is concluded from this study, that not only a careful determination of point recharge data is essential but also an appropriate method for the regionalisation and that results from a single method should be justified by at least one other.

6 Groundwater flow model

In this study a large scale, simple groundwater flow model was set up for basic understanding of the hydrogeological system. It then it turned out that the available data are not sufficient for detailed modelling. Consequently the below presented groundwater flow model was mainly developed as a verification tool for the determined balanced groundwater recharge.

6.1 Method

During this study the modelling software ProcessingModflow 4.10 by CHIANG & KINZELBACH (1991) that is based on the well established source code Modflow by MCDONALD & HARBOUGH (1988) was used. It allows full three dimensional modelling of inhomogeneous groundwater flow systems in steady state and transient simulation with the finite-difference method. Besides the numerical calculation and calibration, pre-processing of the source data in order to develop a geological and hydrogeological model and the post-processing of the calculated data are the most important steps in groundwater flow modelling.

6.1.1 Pre- and post-processing

Required input data for the geological model are the top and the bottom elevation of each aquifer. As hydraulic parameters, porosity and hydraulic conductivity are necessary. The boundary conditions are given by the definition of no-flow cells along the catchment's boundaries. The upper boundary condition of the model is defined by recharge amount and/or abstraction.

All these data can be directly read into the ProcessingModflow input generator as ASCII matrix files. The format of the ASCII files needs to be in row-major order starting with the upper left corner and the last z-value represents the lower right corner. Besides the matrix a header, giving the amount of rows and columns, is expected by the program.

Results calculated by the ProcessingModflow software package are the groundwater levels and the water budget. The water budget file can be viewed by any ASCII editor, while the groundwater levels are only given in the same ASCII matrix format as the input data (see description above). For the visualisation of the calculated levels, it is useful to transform this data set into a surfer grid file by inserting a five line-header, and then mirror the raster along the y-axis so that an up-right ASCII surfer grid file is produced.

6.1.2 Model set-up

Due to the insufficient data availability for the entire study area, the modelling area has been limited to the Eiseb-Epukiro-Catchment (for location see Fig. 4.1.2). It has been assumed that the Kalahari groundwater system is in equilibrium, and a steady state simulation was performed. The interpretation of hydrographs (Chapter 5.4) indicates this to be an appropriate assumption. The calibration of the model is based on the groundwater level map given in Fig. 4.1-1 with the presented limits (Chapter 4.1).

During this simplistic approach the aquifer system has been modelled as a single layer, and the kf-values have been weighted according to the thickness of each formation. The size of the grid cells is approximately 26 km * 28 km. The discretisation of the model area with the boundary conditions is given in Fig. 6.1-1. The model consists of 179 active cells, and four constant head cells have been defined at the eastern border where groundwater flows into Botswana. The inactive no-flow cells (grey areas in Fig. 6.1-1) are defined by the catchment boundaries with no inflow occurring via the mapped groundwater divides (see Chapter 4.1). These cells are not used during the calculation.

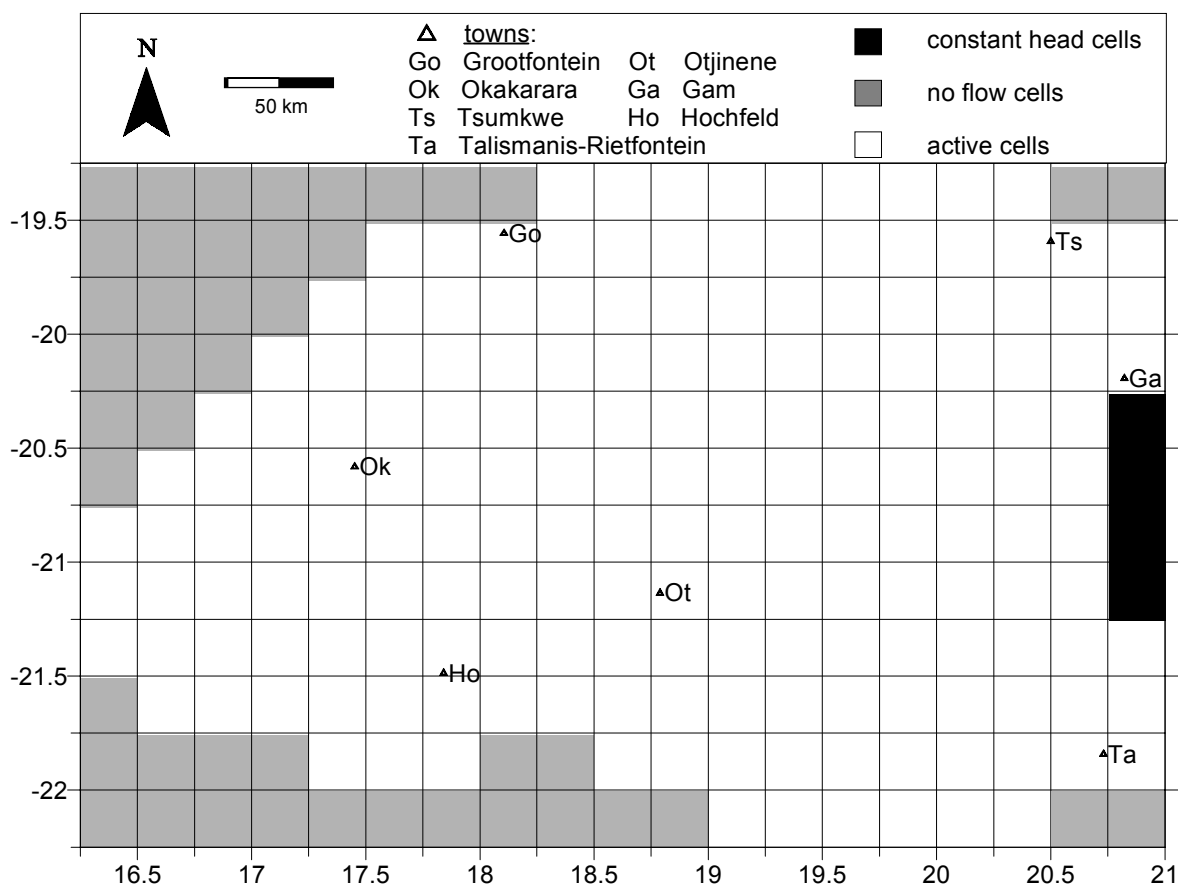


Fig. 6.1-1: Discretisation of the Eiseb-Epukiro-Catchment for the groundwater flow modelling. Constant head cells are given in black, active cells in white and inactive cells in grey.

The thickness of the groundwater system is defined by the top and the bottom of the aquifers. The upper limit for the unconfined aquifer is defined as the topographic elevation for the starting iteration. As the transmissivity is continually recalculated prior to each iteration step during the model run (transmissivity = thickness of the aquifer * hydraulic conductivity), the variable saturated thickness is respected. The bottom of the system is defined as 80 m underneath the Damara topography assuming that deeper groundwater flow is insignificant compared with the above groundwater flow. Thickness of the Kalahari Group (Fig. 3.2-4), Etjo and Rundu (basalts) formations (Fig. 3.2-3) and Omingonde Formation (Fig. 3.2-2) have been subtracted from the topographic elevation to reveal the Damara topography. Subsequent subtraction of another 80 m gives the bottom of the groundwater system. The topographic elevation together with the aquifer thickness is given in Fig. 6.1-2. The greatest thickness occurs in the northern part of the model area. The SW-NE trending trough structure of the aquifer in the western part of the model area is not strictly following the recent topography, that shows a depression slightly east of it.

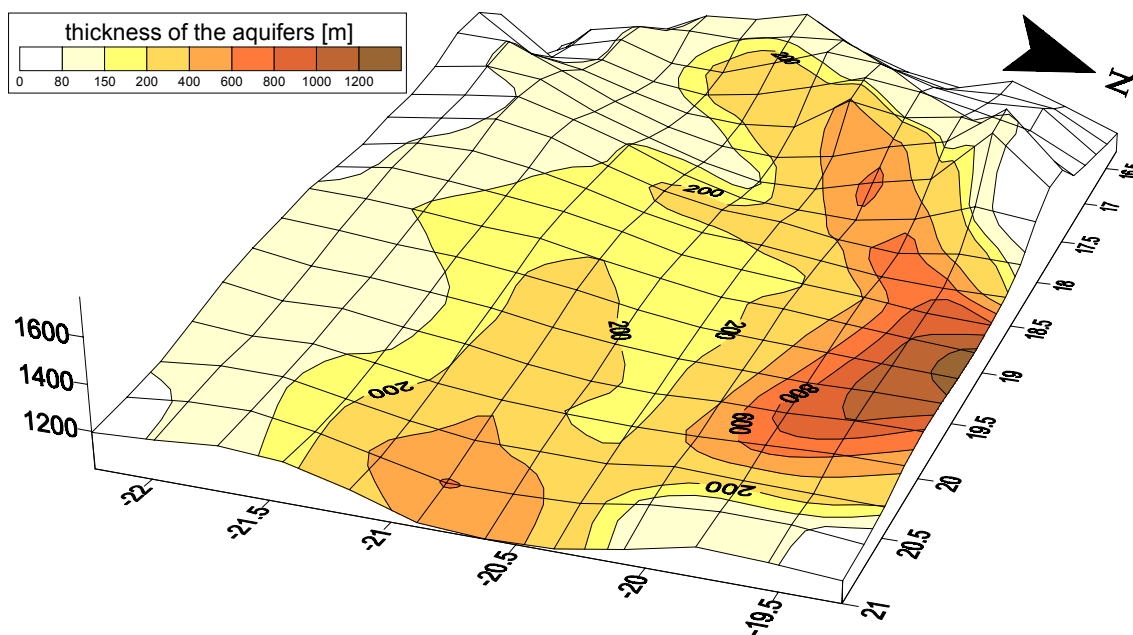


Fig. 6.1-2: Top and bottom of the aquifers for the modelling area. Top of the unconfined aquifer is given as the recent topographic elevation in a 3-d perspective plot. The thickness of the aquifer at start of the model calculation (variable transmissivity in accordance with the wetted thickness is calculated during the model execution) is given as a coloured contour map where the brown colours represent the largest thicknesses.

Porosities for the aquifers are presented in Chapter 4.4. For a steady-state simulation porosity does not cause any head changes and is thus of minor importance. However, the software expects the definition of a porosity value which was set to 0.15.

The hydraulic conductivity for the grid cells have been calculated by weighting the hydraulic conductivity (see Chapter 4.4, Table 4.4-1 and Fig. 4.4-2) for every formation by its thickness contribution to the mixed model aquifer as:

$$kf_{Mi} = \frac{(M_{Ki} * kf_{Ki}) + (M_{Ei} * 1 * 10^{-5} m/s) + (M_{Oi} * 1 * 10^{-7} m/s) + (80 * kf_{Di})}{M_{Ki} + M_{Ei} + M_{Oi} + 80 m} \quad (6.1)$$

where kf_{Mi} means the hydraulic conductivity for the model aquifer at cell i . M_{Ki} , M_{Ei} and M_{Oi} are thickness of the Kalahari aquifer, Etjo and Rundu (basalts) formations and thickness of the Omingonde Formation at cell i . kf_{ki} and kf_{Di} are the hydraulic conductivity for the Kalahari Group and the Damara Sequence at cell i . The results of this calculation are given in Fig. 6.1-3. Green to blue colours indicate relatively high hydraulic conductivities which occur mainly in the western, northern and eastern fringe zone of the model area. Low hydraulic conductivities are documented by pink to orange colours which are dominant in the central part of the basin.

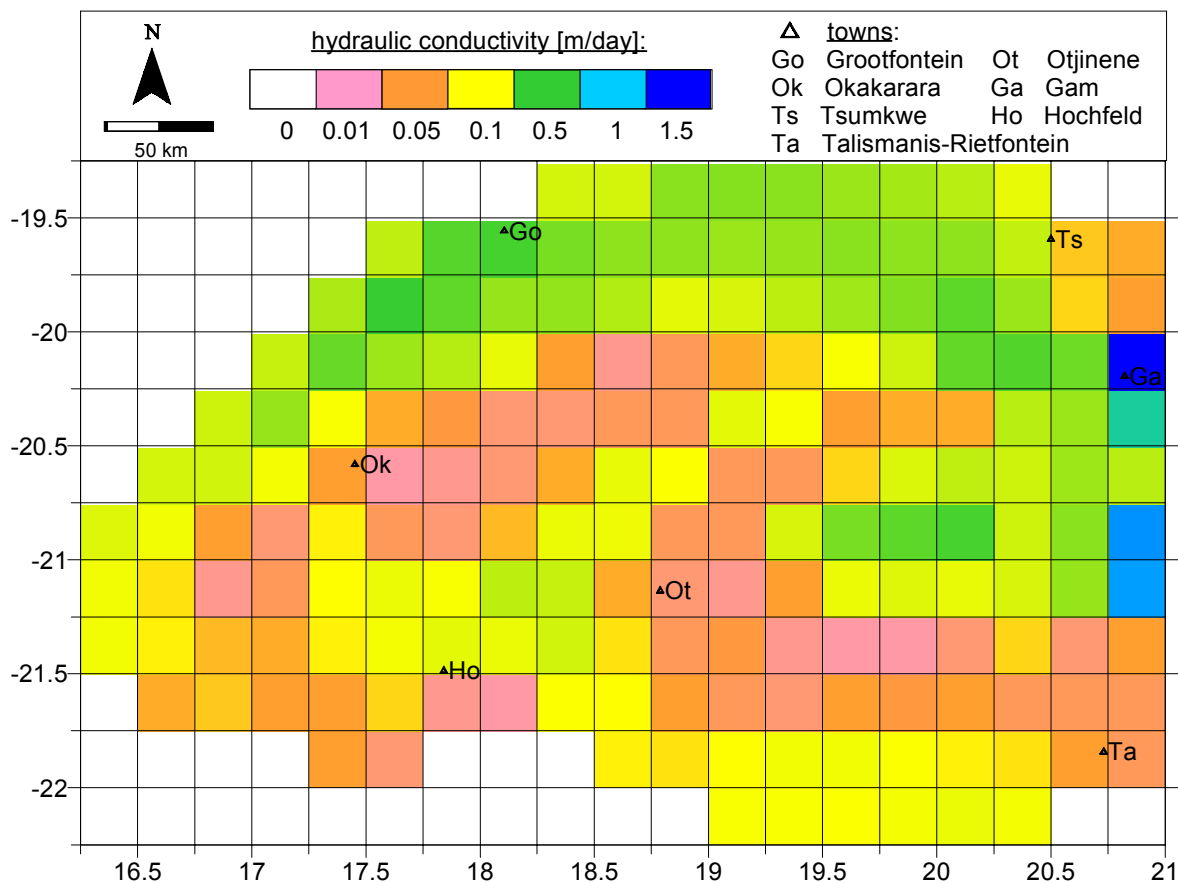


Fig. 6.1-3: Distribution of the hydraulic conductivity for the simplified model aquifer. Kf values have been weighted according to the formation's thickness using equation 6.1.

The calculated hydraulic conductivity for the model aquifer only considers the hydraulic conductivity within the formation and does not respect the hydraulic conductivity of the

unconformities between the formations. Therefore it is likely that the hydraulic conductivity at the basin scale is up to one order of magnitude higher and consequently this possibility was tested during the model execution.

For the areas with large occurrences of basalts it is assumed, that the regional hydraulic conductivity might be increased due to preferred flow along basalt-sandstone-interfaces. Therefore a kf-multiplier raster image was produced which is shown in Fig. 6.1-4. The black areas indicate the region where a multiplied hydraulic conductivity is assumed which is also associated with a smooth hydraulic gradient (see Fig. 4.1-1). This area trends parallel to the Kalahari basin axis (NW-SE), and it is also possible that an increased basin-wide hydraulic conductivity results from prominent faults. Faults in the Eiseb Block are not considered here, as they have already been respected when regionalising hydraulic conductivities for the Kalahari aquifer in Chapter 4.4.

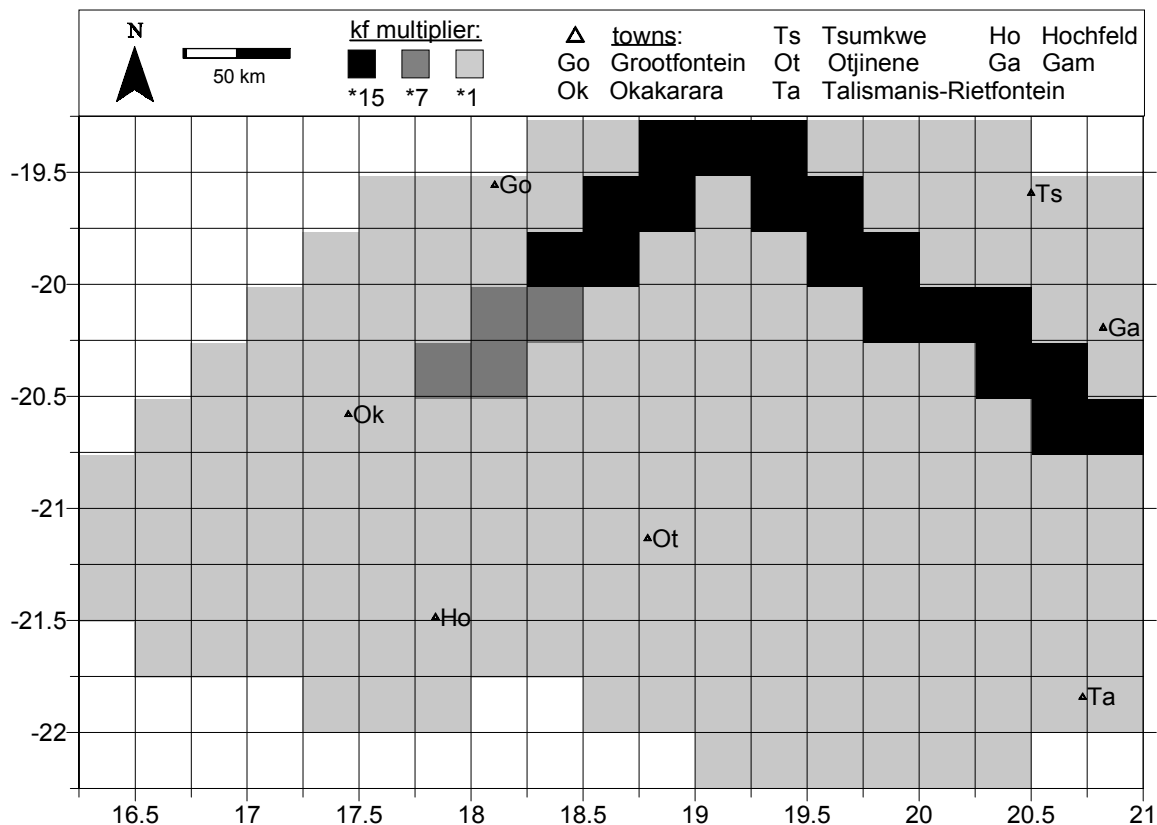


Fig. 6.1-4: Distribution of an assumed kf-multiplier due to basalt occurrence (preferred flow along basalt-sandstone-interfaces), and due to several unconformities between the aquifer forming strata.

For the initial set-up of the model an equally distributed recharge amount of the order of 1 mm/a was used. The distribution and amount of recharge was varied during model execution and calibration and is thus discussed in the according chapter.

6.1.3 Modelling execution and calibration

The major task of the modelling in this study was the inverse determination of recharge. Therefore modelling was started with the above described parameters (Chapter 6.1.2) and consecutive variation of the recharge amount and distribution followed until the calculated groundwater levels fitted with the observed ones. The model was started with a recharge amount of 1 mm/a equally distributed to the catchment. This order of magnitude for the recharge was found to be appropriate during a *maximum kf approach*. The *maximum kf approach* means that the initial kf-values were multiplied by the kf-multiplier and additionally the kf-values were increased by one order of magnitude to respect the groundwater flow in the unconformities. The distribution of the recharge zones was then varied until the resulting groundwater levels fitted with the observed ones.

In a second step it was tested how much recharge the system allows assuming that no additional groundwater flow in the unconformities exists (*minimum kf approach*) by a trial-and-error-procedure. The result indicates the minimum basin wide recharge amount.

During this study more than one hundred model runs have been performed. It was found that the slice-successive overrelaxation was the most stable Modflow solver. Nevertheless often no convergence was reached when setting the acceleration parameters to the recommended values of 1 to 2 (ProcessingModflow help-file). With such acceleration parameters the iteration process became very unstable and large amplitudes of the head change for single cells occurred. Smaller acceleration parameters (mostly between 0.5 and 0.01) avoided this problems, although a larger number of iteration resulted.

6.2 Results

The groundwater level results of the *maximum kf approach* are given in Fig. 6.2-1. The levels fit reasonable well with the regionalised observed levels given in Fig. 4.1-1. During the modelling no lower levels were generated in the hatched area indicated in Fig. 6.2-1 within the full range of plausible parameters. Only unreasonable high kf-values tend to produce some further lowering there. It appears possible that the aquifer thickness following the Kalahari basin axis is larger than expected. The recharge distribution that revealed to the accepted groundwater levels (Fig. 6.2-1) is given in Fig. 6.2-2. The highest recharge amount is assumed in the Otavi area (grey cells, number 10 in Fig. 6.2-2). Areas for which an recharge amount higher than 1 mm/a (for an simplified integrated approach it is assumed that recharge is equally distributed in these areas) is assumed, are the Hochfeld region (class 9), the region around Tsumkwe (class 9), and areas

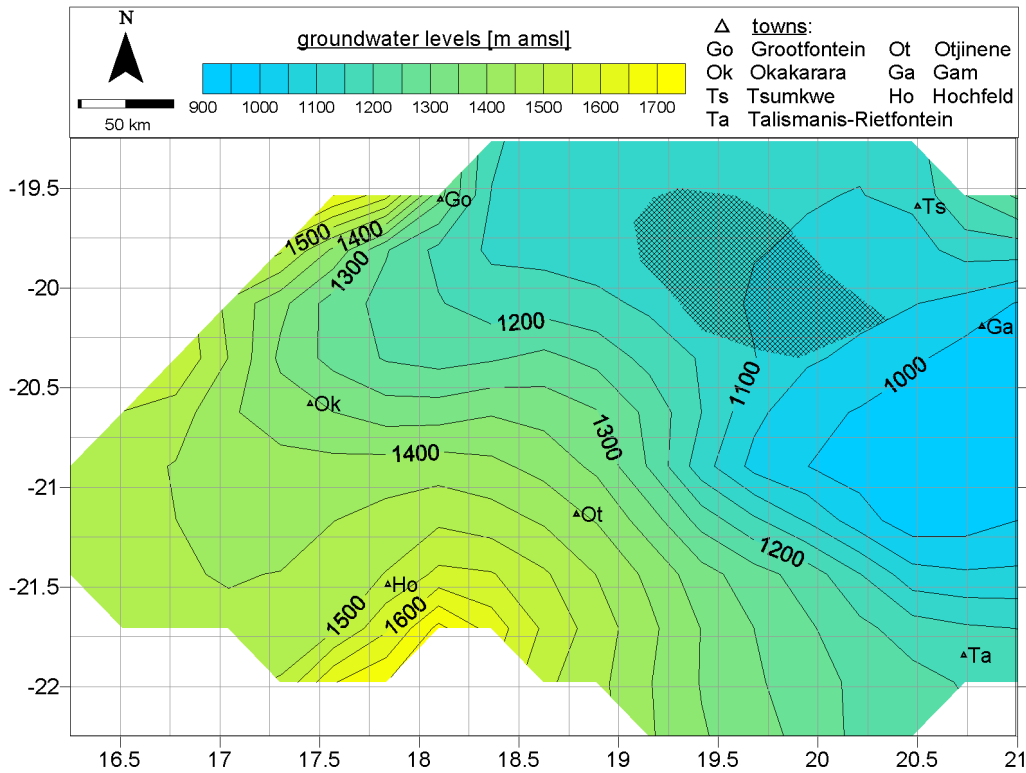


Fig. 6.2-1: Calculated groundwater levels for the model area with *maximum kf-values* and recharge distribution given in Fig. 6.2-2. The area where a discrepancy between calculated and observed levels is not further diminishable by reasonable parameter change is marked by a hatched pattern.

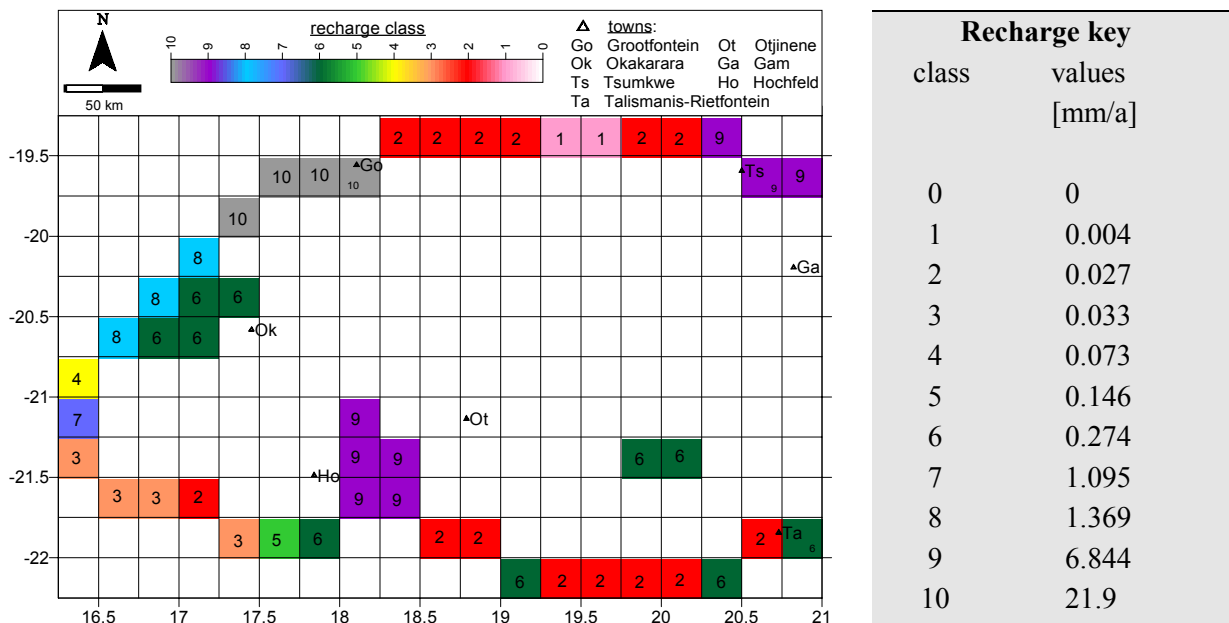


Fig. 6.2-2: Recharge distribution used for the final model run with the *maximum kf-values*. Recharge values corresponding to the colours and numbers in the figure are given in the grey table on the right-hand side. Highest values are marked in greyish to bluish colours, while the cells with a low recharge amount are indicated by reddish to yellowish colours. Cells without recharge or outside the model area are not coloured.

near the western water divide (class 8 and 7). The Waterberg area (dark green cells in Fig. 6.2-2, recharge class 6, located west of Okakarara) influences the regional groundwater system less significant. Areas that are dominated by Damara gneisses or thick Kalahari cover (recharge class 1, 2 and 3, given in pink, red and orange, respectively, in Fig. 6.2-2) are the least significant recharge zones. A total recharge amount of $1.2 \cdot 10^8 \text{ m}^3/\text{a}$ is determined during the *maximum kf approach*. The calculated water balance error of this model is -0.77 %.

The recharge distribution that best fits with the initial *minimum kf distribution* to the observed groundwater levels is given in Fig. 6.2-3. With such hydraulic conductivities a recharge volume of $5.4 \cdot 10^6 \text{ m}^3/\text{a}$ was calculated. The water balance error was very large with more than -20 %. Better water balance errors were only achieved by setting very small head change criterions and not by parameter change. Therefore the modelling result was nevertheless accepted. The recharge zones in this approach (Fig. 6.2-3) are distributed similarly to the *maximum kf approach* (Fig. 6.2-2), but the corresponding recharge values are significantly smaller, which is also reflected in the basin wide recharge amount that appears more than one order of magnitude smaller.

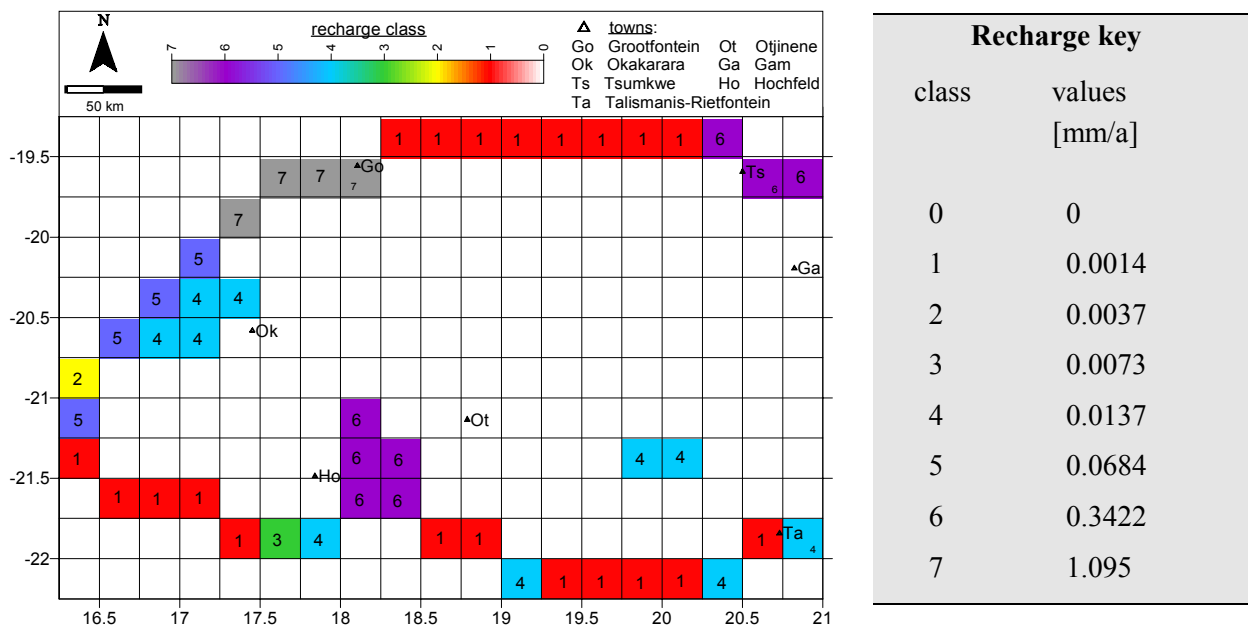


Fig. 6.2-3: Recharge distribution used for the final model run with the *minimum kf-values*. Recharge values corresponding to the colours and numbers in the figure are given in the grey table on the right-hand side. Highest values are marked in greyish to bluish colours, while the cells with a low recharge amount are indicated by reddish to yellowish colours. Cells without recharge or outside the model area are not coloured.

During any of the modelling attempts it was found that without the introduction of the k_f -multiplier, the shape of the groundwater surface cannot be reproduced. It is thus concluded, that the unconformities between the presented formations (Chapter 3) serve as more significant groundwater paths than initially expected.

6.3 Sensitivity analysis

For a sensitivity analysis of the *maximum k_f approach* model, the values of calibrated recharge and hydraulic conductivity have been changed and the magnitude of change in hydraulic heads has thus been examined. 20 sensitivity model runs have been performed by multiplying the calibrated hydraulic conductivity by the factors 0.1, 0.5, 0.8, 0.9, 1.1, 1.2, 1.5, 2, 5 and 10. The recharge amount have been multiplied by the same factors.

A mean water level and the standard deviation has been calculated from the head matrix of each sensitivity-test-run and compared to the mean water level of the calibrated model and its standard deviation. The results are given in Fig. 6.3-1.

The analysis shows that the model is sensitive for both parameters. Recharge changes by factors up to 0.5 (filled triangle in the upper plot of Fig. 6.3-1) calculated several additional dry cells and model runs with even smaller recharge amounts (factor smaller than 0.5) failed to converge. Enlarging the recharge amounts by factors of 5 to 10 (with respect to the calibrated recharge amount) resulted in a mean water level more than 150 m above the calibrated

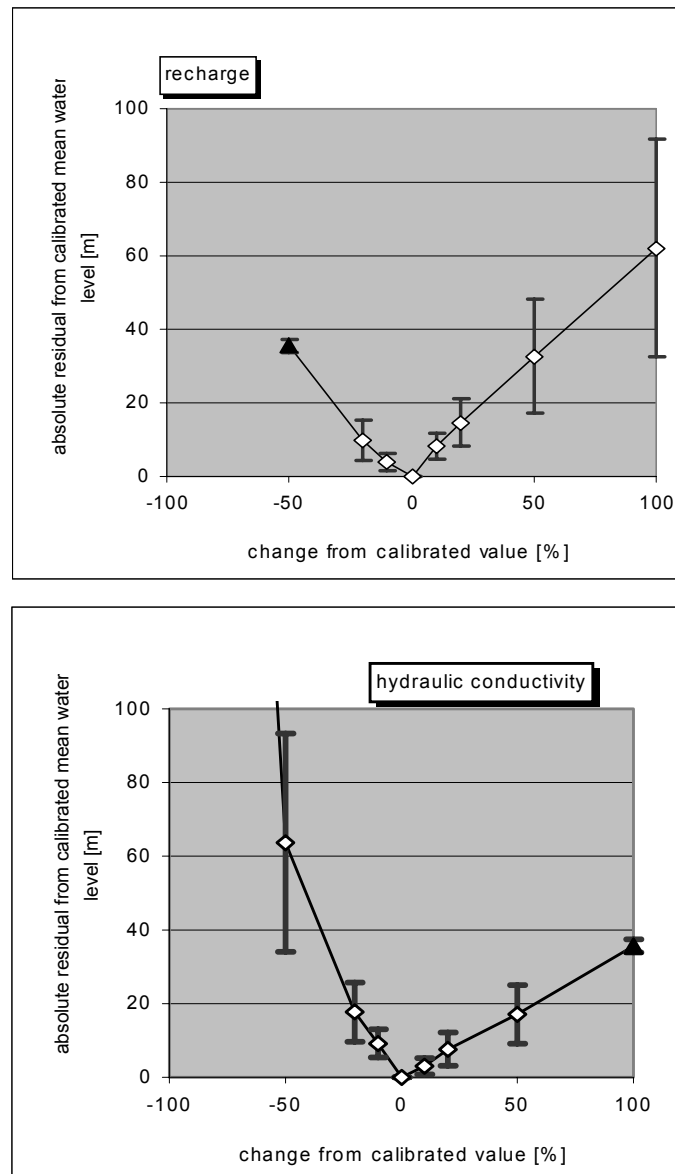


Fig. 6.3-1: Sensitivity analysis of the effect of the value of hydraulic conductivity and recharge on the values of mean water level. Residual standard deviations are also given.

one. It was also found that the standard deviation increase rapidly with the enlarged recharge. Lowering the hydraulic conductivity of about 90 % resulted in a dramatically higher mean water level (+ 484.9 m) which is not indicated in Fig. 6.3-1. Multiplying the hydraulic conductivity by a factor of 2 causes some cells to run dry (filled triangle in the lower plot in Fig. 6.3-1). The tested changes of the calibrated parameters indicated that the model calibration was executed on a sensitive model and is reasonable from this point of view.

6.4 Interpretation and recommendation for further water resource planning

The recharge amount which has been determined by the use of a calibrated groundwater flow model ranges from $5.4 \cdot 10^6 \text{ m}^3/\text{a}$ (*minimum kf approach*) to $1.2 \cdot 10^8 \text{ m}^3/\text{a}$ (*maximum kf approach*). The latter figure lies only slightly above the results from the inverse hydrochemical ($1.04 \cdot 10^8 \text{ m}^3/\text{a}$) and the minimum satellite image ($1.13 \cdot 10^8 \text{ m}^3/\text{a}$) recharge regionalisation approach for the Eiseb-Epukiro-Catchment (chapters 5.7 and 5.8). It also fits within the discharge volume assumed for the entire Kalahari-Makgadikgadi-Okavango-catchment at the Makgadikgadi depression in Botswana ($3\text{-}6 \cdot 10^8 \text{ m}^3/\text{a}$). The *minimum kf approach* reveals a recharge amount that is more than one order of magnitude smaller than any of the other estimates and is therefore not assumed as the appropriate basin wide result.

The major recharge for the Eiseb-Epukiro-Catchment occurs at the western fringe and secondary in the Hochfeld and the Tsumkwe region. Recharge within the catchment is almost negligible.

It was found during the modelling study that any future modelling predictions strongly requires further input data, especially for the hydraulic conductivity distribution. It is as well concluded that detailed modelling with several distinctive aquifers is only possible when more detailed studies of the Kalahari lithology and their distribution within the basin are available. A further questionable parameter is the dispersal of Karoo strata which also appeared during a groundwater flow modelling project in the Otavi area by BÄUMLE ET AL. (2001).

As no prediction with the available basic data are meaningful, only more general interpretation of the current and future water resource management are possible. The present supply and demand situation in the eastern part of the Eiseb-Epukiro-Catchment gives an abstraction volume of $2 - 4.5 \cdot 10^6 \text{ m}^3/\text{a}$ (DWA, 1993c). The western and southern part of the catchment is used for extensive cattle farming which requires under the present conditions 8-12 ha per large stock unit. Assuming that a large stock unit consumes a water amount of 40 - 50 l/day this gives an abstraction amount for cattle watering of $1 - 2 \cdot 10^7 \text{ m}^3/\text{a}$. The water demand has to be topped up by some amount for human consumption and small industries in the major towns. This reveals a total abstraction for the Eiseb-Epukiro-Catchment of at least $2 - 4 \cdot 10^7 \text{ m}^3/\text{a}$. The abstraction

figure corresponds to 20 - 40 % of the modelled recharge amount, but in this calculation no consumption of the water resource from outside the catchment has been considered nor any irrigation.

With the present situation it seems as the water consumption is in accordance with the available water resource. But the results of a steady state situation reflect only the averaged case and in some very dry years the abstraction might be increased, while recovery of the groundwater levels during the wet season was limited. Over-exploitation of single wells during such periods might cause some loss of well yield which will take longer to recover than the over-exploitation time. And it has also to be kept in mind, that the recharge volume of $1.2 \cdot 10^8 \text{ m}^3/\text{a}$ is the calculated upper range and that the total recharge amount might also be smaller than this figure.

Increasing abstraction at the fringe of the catchment might not only cause decreasing groundwater levels there, but also allow no development of additional grassing areas in the eastern part of the catchment which strongly depends on the recharge potential of the fringe areas. A lowering of groundwater levels in the fringe areas could smooth the hydraulic gradient further which would result in slower groundwater movements and thus reduce borehole yield in the eastern part of the catchment. A lowering of the groundwater level in the eastern part of the catchment of the order of 50 m might reveal to a stagnant groundwater system (the discharge area at the Makgadikgadi depression has a lowest elevation at 890 m asl) or even a change of the groundwater flow direction. Such dramatic changes demand for a detailed simulation for the entire catchment which must also include the Botswana part of the basin. For any future water resource management it is recommended to develop further data sources, e.g. hydrographs without abstraction, more detailed basin wide lithology studies and hydraulic parameter tests, followed by detailed modelling including calibration for both steady state and transient, and predictions.

The provided model is not acceptable for planing of further water development as its resolution is insufficient for the finding of water bearing structures. All that is concluded in the sense of well development is to focus on unconformities and fault zones which could result from more detailed geological basic research and an improved data accessibility. It is as well recommendable to provide better training for the local drillers for the borehole lithological description. A further improvement for a hydrogeological model could also be obtained by providing more detailed reports on borehole tests that have been performed by third parties and by providing updated resources to improve the efficiency of the existing DWA database.

7 Hydrochemistry

7.1 Methodological aspects

The major task of a hydrochemical assessment in this study is to understand some of the processes that take place in the catchment and that influence the hydrochemical compositions and developments. Therefore it is initially required to develop a reliable database of hydrochemical parameters. Hydrochemical analyses for the study area are available from HUYSER (1982), from the DWA database and a report by the DWA (1993d). Additional data were obtained during field work by sampling wells and receiving some hydrochemical analyses from farmers. All analyses have been checked for the charge balance error:

$$Error(\%) = \frac{\sum cations(meq/l) - \sum anions(meq/l)}{\sum cations(meq/l) + \sum anions(meq/l)} * 100 \quad (7.1)$$

Only those data with an error below 6 % (this is assumed as the maximum analysing error) went into the database (Appendix D). Most analyses have charge balance errors below 2 - 3 %. The samples obtained during the field work have been analysed directly in the field for pH by an electric pH-meter and for electric conductivity (EC) by a conductivity-meter, while the major ions were quantified in the laboratory of the LFB Hydrogeologie in Würzburg. Analysing methods are summarised in Table 7.1-1.

Table 7.1-1: Summary of analysing methods used for determination of the quantity of major ions in groundwater samples from the study area

Ion	Analysing method	Apparatus	Detection limit [mg/l]
Ca ²⁺	High Performance Liquid Chromatography	Biotronic BT 7000	0.1
Mg ²⁺	High Performance Liquid Chromatography	Biotronic BT 7000	0.1
Na ⁺	High Performance Liquid Chromatography	Biotronic BT 7000	0.1
K ⁺	High Performance Liquid Chromatography	Biotronic BT 7000	0.1
HCO ₃ ⁻	Titrimetry		0.1
SO ₄ ²⁻	Ion Chromatography	Biotronic IC 1000	0.1
NO ₃ ⁻	Ion Chromatography	Biotronic IC 1000	0.1
Cl ⁻	Ion Chromatography	Biotronic IC 1000	0.1

Available tools for understanding the basin-wide distribution of hydrochemical parameters are mathematical regionalisation (Chapter 2.2), hierarchical cluster analysis and principle component analysis. During this study several cluster analyses with or without preliminary factor minimisation by principle component analysis using different data sets (including all major ions or a selection) and different spatial resolution (entire study area, smaller river catchments, administrative regions) have been conducted. None of these cluster analyses revealed groups that were assignable to a specific process or limited to specific (geological) areas. It appears that the distribution of hydrochemical parameters is induced by several processes and that specific water types are not well definable by clustering. Therefore the process of cluster analysis was abandoned although it has been demonstrated to be a powerful tool for the definition of groups produced by specific processes in the western part of this study area by KÜLLS (2000). It was thus decided to "group" the samples according to their appearances in Piper plots, to their electric conductivity and to specific ion ratios with the background of well known processes. The following processes were recognised during this study and some background is given in the next paragraphs: open system calcite dissolution, dolomite dissolution, gypsum dissolution, calcite precipitation, dedolomitisation, evaporation, hydrolyse of mafic minerals, hydrolyse of feldspar and cation exchange.

A very common process in the study area is the open system dissolution of calcite in the unsaturated zone and surface of the saturated zone (for carbonate-carbon-dioxide-water-reactions and -equilibrium-constants see common textbooks, e.g. MATTHEB, 1994; FREEZE & CHERRY, 1979; APPELO & POSTMA, 1996). Rain water infiltrates into the unsaturated zone where the CO₂ partial pressure increases due to root respiration and aerobic decay of organic material. The increasing CO₂ partial pressure causes the reaction given in equation 7.2 to proceed farther to the right to achieve equilibrium. Solution in the carbonate system writes as:



As the soil water leaves the root zone, the CO₂ partial pressure is decreasing during the deeper soil passage and hence calcite becomes supersaturated. Precipitation of calcite underneath the root zone was observed in some soil profiles of the study area as calcrete nodules or horizons.

A common case of closed system dissolution (no contact to a gaseous reservoir) in the study area is dolomite dissolution which typically leads to a Ca²⁺/Mg²⁺ ratio of 1. If both, calcite and dolomite, are available in the aquifer the equilibrium reaction is given as:

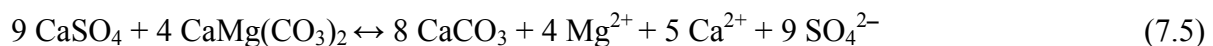


Gypsum dissolution writes as:



Through the dissolution of gypsum the concentration of Ca^{2+} and SO_4^{2-} in the solution is increased. If groundwater, which is saturated with respect to calcite, is entering a zone which contains gypsum, the increased Ca^{2+} -amount is causing calcite to precipitate in order to achieve an equilibrium state for the solution with respect to calcite. Therefore gypsum dissolution is only increasing the SO_4^{2-} -content of a groundwater and HCO_3^- -content is likely to decrease while Ca^{2+} -content should stay approximately constant, assuming that the solution was initially in equilibrium with respect to calcite.

A common case is the process of dedolomitisation if dolomite, calcite and gypsum are available in an aquifer, which is expressed as:



In this case the solution, in equilibrium with dolomite, calcite and gypsum, receives increased amounts of Mg^{2+} , Ca^{2+} and SO_4^{2-} while dolomite is replaced by calcite. Typical ion ratios occurring with this process are $\text{Ca}^{2+}/\text{Mg}^{2+}$ at 1.25 and $\text{Mg}^{2+}/\text{SO}_4^{2-}$ at approximately 0.4.

As presented in chapters 5.7 and 5.8 evaporation from groundwater occurs in some parts of the study area. In these areas evaporation is mostly not reaching concentration factors above 3 (assuming an integrated recharge amount of 100 mm compared to an evaporation amount of 30 mm). It is thus concluded that the evaporation with a maximum factor of 3 causes only calcite to precipitate according to concepts presented and reviewed in DREVER (1982), e.g. GARRELS & MACKENZIE (1967). Calcite precipitation leads to a relative enrichment of Mg^{2+} - and Na^+ -ratio on the cation side and SO_4^{2-} - and Cl^- -enrichment on the anion side of a Piper plot. Whenever calcite precipitates, the $\text{Ca}^{2+}/\text{Mg}^{2+}$ -ratio in the groundwater increases as dolomite is very unreactive at low temperature; e.g. GARRELS & MCKENZIE (1967) assume in their evaporation model that sepiolite ($\text{MgSi}_3\text{O}_6(\text{OH})_2$) instead of dolomite precipitates after calcite. Further evaporation could as well induce the precipitation of either dolomite, sepiolite or gypsum according to the available species following the Hardie-Euster-Model (HARDIE & EUGSTER, 1970 in DREVER, 1982). Evaporation is as well recognisable by increasing Cl^- -content while groundwater levels are shallow.

ions have stronger adsorption affinity than the monovalent ions and the affinity for adsorption is stronger for K^+ than for Na^+ and stronger for Ca^{2+} than for Mg^{2+} .

To verify if the Na^+ - HCO_3^- -water type results from either reaction (eq. 7.7 or eq. 7.8) it is not reasonable to use the development of HCO_3^- as it underlies significant changes by the carbonate-equilibrium-system, and therefore balancing the alkali ions and alkaline earth ions against HCO_3^- is not recommendable. JAHNKE (1999) proposed to use the alkali excess over chloride for the distinction between the genesis of Na^+ - HCO_3^- -water by cation exchange or by weathering of feldspar. Therefore a plot of HCO_3^- and alkaline earth elements ($Ca^{2+} + Mg^{2+}$) versus alkali excess over chloride ($Na^+ + K^+ - Cl^-$) is used. With cation exchange the alkaline earths should decrease 1:1 compared to the alkali excess. Anions are not influenced by this process but a change in the Ca^{2+} - or Mg^{2+} -content influences the carbonate-equilibrium-system and thus a slight decrease in HCO_3^- -content might occur if carbonate is available in the aquifer. During feldspar weathering the alkaline earth content should be rather uninfluenced while the HCO_3^- -content should increase with a stoichiometric relation of 1:1 compared to the alkali excess.

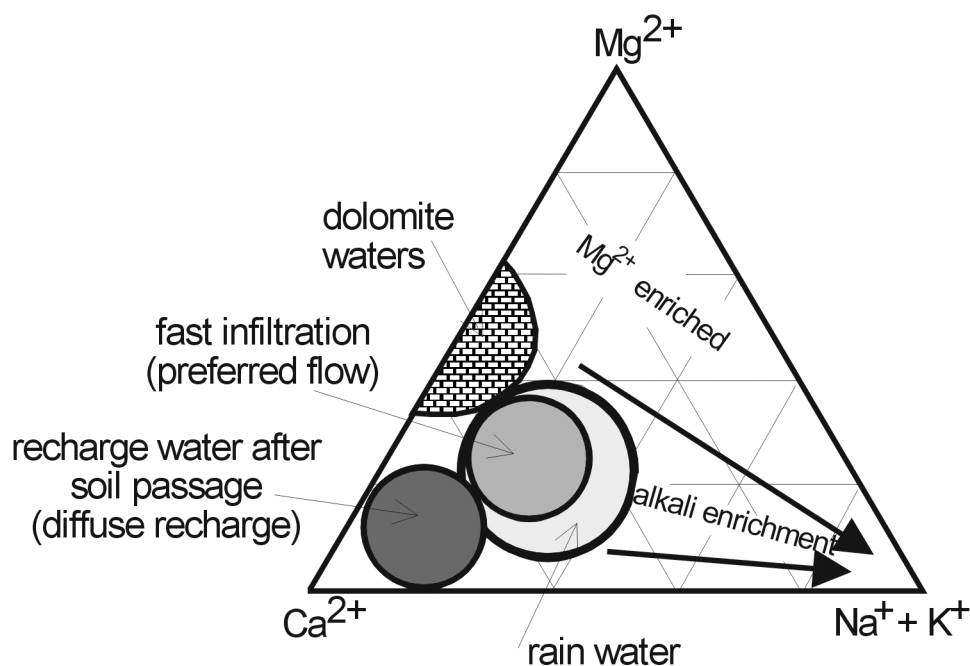


Fig. 7.1-1: Appearance of cation compositions for some typical waters. Grey values are increasing with electric conductivity.

Some water types are defined by certain cation ratios. Therefore such waters are recognisable from the plot in the Piper diagram, and the common water types of rain water, recharge water after soil passage (RASP-water), recharge water from fast infiltration (RFI-water) and dolomitic waters are indicated in Fig. 7.1-1. In the anion field the mentioned water types are characterised by a very dominant HCO_3^- -component.

7.2 Spatial distribution of hydrochemical parameters in the study area

All hydrochemical data for the study area of north-eastern Namibia are plotted in a Piper diagram (Fig. 7.2-1), which indicates the large variation of hydrochemical processes and water types in the research area. Working with such an amount of data is only practicable if simplifications are possible.

The spatial data distribution has been examined in raw variograms for all major ion contents, pH and electric conductivity (Fig. 7.2-2 and 7.2-3). pH (Fig. 7.2-3) shows a particularly bad regional reproducibility. The plots of EC, Na^+ , Cl^- , HCO_3^- and SO_4^{2-} are as well indicating, that any mathematical regionalisation is questionable. The variograms of NO_3^- and K^+ indicate that the distribution of these parameters has no regional component and is thus appearing as a plot of random noise. Only the Ca^{2+} - and Mg^{2+} -distributions would allow meaningful regionalisation. It is concluded that hydrochemical data in general cannot be examined in a *Kalahari basin-wide* approach. This might result on the one hand from very heterogeneous spatial distribution of the available data (upper right lot in Fig. 7.2-2) and on the other hand very variable aquifer lithologies overprint a basin wide pattern. Therefore it was decided to divide the catchment into three main hydrochemical study areas and to examine the hydrochemical distributions there in more detail and then to develop some basin wide understanding that is based on the results of the single study areas.

The western part (west of Longitude E18.6°) of the study area has been studied hydrochemically in detail by KÜLLS (2000) and is thus not further included in this study. As this entire project focuses on the groundwater under Kalahari conditions (Eiseb-Epukiro-catchment), the northern most part of the study area has as well not been further considered. The climate there is wetter and the groundwater near the Okavango might locally be influenced by river-groundwater-interaction and is thus even further overprinting the typical hydrochemical processes in the Kalahari. The eastern part of the catchment has been divided in three main hydrochemical study areas:

- Northern hydrochemical study area (NHSA) between Latitude S19.3° and S20° and east of Longitude E18.6° which includes parts of the Grootfontein and Tsumkwe district.
- Southern hydrochemical study area (SHSA) including samples from the farmland of the district Gobabis, the southern fringe of the Kalahari communal land (former Hereroland East) and samples of the Talismanis-Rietfontein Block.
- Central hydrochemical study area (CHSA) which includes groundwater samples from the lower Epukiro and Eiseb catchments.

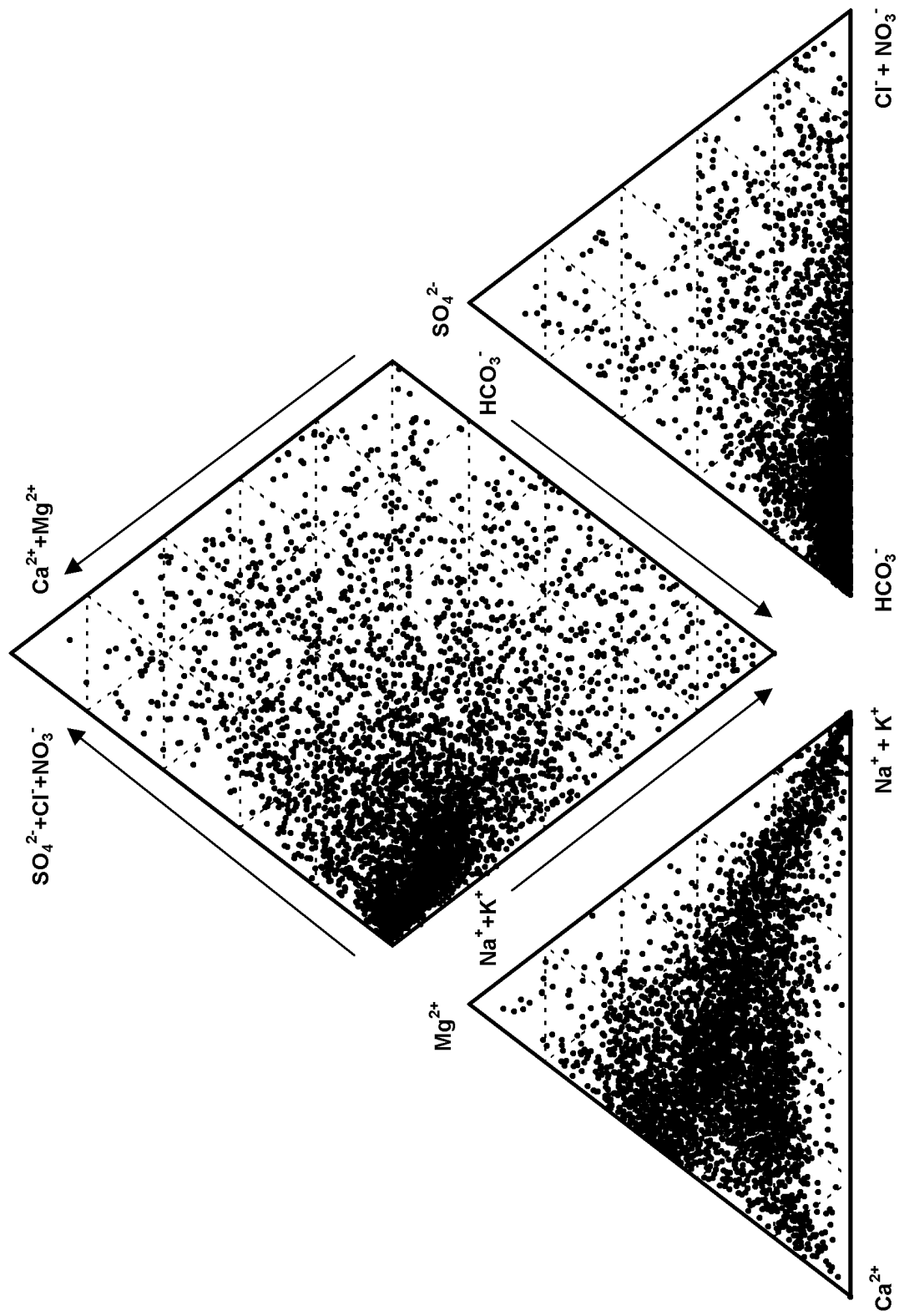


Fig. 7.2-1: Piper diagram of the samples in the entire research area. The spatial distribution of the data points is shown in the upper right plot in Fig. 7.2-2.

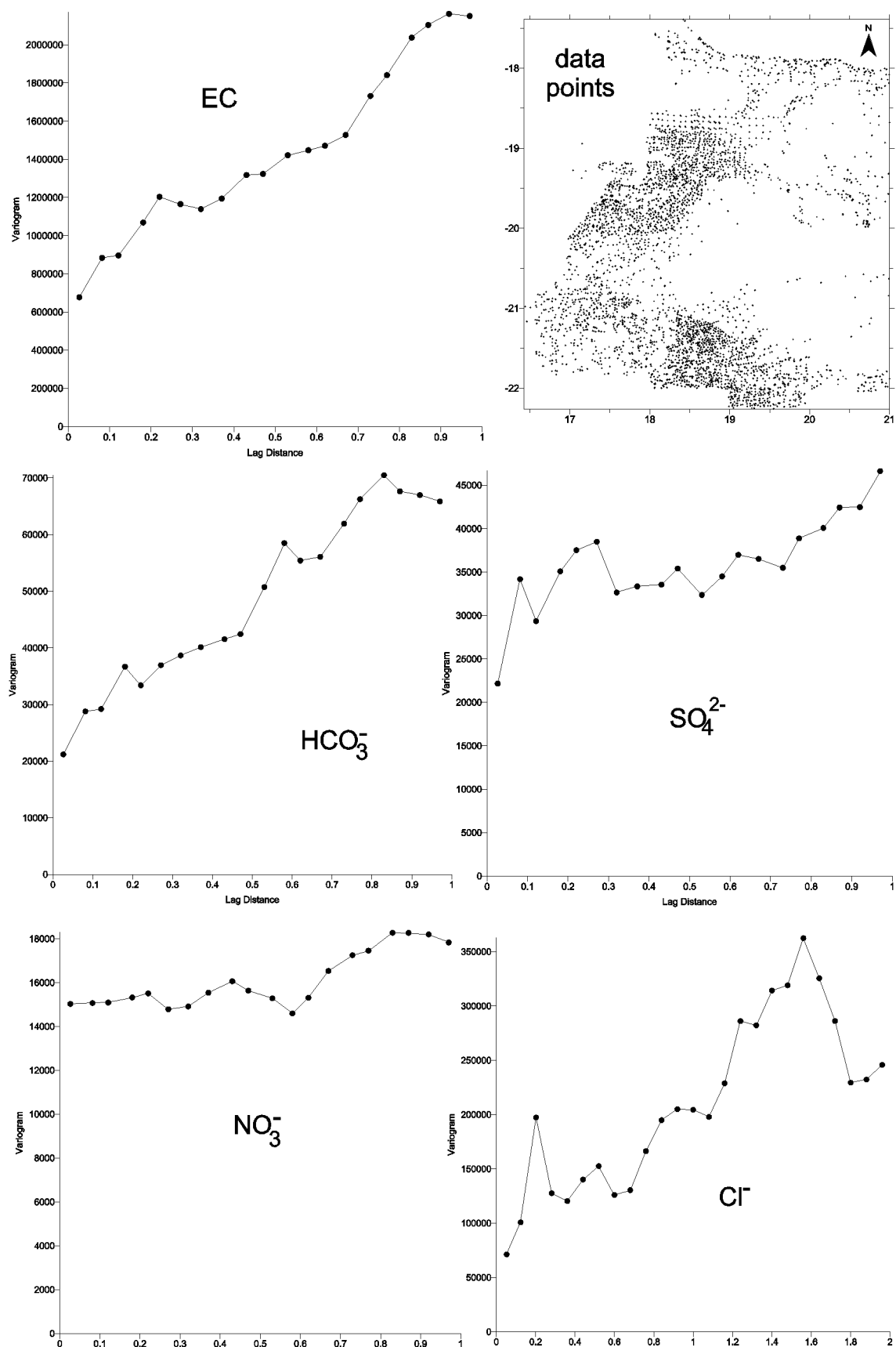


Fig. 7.2-2: Raw variograms of the major anion contents and electric conductivity (EC) in the study area. The spatial distribution of the data points is given in the upper right plot. Used number of data points: 4296 for EC, 4296 for HCO₃⁻ and NO₃⁻, 4137 for SO₄²⁻ and 4123 for Cl⁻.

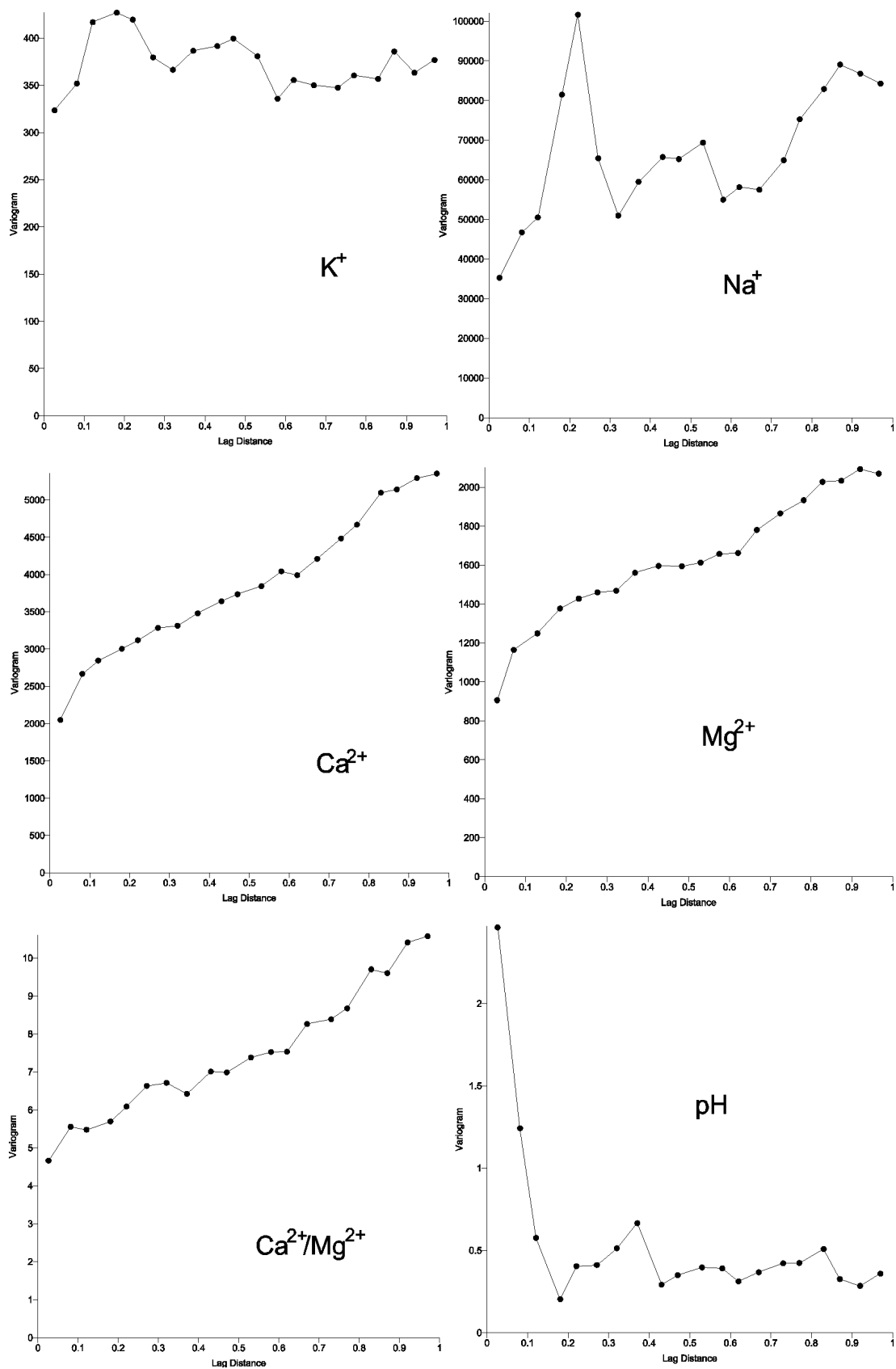


Fig. 7.2-3: Raw variograms of the major cation contents and pH in the study area. The spatial distribution of the data points is given in the upper right plot in Fig. 7.2-2. Used number of data points: 4155 for pH, 4296 for Ca²⁺, Mg²⁺ and Ca²⁺/Mg²⁺-ratio, 4158 for Na⁺ and 4106 for K⁺. Difference from the data amount appears from missing data in the provided data sets by HUYSER (1982) and in the DWA database.

7.2.1 The northern hydrochemical study area (NHSA)

Aquifers of the Kalahari Group, Rundu Formation, Damara Sequence and the Grootfontein Complex appear in the NHSA (Chapter 3). Hydrochemical data plot almost everywhere in the Piper diagram (Fig. 7.2-4), only the Mg^{2+} - and SO_4^{2-} -dominated fields are not occupied.

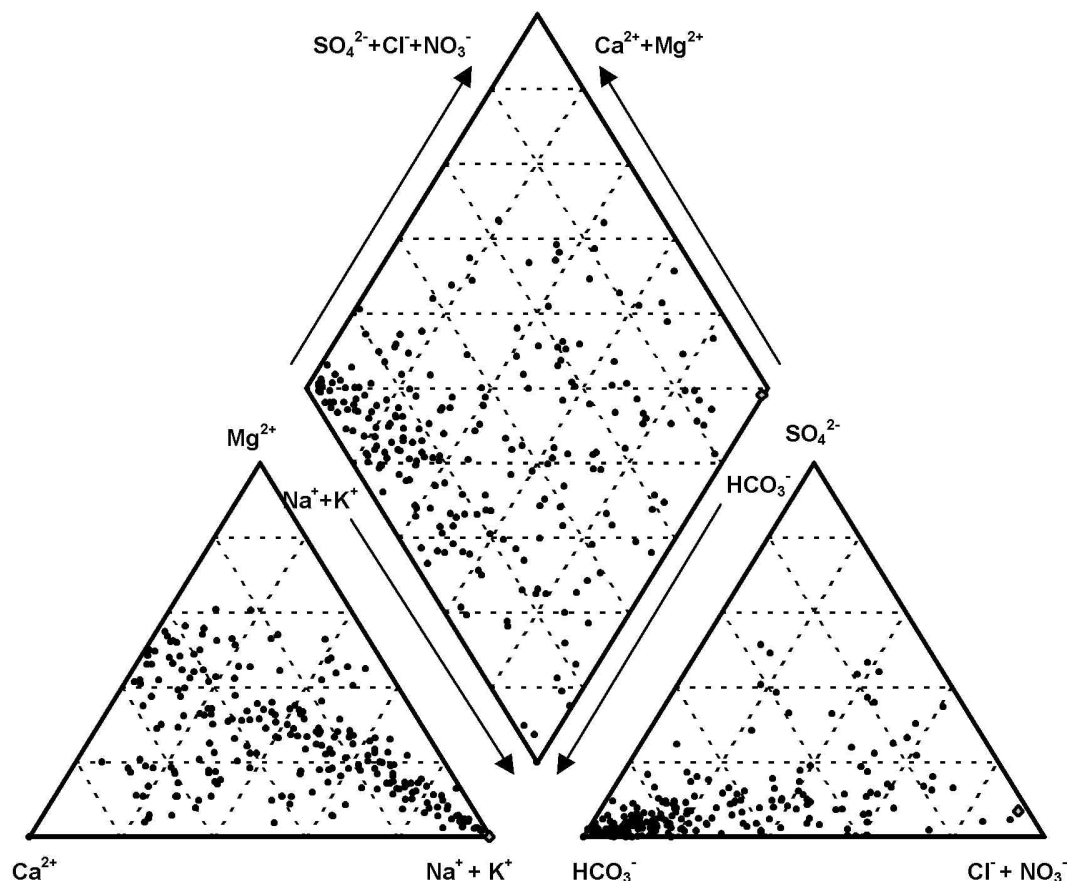


Fig. 7.2-4: Piper plot of groundwater samples from the NHSA. The water sample with the highest EC (42500 $\mu\text{S}/\text{cm}$) at Dobe Pan is indicated by a grey filled \diamond (Na^+ - Cl^- -field).

Electric conductivity for the 241 samples from this area ranges from 220 to 42 500 $\mu\text{S}/\text{cm}$. More than half of the samples (134) show electric conductivities below 1 000 $\mu\text{S}/\text{cm}$, only 5 samples are above 5 000 $\mu\text{S}/\text{cm}$. The distribution of EC is given in Fig. 7.2-5. The highest electric conductivity (pink \diamond in Fig. 7.2-5) occurs in the eastern part of the research area and it is associated with the Dobe Pan (EC = 42 500 $\mu\text{S}/\text{cm}$) where basalts are covered by Kalahari sediments. The sample plots in the Na^+ - Cl^- -field (grey filled \diamond in Fig. 7.2-4) and presents most probably some stagnant water.

The water samples in the NHSA have been subdivided into several groups according to the electric conductivity, distribution in Piper plots and spatial distribution (samples with very high EC are not considered). 3 main groups are further discussed:

- Groundwater with low electric conductivity ($\leq 550 \mu\text{S/cm}$) in the central part of the NHSA
- Groundwater in the western part of the NHSA (5 subgroups)
- Groundwater in the eastern part of the NHSA (7 subgroups)

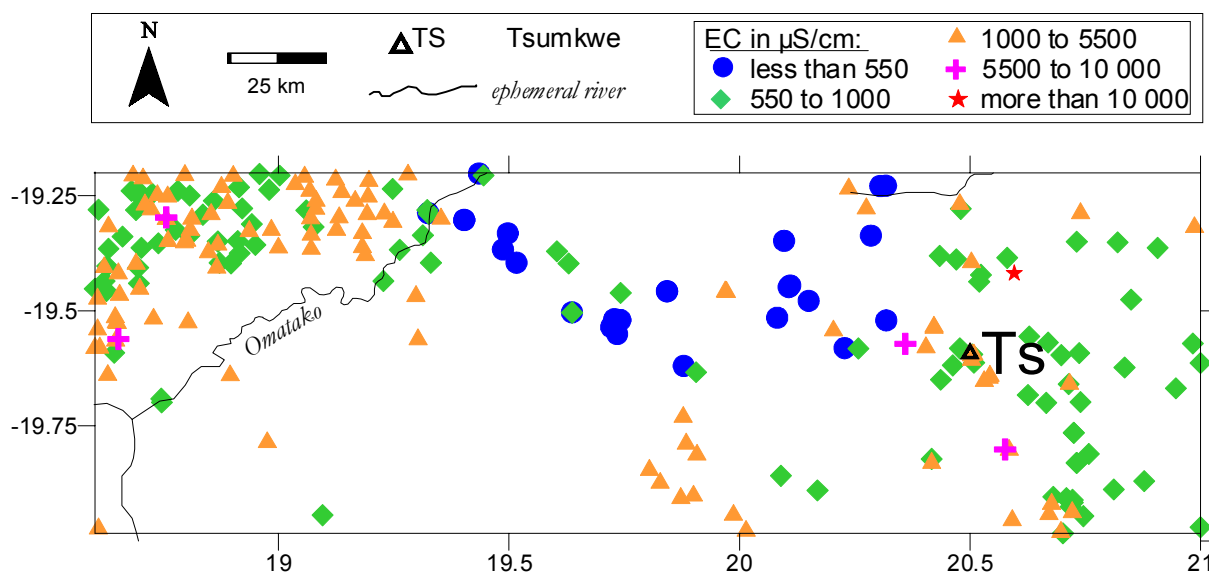


Fig. 7.2-5: Distribution of electric conductivity in the NHSA. The groundwater samples with EC below $550 \mu\text{S/cm}$ are constrained to the central part of the NHSA.

Groundwater with low electric conductivity

Groundwater with EC up to $550 \mu\text{S/cm}$ (dark blue ● in Fig. 7.2-5) appears only in the central northern part of the NHSA and all samples of this group are associated with Kalahari lithologies. All samples appear in the HCO_3^- -field of the Piper plot and only two samples show a slightly increased SO_4^{2-} - or Cl^- -component compared with the others and are respectively indicated as black x and + in Fig. 7.2-6. The SO_4^{2-} -enriched sample (x in Fig. 7.2-6) is constrained to the bench of a flood course.

Most of the samples plot in the field of RFI-waters and RASP-water in the cation triangle of Fig. 7.2-6. In the Piper plot a development from Ca^{2+} - towards Na^+ -dominated waters appears without significant Mg^{2+} -enrichment. A single sample, that is constrained to a flood course, shows a slightly increased $\text{Mg}^{2+}/\text{Ca}^{2+}$ -ratio (Δ in Fig. 7.2-6).

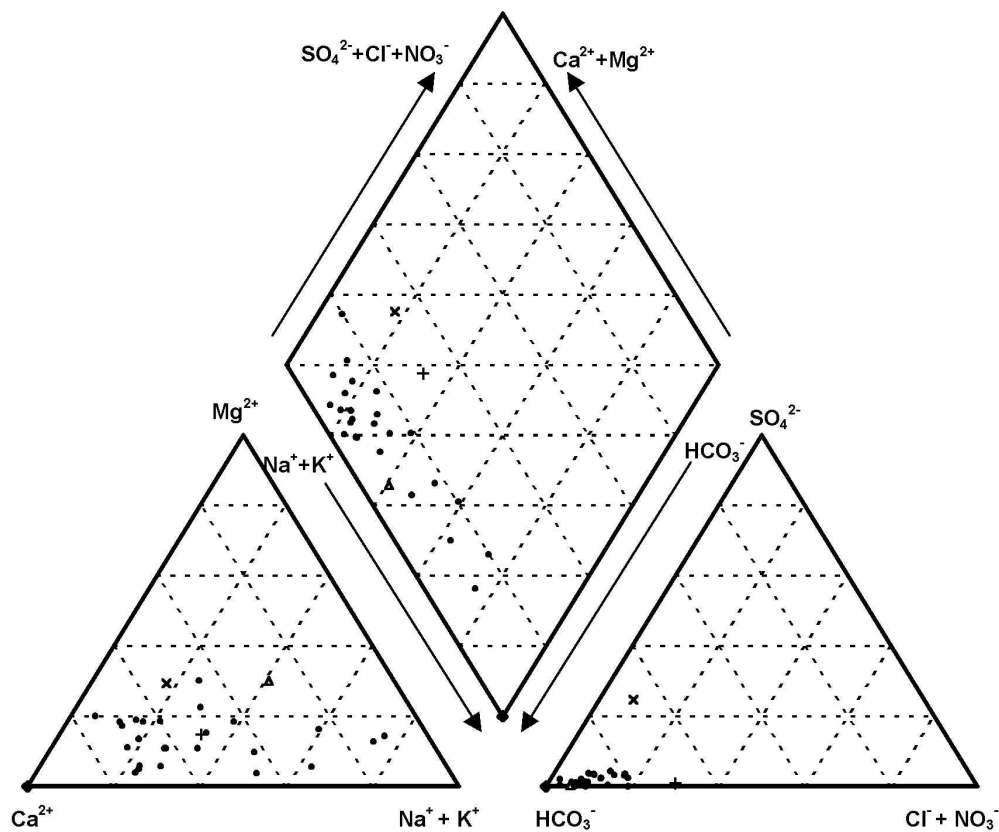


Fig. 7.2-6: Piper plot of groundwater samples with low electric conductivity ($< 550 \mu\text{S}/\text{cm}$) in the NHSA. Samples with extraordinary composition are marked by x (SO_4^{2-} -enriched), + (Cl^- -enriched) and Δ (increased $\text{Mg}^{2+}/\text{Ca}^{2+}$ -ratio).

As some samples plot in the $\text{Na}^+/\text{HCO}_3^-$ -field, the alkaline earths have been plotted against the alkali excess to verify the genesis of this water type (Fig. 7.2-7). For the samples with low alkali excess no correlation appears but samples with an alkali excess of more than $2 \text{ mmol}(\text{eq})/\text{l}$ show a decrease of the alkaline earths with a stoichiometric ratio of approximately 1:1. It is thus concluded that the Na^+ -enrichment for the considered samples results from cation exchange. Clay layers occur locally in the Kalahari Group and thus the

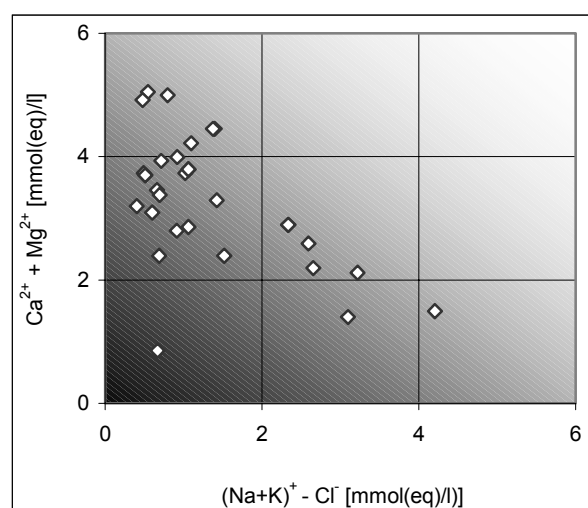


Fig. 7.2-7: Plot of alkaline earths versus alkali excess over chloride for water samples with low hydraulic conductivity in NHSA.

result is consistent with geological observations.

It is concluded that the water samples with low EC in the NHSA represent young recharge water in the Kalahari which has only received minor evaporation. The recharge is of a diffuse nature and Na^+ -enrichment results from cation exchange.

Groundwater in the western part of the NHSA

Groundwater samples with EC between 550 and 5 000 $\mu\text{S}/\text{cm}$ are dominant in the western part of the NHSA and higher conductivities are only reported twice (6 500 - 7 420 $\mu\text{S}/\text{cm}$). The samples with the high EC are marked as grey filled \diamond in Fig. 7.2-8. They are constrained to areas where gneisses of the Grootfontein Complex or undifferentiated Damara lithologies are overlain by Kalahari sediments. Samples with intermediate EC have been divided into five groups: dolomitic waters, Mg^{2+} -enriched samples, Na^+ - HCO_3^- -type, RFI-water and Na^+ -enriched water which is mostly Cl^- -dominated with only a minor SO_4^{2-} -component. The spatial distribution of these groups is given in Fig. 7.2-9.

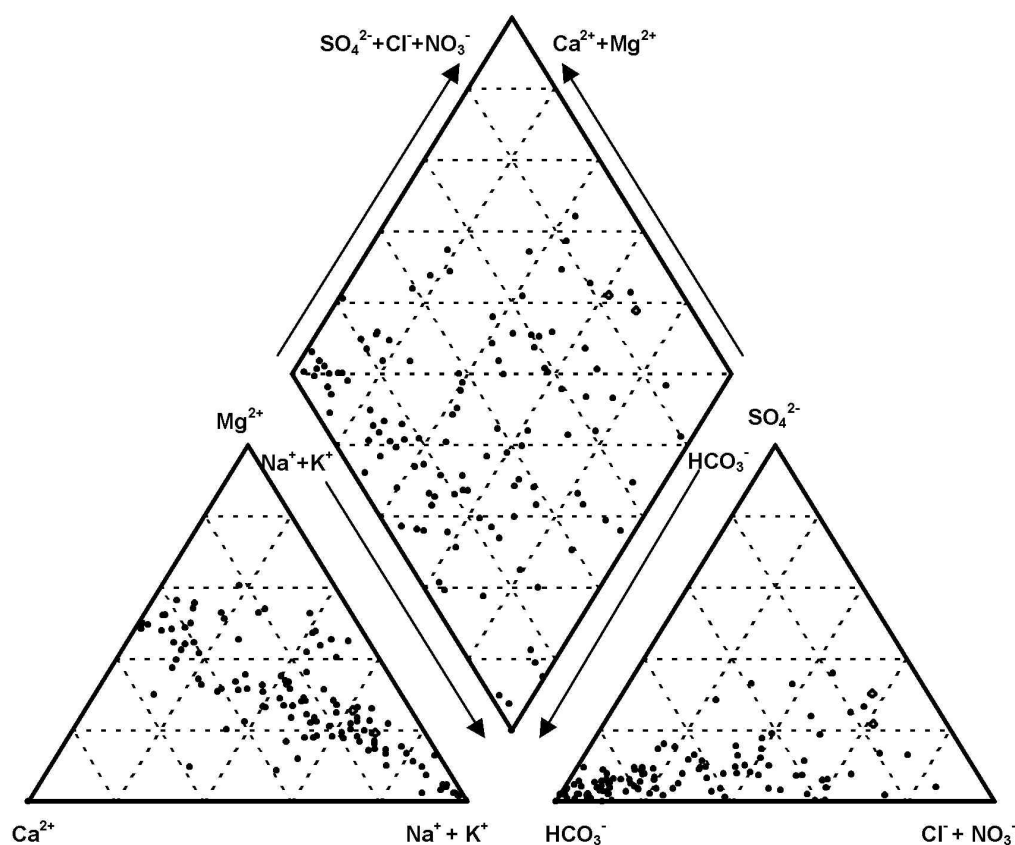


Fig. 7.2-8: Piper plot of groundwater samples in the western part of the NHSA.

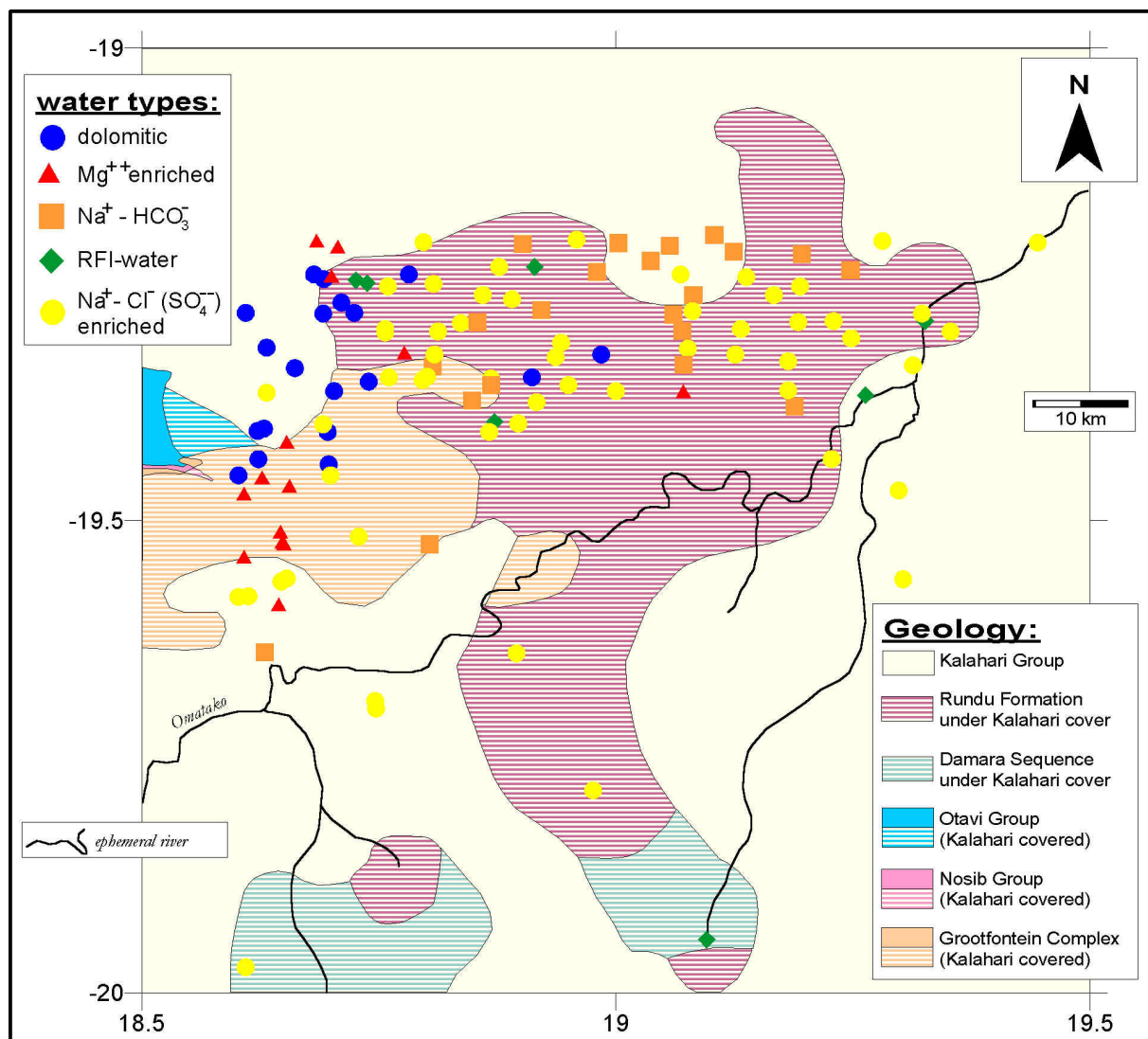


Fig. 7.2-9: Spatial distribution of water types in the western part of the NHTSA with a reference frame of the geology and the major ephemeral rivers.

Most of the samples plot in a balanced $\text{Ca}^{2+}/\text{Mg}^{2+}$ -ratio (Fig. 7.2-8) which indicates dolomite dissolution as described to be typical for water in the Otavi foreland by KÜLLS (2000). 18 samples plot in the proper dolomite field and show electric conductivities from 570-1700 $\mu\text{S}/\text{cm}$. Almost no SO_4^{2-} -component occurs in these samples. This group is constrained to the north-eastern part of the NHTSA and is likely to derive from the Otavi foreland. With a flow towards the east and the south it appears soon that an overprint towards Na^+ - Cl^- -waters takes place, which might result from mixing with an end-member of the Na^+ - Cl^- -water type or by a significantly decreased recharge inflow.

Some Mg^{2+} -enriched waters with respect to dolomite waters appear. EC ranges from 930 - 3000 $\mu\text{S}/\text{cm}$. This small group (14 samples) can be further subdivided into two subgroups. The first group is characterised by the higher Mg^{2+} -ratio, some increased Cl^- -ratio (30-40 %) while

almost no SO_4^{2-} -component appears. In this subgroup all anion-contents and the Mg^{2+} -content increase with EC. This subgroup is constrained to areas where the Rundu Formation is covered by Kalahari sediments. It appears that the Mg^{2+} -enrichment results most likely from weathering of mafic minerals of the underlying basalts and/or its transported weathering products in the Kalahari Group.

The second group with relative Mg^{2+} -enrichment is constrained to an area with shallow groundwater (less than 20 m) where gneisses of the Grootfontein Complex are overlain by 50 - 100 m of Kalahari sediments. In this group the dominant anion is HCO_3^- . The HCO_3^- -content stays almost constant, while all other ions increase with EC. It appears most likely that the relative Mg^{2+} -enrichment results from evaporation and the subsequent precipitation of calcite.

In the western part of the NHSA alkali enriched waters appear including the Na^+ - HCO_3^- -type (21 samples). From the plot of HCO_3^- and alkaline earths versus alkali excess (Fig. 7.2-10) it appears that the Na^+ -enrichment results from feldspar weathering (equation 7.7) due to a stoichiometric 1:1 increase of HCO_3^- versus alkali excess, and alkaline earths versus alkali excess plotting without stoichiometric respect. Most of these samples are located in areas where thick Kalahari sediments overlay the Rundu Formation and only two samples are found within the Grootfontein Complex.

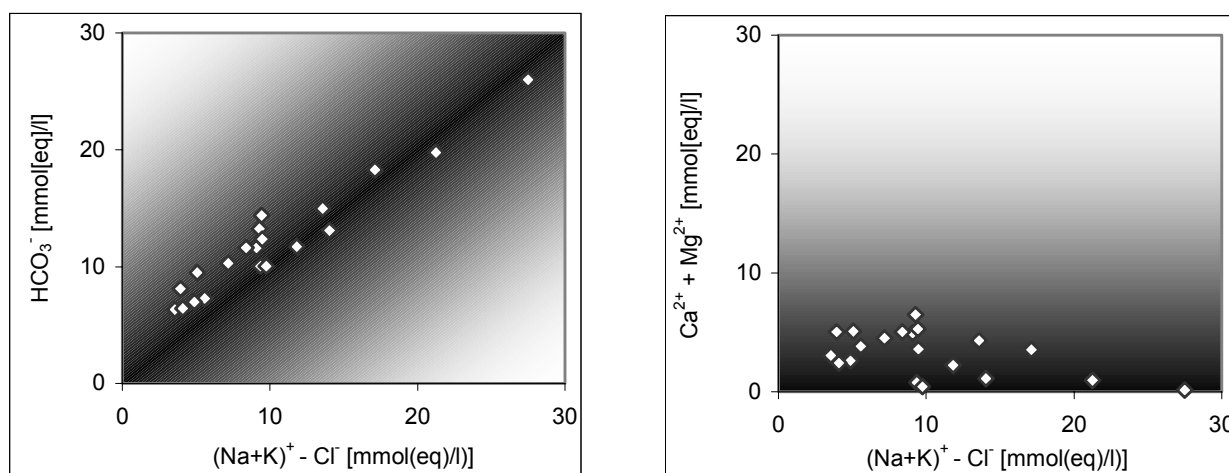


Fig. 7.2-10: Plots of HCO_3^- (left plot) and alkaline earths (right plot) versus alkali excess over chloride for water samples in the western part of NHSA.

The RFI-field is represented by 7 samples only. In this group EC ranges from 650 - 1190 $\mu\text{S}/\text{cm}$. The two samples with the lowest EC are constrained to the flood course of the Omuramba Omatako and one of its tributaries. For this group it was observed that the increase of the Cl^- -ratio correlates well with the total dissolved ion amount and thus reflects the amount of evaporation.

The largest group that occurs in this part of the study area is dominated by a balanced Mg^{2+}/Ca^{2+} -ratio with increased alkali content and an anion development towards $Cl^{-}SO_4^{2-}$ - or Cl^{-} -waters. These waters might partly result from the mixing of any class described above with a water type of increased Cl^{-} - or $Cl^{-}SO_4^{2-}$ -content. This class is not constrained to any specific lithology or surface morphology.

Groundwater in the eastern part of the NHSA

In the eastern part of the NHSA a large variety of water samples occurs with electric conductivity ranging from 560 to 7100 $\mu S/cm$ (not concerning the highly mineralised sample at Dobe Pan mentioned above). A Piper diagram is given in Fig. 7.2-11. Compared with the samples from the western part of the NHSA (Fig. 7.2-8) additional data plot in the field of RASP-water in the data set from the eastern part. Water with a significant increase in Mg^{2+} -ratio are less common here. Some samples with a SO_4^{2-} -ratio above 40 % occur.

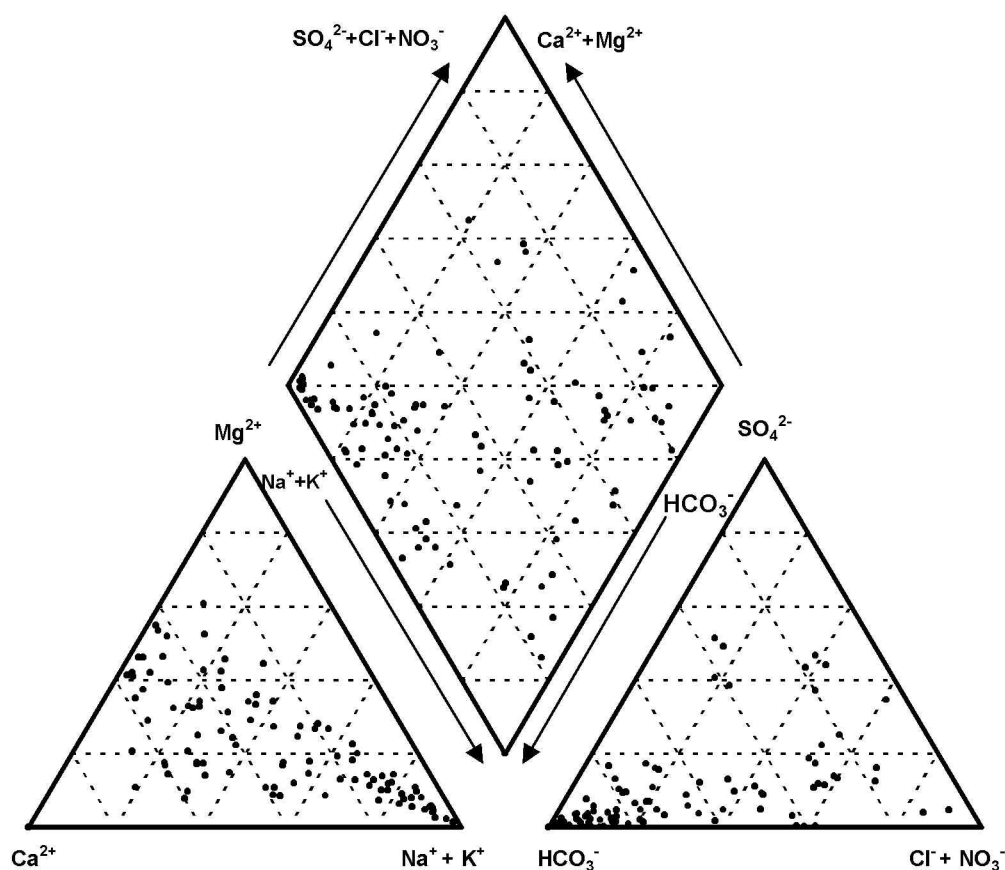


Fig. 7.2-11: Piper plot of groundwater samples in the eastern part of the NHSA.

The water samples have been subdivided into 7 major groups that result from the appearance in the Piper plot: Dolomite waters, RFI-water, RASP-water, Mg^{2+} -enriched waters, $Na^+HCO_3^-$ -

waters, "divas" (examples that do not fit in any other group) from the anion composition and a group of Na^+ - Cl^- -water and two water types that are representing altering water types. The distribution of the groups is given in Fig. 7.2-12.

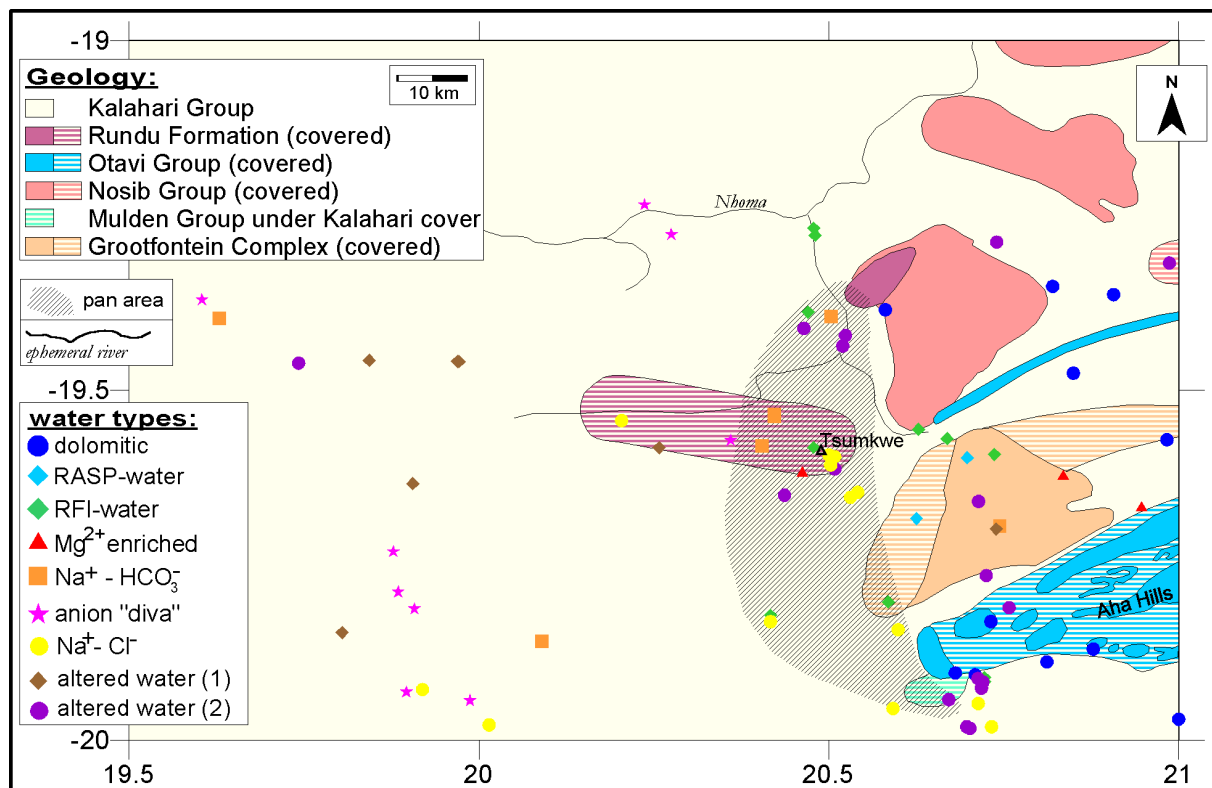


Fig. 7.2-12: Spatial distribution of water types in the eastern part of the NNSA with a reference frame of the geology and the major ephemeral rivers.

Samples that plot in the field of dolomite waters show a very dominant HCO_3^- -component. EC ranges from 560 - 970 $\mu\text{S}/\text{cm}$. From the distribution of the samples which is within or near the Aha Hills and the narrow strip of Otavi Group north-east of Tsumkwe, it is concluded that the fingerprint of these waters results from dissolution of dolomites and the samples in the south-eastern quadrant of the NNSA present recharge water from the Aha Hills.

The field of RASP-water is presented by 2 samples with an electric conductivity range from 585-780 $\mu\text{S}/\text{cm}$. These samples are characterised by a high Ca^{2+} -ratio and very prominent HCO_3^- -amount and it is thus concluded that such waters represent young diffuse recharge waters that are not far from the primary recharge area. Such samples were found east and south-east of Tsumkwe in an area that is dominated by gneisses of the Grootfontein Complex with a fairly thin cover of Kalahari sands only.

Samples that plot in the field of RFI-water in Fig. 7.2-11 are constrained to flood courses of the Omuramba Nhamo or its tributaries and to the pan field around Tsumkwe (Fig. 7.2-12). Electric

conductivity ranges from 698 - 2400 $\mu\text{S}/\text{cm}$, but most of the reported values are below 810 $\mu\text{S}/\text{cm}$. The dominant cation is HCO_3^- with some development towards a Cl^- -component. It is assumed that this group represents water that is quickly recharged by preferred flow path occurring most likely in hardrock areas or unvegetated structured soils. It seems as well reasonable that this water type reflects recharge in hardrock areas that is quickly transported towards the pan field.

Na^+ - HCO_3^- -waters occur in the vicinity of basalts and in areas with thick Kalahari sediments. Conductivity ranges from 650 - 2225 $\mu\text{S}/\text{cm}$. The plots of HCO_3^- and alkaline earths versus alkali excess (Fig. 7.2-13) indicate that feldspar weathering (eq. 7.7) is the major cause of the development. The feldspar source might either be represented by the basalt directly or by its erosional products in the Kalahari Group.

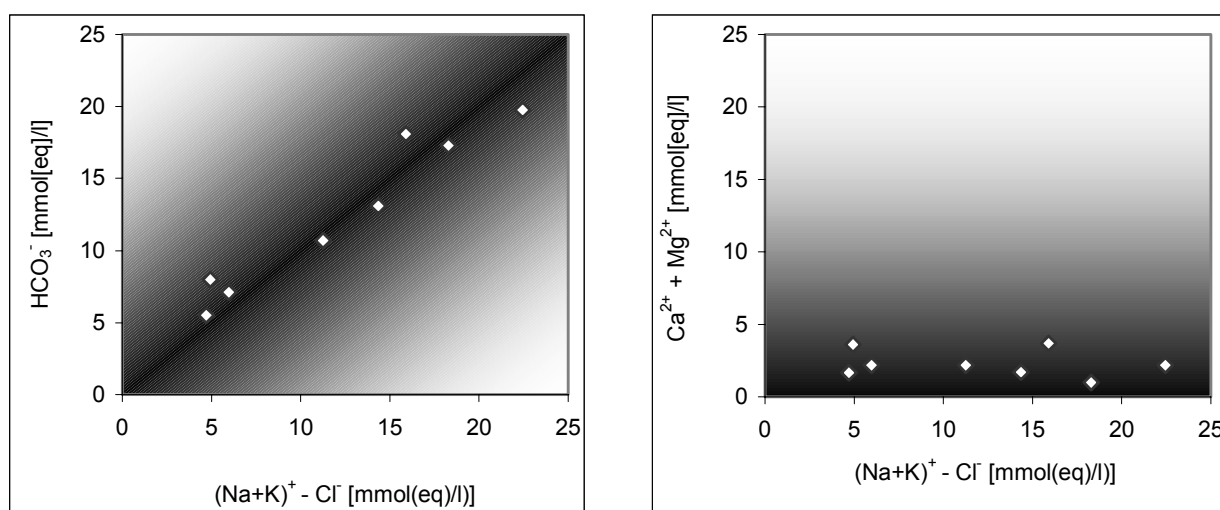


Fig. 7.2-13: Plots of HCO_3^- (left plot) and alkaline earths (right plot) versus alkali excess over chloride for water samples in the western part of NHSA.

Three samples were found that indicate an increased $\text{Mg}^{2+}/\text{Ca}^{2+}$ -ratio. As those samples are characterised by low electric conductivities (585 - 780 $\mu\text{S}/\text{cm}$) and HCO_3^- is dominating the anion composition, it is assumed that the Mg^{2+} -enrichment is not induced by major evaporation but from weathering of mafic minerals from gneisses (Grootfontein Complex) or basalts (dykes for the two eastern most samples or flood basalt for the sample near Tsumkwe).

Two exceptional groups ("anion divas") were found by showing a significant SO_4^{2-} -ratio (more than 35 %). In these samples the Mg^{2+} -ratio is well below 20 %. The first group includes samples that are Na^+ -dominated. EC in this group is between 950 and 3350 $\mu\text{S}/\text{cm}$. The according samples occur in some distance to the hardrock areas and are likely to present some altered waters. The second group (2 samples) is constrained to the Omuramba Nhoma. The samples

there are Ca^{2+} -dominated to Ca^{2+} - Na^+ -dominated while the largest SO_4^{2-} -ratio in this area occurs with 49 - 51 %. Electric conductivity ranges from 1895 - 2000 $\mu\text{S}/\text{cm}$. This water type might result from some dissolution of gypsum in the lower Kalahari Group. For these two samples a $\text{Mg}^{2+}/\text{SO}_4^{2-}$ -ratio of 0.4 occurs which is typical for the process of dedolomitisation. Anyway, the high $\text{Ca}^{2+}/\text{Mg}^{2+}$ -ratio of 3 - 7 indicates a more gypsum and calcite dominated process.

The remaining samples plot in the field of the Na^+ - Cl^- -endmember or altering water that is transposed towards Na^+ - Cl^- -water. The Na^+ - Cl^- -water type occurs mainly in areas that are covered by Kalahari sediments. EC for this group ranges from 1370 to 7100 $\mu\text{S}/\text{cm}$, with the majority showing values below 3000 $\mu\text{S}/\text{cm}$. The two water types labelled as altered water of type 1 and type 2 in Fig. 7.2-12 show electric conductivities between 550 and 1500 $\mu\text{S}/\text{cm}$. Type 1 is characterised by low Mg^{2+} -contents with mostly less than 20 mg/l and a $(\text{Ca}^{2+}+\text{Na}^+)/\text{Mg}^{2+}$ -ratio of 8 - 9. SO_4^{2-} -ratio is always below 20 % and Cl^- -ratio below 40 %, while the Cl^- -content increases with EC. It is assumed that this water type represents the mixing of RASP-water with the Na^+ Cl^- -water type. Altered water of type 2 is characterised by a $\text{Mg}^{2+}/\text{Ca}^{2+}$ -ratio of approximately 1 (0.7 to 1.2), HCO_3^- as the major anion, relatively low Cl^- -content (5 - 40 mg/l with EC below 900 $\mu\text{S}/\text{cm}$, 50 - 90 mg/l above 900 $\mu\text{S}/\text{cm}$) and increasing Na^+ -content with EC. From the appearance in the Piper plot it is concluded that this water represents the mixing path between dolomitic water or RFI-water with a Na^+ - Cl^- -dominated water type. This water type (violet ●) appears in the south-easteren part of Fig. 7.2-12 associated with dolomitic water (blue ●) and Na^+ - Cl^- -water (yellow ●).

7.2.2 The southern hydrochemical study area (SHSA)

1396 samples are available for the SHSA. While the anion ratio covers almost the entire Piper triangle, the distribution of the cations is more constrained to a central area without Mg^{2+} -dominated samples (Fig. 7.2-14). The dolomite field and the proper Ca^{2+} -field are not much frequented. The distribution of samples with low EC in the Piper plot is constrained to HCO_3^- -dominated waters while on the cation plot no specific ion is dominating. It is observed that the cation distribution scatters further in the Piper plot with increasing EC. It is also observed that increasing Mg^{2+} - and Na^+ -ratio correlate positively with electric conductivity. For the anions it was observed that a SO_4^{2-} -enrichment path and a Cl^- -enrichment path appear. While the SO_4^{2-} -ratio increases significantly for samples with an EC between 500 and 1 000 $\mu\text{S}/\text{cm}$ (royal blue area in Fig. 7.2-14c), the Cl^- -dominance occurs more often for samples with EC above 1 000 $\mu\text{S}/\text{cm}$ (light blue area in Fig. 7.2-14c). The samples with EC above 10 000 $\mu\text{S}/\text{cm}$ (white area in Fig. 7.2-14c) are all Cl^- -dominated.

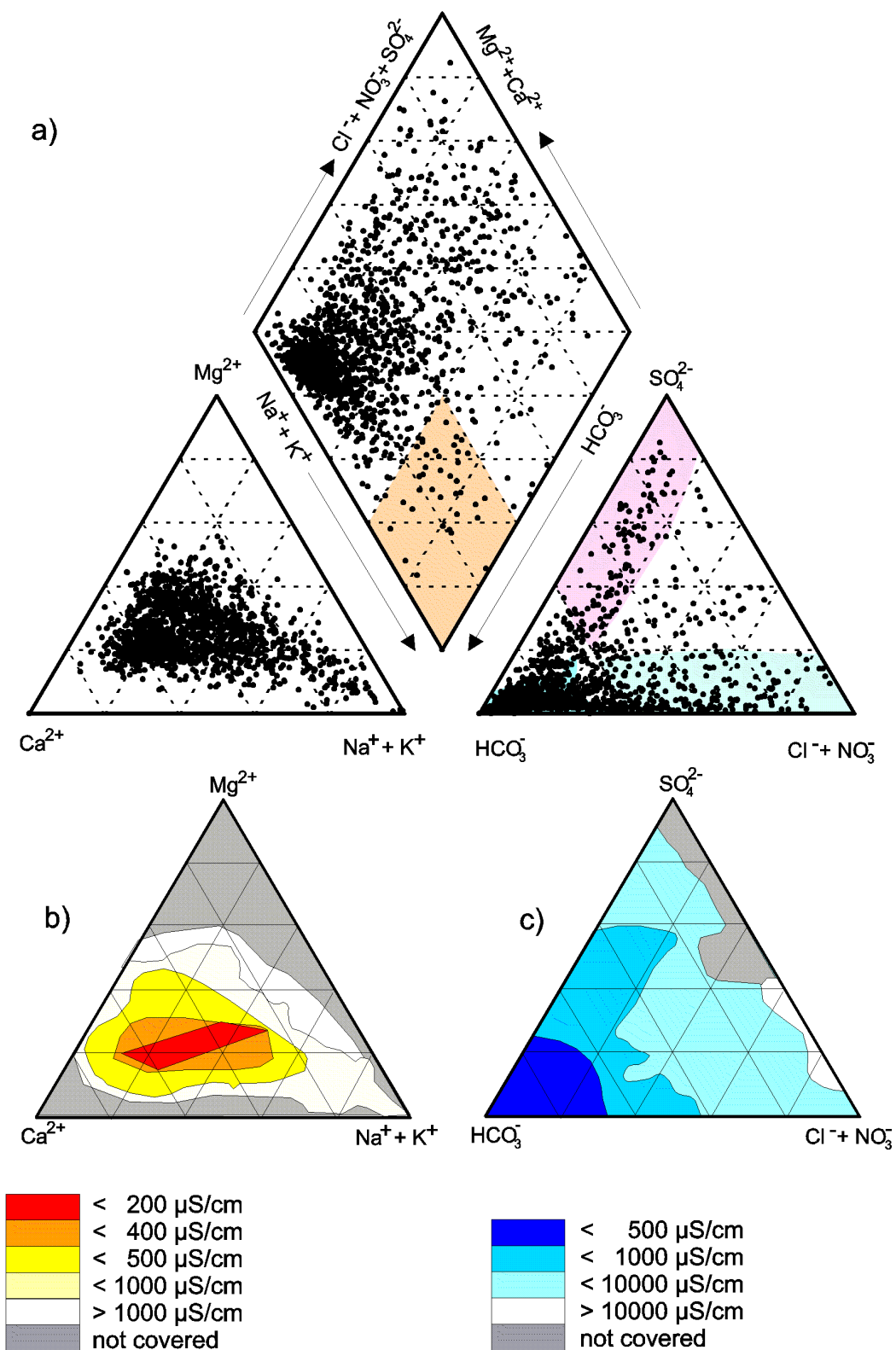


Fig. 7.2-14: Piper plot of groundwater samples in the SHSA. The correlation between electric conductivity and ion ratios is indicated in the lower part (plot b) and c)). Na^+ - HCO_3^- -waters are underlain in orange in the diamond of the upper part (plot a)), while the SO_4^{2-} - and Cl^- -dominated groups are underlain in pink and green, respectively, in the anion plot.

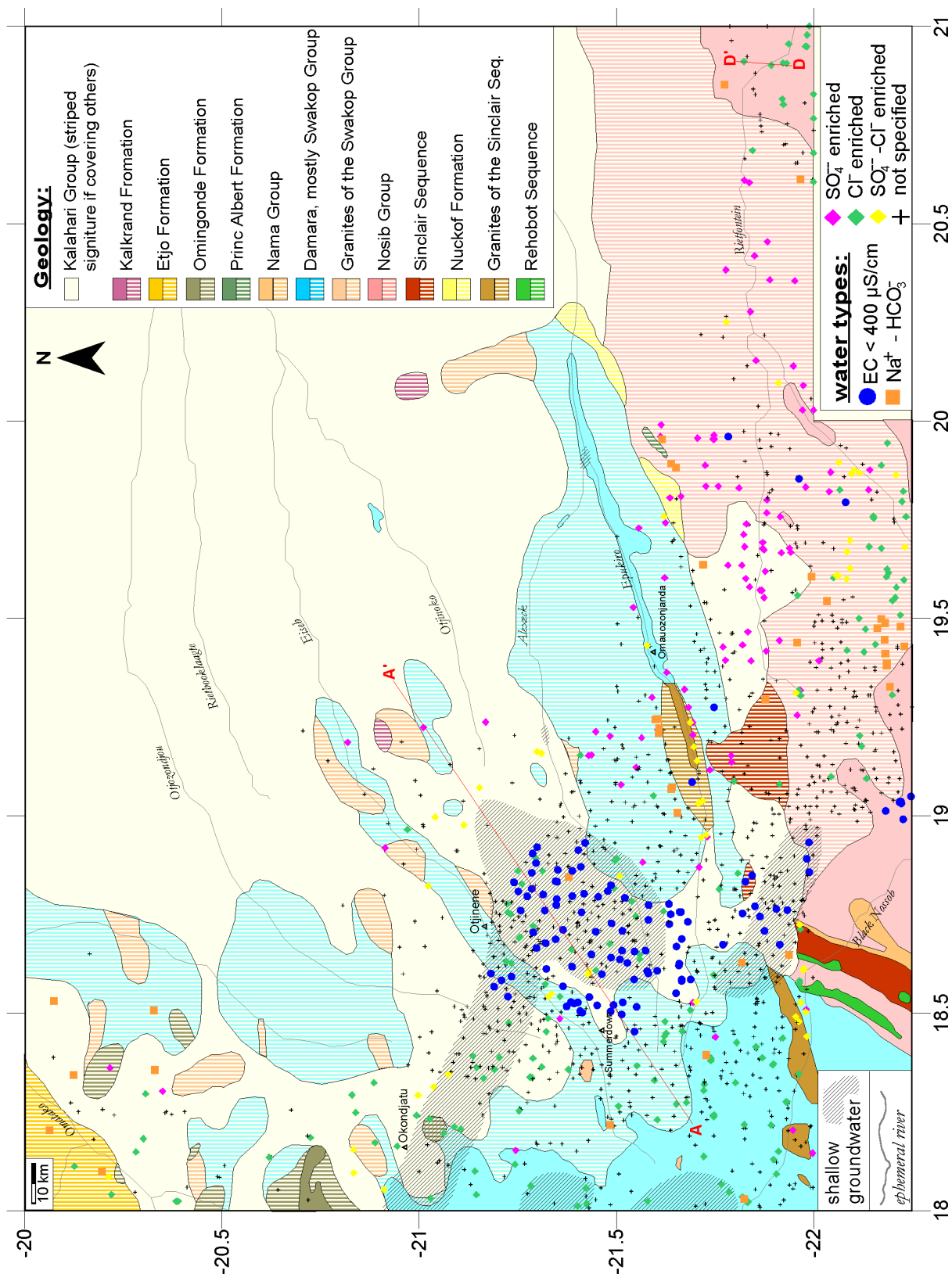


Fig. 7.2-15: Spatial distribution of water types in the SHSA with a reference frame of the geology, the major ephemeral rivers and shallow groundwater. Profile location for Fig. 7.2-18 and Fig. 7.2-19 are indicated by red lines labelled with A-A' and D-D'.

Six groups have been defined according to their electric conductivity and their distribution in the Piper diagram: waters with low electric conductivity ($EC \leq 40 \mu\text{S}/\text{cm}$), Na^+ - HCO_3^- -waters, SO_4^{2-} -enriched samples, Cl^- -enriched type, SO_4^{2-} - to Cl^- -enriched group and a group which could not be further subdivided or specified. The distribution of these groups is given in Fig. 7.2-15.

A variable wise cluster analysis based on Ward's method of Euclidean distances (WARD, 1963) of the major ions (Ca^{2+} , Mg^{2+} , Na^+ , HCO_3^- , SO_4^{2-} , Cl^-) indicated that the variables Na^+ and Cl^- are underlain by one process, while another process is controlling the Ca^{2+} - and Mg^{2+} -distribution (Fig. 8.2-

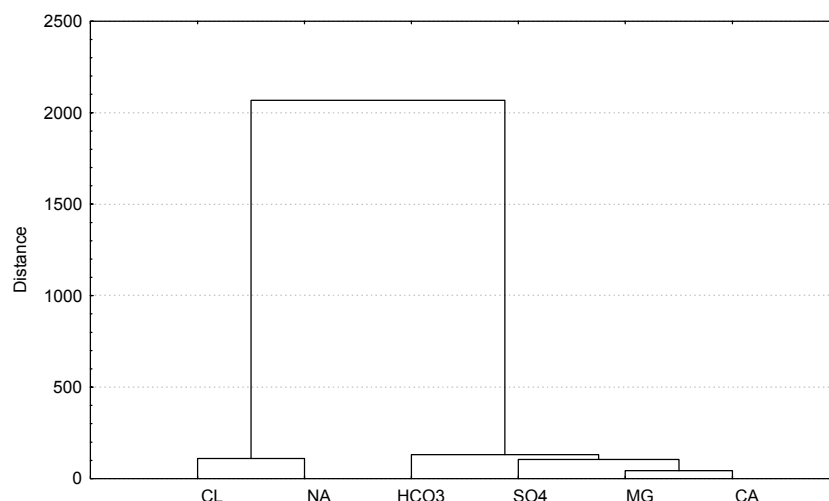


Fig. 7.2-16: Dendritic representation of similarity of hydrochemical variables for the SHSA.

16). A factor analysis was also used to define parameters that are depending on one-another. Factor analysis with a Kaiser criteria (eigenvalue ≥ 1) resulted in two factors which explained only 79 % of the total variance (upper part of Table 7.2-1, marked as a). The introduction of two additional factors explained 96.97 % of the total variance, but the two additional factors are only having low eigenvalues (0.56 and 0.52 respectively). In the latter analysis the two factors with the highest eigenvalue explain mainly the variance of SO_4^{2-} and HCO_3^- , while factor 3 groups Ca^{2+} and Mg^{2+} and factor 4 reflects the Na^+ - and Cl^- -distribution (lower part of Table 7.2-1, marked with b).

Table 7.2-1: Results of two factor analyses (a with, b without Kaiser criterion) for the hydrochemical data for the SHSA. Factor loadings above 0.7 are grey shaded

		Ca^{2+}	Mg^{2+}	Na^+	HCO_3^-	SO_4^{2-}	Cl^-	% of total variance explained	Eigenvalue
a	Loading of factor 1	0.79	0.56	0.92	-0.02	0.8	0.94	60.36	3.62
a	Loading of factor 2	0.29	0.67	0.11	0.94	0.07	0.79	18.67	1.12
b	Loading of factor 1	0.04	0.34	0.44	0.01	0.89	0.23	60.36	3.62
b	Loading of factor 2	0.01	0.33	0.14	0.98	-0.01	0.01	18.67	1.12
b	Loading of factor 3	0.71	0.84	0.12	0.16	0.24	0.29	9.27	0.56
b	Loading of factor 4	0.64	0.16	0.87	0.05	0.37	0.92	8.67	0.52

It is concluded from these tests that the processes dominating the hydro-chemical variance in the SHSA are alteration with Na^+ - Cl^- -enrichment and HCO_3^- -lowering or mixing with such water types. A further dominant process correlates Ca^{2+} - and Mg^{2+} -variations which is probable calcite and dolomite precipitation and dissolution.

The occurrence of samples with electric conductivity below 400 $\mu\text{S}/\text{cm}$ is constrained to areas that are dominated by ephemeral rivers originating in hardrock areas and passing areas where the Kalahari Group forms the topmost aquifer (blue • in Fig. 7.2-15). Most of these samples are associated with shallow groundwater. This group plots in the field of RFI-waters with some Na^+ - and Mg^{2+} -enrichment which is likely to result from some calcite precipitation and cation exchange or feldspar weathering. No correlation to electric conductivity appears for any of the cation contents or cation ratios, including the $\text{Ca}^{2+}/\text{Mg}^{2+}$ -ratio. For the anions only HCO_3^- -content correlates positively with the EC. The Ca^{2+} -content ranges from 11 to 52 mg/l. It is thus concluded that a complicated trade-off of carbonate dissolution and precipitation and cation exchange or feldspar weathering exists in this group. The samples with the lowest EC in this group are constrained to the area of a shallow groundwater between the Omiramba Alexeck and Eiseb (Fig. 7.2-15). In this area well yield is mostly between 5 - 20 m^3/h which allows the area to provide a major water resource.

The group of SO_4^{2-} -enriched water samples is underlain in pink in Fig. 7.2-14a and samples are indicated by pink \diamond in Fig. 7.2-15. Most of these samples are constrained to areas where hardrock aquifers are overlain by Kalahari sediments. This water type was found in the Kalahari aquifers only in the western part of the SHSA. Thus it appears that the SO_4^{2-} -enrichment results from Kalahari lithologies and this group most probably gets its fingerprint during the inflow of recharge water through Kalahari strata. All SO_4^{2-} -enriched samples have an alkali ratio above 20 % and the $\text{Mg}^{2+}/\text{Ca}^{2+}$ -ratio is not significantly increased (below 1.3). The SO_4^{2-} - and Cl^- -content both increase with the EC as well as the Cl^- -ratio.

The group of Cl^- -enriched water samples is underlain in green in Fig. 7.2-14a and indicated by green \diamond in Fig. 7.2-15. Samples of this group occur more often in the hardrock areas than the SO_4^{2-} -enriched samples and the Cl^- -enriched water type occurs in areas that are closer to the groundwater divide compared with the spatial distribution of the SO_4^{2-} -enriched samples. The cation composition of this group covers almost the entire range found in the SHSA. Only the alkali ratio is limited to more than 10 % while the $\text{Ca}^{2+}/\text{Mg}^{2+}$ -ratio ranges from 0.8 to 6. The majority of EC values ranges from 500 - 5 000 $\mu\text{S}/\text{cm}$. In this group the Na^+ - and Cl^- -content increases with the EC. Mg^{2+} -content correlates with EC only below 5 000 $\mu\text{S}/\text{cm}$ while the SO_4^{2-} -content correlates with EC only above 5 000 $\mu\text{S}/\text{cm}$.

A group in which increased SO_4^{2-} - and Cl^- -ratio are dominant plots in the anion field between the groups of SO_4^{2-} - and Cl^- -enrichment in the Piper diagram (Fig. 7.2-14a). The Mg^{2+} -content is always lower than 40 % and the Ca^{2+} -content is always below 75 %. The Na^+ -, Cl^- - and SO_4^{2-} -content correlate positively with the electric conductivity while no correlation exists for the HCO_3^- -, Ca^{2+} - and Mg^{2+} -content. It appears that the Ca^{2+} -content increases until EC reaches approximately 3 000 $\mu\text{S}/\text{cm}$ and then decreases while the Mg^{2+} -content increases. For the Ca^{2+} -ratio a positive correlation appears to the electric conductive below 4 000 $\mu\text{S}/\text{cm}$. This pattern reflects a typical evaporation path. The spatial distribution of this SO_4^{2-} - Cl^- -enriched group is indicated by yellow filled \diamond in Fig. 7.2-15. Some of these water samples occur between the Cl^- -group and the SO_4^{2-} -enriched group, and there they are thought to present the development from the Cl^- -dominated group to the SO_4^{2-} -dominated group. This occurs in the area south of the Omuramba Rietfontein between Longitude E19.5° and E20°. Such development along an assumed flow paths indicates a "backward evaporation path" and is thus thought to result from the gradual mixing of a fresher water with an evaporated water type and indicates probably increasing recharge along a flow path. Other samples are likely to result from direct mixing of the two water types, e.g. the samples near the upper part of the Omuramba Eiseb between Summerdown and Otjinene.

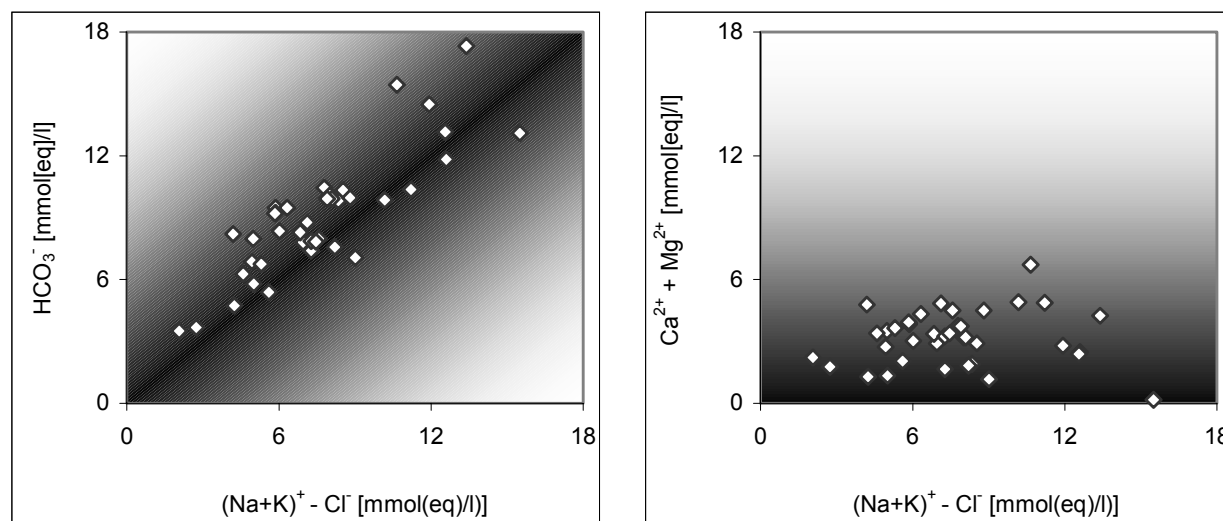


Fig. 7.2-17: Plots of HCO_3^- (left plot) and alkaline earths (right plot) versus alkali excess over chloride for water samples in the NHA plotting in the Na^+ - HCO_3^- -field of the Piper plot in Fig. 7.2-15.

Na^+ - HCO_3^- -water types (orange \blacksquare in Fig. 7.2-15) are mainly constrained to areas with Kalahari sediments with only 4 exceptions. In this group electric conductivity ranges from 480-1770 $\mu\text{S}/\text{cm}$. The Na^+ -content and the upper boundary of SO_4^{2-} - and Cl^- -content correlates positively with EC. Mg^{2+} - and Ca^{2+} -content and alkali ratio is not correlating with the EC

increase. The alkaline earths and the HCO_3^- -content are plotted versus the alkali excess in Fig. 7.2-17. While the HCO_3^- -content correlates with the alkali excess with a slope of approximately one, for the alkaline earths no correlation appears. It is thus concluded that the Na^+ - HCO_3^- -waters are produced by the weathering of feldspar. Possible source rocks exist by various metamorphic rocks and granites (granites of the Damara Group and Sinclair Sequence, Damara Sequence in general, Sinclair Sequence, Nuckof Formation and Rehoboth Sequence as indicated in Fig. 7.2-14) and their erosional products in the Kalahari Group.

The residual group (samples that could not be assigned to any of the other groups) is marked as black + in Fig. 7.2-15. This group is defined by having a HCO_3^- -ratio above 60 % and a Na^+ -ratio below 60 %. No further specific trend in the cation or anion field appears and the spatial distribution indicates no specific correlation. No further subdivision of this group was achieved neither by cluster analysis nor by attempting to define samples that underlay any specific process, e.g. dolomite solution with a $\text{Ca}^{2+}/\text{Mg}^{2+}$ -ratio of 1 or evaporation by increased $\text{Mg}^{2+}/\text{Ca}^{2+}$ -ratio. The occurrence of this group is not constrained to any specific geological unit or ephemeral rivers. It is likely that this group represents the mixing products of any water type combination.

Profiles in the southern hydrochemical study area

Two example profiles along assumed flow paths have been examined in the SHSA to document the development from the fringe towards more central parts of the catchment. One profile which documents a development within the Cl^- -enriched group is situated in the Talismanis-Rietfontein Block (labelled as profile D-D' in Fig. 7.2-15). The aquifer within this profile is always presented by lithologies of the Nosib Group. The second profile is rather complex as it passes from a Damara aquifer into a Kalahari aquifer and changes from fairly deep groundwater to the shallow area between the Omiramba Eiseb and Alexeck (labelled as profile A-A' in Fig. 7.2-15).

The development of the major cation and anion contents and ratios is documented in plots in Fig. 7.2-18 and 7.2-19. In profile D-D' the Cl^- -content is decreasing between the first two sample points which is indicating recharge influence. While the recharge influences the groundwater, the Ca^{2+} - and the Mg^{2+} -content increase and the HCO_3^- - and SO_4^{2-} -content stay almost constant. The Ca^{2+} - and Cl^- -ratio decrease while the HCO_3^- - and the Na^+ -ratio increase. An increasing Na^+ -content is likely to result from weathering of feldspar. During the further flow of the groundwater, the Cl^- -content and -ratio are continuously increasing, while SO_4^{2-} -, HCO_3^- - and Na^+ -content are staying almost constant. Ca^{2+} - and Mg^{2+} -content and ratios are continuously increasing. The very significant increase in the Ca^{2+} -content without increasing HCO_3^- - or SO_4^{2-} -

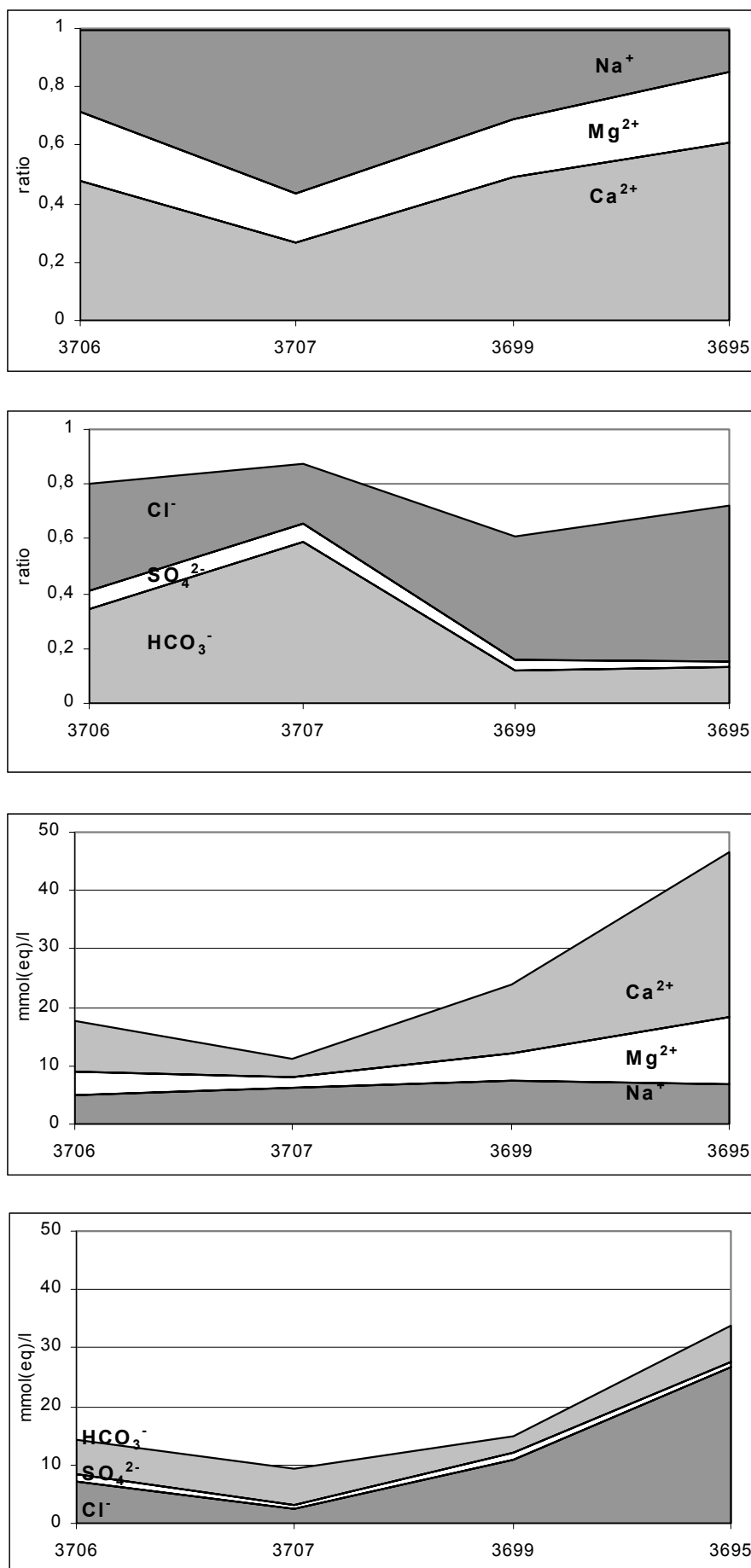
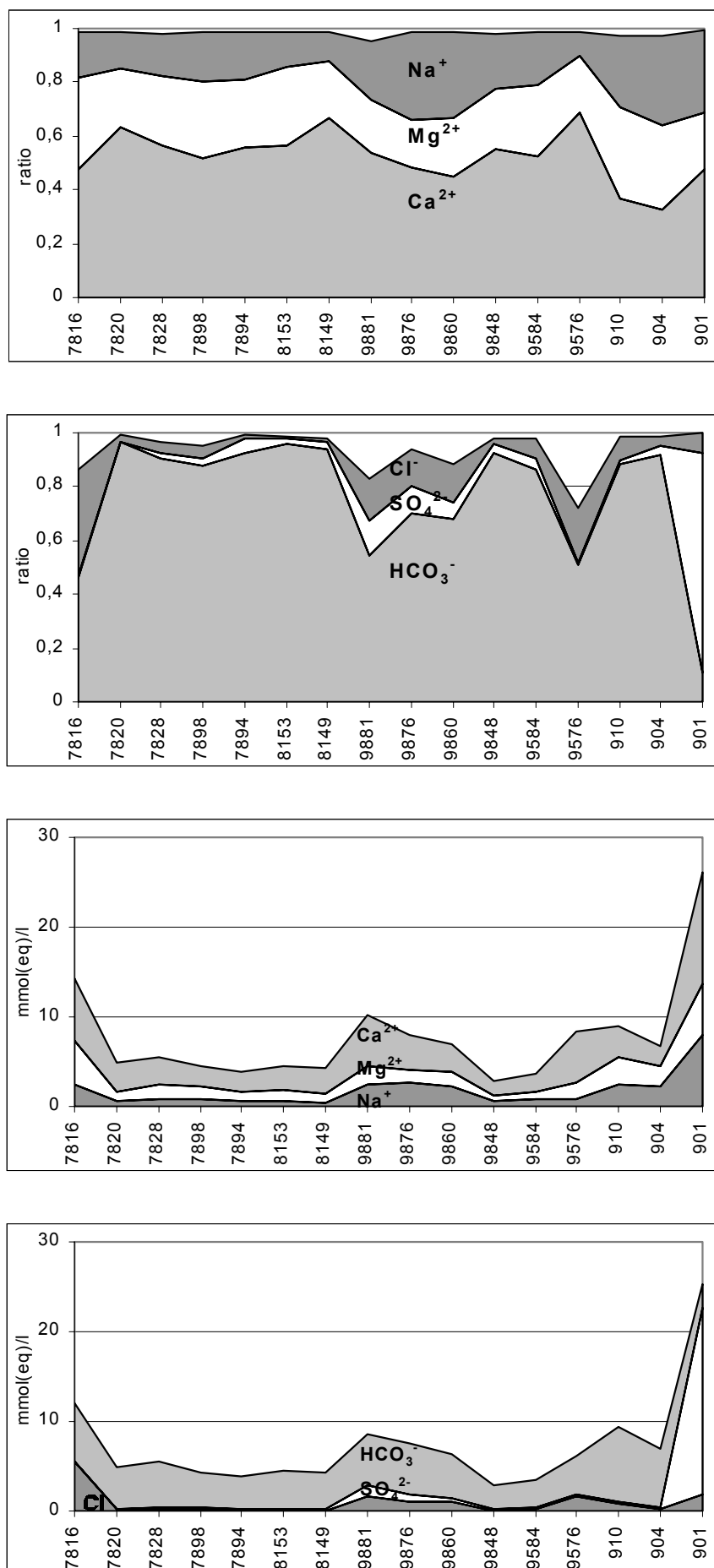


Fig. 7.2-18: Hydrochemical profile D-D' (location shown in Fig. 7.2.15) in the Talismanis-Rietfontein Block. Ion ratios are given in the two upper plots, ion contents in the two lower plots. The flow path is within lithologies of the Nosib Group and the Kalahari cover is becoming thicker from D towards D'. Labels refer to well numbers (for full hydrochemical analysis see Appendix D).

**Fig. 7.2-19:**

Hydrochemical profile A-A' (location shown in Fig. 7.2.15) in the SHSA. Ion ratios are given in the two upper plots, ion contents in the two lower plots. The profile documents the flow path from the Damara aquifer into Kalahari strata and changes from rather deep to shallow groundwater. Labels refer to well numbers (for full hydrochemical analysis see Appendix D).

content is not likely to result from any common process such as calcite, dolomite or gypsum dissolution or dedolomitisation.

The Profile A-A' is starting in marbles and schist of the Swakop Group. Between the first two samples a decreasing chloride content is observed (Fig. 7.2-19) indicating the influence of fresh recharge water. All major anions and cations are showing a content decrease while ratios of Ca^{2+} and HCO_3^- are increasing. During the further flow in the Damara aquifer no major changes in content or ratio of any ion occur and the Cl^- -content stays very low. The groundwater comes to fairly shallow levels between sample 8149 and 9881 which is joined by an increase in all major ions (Fig. 7.2-19) indicating some evaporation. It also causes the $\text{Ca}^{2+}/\text{Mg}^{2+}$ -ratio to decrease. Within the terrain of shallow groundwater decreasing Cl^- -contents are observed between 9881-9876, 9860-9848 and 9576-910-904 which are always accompanied by increasing HCO_3^- -ratio and are thus clearly indicating freshening. Between the last two sample points 904 and 901 a major change in hydrochemistry is observed and SO_4^{2-} becomes the predominant anion. The groundwater is deeper here and the Kalahari strata is still forming the aquifer. Possibly the groundwater gets its fingerprint from gypsum dissolution or FeS oxidation in the lower parts of the Kalahari Group.

7.2.3 The central hydrochemical study area (CHSA)

For the CHSA only 50 samples are available reflecting the sparsely inhabited central part of the study area including the lower Eiseb and Epukiro catchments. All samples show a $\text{Ca}^{2+}/\text{Mg}^{2+}$ -ratio above 1 (Fig. 7.2-20) but the proper Ca^{2+} -field is not covered. Only the HCO_3^- - to SO_4^{2-} -field in the anion plot is covered and no samples with a Cl^- -ratio above 40 % appears. Four groups have been identified according to the anion development: HCO_3^- -dominated waters, a HCO_3^- - SO_4^{2-} -type ($\text{HCO}_3^- > \text{SO}_4^{2-}$), SO_4^{2-} - HCO_3^- -dominated samples ($\text{HCO}_3^- < \text{SO}_4^{2-}$) and a SO_4^{2-} -type. These groups document either a development from HCO_3^- -waters towards SO_4^{2-} -waters or a mixing of the two end-members. One single sample plots in the Na^+ - HCO_3^- -field and is thus not included in the four main groups.

The distribution of the water types is indicated in Fig. 7.2-21. The Na^+ - HCO_3^- -sample (orange filled ■ in Fig. 7.2-21 and □ in Fig. 7.2-20) occurs in the western part of the CHSA within the Kalahari aquifer and either results from cation exchange or feldspar weathering.

The group of HCO_3^- -dominated waters is indicated by black filled ● in Fig. 8.2-20. The $\text{Ca}^{2+}/\text{Mg}^{2+}$ -ratio is always above 1 with a mean of 1.37. No samples plot in the Ca^{2+} -dominated field and the alkali ratio is always lower than 50 %. EC is below 1180 $\mu\text{S}/\text{cm}$. Ca^{2+} -, Mg^{2+} -, SO_4^{2-} - and Cl^- -content correlate positively and strongly with the EC, while the correlation for

HCO_3^- -content is less obvious. The HCO_3^- -ratio decreases with the EC while for the Ca^{2+} -ratio a decreasing trend is only weakly observable. A weak positive correlation occurs for the SO_4^{2-} - and Cl^- -ratios with EC. The four samples with the lowest Mg^{2+} -ratio are all having EC below $500 \mu\text{S}/\text{cm}$. Most of the samples plot in the field of RFI-water but are also orientated along the typical dolomite dissolution path. It is thus concluded that these samples represent a group of recharge water by preferred flow path associated with dolomite dissolution or mixing of recharge water with water that was in equilibrium with dolomite. Most of these water samples are within the Kalahari aquifer.

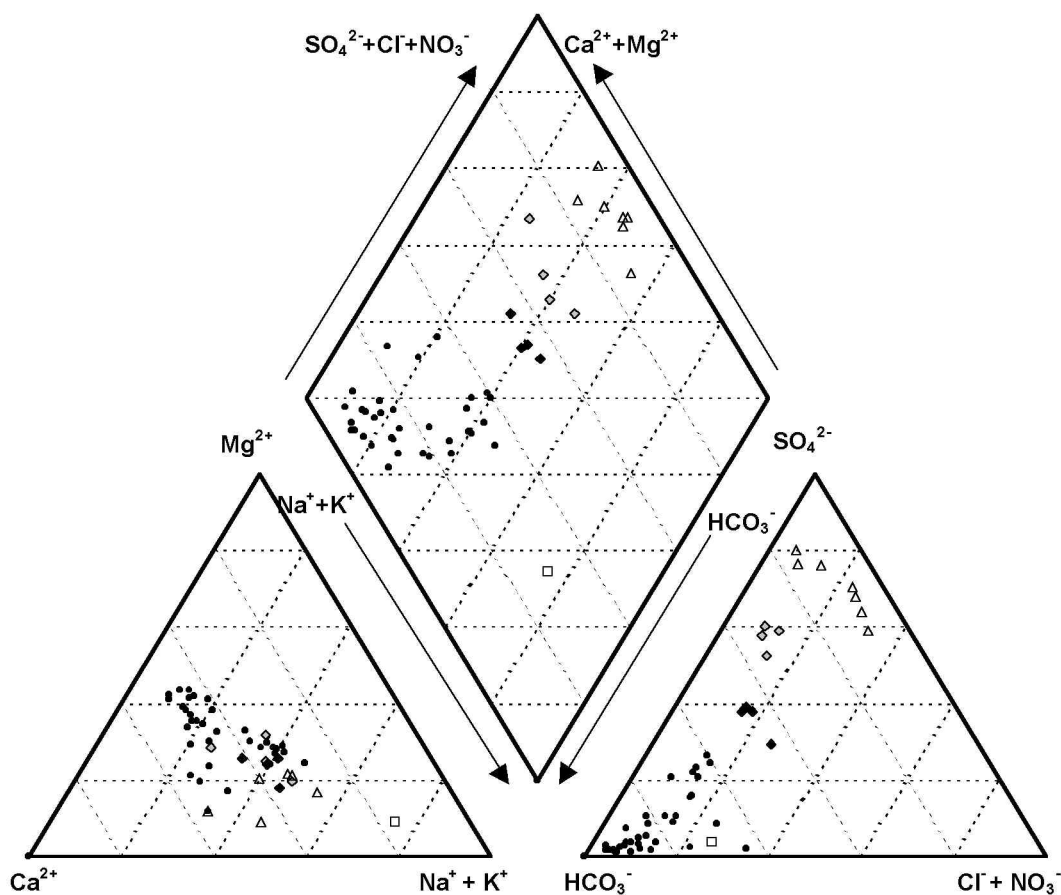


Fig. 7.2-20: Piper plot of the water samples in the CHSA.

Water samples that are dominated by SO_4^{2-} at the anion side occur in the pre-Kalahari aquifer near Ondjora and in the Kalahari aquifer in the eastern part of the CHSA (indicated as pink filled Δ in Fig. 7.2-21). The SO_4^{2-} -content ranges from 711 to 1860 mg/l within this group and the electric conductivity lies between 2399 and 4110 $\mu\text{S}/\text{cm}$. The samples near Ondjora are characterised by the lowest Mg^{2+} -ratio. For all other samples the $\text{Ca}^{2+}/\text{Mg}^{2+}$ -ratio is between 1.9 and 1.5. For the three samples near Ondjora it is observed that the SO_4^{2-} -content increases with

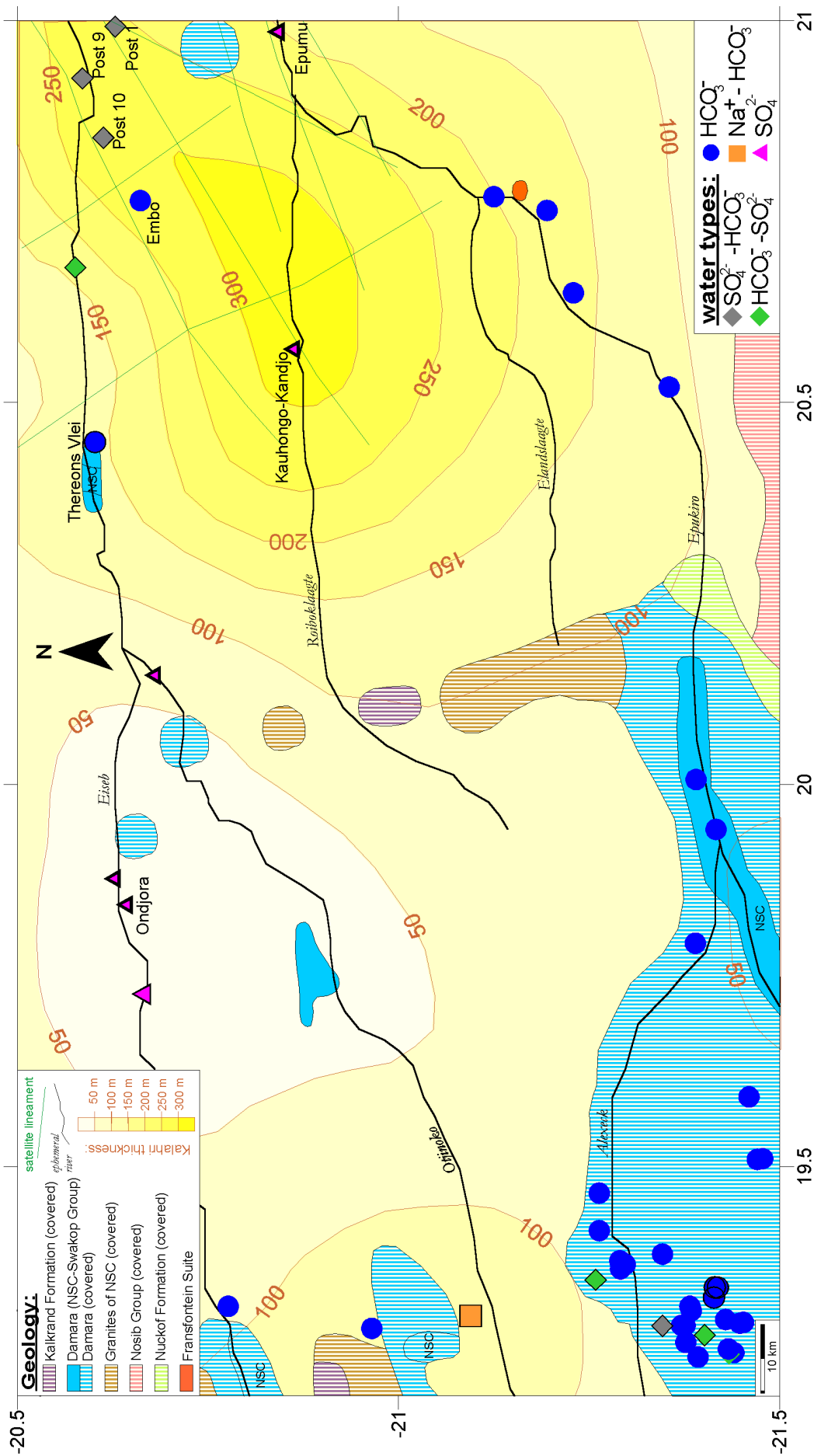


Fig. 7.2-21: Spatial distribution of water types in the CHSA with a reference frame of the geology, including the thickness of the Kalahari Group and the major ephemeral rivers. Samples with electric conductivity below 1000 $\mu\text{S}/\text{cm}$ are marked without frame, 1000-2500 $\mu\text{S}/\text{cm}$ with a thin frame and thick frames indicate values above 2500 $\mu\text{S}/\text{cm}$.

EC, while for the other samples the SO_4^{2-} - and HCO_3^- -ratio increase as well with EC. The two eastern most samples at Epumu (same borehole sampled in 1999 and 2000) and the sample at Kauhongo-Kandjo are from fairly deep boreholes (pump installed at 230 m at Kauhongo-Kandjo, oral information by the local farmer) and it is likely that these samples characterise waters from the lower Kalahari in the eastern part of the study area which might contain gypsum and the composition of the water type thus presents a group that has attained gypsum dissolution.

The samples between the two above presented groups appear as small clusters in the Piper plot and are thus divided into two additional groups. Both groups plot in the HCO_3^- - SO_4^{2-} -field of the Piper diagram (Fig. 7.2-20) and only one sample is slightly shifted towards the HCO_3^- - Cl^- - SO_4^{2-} -field. This sample is situated between Thereons Vlei and Eiseb Post 10 (Fig. 7.2-21). Samples that belong to both groups are constrained to Kalahari aquifers. EC ranges from 1108 to 1429 $\mu\text{S}/\text{cm}$ for the SO_4^{2-} - HCO_3^- -group and from 900 to 1880 $\mu\text{S}/\text{cm}$ for the HCO_3^- - SO_4^{2-} -group. The samples of the SO_4^{2-} - HCO_3^- -group occur more often in the eastern part of the CHSA, while the HCO_3^- - SO_4^{2-} -group is more abundant in the western part of the CHSA.

For the HCO_3^- - SO_4^{2-} -group it is observed that Ca^{2+} - and Cl^- -content correlate positively with the EC. A weak correlation appears only for Mg^{2+} -, Na^+ - and SO_4^{2-} -content. A strong negative correlation is indicated for the HCO_3^- -ratio with EC which points to some calcite precipitation.

For the SO_4^{2-} - HCO_3^- -group a strong positive correlation with EC is observed for Ca^{2+} -, Mg^{2+} -, SO_4^{2-} -content and a weak positive correlation for the HCO_3^- -content. A strong negative correlation appears for the Na^+ -content and -ratio. A negative correlation between the HCO_3^- -ratio and EC is less significant. A decrease in Na^+ -content with increasing EC is either indicating mixing with water of a low Na^+ -content but higher mineralisation or earth-alkalisation during mineralisation of this water type. Earth-alkalisation is very unlikely as Ca^{2+} is stronger adsorbed as Na^+ . It is thus concluded that this group is derived from mixing of the two water types; a SO_4^{2-} -type presented by lower Kalahari waters and a HCO_3^- -dominated water. The latter water type can be either a dolomite type or a RFI-water. The sources is either recharge water within the Kalahari (probably recharge in calcrete terrain, along the Eiseb fault system) or inflow from either the Epukiro catchment in the south or from areas north of the Eiseb, e.g. the Gam area or the Aha Hills where dolomites outcrop.

7.2.4 Implication for the entire catchment

From this study four major hydrochemical processes in the Kalahari catchment are identified:

- 1) Fresh recharge water is observed in all parts of the Kalahari catchment. RASP-water occurs in thick Kalahari strata and also in thin Kalahari strata above hardrocks. The hydrochemical

composition of RFI-water is often preserved in groundwater close to Omiramba. In the pan field around Tsumkwe RFI-waters document preferred flow path recharge from the surrounding hardrocks and indirect recharge in unvegetated pans.

- 2) Dolomite waters occur in the north-western part of the catchment where they originate from the Otavi area. Groundwater occurring in the vicinity of the Aha Hills shows a similar composition.
- 3) All water types originating from the fringe area receive some overprint by mixing with a Cl^- -component during their flow, which most likely documents the decreased recharge amount.
- 4) In the lower part of the Kalahari aquifer in the more central part of catchment mixing with a gypsum-type-water occurs.

Three further processes have been identified that are locally more limited:

- 1) Na^+ - HCO_3^- -water types occur mostly in areas where the Kalahari overlies gneisses or basalts. This water type results mostly from feldspar weathering. Occasionally the hydrolyse of mafic minerals increases Mg^{2+} -content in areas with gneisses.
- 2) Water that has been the subject of evaporation has been identified in areas of shallow groundwater. These areas occur more often in the fringe area of the catchment than in the central part.
- 3) A highly mineralised groundwater of Na^+ - Cl^- -type has been observed in basalts at the Dobe Pan. Mixing with such end-member might locally overprint the basin-wide development.

7.3 Temporal variations of the hydrochemical parameters

Seven wells have been selected to verify the temporal variations of hydrochemical parameters for shallow groundwater and to define typical trends occurring in the study area. Therefore wells that are under different use have been selected:

- a) farm use in the western (Kokasieb-1 and Kokasieb-2) and southern (Ombeameiata-1 Ombeameiata-2 and Amatola) fringe area
- b) urban use as part of a state water scheme (Tsumkwe)
- c) urban use by a small community (Tamboti)

Hydrochemical data for the sampling localities are given in Table 7.3-1 and as Piper plots (triangles only) in Fig. 7.3-1.

The samples from locality 1 on farm Ombeameiata (W-2-1977 & W-2-1999) plot in the cation field between RFI-water and water in equilibrium with dolomite (Fig. 7.3-1a). The Na^+ -component is likely to result from weathering of feldspar in the granites outcropping on the farm. In the anion field a significant $(\text{Cl}^- + \text{NO}_3^-)$ -content is observed, which is mainly caused by a NO_3^-

-component. NO_3^- is in generally attributed to a human impact and as this well is the main well used for cattle watering and cattle dropping is very present here, it appears likely that the NO_3^- -contamination results from the farming and increases with time. This is also underlined by the high K^+ -values (Table 7.3-1) which is also enriched in animal manure. However, the farmer reported that this well had NO_3^- -problems since it was drilled by an earlier generation.

Table 7.3-1: Hydrochemistry for 7 groundwater wells in the study area. The year of sampling is given by the last four digits of the sample's label

Location	No	Depth to GW	pH	EC	Ca^{2+}	Mg^{2+}	Na^+	K^+	HCO_3^-	SO_4^{2-}	NO_3^-	Cl^-
		[m]		[$\mu\text{s}/\text{cm}$]	[mg/l]							
Ombeameiata-1	W-2-1977	~ 10	7.6	1820	121.3	87.9	111	14	430.4	54	363	172
Ombeameiata-1	W-2-1999	~ 10	7.5	2557	188.0	136	130	15.6	250.1	48	657	330
Ombeameiata-2	W-3-1977	~ 10	7.8	880	58.1	45.9	57	11	396.3	17	110.7	36
Ombeameiata-2	W-3-1999	~ 10	7.9	858	70.5	48.2	43.3	10.2	372.1	11.88	113.2	28.7
Amatola	W-10-1976	~ 15	7.3	830	24	22.1	133	16	509.7	11	4.4	6
Amatola	W-10-1999	~ 15	7.9	789	39.6	27.2	100	14.2	477.6	5	5.4	7.4
Kokasieb-2	V-4-1978	34	7.4	1260	109.3	79.9	28	1	598.7	17	101.8	55
Kokasieb-2	V-4-1991	34 - 38	7.4	933	88.1	74.1	24	3	604.8	7	22.6	22
Kokasieb-2	V-4-1994	34 - 38	7.6	1022	88.1	70.9	23	3	612.1	12	39.8	24
Kokasieb-2	V-4-2000	38	6.7	971	78	65.4	24.1	1.1	603	9	25.8	19.2
Kokasieb-1	V-3-1978	~ 25	7.9	1085	66.9	108.1	38	2	807.2	1	< 0.5	14
Kokasieb-1	V-3-2000	~ 25	6.7	1184	91	84	47.7	0.7	688	83	11	47.5
Tamboti	W-22-1999	~ 10	8.1	885	117	63.5	5.8	0.7	617	2.8	13.2	6.2
Tamboti	V-20-2000	~ 10	6.7	904	126	55.8	4.8	0.7	643	2.9	10.8	4.5
Tsumkwe	W-21-1973	6	7.6	630	110.9	18.9	43	10	487.7	16	17.7	25
Tsumkwe	W-21-<1993	7 - 8	7.2	810	105.3	20.2	59	11	430.4	32	4.4	69
Tsumkwe	W-21-1999	7.5	7.7	1514	103.2	32.6	236	10.3	480.1	76.1	8.4	266

In general it was observed for locality 1 on farm Ombeameiata that all cation contents increase during the observation period, but the cation ratio stayed almost constant. The Cl^- -content increases as well, but HCO_3^- -content decreased. This changes are attributed to varying recharge conditions as the rainy seasons 1975/76 and 1976/77 have been very wet in this area (see Fig. 5.3-1, Hochfeld) while the mid 1990s have been drier. Increasing precipitation increases the

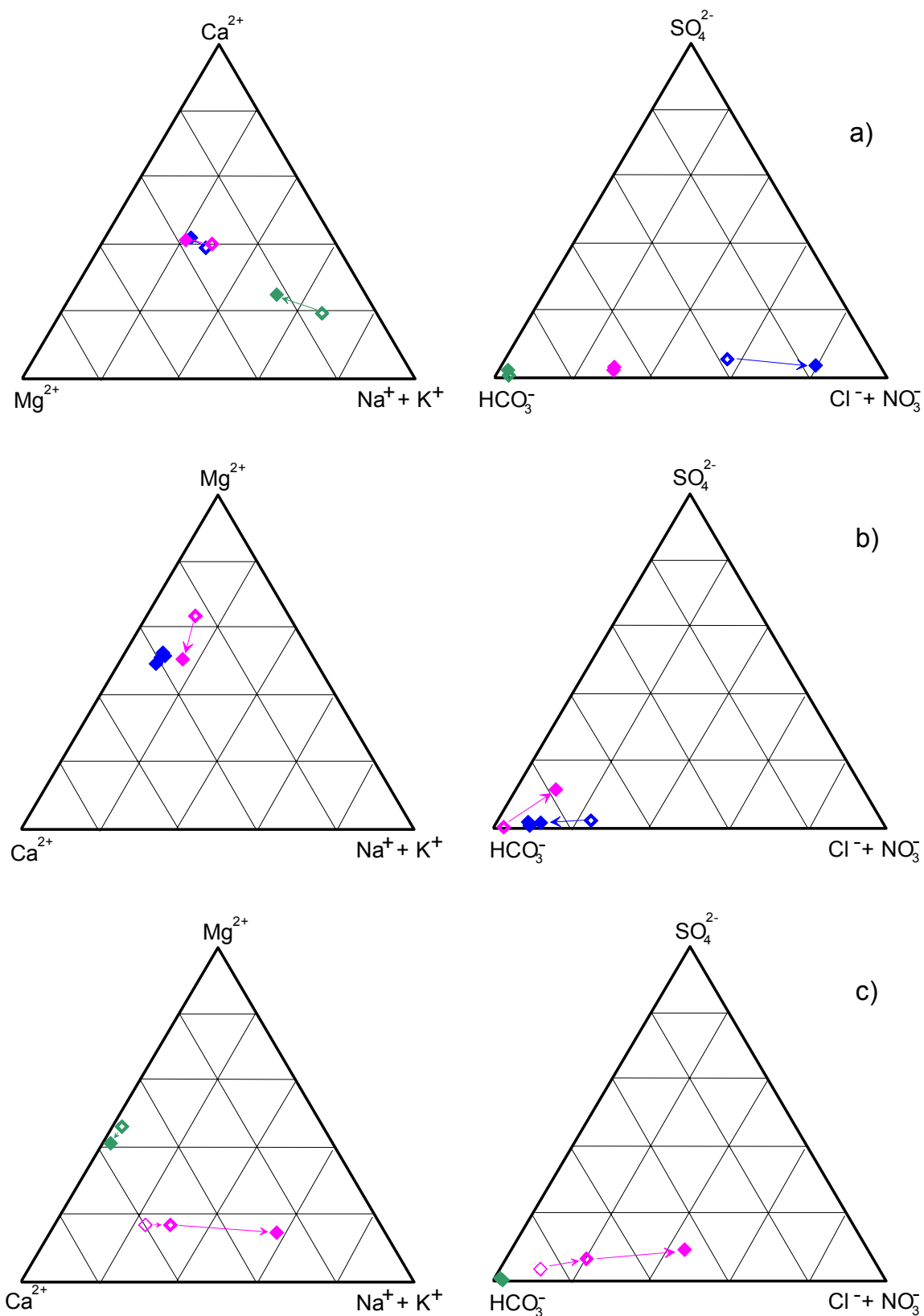


Fig. 7.3-1: Piper plot of the hydrochemical data given in Table 7.3-1. The temporal development is indicated by open \diamond (earlier sample) and filled \blacklozenge (latest sample). Arrows are indicating the direction of change. In plot a) the samples for Ombeimeiaata-1 are given in blue, Ombeimeiaata-2 in pink and Amatola in green. Plot b) gives the ion ratios for Kokasieb-1 in pink and Kokasieb-2 in blue. In plot c) pink is used to present the hydrochemical development at Tsumkwe and green is used for Tamboti.

recharge and the vegetation growth will be promoted. With increased root respiration the dissolution of calcite/dolomite will increase, which can be concluded from the higher HCO_3^- content for the sample from 1977 compared to the sample from 1999.

The samples from locality 2 on farm Ombeameiata (W-3-1977 & W-3-1999 in Table 7.3-1) show only slight variations between the earlier and the recent sample. Cation composition is similar to the samples at Ombeameiata 1. Changes in the Cl^- -concentration are likely to result from the sampling time, as the early sample was taken by the end of the dry season, while the later was taken by the end of the wet season. A NO_3^- -problem, accompanied by high K^+ -contents appears also for this well, although its NO_3^- -content is significantly lower than at Ombeameiata 1. Only a minor increase of the NO_3^- -content occurred in this well during the observation period. Both sampling points at farm Ombeameiata are not far from an assumed major recharge zone near Hochfeld. Groundwater levels at farm Eahero between Hochfeld and farm Ombeameiata are very shallow (4 m below surface) and nowadays the groundwater there is used for some irrigation farming. The variations in hydrochemistry at farm Ombeameiata might thus as well be influenced by the land use change at farm Eahero and other farms.

The samples from farm Amatola (W-10-1976 and W-10-1999) plot both in the field of Na^+ - HCO_3^- -water which is likely to result from weathering of feldspar as the well is located close to the flood course of the upper Eiseb in some Damara lithologies with only very shallow soil cover. As the Omuramba Eiseb is likely to be associated with some fault zones where feldspar weathering is abundant, the hydrochemical interpretation is also consistent with the geological observation. Hydrolyse of feldspar increased due to the wetter season with more vegetation before 1976 than in 1999. The increased Cl^- -concentration reflects as well the changed climatic conditions. For this well fairly high K^+ -values are observed. If high K^+ -contents are combined with high NO_3^- -contents, this is generally attributed to animal manure. Hence, the unique occurrence of high K^+ -contents indicates either that NO_3^- has been reduced in the aquifer or that the K^+ originates from the feldspar weathering.

The groundwater samples from farm Kokasieb plot in the HCO_3^- -field (Fig. 7.3-1). While the cations for V-4-1978 and V-4-2000 plot approximately in the dolomite field, an increased Mg^{2+} -ratio is observed for the samples V-3-1978 and V-3-2000. For Kokasieb-1 it is observed, that Mg^{2+} - and HCO_3^- -content are decreasing from the older to the younger sample while all other parameters increase. The higher HCO_3^- -content is most likely caused by the wetter condition (1976-1978, see Fig. 5.3-1 Maroelaboom) and the resulting denser vegetation with increased root respiration and thus an increased CO_2 -production allowing further calcite/dolomite dissolution. For Kokasieb-2 it is observed that the hydrochemical composition stays temporarily almost

constant if not considering Cl^- and NO_3^- . Although the farm is still used for cattle farming, the NO_3^- -concentration is significantly lowered. It thus appears likely that the initially higher NO_3^- -content was induced by some flushing of previously fixed NO_3^- -amount which might be a relic from a prehistoric pluvial. The only slightly varying Cl^- -concentration for the samples from 1991-2000 indicates that the recharge inflow to deeper groundwater can be assumed as constant over time (Kokasieb-2 is the deepest well in this selection).

The NO_3^- -contents on the two locations on farm Ombeameiata and the oldest water sample at location 2 on farm Kokasieb are above the Namibian maximum allowable limit for drinking water (100 mg/l). They are also well above the WHO (1985) recommendation (45 mg/l). Values above the WHO limit may cause infant methaemoglobinaemia (blue baby syndrome), hypertension, certain cancers, birth defects and spontaneous abortion (SPALDING & EXNER, 1993). A local farmer reported (orally) that on his farm Malta 10 cattle died due to high NO_3^- -contents in the groundwater after the heavy rains in early 2000. On the same borehole a NO_3^- -content of 44.1 mg/l was measured in November 2000. It appears thus that not everywhere high nitrate contents need last for long periods, but that they cause serious problems.

The samples from the location Tamboti which is used by a small bushman community, plot in the field of recharge water that is in equilibrium with dolomite and shows a very dominant HCO_3^- -component (green \diamond in Fig. 7.3-1c). The older sample (W-22-1999) was taken in the early dry season after a fairly dry year. The younger sample was taken after a good rainy season in 1999/2000 in the early stage of the rainy season 2000/01. Vegetation was a lot denser during the second sampling which is also seen in the increased HCO_3^- - and Ca^{2+} -content. The increased recharge inflow is as well reflected by the decreased Cl^- -content.

The sample from Tsumkwe (W-21-1973, <1993 [meaning earlier than 1993, but no exact date is given] & 1999) shows very significant changes in the Cl^- - and Na^+ -content, with Cl^- -content rising from 25 to 266 mg/l. In the DWA database two further analysis were found which indicated Cl^- -contents of 210 and 220 mg/l but no temporal information is available for these samples. The groundwater levels have fallen about 2 m during the time this well was used for urban consumption in Tsumkwe. Prior to the sampling in 1973 an extraordinary wet rainy season occurred with more than 950 mm while the 1998/1999 season was extraordinary dry with 200 mm only. The hydrograph of this well has already been discussed in Chapter 5.4 and it was found that the groundwater recharge is reacting strongly on the total rain amount per season. It is thus concluded that the increased Cl^- -content is mainly induced by a lower recharge amount due to low rainfall. From the change in the cation composition (Fig. 7.3-1) it appears that only the water sample from 1973 had the character of RASP-water but the other samples are likely to lie

on a mixing path with a $\text{Na}^+\text{-Cl}^-$ -water. The percentage of mixing might be very much influenced by the annual recharge inflow. It is also possible that the lowering of the groundwater level, although not significant, might add to this change by pumping a higher percentage of deeper, higher mineralised water. A possible endmember ($\text{Na}^+\text{-Cl}^-$ -type) for such mixing was found under similar geological conditions (flood basalts under Kalahari cover) north-east of Tsumkwe at the Dobe Pan.

From this study it is concluded that in general the shallow groundwater is very sensitive to varying precipitation amount: the wet middle 1970s are clearly seen in the hydrochemistry. This climatic factor does not only influence the recharge amount but the denser vegetation is also increasing hydrolyse and calcite and dolomite dissolution. The hydrochemistry is as well influenced by the groundwater level depth and thus a function of recharge and abstraction. Land use also affects the hydrochemistry in terms of NO_3^- -pollution. From the very slight hydrochemical changes in the deepest well (Kokasieb 2) of this study it is concluded, that the hydrochemical composition for deeper groundwater is less variable as for shallow groundwater.

7.4 Conclusions

The distribution of hydrochemical data within the Kalahari catchment is rather complex due to an inhomogeneous recharge distribution and variable aquifer lithologies. HCO_3^- -water types are abundant, followed by Cl^- -types and less common SO_4^{2-} -types. The latter is mostly limited to areas with thick Kalahari cover. At the cation side $\text{Ca}^{2+}\text{-Mg}^{2+}\text{-Na}^+$ -water types are abandoned, Ca^{2+} -enrichment occurs often, followed by Na^+ -dominated waters and Mg^{2+} -enriched samples are rather seldom.

The recharge mechanisms that were proposed from the study of hydrographs (Chapter 5.4) and interpretation of soil physical properties and their spatial distribution (Chapter 5.2) are confirmed by the results from this hydrochemical study. For the Tsumkwe area the recharge processes are diffuse recharge with soil passage and recharge from pans that are both demanding for an entire good rainy season. The recharge process proposed for the Epukiro area is infiltration along preferred flow path in hardrocks and calcrete and this mechanism is also seen in the RFI-water composition of the groundwater samples there. For this area the groundwater was reported to be very young by VOGEL & VAN URK (1975) which is consistent with the fast, local recharge process that is concluded from this study.

During this study it was found that feldspar weathering is the major process to develop $\text{Na}^+\text{-HCO}_3^-$ -water types, and cation exchange is less common. MAZOR ET AL. (1980) have also proposed this to be a dominant process in the Kalahari and from the interpretation of ^{14}C

contents in such groundwaters they concluded that this is a fairly fast process which "*may be completed in a few years at most*".

Enrichments of Cl^- along a flow path mostly documents a decrease in recharge amount. It is also concluded that only locally some Na^+ - Cl^- -enrichment results from mixing with a deeper, highly mineralised groundwater, e.g. in the northern part of the study areas where it struck in flood basalts. Similar observations have been made in the Kweneneg district of Botswana where a $\text{Ca}^{2+}/\text{Mg}^{2+}$ - HCO_3^- -water type (RFI-water) is lying on top of a Na^+ - $\text{HCO}_3^-/\text{Cl}^-$ -water type (NEUMANN-REDLIN & SEKWALE, 1982 in VERHAGEN, 1988). MAZOR ET AL. (1987) described as well Na^+ - Cl^- -dominated waters to origin from Ecca shales and basalts covered by Kalahari sediments in Botswana.

From this study it appears that saline waters are mostly having its origin in stagnant, fairly deep parts of the aquifer. Therefore a careful screening of the wells would provide better water quality by not including strikes of higher mineralised water. A more detailed assessment of the hydrochemistry with assignment of specific aquifers would initially require to know where the boreholes are *really* filtered. Unfortunately this information is mostly not anymore available for the Namibian wells.

From the study of the hydrogeological model it is assumed, that the majority of groundwater flow is concentrated at unconformities and in combination with good screening reports it would be possible to find out if these waters are of good quality and if they are usable for drinking water supply.

The temporal variations of hydrochemical parameters in shallow groundwater indicate it to be very sensitive to recharge variations. It provides in general the best water qualities, especially in the central part of the study area. The shallow groundwater is also very sensitive for pollution induced by land use changes. If the population is relying on this water resource, it seems reasonable to carefully, continually survey it and its recharge zones.

NO_3^- -contents above the maximum allowable limit for drinking water are demanding for some on-going research in the field of nitrogen sources and pathways under Kalahari environment. So far nitrate contamination studies have focused on the humid climate, but process understanding in arid environment is limited (TREDoux ET AL., 2001). Basically it is understood that high nitrate concentrations are induced by both natural and anthropogenic sources. In southern Africa nitrate problems occur mainly along the fringe of the Kalahari basin (TREDoux ET AL., 2001) and are thus associated with recharge zones mapped in this study. In Namibia the fringe of the Kalahari basin represents an area used for farming since a fairly long period, which might indicate the agricultural land use to be a cause of high NO_3^- -contents in the groundwater. Stock

farming produces 46 kg N/a and 56 kg K₂O/a per cattle (SRU, 1985). Accordingly the nitrate leaching into the groundwater is primarily a question of stocking rate. A major factor is also the denitrification in the unsaturated zone which is highly influenced by transport processes and thus the recharge mechanism becomes an important factor.

It was fairly often observed during field work that the extraction well and the cattle watering tank are spatially not separated. Cow droppings and urine are accumulated in the direct vicinity of the well. Additional cattle manure is washed into these areas by surface runoff as wells are often located in topographic depressions. It appears fairly obvious that fast infiltration along preferred flow paths or in karstified rocks will transport a high amount of these contaminants into the groundwater close to the extracting well. The areas covered by Kalahari sands with diffuse, slow recharge seem to be less vulnerable. However, it is recommended to separate the cattle and their manure from the vicinity of the wells as a first step to protect and to guarantee a qualitatively reliable groundwater resource for the inhabitants of the Kalahari catchment.

8 Summary

This study has focused on hydrogeological and hydrochemical settings of the Northern Namibian Kalahari Catchment which is the Namibian part of the Makgadikgadi-Kalahari-Catchment. Recharge has been the subject of process-understanding, quantification and regionalisation.

Aquifers of Precambrian to almost Recent age occur within the catchment. The largest part of the study area is covered by sediments of the Kalahari Group (Upper Cretaceous to Quaternary) which were deposited in a fault controlled basin. The terrestrial sediments cannot yet be correlated basin-wide because they show facies variations between stratigraphically equivalent units. The most important hydrogeological features observed during the geological study are the basal pre-Kalahari unconformity and fairly young faults that both provide enhanced groundwater flow conductivities. The fault system in the Eiseb Block was studied in detail by the use of satellite images and some of the faults were also recognised in the field, which indicates that the satellite images are a powerful tool for the definition of fairly young fault lineaments and thus also for further groundwater exploration.

The Kalahari lithologies make up the topmost aquifer in the northern part of the study area, in some western parts and in the Eiseb Block (Eiseb Graben Aquifer). Karoo strata are less commonly serving as the topmost aquifer. Damara strata sometimes form the topmost aquifer, mainly in the central southern part of the study area. In this area the strikes are as deep as 180 m below the topographic surface. The highest well yields occur in the Otavi area. In general, increased well yield is not following geologically significant, but older lineaments, but does correlate with faults of young origin or young reactivation of the older lineament, e.g. in the Eiseb Block.

Five classes of surface properties have been defined besides the hardrock areas: Pans and vleis, brown to red soils, dune sand, soil with an aeolian influence, and calcrete. A soil physical study revealed that aeolian sands are most promising for the development of direct diffuse recharge. Recharge by preferred flow might occur in all surface classes either due to joints in calcrete or structures and rootlets in soils. All substratum classes contribute to indirect recharge because even the dune sand allows, albeit very locally, the generation of runoff.

Precipitation ranges from 350 - 600 mm/a in the study area and potential evaporation is a significantly higher with 2600 - 3200 mm/a. As the annual precipitation is highly variable, a higher potential for diffuse recharge is given during relative wet years. Very heavy rains (>100 mm/day) also occur and are good for the development of preferred flow path recharge and indirect recharge.

Hydrograph interpretation allowed the definition of at least two recharge mechanisms: preferred flow path recharge in hardrock and calcrete areas, e.g. the Epukiro area, and diffuse recharge after an entirely wet rainy season for areas with shallow sand cover and/or with pans, e.g. the Tsumkwe area.

Soil water balance calculations indicate that direct recharge occurs mostly in the second half of the rainy season, most probably during late February. The results of the water balance model indicate that the most crucial parameter of such calculations is the root depth which is also highly variable in a semiarid region with patchy vegetation.

Inverse determination of recharge by the chloride mass balance method gives recharge amounts between 0.2 and locally more than 100 mm/a, but the highest figures are unlikely to represent average situations for the catchment. The least favoured recharge conditions are found for Kalahari covered areas, the largest recharge amount occurs in the Otavi area where dolomitic hardrocks outcrop. Three different mechanisms were identified which influence the spatial recharge variability apart from the rain variations: very fast infiltration in karst areas, recharge from preferred flow and diffuse recharge. They are identified by different slopes in a plot of recharge versus precipitation.

The distribution of recharge areas within the catchment is rather complex and the regionalisation of point recharge data to the entire catchment was done by a forward approach using satellite images and by an inverse approach using hydrochemical data. Both methods also considered areas of evaporation and transpiration. From the inverse hydrochemical approach a basin-wide balanced recharge amount of 1.39 mm/a is calculated. The forward approach gave a basin-wide figure of 0.88 (minimum assumption) to 4.53 mm/a (maximum assumption).

From the testing of three different source materials (satellite images, air photographs and geological maps) during the forward recharge regionalisation it was concluded that satellite images are most powerful for such a process. Geological maps are inappropriate for the spatial projection of recharge data as they do mostly not consider the topmost metre of the ground. Air photographs are only recommended when they are classified by grey values and the shape of specific features, e.g. hardrocks occurring as ridges.

The recharge results of this study fit within the largely varying published data, but in this study the scale of the catchment and the variable distribution of surface and geological features are also heeded.

The regionalised recharge figures are confirmed by a simplistic groundwater flow model which indicates that the result of the minimum recharge regionalisation by satellite images and the result from the inverse hydrochemical approach give realistic values.

The simplistic groundwater flow model also indicates that for further modelling more detailed basic data, mainly geological data such as location and character of the pre-Kalahari unconformity and distribution and character of the Rundu Formation, are required.

The study of hydrochemical parameters confirmed the complex recharge distribution by indicating several areas with fresh groundwater of a recharge by fast infiltration water composition or recharge water characterised by a diffuse soil passage. With these two typical groundwater compositions, at least two recharge mechanisms could again be confirmed: recharge of a diffuse nature produces recharge water that is more dominated by Ca^{2+} and HCO_3^- than water that received a fairly quick soil passage along preferred flow paths.

Other prominent hydrochemical processes in the Kalahari are associated with the carbonate-equilibrium-system, mixing with highly mineralised water that is either SO_4^{2-} (central area) or Cl^- (fringe area) dominated and development of Na^+ - HCO_3^- -water types. The latter are mostly generated by feldspar weathering.

Variations of the hydrochemical compositions were observed for shallow groundwaters. They do not only reflect the recharge amount but also the recharge conditions, e.g. a wetter year promotes vegetation growth with increases the HCO_3^- -content in the groundwater due to enhanced CO_2 partial pressure in the root zone.

The main conclusion from this study is that the quantity of groundwater of the Northern Namibian Kalahari Catchment is not endangered by the present land use situation, although the basin-wide recharge figure is only in the order of 1 mm/a. However, it is recommended that prior to any land use change or increased abstraction for supply outside the catchment, a more comprehensive model needs to be compiled including detailed studies of the geology of north-eastern Namibia. Such a model would be most promising when including the Botswana part in the study and developing some bilateral water resource management plan.

At present the quality of the groundwater resource seems to be at higher risk than the quantity; high NO_3^- -content in groundwater is only one subject that needs further understanding. The fairly young, often also shallow, groundwater is typically the water that provides the population with potable quality and therefore careful, continual surveying of the recharge zones seems to be an advisable measure to take. A spatially separation of the extraction well and the cattle watering tank is proposed as an incipient and fairly easy, but promising groundwater protection progress.

9 Zusammenfassung (German summary)

Diese Dissertation behandelt die hydrogeologischen und hydrochemischen Gegebenheiten des nordnamibischen Kalahari-Einzugsgebiets. Den Schwerpunkt stellte dabei das Prozeßverständnis, die Quantifizierung und die Regionalisierung der Grundwasserneubildung für das gesamte Arbeitsgebiet dar.

Das Arbeitsgebiet befindet sich im Nordosten Namibias und umfaßt 5 Teileinzugsgebiete des endorheischen Makgadikgadi-Kalahari-Einzugsgebiets. Das Klima im Arbeitsgebiet ist als semiarid mit Sommerniederschlägen zu klassifizieren. In dem ca. 160 000 km² großen Arbeitsgebiet treten keine permanenten Oberflächengewässer auf und sowohl die extensive Landwirtschaft als auch die Bevölkerung hängt von der Ressource Grundwasser als einziger Trinkwasserquelle ab.

Innerhalb des Untersuchungsgebiets treten Grundwasserleiter präkambrischen bis quartären Alters auf. Der größte Teil des Einzugsgebiets wird von Sedimenten der Kalahari-Gruppe (Oberkreide bis Quartär) bedeckt, die im Arbeitsgebiet Mächtigkeiten bis zu 400 m erreichen (Abb. 3.2-4). Eine weitere stratigraphische Unterteilung der Kalahari-Gruppe erscheint im Zuge dieser Studie wenig sinnvoll, da die terrestrischen Sedimente lateral starken Fazieswechseln unterliegen, und weiterer Forschungsbedarf zur Korrelation innerhalb des Kalahari-Beckens besteht. Wichtige hydrogeologische Elemente sind zum einen die basale Prä-Kalahari-Diskordanz, zum anderen sehr junge (letzte Aktivität jünger als 4-21 ka) Störungen im Eiseb Block. Beide stellen Bereiche erhöhter Grundwasserwegsamkeiten dar. Die Kartierung des jungen Störungssystems erfolgte hauptsächlich mit Satellitenbildern (Abb. 3.3-4), die in den Geländeaufenthalten überprüft wurden. Satellitenbilder bilden in der Kalahari Lineamente zuverlässig und deutlich ab. Sie stellen somit ein leistungsstarkes Mittel für die Grundwassererkundung dar.

Lithologien der Kalahari-Gruppe stellen den obersten Grundwasserleiter vor allem im Norden und Westen des Arbeitsgebietes sowie im Eiseb Block dar. Karoo- und Damara-Lithologien treten weniger häufig als oberster Grundwasserleiter auf (Abb. 4.2-2). Besonders im zentralen südlichen Teil des Arbeitsgebiets treten große Grundwasserflurabstände mit mehr als 150 m auf. Die Verteilung von Brunneneigenschaften zeichnet vor allem das Otavi-Gebiet als leistungsfähig aus. Überdurchschnittliche Brunneneigenschaften treten auch innerhalb eines Kalahari-Grundwasserleiters bei Goblenz auf (Abb. 4.3-2). Häufig korrelieren relative hohe Brunnenleistungen auch mit jüngeren Störungen.

Zur Charakterisierung der Neubildungseigenschaften der Oberflächenbedeckung wurden neben den Festgesteinen fünf Bodenklassen unterteilt: Pfannen und Vleis, rote bis braune Böden, Dünenande, Böden mit äolischem Einfluß und Kalkkrusten. Diese Bodenklassen wurden physikalisch untersucht, hinsichtlich ihrer zu erwartenden Neubildungseigenschaften charakterisiert und räumlich zueinander in bezug gesetzt (Abb. 5.2-5). Äolische Sande zeigen dabei das größte Potential für direkte diffuse Neubildung. Alle Bodenklassen erlauben eine Neubildung entlang präferentieller Fließwege, die in Form von Schrumpfungsrissen oder Wurzelräumen auftreten. Wahrscheinlich tragen alle Bodenklassen zur indirekten Neubildung in Pfannen bei, da selbst auf den Dünenanden Abflußmarken beobachtet wurden. Allerdings ist die Abflußbildung lokal sehr begrenzt.

Der mittlere jährliche Niederschlag liegt im Untersuchungsgebiet zwischen 350 und 600 mm/a, demgegenüber steht eine potentielle Verdunstung von 2600 bis 3200 mm/a. Die jährlichen Niederschlagsmengen schwanken stark und in relativ niederschlagsreichen Jahren besteht ein Neubildungspotential. Des weiteren begünstigen beobachtete Starkregenereignisse (>100 mm/Tag) in relative niederschlagsreichen Jahren die Wahrscheinlichkeit der Neubildung entlang bevorzugter Fließwege und der indirekten Neubildung.

Die Interpretation von Grundwasserganglinien in fünf Beispielgebieten zeigt, daß auch in dem relativ niederschlagsarmen Zeitraum Ende der 1980er / Anfang der 1990er Jahre (im Vergleich zu den 1970er Jahren, die im allgemeinen als relativ niederschlagsreich zu bezeichnen sind) Grundwasserneubildung im Arbeitsgebiet auftrat. Dabei ist wiederum die Identifikation zweier Neubildungsmechanismen möglich. Im Gebiet bei Tsumkwe tritt in überdurchschnittlich niederschlagsreichen Regenzeiten Neubildung auf, die hauptsächlich über die Matrix erfolgt. Im Gebiet der Epukiro Missions Station, wo eher Festgesteine und Kalkkrusten die Oberfläche gestalten, tritt bereits nach einzelnen relativ niederschlagsreichen Monaten Neubildung auf, die als präferentiell (entlang bevorzugter Fließbahnen) zu deuten ist.

Die Verwendung eines Boden-Wasser-Bilanz-Modells hat die Interpretation der bodenphysikalischen Untersuchungen hinsichtlich der Generation der Neubildung über die Matrix für die einzelnen Bodenklassen bestätigt: In den äolischen Sanden treten die höchsten Neubildungsraten innerhalb der untersuchten 4 Klassen (Kalkkrusten wurden nicht berücksichtigt) auf. Für alle Bodenklassen tritt Neubildung nur in überdurchschnittlich regenreichen Jahren in der zweiten Hälfte der Regenzeit auf. Zu einer absoluten Quantifizierung der Neubildung wurde das Modell nicht genutzt, da keine Kalibrierungsdaten zur Verfügung stehen. Es zeigt sich, daß für die Neubildungsentwicklung die Durchwurzelungstiefe der kritischste Parameter ist, da er zum einen die stärksten Veränderungen auf der Ergebnisseite

verursacht. Zum anderen ist bei einer nicht zusammenhängenden Vegetationsdecke (typisch für semiaride Gebiete) die Bestimmung einer mittleren Durchwurzelungstiefe mit den in diesem Projekt zur Verfügung stehenden Methoden nicht zuverlässig möglich.

Neubildungsraten wurden mittels der Chlorid-Bilanz-Methode sowohl in der ungesättigten als auch in der gesättigten Zone berechnet. Die Anwendung in der gesättigten Zone wurde auf Bereiche der Grundwasserscheide limitiert, da hier kein lateraler Zufluß vorhanden ist. Durch die Anwendung in der ungesättigten Zone ergeben sich Neubildungsraten über die Matrix im Bereich von Hundertsteln von Millimetern in unterdurchschnittlichen Niederschlagsjahren bis Zehnteln von Millimetern in durchschnittlichen Niederschlagsjahren. Bei der Anwendung in der gesättigten Zone reichen die Neubildungsraten über die Matrix plus Neubildung entlang bevorzugter Fließbahnen von 0,2 mm/a bis zu lokal über 100 mm/a. Die niedrigsten Werte treten in Bereichen auf, die durch Lockersedimente der Kalahari-Gruppe bedeckt sind. Die höchsten Neubildungsraten sind an verkarstete Festgesteine im Otavi-Gebiet gebunden. Insgesamt sind die höchsten Neubildungsraten an außerordentliche Gegebenheiten gebunden und spiegeln nicht die Bedingungen in dem gesamten Einzugsgebiet wider. Aus der Darstellung aller mittels Chlorid-Bilanz-Methode ermittelten Neubildungsraten gegen den mittleren jährlichen Niederschlag, unterteilt nach unterschiedlichen Oberflächenbeschaffenheiten, ist abzuleiten, daß sowohl für die verkarsteten Festgesteine im Otavi-Gebiete, als auch für die Bereiche, die Kalahari bedeckt sind, jeweils zwei Mechanismen die Neubildungsmenge beeinflussen:

- (1) Im Otavi-Gebiet tritt zum einen eine *sehr schnelle Neubildung entlang bevorzugter Makro-Fließbahnen* (flache Steigung, Abb. 5.6-5a) in den verkarsteten Bereichen auf und daneben eine *Neubildung entlang "normaler" bevorzugter Fließbahnen* (steile Steigung, Abb. 5.6-5a).
- (2) In Kalahari bedeckten Bereichen tritt neben der *Neubildung über die Matrix* (flache Steigung, Abb. 5.6-5b) auch *Neubildung entlang bevorzugter Fließbahnen* (steile Steigung, Abb. 5.6-5b) auf.

Da die Verteilung der Neubildungsgebiete innerhalb des nordnamibischen Kalahari-Einzugsgebiets als sehr komplex anzunehmen ist, verbietet sich die Projektion eines Durchschnittswerts auf die gesamte Fläche von selbst, besonders da auf der Grundwasserscheide Festgesteine sehr viel häufiger ausstreichen als im zentraleren Bereich des Arbeitsgebiets. Die Regionalisierung der punktuellen Neubildungsdaten erfolgte daher durch zwei detailliertere Ansätze: eine Vorwärtsmethode wurde entwickelt, die Satellitenbilder benutzt und eine inverse Methode, die hauptsächlich die Verteilung des Chlorids im Grundwasser innerhalb des Einzugsgebiets verwendet, um Neubildungszonen zu identifizieren und diesen Neubildungswerte

zuzuordnen. Beide Methoden berücksichtigen Zonen, in denen Evaporation und Transpiration durch Phreatophyten zu erwarten sind. Dabei wurde als zusätzlicher Parameter der Grundwasserflurabstand genutzt. Die Verteilungen von Neubildungs- und Evapotranspirationszonen ist in den Abbildungen 5.7-4 und 5.8-13 dargestellt. Mit dem inversen hydrochemischen Ansatz zeigt sich eine einzugsgebietweite Neubildungsmenge von 1,39 mm/a. Der fernerkundliche Ansatz ergibt eine Neubildung von 0,88 mm/a (Minimum-Ansatz) bis 4,53 mm/a (Maximum-Ansatz).

Im Zuge der Vorwärtsregionalisierung wurden drei unterschiedliche Basisdatensätze (Satellitenbilder, Luftbilder und geologische Karten) benutzt. Es hat sich dabei gezeigt, daß nur Satellitenbilder zuverlässige Medien zur Regionalisierung der Neubildung für das Kalahari-Einzugsgebiet sind, wenn man anwenderunterstützte, halbautomatische Klassifikationen nutzt. Geologische Karten sind ein ungeeignetes Medium, da sie gerade die Beschaffenheit der für die Neubildung kritischen obersten Meter des Untergrundes nicht berücksichtigen. Für Luftbilder bietet sich eine Klassifikation an, die zusätzlich zu den Graustufen die Form der unterschiedlichen Einheiten im Luftbild wiedererkennt und berücksichtigt. Die während dieser Studie zur Verfügung stehende software erlaubt automatische Klassifikation für Luftbilder nur auf Grund der Graustufen, wobei keine Unterscheidung zwischen Festgesteinsausstrichen und dichter Vegetation möglich ist.

Die Ergebnisse der punktuellen und der regionalen Neubildungsdaten passen in den Rahmen der bereits veröffentlichten Neubildungsdaten (Fig. 5.9-1). In dieser Studie werden jedoch die komplexen Verteilungsmuster der Neubildung berücksichtigt. Zusätzlich sind die erarbeiteten regionalen Neubildungsdaten durch ein einfaches Grundwasser-Strömungsmodell bestätigt worden, das im Rahmen der sinnvollen hydraulischen Parameter eine Neubildung im Bereich von $5,4 \cdot 10^6 \text{ m}^3/\text{a}$ bis $1,2 \cdot 10^8 \text{ m}^3/\text{a}$ für das Eiseb-Epukiro-Einzugsgebiet zuläßt. Damit wird das Ergebnis der hydrochemischen Neubildungsregionalisierung bestätigt und ebenfalls der minimale Ansatz aus der Vorwärtsregionalisierung.

Das vereinfachte Grundwasser-Strömungsmodell hat ebenfalls gezeigt, daß für detailliertere Modellierungen bessere geologische Basisdaten nötig sind. Vor allem sind hier weitere Kenntnisse über die Prä-Kalahari-Diskordanz sinnvoll und eine detaillierte Aufnahme der Rundu-Formation, die mit Basalt-Sandstein-Wechselagerungen deutliche Wasserwegsamkeiten darstellt.

Die Verteilung hydrochemischer Parameter innerhalb des Einzugsgebietes spiegelt nicht nur die unterschiedlichen Grundwasserleiter-Lithologien wider, sondern auch die komplexe Neubildungsverteilung. Dabei wurden Grundwässer mit typischer Zusammensetzung von

Flutwasser und von Flutwasser nach einer Bodenpassage identifiziert. Diese beiden Wassertypen dokumentieren wiederum die beiden Neubildungsmechanismen diffus und präferentiell. Dabei zeigen die Wässer der diffusen Grundwasserneubildung erhöhte Ca^{2+} - und HCO_3^- -Gehalte auf, die auf den längeren Aufenthalt im Bereich der Wurzelrespiration hindeuten, wobei der CO_2 -Partialdruck und somit auch die Löslichkeit des Kalzits erhöht wird.

Innerhalb der unterschiedlichen Grundwasserleiter-Lithologien wurden hydrochemische Prozesse in Zusammenhang mit dem Kalk-Kohlensäure-Gleichgewicht (z.B. Lösung von Kalzit und Dolomit und Dedolomitisierung) erkannt. Mischungen mit stärker mineralisierten Grundwässern treten ebenfalls auf. Dabei werden im randlichen Bereich der Kalahari und im Bereich von Festgesteinen häufig Cl^- -dominierte Wässer zugemischt. Im zentralen Bereich tritt häufiger ein SO_4^{2-} -dominiertes Mischungsendglied auf, das wahrscheinlich die Wässer der unteren Kalahari im östlichen Teil des Einzugsgebiets charakterisiert. Na^+ - HCO_3^- -Wassertypen treten immer wieder in der Kalahari auf. Im Arbeitsgebiet sind sie hauptsächlich durch die Verwitterung von Feldspäten entstanden, und nur selten durch Kationenaustausch an Tonlagen innerhalb der Kalahari-Gruppe. Mögliche Ausgangsgesteine für die Feldspatverwitterung sind Gneise unterschiedlicher stratigraphischer Einheiten, Basalte oder ihre Abtragungsprodukte in der Kalahari-Gruppe.

Für flache Grundwasservorkommen treten hydrochemische Veränderungen vor allem durch wechselnde Neubildungsbedingungen auf. Dabei variiert nicht nur die Neubildungsmenge, sondern auch der Charakter des Neubildungswassers. In relativ niederschlagsreichen Jahren trägt die dichtere Vegetation und der dadurch erhöhte CO_2 -Partialdruck im Boden zu erhöhten HCO_3^- - und Ca^{2+} -Gehalten und -Anteilen im Grundwasser bei. Ebenso tritt in solchen Jahren verstärkte Feldspatverwitterung auf.

Die Hauptschlußfolgerung dieser Arbeit ist, daß die Grundwasser-Quantität im nordnamibischen Kalahari-Einzugsgebiet zur Zeit nicht gefährdet ist, obwohl die Neubildung im regionalen Maßstab deutlich unter 1% des mittleren jährlichen Niederschlags liegt und mit ca. 1 mm/a anzunehmen ist. Es ist jedoch zu empfehlen, daß Landnutzungsveränderungen oder einer zusätzlichen Grundwasserentnahme für den Bedarf außerhalb des Einzugsgebietes detailliertere Grundwasser-Strömungsmodellierungen vorausgehen sollten. Dazu muß vor allem der geologische Aufbau Nordost-Namibias besser erfaßt werden. Vorrangig sollten dabei die Faziesvariationen und Mächtigkeiten der Karoo-Supergruppe und der Kalahari-Gruppe untersucht werden. Des weiteren erscheint es sinnvoll, den botswanischen Teil des Einzugsgebiets einzubeziehen und eventuell einen bilateralen Wasser-Ressourcen-Plan zu entwickeln.

Die Qualität der Ressource Grundwasser erscheint zur Zeit stärker gefährdet als die Quantität: So stellen hohe NO_3^- -Gehalte im Grundwasser nur ein Thema dar, das eines besseren Prozeßverständnisses bedarf. Häufig versorgt das relative junge, oft auch flache Grundwasser die Bevölkerung mit Trinkwasser guter Qualität und somit würde die sorgfältige, kontinuierliche Beobachtung der entsprechenden Neubildungszonen einen sinnvollen Schritt in Richtung nachhaltige Ressourcensicherung darstellen. Eine relative einfache, aber erfolgversprechende Trinkwasserschutzmaßnahme stellt hierbei die räumliche Trennung von Brunnen und Viehtränke dar.

10 References

- Adobe (2001): Adobe Photoshop Version 4.0LE. Adobe Systems Inc., San Jose.
- Agnew, C. & Anderson, E. (1992): *Water resources in arid realm*. Routledge, pp. 329.
- Albat, H. (1978): The geology of the Kalahari beds of north eastern S.W.A, pp. 13. De Beers Prospecting.
- Allison, G. B. & Hughes, M. W. (1978): The use of environmental tritium and chloride to estimate total local recharge to an unconfined aquifer. *Aust. J. Soil Res.*, **16**, 181-195.
- Allison, G. B. & Barnes, C. J. (1985): Estimation of the evaporation from the normally dry Lake Frome in South Australia. *J. Hydrol.*, **76**, 229-242.
- Appelo, C. A. J. & Postma, D. (1996) *Geochemistry, groundwater and pollution*. Balkema, Rotterdam, 536 pp.
- Bachmat, Y. C., Gvirtzman, H. & Margaritz, M. (1989): Evaluation of groundwater replenishment coefficients from the record of a borehole penetrating the unsaturated zone. *Water Resource Res.*, **25**(5), 973-978.
- Baillieule, T. A. (1973): A geological survey of the Kihabe and Aha Hills, Ngamiland. Geological Survey of Botswana, Gaborone.
- Baillieule, T. A. (1975): Reconnaissance survey of the cover sands in the Republic of Botswana. *J. Sediment. Petrol.*, **45**, 494-503.
- Baillieule, T. A. (1979): The Makgadikgadi pans complex of central Botswana. *Bull. Geol. Soc. America*, **90**, 133-146.
- Balek, J. (1988): Groundwater recharge concepts. In: *Estimation of natural groundwater recharge* (Ed. by I. Simmers), pp. 3-9. *NATO ASI Series C222*.
- Balfour, D. J., Hegenberger, W., Medlycott, A.S. & Wilson, K.J. (1985): Kimberlites near Sikereti, north-eastern South West Africa/Namibia. *Communs. Geol. Surv. S.W. Africa/Namibia*, **1**, 69-77.
- Bäumle, R., Himmelsbach, T. & Bufler, R. (2001): Conceptual hydrogeological models to assess the groundwater resources of the heterogeneous fractured aquifers in Tsumeb (Northern Namibia). In: *New approaches characterizing groundwater flow* (Ed. by K.-P. Seiler & S. Wohnlich), pp. 245-249. Swets & Zeitlinger, Lisse.
- Beanland, S. & Berryman, K. R. (1989): Style and episodicity of late quaternary activity on the Pisa-Grandview Fault Zone, Central Otago, New Zealand. *New Zealand J. Geology and Geophysics*, **32**, 451-461.
- Beekman, H. E., Selaolo, E. T. & Nijsten, G.-J. (1996): Groundwater recharge at the fringe of the Kalahari - The Letlhakeng-Botlhapatou area. *Botswana J. Earth Sci.*, **3**, 19-23.
- BGR (Bundesanstalt für Geowissenschaften und Rohstoffe) (1998): Re-calibration of the groundwater models in the Otavi Mountain Land. Technical co-operation project no. 1989.2034.0. German-Namibian groundwater exploration project. Follow-up report, Vol. 5.

- Bittner, A. (1999): Data base for further decisions regarding the necessity and feasibility of future geophysical and hydrogeological investigations in the study areas Oshivelo, Eastern Caprivi and Eastern Tsumkwe-Otjinene (North-Eastern Namibia). Technical co-operation project no. 1989.2034.0. BGR-DWA desk study. DWA, Windhoek.
- Boocock, C. & Van Straten, O. J. (1961): A note of the development of potable water supplies at depth in the central Kalahari, Bechuanaland Prot. *Rec. Geol. Surv. Bechuanaland Prot.*, **1957/1958**, 11-14.
- Boocock, C. & Van Straten, O. J. (1962): Notes on the geology and hydrology of the central Kalahari region, Bechuanaland Protectorate. *Trans. Geol. Soc., S. Afr.*, **65**, 125-171.
- Bredenkamp, D. B. (1988): Quantitative estimation of groundwater recharge in dolomite. In: *Estimation of natural groundwater recharge* (Ed. by I. Simmers), pp. 449-460. *NATO ASI Series C 222*.
- Bredenkamp, D. B. & Vogel, J. C. (1970): Study of a dolomitic aquifer with carbon-14 and tritium. In: *Isotope hydrology* (Ed. by IAEA), pp. 349-371.
- Bredenkamp, D. B., Schutte, J. M. & Dutoit, G. (1974): Recharge of a dolomitic aquifer as determined from tritium profiles. In: *Isotope techniques in groundwater hydrology* (Ed. by IAEA), pp. 73-94.
- BRGM (Bureau de Recherches Géologiques et Minières) (1988): Kanye dolomite groundwater basin, hydrogeological investigation, resources assessment and development project- Phase II, Final report, Geol. Surv. Dept., Lobatse, Botswana.
- Brooks, R. H. & Corey, A. T. (1964): Hydraulic properties of porous media. *Hydrol. Pap. of the Colorado State Univ.*, **3**, 1-27.
- Brown, S. G. & Newcomb, R. C. (1963): Ground-water resources of the coastal sand-dune area north of Coos Bay, Oregon. *U.S. Geol. Surv. Water-Supply Pap.*, **1619-D**, 1-32.
- Chamley, H. (1989): *Clay sedimentology*. Springer Verlag, Berlin-Heidelberg, pp. 623.
- Chiang, W.-H. & Kinzelbach, W. (1991): Processing Modflow Version 4.10. Wen-Hsing Chiang, Hamburg.
- Clark Labs (1997): IDRISI for Windows Version 2.007. Clark University, Worcester.
- Coates, J. N. M., Davies, J., Gould, D., Hutchins, D.G., Jones, C.R. Key, R.M., Massey, N.W.D., Reeves, G.V., Stansfield, G. & Walker, I.R. (1979): The Kalahari traverse one report. *Bull. Geol. Surv. Botswana*, **21**, 1-294.
- Cooper, H. H. & Jacob, C. E. (1946): A generalized graphical method for evaluating formation constants and summarizing well field history. *Am. Geophys. Union Trans.*, **27**, 526-534.
- Correia, R. J. & Bredenkamp, G. J. (1987): A reconnaissance survey of the vegetation of the Kavango, South West Africa. *J. Sci. Soc. SWA/Namibia*, **40/41**, 29-45.
- Cressie, N. A. C. (1990): The origins of kriging. *Mathematical Geology*, **22**, 239-252.
- Cressie, N. A. C. (1991): *Statistics for spatial data*. John Wiley & Sons Inc., New York, 900 pp.
- Crockett, R. N. (1968): Shashi: Post Karoo system dykes. Sheet 2127A. Geological Survey of Botswana, Gaborone.

- CSIR (Council for Scientific and Industrial Research) (1982): Geoelectrical survey in the Gam area and Eiseb Omuramba. Compiled by De Beer, J. H., Blume, J., Du Plooy, A. and Kruidenier, J.H.B. for National Physical Research Laboratory/Council for Scientific and Industrial Research, Pretoria.
- Dachroth, W. & Sonntag, C. (1983): Grundwasserneubildung und Isotopendatierung in Südwestafrika/Namibia. *Z. dt. Geol. Ges.*, **134**, 1013-1041.
- Darcy, H. (1856): Les fontaines publiques de la ville de Dijon. Dalmont, Paris, 674 pp.
- Das Gupta, A. & Paudyal, G. N. (1988): Estimating aquifer recharge and parameters from water level observation. *J. Hydrol.*, **99**, 103-116.
- Davis, J. C. (1986): *Statistics and data analysis in geology*. John Wiley & Sons Inc., Singapore, 646 pp.
- Davis, S.N. & DeWiest, R.J.M. (1966): *Hydrogeology*. John Wiley & Sons Inc., New York, 463 pp.
- De Beer, H. J. H. & Blume, J. (1985): Geophysical and hydrogeological investigations of the groundwater resources of western Hereroland/South West Africa/Namibia. *Trans. Geol. Soc. S. Afr.*, **88**, 483-493.
- De Beer, J. H. & van Zijl, J. S. V. (1975): An electrical conductivity anomaly and rifting in Southern Africa. *Nature*, **225**, 687-689.
- De Beer, J. H., van Zijl, J. S. V., Huysen, R. M. J., Hugo, P. L. V., Joubert, S. J. & Meyer, R. (1976): A magnetometer array study in South West Africa, Botswana and Rhodesia. *Geophys. J. R. Astr. Soc.*, **45**, 1-17.
- De Swardt, A. M. J. & Bennet, G. (1974) Structural and physiographic development of Natal since the late Jurassic. *Trans. Geol. Soc. S. Africa*, **77**, 309-322.
- De Vries, J. J. (1984): Holocene depletion and active recharge of the Kalahari groundwaters - A review and an indicative model. *J. Hydrol.*, **70**, 221-232.
- De Vries, J. J. & Hoyer, M. (1988): Groundwater studies in semi-arid Botswana - A review. In: *Estimation of natural groundwater recharge* (Ed. by I. Simmers), pp. 339-348. *NATO ASI Series C* 222.
- De Vries, J. J., Selaolo, E. T. & Beekman, H. E. (2000): Groundwater recharge in the Kalahari, with reference to paleo-hydrologic conditions. *J. Hydrol.*, **238**, 110-123.
- DIN 18 123 (1996): Baugrund, Untersuchung von Bodenproben; Bestimmung der Korngrößenverteilung. Beuth Verlag, Berlin.
- Dingle, R. V., Siesser, W. G. & Newton, A. R. (1983): *Mesozoic and Tertiary geology of Southern Africa*. Balkema, Rotterdam, 375 pp.
- Drever, J. L. (1982): *The geochemistry of natural waters*. Prentice-Hall, Englewood Cliffs, 388 pp.
- Du Plessis, P. I. & Le Roux, J. P. (1995): Late Cretaceous alkaline saline lake complexes of the Kalahari Group in northern Botswana. *J. Afr. Earth Sci.*, **20**, 7-15.
- Durner, W. & Flühler, H. (1993): Modellierung des Transports von Chemikalien in strukturierten Böden mit einem Porenbündelmodell. *Mitt. Dt. Bodenkundl. Gesellschaft*, **72**, 93-94.

-
- Dümmer, M. (1982): Zur Hydrogeologie des Raumes Nürnberg-Bad Windsheim. Ph.D. thesis, Ludwig Maximilians Universität München.
- DWA (Department of Water Affairs) (1988): Evaporation map for Namibia. DWA, Windhoek.
- DWA (Department of Water Affairs) (1991): Groundwater investigations in Kavango and Bushmanland/Namibia. DWA, Windhoek.
- DWA (Department of Water Affairs) (1992): Goblenz State Water Scheme - Memorandum on drilling and test pumping. DWA, Windhoek.
- DWA (Department of Water Affairs) (1993a): Resume of previous work carried out within Hereroland. DWA, Windhoek.
- DWA (Department of Water Affairs) (1993b): Memorandum - Drilling and test pumping of replacement boreholes in the Omuramba Epukiro, 3 km east of Omouozonjanda. DWA, Windhoek.
- DWA (Department of Water Affairs) (1993c): Groundwater resource evaluation of East Herero. DWA, Windhoek.
- DWA (Department of Water Affairs) (1993d): Groundwater investigation in Kavango and Bushmanland, Phase 2, Final Report. DWA, Windhoek.
- DWA (Department of Water Affairs) (1993e): Development of water supply to serve the people repatriated from Botswana and their cattle. DWA, Windhoek.
- DWA (Department of Water Affairs) (1993f): Reconnaissance report on the water supply to settlements along the Omuramba Omatako between Goblenz-Okakarara and Okakarara-Central Reservoir Pipeline. DWA, Windhoek.
- DWA (1996a): Geohydrological evaluation and management strategies for the expanded Otjinene State Water Scheme. DWA, Windhoek.
- DWA (Department of Water Affairs) (1996b): Groundwater exploration in the Eiseb block of eastern Namibia. Phase 1 - Final report. DWA, Windhoek.
- Edmunds, W. M. & Walton, N. R. G. (1980): A geochemical and isotopic approach to recharge evaluation in semi-arid zones - past and present. In: *Arid zone hydrology: Investigations with isotope techniques*, pp. 47-68. IAEA, Vienna.
- Edmunds, W. M., Darling, W. G. & Kinniburgh, D. G. (1988): Solute profile techniques for recharge estimation in semi-arid and arid terrain. In: *Estimation of natural groundwater recharge*, (Ed. by I. Simmers), pp. 313-322. *NATO ASI Series C* 222.
- Encarnación, J., Fleming, T. H., Elliot, D. H. & Eales, H. V. (1996): Synchronous emplacement of Ferrar and Karoo dolerites and the early break-up of Gondwana. *Geology*, **24**, 535-538.
- ESRI (Environmental System Research Institute) (1996). ArcView GIS Version 3.0. ESRI Inc., Redlands.
- Fairhead, J. D. & Henderson, R. W. (1977): The seismicity of southern Africa and incipient rifting. *Tectonophysics*, **41**, T19-T26.

-
- Fielitz, K. (1999): Geophysical Investigation in the study areas Oshivelo, eastern Caprivi, and eastern Tsumkwe-Otjinene. DWA-BGR desk study report. DWA, Windhoek.
- Foster, S. S. D., Bath, A. H., Farr, J. L. & Lewis, W. J. (1982): The likelihood of active groundwater recharge in the Botswana Kalahari. *J. Hydrol.*, **55**, 113-136.
- Freeze, R. A. & Cherry, J. A. (1979): *Groundwater*. Prentice-Hall, Englewood Cliffs, New Jersey, 604 pp.
- Frommurge, H. F. (1953): Hydrological research in arid and semi-arid areas in the Union of South Africa and Angola. *Rev. Res., Arid Zone Hydrol., UNESCO*, 58-77.
- Garrels, R. M. & MacKenzie, F. T. (1967): Origin of the chemical composition of some springs and lakes. Equilibrium concepts in natural water systems. *Am. Chem. Soc. Adv. Chem. Ser.*, **67**, 222-242.
- Gehrels, J. C. & van der Lee, J. (1990): Rainfall and recharge: a critical analysis of the atmosphere-soil-groundwater relationship in Kanye, semi-arid Botswana. M.Sc. thesis, Vrije Universiteit Amsterdam.
- George, Orr & Carr. (1993): Groundwater investigation in Kavango and Bushmanland Phase 2 -Final Report, Volume 2 [Appendices]: Stratigraphic analysis of the Kalahari Group sediments based on the historical (original) borehole logs of Kavango and Bushmanland. DWA, Windhoek.
- Gerschütz, S. (1996): Geology, volcanology, and petrogenesis of the Kalkrand Basalt Formation and the dolerite complex, southern Namibia. Ph.D. thesis, Universität Würzburg.
- Gevers, T. W. (1932): Kaoko eruptives and alkaline rocks at Cape Cross, South West Africa. *Trans. Geol. Soc. S. Afr.*, **35**, 85-96.
- Gieske, A. (1992): Dynamics of groundwater recharge - a case study in semi-arid eastern Botswana. Ph.D. thesis, Vrije Universiteit Amsterdam.
- Gieske, A., Selaolo, E. & Beekman, H. E. (1995): Tracer interpretation of moisture transport in a Kalahari sand profile. In: *Application of tracers in arid zone hydrology* (Ed. by E.M. Adar & C. Leibundgut), pp. 373-382. IAHS Publ. 232.
- GoldenSoftware (1999): Surfer Version 7. GoldenSoftware Inc., Golden.
- Green, W. H. & Ampt, G. A. (1911): Studies on soil physics: 1. The flow of air and water through soil. *J. Agric. Sci.*, **4**(1), 1-24.
- Gvirtzman, H., Ronen, D. & Magaritz, M. (1986): Anion exclusion during transport through the unsaturated zone. *J. Hydrol.*, **87**, 267-283.
- Habetha, E. (1969): Ingenieurgeologie. In: *Lehrbuch der angewandten Geologie, Vol. II/2* (Ed. by A. Bentz & Martini, H.J.), pp. 1547-1758. Enke Verlag, Stuttgart.
- Hardie, L. A. & Eugster, H. P. (1970): The evolution of closed-basin brines. *Mineral. Soc. Am. Spec. Publ.*, **3**, 273-290.
- Harland, W. B., Armstrong, R. L., Cox, A. V., Craig, L. E., Smith, A. G. & Smith, D. G. (1990): *A geological time scale*. Cambridge University Press, Cambridge, 263 pp.
-

-
- Hartge, K. H. & Horn, R. (1991): *Einführung in die Bodenphysik*. Enke Verlag, Stuttgart, 303 pp.
- Hatzsch, P. (1978): Untersuchung der gesteinsphysikalischen und petrographischen Eigenschaften der sedimentären Festgesteine im hangenden des Zechstein-Salinars im oberen Fulda-Gebiet. Ph.D. thesis, Christian Albrechts Universität Kiel.
- Haude, W. (1954): Zur praktischen Bestimmung der aktuellen and potentiellen Evaporation und Evapotranspiration. *Mittl. dt. Wetterdienstes*, **8**, 22.
- Haughton, S. H. (1963): *The stratigraphic history of Africa south of the Sahara*. Oliver and Boyd, London, 365 pp.
- Hedberg, R. M. (1979): Stratigraphy of the Ovamboland Basin, South West Africa. *Bull. Precamb. Res. Unit*, **24**, 1-325.
- Hegenberger, W. (1982): The regional geology of northeastern South West Africa/Namibia. Geological Survey of Namibia, Windhoek.
- Hegenberger, W. (1987): Stand der geologischen Kenntnisse über das Kavangogebiet. *J. Sci. Soc. SWA*, **40/41**, 97-113.
- Heinrich, U. (1992): *Zur Methodik der räumlichen Interpolation mit geostatistischen Verfahren*. Deutscher Universitätsverlag.
- Heynes, P. (1992): Namibia's water resource: A new approach needed. *Namibia Review*, **1**, 17-29.
- Himmelsbach, T. & Wendland, E. (1999): Schwermetalltransport in Sandsteinen unter Bedingungen einer hochsalinaren Porenlösung - Laborversuch und Modellierung. *Grundwasser*, **4**(3), 103-112.
- Hoffmann, P. F. (1991): Did the breakout of Laurentia turn Gondwana inside-out? *Science*, **252**, 1409-1412.
- Holzförster, F. (2000): Sedimentology, stratigraphy and synsedimentary tectonics of the Karoo Supergroup in the Huab and Waterberg-Erongo areas, N-Namibia. Ph.D. thesis, Universität Würzburg.
- Holzförster, F., Stollhofen, H. & Stanistreet, I. G. (1999): Lithostratigraphy and depositional environment in the Waterberg-Erongo area, central Namibia, and correlation with the main Karoo Basin, South Africa. *J. Afr. Earth Sci.*, **29**, 105-123.
- Houston, J. (1982): Rainfall and recharge to a dolomite aquifer in semi-arid climate at Kabwe, Zambia. *J. Hydrol.*, **59**, 173-187.
- Houston, J. (1988): Rainfall-runoff-recharge relationship in the basement rocks of Zimbabwe. In: *Estimation of natural groundwater recharge* (Ed. by I. Simmers), pp. 349-366. *NATO ASI Series C222*.
- Howard, K. W. F. & Lloyd, J. W. (1979): The sensitivity of parameters in the Penman evaporation equation and direct recharge balance. *J. Hydrol.*, **94**, 129-142.
- Hugo, P. J. (1969): Report on the core-drilling program in Owamboland 1967-1968, pp. 46. Geological Survey S. W. Africa.

- Hutchins, D. G., Hutton, L. G., Hutton, S. M., Jones, C. R. & Loehnert, E. P. (1976): A summary of the geology, seismicity, geomorphology and hydrogeology of the Okavango Delta. *Bull. Geol. Surv. Botswana*, **7**, 1-27.
- Hutton, R. M. T. (1996): Groundwater exploration in the Eiseb block of eastern Namibia. Phase 1 - Final report, pp. 15. DWA, Windhoek.
- Huyser, D. J. (1982): Chemiese Kwaliteit van die Ondergronds waters in Suidwes-Afrika/Namibie. Volume 3, parts 2 & 3 - Onverwerkte Data. DWA, Windhoek.
- Hyde, L. W. (1971): Groundwater supplies in the Kalahari area, Botswana. In: *Proc. Conf. on sustained production from semi-arid areas*, pp. 77-87, Gaborone.
- Jacks, G. & Traoré, M. (2000): Mechanisms and rates of groundwater recharge at Tombouctou, Republic of Mali. *J. Afr. Earth Sci.*, **30**(4a), 41.
- Jahnke, C. (1999): Ein neues Klassifikationsystem für Grundwässer und seine Anwendung in känozoischen Porengrundwasserleitern. *Grundwasser*, **4**(2), 62-72.
- James, R. V. & Rubin, J. (1986): Transport of chloride ion in a water-unsaturated soil exhibiting anion exclusion. *Soil Sci. Am. J.*, **50**, 1142-1149.
- JICA (Japan International Cooperation Agency) (2000): The study on the groundwater potential. Evaluation and management plan in the southeastern Kalahari (Stampriet) artesian basin in the Republic of Namibia. Progress report II. DWA, Windhoek.
- Jones, C. R. (1982): The Kalahari of southern Africa. In: *The Geological story of the world's deserts, Vol. 17* (Ed. by Smiley), pp. 20-34. Striae, Uppsala.
- Jones, M. Q. W. (1988): Heat flow in the Witwatersrand basin and environs and its significance for the South African shield geotherm and lithosphere thickness. *J. Geophys. Res.*, **93**, 3243-3260.
- Keller, S. & von Hoyer, M. (1992): Erkundung und Bewirtschaftung von präkambrischen Karstaquiferen im südlichen Afrika. *Z. dt. Geol. Ges.*, **143**, 277-290.
- Key, R. M. & Ayres, N. (2000a): The 1998 edition of the national geological map of Botswana. *J. Afr. Earth Sci.*, **30**(3), 427-451.
- Key, R. M. & Ayres, N. (2000b): Botswana geology map. *J. Afr. Earth Sci.*, **30**(3), CD-ROM Supplement.
- King, L. C. (1962): *The morphology of the Earth*, Edinburgh, 699 pp.
- Kitanidis, P. K. (1997): *Introduction to geostatistics - Application in hydrogeology*. Cambridge University Press, New York, 249 pp.
- Külls, C. (2000): Groundwater of the north-western Kalahari, Namibia - Estimation of recharge and quantification of the flow system. Ph.D. thesis, Universität Würzburg.
- Külls, C. & Udluft, P. (2000): Mapping the availability and dynamics of groundwater recharge Part II: Case studies. In: *Congress regional geological cartography and information systems*, München.

- Külls, C., Constantinou, C. & Udluft, P. (2000): Dynamics of groundwater recharge in natural environments and mining areas: Case studies from Cyprus. In: *Congress regional geological cartography and information systems*, München.
- Leo Hatz Consulting (1993): Groundwater resource evaluation of East Herero, pp. 97. Report to the DWA, Windhoek.
- Litherland, M. (1975): The geology of the area around Maitengwe, Sebine and Tshesebe, northeastern and central districts, Botswana. *Geological Survey of Botswana District Memoir*, **2**, 1-133.
- Lloyd, J. W. (1986): A review of aridity and groundwater. *Hydrological Processes*, **1**, 63-78.
- Maidment, D.R. (1993): *Handbook of hydrology*. McGraw-Hill, Inc., New York.
- Mainardy, H. (1999): Grundwasserneubildung in der Übergangszone zwischen Festgesteinsrücken und Kalahari-Lockersedimentüberdeckung (Namibia). *HU-Forschungsergebnisse aus dem Bereich Hydrogeologie und Umwelt*, **17**, 1-145.
- Mallick, D. I. J., Habgood, F. & Skinner, A. C. (1981): A geological interpretation of Landsat imagery and air photography of Botswana, pp. 36. Institute of Geological Sciences Overseas Geology and Mineral Resources.
- Manger, G. E. (1963): Porosity and bulk density of sedimentary rocks. *U.S. Geol. Surv. Bull.*, **1144-E**, 1-55.
- Martin, H. (1953): Notes on the Dwyka succession and on some pre-Dwyka valley in South West Africa. *Trans. Geol. Soc. S. Africa*, **56**, 37-41.
- Martin, H. (1961a): The Geology and Distribution of the Karoo system in South West Africa. In: *Interim report of the coal commission of South West Africa*, (Ed. by J. W. Brandt, H. Martin and J. G. Kirchner), pp. 17-86.
- Martin, H. (1961b): Hydrology and water balance of some regions covered by Kalahari sands in South West Africa. In: *Inter-Afr. conf. on hydrology*, Nairobi.
- Martin, H. (1975): Structural and palaeogeographical evidence for an Upper Palaeozoic sea between southern Africa and South America. In: *3rd Gondwana symposium on Gondwana stratigraphy and palaeontology* (Ed. by K. W. S. Campbell), pp. 37-51, Canberra.
- Martin, H. (1981): The Late Palaeozoic Dwyka Group of the southern Kalahari basin in Namibia and Botswana and the subglacial valleys of the Kaokofeld in Namibia. In: *Earths pre-Pleistocene glacial record* (Ed. by M. J. Hambrey and W. B. Harland), pp. 61-66. Cambridge University Press, Cambridge.
- Martin, H. & Porada, H. (1977): The intercratonic branch of the Damara Orogen in South West Africa. *Precamb. Res.*, **5**, 311-357.
- Mattheß, G. (1994): *Die Beschaffenheit des Grundwassers*. Gebrüder Bornträger, Berlin-Stuttgart, 499 pp.
- Mattheß, G. & Ubell, K. (1983): *Allgemeine Hydrogeologie - Grundwasserhaushalt*. Gebrüder Bornträger, Berlin-Stuttgart, 438 pp.

-
- Mazor, E. (1982): Rain recharge in the Kalahari. -A note on some approaches to the problem. *J. Hydrology*, **55**, 137-144.
- Mazor, E., Verhagen, B. T. & Sellschop, J. P. F. (1974): Kalahari groundwaters: their hydrogen, carbon and oxygen isotopes. In: *Isotope techniques in groundwater hydrology* (Ed. by IAEA), pp. 203-225.
- Mazor, E., Bielsky, M., Verhagen, B. T., Sellschop, J. P. F., Hutton, L. & Jones, M. T. (1980): Chemical composition of groundwaters in the vast Kalahari flatlands. *J. Hydrol.*, **48**, 147-165.
- McCarthy, T. S., Green, R. W. & Franey, N. J. (1993): The influence of neo-tectonics on water dispersal in the northeastern regions of the Okavango swamps, Botswana. *J. Afr. Earth Sci.*, **17**, 23-32.
- McDonald, M. G. & Harbough, A. W. (1988): A modular three-dimensional finite-difference groundwater flow model. *Techniques of water-resources investigations*, **06-A1**, 576.
- Medlycott, A. S. (1980): Bushmanland and Southern Kavango. Interim report July 1979. CDM Prospecting.
- Meijerink, A. M. J., Lubczynski, M. & Wolski, P. (1999): Remote sensing, hydrological analysis and hydrotopes. In: *Regionalization in hydrology* (Ed. by B. Diekkrüger, M.J. Kirkby & U. Schröder), pp. 137-145. IAHS Publ. 254.
- MicroImages (1996): TNTmips Version 5.4. MicroImages Inc., Lincoln.
- Miller, R. M. (1979): The Okavango Lineament, a fundamental tectonic boundary in the Damara Orogen of South West Africa/Namibia. *Trans. Geol. Soc. S. Afr.*, **82**, 349-361.
- Miller, R. M. (1983): The Pan-African orogen in South West Africa/Namibia. In: *Evolution of the Damara Orogen of South West Africa/Namibia* (Ed. by R. M. Miller), pp. 431-512. Special Publ. Geol. Soc. S. Africa 11.
- Miller, R. M. (1992): Hydrocarbons. In: *Mineral resources of Namibia* (Ed. by G. S. Namibia), pp. 7.3/1-7.3/19, Windhoek.
- Miller, R. M. (1997): The Owambo basin of northern Namibia. In: *African basins* (Ed. by R. C. Selley), pp. 237-258. Sedimentary basins of the world 3 (Series ed. K-J. Hsü).
- Miller, R. G. & Grote, W. (1983): 1 : 500 000 geological map of the Damara Orogen in 2 sheets. In: *Evolution of the Damara Orogen of South West Africa/Namibia* (Ed. by R. M. Miller), back pocket. Special Publ. Geol. Soc. S. Africa.
- Miller, R. M. & Schalk, K. E. L. (1980): Geological map of Namibia. Geological Survey of Namibia, Windhoek.
- Millner, S. C., Le Roex, A. P. & O'Connor, J. M. (1995): Age of Mesozoic igneous rocks in northwestern Namibia, and their relationship to continental break-up. *J. Geol. Soc. London*, **152**, 97-104.
- Millner, S. C., Duncan, A. R., Ewart, A. & Marsh, J. S. (1994): Promotion of the Etendeka Formation to group status: A new integrated stratigraphy. *Commun. Geol. Survey Namibia*, **9**, 5-11.

-
- Modisi, M. P. (2000): Fault system at the southeastern boundary of the Okavango Rift, Botswana. *J. Af. Earth Sci.*, **30**, 569-578.
- Modisi, M. P., Atekwana, E. A., Kampunzu, A. B. & Ngwisanyi, T. H. (2000): Rift kinematics during the incipient stage of continental extension: Evidence from the nascent Okavango rift basin, northwestern Botswana. *Geology*, **28**(10), 939-942.
- Moore, A. E. & Dingle, R. V. (1998): Evidence for fluvial sediment transport of Kalahari sands in central Botswana. *S. Afr. J. Geol.*, **101**, 143-153.
- Morel-Seytoux, H. J. & Khanji, J. (1974): Derivation of an equation of infiltration. *Water Resource Res.*, **10**(4), 796-800.
- Morosini, M. (1996): Chemical-isotopic character, origin and evolution of groundwater in western Ghanzi district, Botswana. Hydrochemical report for the TGLP Ghazi/Makunda groundwater survey. Final report. Geological Survey Department, Gaborone.
- Mortimer, C. (1984): Geological map of Botswana. Geological Survey of Botswana, Gaborone.
- Mubu, M. S. (1995): Aeromagnetic mapping and interpretation of mafic dyke swarms in southern Africa. M.Sc. thesis, ITC Delft.
- Neumann-Redlin, C. & Sekwale, M. (1982): Serowe water supply. Groundwater resource study. Final report. Botswana Geological Survey, Lobatse.
- O'Connor & Thomas, D. S. G. (1999): The timing and environmental significance of Late Quarternary linear dune development in western Zambia. *Quaternary Research*, **52**, 44-55.
- Olea, R. A. (1975): Optimum mapping techniques using variable theory. *Kansas Geol. Surv. Series on Spatial Analysis*, **2**, 1-137.
- Olin, M. H. E. & Svensson, C. (1992): Evaluation of geological and recharge parameters for an aquifer in southern Sweden. *Nordic Hydrology*, **23**, 305-314.
- Olsson, T. (1980): Ground-water-level as a measure of the effective porosity and ground-water recharge. *Sverige Geologiska Undersökning Rapporter & Meddelanden*, **21**.
- Passarge, S. (1906): Probleme in dem Globus, III. *Z. Länder u. Völkerkd.*, **190**, 299-302.
- Paya, B. K. (1996): The geology of the Bobonong area. *Geol. Surv. Botswana Bull.*, **40**, 1-111.
- Philip, J. R. (1992): Falling head ponded infiltration. *Water Resource Res.*, **28**(8), 2147-2148.
- Phillips, F. M., Mattick, J. L., Duval, T. A., Elmore, D. & Kubik, P. W. (1988): Chlorine 36 and tritium from nuclear weapons fallout as tracers for long-term liquid and vapor movement in desert soils. *Water Resource Res.*, **24**(11), 1877-1891.
- Poulimenos, G. & Doutsos, T. (1997): Flexural uplift of rift flanks in central Greece. *Tectonics*, **16**(6), 912-923.
- Pretschold, H. H. (1977): Beiträge zur Methodik der hydrodynamischen Analyse, zur Ermittlung von Wasserhaushaltsgrößen und zur Hydrogeologie des Buntsandsteins. Ph.D. thesis, TU Bergakademie Freiberg.
-

-
- Prinz, T. (1996): Multispectral remote sensing of the Gosses Bluff impact crater, Central Australia (N.T.) by using Landsat-TM and ERS-1 data. *Photogr. & Rem. Sens.*, **51**(3), 137-149.
- Reeves, C. V. (1972): Rifting in the Kalahari? *Nature*, **237**, 95-96.
- Reeves, C. V. (1978a): Reconnaissance aeromagnetic survey of Botswana 1975-77, pp. 199. Geological Survey Botswana, Gaborone.
- Reeves, C.V. (1978b): A failed Gondwana spreading axis in southern Africa. *Nature*, **273**, 222-223.
- Reeves, C.V. (2000): Geophysical mapping of mesozoic dyke swarms in Africa - their origin in the disruption of Gondwana. *J. Afr. Earth Sci.*, **30**, 499-513.
- Reineck, H.-E. (1956): Die Oberflächenspannung als geologischer Faktor in Sedimenten. *Senckenbergiana lethaea*, **37**, 265-287.
- Reineck, H.-E. (1984): *Aktuogeologie klastischer Sedimente*. Waldemar Kramer, Frankfurt a. Main, 348 pp.
- Reineck, H.-E. & Singh, I. B. (1980): *Depositional sedimentary environments*. Springer, Berlin-Heidelberg-New York, 549 pp.
- Rietzler, J. (1979): Zur Hydrogeologie des Raumes südöstlich von Nürnberg unter besonderer Berücksichtigung der Gradabteilungsblätter 6533 Röthenbach, 6633 Feucht und 6733 Allersberg. Ph.D. thesis, Ludwig Maximilians Universität München.
- Ringrose, S. Matheson, W. & Beekman, H.E. (1997): Remotely sensed data at the eastern Botswana Kalahari: Geomorphological features and vegetation cover in the Letlhakeng-Bothlhapatlou area. GRES II Project: Technical report. Department of Geological Survey, Lobatse.
- Rushton, K. R. & Ward, C. (1979): The estimation of groundwater recharge. *J. Hydrol.*, **41**, 345-361.
- Sabins, F. F. (1997): *Remote sensing*. W. H. Freeman and Company, New York, 494 pp.
- SACS (South African Committee for Stratigraphy) (1980): SACS Part 1: Lithostratigraphy of the Republic of South Africa, South West Africa/Namibia, and the Republic of Bothuthatswana, Transkei and Venda, pp 690. Handbook Geological Survey South Africa 8.
- Sami, K. & Hughes, D.A. (1996): A comparison of recharge estimates to a fractured sedimentary aquifer in southern Africa from chloride mass balance and an integrated surface-subsurface model. *J. Hydrol*, **179**, 111-136.
- Scalone, B. R. (1992): Evaluation of liquid and vapour water flow in desert soils based on chlorine 36 and tritium tracers and non-isothermal flow simulations. *Water Resource Res.*, **28**(1), 285-297.
- Schlüter, T. (1997): *Geology of East Africa*. Gebrüder Bornträger, Berlin - Stuttgart, 462pp.
- Scholtz, C. H., Koczyński, T. A. & Hutchins, D. G. (1976): Evidence for incipient rifting in southern Africa. *Geophys. J. Res. Astr. Soc.*, **44**, 135-144.
- Seeger, G. (1990): An evaluation of the groundwater resources of the Grootfontein Karst Area. DWA, Windhoek.

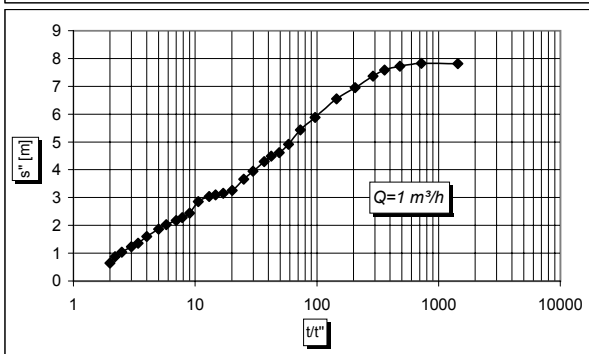
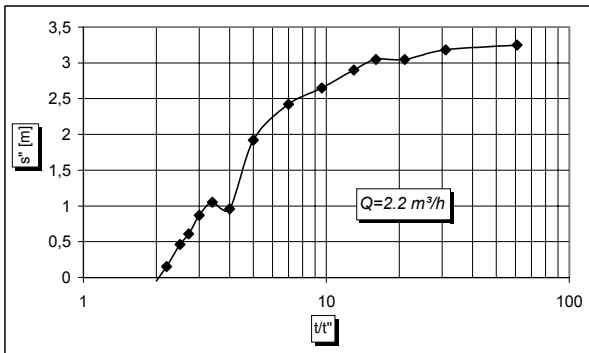
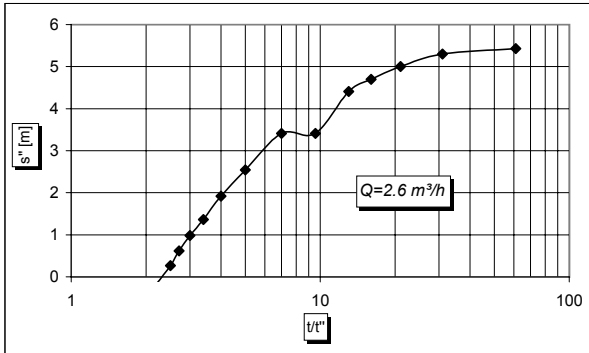
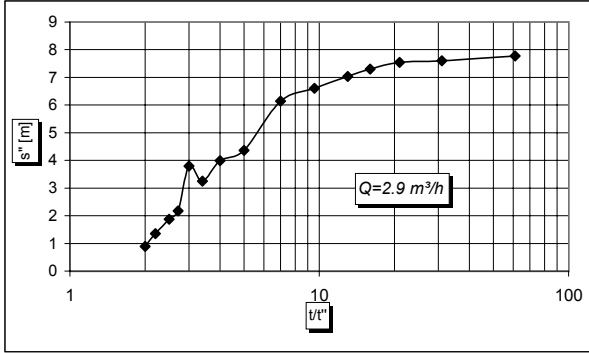
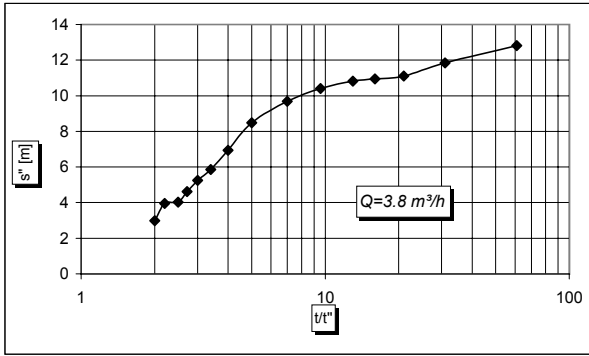
- Selaolo, E. T. (1998): Tracer studies and groundwater recharge assessment in the eastern fringe of the Botswana Kalahari: the Letlhakeng - Botlhapatlou Area. Ph.D. thesis, Vrije Universiteit Amsterdam.
- Selaolo, E. T., Gieske, A. S. M. & Beekman, H. E. (1994): Chloride deposition and recharge rates for shallow groundwater basins in Botswana. In: *25th Cong. IAH*, pp. 502-506, Adelaide.
- Shaw, P. (1986): The palaeohydrology of the Okavango Delta some preliminary results. *Palaeoecol. Afr.*, **17**, 51-58.
- Singhvi, A. K. & Wintle, A. G. (1999): Luminescence dating of aeolian and coastal sand and silt deposits: application and implication. In: *Aeolian environments sediments and landforms* (Ed. by A. S. Goudie, I. Livingstone and S. Stokes). Wiley, Chichester.
- Sloots, R. R. & Wijnen, M. M. (1990): Groundwater recharge to a fractured aquifer in S-E Botswana. Results of a survey of the Molepolole-East wellfield. M. Sc. thesis, Vrije Universiteit Amsterdam.
- Smale, D. (1973): Silcretes and associated silica diagenesis in South Africa. *J. Sed. Petr.*, **4**, 1077-1089.
- Spalding, R.F. & Exner, M.E. (1993): Occurrence of nitrate in groundwater - A review. *J. Environm. Qual.*, **22**, 392-402.
- SRU (Rat von Sachverständigen für Umweltfragen) (1985): *Umweltprobleme der Landwirtschaft*. Kohlhammer, Stuttgart, 423 pp.
- Stansfield, G. (1973): The geology of the area around Dukwe and Tlalambele, central District, Botswana. *Surv. Botswana District Memoir*, **1**, 1-74.
- Stewart, J. W. (1962): Water-yielding potential of weathered crystalline rocks at the Georgia Nuclear Laboratory. *U.S. Geol. Surv. Prof. Pap.*, **450-B**, 106-107.
- Stoer, J. (1983): *Einführung in die Numerische Mathematik I*. Springer Verlag.
- Stonestrome, D. A. & Austin, K. C. (1994): Nonmonotonic matrix pressure histories during constant flux infiltration into homogenous soil profiles. *Water Resource Res.*, **30**, 81-92.
- Summerfield, M. A. (1985): Tectonic background to long-term landform development in tropical Africa. In: *Environmental change and tropical geomorphology* (Ed. by I. Douglas and T. S. O. Spencer), pp. 281-294. BGRG Publ.
- Ten Brink, U. & Stern, T. (1992): Rift flank uplifts and hinterland basins: Comparison of the Transantarctic Mountains with the Great Escarpment of southern Africa. *J. Geophys. Res.*, **97**, 569-585.
- Theis, C. V. (1935): The relation between the lowering of the piezometric surface and the rate and duration of discharge of a well using ground-water storage. *Am. Geophys. Union Trans.*, **16**, 519-524.
- Thomas, D. S. G. (1986): The nature and depositional settings of arid and semi-arid Kalahari sediments, Southern Africa. *J. Arid Environments*, **14**, 17-26.

- Thomas, D. S. G. (1987): Discrimination of depositional environments using sedimentary characteristics in the Mega Kalahari, central southern Africa. In: *Desert sediments: Ancient and modern, Vol. 35* (Ed. by L. Frostick and I. Reid), pp. 293-306. Geological Society Special Publ. 35.
- Thomas, D. S. G. (1988): The nature and depositional setting of arid and semi-arid Kalahari sediments, South Africa. *J. Arid Environment*, **14**, 17-26.
- Thomas, D. S. G. & Shaw, P. A. (1990): The deposition and development of the Kalahari Group sediments, central Southern Africa. *J. Afr. Earth Sci.*, **10**, 187-197.
- Thomas, D. S. G. & Shaw, P. A. (1991): *The Kalahari environment*. Cambridge University Press, Cambridge, 290 pp.
- Thomas, D. S. G., O'Connor, P. W., Bateman, M. D., Shaw, P. A., Stokes, S. & Nash, D. J. (2000): Dune activity as a record of late Quaternary aridity in the northern Kalahari: new evidence from northern Namibia interpreted in the context of regional arid and humid chronologies. *Palaeo.*, **156**(3-4), 243-259.
- Todd, D. K. (1959): *Ground water hydrology*. John Wiley & Sons Inc., New York, 336 pp.
- Tóth, J. (1962): A theory of groundwater motion in small drainage basins. *J. Geophys. Res.*, **68**, 4795-4812.
- Tredoux, G., Engelbrecht, J.F.P. & Talma, A.S. (2001): Nitrate in groundwater in Southern Africa. In: *New approaches characterizing groundwater flow* (Ed. by K.-P. Seiler & S. Wohnlich), pp. 663-666. Swets & Zeitlinger, Lisse.
- Udluft, P. & Külls, C. (2000): Mapping the availability and dynamics of groundwater recharge Part I: Modelling techniques. In: *Congress regional geological cartography and information systems*, Munich.
- Udluft, P. & Zagana, E. (1994): Computer-aided water budget of the Venetikos catchment area. In: *Proc. of the 7th cong. Geol. Soc. Greece, Vol. XXX/4*, pp. 267-274.
- Ullman, W. J. (1985): Evaporation rate from a salt pan: estimates from chemical profiles near surface groundwaters. *J. Hydrol.*, **79**, 365-373.
- UNESCO (1979): Map of the world distribution of arid regions. Paris MAB Technical Notes 7.
- Van Genuchten, M. T. (1980): A closed-form equation for predicting the hydraulic conductivity of unsaturated soils. *Soil Sci. Soc. Am. J.*, **44**, 892-898.
- Van Straten, O. J. (1954): Water supply - south central Kalahari region. *Geol. Surv. Bechuanaland Prot., Annu. Rep.*, **1954**, 31-35.
- Van Straten, O. J. (1961): A note on the chemical composition of some ground waters from the Bechuanaland Protectorate. *Bechuanaland Prot., Rec. Geol. Surv.*, **1957/1958**, 24-35.
- Van Tonder, G. J. & Kirchner, J. (1990): Estimation of natural groundwater recharge in the Karoo aquifer of South Africa. *J. Hydrol.*, **121**, 395-419.

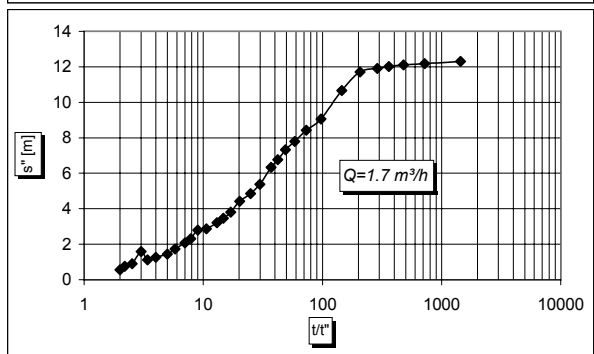
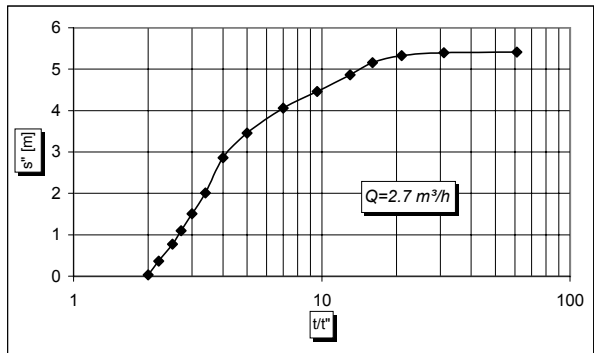
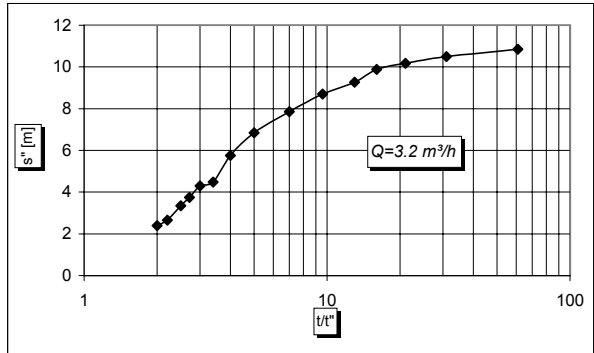
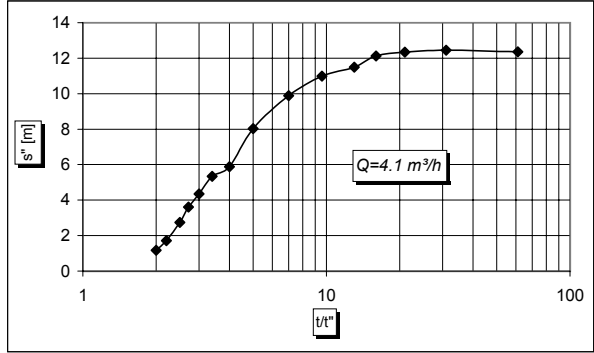
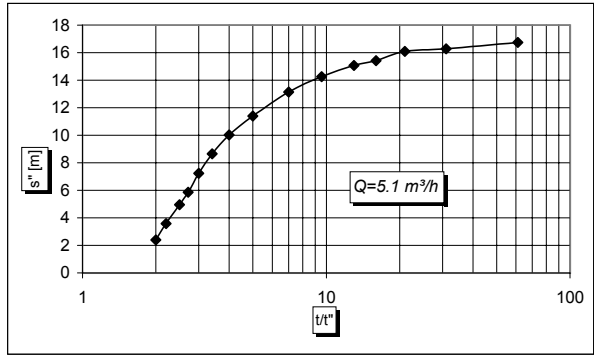
-
- Verhagen, B. T. (1988): Isotope hydrology of the Kalahari: Recharge or no recharge? *Palaeoecol. Africa*, **19**, 143-158.
- Verhagen, B. T. (1995): Semiarid zone groundwater mineralization processes as revealed by environmental isotope studies. In: *Application of tracers in arid zone hydrology* (Ed. E.M. Adar & C. Leibundgut), 245-266. IAHS Publ. 232.
- Vial, J. R. (1967): The southern extension of the East African Rift system and related igneous activity. *Geol. Rundschau*, **57**, 601-614.
- Vogel, J. C. & Van Urk, H. (1975): Isotopic composition of groundwater in semi-arid regions of southern Africa. *J. Hydrol.*, **25**, 23-36.
- Wackerle, R. (1996): Aeromagnetic interpretation map of northern and central Namibia. Geological Survey of Namibia, Ministry of Mines and Energy in cooperation with German Federal Institute for Geosciences and Natural Resources (BGR), Windhoek.
- Wanke, A. W. (2001): Karoo-Etendeka unconformities in NW Namibia and their tectonic implication. Ph.D. thesis, Universität Würzburg.
- Wanke, A., Stollhofen, H., Stanistreet, I. G. & Lorenz, V. (in press): Karoo unconformities in NW-Namibia and their tectonic implications. *Communs. Geol. Surv. Namibia*, **12**.
- Ward, J. H. (1963): Hierarchical grouping to optimize an objective function. *J. Am. Statist. Assoc.*, **58**, 236-244.
- Wasmund, P. (1930): Rieselfelder und Blattflächenabdrücke auf rezentem und fossilem Süßwasserflachstrand. *Senkenbergiana*, **12**, 139-151.
- White, F. (1983): *The vegetation of Africa*. Unesco, Paris.
- WHO (World Health Organization) (1985): Health hazards from nitrates in drinking water. Copenhagen, 102 pp.
- Withers, A. W. (1982): The interpretation of thermal infrared linescanner imagery as an aid to hydrogeological exploration in the north eastern sector of Hereroland, South West Africa/Namibia - The Gam survey area, pp. 31. DWA, Windhoek.
- WMO (World Meteorological Organisation) (1965): Guide to hydrometeorological practices. *WMO-No.*, **168**, 1-82.
- WMO (World Meteorological Organisation) (1966): Measurement and estimation of evaporation and evapotranspiration. *Techn. Notes* 83.
- Worthington, P. F. (1979): A preliminary appraisal of the groundwater resources of Hereroland, South West Africa, pp. 44. National Physical Research Laboratory, Pretoria.
- Wrabel, J. (1999): Ermittlung der Grundwasserneubildung im semiariden Bereich Namibias mittels der Chlorid-Bilanz-Methode. *HU-Forschungsergebnisse aus dem Bereich Hydrogeologie und Umwelt*, **16**, 1-155.
-

- Zausig, J. & Horn, R. (1992): Soil water relation and aeration of single soil aggregates, taken from a gleyic vertisol. *Z. Pflanzenernähr. Bodenk.*, **155**, 237-245.
- Zumsprekel, H. & Prinz, T. (2000): Computer-enhanced multispectral remote sensing data: A useful tool for the geological mapping of Archaean terrains in (semi)arid environments. *Computer and Geosciences*, **26**(1), 87-100.

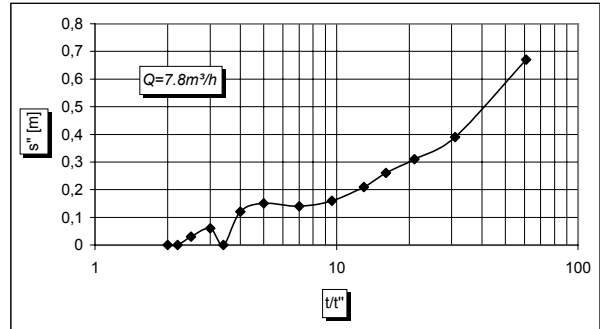
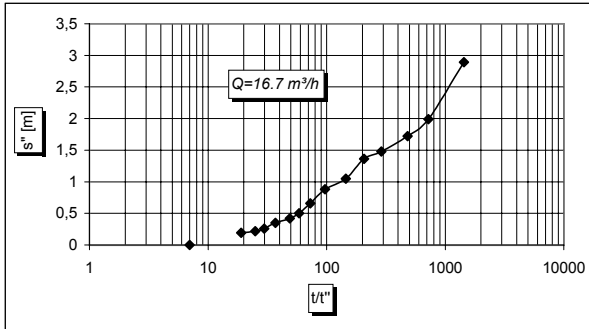
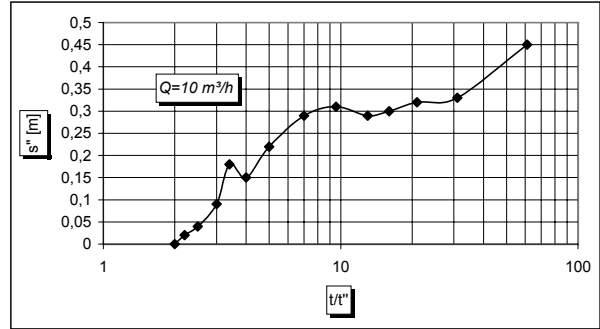
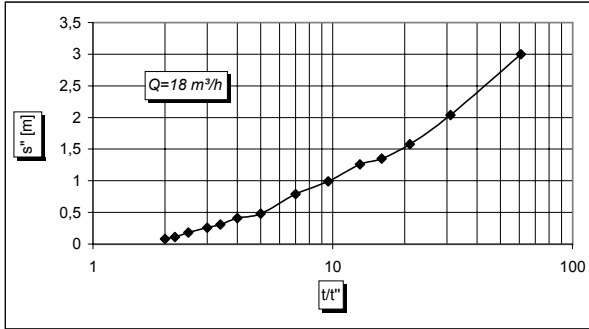
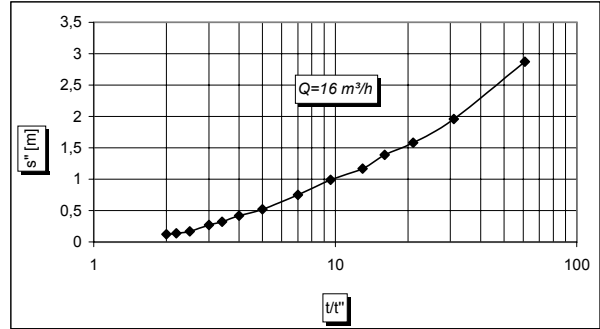
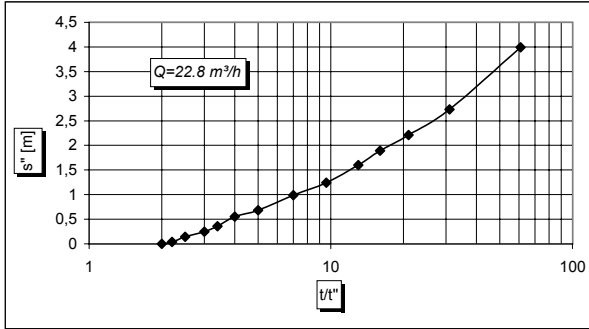
Otjahewita



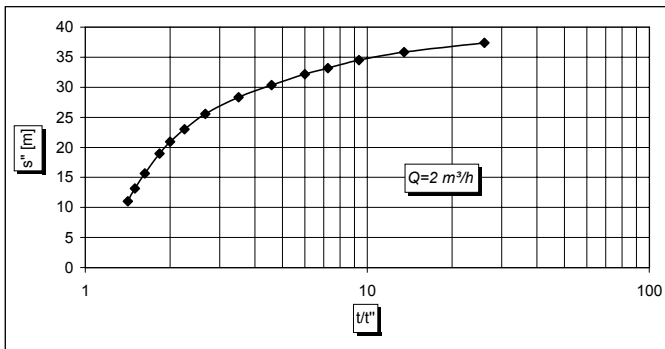
Ringklip



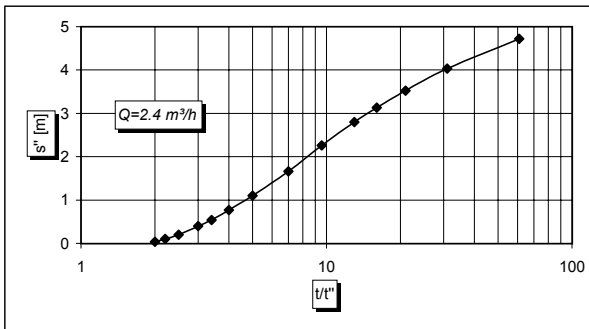
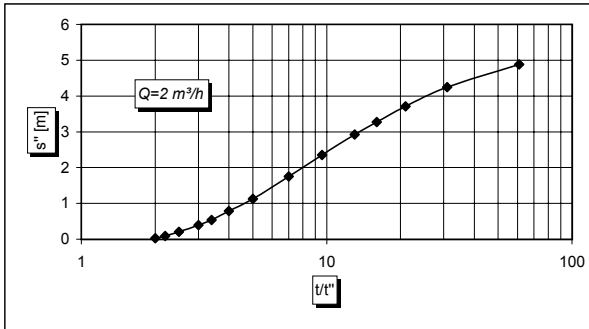
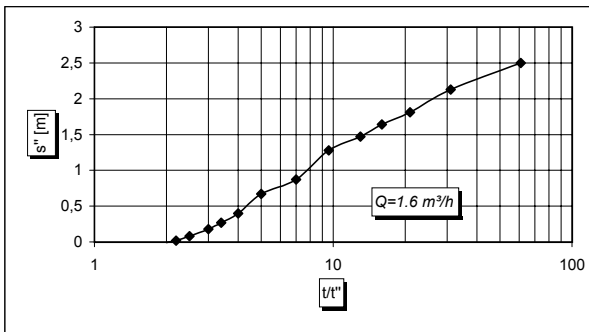
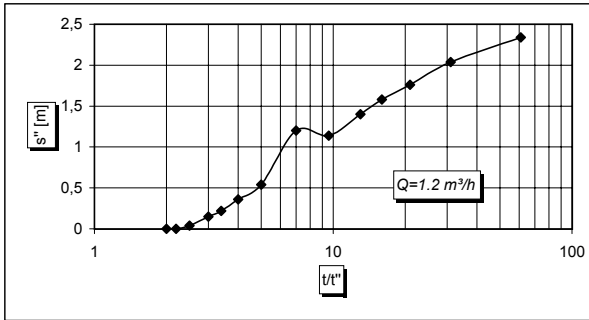
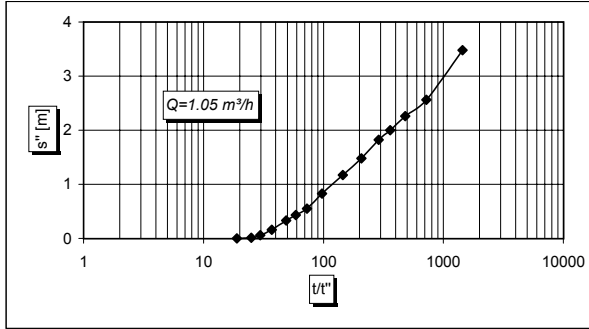
1819DD9



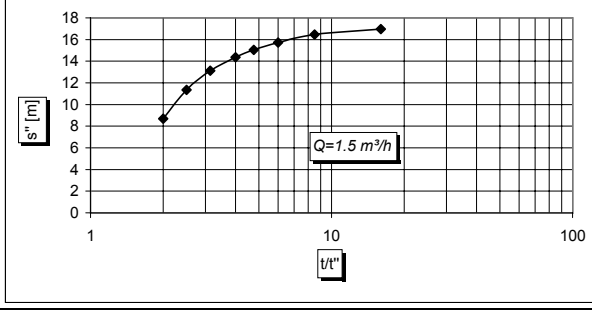
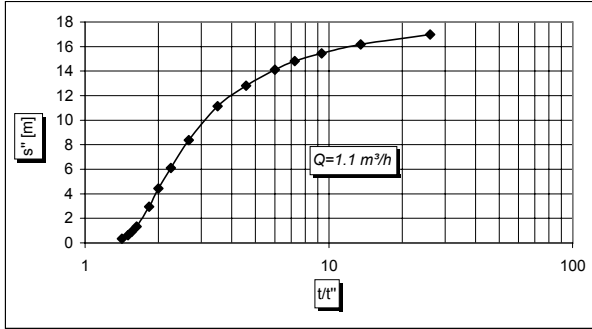
1820CB8



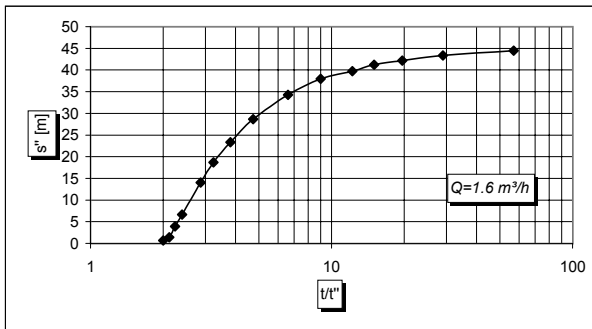
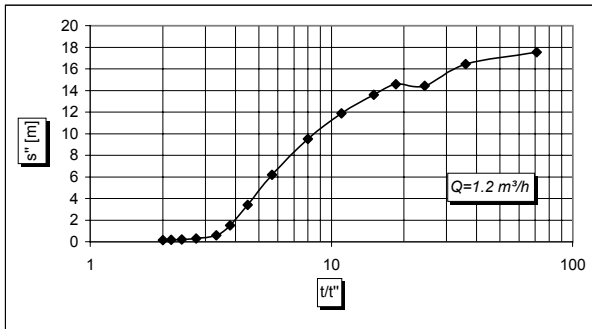
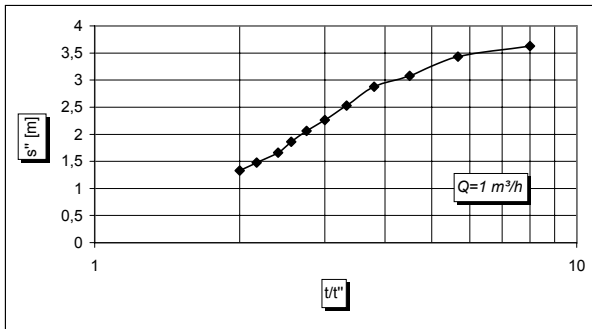
1820BC7



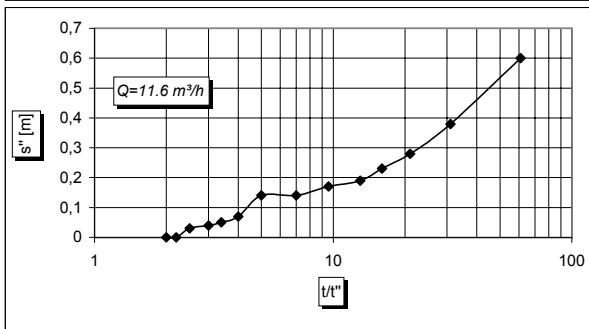
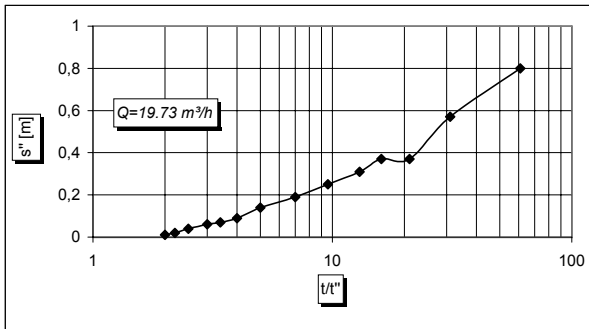
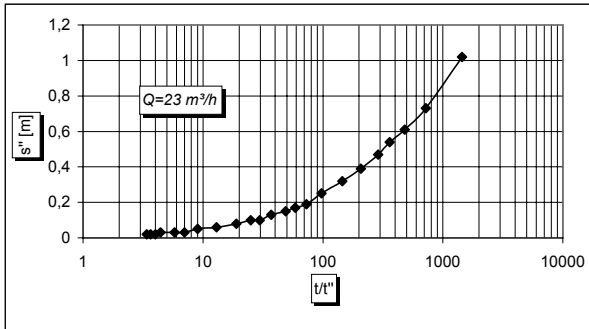
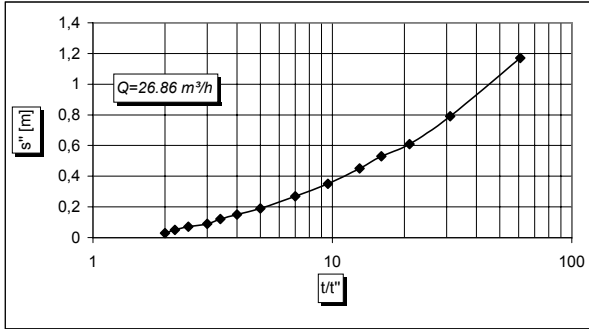
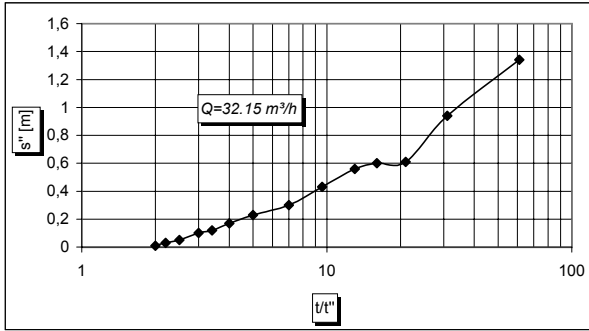
1820AC9



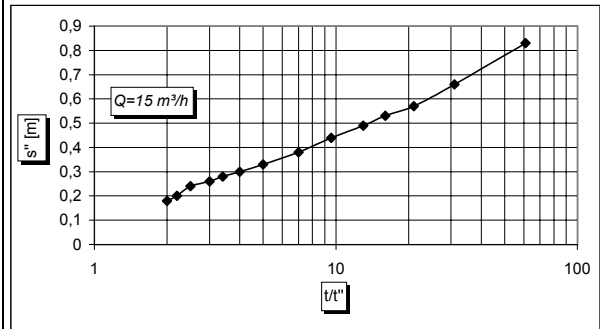
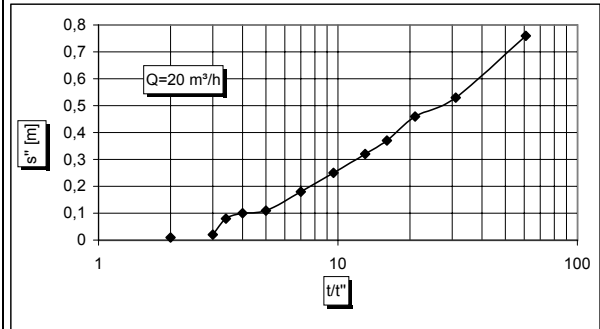
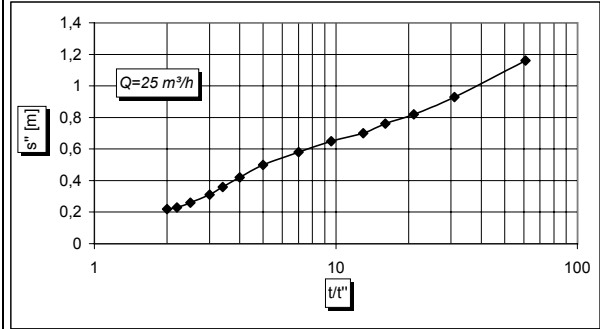
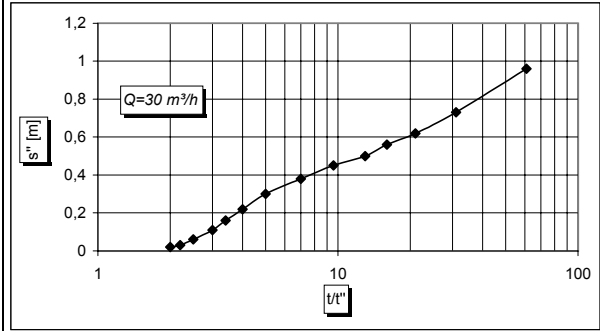
1820AA10



1820BC9



1819BA9



Pans & vleis

No	Longitude	-Latitude	Location	Remarks	Munsell-Colour	av. Kf	d10	d60	u	ctot	n	fine grain ratio
4-a	18,1667	-21,7333	near Steinhausen	dark with crumb structure		2,2E-06				4,61	0,76	
5-a	18,1667	-21,7333	near Steinhausen	dark with crumb structure		3,0E-06				6,59	0,89	
18-a	18,2896	-21,9242	along road 1643	sandy vlei	5YR4/4	4,7E-06	0,06	0,24	4,00	3,86	0,43	11,64
19-a	18,2896	-21,9243	along road 1643	prism to crumb structure, very dark grey, underneath 18-a	10YR2/2	3,1E-06				2,98	0,51	
20-a	18,2897	-21,9245	along road 1643	prism to crumb structure, very dark grey, underneath 18-a	10yr5/2	4,2E-06				5,57	0,69	
25-a	19,3521	-22,2776	along road 1602	grey, sticky vlei sediment	10yr6/2	8,5E-06	0,07	0,27	4,09	8,04	0,65	9,50
31-a	19,7668	-22,2151	along road 1692	with shrinkage cracks	10yr7/2	5,7E-06	0,05	0,28	6,22	1,96	0,42	16,07
42-a	17,4695	-20,6406	along road C22	only slight depression	5yr6/4	8,9E-06	0,09	0,41	4,66	1,55	0,51	4,42
44-a	17,5430	-20,6928	along road C22	dark vlei sediment	10yr4/2	1,3E-06	0,12	0,81	6,71	7,43	0,56	2,33
53-a				vlei sediment	5yr4/1	8,6E-06	0,12	0,41	3,42	3,09	0,63	3,81
76-a	18,2686	-19,5256	20 km east of Grootfontein	crumb structure, contains carbonate grains, brownish grey	5yr4/1	4,9E-07	0,08	0,30	3,85	8,14		6,81
79-a	18,0049	-20,2996	along road 3822, ca 35 km south of Goblenz	with surface crust	10yr4/2	1,1E-06	0,09	0,22	2,59	1,33		5,90
80-a	18,0049	-20,2996	along road 3822, ca 35 km south of Goblenz	similar to 79-a but no crusts	10yr4/2	4,1E-06	0,09	0,25	2,91	1,54		4,64
h-9	20,9958	-20,6291	Buffel Pan (Eiseb Block near the border)	from central part of the pan		4,6E-06	0,10	0,30	3,09	4,06	0,48	2,96
h-10	20,9958	-20,6291	Eiseb Block near the border	greyish pan sediment		9,3E-07	0,11	0,30	2,73	5,42	0,51	1,03
h-13	20,6976	-21,2079	Epukiro Valley	fine brown sand with shrinkage cracks		1,2E-06	0,11	0,29	2,64	1,63	0,53	3,21

Red to brown soils

No	Longitude	-Latitude	Location	Remarks	Munsell-Colour	av. Kf	d10	d60	u	ctot	n	fine grain ratio
1-a	18,2333	-21,8167	Steinhausen, near junction C29/C30	red soil, building aggregates		1,2E-05	0,08	0,29	3,77	1,98	0,44	6,29
2-a	18,2333	-21,8167	Steinhausen, near junction C29/C30	red soil, building aggregates		4,5E-05	0,07	0,28	3,84	1,99	0,44	7,56
3-a	18,2333	-21,8167	Steinhausen, near junction C29/C30	red soil, building aggregates		1,2E-05	0,08	0,22	2,82	1,61	0,41	6,53
35-a	17,5167	-21,6481	along road C31	brown soil, building small aggregates	5yr4/4	6,5E-06	0,08	0,38	4,94	2,04	0,53	7,78
36-a	17,9215	-21,1520	along road 2138	greyish-brownish soil	5yr4/4	9,0E-06	0,09	0,47	5,40	1,00	0,52	5,48
37-a	17,8962	-21,0227	along road 2138	yellowish-red soil	10yr5/4	8,4E-06	0,08	0,39	5,00	1,26	0,56	2,95
69-a			Makuri	very red soil	5yr3/4	8,0E-06	0,10	0,30	3,00	1,51		4,72
72-a	20,7324	-19,8283	road to Gam	red-brown soil with some surface crust	10yr4/4	3,6E-06	0,10	0,21	2,19	1,91		4,80

Aeolian sand

No	Longitude	-Latitude	Location	Remarks	Munsell-Colour	av. Kf	d10	d60	u	ctot	n	fine grain ratio
26-a	19,5593	-22,0089	along road 1825	orange-red dune	10yr7/5	7,2E-05	0,12	0,29	2,42	0,42	0,40	0,76
27-a	19,5593	-22,0089	along road 1825	red dune	10yr7/4	7,8E-05	0,11	0,28	2,67	0,34	0,39	2,08
30-a	19,6483	-22,2615	along road 1776	red dune	10yr5/4	3,0E-05	0,11	0,26	2,48	0,92	0,43	2,28
32-a	20,8797	-21,7976	along road 3814, east of Talismanis	red aeolian sand	10yr5/4	6,9E-05	0,11	0,22	2,00	0,51	0,36	1,55
33-a	20,0601	-21,8494	along road 1692, west of Talismanis	light yellow sand		6,4E-05	0,10	0,23	2,30	0,71	0,42	2,83
38-a	17,8509	-20,9721	along road 2454	red sand	10yr5/4	1,1E-05	0,10	0,31	3,20	0,78	0,53	3,52
39-a	17,8510	-20,9721	along road 2454	red sand	5yr5/4	2,2E-05	0,11	0,35	3,18	0,78	0,50	2,98
46-a	18,0645	-20,9124		dark-red sand	5yr4/4	1,4E-05	0,10	0,31	3,16	1,21	0,37	3,74
47-a	18,4799	-20,9894		red sand	10yr6/4	8,5E-05	0,16	0,42	2,63	0,59	0,33	1,53
48-a			along road 3806, ca 30 km away from Otjinene	red dune sand	5yr5/6	2,9E-05	0,11	0,35	3,18	1,06	0,35	3,14
54-a			near Omuramba Epukiro between Sturmfeld and Mission Station	red sand	5yr4/4	2,6E-05	0,11	0,36	3,27	0,91	0,54	2,64
63-a	18,7884	-19,2767	along road 2845	red dune sand from top of a dune	5yr5/4	1,0E-04	0,11	0,26	2,36	0,65		1,09
71-a	20,7268	-20,1599	road to Gam	dark-red sand	5yr5/4	1,2E-05	0,11	0,26	2,36	1,17	0,58	2,02
78-a	18,3705	-19,9973	along road 3822, ca 50 km south Grootfontein	yellowish-red sand	10yr7/2	2,7E-05	0,11	0,29	2,64	0,80	0,52	2,06
81-a	17,7143	-20,4900	along road 3822, 10 km northeast of Otumborombonga	red sand	10yr5/4	3,9E-05	0,09	0,25	2,72	0,81	0,51	3,46

continued: Aeolian sand

No	Longitude	-Latitude	Location	Remarks	Munsell-Colour	av. Kf	d10	d60	u	ctot	n	fine grain ratio
h-1	21,6696	-18,1158	along the Okavango between Popa Falls and border	light yellow sand		3,1E-05	0,11	0,19	1,73	1,04	0,42	0,77
h-11	20,9986	-20,8366	north of the Epukiro, border trackan der Grenze, nördlich des Epukiro	red sand from dune top		6,8E-05	0,11	0,27	2,45	0,74	0,38	1,12
h-14	20,5284	-21,5225	Epukiro Valley	red sand		9,6E-05	0,12	0,28	2,33	0,75	0,37	1,31
h-2	21,4006	-18,0744		greyish sand		6,9E-05	0,11	0,29	2,64	0,97	0,36	1,54
h-3	20,7727	-18,0531	turn-off to Kaudum National Park from Okavango side	grey, slightly reddish sand		1,3E-04	0,13	0,29	2,23	0,73	0,39	1,10
h-4	18,7068	-19,0386	Farm Ontevrede	greyish to light-pink sand		6,0E-05	0,11	0,33	3,00	0,48	0,37	1,41
h-8			Eiseb Block near the border	light-greyish sand		3,5E-05	0,10	0,26	2,71	0,77	0,37	3,14

Soils with some aeolian influence

No	Longitude	-Latitude	Location	Remarks	Munsell-Colour	av. Kf	d10	d60	u	ctot	n	fine grain ratio
6-a	17,8667	-21,7333	along the road 2170, near the junction with road 2166	sand		4,6E-05	0,07	0,25	3,85	1,55	0,43	9,50
7-a	17,8500	-21,7333	along the road 2170, ca 1 km from the junction with road 2166	sand		1,2E-05	0,08	0,33	4,07	1,35	0,39	1,82
8-a	19,0167	-22,1667	between Gobabis and Drimiopsis	sand	10yr5/4	4,2E-05	0,09	0,29	3,15	1,07	0,37	4,45
9-a	19,0167	-22,1667	between Gobabis and Drimiopsis	sand		8,7E-05	0,10	0,30	3,03	0,95	0,40	3,30
10-a	19,0167	-22,1667	between Gobabis and Drimiopsis	sand		7,6E-05	0,10	0,30	3,06	0,82	0,41	2,97
11-a	19,0333	-22,0667	2 km from Drimiopsis	sand		4,7E-05	0,10	0,26	2,65	0,68	0,37	3,53
12-a	19,0333	-22,0667	200 m west of 11-a	sand		1,4E-05	0,09	0,28	3,26	1,24	0,40	5,32
13-a	18,8500	-21,9833	near junction of roads 1667 und 1636	fine grined red sand	5yr4/4	3,7E-05	0,10	0,30	3,09	1,43	0,39	3,64
14-a	17,3500	-21,0167	along the road C36, ca 1.5 km southeast of the junction with road 2404		5yr4/4	4,5E-05	0,09	0,33	3,67	1,58	0,46	4,63

continued: Soils with some aeolian influence

No	Longitude	-Latitude	Location	Remarks	Munsell-Colour	av. Kf	d10	d60	u	ctot	n	fine grain ratio
15-a	17,2667	-21,2500	along road 2216, distrikt boarder Otjiwarongo-Okahandja		10yr3/4	2,7E-05	0,09	0,29	3,37	0,87	0,38	4,66
16-a	17,7333	-21,9500	along road MR53, 10 km north of sample S8		5yr3/4	1,5E-05	0,08	0,30	3,70	2,49	0,47	5,46
17-a	18,0000	-21,8000	along road MR 53		5yr3/4	3,7E-05	0,09	0,38	4,42	2,09	0,43	5,28
21-a			near junction of roads 1643 and 1639	grey, slightly reddish sand	10yr4/2	1,6E-05	0,09	0,28	3,18	1,90	0,46	4,99
22-a			along 1670, ca 7 km from crossing with road 1825	red sand	5yr4/4	3,2E-05	0,10	0,28	2,89	0,83	0,39	3,55
23-a	19,3030	-21,8031	along road 1668		10yr3/2	3,0E-05	0,10	0,28	2,80	1,81	0,45	3,84
24-a	19,1306	-21,6118		brown sand	5yr3/4	4,1E-05	0,10	0,28	2,89	1,21	0,42	2,64
28-a	19,9937	-21,5761	along road 1830	light sand	10yr7/4	8,1E-05	0,11	0,29	2,64	0,58	0,36	2,36
29-a	19,3776	-21,4035	between Omawewozonyand and Otyjarwa	yellowish-red sand	10yr6/4	8,5E-05	0,11	0,33	3,14	0,91	0,38	3,18
40-a	17,6853	-20,9272	along road 2454	greyish-brown sand	10yr4/2	1,3E-05	0,09	0,25	2,94	2,82	0,56	5,00
41-a	17,4957	-20,8132	along road 2454	nonuniformous yellowish-brown sand	10yr4/2	1,9E-05	0,11	0,44	4,00	0,95	0,56	1,76
43-a	17,4699	-20,6516	1 km from 42-a uphill		5yr5/6	1,4E-05	0,10	0,31	3,26	1,55	0,55	3,84
45-a	17,5430	-20,6929	Grube	greyish sand with some smal aggregates	10yr6/2		0,13	0,65	5,00	1,53		1,61
49-a	18,9260	-21,2149	along road 3806, ca 25 km away from Otjinene		10yr4/4	2,4E-05	0,10	0,29	2,99	1,20	0,37	4,25

continued: Soils with some aeolian influence

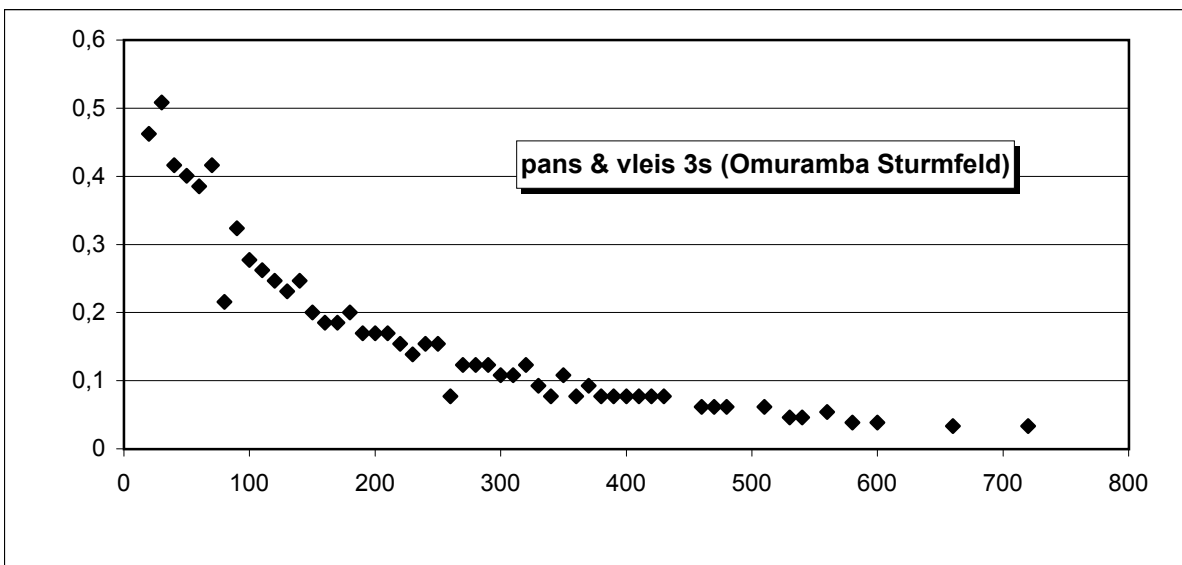
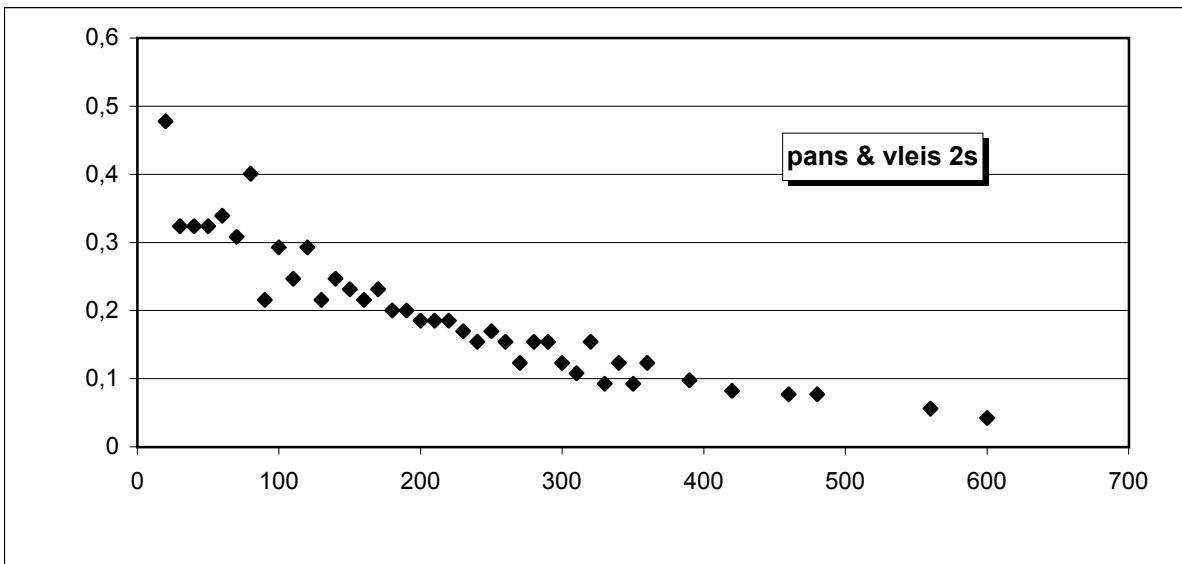
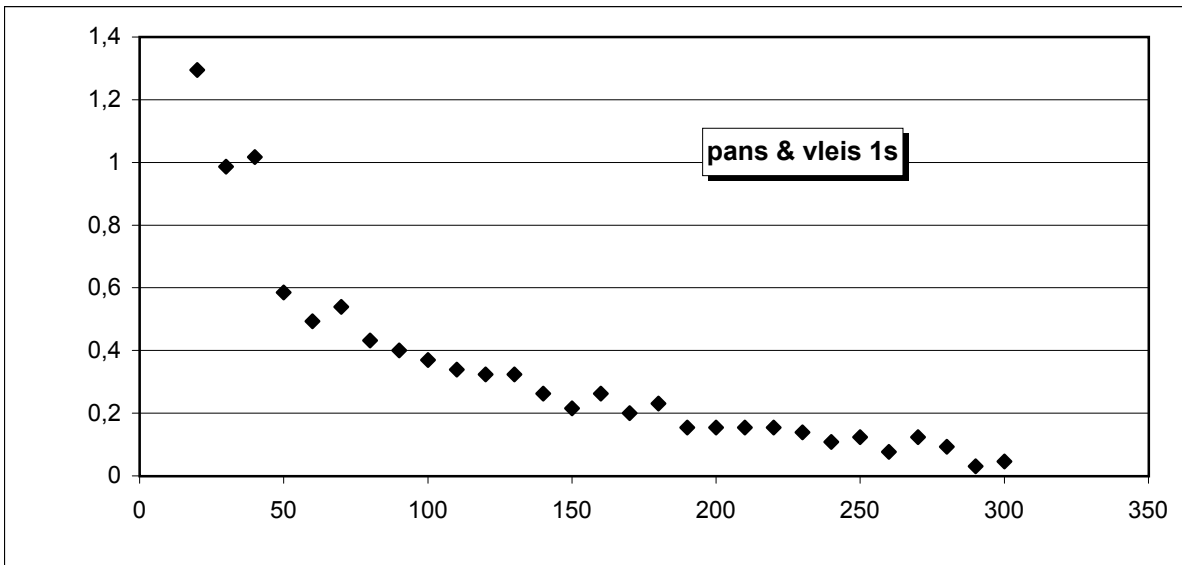
No	Longitude	-Latitude	Location	Remarks	Munsell-Colour	av. Kf	d10	d60	u	ctot	n	fine grain ratio
50-a	18,6926	-21,2632	between Otjinene and Summerdown	fine grained red sand	5yr5/4	2,7E-05	0,10	0,33	3,44	1,20	0,35	3,97
51-a			along road 1663, ca 17 km from Witvley	fine grined red sand with a thin crust under some sand cover	10r4/3	1,0E-05	0,07	0,29	3,92	1,96	0,53	7,58
52-a			Farm Sturmfeld	dark-bown sand	10yr4/2	1,7E-05	0,09	0,29	3,15	0,98	0,57	4,41
56-a	17,6286	-20,5869	20 km west of Okakarara along road 3805			2,5E-05	0,10	0,27	2,70	0,67		3,22
57-a	18,5262	-20,5944	along road 3805, ca 63 km east of Okakarara	light coloured, well sorted sand	10yr7/4	3,4E-05	0,11	0,28	2,67	0,47	0,51	3,06
58-a	18,3770	-20,5887	ca 100 km east Okakarara along road 3805	light fine grained sand	10yr7/4	1,2E-05	0,11	0,29	2,76	0,78		0,45
59-a	18,5262	-20,2168	along road 3805	fine-grained sand	10yr5/4	1,6E-05	0,11	0,29	2,64	1,15	0,50	2,44
60-a	18,5965	-19,8862	along road 3805	red fine-grained sand		1,0E-05					0,55	
61-a	18,5484	-19,5683	between Grootfontein and Otjituuo	light-grey, well sorted sand, with some red-brown small aggregates, lying on top of a dark fine grined sand	10yr5/2	1,7E-05	0,12	0,29	2,42	0,79	0,55	0,55
62-a	18,7943	-19,2886	along raod 2845	grey sand with a dark surface crust and some sand cover	10yr5/2	1,8E-05	0,08	0,29	3,67	3,76	0,70	6,75
64-a	19,2439	-19,3915	track towards Omatako village	red sand	5yr5/6	7,8E-06	0,12	0,35	2,92	0,85	0,51	1,25
65-a	19,2985	-19,4517	track towards Omatako village	grey sand	10yr6/2	8,7E-06	0,09	0,29	3,37	1,20	0,57	4,48
66-a	19,4799	-19,3666	along C44, ca 20 km eastof the Omatako Valley	grey sand	10yr6/2	3,2E-05	0,13	0,33	2,54	0,82	0,46	1,28

continued: Soils with some aeolian influence

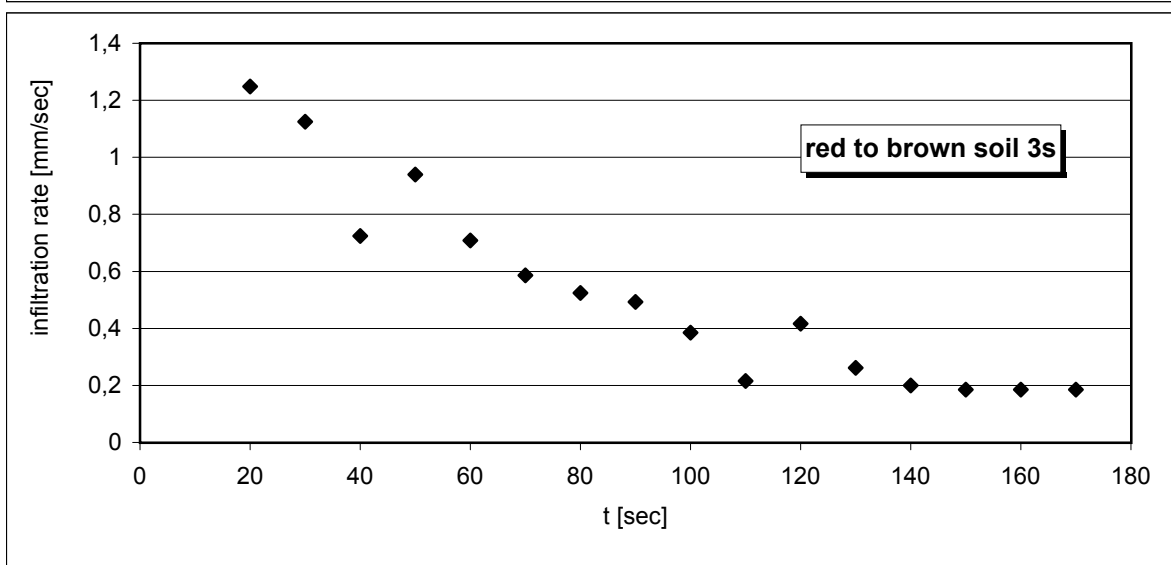
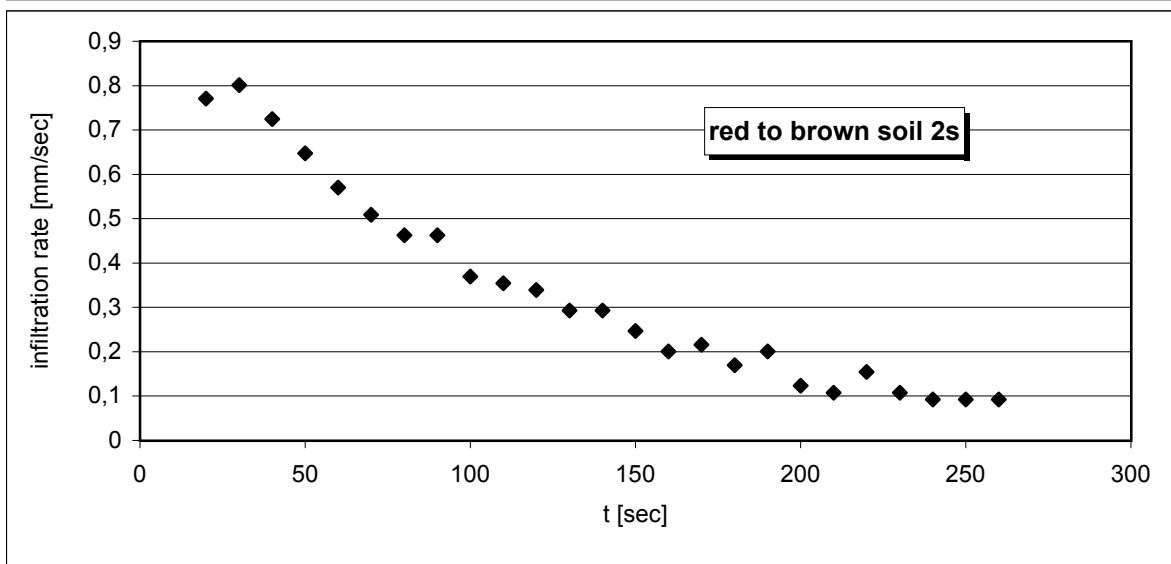
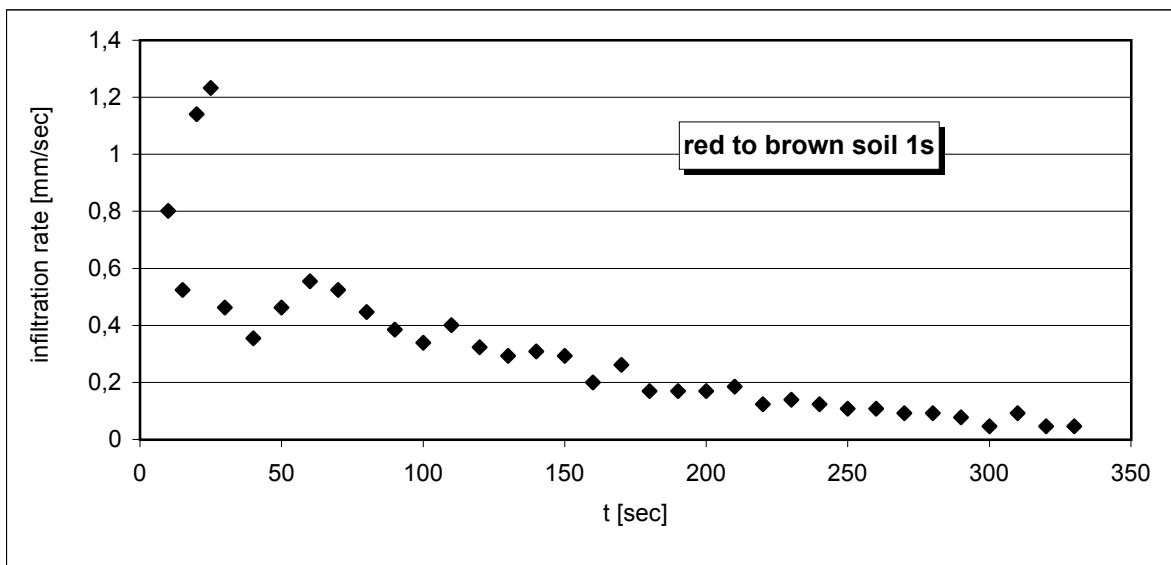
No	Longitude	-Latitude	Location	Remarks	Munsell-Colour	av. Kf	d10	d60	u	ctot	n	fine grain ratio
67-a	20,1130	-19,6031	along road 3301, ca 10 km south of road C44	very light grey sand	10yr7/2	6,1E-05	0,14	0,29	2,07	0,41		0,37
68-a	20,1130	-19,6031	along road 3301, ca 10 km south of road C44	light fine-grined sand	5yr6/4	7,3E-05	0,11	0,25	2,27	0,53		1,48
70-a	20,7533	-20,1965	road to Gam	darkgrey sand	5yr3/2	1,7E-05	0,11	0,26	2,36	1,54	0,67	2,69
73-a	20,4584	-19,5888	road to Tsumkwe	grey sand, building saml aggreagtes in the lower part	10yr4/2	2,0E-05	0,11	0,24	2,18	0,86	0,54	2,62
74-a	20,4584	-19,5888	road to Tsumkwe	grey fine-grained sand	10yr4/2	6,3E-05	0,11	0,24	2,18	0,95		1,46
75-a	20,1616	-19,5228	road to Tsumkwe	gryish-brown sand, building few small aggregates	10yr5/2	6,3E-05	0,11	0,25	2,27	0,67		
77-a	18,5107	-19,7422	along road 3822, ca 15 km south Grootfontein		10yr5/4	4,6E-05	0,11	0,31	2,82	0,92		2,06
h-5	20,0665	-20,6478	Eiseb Valley	brownish sand		8,5E-05	0,11	0,29	2,64	1,05	0,43	2,46
h-6	20,0665	-20,6478	Eiseb Valley	brownish sand		3,7E-05	0,11	0,29	2,64	0,43	0,42	1,69
H-7	20,9504	-20,5616	Eiseb Block near the border	light colourd sand with thin surface crustes		4,6E-05	0,12	0,29	2,52	1,06	0,40	2,81
h-12	20,8584	-20,9605		darkgrey sand		3,3E-05	0,15	0,35	2,33	2,34	0,42	1,45

infiltration test no	(ref-no)	parameters used for fit to GA-model		
		k_{rw} cm/s	he cm	$\theta-\theta_i$
pan 1a	3-1	3,00E-03	125	0,2
pan 2a	3-2	1,80E-03	280	0,2
pan 3a	3-8	1,00E-02	30	0,2
red to brown soil 1a	2-th-41	1,60E-02	12	0,18
red to brown soil 2a	3-9	1,60E-02	16	0,25
red to brown soil 3a	3-10	8,00E-03	10	0,19
red to brown soil 4a	3-11	1,90E-02	12	0,28
red to brown soil 5a	3-15	1,70E-02	28	0,11
red to brown soil 6a	3-16	1,90E-02	18	0,24
red to brown soil 7a	3-17	1,20E-02	8	0,18
red to brown soil 8a	3-18	3,30E-03	8	0,12
red to brown soil 9a	3-21	7,50E-03	8	0,24
red to brown soil 10a	3-22	1,00E-03	32	0,4
red to brown soil 11a	3-23	2,80E-03	12	0,4
aeolian 1a	2-h-18	1,00E-02	12	0,1
aeolian 2a	2-th-39	9,50E-03	10	0,17
aeolian 3a	2-th-40	1,50E-02	10	0,11
aeolian 4a	3-3	1,70E-02	13	0,25
aeolian 5a	3-4	1,20E-02	22	0,11
aeolian 6a	3-5	5,50E-02	8	0,22
aeolian 7a	3-13	3,00E-02	18	0,24
aeolian 8a	3-14	1,90E-02	12	0,08
aeolian 9a	3-19	3,30E-02	12	0,1
aeolian 10a	3-20	3,10E-02	8	0,14
soil with aeolian influence 1a	3-7	3,80E-02	16	0,2
soil with aeolian influence 2a	2-th-26	8,00E-03	12	0,12
soil with aeolian influence 3a	2-th-56	9,00E-03	8	0,24

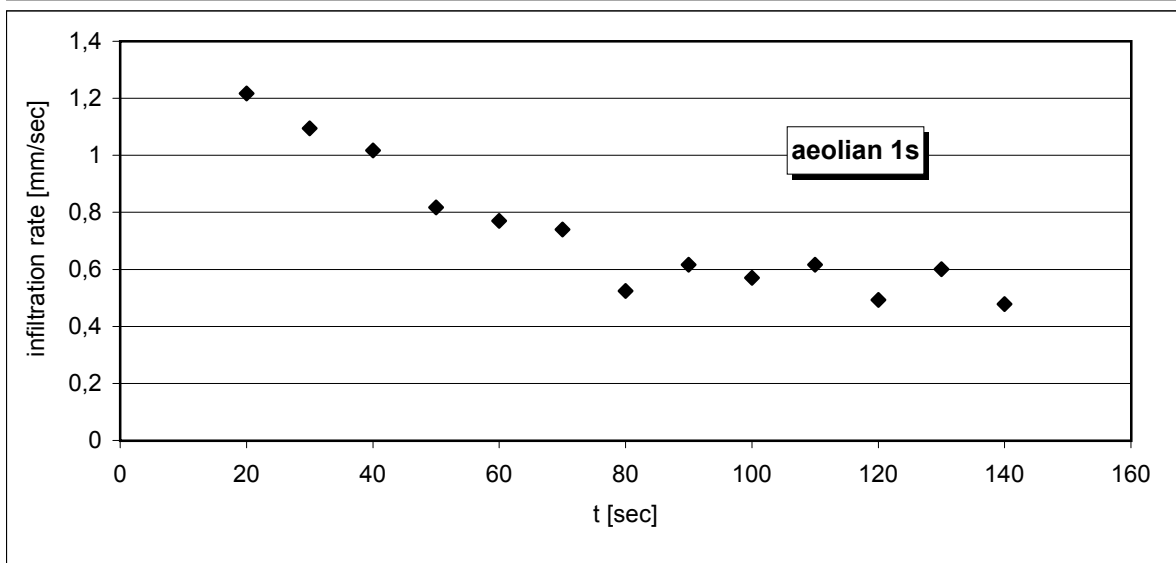
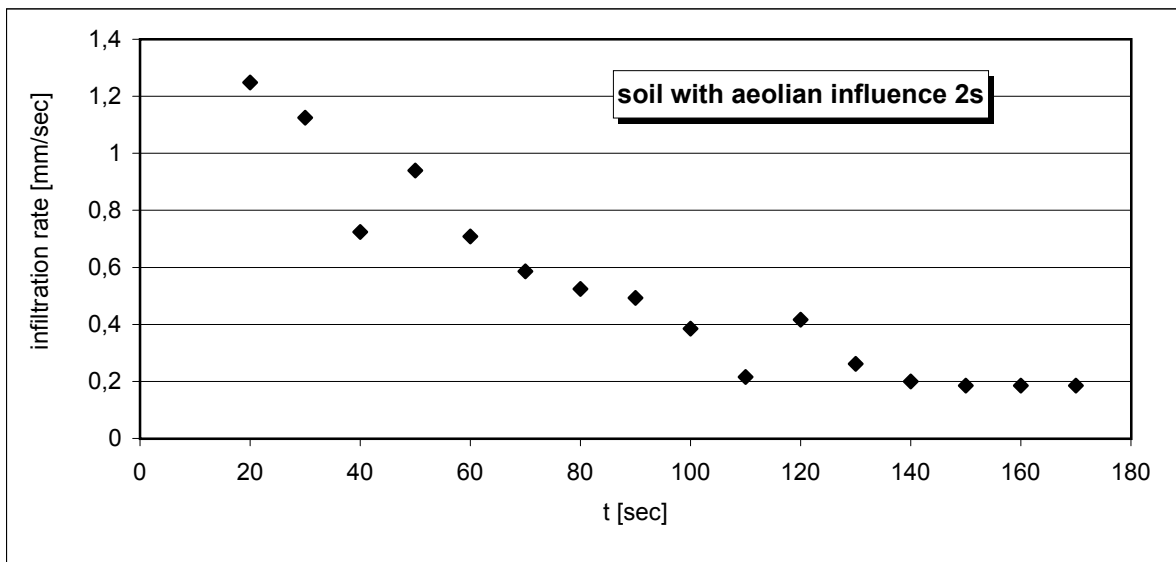
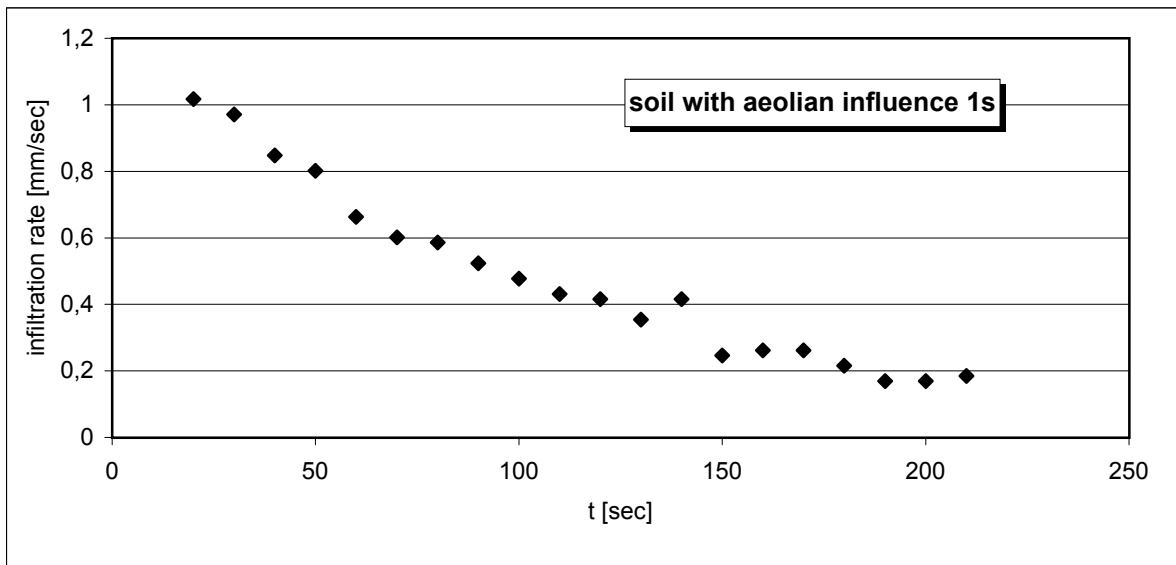
infiltration with continuous ponded height



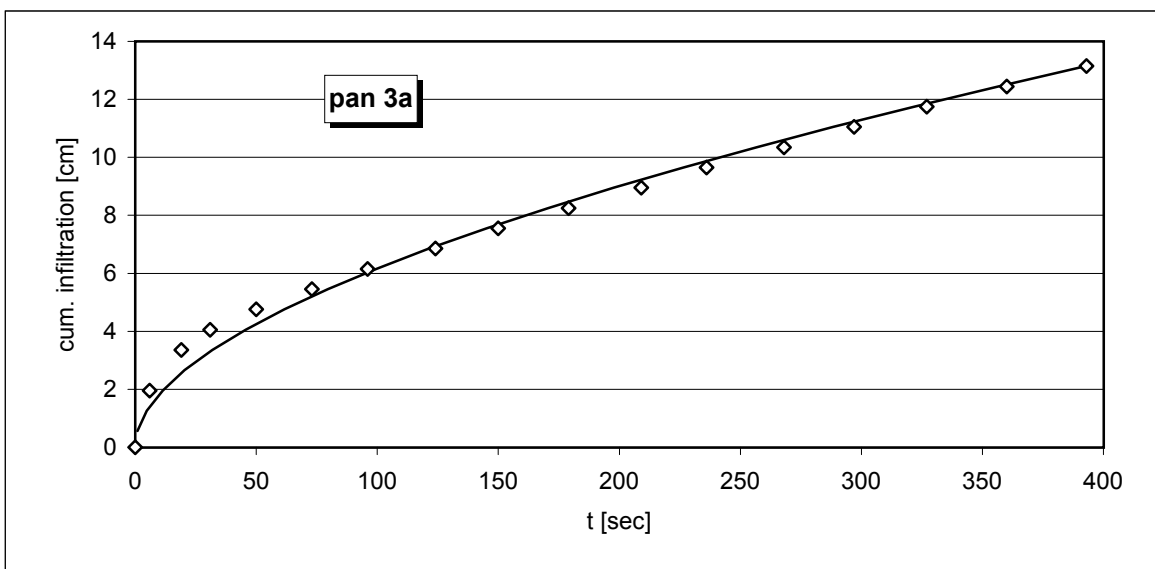
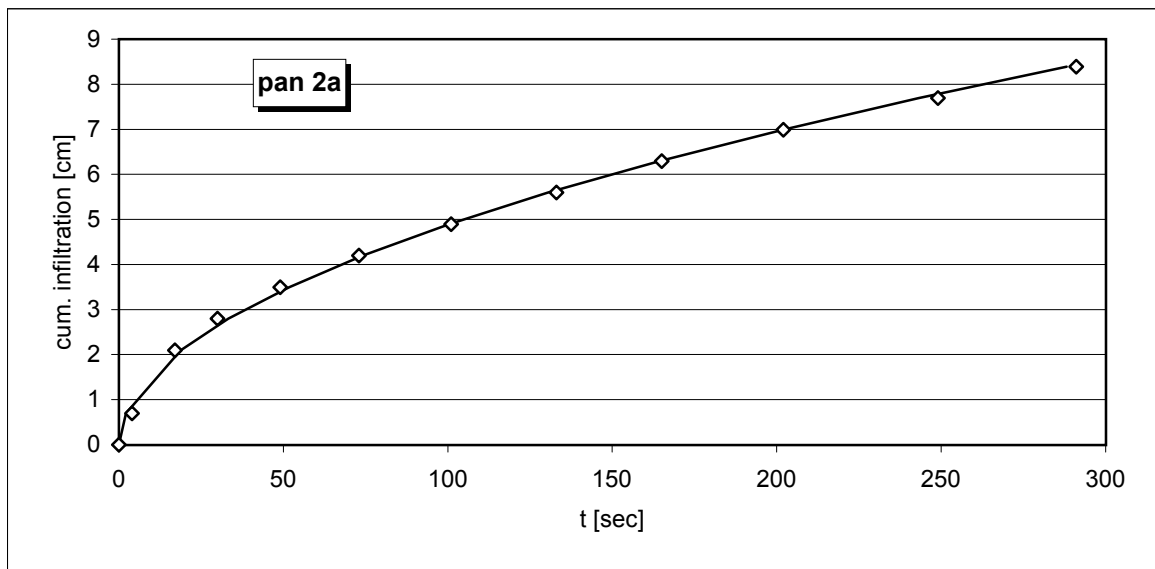
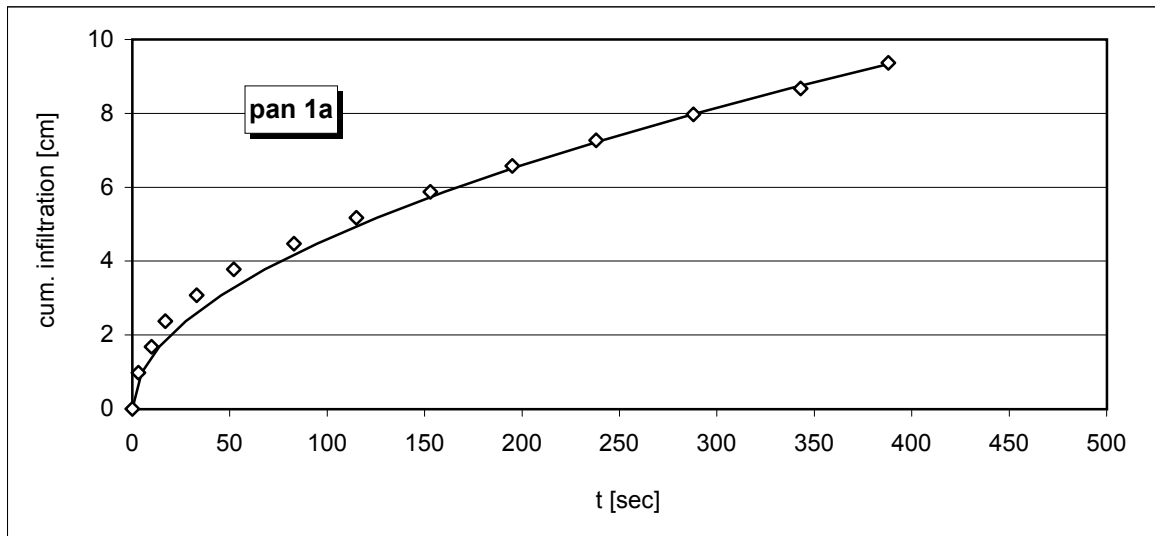
continued: infiltration with continuous ponded height



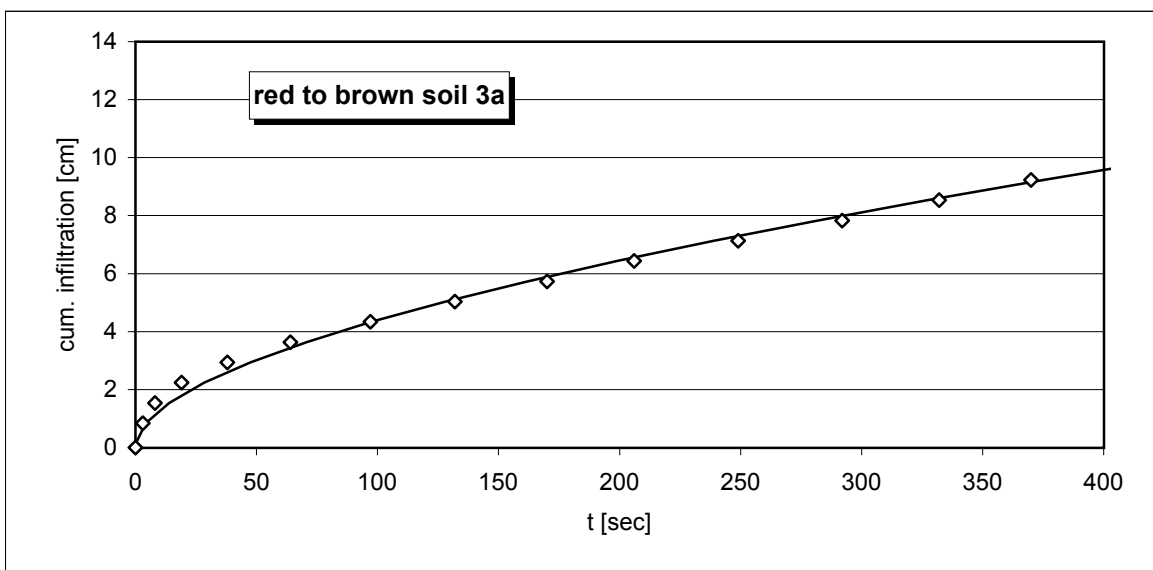
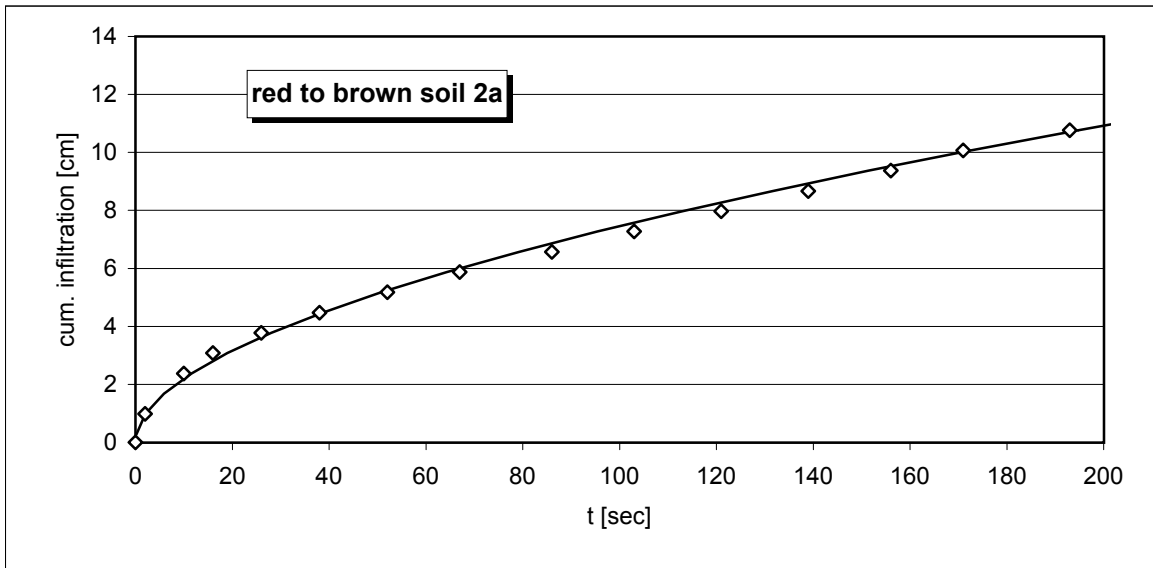
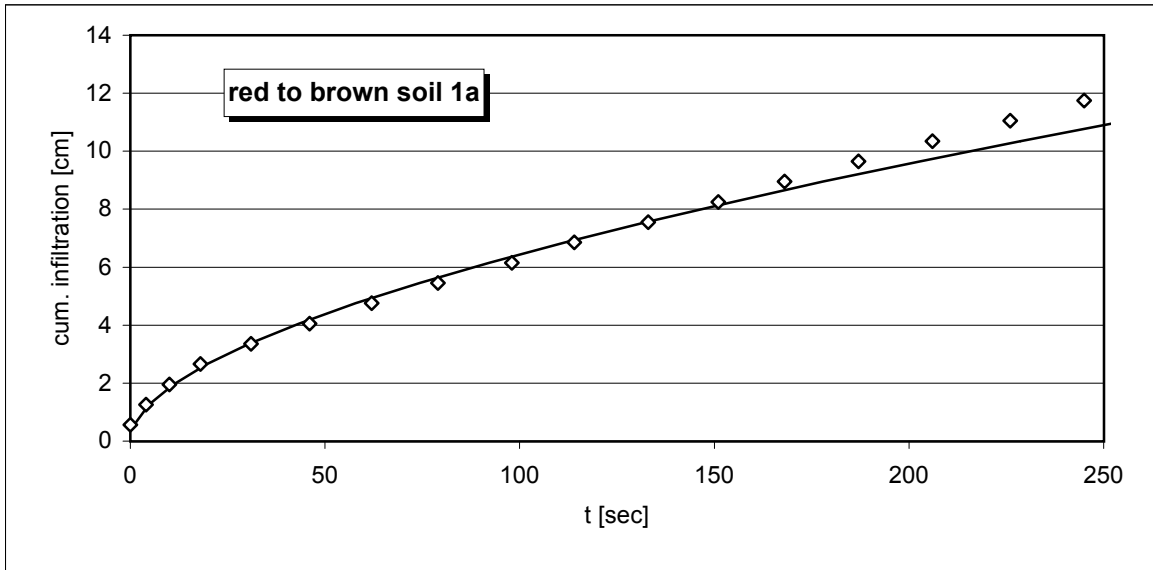
continued: infiltration with continuous ponded height



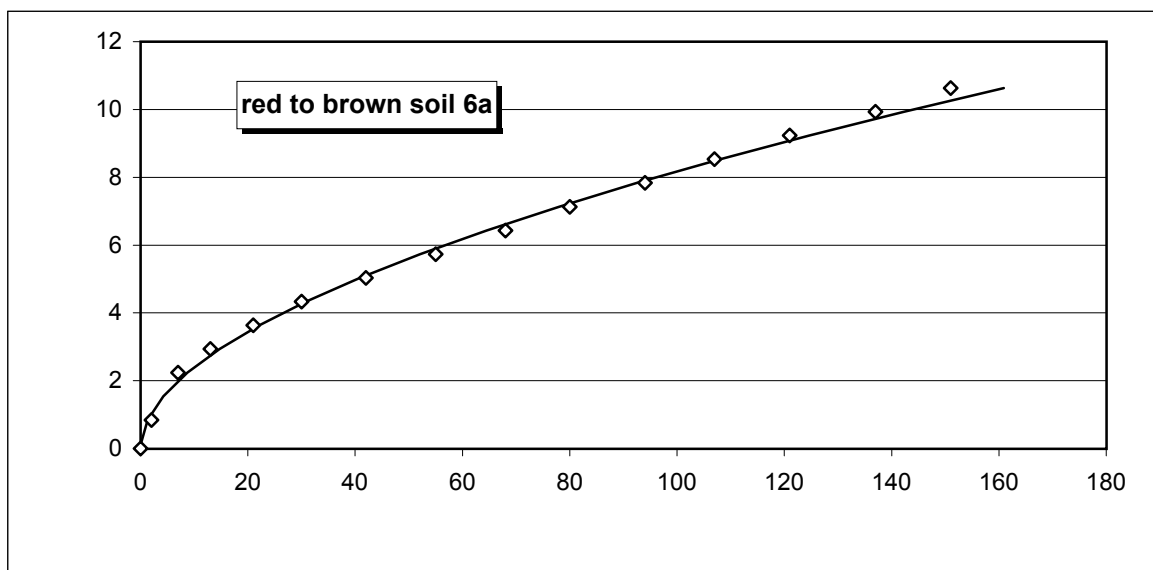
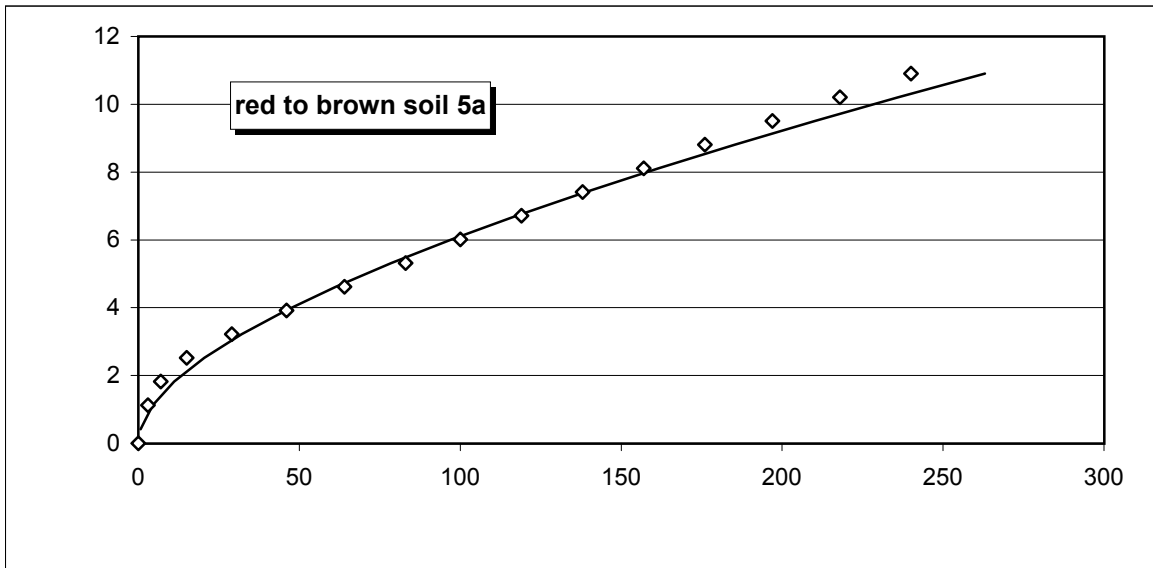
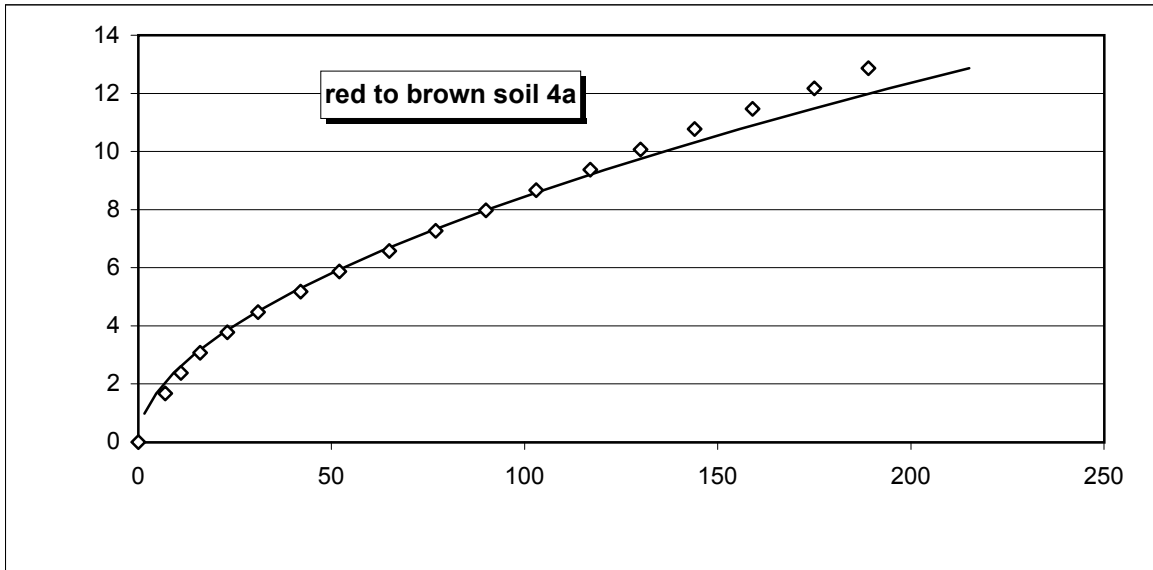
infiltration with falling head permeameter



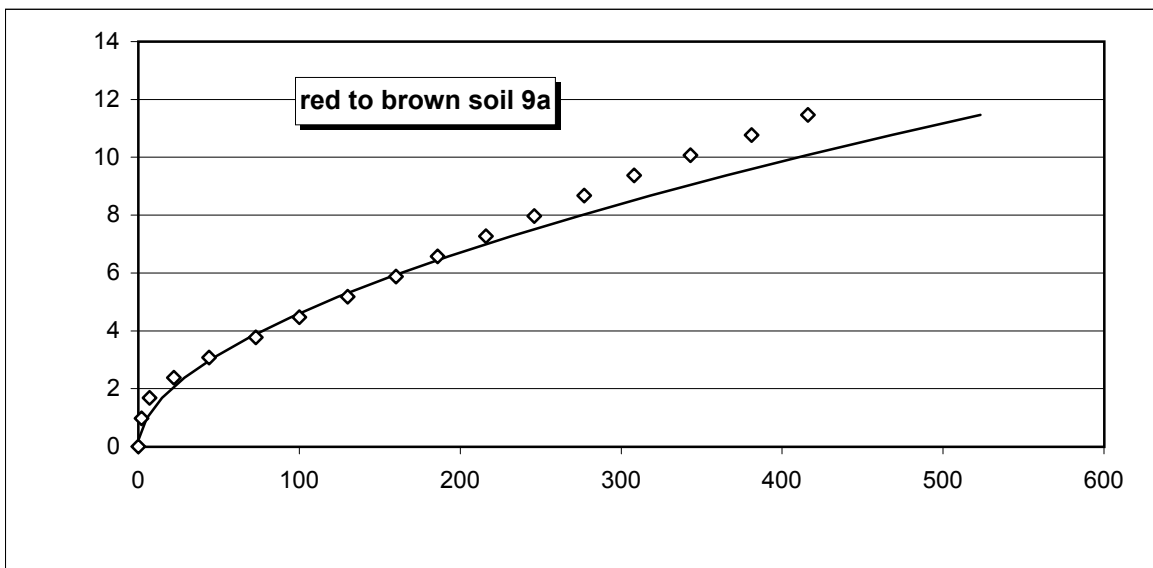
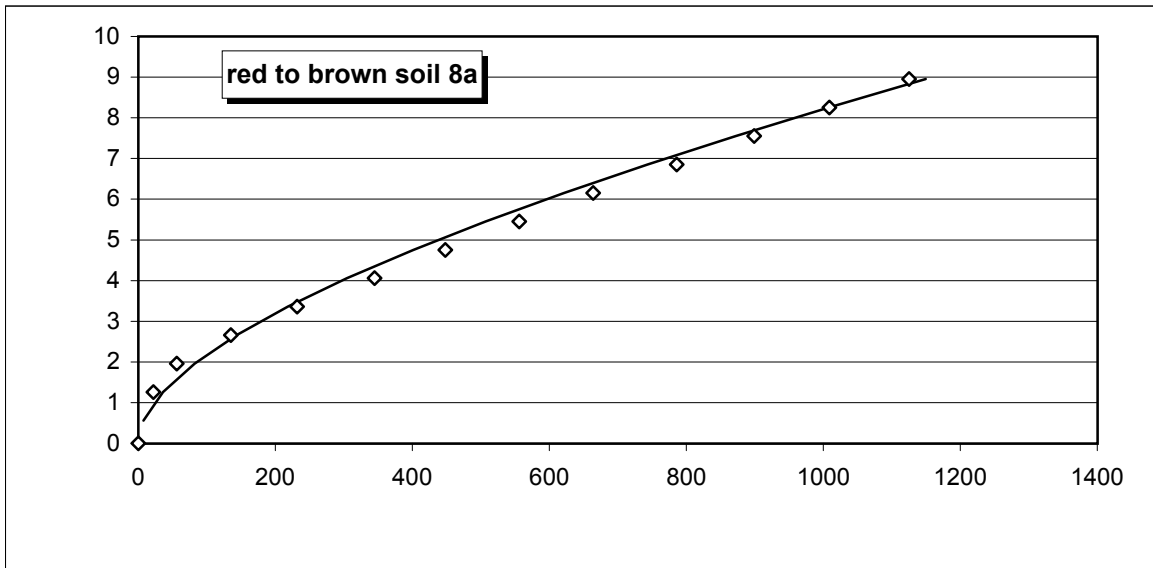
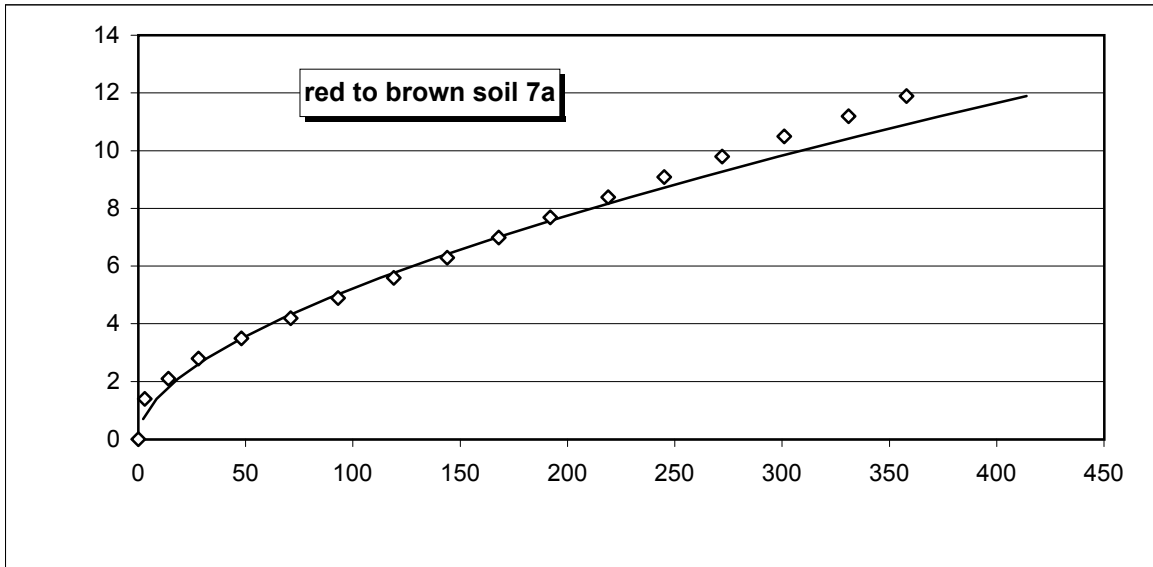
continued: infiltration with falling head permeameter



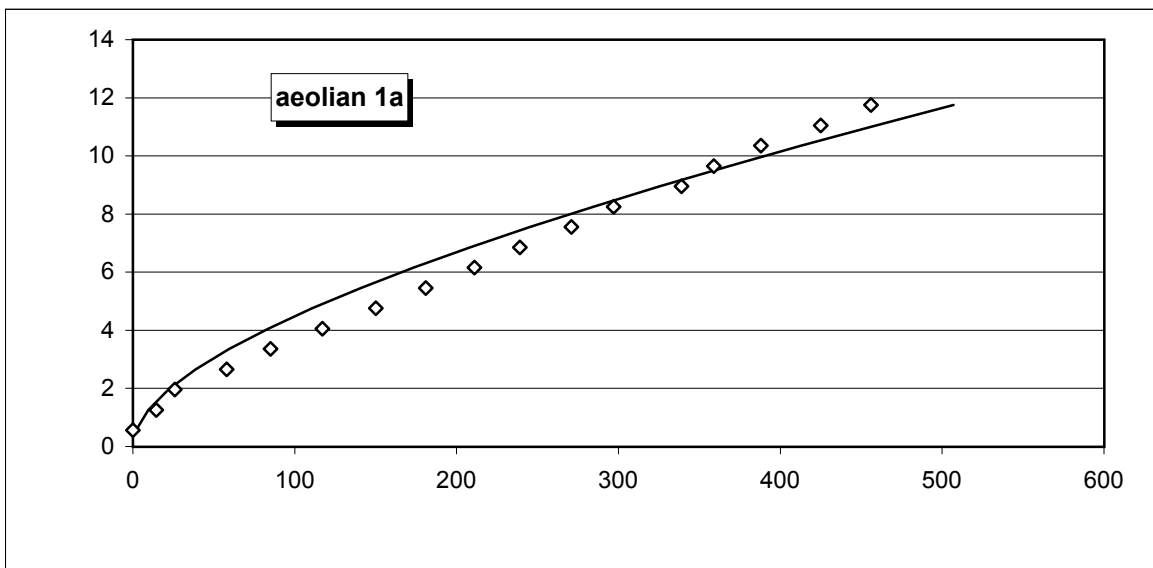
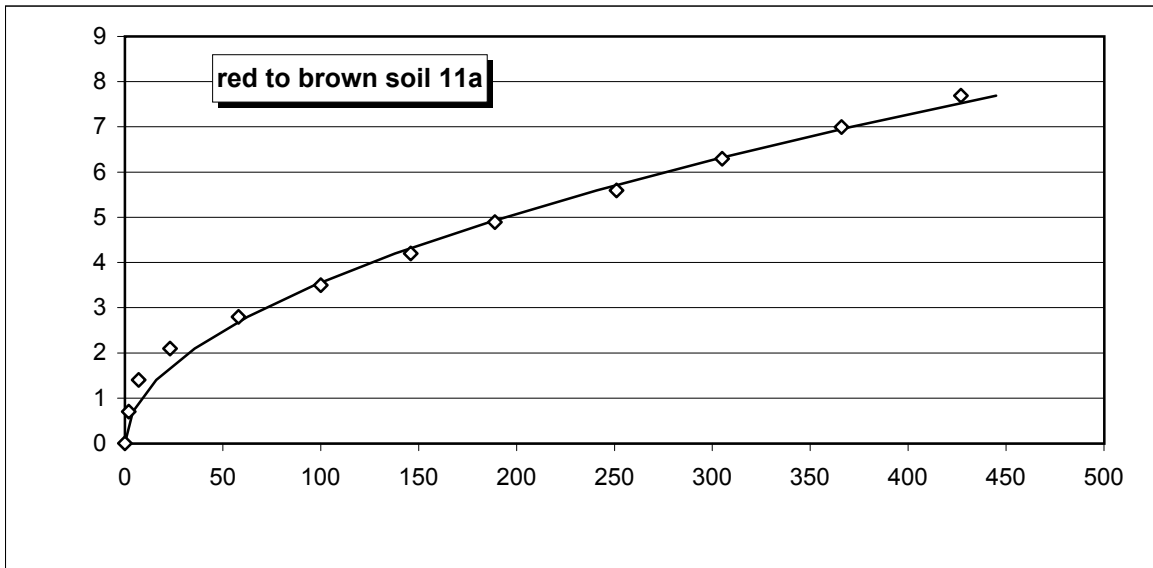
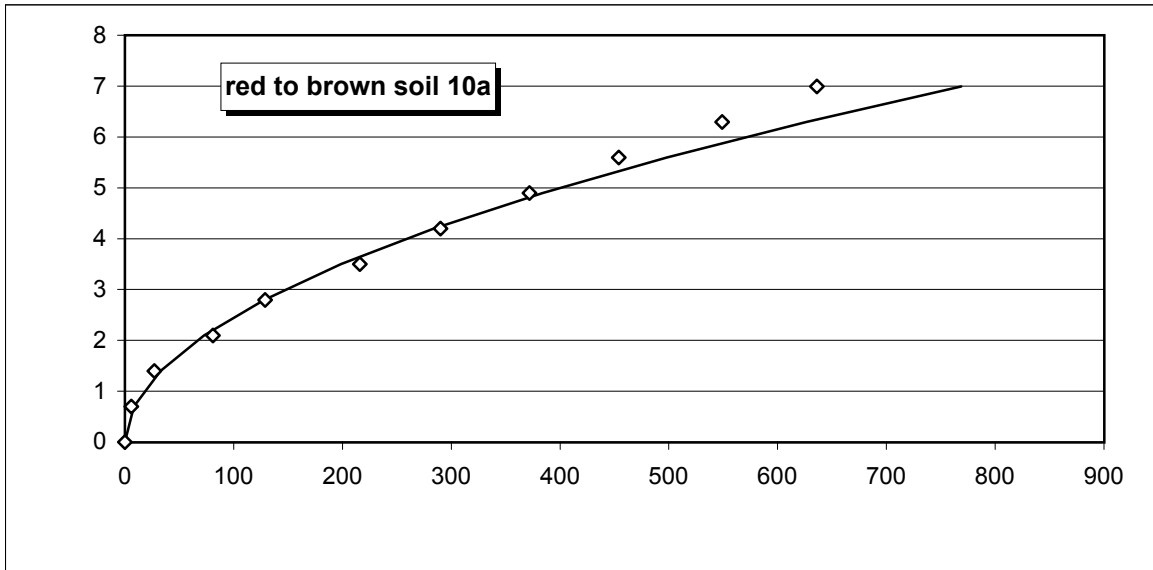
continued: infiltration with falling head permeameter



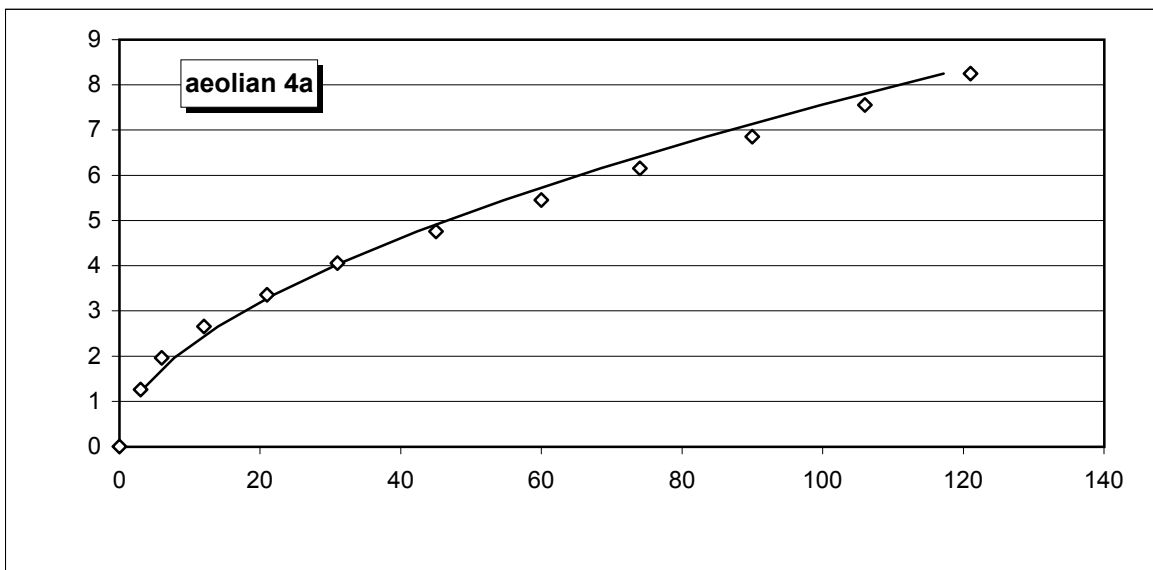
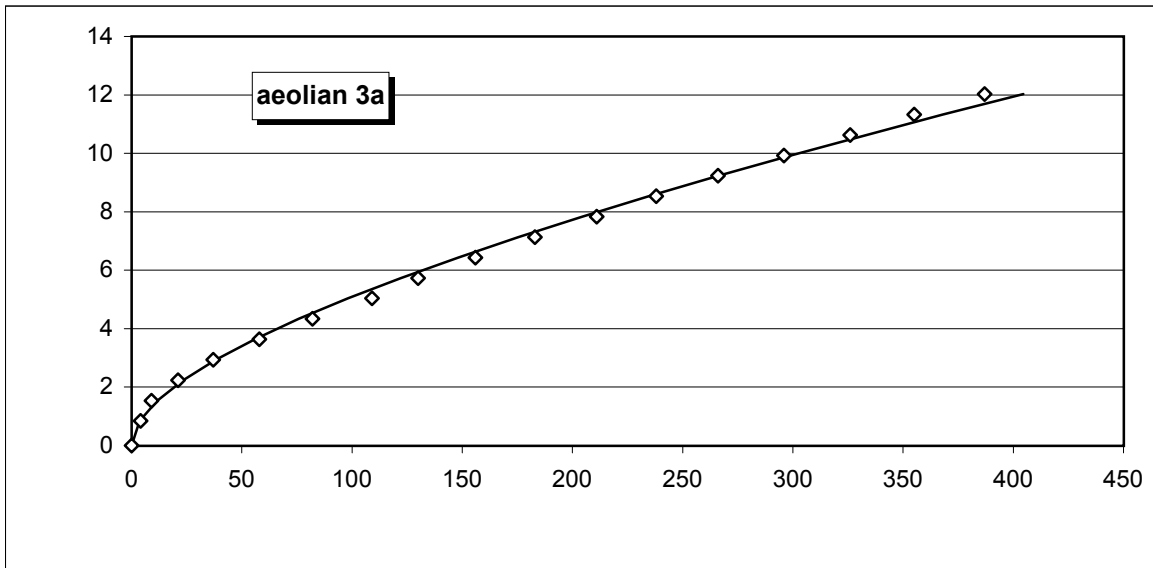
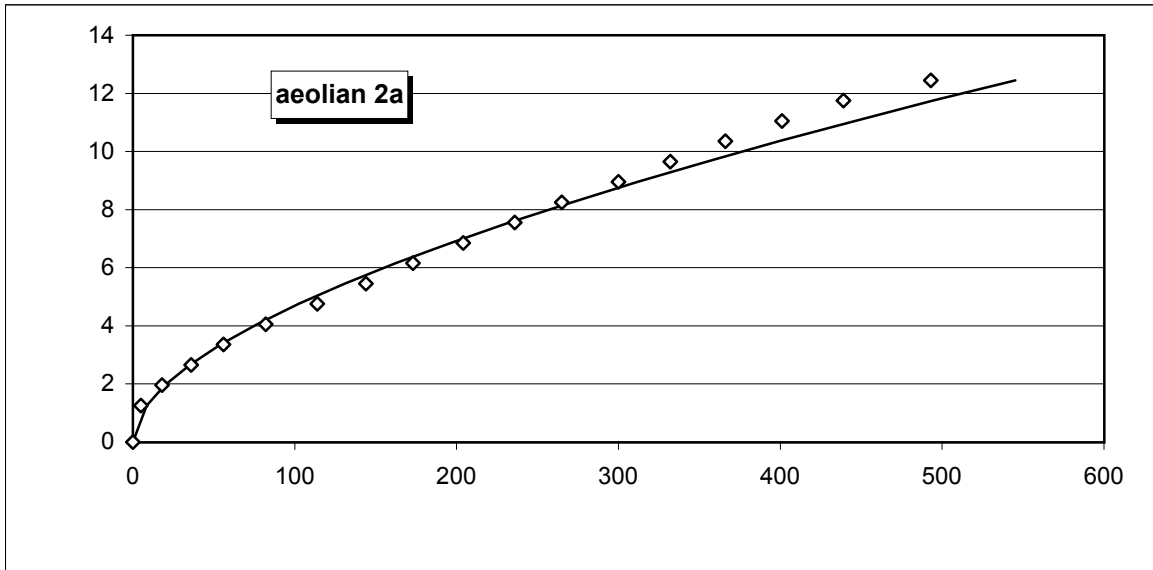
continued: infiltration with falling head permeameter



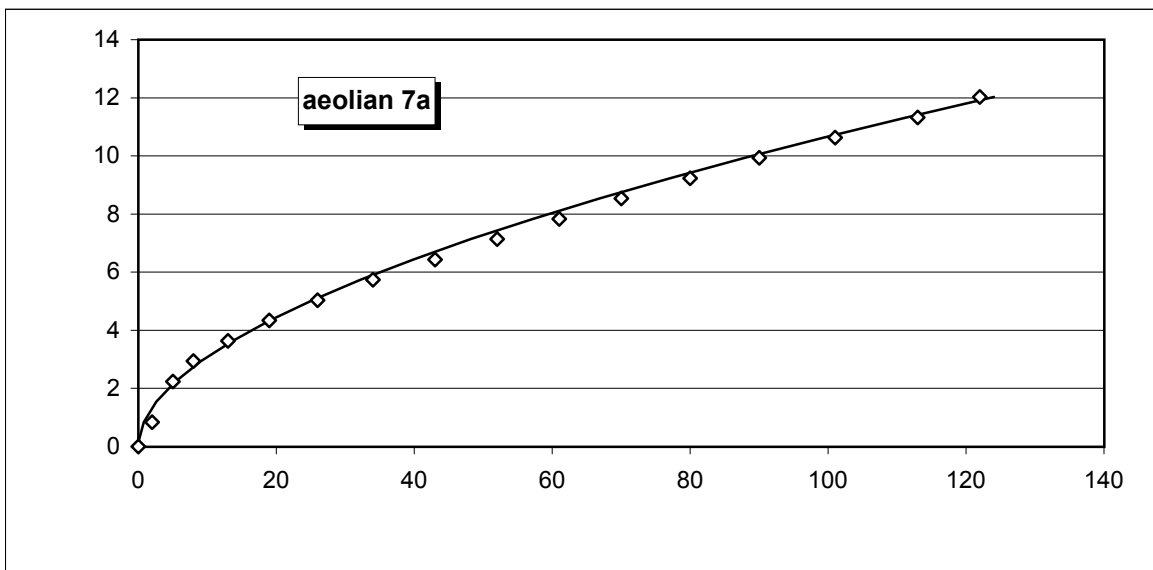
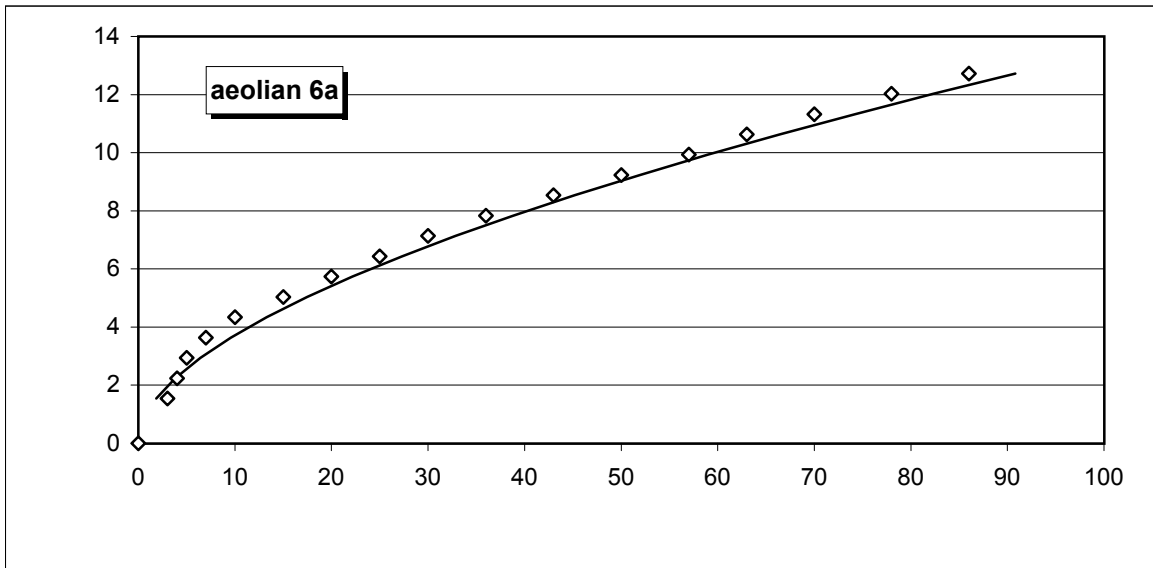
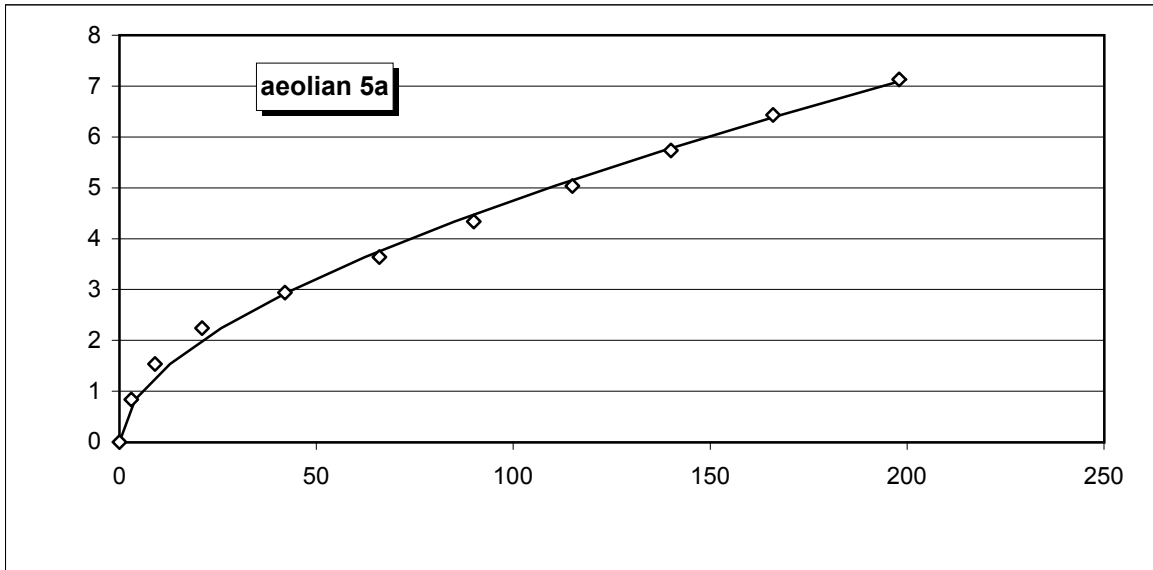
continued: infiltration with falling head permeameter



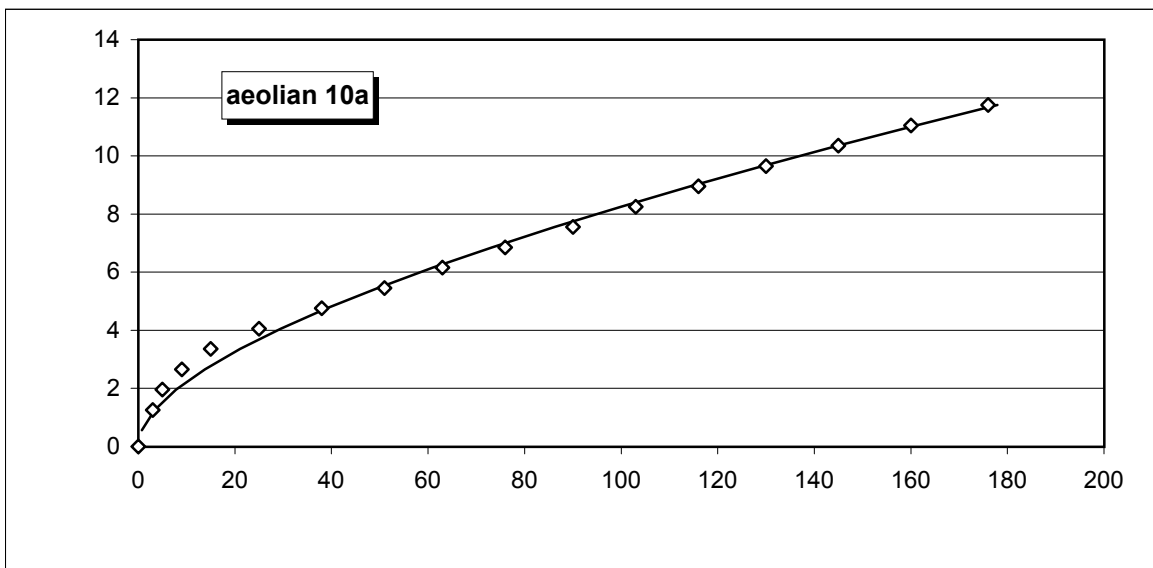
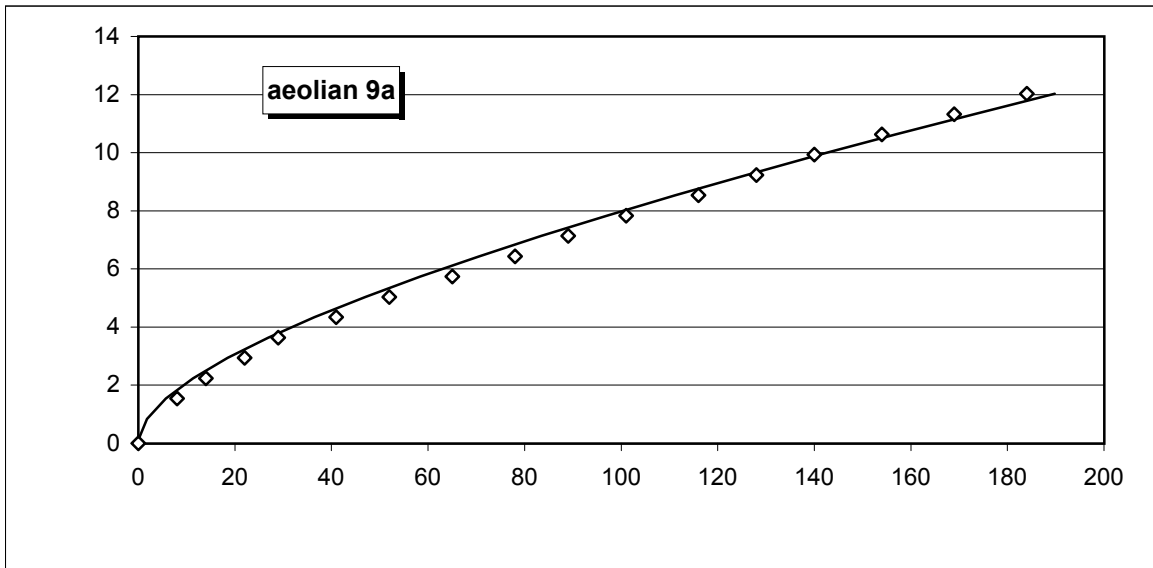
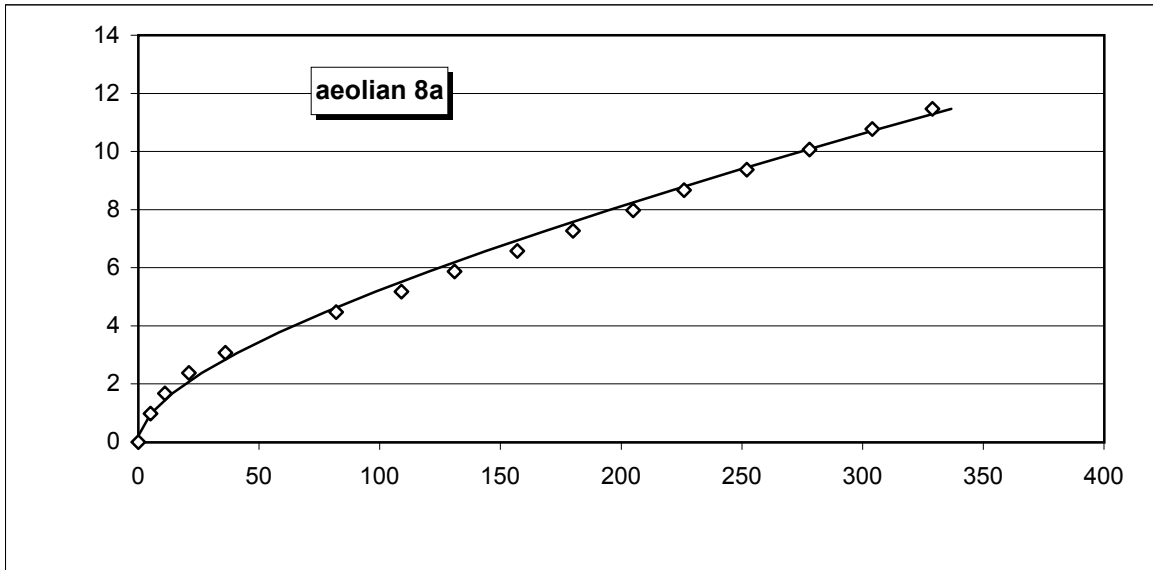
continued: infiltration with falling head permeameter



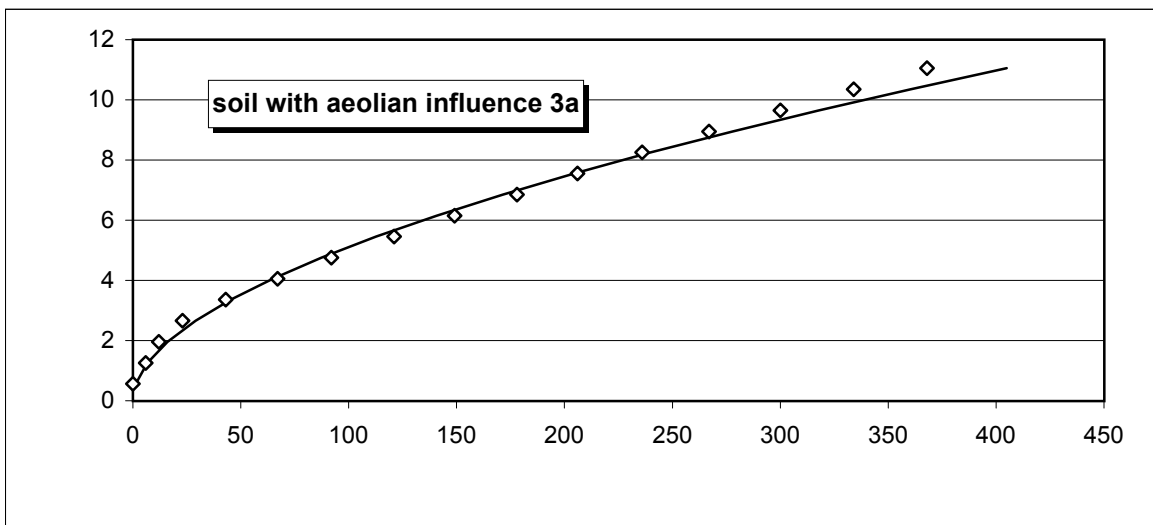
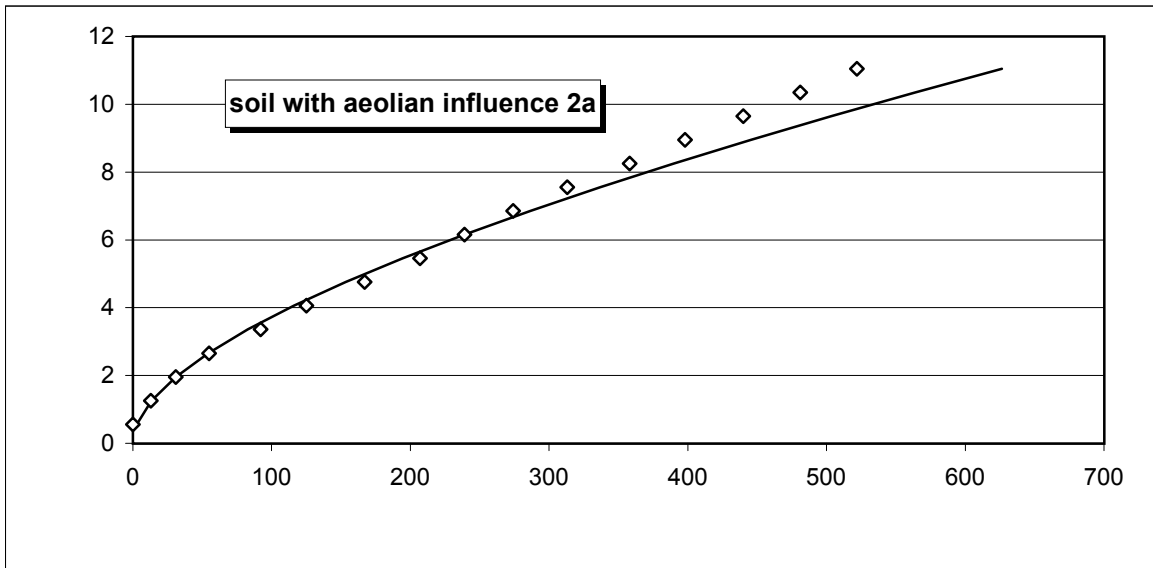
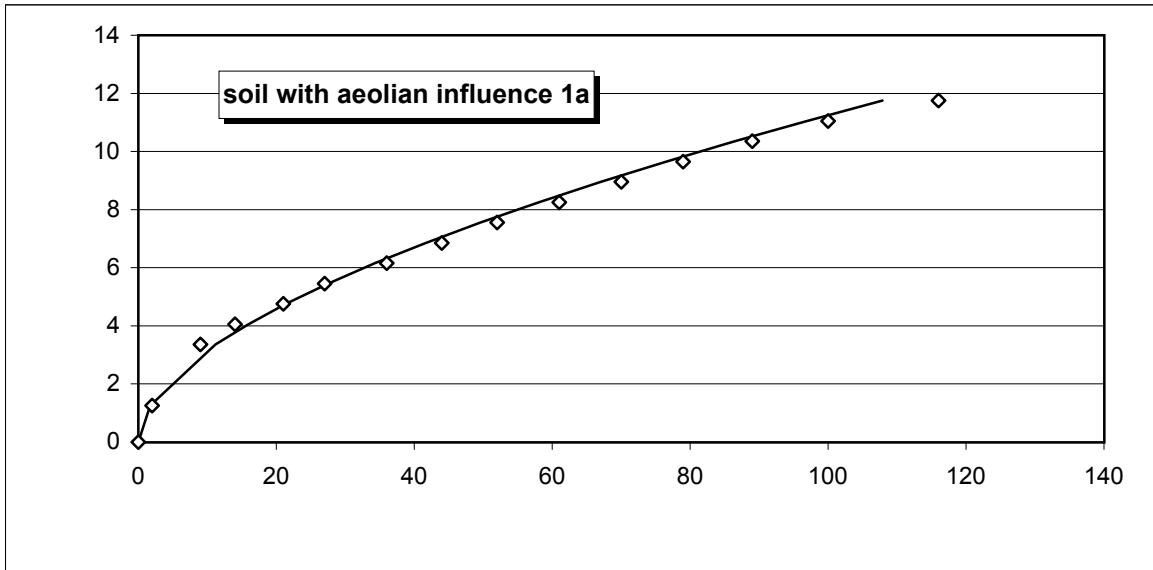
continued: infiltration with falling head permeameter



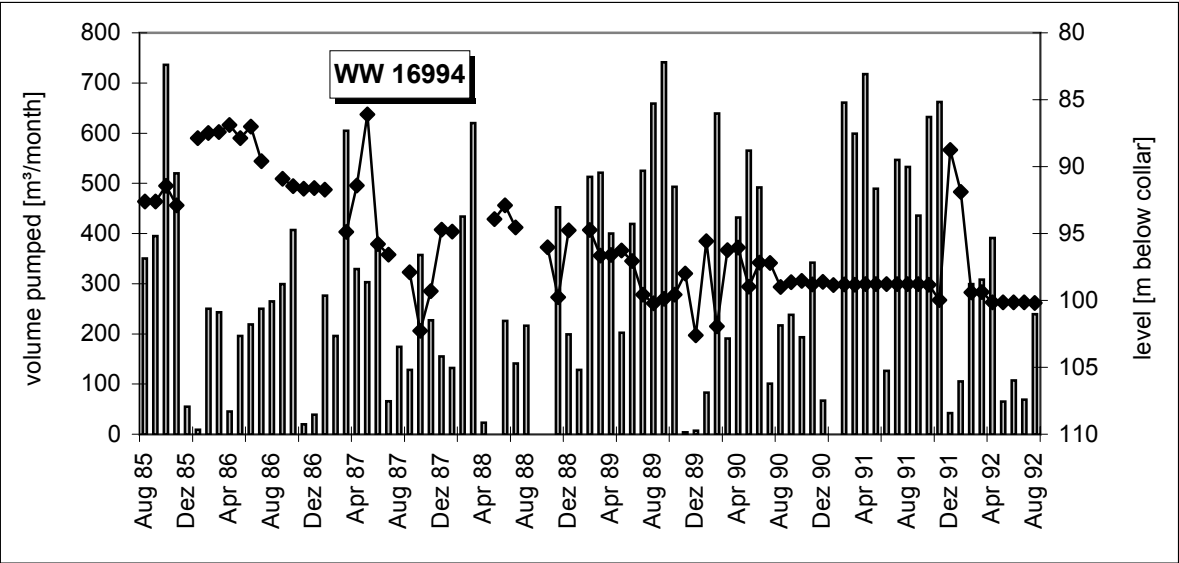
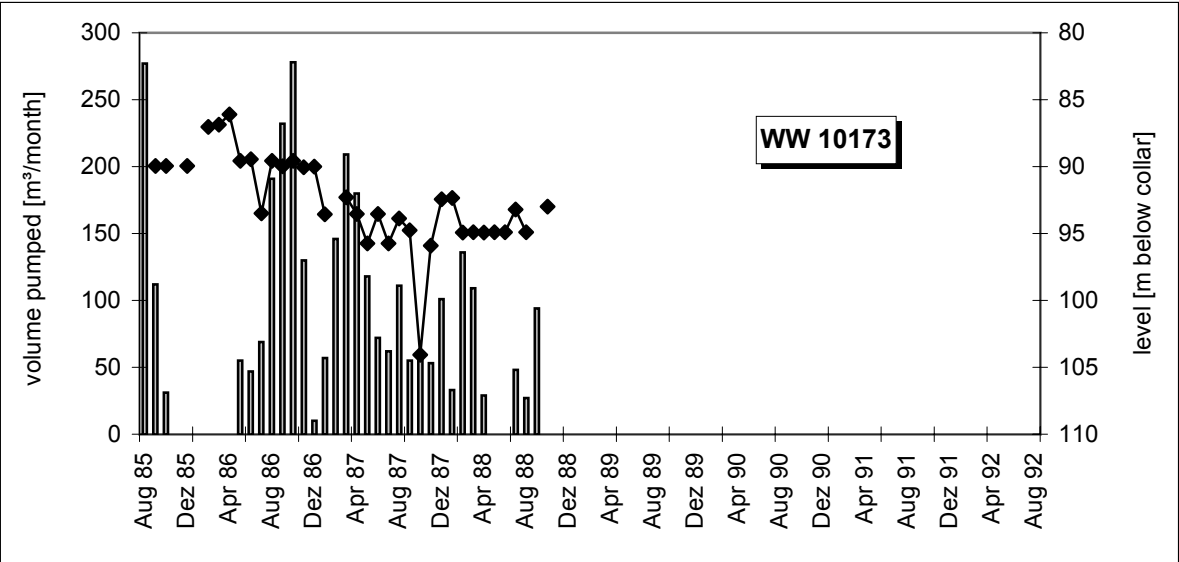
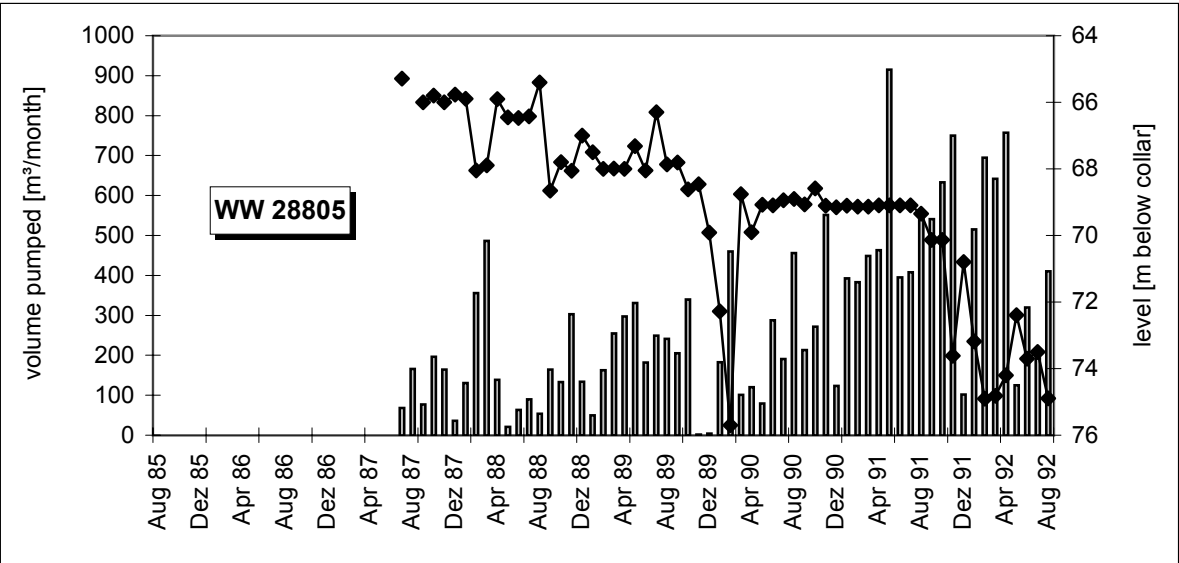
continued: infiltration with falling head permeameter



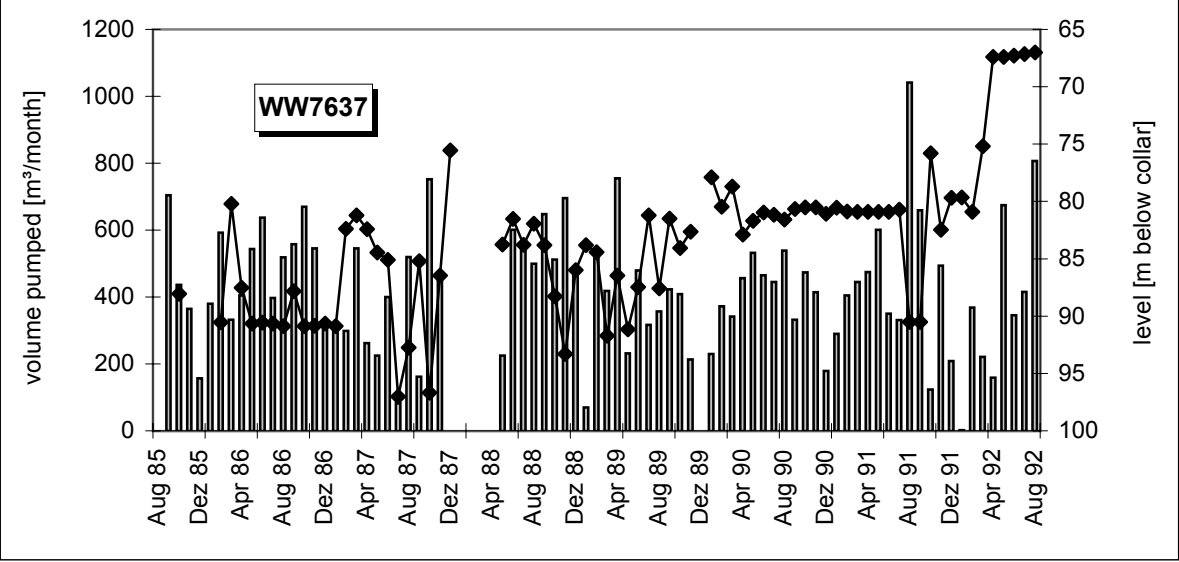
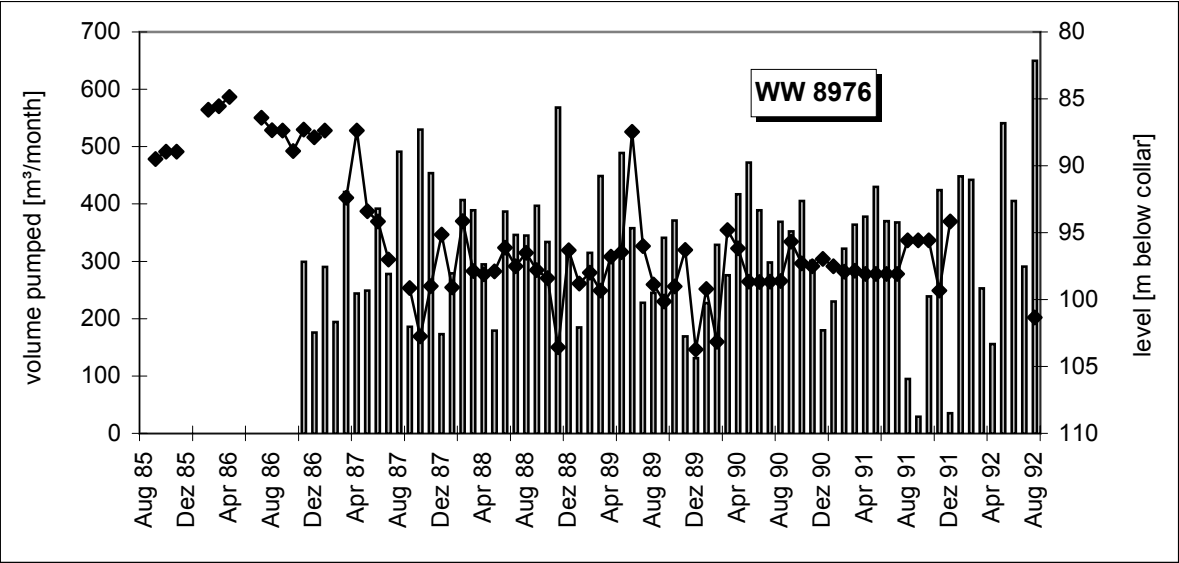
continued: infiltration with falling head permeameter



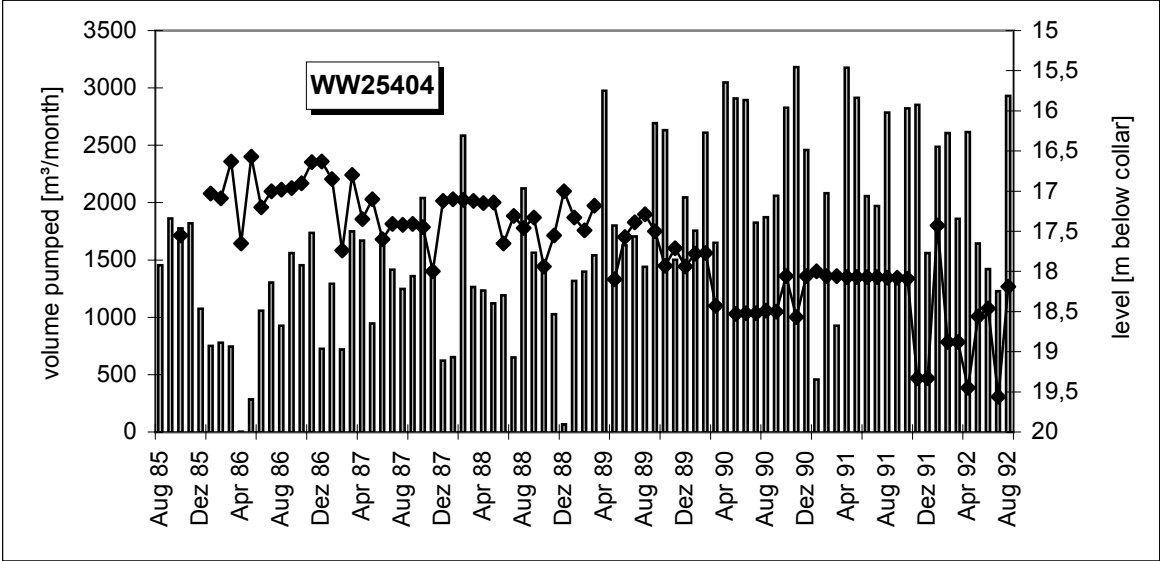
Epukiro



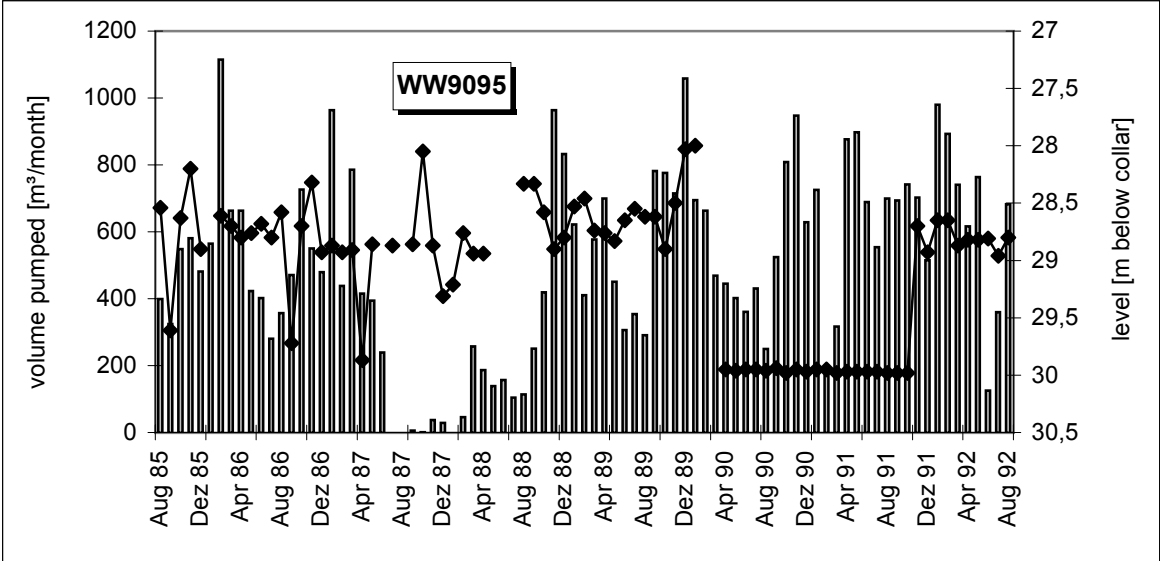
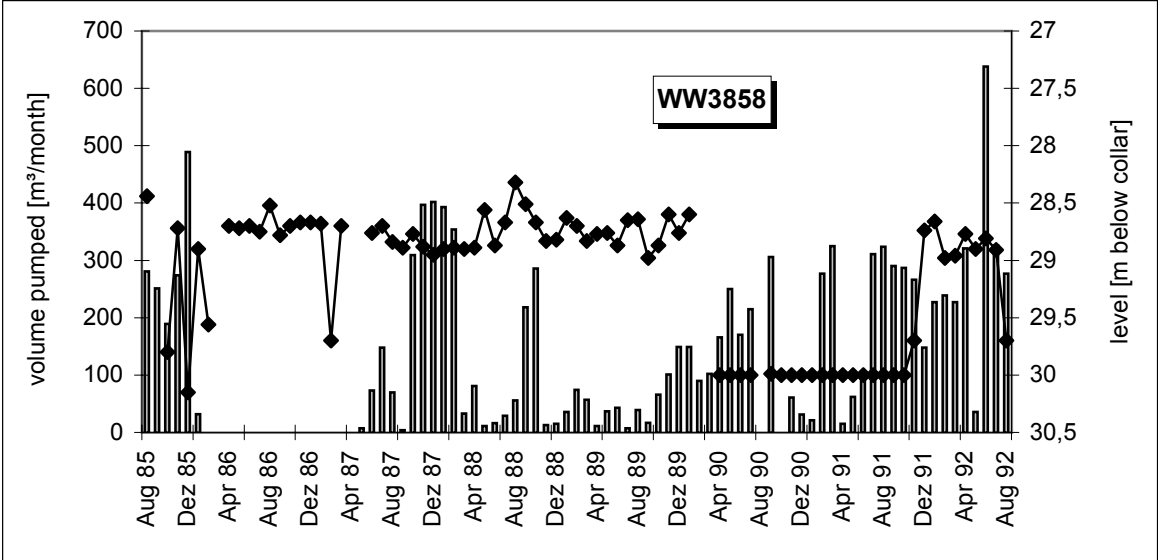
Epukiro



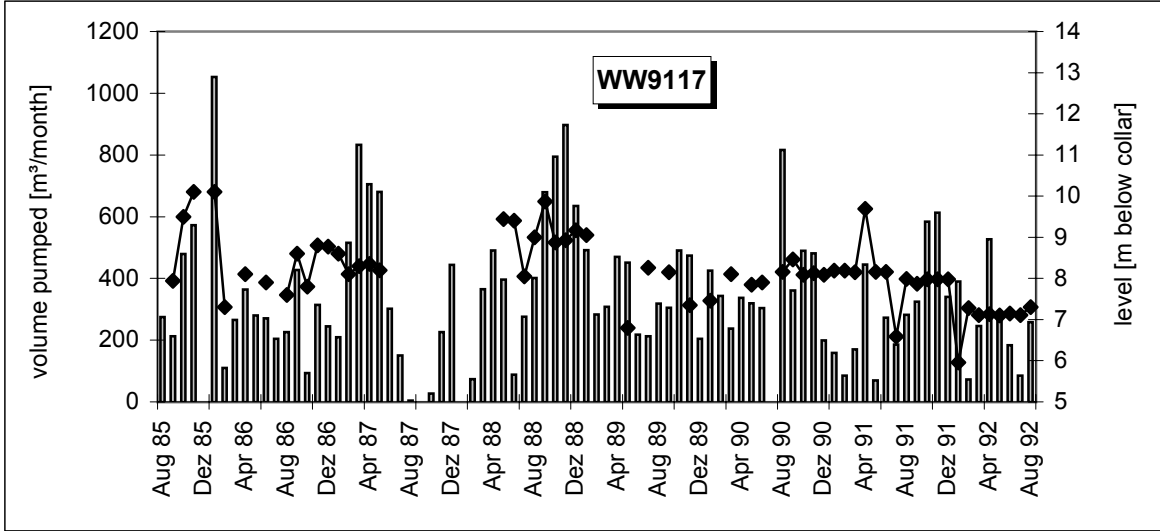
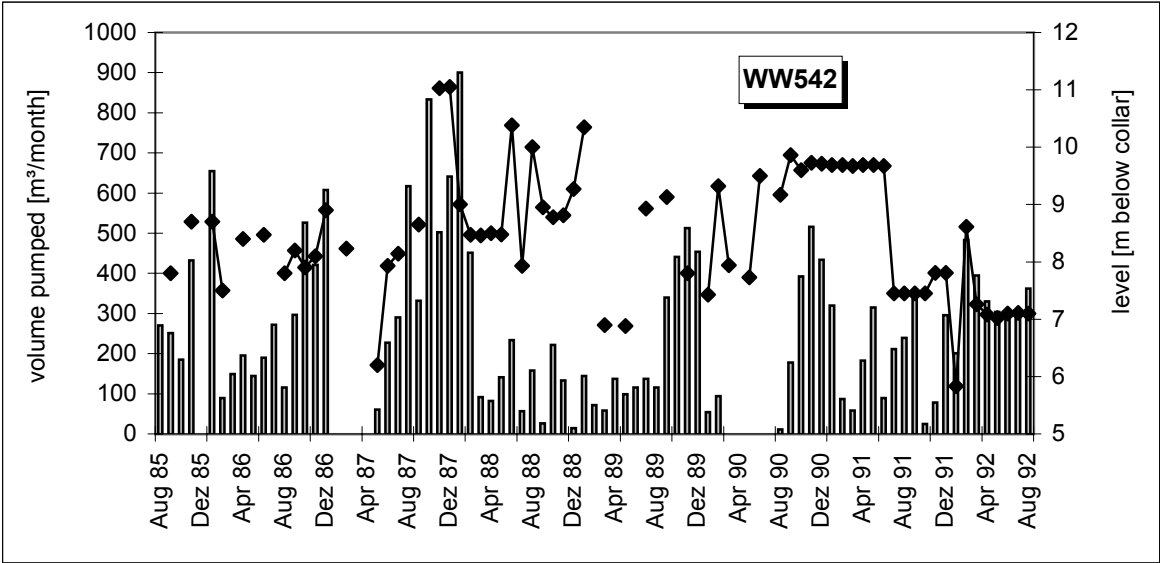
Otjinene



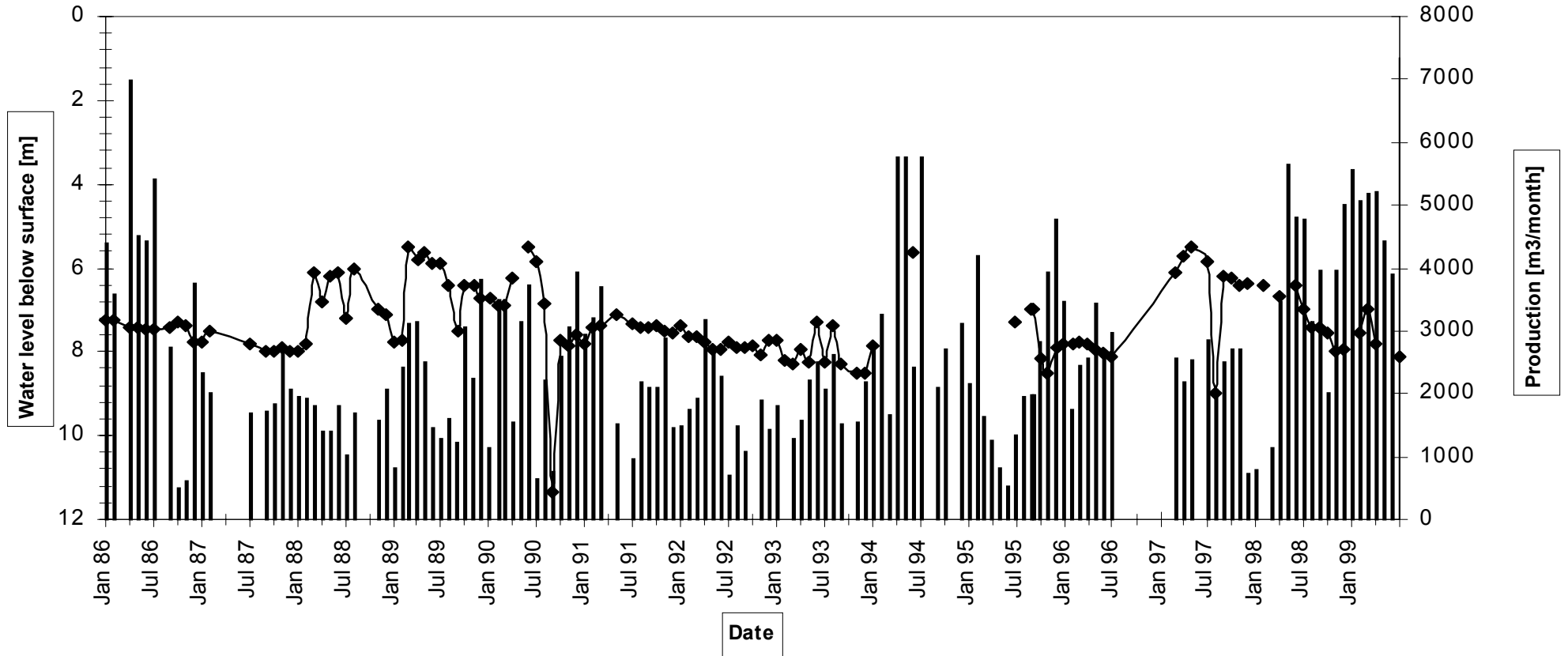
DuPlessis



Hochfeld



Tsumkwe WW 16561



Appendix D: Hydrochemical data

Name	Long	Mlat	pH	ec µS/cm	Ca ²⁺ mg/l	Mg ²⁺ mg/l	Na ⁺ mg/l	K ⁺ mg/l	HCO ₃ ⁻ mg/l	SO ₄ ²⁻ mg/l	NO ₃ ⁻ mg/l	Cl ⁻ mg/l	Balance %
D106/W2276	16,4269	-20,9955	8,0	1060	28,03	12,14	191	43	612,11	22	0,00	21	3,16
D106/W2272	16,4394	-20,9793	7,6	710	63,27	28,17	51	5	335,32	86	0,00	15	0,72
D97/1/W2581	16,4625	-21,1667	7,6	380	59,66	5,83	4	2	181,68	7	13,72	9	1,15
D106/W2269	16,5048	-20,9910	7,6	480	58,46	14,81	19	3	256,06	12	11,51	8	1,84
D99/W2578	16,5683	-21,1450	8,2	420	27,63	23,56	22	4	247,53	8	4,43	1	0,62
D123/W2257	16,5721	-20,9225	7,3	510	64,47	12,14	22	7	274,35	13	10,18	5	2,69
D123/W2256	16,5731	-20,9667	7,3	380	52,06	6,56	2	17	195,10	20	0,44	1	0,33
J22/W4558	16,5779	-21,5441	7,3	1040	76,08	63,62	61	1	499,93	19	57,55	58	2,44
J22/W4557	16,5788	-21,5712	7,6	460	36,04	17,97	33	14	225,58	11	4,43	38	0,01
D124/W2247	16,5817	-20,9856	7,8	550	74,48	10,44	28	5	209,73	13	53,12	38	2,47
J22/W4552	16,5827	-21,5613	7,0	390	50,05	10,93	5	14	234,12	5	0,00	6	-1,70
D100/W2309	16,5837	-21,1928	7,9	1010	56,46	42,01	105	13	496,28	58	0,44	62	0,35
D100/W2308	16,5875	-21,1468	8,1	730	20,82	8,50	137	11	380,44	49	0,00	18	1,37
D132/W2254	16,5981	-20,8270	7,5	790	70,48	22,58	68	4	453,60	3	13,72	20	0,92
D100/W2310	16,6125	-21,1523	7,8	1440	27,23	10,69	284	32	658,45	60	0,44	89	2,84
D103/W2307	16,6144	-21,1090	7,8	890	62,87	35,70	90	4	441,41	33	51,79	54	-0,92
J22/W4556	16,6144	-21,5883	7,4	1530	66,87	65,08	150	10	438,97	74	132,80	144	1,76
J22/W4553	16,6154	-21,5477	7,2	910	86,89	57,07	38	3	584,07	4	22,13	8	2,49
D132/W2253	16,6231	-20,8342	7,6	610	81,69	12,14	33	2	378,00	3	2,21	1	1,98
J254/W3527	16,6404	-21,3486	7,8	1200	53,26	73,82	81	14	652,35	17	57,55	18	0,53
D126/W1904	16,6433	-20,9532	7,7	650	76,48	17,73	62	7	445,06	18	0,44	16	0,15
D103/W2306	16,6452	-21,0631	8,1	2510	20,82	17,00	610	34	1276,66	171	80,57	160	-0,76
J255/W3525	16,6462	-21,3207	7,9	960	64,87	49,30	54	10	537,73	8	35,41	14	-0,24
D128/W2074	16,6471	-20,8613	8,1	370	50,45	5,59	17	8	223,14	12	0,00	1	0,01
J22/W4555	16,6567	-21,5874	7,5	1150	50,05	52,94	148	8	624,31	81	13,28	58	-1,00
J27/W4524	16,6587	-21,7243	6,9	3190	259,88	154,93	181	26	496,28	180	553,35	440	1,54
J27/W4523	16,6683	-21,7225	6,7	3930	315,94	245,76	119	15	556,02	230	996,03	480	-2,30
J254/W3528	16,6712	-21,3559	8,0	1220	58,46	73,82	79	8	624,31	14	75,26	30	0,20
D131/W2072	16,6750	-20,8243	8,0	850	94,10	19,91	76	7	573,10	7	7,08	10	-0,58
J253/W4448	16,6757	-21,4396	7,2	1190	79,69	71,88	67	11	665,77	65	13,28	28	-0,69
D131/W2073	16,6760	-20,8288	7,8	350	46,85	7,77	17	2	203,63	8	13,28	1	0,48
D125/W1609	16,6760	-21,0225	8,2	810	43,65	11,41	141	6	531,64	20	0,00	13	-0,49
D127/W1906	16,6779	-20,9180	7,5	730	99,71	17,24	53	11	512,13	10	19,92	12	-1,53
J256/W2082	16,6856	-21,2495	7,9	1420	43,65	29,38	245	13	554,80	105	11,07	148	-0,15
J28/W4509	16,6962	-21,6126	7,1	1280	100,91	67,02	93	6	542,61	117	30,99	86	1,71
D125/W1610	16,6971	-21,0171	7,5	1380	104,91	43,71	134	13	560,90	50	147,41	90	-0,52
J256/W2083	16,7000	-21,2441	8,3	1150	18,42	3,40	275	4	646,26	47	0,00	55	0,54
D131/W2070	16,7010	-20,7937	7,7	660	80,89	14,57	43	6	432,87	16	5,75	1	-1,86
D189/W2080	16,7019	-21,1595	7,9	1600	39,24	56,34	280	12	925,49	72	92,08	51	-1,32
J255/W3526	16,7067	-21,2973	7,8	1020	36,44	39,58	110	7	445,06	46	24,35	58	-1,19
D127/W1905	16,7183	-20,8874	8,3	630	78,89	8,01	68	8	390,19	14	0,44	34	0,69
D189/W2081	16,7308	-21,1586	8,0	950	46,85	35,94	137	5	673,08	12	0,00	1	0,32
D129/W1688	16,7356	-20,8874	7,1	560	104,91	6,80	11	7	353,61	1	24,35	0	1,93
D171/W1607	16,7356	-21,0459	7,7	890	70,08	14,81	110	11	514,57	25	11,07	33	-1,42
J28/W4511	16,7510	-21,6604	7,8	1000	76,08	89,85	33	6	693,81	30	22,13	12	0,35
J248/W3529	16,7538	-21,3568	8,1	1600	55,66	81,35	161	12	698,69	86	48,69	98	-0,03
D170/W1901	16,7587	-21,0045	7,6	840	54,86	21,13	134	10	536,51	28	0,00	50	-1,06
J259/W4503	16,7606	-21,5919	7,9	1280	88,90	88,88	83	7	707,22	61	26,56	65	1,36
J247/W2017	16,7654	-21,2378	7,9	1080	25,23	33,27	172	6	560,90	47	35,41	40	-1,02
D190/W1831	16,7663	-21,1577	8,0	970	17,62	17,24	245	6	725,51	40	0,00	20	-0,68
J247/W2016	16,7721	-21,2739	7,9	1390	56,86	76,74	141	13	627,97	50	38,96	120	0,88
V-28	16,7728	-21,6523	6,8	1152	90,00	90,90	64	4	680,00	86	41,20	43	0,07
J30/W4513	16,7740	-21,7883	7,0	1620	162,98	71,88	74	4	380,44	88	221,34	180	1,92

Appendix D: Hydrochemical data

Name	Long	Mlat	pH	ec µS/cm	Ca ²⁺ mg/l	Mg ²⁺ mg/l	Na ⁺ mg/l	K ⁺ mg/l	HCO ₃ ⁻ mg/l	SO ₄ ²⁻ mg/l	NO ₃ ⁻ mg/l	Cl ⁻ mg/l	Balance %
J30/W4514	16,7750	-21,6955	7,1	1210	106,92	80,87	71	9	645,04	177	13,28	36	-0,58
D169/W1899	16,7769	-20,9144	7,7	490	85,29	11,90	15	6	310,93	8	15,49	14	1,12
J244/W4434	16,7788	-21,4270	7,0	900	93,70	49,78	18	4	554,80	5	42,05	8	-2,24
D190/W1832	16,7798	-21,2108	8,3	640	13,21	2,91	151	2	238,99	39	13,72	88	0,58
D129/W1689	16,7817	-20,8784	7,3	720	92,10	21,86	46	8	475,55	5	1,33	15	1,52
D170/W1900	16,7817	-20,9919	7,9	740	74,48	47,84	46	6	560,90	14	1,77	12	-0,22
J245/W4427	16,7827	-21,4721	7,4	750	43,65	34,97	63	5	398,73	24	11,07	30	-0,85
J248/W3530	16,7827	-21,3829	8,0	1650	49,25	51,00	216	14	730,39	104	8,85	84	-0,73
J179/W4604	16,7837	-21,6541	6,9	1310	90,10	95,92	69	4	736,49	52	39,84	40	1,87
D171/W1608	16,7865	-21,0288	7,5	810	70,08	38,61	59	6	529,20	10	6,64	8	0,97
J259/W4504	16,7875	-21,5730	7,3	1220	66,07	101,99	81	7	726,73	38	44,27	54	1,50
J245/W4426	16,8096	-21,5027	7,3	970	54,86	74,80	52	6	669,42	6	19,92	10	-1,70
D190/W1830	16,8106	-21,1171	7,5	890	56,86	55,37	102	11	658,45	18	11,07	30	-0,32
D153/W790	16,8163	-20,7018	7,6	630	91,30	23,07	32	6	479,21	3	0,44	5	-0,40
J247/W2018	16,8183	-21,2667	7,8	1540	43,65	42,74	249	14	579,19	110	5,31	172	0,49
J244/W4429	16,8192	-21,4378	7,5	1540	37,64	61,92	238	10	823,06	84	30,99	72	-0,53
D159/1/W1907	16,8202	-20,8901	7,8	860	80,89	34,48	92	11	634,06	14	7,53	20	-0,94
J30/W4516	16,8212	-21,7811	7,8	730	70,88	28,90	52	8	457,26	26	0,00	20	-1,28
D172/W1605	16,8221	-21,0838	7,9	1230	15,22	4,13	259	8	463,35	85	0,00	123	-1,04
D153/W792	16,8231	-20,6820	7,2	760	143,76	23,07	11	2	441,41	9	45,60	42	1,37
J269/Y2156	16,8250	-21,5378	8,0	920	72,08	59,98	44	5	626,75	10	10,62	10	-1,67
D154/W1894	16,8260	-20,7333	8,2	670	122,53	15,54	10	6	380,44	6	38,51	24	2,07
J246/Y2153	16,8269	-21,5721	7,5	1040	58,06	100,05	47	8	757,22	14	32,76	19	-1,42
J179/W4606	16,8269	-21,6495	7,4	1090	64,07	88,88	35	1	647,48	6	53,12	28	-1,32
V-27	16,8276	-21,8276	7,5	1822	96,00	12,90	277	21	577,00	294	1,80	111	-0,84
D154/W1895	16,8279	-20,7423	7,5	620	126,54	12,87	10	4	449,94	2	9,74	6	1,08
J244/W4428	16,8279	-21,4000	7,3	1380	44,85	65,81	177	8	724,29	57	17,71	80	-0,13
V-26	16,8319	-21,6733	6,9	949	89,00	84,00	25	2	619,00	16	51,00	23	2,23
J30/W4517	16,8385	-21,7856	7,3	1090	122,93	43,95	62	8	670,64	38	22,13	34	-1,73
D153/W791	16,8413	-20,7216	7,5	600	98,11	25,01	16	3	412,14	6	11,07	19	0,87
J245/W4424	16,8433	-21,4739	7,3	1290	60,87	81,84	90	7	574,31	20	132,80	52	1,57
J243/1/W2020	16,8500	-21,2901	7,8	4300	37,24	82,08	806	27	538,95	620	20,36	726	2,09
J269/Y2158	16,8548	-21,5270	7,7	790	54,06	59,01	26	4	510,91	9	21,25	10	-2,22
D172/1/W1618	16,8615	-20,9955	7,5	930	54,86	50,51	84	12	609,68	6	25,23	9	0,36
D192/W1833	16,8654	-21,2676	7,8	3150	50,45	10,69	771	46	420,68	544	6,20	643	2,22
D160/W1681	16,8702	-20,8216	7,1	350	52,46	11,90	5	5	219,48	1	8,41	0	2,45
D192/W1835	16,8702	-21,1973	7,9	1020	10,81	6,31	235	5	219,48	115	80,57	156	-1,22
D160/W1680	16,8721	-20,8261	7,2	290	50,45	5,83	4	5	195,10	2	3,54	0	0,05
D192/W1834	16,8817	-21,2153	7,9	700	32,84	33,51	95	8	392,63	30	71,71	20	-0,27
D167/W1686	16,8856	-20,9450	7,3	800	74,48	43,47	44	13	536,51	5	13,72	13	0,29
D160/W1678	16,8865	-20,8297	7,4	410	68,87	11,17	6	6	282,89	2	0,00	0	0,98
D167/W1687	16,8904	-20,9405	7,3	640	72,08	34,73	13	20	445,06	1	3,54	0	1,07
D194/W1602	16,8913	-21,1144	7,7	2400	67,67	38,85	450	31	391,41	405	10,18	410	0,68
D157/W1695	16,8942	-20,7721	7,6	550	63,27	17,48	34	12	373,12	0	0,00	3	1,45
D194/W1600	16,8990	-21,0820	7,8	2700	92,10	43,71	390	20	429,21	360	7,53	385	0,31
J38/Y2368	16,9048	-21,6982	7,7	770	66,07	17,97	75	7	408,48	43	4,43	30	-1,73
J44/Y2132	16,9048	-21,6009	7,2	900	70,08	63,87	48	6	609,68	23	27,00	13	-1,25
D193/W1836	16,9087	-21,1991	8,0	860	30,83	26,47	176	5	634,06	20	17,71	24	-1,16
D167/W1685	16,9106	-20,9054	7,5	840	59,26	33,27	97	11	573,10	15	2,66	16	-0,02
D173/W1614	16,9115	-21,0180	7,2	1220	24,03	1,21	235	11	273,13	110	11,07	160	1,48
D194/W1601	16,9163	-21,1324	7,5	2050	52,46	20,64	405	8	253,63	348	7,53	340	2,37
D166/W1676	16,9183	-20,8676	7,1	580	108,52	9,47	10	6	380,44	2	12,84	1	2,04
D183/W1617	16,9212	-21,0459	7,5	1160	118,13	35,70	74	11	404,82	50	96,95	115	-0,61

Appendix D: Hydrochemical data

Name	Long	Mlat	pH	ec µS/cm	Ca ²⁺ mg/l	Mg ²⁺ mg/l	Na ⁺ mg/l	K ⁺ mg/l	HCO ₃ ⁻ mg/l	SO ₄ ²⁻ mg/l	NO ₃ ⁻ mg/l	Cl ⁻ mg/l	Balance %
D173/W1615	16,9221	-21,0117	7,8	1580	25,23	1,70	313	19	341,42	200	0,00	195	0,78
D325/W3531	16,9269	-20,5838	8,0	710	77,28	22,58	26	4	391,41	5	15,49	4	0,48
J240/W2023	16,9279	-21,3414	8,6	2870	27,23	44,20	565	33	731,61	500	10,18	245	1,57
D160/W1677	16,9356	-20,8216	7,3	1080	144,56	38,61	28	11	376,78	9	222,67	65	0,44
J239/Y2146	16,9423	-21,4640	7,7	3280	75,28	154,93	460	18	737,71	675	7,53	340	1,54
D167/W1684	16,9471	-20,9505	7,2	840	78,89	30,11	59	14	409,70	20	28,77	53	1,35
D196/W1837	16,9471	-21,2568	7,9	3800	37,24	42,98	995	17	1146,19	700	56,66	523	0,09
D174/W1612	16,9490	-21,0306	8,0	1650	32,84	9,23	320	10	487,74	155	32,76	180	-0,76
D174/W1611	16,9500	-21,0261	7,5	1460	46,05	14,33	279	14	697,47	64	45,60	90	-0,21
J38/Y2370	16,9558	-21,7018	7,5	860	94,10	37,88	39	7	540,17	8	16,82	24	-1,42
D183/W1625	16,9567	-21,0982	7,7	1800	50,45	4,37	336	12	365,81	223	0,00	243	0,87
D362/W401	16,9625	-20,3766	7,3	640	126,14	17,00	13	7	469,45	5	8,41	14	0,65
D166/W1675	16,9625	-20,9234	7,3	740	67,67	13,60	88	8	438,97	24	7,53	27	-0,28
D198/W1840	16,9625	-21,2910	7,5	830	67,67	48,81	68	10	499,93	40	19,04	50	-0,64
D149/W2046	16,9654	-20,6414	7,7	600	72,08	21,61	17	5	367,02	10	4,87	1	-0,69
D166/W1674	16,9702	-20,8712	7,4	580	94,10	19,43	10	6	409,70	2	4,87	0	0,35
D362/W399	16,9750	-20,3568	7,3	620	33,24	59,25	46	15	499,93	2	3,54	8	2,30
D174/W1613	16,9788	-20,9883	7,8	1400	85,29	35,70	161	14	402,39	150	0,00	189	-1,67
D156/W1892	16,9808	-20,7577	7,5	840	109,32	26,71	55	9	441,41	10	94,29	50	-0,47
B334/W455	16,9817	-20,1315	7,3	700	144,96	13,60	7	2	520,66	3	4,43	8	-1,05
D361/W3523	16,9846	-20,4297	7,9	800	61,27	37,64	42	13	481,64	6	8,85	6	-0,10
D161/W1672	16,9856	-20,8189	7,6	1220	72,08	21,13	187	8	524,32	53	6,20	138	-0,05
D324/W354	16,9885	-20,5153	7,2	700	81,69	29,63	29	3	396,29	12	37,18	13	0,91
D362/W402	16,9904	-20,3532	7,1	1340	125,34	87,42	74	15	698,69	2	83,66	134	1,28
D324/W355	16,9952	-20,5198	7,1	800	118,93	25,26	28	6	508,47	8	11,95	8	2,55
B334/W453	16,9981	-20,1009	6,9	720	151,77	19,67	7	2	546,27	4	4,87	10	0,80
D198/W1838	17,0000	-21,2423	7,5	840	63,27	36,91	92	9	479,21	30	27,89	60	-0,92
D182/1/W1628	17,0029	-21,0640	7,6	850	85,29	28,17	65	12	512,13	20	16,38	17	0,81
B334/W454	17,0038	-20,0973	7,0	690	136,15	24,04	7	3	515,79	4	5,75	10	1,34
D362/W403	17,0058	-20,3559	7,3	720	69,68	44,68	43	12	509,69	5	10,18	18	1,09
D175/W1651	17,0067	-20,9811	7,3	780	80,89	21,37	69	12	490,18	21	12,84	20	-0,76
D198/W1839	17,0067	-21,2712	7,7	990	28,43	28,90	207	11	596,26	42	19,04	52	2,60
D361/W3522	17,0087	-20,4550	7,6	710	86,09	17,48	15	9	380,44	6	8,85	4	0,02
D149/W2045	17,0096	-20,6396	8,0	620	78,89	12,87	26	4	360,93	11	7,97	1	-0,57
D358/W387	17,0106	-20,2568	7,1	780	167,38	15,30	10	4	519,44	10	30,10	20	1,90
B334/W457	17,0125	-20,1207	7,1	710	146,56	19,67	6	1	541,39	3	4,87	9	-0,26
D358/W388	17,0125	-20,2631	7,1	810	148,56	24,77	8	3	509,69	6	23,90	20	2,32
D162/W1671	17,0135	-20,8297	7,6	600	48,05	23,80	59	8	364,59	9	15,49	14	2,30
J239/Y2143	17,0154	-21,4342	7,9	590	48,05	28,90	32	6	348,73	6	26,56	9	-1,57
D358/W390	17,0212	-20,2045	7,4	720	130,94	17,73	8	3	499,93	4	5,75	12	-1,69
D149/W2047	17,0260	-20,5775	7,4	1170	99,71	23,31	16	4	229,24	19	117,31	60	-0,29
D162/W1670	17,0269	-20,8243	7,6	620	46,05	20,64	72	8	426,77	9	4,87	0	0,50
D164/W1653	17,0308	-20,8982	7,3	580	76,48	11,41	43	6	378,00	12	7,08	8	-0,04
D161/W1673	17,0365	-20,7919	7,9	1180	30,83	12,38	240	7	280,45	102	0,00	200	3,19
B569/W641	17,0375	-20,0775	7,5	800	167,78	3,40	3	1	506,03	5	12,39	8	-0,08
104224	17,0385	-19,2784	8,0	3400	138,95	218,07	275	21	559,68	192	822,47	378	0,38
J172/Y2128	17,0394	-21,5622	7,6	1080	115,33	36,91	53	11	382,88	18	166,00	74	-0,15
D164/W1652	17,0394	-20,9252	7,4	1220	38,44	19,67	245	10	609,68	69	15,05	85	1,34
B569/W2912	17,0433	-20,0757	7,8	690	161,78	15,06	5	2	579,19	5	1,33	5	-0,92
J43/Y2391	17,0433	-21,7955	7,8	700	68,07	32,06	36	7	463,35	3	6,64	8	-1,33
B334/W456	17,0452	-20,1261	7,1	730	160,57	8,26	8	1	541,39	2	8,85	9	-1,33
D200/W1843	17,0471	-21,2099	7,8	930	50,45	32,54	141	8	445,06	90	22,58	74	-0,37
J169/Y2085	17,0500	-21,4360	8,3	570	42,05	28,90	35	6	317,03	7	31,87	6	1,04

Appendix D: Hydrochemical data

Name	Long	Lat	pH	ec μS/cm	Ca ²⁺ mg/l	Mg ²⁺ mg/l	Na ⁺ mg/l	K ⁺ mg/l	HCO ₃ ⁻ mg/l	SO ₄ ²⁻ mg/l	NO ₃ ⁻ mg/l	Cl ⁻ mg/l	Balance %
B94/W468	17,0500	-20,1658	7,0	970	203,82	13,11	12	8	540,17	18	108,01	42	-0,73
D175/W1650	17,0500	-20,9486	7,6	1000	78,89	31,81	110	11	501,15	49	16,38	70	0,64
D200/W1845	17,0510	-21,2153	7,4	880	46,05	30,36	144	8	432,87	90	17,71	68	0,41
J169/Y2090	17,0519	-21,4640	8,6	560	43,25	31,08	31	7	323,13	7	28,33	8	0,97
J168/Y2080	17,0567	-21,3973	8,4	660	38,04	36,91	56	7	385,32	21	18,59	7	2,04
B571/W888	17,0596	-20,0378	7,4	650	130,54	15,78	5	2	491,40	5	0,44	6	-1,54
D358/W389	17,0606	-20,2315	6,9	730	156,97	12,38	6	2	509,69	5	7,53	12	1,37
B569/W639	17,0606	-20,0973	7,0	810	135,75	18,94	7	1	458,48	6	26,56	18	0,51
D180/W1636	17,0606	-21,0748	7,3	900	61,27	28,41	95	13	548,71	20	10,18	20	-1,39
D163/W1641	17,0625	-20,9234	7,2	1250	107,32	23,80	119	13	438,97	59	98,27	112	-1,32
D149/W2048	17,0635	-20,5252	7,6	620	104,11	4,86	6	8	306,06	12	33,64	13	-0,93
B569/W638	17,0644	-20,1009	7,0	720	127,74	13,84	5	1	456,04	4	4,43	8	-0,63
D382/W1667	17,0663	-20,7685	7,7	1120	32,84	3,16	225	10	292,64	76	64,19	145	1,87
J35/Y2358	17,0692	-21,6378	8,4	700	34,04	36,91	56	11	321,91	8	47,81	45	-0,20
D201/W1852	17,0692	-21,1396	7,6	790	39,24	20,40	144	8	504,81	40	17,71	30	-0,65
D364/W393	17,0702	-20,2658	7,1	830	165,78	8,01	10	2	463,35	13	47,37	35	-1,04
D163/W1640	17,0702	-20,8955	7,4	1760	30,83	10,20	400	8	775,51	150	0,00	110	2,69
B98/W472	17,0721	-20,1991	7,1	1170	237,86	14,08	12	3	509,69	25	149,62	72	1,15
D201/W1853	17,0750	-21,1622	7,4	590	48,05	15,30	76	11	406,04	5	2,66	17	-0,25
B572/W2910	17,0817	-20,0081	7,6	620	98,91	23,07	31	6	446,28	21	17,71	11	-0,07
D367/W3521	17,0856	-20,4820	7,8	820	64,07	28,41	57	6	464,57	8	2,21	14	-0,26
D201/W1851	17,0865	-21,1342	7,8	1420	48,05	51,00	265	16	984,02	34	0,00	77	-1,27
B569/W640	17,0894	-20,0865	7,0	700	118,53	14,33	5	2	432,87	4	4,87	10	-1,18
D364/W394	17,0904	-20,2712	7,1	700	142,96	9,47	9	3	493,84	6	0,00	12	-1,04
D201/W1856	17,0904	-21,2117	7,9	950	36,84	23,80	198	7	638,94	60	10,18	28	-0,34
D201/W1854	17,0913	-21,1685	7,6	720	50,45	28,17	100	9	438,97	65	15,49	24	-0,31
D202/W1858	17,0913	-21,2477	7,2	4150	161,78	125,31	700	45	501,15	470	22,58	1082	1,11
B94/W467	17,0962	-20,1405	7,7	740	66,07	25,50	96	18	551,15	12	15,94	13	0,63
J169/Y2088	17,0971	-21,4676	9,0	610	44,05	33,03	48	5	348,73	11	38,96	10	1,98
D382/W1668	17,0990	-20,7793	7,9	1070	19,62	0,24	229	9	274,35	85	0,00	168	0,84
D201/W1857	17,1000	-21,2081	7,6	530	8,81	0,73	122	7	148,76	12	7,53	113	-0,09
D381/W1658	17,1000	-20,8189	7,1	1410	143,36	29,63	141	9	449,94	82	55,33	185	2,45
J43/Y2392	17,1010	-21,7640	7,7	720	70,08	45,90	12	10	482,86	3	12,84	4	-1,50
D180/W1635	17,1019	-21,0775	7,6	960	63,27	29,63	100	11	453,60	43	20,81	50	0,74
D149/W2049	17,1029	-20,5847	7,4	430	57,66	13,36	9	9	237,77	12	7,97	7	1,38
B107/W466	17,1048	-20,1018	7,0	980	193,81	7,53	28	9	408,48	15	132,36	98	-0,70
B98/W473	17,1067	-20,1865	8,3	730	144,96	13,84	6	2	520,66	5	5,75	9	-1,69
D201/W1855	17,1096	-21,1766	7,3	1950	37,24	10,20	459	8	101,21	810	0,00	154	0,00
B573/W886	17,1106	-19,9775	7,4	630	132,94	13,84	5	2	453,60	6	13,72	11	-0,30
D205/W1869	17,1106	-21,1198	7,8	660	41,65	23,31	100	9	445,06	27	15,94	10	1,07
B571/W889	17,1106	-20,0577	7,1	970	183,00	20,16	14	3	482,86	16	96,94	69	-1,21
D163/W1639	17,1106	-20,8910	8,4	1130	32,84	14,57	216	10	677,96	30	21,69	16	-0,19
B571/W890	17,1115	-20,0622	7,3	950	187,00	14,81	18	3	510,91	16	38,95	85	-1,39
B573/W2911	17,1163	-19,9838	7,2	680	156,17	15,54	5	1	551,15	0	6,20	4	0,38
B572/W891	17,1202	-20,0378	7,3	720	145,76	18,94	9	6	540,17	10	0,00	6	0,79
D180/W1637	17,1202	-21,0432	7,3	770	52,46	25,74	84	9	438,97	25	14,61	20	0,62
B572/W892	17,1202	-20,0450	7,1	950	178,59	11,66	13	39	552,37	30	46,04	48	-1,46
D163/W1638	17,1221	-20,9198	7,3	790	72,08	25,74	70	10	463,35	14	19,48	19	1,58
B98/W474	17,1260	-20,2144	6,8	670	140,95	25,26	8	3	526,76	5	10,18	10	1,89
D202/W1863	17,1260	-21,2099	7,5	960	50,45	38,85	158	15	554,80	118	23,90	34	0,30
J189/Y2379	17,1260	-21,7685	7,9	1250	120,53	68,97	40	10	588,95	30	108,46	80	-2,13
B107/W2695	17,1288	-20,1288	7,4	490	60,47	18,21	11	7	310,93	9	4,43	2	-2,24
D382/W1669	17,1288	-20,7613	8,0	1160	18,42	0,97	240	11	231,68	105	0,00	189	1,76

Appendix D: Hydrochemical data

Name	Long	Mlat	pH	ec µS/cm	Ca ²⁺ mg/l	Mg ²⁺ mg/l	Na ⁺ mg/l	K ⁺ mg/l	HCO ₃ ⁻ mg/l	SO ₄ ²⁻ mg/l	NO ₃ ⁻ mg/l	Cl ⁻ mg/l	Balance %
J189/Y2378	17,1298	-21,7802	7,7	1110	78,08	52,94	41	8	588,95	5	7,08	28	-2,01
B575/W762	17,1308	-19,9333	7,6	720	151,36	11,90	4	2	502,37	7	4,87	5	0,92
B98/W475	17,1327	-20,2396	7,0	670	136,15	27,93	8	3	526,76	6	15,05	10	1,25
D178/W1647	17,1337	-20,9937	7,6	600	56,86	20,40	45	10	367,02	6	33,20	8	-1,26
J166/W3541	17,1337	-21,3090	7,5	900	45,65	55,61	40	10	492,62	19	17,71	14	-1,67
D202/W1862	17,1337	-21,2027	7,6	920	37,24	31,33	172	14	579,19	110	7,53	16	-0,32
D179/W1645	17,1346	-21,0225	7,5	610	53,66	23,56	53	8	392,63	21	12,40	8	-1,19
J159/Y2116	17,1356	-21,3874	8,4	640	31,23	31,08	62	11	374,34	18	27,00	10	-0,93
D202/W1861	17,1356	-21,2216	7,6	1080	46,05	42,50	168	19	603,58	121	8,85	54	-1,77
D380/W1654	17,1375	-20,8856	7,4	870	79,69	43,47	63	10	585,29	8	10,18	11	1,52
J159/Y2120	17,1404	-21,4441	8,4	540	33,24	30,11	37	9	314,59	7	28,33	12	-1,00
D206/W1868	17,1413	-21,0892	7,8	660	46,05	23,07	95	8	409,70	47	13,72	20	0,32
B573/W885	17,1433	-19,9955	7,4	660	139,35	10,44	4	2	473,11	5	21,25	6	-2,02
D381/W1659	17,1442	-20,7919	7,4	960	63,27	35,94	122	10	597,48	28	22,58	28	0,64
104746	17,1462	-19,3748	7,6	1050	81,29	88,88	22		666,99	11	0,00	21	2,39
D178/W1646	17,1471	-20,9649	7,5	610	67,67	19,67	42	9	379,22	14	21,25	11	-0,75
J189/Y2376	17,1481	-21,7315	7,9	1110	54,06	70,91	79	17	656,01	10	19,48	53	-1,45
J158/Y2122	17,1490	-21,5171	8,4	640	41,24	30,11	52	11	374,34	3	33,64	15	-0,59
B575/W763	17,1510	-19,9523	7,4	640	124,14	13,84	7	5	415,80	7	11,51	11	2,04
B336/W3505	17,1519	-20,0649	7,4	1450	233,45	8,50	29	3	521,88	34	137,23	96	-1,77
B99/2/W3510	17,1548	-20,2441	7,3	850	141,35	14,57	8	2	486,52	14	19,92	9	-1,08
J189/Y2377	17,1558	-21,7784	7,9	770	109,32	27,93	15	8	517,00	4	15,05	3	-1,56
D205/W1870	17,1558	-21,1703	7,9	5700	452,89	362,80	700	28	398,73	1925	47,81	1136	2,57
D380/W1655	17,1567	-20,8784	7,5	840	52,46	29,38	107	11	518,22	24	17,71	22	0,36
J161/Y2091	17,1577	-21,3459	8,0	810	33,24	35,94	88	16	408,48	30	37,19	24	1,47
D202/W1859	17,1625	-21,2441	8,0	1010	24,03	34,00	191	18	585,29	81	21,69	54	-1,49
D365/W3517	17,1644	-20,3117	7,1	920	147,36	17,73	15	5	518,22	18	6,64	8	2,09
B336/W3506	17,1654	-20,0369	7,3	630	80,49	8,01	10	11	314,59	11	2,21	5	-1,55
D179/W1643	17,1702	-21,0514	8,2	900	59,26	30,60	97	11	460,91	49	5,31	52	-0,75
D383/W1664	17,1712	-20,7649	7,5	870	48,05	26,71	131	7	548,71	15	21,69	23	0,82
B108/W464	17,1721	-20,1027	7,1	920	204,22	10,69	10	2	477,99	15	87,20	83	-1,44
D203/W3569	17,1731	-21,2730	7,8	900	26,83	37,64	116	14	471,89	57	22,13	32	-1,70
D179/W1644	17,1750	-21,0171	7,6	740	42,85	25,01	90	12	403,61	34	33,64	31	-1,87
D179/W1642	17,1769	-21,0712	7,9	1080	56,86	38,85	122	10	414,58	67	6,20	122	-0,57
B106/W471	17,1798	-20,2090	7,2	720	142,56	19,18	15	3	496,28	7	23,02	18	1,42
B482/W3507	17,1798	-20,0189	7,5	920	106,52	34,48	28	10	536,51	16	8,85	14	-0,19
B575/W761	17,1808	-19,9703	7,3	500	104,51	9,47	2	2	359,71	0	0,44	8	0,02
D380/W1657	17,1808	-20,8748	7,7	710	62,47	31,33	56	9	486,52	8	9,74	11	-1,45
D206/W1867	17,1837	-21,1468	7,4	2150	161,78	93,74	220	16	347,52	265	46,48	479	0,57
B576/W655	17,1885	-19,9459	7,2	750	119,73	18,70	8	3	348,73	23	48,69	38	-0,71
D383/W1666	17,1885	-20,7523	7,4	920	54,86	32,30	128	9	548,71	18	34,09	31	1,83
D207/W1864	17,1894	-21,1622	7,6	780	48,05	32,30	110	13	426,77	64	50,47	36	0,08
B486/W760	17,1904	-19,9036	7,6	1090	130,54	33,51	74	9	523,10	110	65,51	45	-1,81
B106/W469	17,1923	-20,2036	7,4	660	122,13	5,59	13	10	375,56	12	20,36	25	-0,42
D383/W1665	17,1923	-20,7613	7,5	860	52,46	30,11	116	9	548,71	14	20,36	21	0,81
B486/W2906	17,1923	-19,9000	7,4	1060	132,14	59,01	55	6	570,66	188	13,72	11	0,71
B576/W656	17,1952	-19,9505	7,5	890	136,15	33,03	7	4	476,77	18	33,64	48	-0,83
B105/W458	17,1962	-20,1901	7,0	660	135,35	12,63	9	5	490,18	7	8,41	10	-1,68
D384/W1660	17,1962	-20,8090	7,5	1240	63,27	43,71	180	11	540,17	152	30,10	80	0,36
B99/2/W3511	17,1971	-20,2793	7,4	770	103,71	20,40	9	3	349,95	14	57,55	22	-1,70
D203/W3568	17,1971	-21,2721	7,6	840	49,65	42,50	84	12	459,70	49	19,92	24	1,97
D365/W3518	17,1971	-20,3315	7,2	950	133,35	24,77	19	5	518,22	9	22,13	10	1,73
B452/Y5692	17,1990	-19,2856	7,5	1000	113,32	62,90	25	1	671,86	31	11,51	12	-0,98

Appendix D: Hydrochemical data

Name	Long	Mlat	pH	ec µS/cm	Ca ²⁺ mg/l	Mg ²⁺ mg/l	Na ⁺ mg/l	K ⁺ mg/l	HCO ₃ ⁻ mg/l	SO ₄ ²⁻ mg/l	NO ₃ ⁻ mg/l	Cl ⁻ mg/l	Balance %
D288/W2037	17,2019	-20,6405	7,9	620	72,88	7,77	49	6	368,24	12	7,53	1	0,97
D204/W1847	17,2029	-21,2360	7,6	650	38,44	25,26	90	14	404,82	29	22,13	24	-0,02
D213/W1878	17,2029	-21,0856	8,3	1200	89,70	33,03	151	10	417,02	70	19,04	190	0,21
D204/W1846	17,2048	-21,2207	7,6	950	39,24	33,51	161	15	499,93	82	26,56	68	-0,59
B99/2/W3512	17,2048	-20,2793	7,4	6400	504,55	66,05	32	8	280,45	109	1083,20	232	2,11
B578/W764	17,2067	-19,8703	7,7	830	126,14	40,07	15	5	575,53	6	20,36	13	0,58
B579/W767	17,2067	-19,8559	7,2	850	106,52	56,58	17	6	607,24	14	2,66	5	2,05
J161/1/Y2103	17,2077	-21,3784	8,7	750	42,05	36,91	77	10	442,62	15	25,68	16	1,80
B482/W3508	17,2087	-20,0108	7,2	980	183,80	7,77	5	3	570,66	8	22,13	6	0,30
B108/W463	17,2096	-20,0847	7,1	910	124,54	38,37	46	14	691,37	1	0,00	8	0,66
D288/W2038	17,2106	-20,6045	7,5	770	92,10	21,86	36	8	481,64	10	2,66	3	-0,39
D380/W1656	17,2125	-20,8874	7,4	700	59,26	21,86	78	7	451,16	21	13,28	16	-1,00
D214/W1885	17,2125	-21,0342	7,7	1510	89,70	64,60	199	11	530,42	175	36,74	204	0,12
D383/W1663	17,2135	-20,7342	8,1	1530	14,42	12,14	351	6	474,33	67	25,23	268	0,01
D383/W1662	17,2144	-20,7595	7,3	1800	74,48	34,97	308	16	518,22	179	0,00	260	2,12
B578/W765	17,2154	-19,8793	7,7	850	115,33	49,30	18	8	665,77	5	0,00	5	-1,63
D203/W3567	17,2163	-21,2658	7,7	1280	24,03	29,87	245	14	593,82	107	24,35	62	1,98
J187/1/Y2381	17,2173	-21,7595	8,5	1840	12,01	97,86	266	32	793,80	62	7,97	250	-1,03
B108/W462	17,2183	-20,0982	6,9	720	101,31	28,66	34	8	520,66	31	0,00	7	-1,51
B486/W758	17,2183	-19,9631	7,4	860	160,98	21,61	10	4	479,21	22	45,59	37	1,26
D213/W1880	17,2183	-21,1279	8,2	1140	32,84	23,80	203	16	792,58	0	8,85	5	-1,67
D207/W1865	17,2183	-21,1892	7,7	1240	50,45	44,68	216	16	603,58	190	29,22	70	-0,91
D427/W3520	17,2212	-20,3640	7,8	990	75,68	37,88	54	10	486,52	18	11,07	34	0,07
D213/W1881	17,2240	-21,1216	7,6	680	63,27	44,20	37	13	475,55	20	1,77	18	-0,06
B486/W759	17,2240	-19,9577	7,2	710	121,73	23,07	6	1	401,17	13	50,91	24	-0,50
D384/W1661	17,2240	-20,8153	7,4	820	59,26	29,63	97	9	536,51	11	16,38	14	0,84
B327/W780	17,2250	-19,8090	7,6	1290	76,08	101,75	95	10	659,67	210	17,71	29	0,82
B482/W3509	17,2288	-19,9874	7,0	830	150,96	8,50	6	3	497,50	5	2,21	5	0,80
B580/W782	17,2298	-19,8090	7,7	700	82,49	44,20	15	5	487,74	7	4,87	5	1,04
B579/W769	17,2308	-19,8459	7,6	780	71,68	58,04	15	10	438,97	4	81,89	24	-0,08
D207/W1866	17,2308	-21,2036	7,7	1950	46,05	31,57	398	26	460,91	266	45,60	334	-0,81
B483/W3504	17,2327	-20,0342	7,4	860	146,16	7,29	8	5	502,37	6	6,64	7	-1,72
D149/W2044	17,2337	-20,5865	7,9	580	32,84	21,86	55	10	354,83	10	2,66	4	-0,77
D427/W3519	17,2337	-20,3568	7,5	930	134,55	11,41	14	1	421,90	16	48,69	18	-1,50
D287/W2042	17,2356	-20,6658	7,5	830	41,65	20,64	57	9	364,59	9	0,00	7	0,98
D389/W2036	17,2385	-20,7144	8,3	1170	43,65	28,66	176	11	554,80	50	21,69	73	-0,28
D214/W1883	17,2404	-21,0784	7,8	2280	161,78	84,02	250	19	417,02	250	32,76	518	-1,55
D214/W1884	17,2413	-21,0595	7,7	1550	126,94	65,81	151	12	445,06	110	31,43	294	0,65
D214/W1882	17,2433	-21,0829	7,6	2950	174,99	100,29	389	22	423,11	430	35,41	673	-1,39
B578/W766	17,2452	-19,9000	7,5	600	86,09	23,80	16	7	399,95	8	6,64	8	0,53
B99/W459	17,2452	-20,2243	6,9	900	159,77	19,67	19	3	462,13	17	49,58	71	-1,11
B486/W2907	17,2471	-19,9441	7,4	840	163,38	25,01	10	4	627,97	5	4,87	9	0,09
B117/W3500	17,2500	-20,0685	7,7	750	93,30	16,27	18	7	360,93	30	2,21	3	2,18
B109/W461	17,2500	-20,1486	7,0	780	90,90	34,00	40	7	530,42	10	14,17	9	-0,70
D287/W2039	17,2510	-20,6396	7,6	700	50,45	15,78	40	4	304,84	6	18,59	10	-0,39
D215/W2029	17,2510	-20,9937	7,6	1480	111,72	38,37	122	11	362,15	60	47,81	230	-0,43
B579/W770	17,2548	-19,8649	7,7	560	55,66	32,54	25	12	388,97	5	0,00	8	1,07
D287/W2041	17,2548	-20,6189	7,2	800	48,05	7,29	116	7	324,35	77	0,00	44	0,38
B99/4/W3516	17,2567	-20,3279	7,5	940	103,31	25,50	46	9	448,72	41	8,85	34	0,93
B99/4/W3515	17,2606	-20,3315	7,6	720	37,24	16,27	90	7	373,12	8	4,43	24	1,82
D385/W3603	17,2635	-20,8703	8,0	650	54,06	30,60	55	6	406,04	16	17,71	9	1,53
D385/W3604	17,2635	-20,8748	7,9	670	54,06	31,08	60	6	412,14	14	19,92	10	2,36
D389/W2035	17,2635	-20,8045	8,0	1500	22,02	12,14	285	7	386,53	125	29,22	190	-0,32

Appendix D: Hydrochemical data

Name	Long	Mlat	pH	ec μS/cm	Ca ²⁺ mg/l	Mg ²⁺ mg/l	Na ⁺ mg/l	K ⁺ mg/l	HCO ₃ ⁻ mg/l	SO ₄ ²⁻ mg/l	NO ₃ ⁻ mg/l	Cl ⁻ mg/l	Balance %
D219/W1872	17,2635	-21,1054	7,0	7500	472,51	441,97	778	56	219,48	1375	88,09	2248	-0,95
D287/W2040	17,2683	-20,6748	7,9	1520	27,23	23,31	275	9	498,71	83	26,56	205	-2,04
D216/W3589	17,2702	-20,9631	7,6	820	59,66	39,83	51	9	414,58	23	30,99	20	2,15
D385/W3605	17,2702	-20,8748	7,6	980	86,09	51,24	51	7	438,97	23	66,40	58	2,49
B581/W778	17,2731	-19,7658	7,5	500	60,87	29,87	9	3	342,64	3	1,33	5	1,04
J163/Y2106	17,2740	-21,4117	8,8	660	47,25	27,93	47	10	334,10	10	45,15	10	1,92
B117/W3499	17,2740	-20,0351	7,3	830	121,33	14,08	25	6	467,01	26	4,43	7	-0,05
J163/Y2105	17,2750	-21,3946	8,7	790	38,04	33,03	82	15	385,32	16	57,55	23	2,03
B583/Y3095	17,2750	-19,7468	7,8	880	54,06	76,01	25	3	574,31	31	0,44	4	-0,30
B582/Y2610	17,2769	-19,7523	7,2	1140	90,10	83,05	22	7	666,99	5	38,95	43	-1,62
D216/W3594	17,2769	-20,9054	8,3	1500	2,00	1,94	350	5	716,98	49	48,69	72	0,08
B581/W777	17,2798	-19,7901	7,5	760	143,76	16,51	6	3	523,10	6	7,08	8	-0,94
B581/W776	17,2808	-19,7964	7,6	450	56,46	25,98	6	2	296,30	6	5,75	8	-0,30
B99/W460	17,2808	-20,2261	6,9	720	137,75	15,78	11	2	499,93	6	16,38	16	-1,87
J187/2/Y2330	17,2808	-21,6468	7,8	980	55,26	58,04	79	14	609,68	40	23,46	19	-1,78
B582/Y2611	17,2817	-19,7667	7,1	940	142,15	28,90	19	1	586,51	17	12,84	16	-1,43
D209/W3566	17,2827	-21,2820	7,9	960	25,63	32,30	154	12	497,50	62	24,35	44	-0,62
D327/W3621	17,2837	-20,4811	6,1	50	2,00	2,43	2	2	18,29	0	0,44	5	-1,13
B485/W3492	17,2846	-19,9739	7,8	740	61,27	26,96	19	29	402,39	5	0,00	5	0,03
B580/W783	17,2846	-19,8477	7,3	1020	141,35	28,90	23	6	336,54	11	94,29	117	0,10
B327/W781	17,2913	-19,8090	7,8	360	52,06	14,08	7	4	214,61	5	4,87	11	1,88
B491/W771	17,2913	-19,9586	7,7	650	54,46	37,64	46	13	453,60	12	0,00	11	0,96
B485/W3494	17,2923	-19,9865	7,6	720	80,49	19,43	30	7	365,81	62	0,00	1	-1,49
J186/2/Y2321	17,2933	-21,5712	8,1	1000	65,27	59,01	68	17	513,35	20	104,03	45	-1,16
D216/W3591	17,2962	-20,9333	7,6	720	33,64	27,93	78	8	373,12	28	0,00	30	0,20
D215/W2028	17,2971	-21,0162	7,5	470	76,08	7,53	15	12	304,84	7	2,21	1	1,61
B99/3/W3514	17,2971	-20,2640	7,1	1320	177,79	17,00	22	13	343,86	32	221,33	68	-0,98
D210/W3561	17,2981	-21,2360	7,6	960	36,84	37,15	137	12	509,69	67	19,92	32	0,86
D388/W3607	17,2981	-20,8198	7,9	960	56,46	41,28	110	8	584,07	19	8,85	22	2,16
B485/W3493	17,2990	-19,9721	7,5	820	93,30	31,57	23	10	493,84	18	0,00	1	0,08
D286/W3611	17,3000	-20,5793	7,4	1220	59,66	29,14	191	13	613,33	57	0,44	83	1,55
B99/3/W3513	17,3000	-20,2604	7,2	1300	199,42	18,21	18	8	512,13	27	106,24	48	1,70
D209/W3565	17,3010	-21,2901	7,6	860	30,03	28,90	125	11	471,89	45	17,71	28	-0,78
D218/W1886	17,3010	-21,0604	7,5	6600	332,76	393,16	813	76	417,02	1550	120,85	1725	-1,96
D215/W2027	17,3019	-21,0495	7,8	500	37,24	25,98	15	11	281,67	15	3,98	1	-0,91
D216/W3588	17,3029	-21,0063	8,7	900	20,82	36,67	74	11	397,51	22	2,21	19	0,08
D219/W1874	17,3029	-21,1279	8,2	910	41,65	50,03	102	17	412,14	80	35,41	70	0,46
D390/W3610	17,3058	-20,7189	8,1	1280	27,23	35,70	200	13	537,73	64	2,21	108	0,38
D286/W3612	17,3077	-20,6099	7,2	940	88,50	33,51	74	10	554,80	31	8,85	28	-0,10
B792/Y2609	17,3077	-19,6928	7,5	1370	119,33	100,05	23	5	673,08	40	123,95	54	-0,23
J163/Y2107	17,3087	-21,4099	8,0	880	37,24	27,93	126	14	453,60	14	59,32	36	1,51
J187/2/Y2329	17,3106	-21,6631	7,4	790	60,07	52,94	10	14	304,84	10	97,39	56	-1,26
D216/W3590	17,3115	-20,9495	7,6	1100	40,04	25,50	165	10	487,74	64	8,85	66	0,87
B492/W773	17,3125	-19,8910	7,3	900	145,76	38,13	6	3	548,71	18	32,31	27	0,46
B581/W779	17,3135	-19,8027	7,3	790	137,35	22,83	8	2	557,24	6	2,21	5	-1,63
D286/W3613	17,3135	-20,6405	7,3	900	74,88	31,08	97	9	586,51	24	6,64	12	0,88
B497/W774	17,3154	-19,8405	7,4	730	92,50	36,91	15	8	409,70	81	0,44	16	-2,01
D210/W3562	17,3154	-21,2423	7,9	1040	17,22	29,14	183	28	536,51	47	44,27	48	0,40
B492/W772	17,3163	-19,8946	7,0	770	139,35	18,46	6	4	447,50	15	38,51	24	-0,61
B582/Y2612	17,3183	-19,7757	7,0	1050	95,30	59,98	50	4	666,99	48	0,44	18	-1,95
D209/W3564	17,3212	-21,2946	7,5	1020	32,03	46,38	119	31	546,27	44	30,99	40	-0,49
J154/Y2332	17,3212	-21,4829	7,8	1950	96,10	68,97	197	19	417,02	95	348,39	184	-0,24
D390/W3609	17,3231	-20,6955	7,9	1750	48,85	22,58	300	12	429,21	118	4,43	280	0,55

Appendix D: Hydrochemical data

Name	Long	Mlat	pH	ec µS/cm	Ca ²⁺ mg/l	Mg ²⁺ mg/l	Na ⁺ mg/l	K ⁺ mg/l	HCO ₃ ⁻ mg/l	SO ₄ ²⁻ mg/l	NO ₃ ⁻ mg/l	Cl ⁻ mg/l	Balance %
B583/Y3094	17,3240	-19,7441	7,0	1040	108,12	63,87	20	3	631,62	40	19,03	6	-0,27
D386/1/W3602	17,3250	-20,8838	7,8	1140	38,44	37,15	180	11	642,60	41	15,49	46	0,59
J186/2/Y2326	17,3279	-21,5306	8,5	1280	29,23	60,95	171	29	590,17	90	23,90	94	0,24
B112/W3503	17,3298	-20,1748	7,8	540	64,87	11,17	11	3	242,65	21	8,85	12	-1,91
B114/W3501	17,3298	-20,1658	7,2	860	139,35	6,31	8	2	332,88	15	84,11	22	0,82
D218/W1888	17,3317	-21,1036	7,6	890	37,24	42,74	131	16	499,93	80	23,90	30	1,74
B793/1/Y2554	17,3327	-19,6820	8,0	620	68,87	55,85	5	1	451,16	20	0,44	13	0,56
D327/W3622	17,3327	-20,5306	7,5	1400	71,68	19,91	204	9	432,87	92	6,64	180	0,44
D286/W3614	17,3337	-20,6234	7,6	550	46,45	16,27	60	6	345,08	17	15,49	6	-0,06
D210/W3563	17,3337	-21,2495	7,7	1220	26,83	38,85	199	23	554,80	119	42,05	48	0,65
D216/W3592	17,3337	-20,9856	7,0	5800	381,21	291,65	300	25	402,39	690	42,50	1303	-1,47
B121/W3498	17,3356	-20,0261	7,6	940	98,51	26,71	28	6	335,32	28	66,40	50	-0,44
D386/1/W3601	17,3356	-20,9063	8,0	1750	14,42	9,71	407	5	881,59	114	4,43	74	0,96
D388/W3608	17,3365	-20,8018	7,7	1040	60,47	46,63	116	12	634,06	23	19,92	24	1,40
D286/W3615	17,3375	-20,6234	7,6	540	44,85	14,33	55	5	325,57	17	11,07	4	-0,37
B485/W3495	17,3375	-19,9820	7,2	880	99,71	23,07	18	6	402,39	15	23,02	25	-1,09
D332/W3623	17,3394	-20,4315	7,0	210	29,63	3,40	9	5	115,84	5	0,89	6	2,06
B485/W3496	17,3394	-19,9676	7,5	820	105,72	20,88	23	10	475,55	10	16,38	4	-0,77
D332/W3626	17,3404	-20,4225	7,7	100	15,22	2,91	3	3	59,75	2	0,44	5	1,57
D286/W3616	17,3404	-20,6234	7,8	490	42,45	14,81	43	6	298,74	13	6,64	4	-0,24
D216/W3593	17,3404	-21,0027	7,5	2550	34,84	42,25	429	18	615,77	343	0,44	285	-1,90
B792/Y2608	17,3433	-19,7144	7,1	1200	120,13	70,91	56	3	677,96	110	0,44	25	0,80
D285/W3620	17,3442	-20,6135	7,3	760	82,89	29,14	54	7	490,18	24	0,44	10	1,34
D332/W3624	17,3452	-20,4225	7,5	210	31,23	3,40	9	4	129,25	0	2,21	7	-0,41
B121/W3497	17,3452	-20,0396	7,4	850	124,94	16,76	21	5	454,82	28	11,07	8	1,25
B583/Y3092	17,3452	-19,7676	7,1	930	93,30	57,07	20	2	608,46	9	9,74	7	-1,16
J84/Y1439	17,3462	-21,6784	7,1	820	65,27	42,01	46	19	424,33	20	42,50	40	0,09
D332/W3625	17,3481	-20,4243	6,9	210	24,83	7,77	8	5	128,03	5	2,21	5	-0,53
D285/W3617	17,3490	-20,6180	7,5	880	87,70	34,00	63	8	534,08	19	28,77	16	0,27
B583/Y3093	17,3500	-19,7622	6,6	2630	275,50	160,03	87	5	552,37	105	469,22	410	0,75
D386/W3598	17,3519	-20,9369	7,5	1440	77,28	60,95	161	10	557,24	143	0,44	120	1,99
B127/W3502	17,3548	-20,1640	7,2	1250	193,01	10,20	16	4	420,68	31	123,95	72	-1,32
J225/Y248	17,3587	-21,5676	7,5	1140	30,03	63,87	117	22	518,22	54	74,37	48	0,96
D386/1/W360C	17,3596	-20,8973	7,8	2000	73,28	76,49	270	12	679,18	237	28,77	173	1,37
B456/Y5717	17,3606	-19,2333	7,8	920	103,31	57,07	23	2	603,58	27	16,38	15	-1,08
D223/Y1207	17,3606	-21,2829	8,0	950	23,23	27,93	153	14	548,71	25	30,10	18	-0,23
B493/W3487	17,3615	-19,9243	7,2	940	168,58	16,27	3	1	573,10	7	0,44	3	1,42
D223/Y1205	17,3615	-21,2865	8,2	990	33,24	32,06	152	13	556,02	42	37,19	18	0,65
D387/Y669	17,3615	-20,8640	7,8	1350	67,27	53,91	163	10	709,66	53	16,38	60	1,50
J83/Y2031	17,3635	-21,6991	7,6	1580	55,26	30,11	280	12	763,31	165	1,77	86	-1,88
D223/Y1206	17,3644	-21,2892	8,1	1110	31,23	34,00	173	13	542,61	35	63,75	47	0,99
D388/W3606	17,3654	-20,8324	7,7	760	62,87	42,74	51	11	479,21	16	15,49	16	1,47
D231/W3585	17,3663	-21,1027	7,7	760	43,25	36,18	60	9	384,10	27	30,99	24	-0,36
D231/W3587	17,3683	-21,1333	7,8	980	50,05	46,14	86	11	420,68	49	77,47	32	1,23
D391/Y676	17,3683	-20,7315	7,5	1350	49,25	32,06	198	10	540,17	43	1,77	131	1,79
B498/W3485	17,3702	-19,8360	7,2	800	130,14	18,94	5	2	481,64	7	8,85	5	-0,01
B501/W3483	17,3702	-19,8063	7,6	900	82,49	62,17	16	8	579,19	6	0,00	2	2,32
B139/Y3778	17,3721	-20,0117	7,0	680	95,30	18,94	40	4	459,70	9	0,00	2	2,38
B456/Y5718	17,3721	-19,2090	7,4	1410	200,22	65,08	18	1	519,44	25	201,41	140	-0,23
B139/Y3777	17,3731	-20,0072	7,6	700	70,08	17,97	57	7	436,53	15	0,00	5	0,17
B498/W3484	17,3740	-19,8252	7,4	700	102,51	19,91	7	2	414,58	8	3,10	4	-0,10
B455/Y5721	17,3740	-19,2468	7,1	1080	147,36	50,03	15	5	637,72	31	57,55	18	-1,14
B793/Y2606	17,3740	-19,7027	6,9	1330	128,14	75,04	80	4	701,13	150	3,54	41	1,01

Appendix D: Hydrochemical data

Name	Long	Mlat	pH	ec µS/cm	Ca ²⁺ mg/l	Mg ²⁺ mg/l	Na ⁺ mg/l	K ⁺ mg/l	HCO ₃ ⁻ mg/l	SO ₄ ²⁻ mg/l	NO ₃ ⁻ mg/l	Cl ⁻ mg/l	Balance %
B493/W3488	17,3750	-19,8838	7,2	910	161,38	15,30	3	1	570,66	8	7,53	2	-1,19
D285/W3618	17,3769	-20,6189	7,8	1240	12,01	10,20	250	8	434,09	79	26,56	120	-0,22
B498/W3486	17,3779	-19,8252	7,6	780	120,93	20,88	7	2	469,45	10	0,00	4	0,58
D386/W3599	17,3788	-20,9297	7,6	3900	73,28	87,67	771	25	1364,45	540	33,20	363	0,75
B335/W3490	17,3798	-19,9856	7,5	800	120,13	21,86	11	11	499,93	8	0,44	4	0,43
J84/Y1438	17,3798	-21,6225	7,6	1020	42,05	71,88	53	25	514,57	9	99,60	38	-1,53
B493/W3489	17,3808	-19,8955	7,4	900	150,96	17,73	3	1	518,22	7	22,13	3	0,37
D387/Y670	17,3808	-20,8396	7,9	1050	70,08	42,98	102	7	574,31	13	25,67	40	1,86
B335/W3491	17,3827	-19,9928	7,2	830	133,35	15,30	14	3	493,84	9	2,21	5	0,83
D392/Y673	17,3827	-20,8045	7,8	1290	60,07	44,93	147	12	553,59	66	21,69	83	0,97
D386/W3596	17,3827	-20,9523	8,0	1300	44,05	41,77	176	9	556,02	85	23,90	82	-0,22
J84/Y1437	17,3837	-21,6595	7,3	1190	81,29	68,00	41	18	452,38	10	172,64	64	-1,31
B133/W3750	17,3856	-20,2279	6,7	90	6,01	2,91	3	8	40,24	3	3,54	2	2,29
D386/W3597	17,3865	-20,9586	7,6	1240	52,46	51,97	168	9	606,02	85	19,92	80	0,53
B793/Y2605	17,3865	-19,7099	7,0	1370	126,14	66,05	99	5	684,06	170	15,49	46	-0,41
D386/W3595	17,3865	-20,9477	7,4	1460	54,06	51,24	168	10	542,61	90	50,91	104	-0,15
B793/Y2607	17,3865	-19,7099	6,9	1560	140,15	76,98	109	5	649,91	220	38,07	77	0,50
D235/Y1025	17,3894	-20,9991	8,3	760	34,04	40,07	81	9	404,82	24	22,13	37	1,24
D392/Y674	17,3894	-20,7622	8,0	1610	40,04	35,94	272	0	608,46	62	25,23	166	1,31
J82/Y2030	17,3894	-21,7000	7,9	1620	10,01	9,96	395	23	796,24	92	24,79	108	1,81
B799/2/Y4973	17,3904	-19,6108	7,1	810	132,14	26,96	8	1	485,30	6	42,50	6	1,40
D391/Y675	17,3904	-20,6982	8,0	1520	86,09	42,98	170	12	363,37	105	10,62	260	-0,36
B505/Y4525	17,3913	-19,7748	7,5	960	97,31	56,10	32	2	616,99	22	3,10	17	-0,84
D334/Y2488	17,3933	-20,4027	7,3	400	59,26	3,89	17	5	235,33	6	5,75	4	-0,51
B799/1/Y4972	17,3933	-19,6162	7,9	960	92,10	59,98	45	3	649,91	30	0,44	6	0,49
D223/Y1203	17,3933	-21,2919	8,3	1740	44,05	67,27	218	17	514,57	170	43,38	185	-0,67
D334/Y2489	17,3942	-20,3991	7,0	270	34,04	2,91	17	5	158,52	7	4,43	2	-1,16
J82/Y2029	17,3942	-21,6991	7,4	1030	50,05	42,01	121	21	646,26	32	27,45	15	-1,54
J224/Y2312	17,3942	-21,5604	7,9	1370	76,08	69,94	109	19	476,77	39	265,61	90	-2,21
B139/Y3774	17,3942	-20,0631	6,9	1730	135,35	44,93	176	8	557,24	73	11,95	255	0,75
J82/Y2027	17,3981	-21,7505	7,7	680	60,07	36,91	35	5	443,84	8	25,68	3	-1,63
B794/Y2603	17,3981	-19,6694	7,8	710	70,08	53,91	2	2	499,93	6	3,10	3	-2,31
B794/5/Y4626	17,3990	-19,6982	7,3	1460	129,34	73,10	110	6	704,79	180	3,10	58	1,23
B136/Y3769	17,3990	-20,0946	7,5	1820	39,24	68,97	250	10	465,79	286	26,56	196	-2,04
D393/Y672	17,4000	-20,8225	7,4	1110	60,07	45,90	116	10	570,66	20	22,13	48	2,53
B799/3/Y4974	17,4010	-19,6144	7,3	940	106,12	59,98	12	1	645,04	7	20,36	4	-1,73
D285/W3619	17,4019	-20,6658	7,9	1260	32,03	21,13	214	10	453,60	70	13,28	140	-0,59
D391/Y678	17,4019	-20,7153	8,0	1590	88,10	43,95	197	12	415,80	124	7,53	265	-0,30
B794/Y2604	17,4038	-19,6604	7,5	650	63,27	50,03	1	1	448,72	6	3,98	2	-1,72
D391/Y677	17,4038	-20,7171	8,4	1820	16,02	11,90	364	7	577,97	140	0,44	215	-1,84
B139/Y3775	17,4038	-20,0423	7,4	3190	149,36	48,08	500	19	660,89	245	0,00	670	-1,73
B488/Y3779	17,4048	-19,9703	7,0	632	105,31	15,06	15	4	434,09	6	0,44	1	-0,17
B488/Y3780	17,4048	-19,9450	7,2	680	135,35	14,08	3	1	457,26	5	0,44	4	2,23
D334/1/Y2490	17,4048	-20,4432	8,2	730	25,23	1,94	107	5	91,45	13	11,51	148	0,58
B505/Y4523	17,4048	-19,7297	7,7	990	100,11	68,97	21	4	640,16	49	0,44	6	-0,01
B799/4/Y4986	17,4048	-19,6090	7,3	1040	100,11	75,04	17	1	710,88	15	5,31	14	-2,08
B505/Y4522	17,4048	-19,7568	7,9	1100	114,12	69,94	30	4	693,81	58	23,02	11	-1,54
B799/5/Y4987	17,4048	-19,6045	7,3	2250	130,14	104,91	225	1	735,27	305	101,81	175	-0,08
B455/Y5722	17,4058	-19,2640	7,3	960	136,15	51,00	10	1	662,11	20	3,54	7	-0,31
B505/Y4521	17,4058	-19,7550	7,4	1120	115,33	71,88	31	4	690,15	57	21,69	8	0,18
D232/Y1081	17,4077	-21,1261	8,5	780	66,07	32,06	61	7	397,51	32	29,22	31	1,39
B502/Y3798	17,4096	-19,8288	6,9	840	156,17	23,07	3	3	557,24	8	0,44	10	1,59
B133/Y3751	17,4106	-20,1802	7,0	750	85,29	22,10	44	5	476,77	7	8,85	6	-0,94

Appendix D: Hydrochemical data

Name	Long	Lat	pH	ec µS/cm	Ca ²⁺ mg/l	Mg ²⁺ mg/l	Na ⁺ mg/l	K ⁺ mg/l	HCO ₃ ⁻ mg/l	SO ₄ ²⁻ mg/l	NO ₃ ⁻ mg/l	Cl ⁻ mg/l	Balance %
B139/Y3776	17,4106	-19,9955	7,0	1270	158,17	26,96	59	6	476,77	20	52,23	140	-0,74
B502/Y3797	17,4115	-19,8342	7,0	790	145,36	20,88	3	1	540,17	5	0,44	7	-0,18
D234/Y1085	17,4125	-21,0414	7,9	650	73,28	25,01	30	5	338,98	11	34,09	20	1,78
B456/Y5719	17,4125	-19,1910	7,4	940	129,34	57,07	11	1	657,23	20	5,75	6	0,89
B794/4/Y4625	17,4125	-19,6757	7,2	1040	102,11	68,00	39	3	686,49	27	16,82	12	0,17
B456/Y5720	17,4135	-19,2153	7,7	680	66,07	51,97	9	1	434,09	15	10,62	6	1,42
B798/1/Y4628	17,4173	-19,6459	7,7	770	88,10	58,04	2	1	543,83	5	4,43	4	0,45
D232/Y1080	17,4173	-21,0955	7,8	880	58,06	34,00	85	7	421,90	53	32,32	33	0,53
D335/Y2491	17,4183	-20,3820	7,3	270	37,24	1,94	13	5	148,76	4	3,98	2	1,30
B794/3/Y4624	17,4202	-19,6658	7,3	1040	104,11	73,10	37	2	688,93	23	40,28	14	0,22
B139/Y3773	17,4202	-20,0486	6,9	1820	159,37	44,93	176	7	540,17	81	24,35	295	0,60
B794/2/Y4622	17,4212	-19,6595	7,4	880	110,12	60,95	1	1	645,04	6	0,44	6	-1,36
B794/1/Y4518	17,4212	-19,6955	7,1	1030	109,32	80,87	6	1	734,05	5	0,44	1	0,92
B130/W3767	17,4221	-20,1216	7,0	830	132,14	13,11	25	7	402,39	34	42,05	28	0,96
B794/2/Y4623	17,4231	-19,6613	7,5	870	110,12	60,95	1	0	615,77	5	10,62	8	-0,17
D235/Y1026	17,4231	-20,9739	7,8	1330	38,04	41,04	200	11	553,59	72	90,75	86	-0,71
B798/Y4627	17,4240	-19,6505	7,4	810	103,31	54,88	1	1	580,41	5	3,54	4	-0,23
827	17,4240	-20,5676	8,0	1620	52,06	46,87	247	11	512,13	185	56,66	124	2,41
B794/1/Y4517	17,4250	-19,6919	7,3	1030	100,11	84,02	10	2	729,17	4	5,31	5	0,55
B488/Y3781	17,4260	-19,9577	7,5	980	160,17	19,91	22	3	445,06	20	104,03	44	0,17
B794/1/Y4516	17,4260	-19,6892	7,4	1030	105,31	76,01	8	1	741,37	4	0,44	1	-1,59
828	17,4269	-20,5568	7,2	2760	136,15	124,09	284	16	374,34	490	35,41	500	-2,05
D223/Y1201	17,4308	-21,2964	8,0	970	75,28	59,98	22	8	371,90	59	52,24	69	-1,29
B509/Y4514	17,4317	-19,7072	7,8	1300	63,27	75,04	116	6	542,61	185	0,44	59	0,40
B457/Y5728	17,4317	-19,1829	7,4	1320	29,23	8,01	305	0	724,29	39	57,55	39	2,25
B138/Y3771	17,4327	-19,9982	6,9	890	104,11	27,93	45	6	529,20	31	17,71	9	-1,30
B505/Y4524	17,4327	-19,7775	7,7	2470	120,13	185,04	99	7	546,27	95	371,84	280	1,74
D229/Y1089	17,4337	-21,1748	7,8	790	59,26	34,97	65	7	387,75	42	44,27	20	1,93
J80/Y2025	17,4346	-21,8243	7,5	1030	150,16	31,08	57	8	671,86	23	9,30	30	0,99
B499/Y3795	17,4356	-19,8450	6,8	910	130,14	26,96	3	35	584,07	10	0,44	5	-0,97
B784/Y4817	17,4375	-19,5793	6,9	860	83,29	57,07	21	3	560,90	9	0,44	1	2,22
B502/Y3799	17,4385	-19,8198	6,9	810	145,36	20,88	3	3	531,64	5	7,97	12	-0,57
D233/Y1072	17,4385	-21,1189	7,9	840	74,08	34,97	51	7	373,12	17	45,60	51	1,87
B798/2/Y4629	17,4394	-19,6414	7,4	810	104,11	51,00	1	1	565,78	8	4,43	1	-0,41
J224/Y2307	17,4394	-21,5099	7,8	1110	70,08	46,87	115	13	609,68	63	46,92	42	-2,15
J85/Y171	17,4413	-21,6234	7,3	1390	100,11	69,94	59	13	402,39	30	243,47	80	0,91
B135/Y3766	17,4423	-20,1135	6,8	860	158,17	10,93	10	4	540,17	27	0,00	4	-1,05
B798/8/Y4631	17,4423	-19,6523	7,7	970	97,31	71,88	29	1	686,49	26	2,66	1	0,81
B494/Y3794	17,4433	-19,8811	7,2	1810	55,26	71,88	265	13	937,68	39	68,61	106	0,63
B506/Y4519	17,4442	-19,7495	7,5	1140	122,13	61,92	40	2	636,50	95	19,92	17	-0,87
B585/Y4829	17,4452	-19,5153	7,3	860	152,17	13,11	9	1	536,51	9	7,97	12	-1,93
D229/Y1094	17,4481	-21,1910	8,1	660	52,06	34,00	52	7	391,41	26	15,05	9	2,51
B495/Y3792	17,4481	-19,9189	7,0	820	156,17	13,11	1	1	537,73	5	0,44	8	-1,15
B509/Y4515	17,4481	-19,7270	7,8	1050	115,33	70,91	21	3	599,92	120	9,74	6	-0,30
B798/4/Y4630	17,4490	-19,6414	7,8	420	45,25	23,07	9	1	275,57	5	3,54	1	-1,43
B798/5/Y4632	17,4490	-19,6423	7,6	510	32,03	31,08	38	0	340,20	7	2,66	6	-1,03
B138/Y3770	17,4529	-20,0360	7,2	1120	122,13	42,98	66	7	597,48	35	15,05	58	1,13
B457/Y5729	17,4538	-19,1865	7,9	1100	124,14	68,00	19	3	604,80	27	101,81	40	-2,13
D234/1/Y1028	17,4548	-21,0027	7,9	820	47,25	32,06	96	7	425,55	47	31,87	30	0,20
D235/Y1027	17,4558	-20,9532	7,7	750	47,25	42,01	55	10	421,90	35	20,36	23	-0,92
B495/Y3793	17,4558	-19,9180	7,1	770	148,16	15,06	2	1	520,66	5	0,44	6	-0,39
B499/Y3796	17,4558	-19,8559	7,0	790	136,15	23,07	2	1	525,54	5	3,54	4	-0,46
B509/Y4513	17,4567	-19,6766	7,4	940	111,32	68,97	4	1	674,30	5	0,44	1	1,06

Appendix D: Hydrochemical data

Name	Long	Lat	pH	ec µS/cm	Ca ²⁺ mg/l	Mg ²⁺ mg/l	Na ⁺ mg/l	K ⁺ mg/l	HCO ₃ ⁻ mg/l	SO ₄ ²⁻ mg/l	NO ₃ ⁻ mg/l	Cl ⁻ mg/l	Balance %
D234/Y1084	17,4577	-21,0405	7,7	840	55,26	36,91	67	14	408,48	32	36,74	32	1,18
D233/Y1070	17,4587	-21,0694	7,8	1030	60,07	36,91	106	26	501,15	47	42,05	37	1,79
B784/Y4816	17,4596	-19,5847	6,9	1090	111,32	75,04	9	1	660,89	5	29,66	22	0,47
D423/1/Y681	17,4596	-20,7153	8,5	2030	16,02	25,98	430	9	875,49	53	16,82	200	1,17
D423/1/Y679	17,4606	-20,7468	7,5	5250	79,29	110,01	930	19	713,32	550	15,49	1020	1,68
B489/Y3782	17,4625	-19,9568	7,0	670	120,13	10,93	9	2	419,46	4	14,17	10	-0,89
B752/Y4818	17,4635	-19,5883	6,9	1370	135,35	94,95	14	1	660,89	4	70,83	90	2,04
D233/Y1073	17,4644	-21,1054	8,3	2250	145,36	84,99	168	64	553,59	120	230,19	260	1,26
B512/3/Y4633	17,4683	-19,6387	7,8	500	32,03	26,96	43	1	337,76	5	0,44	1	0,33
829	17,4692	-20,6541	7,6	1300	102,11	62,90	62	37	568,22	40	154,93	45	0,00
B507/Y4509	17,4692	-19,7414	7,3	1460	150,16	93,01	32	3	632,84	225	44,71	40	-0,86
D233/Y1074	17,4692	-21,0964	8,1	1480	56,06	53,91	182	25	546,27	73	126,16	102	1,30
D336/Y2953	17,4692	-20,5252	7,6	2760	97,31	10,93	465	11	86,57	275	0,44	670	0,41
B49/Y4850	17,4702	-19,4604	7,2	940	86,09	62,90	34	6	601,14	40	2,66	6	0,94
B964/Y3752	17,4740	-20,2117	6,6	70	6,01	1,94	2	6	31,70	4	3,54	2	-1,15
B510/Y4512	17,4740	-19,7243	8,0	900	71,28	76,01	23	3	606,02	48	0,44	6	-1,00
B136/Y3768	17,4750	-20,0568	7,2	2090	200,22	67,02	149	8	476,77	209	227,97	235	-0,62
D393/Y671	17,4750	-20,8225	8,3	6420	16,02	16,03	1480	6	1438,83	650	29,22	920	2,39
B503/Y4520	17,4769	-19,8027	7,6	1850	127,34	125,06	38	5	370,68	20	219,12	315	-1,30
D237/Y1030	17,4769	-20,9117	7,8	2070	31,23	40,07	408	19	634,06	305	46,04	200	-0,08
J80/Y2023	17,4798	-21,8207	7,3	1090	120,13	35,94	80	11	609,68	83	9,74	44	-1,57
B489/Y3783	17,4808	-19,9414	7,2	1180	186,20	16,03	50	10	548,71	45	37,18	82	0,77
B489/Y3784	17,4817	-19,9441	7,7	550	87,29	8,01	3	26	332,88	5	0,44	2	1,64
J80/Y2024	17,4827	-21,8162	7,4	900	150,16	28,90	19	11	599,92	30	3,98	14	0,29
B138/Y3772	17,4837	-20,0018	7,0	750	131,34	4,61	13	15	379,22	17	66,40	6	0,47
B510/Y4511	17,4837	-19,6802	7,5	880	110,12	58,04	1	1	640,16	4	3,54	1	-1,52
D233/Y1069	17,4846	-21,0802	7,6	690	68,07	19,91	54	6	349,95	29	20,36	20	2,07
D291/Y2957	17,4856	-20,3252	6,9	70	2,00	0,97	1	8	14,63	4	1,77	2	2,38
B586/Y4832	17,4856	-19,4847	7,0	940	88,10	57,07	25	4	582,85	32	0,44	3	-0,14
B135/Y3765	17,4865	-20,0865	6,9	780	138,15	11,90	15	3	431,65	28	10,62	16	1,91
B586/Y4833	17,4865	-19,4874	7,1	1040	83,29	69,94	38	3	637,72	46	1,77	6	0,15
B135/Y3764	17,4894	-20,0802	7,0	1330	210,23	18,94	41	5	359,71	86	201,41	94	1,36
B585/Y4828	17,4904	-19,5297	6,8	930	156,17	17,00	9	1	523,10	8	35,41	20	-1,36
B586/Y4830	17,4904	-19,5216	6,8	1000	190,21	10,93	8	1	523,10	10	43,82	32	1,77
D304/Y2952	17,4923	-20,3703	5,9	60	5,21	1,94	2	5	29,26	4	0,44	2	0,64
J221/Y222	17,4923	-21,4847	7,9	1330	53,26	34,97	195	3	765,75	37	24,35	11	0,25
D336/Y2954	17,4923	-20,4613	7,9	4420	255,48	24,04	660	15	143,88	340	5,75	1200	0,51
D423/1/Y680	17,4923	-20,7477	7,8	6100	120,13	70,91	1127	19	1099,85	370	4,43	1320	-1,36
J85/Y173	17,4933	-21,6189	8,2	1070	52,06	65,08	81	18	595,04	36	6,64	28	2,31
B49/Y4851	17,4942	-19,4703	7,2	890	102,11	52,94	27	4	593,82	29	0,44	6	1,02
D237/Y1031	17,4962	-20,9748	7,6	910	38,04	42,98	106	12	474,33	43	54,01	29	-0,02
B144/Y3763	17,4962	-20,0369	7,2	1540	106,12	60,95	167	7	637,72	193	0,00	98	1,49
D423/Y682	17,4962	-20,8036	7,3	5670	142,15	101,02	1090	10	954,75	1150	13,72	760	1,47
B586/Y4831	17,4971	-19,5252	6,8	980	180,20	10,93	5	1	523,10	8	38,51	29	-0,22
D423/Y684	17,4981	-20,8090	8,3	2780	31,23	23,07	620	5	1073,03	405	1,77	124	1,68
826	17,5000	-20,5505	7,4	2430	90,10	85,97	346	20	485,30	450	61,97	325	-0,65
B49/Y4849	17,5010	-19,4432	7,1	910	127,34	42,01	18	4	593,82	48	0,44	4	-0,72
J87/1/Y174	17,5010	-21,7306	7,2	970	71,28	48,08	66	11	562,12	16	11,95	18	2,01
B510/Y4510	17,5010	-19,7117	7,7	1030	90,10	78,92	25	2	707,22	40	0,44	5	-1,79
D243/Y1079	17,5019	-21,1180	8,3	770	75,28	30,11	40	7	352,39	12	52,24	43	0,45
B459/Y5758	17,5019	-19,2018	7,4	940	105,31	59,01	11	1	615,77	20	6,64	4	-0,53
D423/Y687	17,5019	-20,8144	7,9	2140	22,02	16,03	465	4	969,38	185	0,44	84	1,41
B459/Y5759	17,5029	-19,1703	6,8	1000	115,33	61,92	10	1	670,64	20	0,44	4	-0,95

Appendix D: Hydrochemical data

Name	Long	Mlat	pH	ec µS/cm	Ca ²⁺ mg/l	Mg ²⁺ mg/l	Na ⁺ mg/l	K ⁺ mg/l	HCO ₃ ⁻ mg/l	SO ₄ ²⁻ mg/l	NO ₃ ⁻ mg/l	Cl ⁻ mg/l	Balance %
D237/Y1032	17,5029	-20,9721	7,4	2010	117,33	107,09	167	25	660,89	100	287,73	166	0,75
B752/Y4826	17,5058	-19,6018	7,2	1200	101,31	100,05	13	1	718,20	9	36,30	35	1,27
B514/Y4646	17,5067	-19,6423	7,4	480	33,24	24,04	36	0	320,69	7	0,44	1	-2,17
D238/Y695	17,5067	-20,8883	7,5	5030	69,28	105,88	885	27	536,51	630	163,79	990	-1,08
B459/Y5757	17,5077	-19,2018	8,0	620	38,04	53,91	10	1	385,32	20	6,20	4	-1,08
B500/Y3800	17,5077	-19,8342	7,3	860	150,16	17,73	10	5	493,84	18	38,95	14	0,13
D304/Y2951	17,5077	-20,4018	7,9	1710	138,15	20,88	141	9	91,45	20	3,54	450	1,05
B758/Y4639	17,5087	-19,6559	7,8	1100	161,38	41,04	14	1	469,45	5	75,70	92	1,90
D243/Y1078	17,5106	-21,1009	7,9	900	72,08	42,01	49	8	346,30	26	84,11	62	0,36
B49/Y4852	17,5135	-19,4550	7,0	910	133,35	39,10	17	4	581,63	49	0,44	4	0,19
B585/Y4827	17,5135	-19,5477	6,8	910	175,39	11,90	4	1	579,19	4	2,66	4	1,02
B5111/Y4508	17,5135	-19,7126	7,5	1080	105,31	74,07	27	2	707,22	34	10,62	10	-0,69
B752/Y4821	17,5154	-19,5865	7,0	980	81,29	75,04	17	1	627,97	4	12,39	6	1,16
B48/Y5670	17,5154	-19,4216	7,6	2110	113,32	154,93	141	48	1055,96	125	41,17	150	1,90
D423/Y685	17,5163	-20,8045	8,0	1350	33,24	16,03	268	4	674,30	54	19,92	58	2,09
D423/Y683	17,5163	-20,7919	7,4	3210	94,10	69,94	560	6	629,19	450	37,18	470	2,08
B146/Y3789	17,5192	-19,9865	7,6	810	164,18	5,10	3	4	476,77	5	14,17	26	-0,19
B496/Y3801	17,5212	-19,8676	7,3	820	140,15	16,03	7	7	436,53	12	40,73	32	-0,94
B144/Y3761	17,5212	-20,0757	7,0	1010	175,39	16,03	15	4	413,36	30	72,15	67	1,76
B752/Y4825	17,5221	-19,6072	7,7	840	57,26	80,87	3	1	560,90	5	0,44	4	1,32
B147/Y3790	17,5231	-19,9198	7,2	870	140,15	31,08	4	3	540,17	10	17,71	16	0,02
B508/Y4495	17,5231	-19,7649	7,3	1230	100,11	87,91	48	6	787,70	81	0,44	3	-0,74
B49/Y4846	17,5269	-19,4874	7,2	910	97,31	51,97	25	7	564,56	27	13,28	14	-0,12
D238/Y696	17,5269	-20,8874	8,5	1580	3,20	22,10	324	22	747,46	100	0,44	72	0,80
B147/Y3791	17,5308	-19,9171	7,4	820	140,15	26,96	3	1	543,83	5	10,62	5	0,21
B752/Y4824	17,5317	-19,5964	7,6	500	34,04	41,04	4	1	304,84	5	7,97	6	-1,15
B752/Y4823	17,5317	-19,5892	7,0	770	68,07	59,98	4	1	493,84	4	11,51	4	0,34
B761/Y7841	17,5317	-19,2892	7,5	810	79,29	60,95	8	1	540,17	14	7,53	4	-0,17
B49/Y4853	17,5317	-19,4676	7,5	860	128,14	37,88	16	4	574,31	26	0,44	3	1,30
D338/Y2955	17,5317	-20,4802	7,4	2760	225,45	18,94	285	11	112,18	215	0,44	660	1,09
B758/Y4640	17,5337	-19,6459	7,7	800	127,34	24,04	14	1	462,13	4	37,63	21	0,62
D239/Y1041	17,5337	-20,9486	8,0	1960	117,33	84,02	200	12	391,41	245	69,06	310	0,93
B144/Y3762	17,5346	-20,0739	6,8	1040	200,22	15,06	11	3	540,17	25	33,64	52	1,74
D238/Y694	17,5346	-20,9135	7,5	1410	45,25	42,01	214	12	512,13	155	70,83	80	1,03
B49/Y4847	17,5356	-19,5045	7,4	850	115,33	37,88	17	3	574,31	26	0,44	4	-1,95
B504/Y4493	17,5375	-19,8126	7,5	590	98,11	17,00	6	2	360,93	5	30,54	8	-0,98
D243/Y1076	17,5375	-21,1090	8,5	1390	37,24	41,04	226	15	636,50	110	45,60	68	0,24
B508/Y4496	17,5385	-19,7477	7,4	1030	108,12	74,07	14	3	701,13	32	0,44	8	-0,87
B761/Y6413	17,5385	-19,1937	7,2	1120	104,11	84,99	14	1	756,00	6	16,82	17	-1,69
B967/Y3753	17,5404	-20,2081	6,8	160	12,01	2,91	6	8	69,50	4	2,66	3	-1,69
B5111/Y4507	17,5404	-19,6883	7,3	860	100,11	54,88	4	1	599,92	5	2,66	4	-1,92
D244/Y1066	17,5413	-21,0640	7,7	1090	67,27	45,90	115	11	425,55	170	27,00	59	-0,78
B508/Y4494	17,5423	-19,7631	7,5	830	58,06	41,04	70	4	518,22	15	28,77	8	-0,39
D227/Y1107	17,5423	-21,2000	7,8	1290	103,31	84,99	32	15	380,44	17	258,97	94	1,86
B148/Y4813	17,5433	-19,9108	7,2	940	138,15	25,98	9	5	541,39	9	15,94	18	-1,41
D404/Y691	17,5452	-20,8766	7,9	960	37,24	33,03	106	14	380,44	42	36,30	68	-0,35
D227/Y1106	17,5452	-21,2036	7,7	1080	85,29	70,91	33	14	380,44	10	192,57	68	1,79
B148/Y4814	17,5462	-19,9072	6,7	910	134,15	26,96	12	7	515,79	11	20,81	24	-0,42
B5111/Y4506	17,5471	-19,6883	7,4	790	99,31	50,03	1	1	546,27	6	3,54	1	-0,12
B49/Y4848	17,5471	-19,4793	7,2	840	114,12	28,90	24	8	496,28	25	17,71	18	-0,67
B148/Y4815	17,5481	-19,9414	6,9	1070	140,15	31,08	17	13	481,64	11	90,75	50	-1,72
D243/Y1077	17,5490	-21,0928	8,4	880	55,26	30,11	108	11	425,55	92	6,64	26	2,43
D225/Y1114	17,5490	-21,2306	7,5	1540	103,31	90,09	95	23	532,86	61	192,57	122	2,19

Appendix D: Hydrochemical data

Name	Long	Mlat	pH	ec µS/cm	Ca ²⁺ mg/l	Mg ²⁺ mg/l	Na ⁺ mg/l	K ⁺ mg/l	HCO ₃ ⁻ mg/l	SO ₄ ²⁻ mg/l	NO ₃ ⁻ mg/l	Cl ⁻ mg/l	Balance %
B785/Y5672	17,5510	-19,4090	7,9	900	60,07	76,98	32	2	524,32	120	0,44	5	-2,11
B146/Y3788	17,5519	-19,9937	7,0	1360	168,18	62,90	35	7	584,07	14	148,29	100	0,64
B48/Y5669	17,5548	-19,4387	7,4	840	95,30	48,08	26	2	513,35	36	25,23	12	-0,07
D225/Y1112	17,5548	-21,2577	8,1	3640	355,59	178,00	154	56	491,40	225	1062,43	340	1,33
J228/Y208	17,5558	-21,5351	7,5	930	50,05	42,98	70	13	419,46	25	44,27	46	0,03
B511/Y4505	17,5577	-19,7054	7,3	770	70,08	56,10	15	3	502,37	12	0,44	1	1,86
D239/Y1042	17,5577	-20,9234	8,0	1850	103,31	119,96	147	18	429,21	400	81,45	182	0,17
B504/Y4492	17,5587	-19,7865	7,8	1230	97,31	78,92	71	15	701,13	145	0,44	4	0,65
830	17,5606	-20,6685	7,4	730	87,29	41,04	40	3	491,40	20	55,33	18	-1,65
D227/Y1108	17,5606	-21,1829	8,5	740	42,05	50,03	48	14	404,82	18	45,60	20	2,07
J228/Y207	17,5615	-21,5378	7,2	990	74,08	50,03	50	12	463,35	14	69,06	34	1,66
B758/Y4638	17,5625	-19,6613	7,4	850	92,10	57,07	17	1	595,04	5	7,08	1	0,29
B758/Y4637	17,5625	-19,6640	7,3	930	100,11	63,87	16	1	631,62	5	30,99	4	-0,43
D243/Y1075	17,5635	-21,1099	8,3	860	38,04	33,03	102	12	401,17	28	34,09	53	0,85
D239/Y1044	17,5635	-20,9604	8,0	1410	69,28	52,94	165	15	495,06	115	123,95	98	0,34
D241/Y1036	17,5635	-21,0207	7,4	1460	79,29	59,98	174	14	595,04	190	20,36	92	0,56
J229/1/Y219	17,5644	-21,5018	7,9	820	34,04	45,90	64	14	441,41	13	15,05	22	1,47
B145/Y3786	17,5654	-20,0432	7,0	860	136,15	14,08	38	3	537,73	17	0,44	12	0,89
D241/Y1040	17,5663	-20,9955	7,7	1410	38,04	36,91	241	23	536,51	155	70,83	81	1,78
D404/Y692	17,5663	-20,8847	7,5	1660	87,29	84,99	125	17	449,94	235	68,17	152	-1,24
D291/Y2958	17,5673	-20,3396	8,1	600	41,24	7,04	75	5	332,88	5	1,77	15	0,14
B786/Y5676	17,5673	-19,3793	7,6	900	88,10	65,08	20	2	567,00	53	9,74	6	-0,23
D432/Y688	17,5673	-20,8550	8,0	1220	45,25	61,92	116	14	491,40	61	39,84	96	0,33
D432/Y689	17,5673	-20,8712	7,8	1390	51,26	59,01	145	14	408,48	145	52,23	140	-1,49
B145/Y3787	17,5673	-20,0360	6,8	1760	300,33	26,96	18	4	468,23	43	402,82	100	0,57
D249/Y1126	17,5683	-21,1396	8,3	960	48,05	33,03	118	21	484,08	28	35,41	47	1,76
B566/3/Y4491	17,5692	-19,7820	7,9	1190	51,26	76,98	100	7	619,43	88	28,77	36	-0,16
D338/Y2956	17,5692	-20,4721	7,2	7730	748,81	114,86	630	23	207,29	430	150,51	2200	-1,33
B758/Y4636	17,5702	-19,6703	7,9	880	97,31	63,87	13	0	625,53	5	13,28	1	0,38
B566/2/Y4487	17,5702	-19,8117	7,7	1010	66,07	90,09	20	15	653,57	50	0,44	4	0,39
D225/Y1113	17,5702	-21,2766	7,9	1770	135,35	73,10	155	9	525,54	160	154,94	166	1,59
D404/Y693	17,5712	-20,8982	7,6	1030	50,05	48,08	104	12	457,26	68	33,64	51	1,78
B752/Y4822	17,5721	-19,5117	6,8	1070	132,14	68,00	2	1	718,20	4	1,77	4	1,26
D239/Y1043	17,5740	-20,9577	7,3	2720	129,34	137,93	282	21	474,33	450	177,07	375	0,05
D423/Y686	17,5760	-20,8081	7,3	8560	105,31	162,95	1575	98	947,44	960	181,49	1700	1,87
B517/Y4634	17,5769	-19,6486	7,7	740	88,10	52,94	1	1	517,00	4	0,44	0	1,48
B517/Y4635	17,5769	-19,6514	7,5	1710	170,19	65,08	95	2	480,42	50	150,51	255	-1,38
B316/Y4497	17,5779	-19,7541	7,5	770	63,27	68,00	2	2	525,54	9	0,44	4	-0,17
B316/Y4503	17,5779	-19,7216	7,2	1080	110,12	62,90	27	1	666,99	6	44,27	22	-2,14
B145/Y3785	17,5788	-20,0685	7,2	600	78,08	15,06	38	3	393,85	8	0,00	12	-0,68
B566/3/Y4490	17,5788	-19,7595	7,7	770	67,27	62,90	8	4	531,64	5	0,44	6	-0,06
B566/1/Y4482	17,5798	-19,8640	7,2	1090	85,29	82,08	22	6	752,34	5	0,44	1	-1,42
B761/Y6411	17,5837	-19,2523	7,0	910	109,32	53,91	8	2	609,68	20	7,08	6	-1,91
J215/Y1221	17,5837	-21,3027	7,6	1030	39,24	33,03	135	12	469,45	80	40,73	43	-1,69
J229/1/Y220	17,5837	-21,4883	7,5	1540	87,29	79,89	68	15	352,39	35	236,83	148	-0,79
B761/Y7842	17,5856	-19,3045	7,8	670	57,26	56,10	3	1	435,31	12	10,18	4	-0,21
B521/Y4641	17,5865	-19,6730	7,4	1040	108,12	59,98	43	1	751,12	6	0,44	1	-0,98
B967/Y3754	17,5875	-20,2063	6,8	140	8,01	2,91	3	8	46,34	5	3,10	2	0,24
D241/Y1037	17,5875	-21,0126	8,2	830	35,24	34,97	99	13	425,55	45	15,94	46	-1,02
B785/Y5673	17,5875	-19,4189	7,5	980	125,34	61,92	17	2	674,30	36	8,85	5	0,23
825	17,5875	-20,5153	7,8	1320	139,35	62,90	42	14	506,03	115	10,18	128	-0,51
B316/Y4504	17,5885	-19,7135	7,5	650	68,07	42,01	14	2	460,91	7	5,31	1	-1,95
B787/Y4837	17,5885	-19,4658	7,5	820	100,11	48,08	13	2	554,80	20	0,44	8	-0,90

Appendix D: Hydrochemical data

Name	Long	Lat	pH	ec µS/cm	Ca ²⁺ mg/l	Mg ²⁺ mg/l	Na ⁺ mg/l	K ⁺ mg/l	HCO ₃ ⁻ mg/l	SO ₄ ²⁻ mg/l	NO ₃ ⁻ mg/l	Cl ⁻ mg/l	Balance %
D225/Y1111	17,5885	-21,2324	8,0	890	75,28	53,91	52	12	546,27	16	30,54	2	4,51
D244/Y1061	17,5894	-21,0468	8,3	840	42,05	37,88	85	12	395,07	53	10,18	54	-0,25
B518/Y4643	17,5913	-19,6604	7,6	990	98,11	66,05	36	1	697,47	13	7,53	6	-0,29
J229/1/Y218	17,5923	-21,5189	7,8	770	50,05	34,97	52	11	363,37	35	42,94	15	0,76
B518/Y4642	17,5923	-19,6577	7,5	780	80,09	50,03	21	0	551,15	4	7,53	6	-2,05
B48/Y5671	17,5933	-19,4559	7,4	980	133,35	53,91	15	2	662,11	31	16,38	4	-0,34
B566/2/Y4486	17,5952	-19,8144	7,5	1230	21,22	139,88	15	19	626,75	17	122,18	36	0,35
J150/Y178	17,5990	-21,6270	7,5	1140	88,10	46,87	74	11	426,77	20	139,44	88	-1,63
D227/Y1110	17,5990	-21,2090	7,4	4160	320,35	249,88	169	31	370,68	275	23,46	1110	1,37
B566/3/Y4489	17,6010	-19,7820	7,4	940	80,09	63,87	18	12	531,64	15	68,61	16	-1,15
B566/1/Y4483	17,6029	-19,8829	7,5	870	77,28	42,01	47	6	545,05	13	15,05	10	-1,13
B566/1/Y4484	17,6038	-19,8333	7,4	1010	73,28	71,88	38	13	521,88	95	42,50	10	0,26
B566/3/Y4488	17,6038	-19,7676	7,4	1140	92,10	87,91	46	4	815,75	22	0,44	4	-0,05
B968/Y2959	17,6048	-20,2748	7,5	230	20,02	5,10	14	13	125,59	4	2,21	7	-0,31
B566/2/Y4485	17,6058	-19,8144	7,8	820	54,06	68,00	18	9	491,40	8	48,25	13	-0,32
B519/Y4647	17,6067	-19,6685	7,4	950	90,10	56,10	55	1	656,01	22	12,84	1	0,37
B345/Y2960	17,6077	-20,3405	8,0	3200	63,27	13,11	550	7	126,81	210	7,97	730	2,11
B520/Y4645	17,6087	-19,6784	7,5	620	46,05	34,00	44	1	413,36	10	10,62	1	-1,03
B520/Y4644	17,6087	-19,6757	7,4	990	96,10	54,88	64	1	687,71	15	9,74	1	1,48
D240/Y1048	17,6089	-20,9685	7,9	800	53,26	43,95	58	12	425,55	30	34,97	30	0,53
B969/Y3758	17,6096	-20,0901	7,4	150	12,01	2,91	7	8	63,41	7	0,44	4	1,64
B150/Y4444	17,6096	-20,0252	6,9	910	190,21	7,04	5	2	602,36	5	0,44	6	0,92
D240/Y1045	17,6115	-20,9414	7,5	770	51,26	44,93	58	11	436,53	37	23,90	20	1,03
D434/Y699	17,6115	-20,8946	8,0	1370	50,05	59,98	180	13	560,90	165	43,38	54	2,45
D227/Y1109	17,6125	-21,1991	7,8	1100	76,08	42,98	117	11	508,47	87	19,48	62	1,99
B150/Y4445	17,6135	-19,9973	7,5	420	68,07	8,99	5	2	236,55	4	0,44	8	2,47
B787/Y4838	17,6135	-19,5288	7,1	1000	132,14	48,08	26	3	601,14	80	0,44	3	0,64
B316/Y4502	17,6135	-19,7550	7,4	1050	112,12	78,92	7	1	768,19	5	0,44	5	-1,67
D434/Y698	17,6135	-20,8910	8,4	1390	45,25	48,08	204	14	567,00	165	43,82	48	2,18
J231/Y231	17,6154	-21,5829	7,6	720	34,04	30,11	76	10	402,39	22	12,84	8	1,66
B752/Y4819	17,6163	-19,5694	7,6	760	66,07	57,07	12	0	513,35	4	7,08	1	-0,71
B589/Y4843	17,6163	-19,4468	7,0	960	122,13	49,05	12	3	640,16	28	0,44	4	-2,12
B150/Y4446	17,6173	-19,9856	7,1	830	150,16	14,08	7	5	569,44	4	0,44	1	-1,98
B786/1/Y5675	17,6173	-19,4081	7,9	860	82,09	69,94	16	2	603,58	32	0,44	3	-0,24
J218/Y1358	17,6183	-21,4865	8,3	700	41,65	37,88	66	11	360,93	35	25,68	36	1,67
B149/Y5502	17,6192	-19,8973	7,3	710	89,30	42,98	6	2	495,06	5	0,00	10	-1,16
B752/Y4820	17,6221	-19,5865	7,0	860	105,31	54,88	1	1	569,44	4	1,77	1	1,91
B787/Y4839	17,6231	-19,5081	7,5	730	109,32	28,90	12	2	470,67	30	2,66	2	-0,19
B589/Y4844	17,6231	-19,4171	7,6	890	114,12	49,05	10	2	581,63	17	17,71	8	-0,87
B316/Y4498	17,6231	-19,7279	7,2	1100	98,11	79,89	28	2	707,22	40	9,74	12	-0,70
B787/Y4834	17,6231	-19,4865	7,0	1390	132,14	65,08	55	4	570,66	117	101,81	16	1,99
B970/Y3755	17,6240	-20,1766	6,7	130	9,21	2,91	4	9	51,21	3	4,43	5	-0,48
B787/Y4835	17,6240	-19,4901	7,1	1350	139,35	65,08	41	4	586,51	93	132,80	29	-1,09
B761/Y6412	17,6260	-19,2685	6,8	900	108,12	54,88	5	1	621,87	14	0,89	4	-2,19
B787/Y4836	17,6269	-19,4784	7,0	1170	136,15	53,91	31	3	599,92	94	42,50	12	-0,62
B800/Y4481	17,6288	-19,8748	7,4	980	105,31	34,97	53	5	616,99	8	15,94	13	-1,56
D249/Y1122	17,6308	-21,1622	8,1	610	50,05	27,93	45	12	359,71	13	13,28	13	2,27
B805/Y4657	17,6317	-19,6910	7,3	1280	78,08	90,09	90	1	586,51	225	12,39	8	1,76
B969/Y3757	17,6327	-20,1270	6,8	190	24,03	2,91	4	5	97,55	5	0,44	3	-1,53
831	17,6346	-20,7153	7,4	1500	116,13	39,10	158	3	512,13	33	278,88	82	0,22
824	17,6346	-20,4820	8,2	3360	34,04	24,04	730	6	1010,84	360	12,39	380	0,86
B801/Y4479	17,6356	-19,7820	7,2	1360	70,08	84,99	98	12	745,02	73	41,17	37	-1,24
J230/Y234	17,6365	-21,5135	8,1	710	38,04	32,06	55	15	374,34	12	34,97	13	-0,02

Appendix D: Hydrochemical data

Name	Long	Lat	pH	ec µS/cm	Ca ²⁺ mg/l	Mg ²⁺ mg/l	Na ⁺ mg/l	K ⁺ mg/l	HCO ₃ ⁻ mg/l	SO ₄ ²⁻ mg/l	NO ₃ ⁻ mg/l	Cl ⁻ mg/l	Balance %
B786/1/Y5674	17,6394	-19,3802	7,6	980	135,35	53,91	15	3	669,42	16	28,77	6	-0,08
B802/1/Y4480	17,6413	-19,8577	7,6	990	150,16	39,10	76	4	575,53	61	154,93	52	-1,91
B805/Y4659	17,6413	-19,6613	7,0	5350	520,57	359,89	95	1	724,29	150	1257,17	800	1,63
B589/Y4842	17,6433	-19,4586	7,0	1020	123,33	65,08	11	2	692,59	15	3,54	8	0,39
B770/Y6399	17,6433	-19,3171	6,7	1250	127,34	84,02	16	1	602,36	22	79,68	82	0,22
B345/1/Y3281	17,6442	-20,3712	7,9	700	79,29	12,87	86	7	391,41	30	13,28	55	0,74
B149/Y5504	17,6452	-19,9477	7,7	4490	155,37	83,05	660	14	497,50	40	38,07	1200	0,24
823	17,6452	-20,4928	8,0	2490	9,21	11,90	580	7	886,47	105	18,59	300	2,62
B316/Y4501	17,6462	-19,7595	7,4	1370	65,27	144,98	30	7	970,60	5	13,28	16	-0,02
B149/Y5503	17,6471	-19,9000	7,3	1530	210,23	48,08	55	1	518,22	88	230,19	118	-1,46
D240/Y1047	17,6481	-20,9721	7,8	1790	88,10	84,99	172	16	415,80	230	37,63	250	0,05
D256/Y1143	17,6500	-21,1063	7,7	850	43,25	20,88	111	10	458,48	34	25,68	20	-1,32
B761/Y6414	17,6510	-19,2135	7,4	860	57,26	67,02	20	1	454,82	52	23,90	21	-1,31
B151/Y4452	17,6510	-19,9766	7,1	870	150,16	15,06	15	2	541,39	5	0,44	18	-0,29
B801/Y4478	17,6510	-19,8081	7,3	970	63,27	76,98	28	10	657,23	9	14,17	1	-1,13
J231/Y225	17,6510	-21,5477	7,6	1150	64,07	57,07	80	19	435,31	50	110,67	76	-1,02
D240/Y1046	17,6510	-20,9378	8,1	2340	102,11	118,02	241	17	395,07	320	28,33	390	2,25
D435/Y701	17,6519	-20,8874	8,1	2780	95,30	118,99	370	18	477,99	450	55,78	430	1,42
D256/Y1145	17,6538	-21,1568	7,7	740	50,05	32,06	60	9	382,88	13	47,81	12	2,05
D256/Y1144	17,6538	-21,1423	7,9	950	47,25	34,00	97	10	448,72	20	44,27	40	0,09
B151/Y4451	17,6538	-20,0333	7,6	1140	170,19	26,96	27	2	460,91	29	132,80	66	-0,93
D254/Y1120	17,6538	-21,2000	7,6	2600	370,40	100,05	31	8	387,75	84	849,94	186	2,19
B589/Y4841	17,6548	-19,4676	7,1	1300	140,15	78,92	20	10	682,84	37	90,75	56	-1,32
D435/Y705	17,6548	-20,8820	7,7	3890	148,16	197,92	494	24	495,06	770	60,65	790	-1,74
833	17,6558	-20,6532	7,6	860	68,07	36,91	54	21	415,80	20	68,17	40	-0,74
J95/Y199	17,6587	-21,6622	7,6	840	50,05	42,01	55	18	474,33	13	16,82	10	1,21
B316/Y4499	17,6596	-19,7243	7,3	920	85,29	69,94	11	2	640,16	8	4,87	1	-1,05
B589/Y4840	17,6596	-19,4640	7,3	1260	135,35	79,89	20	9	663,33	38	84,11	52	-0,20
D254/Y1121	17,6596	-21,2054	7,5	3530	510,56	90,09	106	37	367,02	300	1062,43	275	1,71
D254/Y1116	17,6606	-21,1991	7,3	1000	145,36	34,00	22	6	546,27	7	64,63	38	-0,23
D254/Y1118	17,6606	-21,1784	8,2	2810	340,37	94,95	101	10	346,30	67	637,46	400	1,40
D435/Y702	17,6606	-20,8964	7,9	6530	213,43	314,96	780	35	380,44	1220	110,67	1320	0,52
B151/Y4453	17,6615	-19,9766	7,3	510	67,27	15,06	6	4	293,86	5	0,44	1	0,04
854	17,6625	-20,8144	7,1	8500	344,37	284,85	1360	42	526,76	1800	28,33	1778	2,10
D256/Y1146	17,6635	-21,1577	8,0	1100	103,31	42,01	52	6	417,02	20	88,54	82	0,16
J230/Y236	17,6654	-21,4676	7,7	730	49,25	31,08	46	12	380,44	8	42,05	16	-1,40
D254/Y1115	17,6654	-21,2000	7,5	1100	150,16	45,90	30	5	529,20	9	123,95	48	1,97
B761/Y6422	17,6683	-19,2495	7,5	890	80,09	56,10	11	2	512,13	20	8,85	6	0,11
B971/Y2961	17,6702	-20,3108	8,0	610	52,06	2,91	65	3	220,70	63	10,18	22	0,25
D261/Y725	17,6702	-20,9838	7,6	2660	113,32	116,08	344	20	477,99	470	33,64	420	1,11
B970/Y3756	17,6712	-20,2000	6,7	150	9,21	2,91	8	10	57,31	5	3,10	8	-0,60
B770/Y6398	17,6721	-19,3225	6,8	890	106,12	57,07	9	1	602,36	16	0,44	6	0,13
J218/Y1360	17,6721	-21,4171	8,3	950	82,09	56,34	39	9	257,28	33	119,08	127	1,20
D437/Y709	17,6740	-20,9559	7,9	2050	96,10	94,95	207	19	408,48	250	23,90	360	-0,76
D434/Y700	17,6740	-20,8577	8,0	4710	166,18	179,95	685	34	491,40	1080	132,80	710	0,99
B972/Y3283	17,6750	-20,3964	7,6	10000	524,57	41,77	1598	63	117,06	543	0,44	3069	0,47
B972/Y3282	17,6760	-20,3703	7,9	2700	166,98	51,97	427	16	307,28	191	1,33	768	1,44
B805/Y4658	17,6769	-19,6495	7,5	760	83,29	56,10	1	1	538,95	3	0,44	1	-0,50
J98/Y2006	17,6779	-21,8180	7,8	2480	68,07	69,94	450	8	1298,61	44	54,45	188	0,96
D437/Y708	17,6788	-20,9342	8,3	1890	75,28	66,05	225	17	421,90	175	104,03	230	1,81
B656/1/Y4648	17,6798	-19,7009	7,4	760	92,10	50,03	2	1	529,20	5	2,66	1	-0,13
J103/Y206	17,6808	-21,7108	7,6	1070	66,07	63,87	29	19	418,24	13	128,38	46	-0,93
B153/Y4450	17,6827	-19,8991	7,1	890	133,35	35,94	10	2	596,26	10	4,43	4	-0,33

Appendix D: Hydrochemical data

Name	Long	Lat	pH	ec µS/cm	Ca ²⁺ mg/l	Mg ²⁺ mg/l	Na ⁺ mg/l	K ⁺ mg/l	HCO ₃ ⁻ mg/l	SO ₄ ²⁻ mg/l	NO ₃ ⁻ mg/l	Cl ⁻ mg/l	Balance %
B656/Y4650	17,6827	-19,7198	7,4	1020	103,31	79,89	5	1	612,11	14	71,71	16	0,17
D256/Y1142	17,6827	-21,1171	7,5	5550	335,57	249,88	380	21	360,93	320	991,60	900	0,39
D253/Y1148	17,6837	-21,2261	7,9	4980	240,26	197,92	430	17	510,91	355	1027,02	600	-1,90
B761/Y6417	17,6846	-19,2946	7,5	680	59,26	56,10	6	1	454,82	16	9,74	6	-1,59
D254/Y1117	17,6846	-21,1694	8,0	730	59,26	57,07	10	16	436,53	5	30,99	12	2,42
B656/Y4649	17,6856	-19,7171	7,3	830	97,31	58,04	4	1	569,44	11	0,44	6	0,48
D261/Y724	17,6856	-20,9982	7,6	2250	96,10	99,08	270	20	459,70	305	154,94	290	1,29
J103/Y204	17,6865	-21,7063	7,1	2110	138,15	110,01	69	24	441,41	33	387,34	200	-0,63
D253/Y1149	17,6875	-21,2297	7,5	4580	390,42	212,00	124	10	337,76	250	1027,02	600	-1,90
D437/Y710	17,6885	-20,9577	7,4	4100	152,17	177,03	583	29	553,59	820	46,92	810	-1,52
B976/Y3760	17,6894	-20,0991	6,8	130	10,01	2,91	6	8	63,41	5	0,44	3	-1,23
J103/Y203	17,6894	-21,6802	7,2	780	80,09	31,08	34	8	419,46	27	7,97	16	1,36
B589/Y4845	17,6894	-19,4739	7,5	800	89,30	48,08	14	3	554,80	7	0,44	6	-1,71
B761/Y6416	17,6913	-19,1838	7,1	1250	135,35	79,89	29	1	609,68	100	37,18	62	0,67
B761/Y6421	17,6942	-19,2441	7,7	800	52,06	60,95	6	1	475,55	10	0,44	5	-1,56
B316/Y4500	17,6962	-19,7703	7,2	1230	103,31	96,89	14	2	697,47	38	64,63	35	-1,65
D437/Y711	17,6971	-20,9622	7,5	2770	107,32	125,06	340	25	438,97	500	28,77	450	0,51
B152/Y4447	17,7010	-20,0126	7,3	480	65,27	10,93	10	6	284,11	5	8,41	1	-1,85
B801/Y4477	17,7019	-19,8108	7,2	1240	94,10	104,91	32	3	808,43	77	11,51	6	-1,37
D435/Y703	17,7029	-20,8829	7,9	2510	101,31	94,95	343	21	463,35	470	50,46	380	-1,02
B656/Y4651	17,7038	-19,7072	8,0	730	70,08	61,92	4	1	475,55	33	7,97	6	0,08
B152/Y4448	17,7038	-19,9712	7,2	1260	185,40	30,11	33	5	535,30	30	201,41	44	-2,18
B976/Y3759	17,7048	-20,1486	6,6	130	8,01	5,10	5	9	63,41	5	0,44	4	0,15
B761/Y6425	17,7058	-19,1964	7,5	630	46,05	57,07	7	1	423,11	14	5,31	2	-0,30
B761/Y6424	17,7058	-19,1928	7,4	1710	148,16	79,89	135	1	571,88	260	48,25	135	1,26
D437/Y712	17,7058	-20,9396	7,7	2300	81,29	86,94	348	25	519,44	420	37,63	290	1,78
B975/Y2962	17,7067	-20,1685	7,0	160	8,01	2,91	10	11	46,34	5	3,98	14	1,24
B46/Y4980	17,7077	-19,5991	7,3	610	98,11	22,10	2	0	420,68	3	0,44	2	-1,57
B46/Y4979	17,7077	-19,6063	7,4	630	87,29	32,06	2	1	432,87	4	0,44	3	-1,13
D437/Y706	17,7087	-20,9252	7,9	2560	90,10	93,98	400	25	512,13	530	29,66	325	2,01
B771/Y6397	17,7096	-19,3180	6,8	890	98,11	60,95	4	1	618,21	6	9,74	4	-2,01
B761/Y6426	17,7096	-19,1955	7,5	1600	116,13	79,89	120	2	479,21	248	57,55	115	1,30
D437/Y707	17,7096	-20,9351	7,8	3380	157,37	180,92	380	32	495,06	780	72,15	550	-1,16
B46/Y4978	17,7106	-19,6036	7,6	510	60,07	30,11	4	1	340,20	7	0,44	3	-1,20
B761/Y6427	17,7106	-19,1928	7,2	800	78,08	59,98	8	1	536,51	16	6,20	4	-0,72
J98/Y2004	17,7115	-21,8360	7,4	840	70,08	40,07	51	20	531,64	28	8,85	15	-1,74
832	17,7115	-20,6784	8,4	930	99,31	49,05	27	15	526,76	7	68,61	33	-1,24
D261/Y723	17,7135	-20,9847	7,7	2200	58,06	84,02	328	24	508,47	340	30,99	280	1,82
B47/Y4858	17,7144	-19,4748	7,7	980	132,14	52,94	10	2	685,28	15	0,44	4	-0,98
D253/Y1147	17,7144	-21,2505	7,8	2890	86,09	59,01	416	13	452,38	420	30,99	420	-1,65
J98/Y2005	17,7154	-21,7991	7,9	630	56,06	31,08	27	18	378,00	9	25,23	12	-0,97
D435/Y704	17,7192	-20,8712	7,5	3070	207,43	144,00	334	25	387,75	460	62,86	680	1,69
B344/3/Y4468	17,7202	-19,8333	7,2	1490	90,10	119,96	66	6	853,55	125	22,58	18	-0,20
B767/Y4449	17,7212	-20,0676	7,5	190	22,02	3,89	9	7	98,77	5	0,44	8	0,85
B344/5/Y4661	17,7212	-19,7811	7,2	2040	200,22	100,05	132	13	692,59	530	0,44	60	0,44
B344/5/Y4660	17,7221	-19,7631	7,4	1520	106,12	127,49	40	2	686,49	100	168,21	55	-0,06
B771/2/Y6390	17,7240	-19,3901	6,8	800	102,11	44,93	2	0	529,20	6	0,44	2	0,12
836	17,7250	-20,6162	7,4	1520	62,07	59,98	202	11	512,13	185	26,56	136	1,76
B344/5/Y4662	17,7279	-19,8000	7,3	2760	96,10	262,27	194	7	760,88	990	3,54	62	0,15
853	17,7288	-20,8216	6,9	11040	806,88	429,83	970	35	374,34	580	106,24	3570	-0,79
B975/Y2963	17,7288	-20,2054	7,3	110	6,01	0,97	9	11	51,21	5	0,44	4	-0,51
D257/1/Y736	17,7288	-21,1180	8,4	1330	35,24	39,10	226	12	525,54	130	19,48	108	1,45
B761/Y6420	17,7288	-19,1946	7,3	2050	120,13	75,04	206	4	352,39	450	1,77	250	-2,28

Appendix D: Hydrochemical data

Name	Long	Mlat	pH	ec µS/cm	Ca ²⁺ mg/l	Mg ²⁺ mg/l	Na ⁺ mg/l	K ⁺ mg/l	HCO ₃ ⁻ mg/l	SO ₄ ²⁻ mg/l	NO ₃ ⁻ mg/l	Cl ⁻ mg/l	Balance %
B974/Y3287	17,7317	-20,2369	8,1	240	17,62	5,34	33	4	121,94	10	1,77	21	0,51
B46/Y4981	17,7317	-19,5838	7,7	590	74,08	37,88	2	0	419,46	3	0,44	1	-0,49
822	17,7317	-20,4703	6,4	3790	415,65	245,03	130	25	816,97	375	3,54	1000	-2,34
D272/Y766	17,7327	-21,2838	7,9	1740	82,09	43,95	220	9	409,70	86	296,60	160	-0,82
D437/Y716	17,7337	-20,9243	7,4	3690	172,19	157,85	426	31	432,87	840	61,97	600	-1,92
821	17,7356	-20,4270	7,3	19110	610,66	169,99	3620	95	395,07	1250	0,00	5920	1,21
B154/Y4459	17,7365	-19,8847	7,2	950	150,16	32,06	6	4	632,84	8	6,20	6	-1,47
D437/Y713	17,7365	-20,9514	7,6	1690	53,26	45,90	278	17	536,51	250	24,79	141	1,57
D272/Y767	17,7385	-21,2604	7,7	1030	46,05	28,90	143	8	424,33	67	24,79	80	0,43
B977/Y3303	17,7394	-20,0775	7,9	220	31,63	2,19	13	6	101,21	4	7,53	21	0,44
D437/Y714	17,7394	-20,9577	8,0	1590	45,25	44,93	260	17	519,44	235	23,90	130	0,69
D436/Y718	17,7394	-20,8973	8,1	1890	86,09	69,94	264	19	438,97	390	27,45	210	0,78
B155/Y4458	17,7404	-19,9973	7,1	1760	195,41	42,98	128	4	556,02	32	265,60	141	2,48
J144/Y1381	17,7413	-21,5613	8,0	460	15,62	36,43	35	8	258,50	26	2,21	24	0,12
B47/Y4857	17,7413	-19,4829	7,1	1040	136,15	52,94	13	2	685,28	17	7,08	16	-1,60
834	17,7413	-20,7054	7,8	1990	127,34	78,68	215	14	526,76	305	119,52	186	0,85
B761/Y6418	17,7433	-19,2883	7,6	800	88,10	57,07	6	1	569,44	8	0,89	2	-1,01
J137/Y1163	17,7433	-21,3766	8,3	2580	36,04	86,94	366	30	573,10	210	214,70	310	-0,64
B317/Y4865	17,7442	-19,5252	7,2	960	113,32	53,91	6	1	531,64	5	53,12	40	-2,00
B46/Y4975	17,7452	-19,6252	7,4	600	98,11	22,10	2	0	414,58	3	0,44	2	-0,85
B973/Y3284	17,7452	-20,3937	7,8	8750	488,53	42,50	1492	61	124,37	488	0,44	2829	1,25
D273/Y1185	17,7462	-21,2991	7,6	2060	140,15	80,87	168	13	364,59	150	236,83	270	1,81
B47/Y4854	17,7471	-19,4694	7,5	1220	195,41	57,07	8	1	891,35	12	0,44	1	-0,24
B155/Y4457	17,7500	-19,9631	7,1	1020	96,10	60,95	38	2	710,88	5	0,44	6	-1,77
B977/Y3302	17,7510	-20,0378	7,9	200	19,62	2,43	26	5	76,82	0	0,44	42	-0,27
B757/Y4988	17,7510	-19,6739	7,8	550	68,07	31,08	3	2	368,24	9	3,54	1	-1,38
B47/Y4855	17,7510	-19,4712	6,9	1220	185,40	57,07	10	2	868,18	15	0,44	2	-0,59
B344/3/Y4466	17,7510	-19,8288	7,1	1540	105,31	119,96	60	5	815,75	165	0,44	14	1,88
J147/Y185	17,7519	-21,5703	7,5	740	38,04	35,94	60	9	426,77	16	7,97	8	0,09
B155/Y4454	17,7529	-20,0108	7,4	210	24,03	6,07	8	7	114,62	5	0,44	8	0,23
D270/Y754	17,7538	-21,1775	8,0	960	40,04	34,00	125	12	437,75	61	29,66	58	-0,09
D273/Y1181	17,7538	-21,3207	7,6	1400	52,06	34,00	187	10	445,06	135	18,59	140	-2,02
B344/3/Y4467	17,7538	-19,8360	7,3	1610	106,12	129,92	64	5	846,23	175	38,07	26	0,10
B344/5/Y4663	17,7548	-19,7577	7,2	1080	153,37	41,04	17	6	616,99	23	26,12	31	0,16
D437/Y715	17,7558	-20,9342	8,2	1890	78,08	63,87	266	17	449,94	340	28,33	210	0,77
B46/Y4977	17,7567	-19,6045	7,6	560	66,07	33,03	4	1	369,46	4	9,74	6	-1,97
J102/Y1997	17,7567	-21,7360	8,0	840	73,28	40,07	57	12	537,73	25	16,82	14	-1,31
B974/Y3288	17,7577	-20,2685	7,8	230	20,02	4,13	29	7	120,72	2	0,44	27	-0,17
B46/Y4976	17,7625	-19,6072	7,7	550	62,07	33,03	4	1	345,08	5	9,30	6	-0,53
B771/1/Y6389	17,7635	-19,3342	7,1	820	84,09	56,10	5	1	545,05	6	1,77	4	-0,79
B761/Y6415	17,7635	-19,1919	7,6	1570	135,35	84,99	89	1	569,44	210	9,74	140	-0,47
D257/1/Y737	17,7644	-21,1135	7,9	860	42,05	25,98	117	12	421,90	44	39,84	28	1,96
D257/1/Y738	17,7644	-21,1180	7,8	980	34,04	37,88	130	15	449,94	60	46,48	43	1,25
B344/2/Y4464	17,7644	-19,7892	7,3	1120	100,11	69,94	40	4	643,82	120	0,44	1	-1,92
D436/Y719	17,7663	-20,9234	7,6	2100	80,09	73,10	278	23	449,94	280	108,45	260	0,90
B155/Y4456	17,7673	-19,9523	7,3	1040	85,29	73,10	34	4	727,95	5	0,44	6	-1,49
835	17,7673	-20,6414	7,3	2480	67,27	109,04	364	26	796,24	290	39,84	280	2,13
J138/W2171	17,7683	-21,4135	8,1	1780	42,45	42,25	282	28	499,93	205	15,05	190	1,40
B978/Y2968	17,7692	-20,1315	6,9	120	4,00	1,94	4	8	31,70	5	0,44	3	1,57
B973/Y3285	17,7692	-20,3180	7,7	250	16,82	7,77	23	8	70,72	59	0,44	10	0,13
B771/1/Y6388	17,7692	-19,3153	6,7	910	103,31	58,04	4	1	626,75	6	0,44	2	-1,60
B155/Y4455	17,7712	-19,9694	7,4	500	50,05	25,98	12	3	325,57	5	0,44	1	-2,24
J102/Y1993	17,7750	-21,6874	8,4	860	2,00	77,95	55	23	441,41	70	37,19	17	-1,43

Appendix D: Hydrochemical data

Name	Long	Lat	pH	ec µS/cm	Ca ²⁺ mg/l	Mg ²⁺ mg/l	Na ⁺ mg/l	K ⁺ mg/l	HCO ₃ ⁻ mg/l	SO ₄ ²⁻ mg/l	NO ₃ ⁻ mg/l	Cl ⁻ mg/l	Balance %
D264/Y656	17,7750	-21,0685	7,6	2400	132,14	80,87	250	15	380,44	200	354,14	260	2,22
J144/Y1385	17,7760	-21,5568	8,1	600	43,65	35,94	31	7	292,64	28	23,46	29	0,66
B761/Y6423	17,7760	-19,2865	7,0	960	114,12	53,91	5	0	585,29	10	18,59	10	-0,15
D273/Y1180	17,7769	-21,3072	7,9	800	46,05	27,93	86	10	392,63	35	20,36	42	-0,49
J102/Y1998	17,7769	-21,7279	7,8	1260	105,31	49,05	114	15	623,09	160	6,20	54	-1,78
D273/Y1179	17,7788	-21,3135	7,8	890	31,23	16,03	150	8	448,72	41	23,90	36	-0,01
D264/Y657	17,7798	-21,0712	7,3	2630	143,36	80,87	280	16	401,17	220	336,44	310	2,07
B977/Y3301	17,7808	-20,0784	8,0	200	22,42	8,74	8	7	103,64	2	0,44	23	-0,64
B344/2/Y4465	17,7808	-19,7937	6,9	840	87,29	60,95	32	6	535,30	56	38,07	28	-1,91
D264/Y655	17,7808	-21,0649	7,6	1560	60,07	37,88	222	13	408,48	155	95,18	156	0,77
B344/1/Y3314	17,7817	-19,8486	7,9	1040	191,81	41,53	8	2	558,46	43	56,66	83	0,32
D264/Y654	17,7817	-21,1009	7,7	1290	62,07	37,88	165	13	401,17	145	34,97	124	0,25
J144/Y1386	17,7827	-21,5748	7,8	680	49,25	50,75	33	7	295,08	86	1,77	50	1,12
B344/1/Y3315	17,7837	-19,8577	8,0	1500	234,25	51,24	26	4	514,57	106	232,40	93	0,38
J147/Y191	17,7846	-21,6432	7,3	880	70,08	44,93	41	9	448,72	47	0,44	30	0,12
D269/Y667	17,7846	-21,1261	7,5	1770	34,04	35,94	330	8	587,73	210	21,25	144	2,14
B156/Y3308	17,7856	-19,9874	8,0	390	62,47	10,44	20	6	253,63	0	0,89	25	1,25
B761/Y6410	17,7856	-19,2604	7,5	1030	132,14	52,94	19	1	620,65	90	9,74	4	-2,13
D436/Y717	17,7856	-20,8865	7,6	2100	78,08	66,05	322	21	525,54	300	29,22	270	1,99
J143/Y1369	17,7865	-21,4910	8,4	2100	110,12	67,75	261	19	323,13	235	260,30	289	0,82
B47/Y4856	17,7875	-19,4892	7,0	1200	190,21	51,97	12	2	823,06	24	7,97	4	0,39
B317/Y4864	17,7885	-19,5604	7,3	710	86,09	40,07	3	1	460,91	5	7,97	8	-1,67
D271/Y757	17,7923	-21,2207	7,6	1640	91,30	65,08	163	16	452,38	88	234,62	156	-0,06
J138/W2168	17,7933	-21,4198	8,3	980	37,24	19,67	144	14	338,98	76	53,12	68	0,93
B344/2/Y4463	17,7933	-19,7928	6,6	2480	250,27	204,96	59	5	1537,60	305	0,44	16	0,06
841	17,7942	-20,5793	7,8	1080	81,29	52,94	76	3	443,84	50	101,81	73	-0,93
B979/Y2965	17,7952	-20,2018	7,1	180	8,01	6,07	5	12	56,09	5	0,44	14	-0,06
B47/Y4860	17,7952	-19,4739	7,0	1330	200,22	61,92	8	1	957,19	10	0,44	1	-1,50
B344/4/Y4469	17,7981	-19,7703	7,1	3360	265,49	264,94	49	1	521,88	155	495,78	650	-1,20
B47/Y4859	17,7990	-19,4694	7,2	1170	170,19	59,98	9	2	835,26	11	0,44	2	-0,40
B156/Y3307	17,8000	-19,9189	8,2	900	126,14	55,37	22	4	632,84	42	0,44	20	0,39
B156/Y3309	17,8000	-20,0036	8,0	1100	138,55	23,31	42	21	184,12	43	249,66	122	-0,82
D264/Y648	17,8000	-21,0775	7,7	2460	77,28	54,88	402	18	467,01	400	29,66	310	2,16
B344/2/Y4461	17,8010	-19,8162	7,2	1690	114,12	144,98	41	4	653,57	315	75,25	43	-0,47
B317/Y4866	17,8019	-19,5000	7,7	620	50,05	53,91	2	1	430,43	5	0,44	4	-1,62
J148/Y1773	17,8029	-21,6532	8,1	800	84,09	41,04	30	8	473,11	22	37,19	10	-0,06
B161/Y2998	17,8038	-19,8198	7,7	1080	80,09	86,94	15	1	631,62	15	43,38	21	-0,54
9163	17,8048	-21,8009	6,9	660	83,29	9,96	24	4	282,89	13	44,27	23	-1,19
842	17,8048	-20,5649	7,4	1170	92,10	62,90	65	4	596,26	20	115,09	36	-1,39
820	17,8058	-20,4090	7,5	1910	158,17	84,02	100	15	692,59	21	37,18	275	-1,52
B344/2/Y4460	17,8058	-19,8144	8,0	1220	45,25	110,01	60	4	596,26	135	33,20	30	0,21
B159/Y3312	17,8067	-19,8784	7,8	500	116,93	3,89	2	1	343,86	0	1,33	19	0,60
B977/Y3300	17,8077	-20,0694	7,4	160	20,82	2,91	12	7	84,14	4	0,44	18	0,07
D375/1/W2182	17,8096	-21,1829	8,1	1180	56,46	56,10	119	19	426,77	135	36,74	95	0,07
819	17,8115	-20,4045	7,6	1910	63,27	53,91	264	32	609,68	210	36,30	182	-0,47
J148/Y1774	17,8125	-21,6892	7,4	750	60,07	34,97	40	11	388,97	12	64,63	19	-1,91
D267/Y627	17,8125	-21,1441	7,9	1020	50,05	32,06	125	12	418,24	62	39,84	70	0,54
B978/Y2966	17,8135	-20,1622	7,5	130	7,21	5,10	8	11	54,87	5	0,44	12	2,16
B158/1/Y3304	17,8135	-20,0009	7,8	2700	315,14	54,40	143	33	135,35	262	495,34	401	0,54
D375/1/W217E	17,8144	-21,2135	7,7	1090	41,24	32,06	141	18	398,73	107	38,96	75	-0,95
B158/1/Y3305	17,8154	-20,0054	7,9	280	44,45	7,53	10	6	146,32	2	12,39	25	1,20
J135/W2144	17,8154	-21,3207	8,0	1100	50,45	43,95	97	18	374,34	35	79,24	93	0,23
B980/Y3286	17,8173	-20,3315	7,9	2700	69,68	47,35	531	18	685,28	167	33,20	519	1,72

Appendix D: Hydrochemical data

Name	Long	Mlat	pH	ec µS/cm	Ca ²⁺ mg/l	Mg ²⁺ mg/l	Na ⁺ mg/l	K ⁺ mg/l	HCO ₃ ⁻ mg/l	SO ₄ ²⁻ mg/l	NO ₃ ⁻ mg/l	Cl ⁻ mg/l	Balance %
J148/Y1770	17,8202	-21,6613	7,9	690	55,26	39,10	26	14	407,26	7	34,53	8	-0,92
B157/Y3291	17,8212	-20,0450	7,8	260	39,64	5,59	11	12	142,66	4	0,00	24	1,98
B761/Y6419	17,8212	-19,2910	6,8	890	124,14	53,91	6	1	618,21	12	1,77	2	2,11
D264/Y653	17,8212	-21,0991	7,5	4070	79,29	78,92	680	26	570,66	620	106,24	550	1,51
D264/Y651	17,8212	-21,0856	7,5	4790	97,31	116,08	850	30	540,17	910	74,37	740	2,23
J148/Y1771	17,8221	-21,6658	7,8	860	72,08	42,01	32	14	410,92	7	106,24	18	-1,66
J101/1/Y1767	17,8221	-21,7441	7,5	1530	140,15	57,07	98	15	576,75	240	4,43	82	-1,50
D267/Y628	17,8269	-21,1261	7,8	2370	63,27	52,94	398	15	487,74	300	130,59	310	0,24
805	17,8279	-20,3721	7,0	6730	124,14	116,08	1600	60	3795,84	220	18,59	679	0,37
D374/W2110	17,8288	-21,2387	7,8	1800	53,26	41,77	256	26	421,90	275	55,33	158	-0,26
B45/2/Y4673	17,8298	-19,6306	7,8	700	62,07	53,91	7	1	454,82	7	4,43	6	0,15
D374/W2116	17,8308	-21,2955	7,9	1410	62,47	36,18	172	17	398,73	165	75,70	102	-0,20
B982/Y2971	17,8308	-20,1964	6,8	2210	80,09	42,98	102	225	152,42	85	442,66	200	1,95
B159/Y3313	17,8317	-19,8982	8,0	1250	164,18	71,40	39	5	558,46	74	116,86	117	0,04
B317/Y4861	17,8327	-19,5072	7,8	800	93,30	51,97	4	1	519,44	5	17,26	12	-0,56
B317/Y4862	17,8327	-19,5117	7,2	870	108,12	57,07	1	1	607,24	5	3,54	1	0,09
D264/Y652	17,8337	-21,0928	7,5	3350	77,28	62,90	580	24	519,44	560	28,33	450	2,28
D438/Y720	17,8346	-20,9027	7,5	4100	182,20	174,85	535	28	352,39	900	12,39	800	0,20
B344/2/Y4462	17,8356	-19,8045	7,1	1460	84,09	119,96	66	2	927,93	85	3,54	12	-1,11
B978/Y2967	17,8365	-20,1297	7,0	220	15,22	8,01	9	12	54,87	5	31,87	20	0,85
J148/Y1776	17,8365	-21,6757	8,1	940	76,08	46,87	53	13	426,77	63	47,81	53	-1,35
B344/4/Y4470	17,8375	-19,7613	7,3	810	83,29	51,97	4	3	541,39	4	0,44	1	-1,74
B344/1/Y3316	17,8375	-19,8441	7,9	1150	93,30	113,89	35	4	791,36	77	10,18	24	0,77
B979/Y2964	17,8404	-20,2477	7,0	140	4,00	1,94	12	7	42,68	5	4,43	7	-0,55
J133/W2152	17,8404	-21,3865	8,1	620	32,03	30,84	44	13	325,57	14	20,36	18	-0,63
B158/2/Y3306	17,8404	-19,9279	7,8	850	116,93	59,98	17	3	616,99	37	0,00	21	0,49
B159/Y3311	17,8423	-19,8703	8,4	900	85,69	90,09	23	3	687,71	15	0,44	24	2,00
B45/1/Y4672	17,8423	-19,6613	7,5	970	155,37	25,98	16	1	492,62	5	61,09	37	1,95
D375/W2183	17,8423	-21,2153	8,2	2020	60,47	49,54	315	26	476,77	245	45,60	261	1,06
D443/Y584	17,8433	-20,9387	7,4	2720	108,12	83,05	380	21	436,53	420	18,59	455	0,45
B157/Y3290	17,8442	-20,0459	7,6	400	64,87	7,04	13	7	153,64	63	5,75	21	0,51
B158/Y3294	17,8452	-20,0324	7,8	230	25,23	7,53	13	7	106,08	6	4,87	23	0,62
B45/Y4671	17,8462	-19,6622	7,4	770	118,13	25,98	12	1	454,82	5	30,10	16	0,50
B157/Y3289	17,8471	-20,0775	7,8	190	21,22	5,59	11	7	90,23	4	0,44	20	0,99
B158/Y3295	17,8490	-20,0315	7,5	240	37,64	3,64	10	7	132,91	2	1,33	20	-0,24
855	17,8490	-20,8468	7,4	2100	52,06	53,91	348	11	581,63	220	11,51	260	1,86
J131/Y1404	17,8510	-21,4829	7,6	990	66,07	37,88	73	36	406,04	36	88,54	58	0,20
J131/Y1403	17,8529	-21,4847	7,2	2370	155,37	100,05	164	15	399,95	20	442,68	295	2,33
D438/Y721	17,8548	-20,9063	7,9	2870	115,33	110,01	375	21	401,17	530	10,62	490	0,09
J131/Y1402	17,8567	-21,4649	7,4	590	49,25	25,01	37	13	323,13	5	44,27	14	-0,39
B980/2/Y2977	17,8577	-20,2658	7,2	140	6,01	1,94	17	6	54,87	5	0,44	13	-0,90
J133/W2154	17,8577	-21,3838	8,2	740	37,24	36,91	62	15	410,92	23	16,38	22	-0,76
J134/W2121	17,8577	-21,3045	7,9	2250	58,46	45,17	360	39	451,16	400	25,23	228	1,59
B982/Y2970	17,8587	-20,1901	7,6	130	6,01	2,91	9	8	37,80	6	3,10	10	2,68
J131/Y1394	17,8596	-21,5000	8,0	600	19,22	28,90	76	14	347,52	20	14,17	22	0,29
B158/Y3299	17,8596	-19,9730	7,5	900	118,53	62,41	18	4	612,11	66	0,44	17	0,18
B159/Y3310	17,8615	-19,9081	8,1	1070	137,75	84,27	18	3	752,34	63	5,31	30	0,32
B158/Y3297	17,8625	-20,0297	7,4	380	61,67	8,74	13	6	173,15	14	17,71	38	0,32
B158/Y3296	17,8625	-20,0216	7,5	400	70,88	6,56	11	9	201,19	16	22,58	25	0,90
J148/Y1778	17,8625	-21,6568	7,5	750	76,08	35,94	31	12	463,35	13	38,07	8	-1,72
B344/7/Y4674	17,8635	-19,6532	7,5	740	107,32	30,11	12	1	504,81	9	2,66	6	-1,71
B44/Y4621	17,8644	-19,7505	7,4	720	87,29	51,00	1	0	530,42	5	2,66	0	-1,40
B317/Y4863	17,8644	-19,5514	7,3	740	84,09	50,03	1	1	512,13	4	2,66	2	-1,14

Appendix D: Hydrochemical data

Name	Long	Lat	pH	ec µS/cm	Ca ²⁺ mg/l	Mg ²⁺ mg/l	Na ⁺ mg/l	K ⁺ mg/l	HCO ₃ ⁻ mg/l	SO ₄ ²⁻ mg/l	NO ₃ ⁻ mg/l	Cl ⁻ mg/l	Balance %
J104/Y1765	17,8654	-21,7081	7,9	620	55,26	34,00	25	12	378,00	7	22,13	8	0,19
B44/2/Y4471	17,8654	-19,7360	7,4	980	84,09	75,04	10	1	649,91	5	9,74	13	-2,02
J131/Y1395	17,8673	-21,5315	8,0	650	57,26	30,11	39	10	375,56	12	35,41	20	-1,70
B44/Y4620	17,8673	-19,7514	7,5	750	88,10	56,10	1	0	558,46	5	0,00	0	-1,10
B744/Y4867	17,8702	-19,5198	7,5	910	112,12	58,04	1	1	636,50	5	6,20	4	-1,45
D274/1/W2136	17,8712	-21,2414	7,6	1740	70,48	43,47	215	22	385,32	161	102,26	200	0,15
B44/3/Y2997	17,8721	-19,8036	7,8	950	82,09	74,07	8	1	608,46	4	0,00	29	-1,44
B44/2/Y4772	17,8740	-19,7225	7,8	930	73,28	83,05	5	2	670,64	4	0,00	6	-2,20
B982/Y2969	17,8750	-20,2333	6,8	130	5,21	2,91	9	8	31,70	5	5,75	14	-0,71
B158/Y3298	17,8750	-19,9928	7,7	560	78,08	33,03	17	3	381,66	25	0,44	22	0,18
843	17,8769	-20,5315	7,6	1210	92,10	61,92	87	8	596,26	57	80,56	64	-1,38
J131/Y1399	17,8779	-21,4757	7,5	780	75,28	33,03	41	8	354,83	8	78,80	48	-0,84
B983/Y3292	17,8788	-20,1595	7,1	170	10,81	13,11	5	7	71,94	11	0,44	22	-0,51
B162/Y2995	17,8788	-19,8775	7,5	1190	92,10	85,97	34	3	758,44	28	0,44	13	-0,61
B160/Y3317	17,8798	-19,8523	7,8	1600	153,37	118,99	43	5	604,80	166	153,60	121	0,48
B344/7/Y4675	17,8808	-19,6432	7,4	760	113,32	27,93	12	1	499,93	4	3,98	8	-0,39
B655/Y6394	17,8817	-19,4622	8,1	700	12,01	90,09	8	2	508,47	6	0,44	8	-1,63
D438/Y722	17,8817	-20,9270	8,3	1890	71,28	51,00	276	46	477,99	250	26,56	250	1,01
J133/W2151	17,8827	-21,3667	8,1	840	37,24	39,10	72	16	392,63	23	41,61	47	-1,68
J132/W2156	17,8846	-21,4108	8,1	650	33,24	33,75	45	14	352,39	12	17,26	19	-0,65
B44/3/Y2996	17,8856	-19,8162	7,4	1390	118,13	110,01	13	1	695,03	24	86,32	76	0,36
D274/W2119	17,8885	-21,2748	8,2	710	27,23	45,41	44	15	335,32	15	28,33	34	1,16
J108/Y1746	17,8923	-21,6901	8,0	630	72,08	20,88	38	10	410,92	7	13,28	6	-0,27
J104/Y1764	17,8923	-21,7360	7,7	3340	350,38	150,08	132	19	410,92	105	779,12	480	1,46
B984/Y2987	17,8933	-20,0505	8,0	1550	82,09	59,01	82	71	436,53	110	48,69	164	-1,78
803	17,8942	-20,3279	7,8	7840	13,21	189,90	2140	112	5420,02	370	0,00	490	0,85
B980/2/Y2978	17,8952	-20,2640	6,8	100	6,01	1,94	7	7	29,26	4	2,21	10	3,43
B984/Y2988	17,8952	-20,0559	7,6	620	35,24	18,94	33	38	298,74	15	19,03	11	-0,88
B164/Y2991	17,8952	-19,9459	7,6	990	90,10	75,04	15	3	643,82	18	22,13	9	-0,60
J104/Y1763	17,8952	-21,7378	7,9	1530	132,14	68,00	35	84	527,98	58	216,91	90	-0,12
B984/Y2989	17,8962	-20,0901	7,5	140	10,01	2,91	8	11	57,31	7	0,44	10	-0,20
D274/1/W2134	17,8962	-21,2514	7,7	1380	50,45	47,60	144	23	465,79	106	32,76	96	0,79
D267/Y622	17,8981	-21,1441	7,4	2760	102,11	65,08	445	26	477,99	460	24,35	440	0,43
B983/Y3293	17,8990	-20,1351	7,9	250	38,04	6,31	7	7	131,69	6	1,33	24	-1,36
B44/4/Y4474	17,8990	-19,7441	7,5	830	67,27	70,91	8	1	586,51	4	0,00	6	-1,54
B162/Y2993	17,9010	-19,9036	6,8	2210	230,25	110,01	102	12	1212,04	78	90,75	78	0,27
B44/4/Y4476	17,9048	-19,7171	8,5	790	10,01	104,91	6	4	575,53	5	0,00	12	-1,96
B380/Y4682	17,9048	-19,6604	7,8	990	54,06	94,95	9	1	558,46	8	26,56	42	-0,02
J131/Y1400	17,9058	-21,4685	8,2	710	42,05	33,03	69	12	368,24	15	41,61	33	1,09
B655/Y6393	17,9058	-19,4568	6,8	890	105,31	57,07	2	0	621,87	4	0,44	2	-1,46
B164/Y2992	17,9058	-19,9667	7,6	1170	80,09	90,09	22	2	625,53	9	130,59	13	-1,95
B14/Y4677	17,9077	-19,6351	7,4	1550	106,12	119,96	57	0	810,87	22	62,42	110	-0,58
B44/4/Y4475	17,9077	-19,7505	7,6	3100	130,14	264,94	92	16	727,95	150	407,25	400	-0,30
B14/Y4676	17,9106	-19,6387	7,6	730	74,08	43,95	16	0	497,50	5	0,44	3	-2,06
B161/Y2999	17,9106	-19,8505	7,7	1660	98,11	139,88	45	17	809,65	87	30,99	99	1,14
B161/Y3000	17,9144	-19,8486	7,6	1410	80,09	119,96	47	5	855,98	82	4,43	14	-0,50
B162/Y2994	17,9154	-19,8964	7,5	1770	91,30	150,08	102	5	947,44	190	0,44	34	2,44
852	17,9163	-20,6730	7,6	1880	79,29	40,07	256	13	436,53	65	15,94	365	-0,90
D267/Y621	17,9163	-21,1568	7,4	2370	75,28	48,08	374	27	421,90	360	32,32	330	0,89
B984/Y2990	17,9183	-20,0351	7,8	620	41,24	36,91	23	3	362,15	7	0,44	7	-0,90
D443/Y568	17,9183	-21,0306	7,5	670	70,08	17,97	50	5	318,25	13	28,33	47	0,06
B533/Y6396	17,9192	-19,3919	6,9	910	135,35	43,95	4	1	645,04	6	1,77	6	-1,51
D376/1/W2173	17,9212	-21,1991	8,2	2600	76,48	41,04	418	53	557,24	340	42,94	330	0,98

Appendix D: Hydrochemical data

Name	Long	Mlat	pH	ec µS/cm	Ca ²⁺ mg/l	Mg ²⁺ mg/l	Na ⁺ mg/l	K ⁺ mg/l	HCO ₃ ⁻ mg/l	SO ₄ ²⁻ mg/l	NO ₃ ⁻ mg/l	Cl ⁻ mg/l	Balance %
D377/1/W2133	17,9221	-21,2577	8,0	2000	56,46	47,60	288	26	465,79	250	46,48	225	-0,02
B591/Y4873	17,9231	-19,5090	7,4	730	77,28	53,91	1	1	506,03	7	3,54	4	-1,46
B744/Y4868	17,9240	-19,5207	7,3	790	95,30	53,91	2	1	545,05	5	2,66	4	0,61
844	17,9269	-20,5126	7,9	5300	348,38	225,84	470	4	110,96	1080	119,52	1170	-2,35
B534/Y6387	17,9288	-19,3883	7,6	1030	135,35	53,91	10	1	609,68	8	20,36	33	1,01
810	17,9298	-20,3180	7,0	11810	248,27	415,02	1860	88	1891,21	940	11,51	2920	-1,30
J128/W2163	17,9308	-21,3694	8,0	710	45,25	33,51	54	16	393,85	15	26,56	17	0,64
J112/Y1434	17,9327	-21,5856	8,0	1060	120,13	42,98	30	13	434,09	9	110,67	85	-1,39
B322/Y4698	17,9337	-19,5739	7,1	780	80,09	59,98	1	1	534,08	3	6,20	3	0,01
B986/Y2974	17,9356	-20,1793	6,8	160	13,21	2,91	6	10	60,97	5	2,21	10	-0,18
J127/Y2142	17,9356	-21,2874	8,0	970	43,25	47,84	90	18	434,09	47	42,94	42	2,45
D267/Y620	17,9356	-21,1225	7,7	1130	77,28	56,10	80	13	438,97	19	146,08	76	0,80
B985/Y2979	17,9394	-20,1459	6,7	90	3,20	1,94	7	9	26,83	7	0,44	10	-1,17
B986/Y2972	17,9404	-20,2117	6,7	310	6,01	3,89	20	20	74,38	20	0,44	13	-0,21
B531/Y6395	17,9413	-19,4459	7,5	740	67,27	59,98	3	1	520,66	6	0,44	2	-1,59
B984/Y2986	17,9442	-20,0559	7,7	1190	89,30	25,98	84	32	402,39	71	11,07	111	-1,41
B163/Y3003	17,9442	-19,8721	7,3	5520	235,46	245,03	525	47	1935,11	255	0,44	680	-0,23
B980/1/Y2976	17,9452	-20,2586	6,8	220	15,22	5,10	10	11	91,45	2	0,44	14	-1,23
D275/Y641	17,9481	-21,1739	7,9	2520	235,46	117,05	91	18	338,98	195	309,88	360	2,04
B322/Y4699	17,9500	-19,5658	7,9	720	70,08	62,90	1	1	502,37	4	3,54	3	1,65
J105/Y1753	17,9500	-21,7342	7,7	880	79,29	43,47	35	13	368,24	19	92,96	50	0,26
B591/Y4872	17,9500	-19,4541	7,6	1020	100,11	84,99	4	0	751,12	5	0,44	4	-1,49
J129/Y1660	17,9510	-21,4541	8,2	640	44,05	24,04	58	9	360,93	20	31,87	12	-1,80
J111/Y1423	17,9529	-21,5640	7,7	840	39,24	41,04	75	18	427,99	16	29,66	44	-0,05
D275/Y642	17,9529	-21,1856	7,7	1250	85,29	42,01	124	14	441,41	130	35,41	100	0,50
Y105/Y1754	17,9548	-21,7234	7,9	760	73,28	35,94	40	16	518,22	10	5,31	10	-1,71
J107/Y1740	17,9558	-21,6405	7,7	630	66,07	32,06	22	13	420,68	8	10,62	6	-1,21
B985/Y2980	17,9577	-20,0874	6,6	100	6,01	1,94	5	10	36,58	4	2,66	6	2,08
B175/Y3326	17,9577	-19,8153	7,3	1620	170,19	79,89	48	19	635,28	30	100,93	160	1,33
J107/Y1741	17,9587	-21,6369	7,9	660	63,27	33,03	29	11	417,02	15	8,85	8	-0,65
D394/Y613	17,9587	-21,1414	8,3	750	55,26	51,97	16	20	384,10	8	88,54	13	-0,09
B7/Y4969	17,9606	-19,3577	7,3	880	102,11	37,88	17	1	398,73	8	70,83	35	0,83
106140	17,9615	-18,9243	7,8	1080	84,09	93,98	45	4	580,41	161	0,00	43	-0,31
104871	17,9625	-19,4514	7,8	700	57,26	59,98	1	1	476,77	5	0,00	3	-0,88
B591/Y4871	17,9625	-19,4514	7,8	700	57,26	59,98	1	1	476,77	5	0,44	3	-0,93
B166/Y2984	17,9625	-19,9532	7,6	1070	63,27	82,08	35	3	695,03	5	3,54	5	-0,79
B591/Y4870	17,9625	-19,5162	7,1	1200	122,13	74,07	17	3	632,84	16	61,53	58	-1,24
J112/Y1432	17,9635	-21,6252	8,0	690	53,26	35,94	37	12	414,58	10	32,32	9	-1,61
J126/Y443	17,9635	-21,3099	7,5	790	41,24	36,91	66	15	387,75	38	30,54	26	-0,13
B175/Y3327	17,9654	-19,8144	7,3	2260	200,22	119,96	94	6	510,91	61	309,87	300	2,12
106403	17,9663	-19,2036	7,3	1350	117,33	90,09	25	1	630,40	6	45,59	110	0,30
B163/Y3002	17,9663	-19,9162	7,7	1570	54,06	95,92	150	12	975,48	9	36,30	31	-0,60
B532/Y4966	17,9673	-19,4414	7,3	970	107,32	66,05	2	1	684,06	5	0,44	2	-2,13
J130/Y1406	17,9692	-21,4892	7,5	1780	122,13	76,01	72	12	334,10	20	230,19	200	1,75
B591/Y4869	17,9712	-19,4802	7,7	730	61,27	57,07	9	2	476,77	10	7,08	10	-1,34
106377	17,9721	-19,2162	6,9	1030	102,11	75,04	8	1	713,32	6	2,66	4	-1,39
B166/Y2985	17,9740	-20,0550	8,2	660	50,05	31,08	35	7	345,08	23	27,00	11	-0,90
106136	17,9740	-18,8703	8,1	1300	74,08	58,04	88	65	453,60	28	121,73	140	0,12
B8/Y4971	17,9779	-19,4126	7,7	780	68,07	61,92	7	0	510,91	3	28,77	7	-1,66
B986/Y2973	17,9788	-20,2225	6,9	250	14,02	5,10	21	21	131,69	4	5,75	9	-0,36
106372	17,9788	-19,3108	7,3	830	90,10	52,94	12	6	532,86	6	12,84	3	2,03
J111/Y1428	17,9788	-21,5667	7,3	910	65,27	45,90	55	11	451,16	10	34,53	68	-1,87
106376	17,9798	-19,2297	7,4	960	95,30	69,94	5	2	670,64	6	2,66	2	-1,98

Appendix D: Hydrochemical data

Name	Long	Lat	pH	ec µS/cm	Ca ²⁺ mg/l	Mg ²⁺ mg/l	Na ⁺ mg/l	K ⁺ mg/l	HCO ₃ ⁻ mg/l	SO ₄ ²⁻ mg/l	NO ₃ ⁻ mg/l	Cl ⁻ mg/l	Balance %
106404	17,9798	-19,1730	6,7	1050	132,14	60,95	8	0	714,54	20	0,00	6	-1,39
B166/Y2983	17,9798	-19,9811	7,7	1460	74,08	100,05	94	10	812,09	38	0,44	78	-0,10
B166/Y2982	17,9808	-20,0000	7,6	1410	70,08	110,01	66	6	798,68	91	0,44	42	-1,90
B163/Y3004	17,9817	-19,8865	7,8	1930	83,29	169,99	59	3	824,28	50	5,31	220	-0,13
B42/Y4668	17,9827	-19,7180	7,4	730	83,29	49,05	3	1	506,03	4	0,00	4	-0,83
B41/1/Y4807	17,9846	-19,6703	7,0	890	96,10	62,90	1	1	584,07	4	3,54	4	1,08
B985/Y2981	17,9856	-20,1360	6,9	100	4,00	0,97	5	10	24,39	5	5,31	5	1,52
B986/Y2975	17,9865	-20,1784	6,5	190	8,01	1,94	8	20	54,87	8	0,44	11	1,28
B175/Y3325	17,9865	-19,7811	7,3	1910	210,23	67,02	74	1	593,82	18	141,65	240	0,23
7800	17,9894	-21,8108	7,4	480	82,09	15,06	6	11	306,06	15	0,00	12	1,83
B12/Y4701	17,9904	-19,5559	7,7	750	80,09	61,92	1	1	534,08	4	0,44	1	1,61
106348	17,9913	-19,0054	7,0	1460	104,11	56,10	140	3	748,68	6	70,83	88	-0,13
106374	17,9923	-19,2730	6,8	930	103,31	59,98	3	1	625,53	6	12,39	4	-2,11
B7/Y4970	17,9923	-19,3964	7,6	880	68,07	86,94	4	1	614,55	4	7,97	12	0,60
B9/1/Y4718	17,9933	-19,4739	7,8	700	42,05	71,88	2	1	487,74	3	0,44	4	-0,31
106347	17,9933	-19,0396	6,9	940	120,13	52,94	11		663,33	4	0,00	6	-1,34
B10/Y4714	17,9942	-19,4829	7,9	720	70,08	59,01	2	1	512,13	3	0,44	4	-0,65
B41/Y3448	17,9942	-19,6946	7,4	750	86,09	57,07	1	1	559,68	4	4,43	2	-1,75
B177/Y3331	17,9942	-19,7613	7,3	1740	180,20	110,01	25	1	599,92	10	367,41	96	1,28
B175/Y3323	17,9952	-19,8297	7,8	930	112,12	54,88	7	1	620,65	7	2,21	6	-0,39
106375	17,9971	-19,2432	6,8	930	107,32	50,03	10	1	547,49	6	54,89	15	-2,33
106383	17,9981	-19,3153	7,0	930	106,12	54,88	4	1	536,51	24	51,35	9	-1,78
106071	18,0010	-18,9387	8,1	1000	81,69	89,37	33	3	647,48	4	22,13	64	0,33
B164/1/Y3014	18,0010	-19,9559	7,5	2210	94,10	164,89	106	22	781,60	41	208,05	200	1,69
C383	18,0029	-18,7063	8,2	850	72,08	43,23	59	11	475,55	33	1,33	39	2,04
B177/Y3332	18,0038	-19,7631	7,2	2550	320,35	59,98	18	1	418,24	27	451,52	260	-0,69
106373	18,0038	-19,3081	7,8	840	70,08	70,91	11	2	532,86	52	6,20	2	-0,56
106384	18,0048	-19,3135	7,0	900	99,31	56,10	5	1	553,59	14	26,56	10	-1,31
106345	18,0058	-19,0550	6,8	1050	140,15	57,07	16	1	669,42	8	20,36	19	1,68
106344	18,0058	-19,0595	6,9	1410	150,16	59,98	38	60	696,25	52	84,55	56	0,58
J122/Y1675	18,0067	-21,4306	7,8	1160	79,29	59,01	72	15	417,02	40	154,94	80	-0,38
7803	18,0087	-21,8640	7,4	880	59,26	34,00	86	11	498,71	13	13,28	38	0,24
B7/Y4967	18,0096	-19,3820	7,2	1060	103,31	84,99	4	0	737,71	5	5,75	6	-0,53
B167/Y3015	18,0106	-19,9739	7,7	1100	81,29	78,92	45	1	695,03	16	25,67	18	-0,44
B174/Y3322	18,0106	-19,8495	7,1	5180	250,27	249,88	550	43	1044,98	370	725,97	700	1,57
J106/Y1750	18,0115	-21,7009	7,9	760	97,31	37,88	23	11	547,49	7	0,44	9	-0,67
J122/Y1671	18,0115	-21,4018	7,9	1040	88,10	52,94	36	11	354,83	11	110,67	110	-1,54
7802	18,0135	-21,8622	7,3	840	66,07	42,98	46	19	467,01	12	28,33	32	0,31
106349	18,0135	-18,9829	7,0	1190	95,30	85,97	48	1	820,62	10	0,00	27	-1,68
B175/Y3324	18,0144	-19,8162	7,4	920	111,32	42,98	18	1	545,05	5	0,44	30	0,05
106346	18,0144	-19,0450	7,0	1070	126,14	54,88	24		663,33	6	6,20	43	-1,88
B163/Y3001	18,0144	-19,9405	7,3	2980	180,20	189,90	108	1	608,46	69	309,87	460	-0,07
7782	18,0154	-21,9153	7,0	830	66,07	33,03	67	13	498,71	10	6,64	25	0,37
106407	18,0154	-19,1748	7,4	880	97,31	57,07	6	1	552,37	28	27,45	8	-2,31
106369	18,0154	-19,2216	7,0	1000	96,10	73,10	7	1	649,91	6	0,00	4	1,14
B177/Y3330	18,0154	-19,7748	7,5	1740	190,21	65,08	63	1	568,22	57	278,88	120	-2,13
J114/Y1680	18,0154	-21,4847	8,0	1960	68,07	56,10	286	14	657,23	67	336,44	130	-1,06
B167/Y3016	18,0163	-20,0396	7,6	1410	77,28	114,86	70	7	786,48	95	3,98	36	1,80
B12/Y4700	18,0173	-19,5577	7,6	720	80,09	54,88	2	0	499,93	4	0,44	1	1,72
Y106/Y1749	18,0173	-21,7252	8,0	800	46,05	31,08	96	17	515,79	12	6,20	8	2,37
J125/Y431	18,0183	-21,3423	7,8	730	49,25	36,91	52	12	403,61	20	37,19	13	0,42
J122/Y1677	18,0183	-21,4243	7,6	1820	121,33	87,91	111	14	430,43	54	363,00	172	-1,10
B11/Y4875	18,0212	-19,5324	7,5	820	90,10	56,10	4	2	571,88	4	0,44	6	-1,55

Appendix D: Hydrochemical data

Name	Long	Lat	pH	ec µS/cm	Ca ²⁺ mg/l	Mg ²⁺ mg/l	Na ⁺ mg/l	K ⁺ mg/l	HCO ₃ ⁻ mg/l	SO ₄ ²⁻ mg/l	NO ₃ ⁻ mg/l	Cl ⁻ mg/l	Balance %
7805	18,0212	-21,8324	7,2	2170	137,35	83,05	214	10	531,64	200	161,57	305	-1,76
B10/Y4713	18,0221	-19,5063	7,7	880	90,10	69,94	2	1	615,77	3	0,44	6	0,16
106076	18,0231	-18,8685	8,0	820	78,89	52,21	20	11	360,93	6	73,48	81	-0,67
C385	18,0231	-18,5658	7,3	910	51,66	46,38	83	17	530,42	8	22,13	25	2,54
7806	18,0231	-21,8342	7,1	2740	207,43	113,89	218	15	471,89	220	145,64	515	0,68
7804	18,0240	-21,8297	7,5	570	57,26	32,06	6	12	359,71	5	6,20	2	-0,76
807	18,0240	-20,3892	6,7	4530	288,31	137,93	550	19	803,55	450	6,64	980	-0,14
806	18,0240	-20,3838	6,9	6070	263,49	203,99	970	42	2369,20	280	14,61	994	0,19
B7/Y4968	18,0240	-19,3955	7,6	990	86,09	92,04	2	0	701,13	5	3,54	3	0,94
J113/Y1737	18,0240	-21,5793	7,7	2010	175,39	129,92	35	18	410,92	24	407,26	260	0,68
B174/Y3320	18,0260	-19,8847	7,9	750	94,10	47,60	31	8	515,79	44	26,56	24	-1,50
B11/Y4874	18,0269	-19,5297	7,5	780	86,09	53,91	2	2	545,05	4	0,44	2	-1,16
7781	18,0269	-21,9243	7,2	910	64,07	30,11	101	11	509,69	19	4,43	46	1,13
851	18,0269	-20,7189	7,6	1100	69,28	34,97	119	20	540,17	56	45,15	48	-0,33
J121/Y1694	18,0279	-21,4477	7,8	570	53,26	26,96	22	7	319,47	3	41,61	9	-1,73
B41/1/Y4808	18,0288	-19,6523	7,7	590	20,02	50,03	16	2	251,19	4	16,82	43	1,55
7798	18,0298	-21,8243	8,0	1570	26,03	35,94	300	27	1057,18	17	5,75	12	-0,32
D446/Y599	18,0308	-21,0297	7,4	2650	305,53	110,01	59	7	449,94	32	708,29	290	-1,09
B174/Y3319	18,0346	-19,8775	7,8	1200	119,33	75,28	66	9	707,22	67	21,25	62	0,57
7799	18,0346	-21,8198	7,4	4670	163,38	179,95	650	24	616,99	275	863,20	700	2,31
B177/Y3333	18,0356	-19,7541	7,2	970	112,12	62,90	5	1	632,84	5	2,66	8	1,24
J122/Y1674	18,0365	-21,4234	7,8	620	54,06	32,06	30	9	354,83	10	36,30	10	-0,15
C384	18,0365	-18,6378	7,5	1000	94,90	56,58	31	8	378,00	4	48,69	125	1,65
B9/Y4715	18,0375	-19,4414	7,2	940	96,10	80,87	2	0	682,84	3	0,44	4	0,73
B168/Y3013	18,0375	-20,0577	7,9	1210	60,07	84,99	75	6	706,00	41	1,33	42	-0,83
B177/Y3328	18,0404	-19,8009	7,4	1390	124,14	76,98	53	1	626,75	61	55,78	80	0,55
D395/Y383	18,0404	-21,1450	7,6	1480	115,33	100,05	20	14	370,68	8	292,17	138	1,23
800	18,0413	-20,2198	7,1	25640	1171	113,89	5400	108	338,98	1650	0,00	9000	1,95
B167/Y3017	18,0423	-20,0144	7,9	970	50,05	76,01	41	6	619,43	19	0,44	16	-1,46
D277/Y417	18,0433	-21,2748	7,6	920	67,27	40,07	55	11	354,83	37	67,29	68	-1,38
B174/Y3321	18,0452	-19,8676	7,8	1340	104,11	59,98	55	5	638,94	7	19,92	56	0,53
106069	18,0452	-18,9378	8,1	1500	153,37	67,75	108	14	946,22	12	80,12	54	-0,78
7797	18,0471	-21,7856	7,5	820	66,47	41,04	23	16	263,38	15	81,01	86	-1,56
106068	18,0471	-18,9333	7,4	1110	94,10	77,95	35	1	615,77	24	79,68	32	-0,47
106067	18,0471	-18,9892	7,1	1170	121,33	65,08	36	2	680,40	33	35,41	40	-1,92
809	18,0471	-20,2802	7,2	1230	84,09	68,00	94	2	602,36	45	108,45	47	0,17
B9/1/Y4717	18,0481	-19,4577	7,8	700	73,28	57,07	1	1	481,64	4	1,77	1	2,36
B178/Y3082	18,0481	-19,8324	7,5	1210	99,31	80,87	38	2	654,79	7	69,06	56	-0,95
105380	18,0490	-19,2640	7,9	660	35,24	70,91	5	1	456,04	23	5,31	3	-1,80
J114/Y1688	18,0490	-21,5378	8,3	690	64,07	27,93	52	8	448,72	16	0,44	16	-1,14
106075	18,0500	-18,8595	7,9	640	74,08	57,55	10	2	460,91	10	0,00	28	2,10
106406	18,0500	-19,1766	6,9	1440	149,36	90,09	11	1	682,84	6	61,97	115	-0,61
B10/Y4712	18,0510	-19,5027	7,5	700	74,08	51,97	2	1	481,64	4	0,44	4	-0,07
106072	18,0519	-18,8901	8,1	600	58,46	58,52	11	2	419,46	11	0,00	39	0,36
B9/Y4716	18,0519	-19,4514	7,7	750	85,29	57,07	2	1	536,51	4	2,66	1	0,65
106064	18,0519	-19,0216	6,9	1030	99,31	74,07	28		684,06	47	5,31	11	-1,28
B178/Y3081	18,0529	-19,8288	7,3	1130	91,30	88,88	18	3	585,29	7	104,03	37	1,07
106368	18,0529	-19,2378	7,1	960	90,10	73,10	9	1	618,21	8	0,00	8	1,88
850	18,0529	-20,6423	7,8	970	57,26	33,03	90	40	449,94	20	32,76	74	0,51
7784	18,0538	-21,8523	7,3	730	103,31	33,03	3	6	451,16	9	23,90	6	0,13
B600/Y4731	18,0538	-19,6477	7,2	860	106,12	52,94	6	0	530,42	4	26,12	20	0,78
B173/2/Y3318	18,0538	-19,9108	7,9	950	113,72	73,82	33	4	673,08	52	0,44	33	0,90
106405	18,0538	-19,2081	7,2	1320	125,34	94,95	10	1	609,68	6	49,58	124	0,40

Appendix D: Hydrochemical data

Name	Long	Mlat	pH	ec µS/cm	Ca ²⁺ mg/l	Mg ²⁺ mg/l	Na ⁺ mg/l	K ⁺ mg/l	HCO ₃ ⁻ mg/l	SO ₄ ²⁻ mg/l	NO ₃ ⁻ mg/l	Cl ⁻ mg/l	Balance %
856	18,0538	-20,9117	7,4	10600	152,17	195,97	2020	25	359,71	2200	0,00	2280	-1,66
106073	18,0558	-18,8685	8,2	680	77,68	54,64	5	2	436,53	34	0,00	35	-1,19
7778	18,0558	-21,9477	7,4	1270	77,28	45,90	130	16	552,37	5	121,73	83	0,87
J121/Y1691	18,0577	-21,4613	8,0	490	45,25	27,93	18	11	315,81	4	10,62	8	-0,32
J122/Y1673	18,0577	-21,4225	8,2	1350	76,08	76,01	74	20	368,24	20	141,66	192	-1,32
8206	18,0587	-21,9982	8,1	1230	65,27	36,91	165	15	795,02	17	0,00	16	0,07
808	18,0596	-20,4117	7,0	970	90,10	61,92	40	1	679,18	12	0,00	8	-1,09
B172/Y3005	18,0596	-19,9730	7,4	1280	134,15	34,00	47	42	574,31	36	70,38	64	-1,91
8205	18,0596	-21,9928	7,2	1560	85,29	46,87	177	11	609,68	72	54,45	128	0,36
106070	18,0606	-18,9288	8,0	600	96,50	25,26	11	2	397,51	6	0,00	34	-1,16
106074	18,0635	-18,8685	8,1	1100	82,89	53,18	116	4	577,97	2	72,15	105	0,08
D277/Y411	18,0635	-21,2829	7,1	3810	330,36	204,96	150	21	376,78	180	903,07	500	2,31
B6/Y4960	18,0644	-19,3703	7,1	1080	89,30	100,05	5	0	753,56	5	4,43	8	0,62
7783	18,0654	-21,8901	7,4	780	67,27	42,01	27	7	330,44	7	73,48	49	0,24
7780	18,0654	-21,9387	7,5	1010	76,08	37,88	106	14	579,19	16	14,17	66	-0,14
B177/Y3329	18,0654	-19,7847	8,0	1040	72,08	53,91	77	7	568,22	68	0,44	18	1,40
D395/Y381	18,0663	-21,1306	7,5	970	96,10	46,87	33	5	492,62	6	26,56	70	-1,85
7801	18,0663	-21,7667	7,2	1710	191,41	88,88	19	17	418,24	15	338,64	200	-0,39
C267	18,0673	-17,5685	7,9	550	56,06	29,14	31	7	396,29	2	0,00	10	-0,70
B168/Y3011	18,0683	-20,0297	7,5	860	76,08	60,95	10	2	585,29	4	0,44	2	-2,31
7779	18,0683	-21,9532	7,3	1490	82,09	61,92	162	15	652,35	20	13,28	172	1,37
1718ca1	18,0690	-17,5830	7,9	545	56,06	29,14	31	7	396,29	2	0,00	10	-0,70
B178/Y3080	18,0702	-19,8027	7,0	2870	250,27	119,96	171	1	625,53	40	301,01	500	-0,36
B178/Y3079	18,0721	-19,7955	7,5	930	77,28	59,98	38	1	580,41	6	0,44	46	-2,20
B172/Y3007	18,0731	-19,9532	8,0	2210	80,09	129,92	172	47	924,27	69	82,34	190	0,21
106100	18,0740	-18,7486	8,1	450	34,44	41,04	17	5	301,18	2	3,54	39	-1,42
B5/A4944	18,0740	-19,4360	7,4	860	95,30	61,92	1	2	607,24	4	4,43	4	-1,35
B5/Y4945	18,0760	-19,4306	7,6	750	71,28	59,98	1	1	532,86	5	0,44	2	-1,94
106363	18,0769	-19,1667	6,9	1150	105,31	94,95	13		730,39	4	41,17	26	0,68
B172/Y3006	18,0769	-19,9874	8,2	720	46,05	59,98	10	2	476,77	5	0,44	3	-1,84
C382	18,0788	-18,7126	7,5	780	62,07	38,85	35	7	396,29	9	30,99	25	0,69
B178/Y3078	18,0788	-19,8550	7,1	1330	124,14	71,88	67	10	706,00	38	29,22	70	1,57
J122/Y1672	18,0817	-21,4216	7,6	750	54,06	34,97	43	10	438,97	9	15,05	12	-1,67
B186/Y3091	18,0817	-19,7081	7,2	1170	74,08	101,99	14	1	731,61	7	12,39	33	-2,09
B600/Y4733	18,0827	-19,6306	7,6	650	54,06	45,90	14	0	393,85	3	23,46	16	-1,81
105385	18,0827	-19,2099	7,1	1450	152,17	100,05	15	1	756,00	8	61,97	110	-0,47
B808/Y4938	18,0837	-19,4910	7,6	770	61,27	69,94	5	1	551,15	4	1,77	6	-1,41
106364	18,0846	-19,1802	7,0	1100	110,12	95,92	7		810,87	4	0,00	8	0,35
845	18,0846	-20,4937	7,3	1210	103,31	49,05	99	7	519,44	53	97,39	72	1,71
B600/Y4732	18,0856	-19,6342	7,5	900	105,31	50,03	16	1	499,93	4	62,86	26	0,35
B179/Y3075	18,0856	-19,8712	7,3	2260	114,12	110,01	218	2	752,34	110	7,97	350	-0,70
799	18,0856	-20,2126	7,4	2620	98,11	73,10	418	19	453,60	480	0,00	410	1,00
D279/Y420	18,0865	-21,2162	7,7	900	44,05	44,93	82	12	517,00	27	34,53	20	-1,95
104958	18,0865	-19,3324	7,2	1390	56,06	164,89	16	12	975,48	15	5,31	19	1,31
846	18,0865	-20,4883	7,2	2040	141,35	60,95	196	12	443,84	46	566,61	122	0,22
B5/Y4943	18,0875	-19,4495	7,5	930	73,28	79,89	9	1	606,02	4	1,77	26	-0,60
106063	18,0885	-19,0216	7,0	950	103,31	66,05	12	1	671,86	4	7,53	8	-1,34
B171/Y3010	18,0904	-20,0045	7,9	810	85,29	42,98	6	9	465,79	5	30,99	14	-2,06
106065	18,0923	-18,9910	7,0	910	109,32	57,07	8		651,13	5	0,00	6	-2,08
J115/Y1699	18,0933	-21,5063	7,6	590	78,08	17,00	29	4	298,74	12	46,04	16	2,46
7777	18,0933	-21,9054	7,4	4490	204,22	181,89	520	12	692,59	188	411,68	1000	-2,06
B180/Y3020	18,0942	-19,9189	7,8	880	84,09	53,91	21	2	568,22	8	0,44	11	-1,03
C380	18,0952	-18,5685	7,3	1100	51,66	40,31	141	18	548,71	14	30,99	80	1,83

Appendix D: Hydrochemical data

Name	Long	Mlat	pH	ec µS/cm	Ca ²⁺ mg/l	Mg ²⁺ mg/l	Na ⁺ mg/l	K ⁺ mg/l	HCO ₃ ⁻ mg/l	SO ₄ ²⁻ mg/l	NO ₃ ⁻ mg/l	Cl ⁻ mg/l	Balance %
106078	18,0952	-18,8568	8,1	1180	56,06	118,75	73	4	759,66	53	0,00	64	1,56
B168/Y3012	18,0962	-20,0495	7,5	830	80,09	56,10	8	2	551,15	5	1,77	6	-1,76
106367	18,0962	-19,2541	7,5	980	77,28	84,99	9	1	654,79	8	0,00	5	1,03
858	18,0962	-20,8342	7,1	3090	123,33	71,88	490	14	664,55	530	37,63	410	-0,52
1818ca1007	18,0975	-18,5663	7,5	1110	46,05	41,04	134	18	521,88	13	39,84	84	0,54
106099	18,0981	-18,7604	8,0	710	46,85	76,25	4	5	388,97	0	55,33	53	0,86
7795	18,0981	-21,8640	7,5	1000	66,07	53,91	51	21	563,34	8	60,65	14	-1,33
798	18,0990	-20,1955	8,3	1320	37,24	32,06	245	16	608,46	155	0,00	80	0,34
D280/1/Y376	18,0990	-21,0000	7,1	1330	115,33	61,92	71	3	503,59	27	177,07	92	-0,89
105381	18,1000	-19,2946	7,9	970	42,05	117,05	8	1	729,17	11	4,87	4	-1,09
D398/Y384	18,1000	-21,1414	7,5	1680	110,12	104,91	75	9	464,57	74	250,11	182	-1,95
7785	18,1010	-21,7937	7,0	1050	147,36	34,97	30	13	434,09	15	177,07	41	1,84
B180/Y3021	18,1010	-19,9288	7,7	1440	90,10	104,91	93	2	838,91	37	0,44	72	1,98
B754/1/Y4810	18,1019	-19,5811	7,2	840	98,11	54,88	3	0	556,02	4	0,44	1	1,67
D398/Y385	18,1038	-21,1144	7,8	940	110,12	50,03	20	3	359,71	5	168,22	47	2,53
B178/Y3077	18,1048	-19,8243	7,0	2150	150,16	135,02	133	7	855,98	26	75,25	270	2,44
B184/Y3084	18,1058	-19,8072	7,4	990	92,10	69,94	21	1	682,84	5	0,44	15	-1,89
B376/Y4725	18,1067	-19,6604	7,8	840	91,30	58,04	10	1	565,78	3	10,62	4	0,89
C381	18,1067	-18,6369	7,5	860	73,28	45,41	38	10	402,39	19	48,69	48	0,94
B754/1/Y4811	18,1067	-19,5793	7,3	870	84,09	68,00	3	1	581,63	4	0,44	3	1,22
B376/Y4726	18,1077	-19,6550	7,3	840	88,10	58,04	10	1	567,00	4	9,74	4	-0,07
106080	18,1096	-18,8874	7,8	690	61,67	62,17	13	2	440,19	27	0,00	34	0,42
104940	18,1106	-19,3847	7,4	910	73,28	79,89	5	1	642,60	4	0,00	10	-1,98
104959	18,1106	-19,3153	8,0	1190	72,08	129,92	10	1	864,52	10	2,66	10	0,16
B754/1/Y4812	18,1115	-19,5775	7,3	840	84,09	60,95	3	1	552,37	4	1,77	4	0,49
B179/Y3076	18,1115	-19,8946	7,5	1170	137,35	42,98	47	1	603,58	24	4,43	88	-1,91
106060	18,1125	-19,0261	7,0	1030	89,30	78,92	28	1	709,66	16	5,31	19	-1,58
B184/Y3083	18,1125	-19,8090	7,2	1100	86,09	79,89	37	3	697,47	10	9,30	35	-0,87
104941	18,1125	-19,3604	7,5	1190	64,07	134,05	8		836,48	4	1,77	24	0,27
797	18,1125	-20,1261	8,3	8550	179,40	187,96	1600	56	927,93	560	44,27	2280	1,90
B808/Y4937	18,1135	-19,4640	7,5	930	75,28	84,99	18	0	691,37	5	0,44	2	0,16
104937	18,1135	-19,4640	7,5	930	75,28	84,99	18		691,37	5	0,00	2	0,18
847	18,1144	-20,5063	7,3	1020	92,10	43,95	49	8	443,84	14	65,96	71	-0,39
B179/Y3074	18,1144	-19,8559	7,7	5080	220,24	270,04	375	110	487,74	300	690,56	920	0,97
D280/1/Y375	18,1154	-21,0739	7,5	720	68,07	34,00	29	3	409,70	8	29,22	16	-1,77
106077	18,1154	-18,8757	8,1	980	70,48	91,55	20	4	437,75	14	115,54	98	-0,29
B5/Y4942	18,1163	-19,4432	7,4	1370	89,30	119,96	18	1	614,55	4	119,52	120	-1,08
D279/Y421	18,1173	-21,2432	7,5	1850	97,31	76,01	165	26	453,60	79	283,31	193	-0,37
D279/Y425	18,1192	-21,2676	7,5	620	52,06	26,96	34	10	348,73	14	19,04	18	-2,03
7796	18,1192	-21,8441	7,1	1030	108,12	36,91	52	20	585,29	13	0,00	36	1,48
106094	18,1202	-18,7550	8,2	900	70,08	66,30	42	6	354,83	34	41,61	127	0,72
D280/1/Y374	18,1212	-21,0468	7,3	1040	98,11	53,91	29	2	401,17	17	174,86	46	-1,85
106079	18,1231	-18,8820	8,1	800	110,12	34,73	17	16	431,65	37	3,54	54	0,41
106098	18,1231	-18,7595	8,0	930	62,07	80,62	36	6	378,00	35	64,19	115	1,10
7774	18,1231	-21,9063	7,7	1030	51,26	34,00	154	3	606,02	60	0,00	29	0,55
B186/Y3090	18,1231	-19,7297	7,4	2320	112,12	169,99	109	6	695,03	50	309,87	260	-0,58
B808/Y4939	18,1260	-19,5009	7,8	880	53,26	104,91	5	1	685,28	4	0,44	10	-0,30
105386	18,1260	-19,1676	7,2	1100	122,13	84,99	11		796,24	5	5,31	13	-0,14
106097	18,1260	-18,7847	8,2	2000	160,98	98,59	154	10	330,44	163	101,81	449	-0,03
B171/Y3009	18,1269	-20,0243	8,2	550	40,04	46,87	4	2	364,59	5	3,98	4	-1,43
104950	18,1269	-19,4090	7,4	910	94,10	67,02	1		629,19	5	0,00	2	-1,05
104951	18,1269	-19,4045	7,5	930	106,12	65,08	2		654,79	5	0,00	3	-0,84
D280/1/Y373	18,1269	-21,0514	7,3	1110	91,30	43,95	31	50	437,75	48	108,46	47	-2,03

Appendix D: Hydrochemical data

Name	Long	Lat	pH	ec µS/cm	Ca ²⁺ mg/l	Mg ²⁺ mg/l	Na ⁺ mg/l	K ⁺ mg/l	HCO ₃ ⁻ mg/l	SO ₄ ²⁻ mg/l	NO ₃ ⁻ mg/l	Cl ⁻ mg/l	Balance %
7772	18,1298	-21,8982	7,5	960	60,07	25,98	108	9	359,71	43	14,17	110	-0,29
105384	18,1298	-19,2072	7,2	1160	125,34	86,94	8	1	768,19	5	48,69	22	-1,14
104952	18,1346	-19,3739	7,7	1020	76,08	100,05	4	1	712,10	10	2,66	8	0,34
B754/1/Y4809	18,1356	-19,6270	7,4	940	105,31	60,95	9	1	593,82	5	5,75	14	1,73
849	18,1356	-20,6261	7,2	1630	142,15	84,99	58	4	401,17	20	442,66	83	0,73
848	18,1356	-20,6198	7,2	1770	105,31	110,98	105	1	596,26	57	210,27	170	-0,43
104957	18,1356	-19,4559	7,6	2980	200,22	195,00	107		587,73	32	393,97	470	1,29
104953	18,1365	-19,3766	7,5	850	68,07	77,95	4		587,73	5	0,00	8	0,12
105382	18,1375	-19,2712	7,5	910	98,11	69,94	10	2	608,46	12	24,79	13	0,67
B180/Y3022	18,1375	-19,9234	7,4	990	113,32	42,98	30	1	603,58	5	0,44	29	-1,40
B184/Y3086	18,1375	-19,7532	7,7	1060	66,07	100,05	19	1	746,24	6	0,44	12	-1,27
7786	18,1375	-21,7216	8,5	1140	28,03	48,08	145	20	440,19	68	4,43	128	-0,56
105383	18,1385	-19,2324	7,7	970	20,02	129,92	17	2	699,91	20	0,00	23	-0,22
106087	18,1413	-18,9396	8,2	800	100,91	57,07	13	6	440,19	82	2,66	46	0,91
B111/1/Y4736	18,1433	-19,4964	7,2	1390	64,07	160,03	24	1	965,73	10	8,85	26	1,53
B179/1/Y3072	18,1433	-19,8640	7,2	1500	92,10	96,89	74	1	741,37	18	75,25	100	-2,30
B180/Y3019	18,1433	-19,9667	7,3	2040	150,16	110,01	90	1	625,53	50	296,59	154	0,16
B180/Y3018	18,1433	-19,9712	7,6	2150	150,16	125,06	101	3	608,46	55	309,87	180	2,45
B171/Y3008	18,1442	-20,0324	8,2	830	51,26	62,90	13	2	436,53	6	26,56	31	-1,37
106095	18,1452	-18,7991	7,7	680	49,25	45,65	48	5	371,90	34	17,71	46	0,26
106086	18,1452	-18,8928	8,0	800	88,90	55,37	13	8	371,90	108	0,00	41	1,36
104961	18,1452	-19,3180	7,1	1300	73,28	135,02	20	4	857,20	20	14,61	22	1,35
B179/1/Y3073	18,1452	-19,8495	7,5	1880	71,28	150,08	85	1	752,34	11	39,84	245	-1,22
106183	18,1462	-19,2928	7,8	800	36,44	111,95	9	1	602,36	2	0,00	39	1,93
7776	18,1462	-21,9973	7,3	2300	130,14	59,98	385	10	487,74	720	16,82	150	1,69
B179/1/Y3071	18,1471	-19,8739	7,6	1210	109,32	68,97	39	1	527,98	8	92,96	78	1,31
801	18,1490	-20,2820	7,2	15040	590,64	82,08	2750	130	221,92	1100	3,54	4800	-0,88
106061	18,1500	-19,0153	7,2	760	93,30	41,04	10	1	498,71	20	0,00	9	-2,02
B186/Y3087	18,1500	-19,7387	7,4	970	84,09	76,01	12	1	643,82	6	7,97	17	-1,28
B186/Y3088	18,1500	-19,7333	7,4	1130	97,31	90,09	21	1	631,62	16	39,84	52	1,59
7773	18,1500	-21,9108	7,6	1640	53,26	44,93	255	7	590,17	145	4,87	164	0,66
106083	18,1510	-18,8631	8,0	650	64,47	51,97	10	2	315,81	18	65,07	47	0,34
104956	18,1510	-19,4622	7,7	860	59,26	79,89	10		615,77	5	0,00	3	-1,55
J118/1/W9921	18,1510	-21,3991	7,6	1140	55,26	84,99	52	22	553,59	18	95,18	52	0,51
B186/Y3089	18,1510	-19,7288	7,2	2040	160,17	114,86	68	1	568,22	62	243,47	240	-2,09
7775	18,1519	-21,9135	7,5	880	75,28	32,06	96	4	440,19	110	0,00	25	2,22
D279/Y422	18,1529	-21,2450	8,0	1120	88,10	53,91	77	9	442,62	130	29,66	72	-0,23
104955	18,1529	-19,4315	7,3	1130	61,27	114,86	20		819,40	5	0,00	4	-0,99
C377	18,1548	-18,7198	7,3	590	64,47	39,34	19	5	388,97	7	19,92	15	0,98
106096	18,1548	-18,7784	7,8	2100	133,35	93,49	224	13	360,93	140	252,76	402	0,37
857	18,1548	-20,8333	7,3	7840	62,07	148,86	1600	21	664,55	1560	0,00	1580	-1,42
C378	18,1567	-18,6468	7,5	990	94,90	55,37	33	8	378,00	4	53,12	125	1,26
106366	18,1587	-19,1982	6,7	1480	111,32	110,01	32	1	740,15	18	110,67	80	-1,60
C379	18,1596	-18,5685	8,2	800	59,66	41,53	84	15	499,93	16	26,12	35	2,44
104954	18,1615	-19,3820	7,3	1130	90,10	104,91	7		816,97	5	0,00	14	-1,67
7557	18,1635	-21,9676	6,9	680	76,08	22,10	38	9	290,21	55	37,63	40	-0,91
106062	18,1635	-18,9946	7,1	830	99,31	49,05	13	1	540,17	12	13,72	16	-0,99
B181/Y3027	18,1635	-19,9973	7,4	1130	125,34	62,90	26	4	563,34	32	66,40	58	0,23
B184/Y3085	18,1635	-19,7973	7,2	3310	250,27	114,86	295	34	527,98	115	345,28	630	1,79
862	18,1635	-20,9441	7,5	5300	780,85	167,07	124	20	193,88	530	6,64	1580	-0,23
104962	18,1644	-19,3423	7,6	1100	83,29	104,91	6		782,82	5	0,00	10	-0,63
7787	18,1663	-21,7000	7,8	700	70,08	31,08	36	10	440,19	8	9,30	6	1,13
D280/1/Y378	18,1673	-21,0207	8,0	810	80,09	39,10	30	3	415,80	21	60,20	20	-1,10

Appendix D: Hydrochemical data

Name	Long	Lat	pH	ec µS/cm	Ca ²⁺ mg/l	Mg ²⁺ mg/l	Na ⁺ mg/l	K ⁺ mg/l	HCO ₃ ⁻ mg/l	SO ₄ ²⁻ mg/l	NO ₃ ⁻ mg/l	Cl ⁻ mg/l	Balance %
B183/Y3070	18,1673	-19,8919	7,7	1440	58,06	70,91	143	1	591,39	46	46,04	136	-0,83
B195/Y3431	18,1673	-19,6829	7,2	1550	78,08	119,96	70	1	737,71	12	42,50	149	-1,14
8898	18,1683	-21,2991	7,5	890	81,29	48,08	19	8	351,17	6	141,65	42	-1,66
9928	18,1692	-21,3622	7,6	1070	68,07	69,94	56	20	532,86	82	32,76	29	1,31
B181/Y3026	18,1702	-20,0243	7,3	1020	90,10	79,89	16	2	568,22	10	17,26	58	1,65
9929	18,1712	-21,3324	7,4	640	71,28	28,90	20	7	379,22	8	31,87	6	-0,58
863	18,1721	-20,8883	7,5	13690	670,73	34,97	2450	65	110,96	940	0,00	4160	2,07
8897	18,1731	-21,2964	7,7	620	60,07	36,91	16	6	349,95	6	46,48	11	-0,26
7558	18,1731	-21,9802	6,8	690	80,09	24,04	42	5	406,04	21	7,97	30	-0,86
106104	18,1750	-18,7946	8,1	550	49,65	35,94	29	4	297,52	2	23,02	42	2,45
B195/Y3434	18,1760	-19,6973	7,9	740	56,06	78,92	14	1	574,31	4	7,08	9	0,32
106365	18,1760	-19,2234	6,9	1070	107,32	84,99	11	1	751,12	4	4,87	17	-0,38
106184	18,1769	-19,2820	7,9	800	42,05	100,29	12	2	525,54	40	0,00	49	0,44
105371	18,1779	-18,9423	7,9	640	96,10	26,96	4	7	419,46	5	14,17	6	-0,06
J118/1/W9923	18,1779	-21,4288	7,5	980	68,07	43,95	84	11	568,22	37	22,13	26	-1,01
B195/Y3433	18,1788	-19,7072	7,7	1440	74,08	129,92	47	1	713,32	17	61,97	106	1,30
B195/Y3432	18,1788	-19,7018	7,4	1670	73,28	144,98	82	25	934,02	36	29,22	105	0,77
106085	18,1788	-18,8874	8,1	850	61,67	64,11	41	8	406,04	35	42,05	83	-0,30
7559	18,1798	-21,9532	7,1	1100	127,34	39,10	44	7	352,39	23	288,62	28	-0,15
795	18,1808	-20,1748	7,9	580	60,07	28,90	18	15	391,41	5	9,74	3	-1,64
106084	18,1808	-18,8658	8,1	800	100,91	49,05	17	3	440,19	22	15,49	64	0,82
B1/Y4738	18,1817	-19,5153	7,3	800	87,29	58,04	2	1	560,90	4	1,77	4	-0,92
7790	18,1817	-21,8252	7,3	970	77,28	48,08	44	14	451,16	13	63,30	56	-0,88
B1/Y4739	18,1827	-19,5099	7,4	780	88,10	54,88	1	0	537,73	3	2,66	1	0,07
104744	18,1827	-19,4090	7,8	900	68,07	85,97	16		637,72	5	0,00	12	1,24
802	18,1827	-20,3009	6,9	12540	364,40	152,99	2260	68	470,67	910	57,55	3840	-1,91
105370	18,1856	-18,9117	7,1	780	60,07	33,03	45	23	458,48	6	0,00	7	2,64
859	18,1856	-20,7243	7,0	2430	185,40	53,91	250	11	540,17	49	460,37	265	0,14
B183/Y3068	18,1894	-19,9063	7,1	1880	107,32	80,87	186	1	855,98	52	86,76	136	-0,55
7788	18,1894	-21,6856	7,6	420	60,07	11,90	10	5	276,79	5	2,21	2	-2,08
7789	18,1894	-21,7468	7,4	720	66,07	27,93	41	6	246,31	17	162,46	26	-1,39
860	18,1894	-20,7171	7,2	1040	119,33	22,10	58	8	387,75	40	24,79	102	0,17
104964	18,1894	-19,3514	7,4	1660	95,30	135,02	88	1	836,48	96	0,00	124	1,32
106101	18,1904	-18,7955	7,8	700	44,45	66,54	12	4	297,52	0	76,14	73	0,94
106103	18,1923	-18,7694	8,2	900	71,68	53,18	51	8	284,11	0	142,98	107	1,94
B194/Y3065	18,1942	-19,7550	7,1	1020	93,30	68,00	16	11	677,96	7	1,77	13	-1,85
106047	18,1952	-19,0856	7,0	870	119,33	44,93	7		615,77	4	0,00	6	-1,91
B181/Y3024	18,1962	-20,0108	7,3	990	107,32	69,94	10	2	540,17	12	74,37	33	1,59
D280/5/Y370	18,1962	-21,0622	7,1	4240	285,51	169,99	330	4	542,61	115	1009,31	520	0,54
B183/Y3069	18,1990	-19,8937	8,1	830	30,03	51,00	77	1	504,81	8	0,44	26	-0,60
B181/Y3025	18,2010	-20,0180	8,0	910	70,08	84,99	17	4	620,65	8	3,54	14	2,45
106102	18,2019	-18,8135	8,0	570	37,24	67,27	4	6	375,56	0	8,85	43	1,38
105372	18,2019	-18,9595	7,8	870	62,07	73,10	17	9	526,76	18	3,54	24	1,72
B181/Y3023	18,2019	-20,0117	7,5	1060	108,12	59,98	12	2	523,10	10	75,25	32	0,03
104888	18,2019	-19,2910	7,4	3800	200,22	195,00	275	3	496,28	50	593,17	740	-1,98
7561	18,2029	-21,9351	7,2	860	101,31	20,88	68	6	362,15	130	11,95	27	1,49
7834	18,2038	-21,6378	7,4	670	85,29	36,91	20	7	456,04	5	15,94	10	1,37
B183/Y3067	18,2038	-19,8757	8,0	680	49,25	53,91	15	1	442,62	4	0,44	15	-1,27
7560	18,2038	-21,9477	7,4	720	64,07	14,08	71	7	265,82	115	4,43	29	-0,11
104745	18,2038	-19,3721	7,9	1140	80,09	114,86	16	1	786,48	25	0,00	16	1,10
104963	18,2038	-19,3261	7,4	1350	103,31	104,91	24	1	693,81	17	115,09	50	-0,45
104747	18,2038	-19,3775	7,4	1560	69,28	154,93	46	1	820,62	27	61,09	90	1,95
796	18,2038	-20,0631	7,8	1640	75,28	35,94	306	24	941,34	46	15,05	116	1,82

Appendix D: Hydrochemical data

Name	Long	Lat	pH	ec µS/cm	Ca ²⁺ mg/l	Mg ²⁺ mg/l	Na ⁺ mg/l	K ⁺ mg/l	HCO ₃ ⁻ mg/l	SO ₄ ²⁻ mg/l	NO ₃ ⁻ mg/l	Cl ⁻ mg/l	Balance %
B197/3/Y3428	18,2048	-19,6622	7,1	940	84,09	73,10	16	1	638,94	6	0,44	4	1,00
104742	18,2048	-19,4351	7,4	1180	90,10	88,88	26	1	565,78	4	57,55	86	1,00
104965	18,2058	-19,3613	7,3	1820	83,29	154,93	68	30	780,38	83	154,93	98	2,10
104741	18,2067	-19,4441	7,1	770	74,08	86,94	22		631,62	24	21,69	18	0,42
B732/Y4741	18,2067	-19,4441	7,1	770	74,08	86,94	22	0	631,62	24	21,69	18	0,43
D280/5/Y367	18,2067	-21,1054	7,6	1740	133,35	80,87	100	2	490,18	29	234,62	210	-1,76
1818ca1030	18,2083	-18,5350	8,1	1450	34,04	44,93	220	33	658,45	25	12,84	144	0,73
7793	18,2087	-21,8279	7,3	800	71,28	23,07	70	8	380,44	21	86,32	26	-0,53
7794	18,2087	-21,8225	7,4	920	72,08	19,91	32	9	378,00	11	7,53	4	1,48
B732/Y4740	18,2096	-19,5162	7,3	850	90,10	67,02	2	1	577,97	24	2,66	9	-0,71
106055	18,2106	-19,0063	7,0	870	94,10	54,88	21		598,70	6	1,77	18	-1,69
104887	18,2106	-19,2883	7,0	1000	97,31	68,97	17	1	665,77	5	2,66	10	-0,20
B182/Y3028	18,2125	-19,9541	7,8	1820	78,08	139,88	94	37	726,73	112	137,23	148	-0,46
D280/5/Y369	18,2125	-21,0892	7,0	4290	300,33	195,00	295	11	501,15	120	885,36	710	-0,98
7611	18,2135	-21,9910	6,9	1070	104,11	59,98	56	6	657,23	42	2,21	28	0,99
7846	18,2144	-21,4946	7,5	670	45,25	45,90	38	9	467,01	8	4,87	8	-1,29
7555	18,2144	-21,8973	7,1	700	86,09	30,11	15	9	410,92	6	32,76	10	-0,08
7612	18,2144	-21,9937	7,2	1070	100,11	54,88	55	5	627,97	42	0,00	27	0,44
106056	18,2144	-19,0045	7,7	1410	105,31	104,91	47	12	680,40	43	132,80	70	0,24
106109	18,2163	-18,8928	8,1	630	41,65	70,67	11	2	413,36	0	7,08	54	0,07
B194/Y3064	18,2163	-19,7748	8,7	930	16,02	104,91	28	1	453,60	7	0,00	124	-1,85
8118	18,2173	-21,4838	7,3	830	24,03	22,10	133	16	509,69	11	4,43	6	2,16
106054	18,2173	-19,0018	7,0	950	99,31	62,90	24		638,94	27	0,00	20	-1,86
B183/Y3066	18,2173	-19,8901	7,8	1130	65,27	76,98	74	1	677,96	6	0,44	62	-0,60
7556	18,2173	-21,8919	7,2	1500	159,37	59,98	42	30	396,29	32	143,42	202	1,02
B193/Y3062	18,2173	-19,8189	7,0	2870	170,19	189,90	155	1	803,55	61	548,90	290	-0,94
1718cc1001	18,2180	-17,7530	7,7	1040	38,84	35,94	153	13	604,80	21	2,21	48	0,61
7791	18,2183	-21,8243	7,2	2450	275,50	68,00	90	14	317,03	62	590,96	300	-1,79
1718cc2	18,2188	-17,7516	8,6	2300	8,41	7,29	604	13	1146,19	171	2,66	185	0,03
B197/2/Y3437	18,2192	-19,6541	7,4	970	95,30	68,97	16	1	643,82	7	0,44	3	1,66
B197/3/Y3429	18,2192	-19,6829	7,2	5650	270,29	334,88	425	30	673,08	420	885,33	930	0,01
106108	18,2212	-18,8703	8,1	700	42,05	71,15	24	3	463,35	13	0,00	44	-0,17
B197/2/Y3436	18,2212	-19,6514	7,5	910	90,10	61,92	15	1	603,58	8	0,44	3	0,59
B193/Y3063	18,2221	-19,8270	8,8	970	9,21	110,01	60	1	591,39	8	0,44	62	2,24
B197/3/Y3430	18,2221	-19,6856	7,2	3180	116,13	214,91	222	10	690,15	195	424,96	440	-1,83
106107	18,2231	-18,8423	8,0	470	27,23	49,05	21	3	306,06	13	0,00	34	1,11
C375	18,2240	-18,6541	7,3	1000	66,87	48,08	94	11	499,93	17	35,41	80	1,25
104743	18,2240	-19,4171	7,3	1050	87,29	92,04	14		663,33	4	20,36	30	1,66
1818ca1003	18,2250	-18,7277	7,2	1170	80,09	50,03	98	9	468,23	33	146,08	64	0,33
105369	18,2260	-18,9171	7,3	1460	117,33	62,90	120	5	588,95	95	79,68	100	2,00
C374	18,2279	-18,5838	7,5	1380	55,66	45,17	230	37	804,77	46	35,41	125	-2,24
1718ca10	18,2286	-17,6642	8,8	1420	8,01	16,27	310	9	681,62	85	19,48	60	1,66
7842	18,2288	-21,5180	7,3	480	48,05	24,04	33	4	317,03	8	6,64	11	1,15
105373	18,2288	-18,9568	7,2	950	108,12	58,04	24	7	598,70	21	5,75	32	0,66
1718caq1002	18,2291	-17,6045	8,0	380	36,04	20,88	10	5	238,99	1	2,21	7	-1,10
C376	18,2298	-18,7180	7,3	830	59,66	38,61	96	10	515,79	46	28,33	20	0,73
105374	18,2298	-18,9297	7,5	1300	120,13	77,95	42	53	706,00	55	55,78	49	1,94
105368	18,2298	-18,9144	7,6	3300	215,43	139,88	270	32	562,12	260	664,00	320	0,67
1718ca1005	18,2300	-17,6710	7,9	490	22,02	17,97	55	14	307,28	1	2,21	8	0,10
1718ca7	18,2306	-17,6645	7,8	485	22,42	20,40	59	14	329,22	6	0,00	10	-0,70
7814	18,2308	-21,7297	7,0	580	81,29	19,91	25	8	353,61	7	47,37	11	-0,20
7835	18,2308	-21,6036	7,2	1250	121,33	82,08	30	13	420,68	6	194,77	150	0,19
B182/Y3029	18,2308	-19,9946	7,0	2710	210,23	189,90	42	1	637,72	15	442,66	360	-0,16

Appendix D: Hydrochemical data

Name	Long	Mlat	pH	ec µS/cm	Ca ²⁺ mg/l	Mg ²⁺ mg/l	Na ⁺ mg/l	K ⁺ mg/l	HCO ₃ ⁻ mg/l	SO ₄ ²⁻ mg/l	NO ₃ ⁻ mg/l	Cl ⁻ mg/l	Balance %
1718ca6	18,2309	-17,6633	7,6	1800	18,42	19,18	455	14	1310,80	12	5,31	20	0,59
B593/2/Y4752	18,2317	-19,4865	7,8	1520	90,10	125,06	68	1	791,36	6	52,68	120	1,26
W-10	18,2323	-21,4870	8,0	789	39,60	27,20	100	14	477,63	5	5,44	7	4,08
7569	18,2327	-21,9315	7,4	840	76,08	34,00	79	5	508,47	65	0,00	11	0,80
106048	18,2327	-19,1000	7,1	1110	124,14	68,00	27	5	697,47	15	29,22	35	-0,42
868	18,2327	-21,0270	7,3	3200	62,07	37,88	615	11	532,86	285	5,75	660	-0,19
B188/Y3034	18,2337	-19,9189	7,9	1280	90,10	53,91	137	1	763,31	6	0,44	82	-0,13
106049	18,2356	-19,0964	6,9	1050	120,13	52,94	17	4	563,34	12	30,10	25	2,38
1718ca1001	18,2370	-17,5370	7,6	710	46,85	57,07	16	13	473,11	1	2,21	10	-0,18
1718cc1002	18,2375	-17,8650	7,9	670	34,04	25,98	72	16	434,09	1	2,21	7	0,07
8117	18,2375	-21,4784	7,2	770	33,24	34,97	83	13	467,01	11	8,41	8	1,40
1718ca13	18,2377	-17,7473	7,9	950	36,84	35,94	148	20	603,58	24	0,00	45	0,36
C259	18,2385	-17,6712	8,4	730	12,01	9,71	140	10	432,87	10	1,77	15	-0,06
7808	18,2385	-21,7468	7,4	880	76,08	42,01	26	12	306,06	10	84,11	72	0,46
B192/1/Y3046	18,2385	-19,8495	7,0	950	110,12	53,91	16	1	660,89	5	0,44	6	-2,11
1718cc5	18,2391	-17,8636	8,6	285	30,83	16,51	13	5	207,29	0	0,00	10	-1,22
7567	18,2394	-21,8937	7,3	770	77,28	25,01	27	9	390,19	6	28,33	12	0,03
7833	18,2394	-21,6459	7,3	1210	92,10	76,98	51	15	456,04	12	199,20	96	-0,41
106105	18,2404	-18,8811	8,1	690	59,26	55,37	25	4	458,48	26	0,00	34	-1,75
C258	18,2404	-17,6595	8,6	2300	5,21	2,91	734	7	1743,67	43	22,13	80	0,80
104876	18,2404	-19,3315	7,3	2660	106,12	169,99	255	4	1064,49	65	15,94	445	-1,82
7836	18,2413	-21,5775	7,2	570	52,06	19,91	57	8	386,53	7	2,66	11	0,63
7807	18,2413	-21,7432	7,4	640	77,28	13,11	33	12	299,96	6	59,76	24	-0,03
867	18,2413	-20,9937	7,7	1990	67,27	31,08	340	11	553,59	125	10,62	330	-0,40
7845	18,2423	-21,5387	8,4	560	56,06	34,00	28	8	397,51	6	10,18	7	0,12
D402/Y366	18,2423	-21,1613	7,3	910	48,05	51,00	78	10	557,24	30	2,21	25	-1,23
793	18,2423	-20,2270	7,0	1480	165,38	54,88	103	11	823,06	60	3,54	108	-0,88
B197/2/Y3435	18,2423	-19,6730	7,2	3050	80,09	239,93	230	1	826,72	160	499,33	276	1,58
104889	18,2433	-19,2703	7,8	780	88,10	41,04	13		476,77	9	17,71	14	-2,01
7809	18,2433	-21,7477	7,2	1070	114,12	51,97	28	13	332,88	12	192,56	84	1,50
B593/2/Y4753	18,2433	-19,4658	8,8	1660	20,02	189,90	82	1	874,27	5	13,28	190	0,53
105361	18,2442	-18,8045	7,4	720	61,27	45,90	20	4	398,73	6	38,51	16	0,48
837	18,2442	-20,3730	7,6	1060	55,26	58,04	92	8	625,53	45	15,94	27	-1,95
B192/1/Y3047	18,2442	-19,8441	7,1	1210	101,31	82,08	42	1	695,03	6	20,36	78	-1,38
104891	18,2452	-19,2757	7,4	940	100,11	36,91	26	24	470,67	20	57,99	27	-0,25
C260	18,2452	-17,6667	8,3	1900	22,02	19,43	439	12	1280,32	8	15,05	20	0,33
C392	18,2462	-17,8703	8,5	290	30,83	16,51	13	5	207,29		0,00	10	-1,22
B213/Y3439	18,2462	-19,6099	7,0	2180	126,14	179,95	60	1	748,68	6	203,63	260	1,55
B188/Y3035	18,2481	-19,9360	7,3	1040	88,10	40,07	42	31	402,39	27	101,81	67	-1,79
838	18,2481	-20,3559	7,3	1060	70,08	50,03	100	9	637,72	60	14,61	27	-2,03
105362	18,2490	-18,7649	7,6	830	59,26	45,90	52	6	445,06	7	14,61	44	1,29
106106	18,2490	-18,8658	8,1	3200	115,33	170,96	390	13	548,71	841	14,61	347	0,81
864	18,2490	-20,8387	7,8	4640	232,25	17,00	770	37	485,30	240	0,00	1260	-1,11
C261	18,2500	-17,6766	7,8	490	22,42	20,40	59	14	329,22	6	0,00	10	-0,70
7843	18,2500	-21,5090	7,3	550	50,05	27,93	30	7	367,02	7	6,64	9	-1,89
7815	18,2500	-21,7162	7,1	800	108,12	31,08	30	6	471,89	11	41,61	35	-1,10
794	18,2510	-20,1360	7,8	790	55,26	19,91	97	9	401,17	15	16,38	58	0,33
B593/Y3443	18,2510	-19,5243	7,7	800	78,08	56,10	5	1	470,67	34	14,61	5	-0,24
839	18,2510	-20,3595	7,3	970	136,15	39,10	16	2	506,03	8	88,53	33	-0,28
840	18,2510	-20,4054	7,5	1020	91,30	50,03	71	3	581,63	32	44,27	37	-0,50
7568	18,2519	-21,8883	7,0	720	75,28	25,98	47	9	421,90	8	29,22	23	-0,19
104890	18,2519	-19,2730	7,8	820	100,11	46,87	9	1	515,79	7	13,28	16	0,03
B199/Y3059	18,2519	-19,7757	7,6	5080	275,50	309,87	242	167	585,29	280	1434,23	520	0,77

Appendix D: Hydrochemical data

Name	Long	Lat	pH	ec µS/cm	Ca ²⁺ mg/l	Mg ²⁺ mg/l	Na ⁺ mg/l	K ⁺ mg/l	HCO ₃ ⁻ mg/l	SO ₄ ²⁻ mg/l	NO ₃ ⁻ mg/l	Cl ⁻ mg/l	Balance %
8896	18,2529	-21,2532	7,6	1920	205,42	68,97	40	4	301,18	12	398,40	210	0,66
104886	18,2538	-19,3018	7,3	2450	147,36	154,93	103	45	714,54	70	278,88	275	0,61
861	18,2548	-20,6757	7,1	1150	122,13	57,07	35	10	553,59	43	8,41	89	-0,18
104883	18,2548	-19,3550	7,8	1280	70,08	114,86	61	1	855,98	5	4,43	42	0,77
B199/Y3060	18,2548	-19,7928	7,7	1370	91,30	119,96	47	1	919,39	7	24,79	25	0,55
B199/Y3061	18,2548	-19,7802	7,3	5520	330,36	419,87	227	39	712,10	235	1770,66	520	1,74
B213/Y3440	18,2558	-19,6405	7,7	970	83,29	74,07	21	1	626,75	9	6,20	7	1,98
104884	18,2558	-19,3811	7,2	2340	210,23	129,92	93	7	679,18	50	318,72	260	1,52
8894	18,2567	-21,2586	7,7	530	31,23	35,94	24	4	323,13	10	4,43	11	-1,93
792	18,2567	-20,1973	7,0	870	77,28	43,95	56	9	595,04	5	6,20	15	-1,17
104803	18,2567	-19,4189	7,3	1790	71,28	144,98	98	10	912,07	28	44,27	120	0,95
B198/Y3338	18,2577	-19,7541	7,4	1140	64,07	110,01	24	1	760,88	5	0,44	7	2,07
104804	18,2587	-19,4144	7,8	1130	34,04	57,07	79	73	527,98	30	0,00	75	1,32
104892	18,2587	-19,2874	7,2	1390	138,15	49,05	51	70	669,42	35	59,76	56	2,39
7613	18,2596	-21,9351	7,3	670	63,27	20,88	53	7	373,12	29	0,00	17	1,11
8895	18,2596	-21,2550	7,5	930	101,31	50,03	29	4	588,95	10	14,61	16	-0,05
B593/2/Y4751	18,2596	-19,4793	7,5	790	84,09	59,01	2	0	540,17	5	8,85	4	-0,39
B198/Y3335	18,2596	-19,7135	7,8	4290	122,13	355,52	235	2	824,28	61	655,14	660	1,85
B192/1/Y3049	18,2606	-19,8270	7,2	1210	90,10	100,05	34	1	862,08	5	0,44	18	-1,77
B199/Y3058	18,2606	-19,7775	7,4	2710	152,17	210,06	103	1	729,17	55	566,61	240	0,65
7813	18,2625	-21,7378	7,2	670	67,27	31,08	44	12	434,09	5	14,61	16	1,44
105306	18,2625	-19,0694	7,2	940	100,11	67,02	15		665,77	4	0,00	14	-1,00
B198/Y3336	18,2625	-19,7090	7,1	3820	136,15	335,85	143	1	824,28	42	500,21	650	-0,13
7844	18,2635	-21,5351	7,6	550	59,26	27,93	22	7	375,56	6	6,20	5	-1,00
B213/Y3438	18,2635	-19,6523	7,3	1150	71,28	100,05	33	15	753,56	17	3,54	11	2,02
B191/Y3045	18,2644	-19,8721	7,4	1370	109,32	90,09	42	1	677,96	7	64,63	103	-1,61
B593/Y3442	18,2654	-19,5595	9,6	310	4,00	35,94	12	0	203,63	3	0,44	6	1,42
8119	18,2654	-21,3441	7,2	800	60,07	45,90	48	7	487,74	5	8,85	16	1,97
B198/Y3334	18,2654	-19,7153	7,5	2490	62,07	207,63	142	1	847,45	12	208,05	280	1,92
7838	18,2654	-21,5054	6,9	2850	225,45	173,87	164	10	590,17	175	517,92	450	-2,10
B192/1/Y3048	18,2673	-19,8423	8,4	440	11,21	43,95	16	1	281,67	5	0,44	13	-1,96
104877	18,2683	-19,3261	7,6	1240	70,08	110,01	49		731,61	10	70,83	36	1,12
7819	18,2702	-21,6523	7,0	910	103,31	28,90	50	6	290,21	5	94,73	120	0,45
7562	18,2712	-21,9342	7,3	660	35,24	16,03	101	3	390,19	37	2,21	6	1,19
B189/Y3032	18,2712	-20,0072	7,5	810	66,07	71,88	10	4	563,34	7	0,44	2	1,60
B198/Y3337	18,2712	-19,7315	7,3	5560	145,36	444,64	305	1	899,88	60	584,32	1120	0,11
1718cd1006	18,2720	-17,8940	8,6	880	2,00	0,97	210	5	548,71	1	0,44	21	-0,90
D280/2/Y348	18,2721	-21,1541	7,5	1040	49,25	56,10	102	7	551,15	84	13,28	34	-1,12
105375	18,2721	-18,9495	6,9	730	66,07	10,93	62	15	430,43	8	4,43	4	-0,87
7792	18,2731	-20,1171	7,2	910	105,31	24,04	42	32	375,56	29	100,93	48	0,71
105366	18,2731	-18,9108	8,2	920	41,24	77,95	62	3	590,17	28	0,89	20	1,87
8893	18,2740	-21,2739	7,6	930	95,30	48,08	37	3	609,68	14	3,54	11	-1,20
7816	18,2740	-21,6775	7,1	1210	138,15	60,95	55	9	391,41	6	116,42	192	2,47
B593/1/Y4750	18,2740	-19,4793	7,8	710	63,27	58,04	2	1	484,08	4	0,44	8	-1,25
7841	18,2750	-21,5333	7,2	550	52,06	28,90	25	7	353,61	5	22,13	5	-1,23
B188/Y3033	18,2750	-19,9676	7,7	820	55,26	74,07	15	2	504,81	8	18,59	18	1,64
B214/Y3446	18,2750	-19,5919	8,5	1130	21,22	135,02	36	1	609,68	15	54,45	72	2,03
104878	18,2760	-19,3288	7,2	2280	139,35	160,03	88	9	673,08	40	354,13	255	-1,20
7564	18,2760	-21,9297	7,5	2920	167,38	92,04	365	2	601,14	275	110,67	510	0,17
7563	18,2760	-21,9324	7,1	5140	295,52	220,01	580	3	574,31	420	619,73	1020	1,07
789	18,2769	-19,9991	7,2	1100	96,10	48,08	83	7	657,23	40	6,64	26	0,39
105352	18,2779	-18,8396	7,6	680	45,25	50,03	29	5	462,13	6	0,00	1	0,24
105363	18,2779	-18,8811	8,2	1280	62,07	87,91	80	6	452,38	125	0,00	125	1,53

Appendix D: Hydrochemical data

Name	Long	Lat	pH	ec µS/cm	Ca ²⁺ mg/l	Mg ²⁺ mg/l	Na ⁺ mg/l	K ⁺ mg/l	HCO ₃ ⁻ mg/l	SO ₄ ²⁻ mg/l	NO ₃ ⁻ mg/l	Cl ⁻ mg/l	Balance %
105379	18,2788	-18,9838	7,1	830	106,12	57,07	5		607,24	3	0,00	6	0,12
7810	18,2798	-21,7306	7,6	680	58,06	31,08	44	9	413,36	11	1,33	18	0,44
105311	18,2798	-19,0216	7,3	1190	103,31	100,05	34		826,72	9	0,00	20	1,94
105357	18,2817	-18,7901	8,1	660	29,23	34,00	80	6	457,26	7	0,00	3	1,06
104897	18,2817	-19,2306	7,6	840	104,11	52,94	5		560,90	5	12,84	12	-0,37
105356	18,2817	-18,8072	8,5	850	18,02	59,01	94	6	535,30	20	0,00	20	1,23
104896	18,2817	-19,2261	7,4	910	107,32	54,88	8		587,73	5	13,72	12	-0,37
104749	18,2817	-19,4595	7,2	1370	75,28	150,08	20	1	951,09	4	3,98	21	2,02
B593/1/Y4749	18,2817	-19,4595	7,2	1370	75,28	150,08	20	1	951,09	4	3,98	21	2,02
B593/Y3441	18,2827	-19,5541	7,2	860	85,29	59,98	5	1	551,15	6	7,08	7	-0,18
7811	18,2837	-21,7261	7,3	790	56,06	30,11	57	10	424,33		3,98	23	2,19
8120	18,2837	-21,4595	7,2	830	42,05	28,90	105	6	498,71	26	3,10	8	1,14
7817	18,2865	-21,6766	7,4	460	40,04	19,91	24	16	295,08	7	6,64	5	-1,36
7837	18,2865	-21,5919	7,3	670	97,31	22,10	30	5	429,21	6	5,31	25	0,98
B200/Y3050	18,2865	-19,8072	7,3	970	87,29	75,04	13	1	677,96	5	0,44	5	-1,07
B191/Y3044	18,2865	-19,8622	7,0	1210	119,33	76,98	23	1	660,89	6	27,89	81	-1,39
7818	18,2875	-21,6811	7,5	430	40,04	25,01	13	6	284,11	8	4,43	2	-1,80
7839	18,2875	-21,4874	7,4	650	53,26	37,88	40	6	440,19	6	11,07	9	-0,67
105304	18,2875	-19,0784	7,4	880	91,30	69,94	18		669,42	7	0,00	15	-1,97
104893	18,2875	-19,2739	7,7	1020	97,31	76,98	20	1	659,67	5	0,00	30	1,36
7856	18,2894	-21,8387	7,1	900	63,27	46,87	34	11	397,51	10	64,19	42	-0,95
105376	18,2894	-18,9586	7,9	1650	71,28	96,89	141	4	530,42	57	246,56	160	-1,67
B212/Y3341	18,2894	-19,6910	8,2	2550	56,06	220,01	112	1	690,15	23	185,92	380	0,57
V-3	18,2900	-19,3973	6,7	1184	91,00	84,00	48	1	688,00	83	11,00	48	-3,47
B189/Y3030	18,2913	-20,0126	9,0	830	10,01	68,00	90	19	568,22	27	0,44	8	1,88
1718cb1004	18,2920	-17,7080	7,1	610	26,83	9,96	30	75	99,99	50	121,73	40	-3,50
105305	18,2923	-19,0802	7,2	960	97,31	71,88	14	1	675,52	6	0,00	16	-1,05
869	18,2923	-20,9973	7,9	2150	107,32	56,10	296	11	565,78	320	8,41	245	0,32
865	18,2933	-20,8297	6,9	18210	931,01	171,93	2940	71	221,92	900	0,00	6240	-2,08
B191/Y3043	18,2933	-19,9054	7,1	190	30,03	2,91	1	2	97,55	6	0,44	1	2,07
B199/Y3056	18,2933	-19,7369	7,3	2870	150,16	150,08	235	5	741,37	170	469,22	290	-2,02
B593/1/Y4748	18,2942	-19,4784	7,2	800	84,09	57,07	4	1	547,49	4	6,20	8	-1,57
105307	18,2942	-19,1180	7,3	960	106,12	76,01	12		697,47	7	0,00	15	0,30
104879	18,2942	-19,2982	7,1	980	136,15	42,98	12	1	659,67	5	0,00	0	-0,17
104754	18,2942	-19,4351	7,1	1260	123,33	92,04	12		741,37	6	5,75	74	-0,71
104894	18,2952	-19,2631	7,0	980	136,15	48,08	6		665,77	4	0,00	6	-0,69
104791	18,2962	-19,3514	7,2	1280	85,29	76,98	79	4	749,90	18	19,03	39	0,20
812	18,2962	-20,3063	6,7	5560	336,37	229,97	620	27	1246,18	440	5,31	1240	-1,00
B214/Y3447	18,2962	-19,5973	8,6	860	6,01	100,05	27	24	574,31	17	0,44	13	0,88
D402/Y360	18,2962	-21,1775	7,9	970	84,09	51,00	73	3	584,07	41	15,05	25	1,18
7857	18,2971	-21,8225	7,4	600	66,07	19,91	31	7	326,79	15	19,03	9	1,85
105365	18,2990	-18,9090	8,0	940	85,29	61,92	34	5	520,66	44	0,00	42	1,50
105358	18,3000	-18,7811	7,5	830	54,06	63,87	24	4	486,52	7	19,48	20	0,56
8892	18,3000	-21,2766	7,8	970	59,26	61,92	66	4	515,79	22	39,84	41	1,45
B189/Y3031	18,3000	-19,9847	7,3	1040	110,12	73,10	4	3	493,84	6	70,83	66	2,34
105355	18,3010	-18,8126	7,6	870	60,07	52,94	48	12	502,37	13	36,30	22	0,20
C373	18,3010	-18,5919	7,3	1850	66,87	51,73	413	28	981,58	56	35,41	315	-0,82
B199/Y3057	18,3019	-19,7739	7,2	1130	101,31	90,09	26	1	798,68	5	0,44	10	0,53
104898	18,3019	-19,2486	7,4	870	122,13	46,87	3		607,24	5	0,00	4	-0,43
105312	18,3019	-19,0207	7,6	1090	113,32	68,97	18	23	688,93	16	31,43	24	-0,42
C372	18,3019	-18,6568	7,4	1180	95,70	60,95	136	14	463,35	7	0,00	270	2,26
104882	18,3019	-19,3117	7,1	1480	96,10	84,99	115	1	848,67	7	0,00	93	0,42
7614	18,3029	-21,9505	7,4	790	83,29	33,03	40	13	427,99	23	19,92	36	0,66

Appendix D: Hydrochemical data

Name	Long	Mlat	pH	ec µS/cm	Ca ²⁺ mg/l	Mg ²⁺ mg/l	Na ⁺ mg/l	K ⁺ mg/l	HCO ₃ ⁻ mg/l	SO ₄ ²⁻ mg/l	NO ₃ ⁻ mg/l	Cl ⁻ mg/l	Balance %
104906	18,3029	-19,2081	7,5	1170	112,12	65,08	31	14	629,19	19	36,74	58	-1,09
104801	18,3029	-19,3919	7,3	1240	78,08	110,01	33		831,60	9	0,00	15	0,51
811	18,3029	-20,3495	7,4	2090	80,09	36,91	322	72	671,86	430	24,79	84	0,33
104880	18,3029	-19,3054	7,0	6060	280,30	234,83	640	3	685,28	160	929,60	1100	0,53
7840	18,3038	-21,5315	7,3	520	58,06	31,08	16	5	348,73	6	10,62	4	1,25
7565	18,3038	-21,9126	7,2	690	56,06	39,10	32	11	406,04	5	28,77	12	0,83
B191/Y3042	18,3038	-19,9288	7,5	2370	124,14	100,05	141	160	643,82	145	123,95	325	-0,17
105351	18,3048	-18,8658	7,9	1060	50,05	75,04	75	6	527,98	77	1,77	58	0,70
7812	18,3048	-21,7216	7,2	1710	112,12	60,95	174	16	429,21	16	332,00	210	-0,15
B200/Y3051	18,3048	-19,7892	7,3	2210	66,07	160,03	140	100	1177,89	79	119,52	88	-0,49
105378	18,3058	-18,9883	8,1	640	86,09	31,08	8	8	419,46	5	5,75	9	0,55
C371	18,3058	-18,7279	7,8	1100	117,73	82,81	27	7	542,61	4	79,68	150	-1,58
104800	18,3067	-19,3775	7,5	1790	66,07	164,89	109		1182,77	4	0,00	46	1,99
B214/Y3444	18,3067	-19,6153	7,3	1460	86,09	108,06	71	1	719,42	20	69,94	88	1,51
1718cd1004	18,3070	-17,8070	8,1	1830	4,00	5,10	430	8	902,32	83	2,21	122	-1,18
7566	18,3077	-21,8793	7,0	910	92,10	44,93	48	13	557,24	6	27,00	27	1,22
8121	18,3077	-21,4613	7,2	940	67,27	39,10	78	6	460,91	25	48,69	35	1,37
104895	18,3077	-19,2757	7,0	1000	132,14	50,03	14		673,08	4	0,00	12	-0,58
B200/Y3052	18,3077	-19,7847	7,5	1820	74,08	139,88	86	100	1137,65	68	37,18	40	-0,65
105303	18,3096	-19,0919	7,6	940	78,08	68,97	21	15	615,77	20	0,00	22	-1,18
104799	18,3096	-19,3739	8,0	1150	24,03	114,86	67		736,49	4	0,00	30	2,13
B212/Y3339	18,3096	-19,6937	7,9	2660	115,33	125,06	245	11	708,44	78	305,44	280	1,75
B201/Y3054	18,3106	-19,8450	8,4	1100	29,23	119,96	42	10	724,29	7	0,44	48	0,13
105377	18,3106	-18,9640	7,6	1740	173,39	79,89	72	21	530,42	69	265,60	160	-0,08
B212/Y3340	18,3106	-19,6892	7,6	3130	100,11	169,99	290	1	905,98	60	349,70	320	1,38
790	18,3115	-20,0288	7,1	540	70,08	15,06	9	12	325,57	3	7,08	2	-1,22
1718cb2	18,3120	-17,5630	7,1	545	57,66	35,45	5	5	371,90	0	0,00	5	-0,77
105354	18,3135	-18,8324	8,0	650	51,26	46,87	17	2	384,10	5	23,90	9	1,17
105364	18,3135	-18,9072	7,5	770	90,10	45,17	14	2	457,26	12	20,36	15	2,18
870	18,3135	-21,0369	7,8	5520	120,13	44,93	1075	11	457,26	900	12,84	1080	-0,15
104793	18,3144	-19,3595	7,0	1090	103,31	76,01	9	1	707,22	4	7,97	10	-1,08
B214/Y3445	18,3163	-19,6306	8,4	1940	28,03	110,01	300	1	1219,35	54	4,87	60	1,39
7855	18,3173	-21,8288	7,4	560	65,27	16,03	40	6	359,71	6	24,79	9	-1,55
V-1	18,3173	-19,4396	6,7	1365	105,00	95,00	32	6	769,00	31	9,40	74	-3,04
1718cd1005	18,3180	-17,8530	8,4	1410	10,01	6,07	330	5	931,58	18	2,21	9	-1,43
V-4	18,3187	-19,3791	6,7	971	78,00	65,40	24	1	603,00	9	25,80	19	-3,17
B212/Y3342	18,3192	-19,6604	8,4	1510	10,01	100,05	200	1	963,29	27	0,44	28	0,90
7820	18,3192	-21,6423	7,5	430	63,27	13,11	15	3	292,64		2,66	4	0,14
104910	18,3202	-19,1613	8,1	1130	72,08	90,09	37	37	699,91	24	7,97	37	1,59
7823	18,3202	-21,7225	7,1	1880	212,23	59,98	168	14	460,91	165	265,60	291	-0,62
V-2	18,3204	-19,4384	6,7	1081	99,00	87,60	12	1	604,00	10	44,10	71	-0,57
8122	18,3212	-21,4811	7,3	880	42,05	42,98	84	10	536,51	17	6,20	11	-0,06
7854	18,3221	-21,7802	7,4	590	71,28	23,07	34	8	407,26	7	11,51	11	-1,23
104755	18,3221	-19,4414	7,3	1050	98,11	80,87	14	1	712,10	4	0,00	14	0,15
104881	18,3221	-19,3288	7,2	1440	127,34	75,04	59	2	743,80	19	61,09	76	-1,84
7822	18,3240	-21,7234	7,2	860	90,10	25,01	104	9	493,84	51	30,99	48	1,34
7853	18,3240	-21,8018	7,4	1000	130,14	28,90	33	10	330,44	10	146,08	94	-0,32
866	18,3240	-20,8856	7,0	10160	615,87	274,90	1355	32	291,42	900	0,00	3120	0,71
105367	18,3250	-18,8775	8,0	740	38,04	76,01	14	4	504,81	5	0,00	8	1,50
1818ab2	18,3252	-18,1867	7,7	3050	32,84	50,51	630	42	1054,74	104	39,84	530	-1,11
105359	18,3260	-18,7685	7,9	920	35,24	46,87	104	11	562,12	20	23,90	10	0,60
105353	18,3260	-18,8586	7,4	5810	370,40	239,93	535	12	436,53	520	40,73	1440	2,11
105308	18,3269	-19,0703	7,4	890	105,31	57,07	12	2	571,88	28	6,20	19	-0,32

Appendix D: Hydrochemical data

Name	Long	Lat	pH	ec µS/cm	Ca ²⁺ mg/l	Mg ²⁺ mg/l	Na ⁺ mg/l	K ⁺ mg/l	HCO ₃ ⁻ mg/l	SO ₄ ²⁻ mg/l	NO ₃ ⁻ mg/l	Cl ⁻ mg/l	Balance %
104802	18,3269	-19,3964	7,6	910	72,08	73,10	16	2	582,85	5	2,66	10	1,86
7821	18,3288	-21,7234	7,5	950	72,08	25,01	109	8	402,39	35	104,03	40	2,28
104792	18,3288	-19,3541	7,5	1020	96,10	67,02	15		627,97	4	29,22	20	-2,00
105326	18,3288	-18,9387	7,7	1460	75,28	61,92	157	10	495,06	225	10,62	120	-1,29
7832	18,3298	-21,5964	7,3	1260	183,40	45,90	35	5	343,86	9	265,60	142	1,63
105360	18,3308	-18,7928	7,8	660	60,07	37,88	19	3	374,34	5	6,64	26	-0,44
104798	18,3308	-19,3802	7,4	1260	109,32	79,89	28	1	598,70	17	101,81	55	-0,32
8885	18,3327	-21,3297	7,9	580	37,24	37,88	39	4	371,90	8	5,31	14	0,24
1718cb1003	18,3330	-17,6920	8,1	710	10,81	8,99	153	5	399,95	20	2,21	23	2,59
8918	18,3337	-21,1432	7,7	900	82,09	60,95	56	3	637,72	24	7,97	19	0,04
8889	18,3337	-21,2883	7,6	970	101,31	44,93	44	2	429,21	10	190,35	10	0,58
1718cb6	18,3338	-17,6873	8,8	465	14,42	13,11	92	13	335,32	9	0,00	10	1,39
7831	18,3346	-21,5982	7,0	920	117,33	35,94	33	6	467,01	9	56,22	56	0,36
104885	18,3346	-19,3604	7,3	1200	73,28	125,06	23	1	835,26	14	0,00	14	2,04
8137	18,3356	-21,3901	7,1	600	66,07	26,96	19	2	380,44	5	1,33	5	-0,84
7850	18,3356	-21,7658	7,3	860	106,12	34,97	38	13	375,56	10	92,96	66	2,18
104907	18,3356	-19,1964	7,3	1060	82,09	90,09	11	9	749,90	6	0,00	8	-1,70
8917	18,3356	-21,1631	7,6	2120	145,36	108,06	133	30	708,44	78	221,33	185	1,51
104534	18,3365	-19,4730	7,8	830	75,28	68,97	2		579,19	5	0,00	10	-1,85
7587	18,3365	-21,9081	7,4	880	65,27	51,97	35	16	437,75	7	70,83	35	0,08
7585	18,3365	-21,8649	7,2	960	88,10	44,93	54	10	454,82	9	86,32	42	2,29
8890	18,3375	-21,2856	7,2	2050	198,22	105,88	99	5	512,13	20	464,80	240	-0,08
8891	18,3385	-21,2811	7,3	1210	158,17	80,87	70	3	532,86	18	309,87	130	-0,29
8124	18,3394	-21,4847	7,2	930	51,26	50,03	80	9	487,74	23	44,27	24	2,57
8922	18,3394	-21,1189	7,7	1170	62,07	77,95	85	6	693,81	48	19,92	26	-0,23
B748/Y3358	18,3394	-19,7360	7,9	1410	75,28	90,09	80	15	632,84	36	70,83	89	0,87
104533	18,3404	-19,4766	7,7	810	70,08	68,00	2	1	562,12	4	0,00	8	-1,69
8923	18,3404	-21,1234	7,7	1370	70,08	80,87	120	8	687,71	82	54,01	58	0,29
7824	18,3413	-21,6838	7,2	600	100,11	13,11	26	5	370,68	7	7,97	28	1,34
7849	18,3413	-21,7649	7,5	670	88,10	30,11	27	10	477,99	5	11,07	5	0,28
104794	18,3413	-19,3405	7,2	1170	94,10	90,09	34		787,70	4	0,00	13	0,85
B748/Y3359	18,3413	-19,7405	7,2	2090	140,15	110,01	117	25	777,95	53	146,08	180	1,13
7588	18,3433	-21,9568	7,7	640	40,04	19,91	85	4	410,92	13	12,84	8	-0,01
8125	18,3433	-21,4856	7,6	720	31,23	28,90	88	7	424,33	21	8,85	5	1,72
B190/Y3041	18,3433	-19,9459	8,5	1060	15,22	80,87	111	3	614,55	41	6,20	51	-0,59
B215/Y3366	18,3433	-19,6342	7,3	1510	72,08	100,05	99	1	788,92	40	54,89	64	-0,89
8126	18,3442	-21,4820	7,3	680	36,04	34,00	56	8	413,36	15	7,53	4	-0,58
105309	18,3442	-19,0450	8,0	730	49,25	66,05	14		441,41	33	0,00	25	-0,72
7586	18,3442	-21,8459	7,0	740	98,11	17,97	38	6	459,70	5	17,71	12	-0,49
104911	18,3442	-19,1360	8,3	1020	96,10	79,89	16	6	670,64	49	2,66	16	-1,16
791	18,3442	-20,1243	7,6	1280	23,23	19,91	273	23	885,25	5	8,85	19	-0,10
8123	18,3452	-21,5495	7,0	700	85,29	25,98	24	3	456,04	4	0,00	7	-1,57
104785	18,3452	-19,3784	7,3	1070	123,33	52,94	6	1	476,77	4	132,80	30	-0,40
104786	18,3452	-19,3829	7,2	2070	240,26	100,05	15	3	447,50	16	398,40	215	1,93
871	18,3452	-21,0739	7,1	5520	134,15	87,91	980	15	470,67	1040	21,25	896	1,75
B748/Y3361	18,3462	-19,7721	8,5	730	13,21	77,95	26	1	493,84	4	0,44	4	-0,40
8136	18,3462	-21,4072	7,0	860	80,09	34,97	61	8	482,86	44	6,64	31	-0,40
8908	18,3462	-21,2162	7,7	1430	114,12	63,87	97	3	673,08	34	101,81	82	-1,45
105315	18,3462	-18,9946	7,4	1600	117,33	104,91	69	30	579,19	65	203,63	130	1,28
105316	18,3462	-18,9982	7,4	1790	120,13	110,01	61	70	570,66	63	247,89	165	0,45
B201/Y3053	18,3462	-19,8423	7,7	2150	118,13	160,03	76	2	660,89	9	323,14	250	-1,88
7590	18,3462	-21,9622	7,1	2850	172,19	102,96	320	2	568,22	215	407,25	370	0,39
1718cb1005	18,3470	-17,6140	7,9	390	42,85	23,07	3	4	253,63	1	2,21	2	0,00

Appendix D: Hydrochemical data

Name	Long	Mlat	pH	ec µS/cm	Ca ²⁺ mg/l	Mg ²⁺ mg/l	Na ⁺ mg/l	K ⁺ mg/l	HCO ₃ ⁻ mg/l	SO ₄ ²⁻ mg/l	NO ₃ ⁻ mg/l	Cl ⁻ mg/l	Balance %
7589	18,3471	-21,9577	7,5	560	62,07	24,04	24	6	368,24	7	7,08		-0,18
105314	18,3471	-19,0027	7,5	980	97,31	65,08	16	18	625,53	18	1,77	20	0,66
C255	18,3481	-17,5874	7,1	550	57,66	35,45	5	5	371,90	0	0,00	5	-0,77
7852	18,3481	-21,7919	7,3	630	96,10	17,00	28	7	397,51	15	24,35	9	0,78
B748/Y3362	18,3500	-19,7297	7,2	1300	98,11	73,10	65	1	765,75	8	5,75	36	-0,22
B228/Y4531	18,3500	-19,5685	7,3	1640	83,29	114,86	89	1	701,13	74	12,39	134	1,43
W-5	18,3506	-21,3506	7,7	754	74,40	38,72	37	3	481,90	4	6,88	12	1,00
B201/Y3055	18,3510	-19,8730	7,6	860	82,09	65,08	13	1	603,58	5	1,77	5	-0,61
B215/Y3365	18,3510	-19,6811	7,2	1180	93,30	79,89	30	1	765,75	4	0,44	16	-2,07
8924	18,3510	-21,0523	7,9	1560	80,09	84,02	167	5	693,81	200	59,32	72	-0,60
8920	18,3519	-21,0811	7,6	850	74,08	35,94	65	4	371,90	38	95,17	50	-1,27
104934	18,3538	-19,2721	7,8	1080	54,06	56,10	111	2	621,87	35	18,15	37	-0,26
7851	18,3548	-21,7685	7,4	580	76,08	19,91	34	8	359,71	10	25,67	10	2,29
8912	18,3548	-21,2225	7,8	790	82,09	37,88	28	2	491,40	8	13,28	13	-1,84
7826	18,3558	-21,6874	7,1	640	95,30	15,06	34	6	397,51	8	19,03	16	1,25
8925	18,3558	-21,0333	7,8	1390	67,27	73,10	140	4	680,40	172	7,53	32	-0,61
105350	18,3567	-18,8000	7,7	740	45,25	66,05	15	10	503,59	7	5,75	2	0,31
813	18,3567	-20,3297	8,0	1770	23,23	15,06	365	53	803,55	103	23,46	166	-1,86
B228/Y4530	18,3567	-19,5342	7,2	2920	175,39	224,87	84	2	659,67	62	677,28	310	-1,29
C262	18,3577	-17,6811	8,4	590	2,40	1,94	140	28	378,00	10	11,95	5	2,52
8134	18,3577	-21,4414	7,1	1060	64,07	34,97	118	6	547,49	45	19,92	40	0,01
8138	18,3577	-21,3784	7,3	1120	124,14	48,08	34	3	393,85	5	154,93	94	-0,01
B227/Y4526	18,3577	-19,5793	7,9	1120	62,07	76,01	77	2	734,05	5	30,99	18	-1,50
8911	18,3577	-21,1910	7,6	3330	290,32	160,03	197	5	918,17	175	442,66	320	2,10
7828	18,3587	-21,6153	7,3	480	64,07	17,97	21	4	317,03	6	11,51	9	-0,60
8887	18,3596	-21,3054	7,9	820	43,25	51,97	62	4	448,72	24	11,07	43	-0,06
104797	18,3596	-19,3550	7,7	1090	91,30	65,08	29	1	475,55	19	106,24	48	-0,26
B227/Y4527	18,3596	-19,5829	7,6	1440	82,09	125,06	56	2	701,13	4	160,24	80	1,38
8127	18,3606	-21,5306	7,1	610	78,08	19,91	19	3	391,41	4	0,00	3	-1,11
B202/Y3040	18,3606	-19,8856	7,4	1130	65,27	104,91	32	1	781,60	7	5,75	18	-0,93
B202/Y3036	18,3606	-19,9126	7,9	1350	54,06	100,05	87	1	603,58	15	161,57	68	0,04
B202/Y3038	18,3615	-19,9081	7,5	840	52,06	63,87	18	13	396,29	12	97,39	22	0,18
8910	18,3615	-21,1757	8,0	1770	149,36	85,97	93	11	609,68	64	278,88	106	0,11
818	18,3615	-20,2162	7,4	2870	320,35	128,95	230	34	291,42	1200	2,21	220	2,00
8135	18,3625	-21,4126	7,0	660	79,29	27,93	17	5	418,24	5	1,77	4	0,16
8913	18,3625	-21,2117	7,7	890	106,12	42,01	30	1	575,53	10	13,72	14	-0,85
105310	18,3625	-19,0405	7,9	980	79,29	90,09	38		738,93	29	0,00	16	-0,54
8919	18,3625	-21,1459	7,6	1820	141,35	91,07	70	5	512,13	36	309,87	152	-1,96
8914	18,3635	-21,1306	7,8	630	31,23	46,87	38	3	413,36	14	3,54	5	-0,83
109435	18,3635	-19,2279	7,5	930	96,10	54,88	16	1	576,75	4	23,90	18	-1,93
7825	18,3644	-21,6856	7,2	620	102,11	14,08	27	7	397,51	7	21,69	10	2,12
8886	18,3644	-21,3108	7,7	1330	73,28	66,05	111	4	476,77	56	36,74	152	0,59
105324	18,3644	-18,9405	7,4	1790	118,13	114,86	81	21	495,06	43	292,16	220	-1,32
B202/Y3039	18,3654	-19,9135	7,4	1710	73,28	139,88	64	3	419,46	19	442,66	106	1,77
8916	18,3654	-21,1550	7,7	930	98,51	50,03	34	2	616,99	10	4,87	16	-1,34
8909	18,3654	-21,1865	7,8	940	104,11	48,08	44	1	603,58	16	22,13	19	-0,12
104908	18,3654	-19,2072	7,2	2250	134,15	150,08	146	7	642,60	73	303,23	300	0,33
7829	18,3663	-21,5883	7,3	520	72,08	22,10	15	3	359,71	5	4,87	3	-0,15
105302	18,3663	-19,1063	7,3	880	88,10	65,08	13	1	602,36	22	0,00	12	-1,55
104909	18,3673	-19,1532	7,9	1100	72,08	90,09	25	12	692,59	14	11,51	34	-1,52
104795	18,3673	-19,3036	7,2	1170	111,32	79,89	28		786,48	5	0,00	13	-0,05
7830	18,3673	-21,5523	7,5	1570	190,21	71,88	46	6	407,26	10	172,64	270	0,80
B202/Y3037	18,3673	-19,9090	7,5	1660	78,08	129,92	83	2	682,84	8	227,97	105	0,70

Appendix D: Hydrochemical data

Name	Long	Mlat	pH	ec µS/cm	Ca ²⁺ mg/l	Mg ²⁺ mg/l	Na ⁺ mg/l	K ⁺ mg/l	HCO ₃ ⁻ mg/l	SO ₄ ²⁻ mg/l	NO ₃ ⁻ mg/l	Cl ⁻ mg/l	Balance %
7827	18,3683	-21,6514	7,2	650	100,11	18,94	19	3	290,21	5	34,09	66	1,26
105328	18,3683	-18,9180	7,8	1210	39,24	78,92	138	3	649,91	93	9,30	41	2,25
8129	18,3692	-21,4631	7,3	820	30,03	36,91	94	12	482,86	25	2,66	10	0,98
105301	18,3692	-19,1225	7,2	960	84,09	75,04	18	2	626,75	20	9,74	22	-1,15
872	18,3692	-20,9721	7,3	1100	72,08	48,08	103	10	553,59	93	14,61	37	0,01
7570	18,3692	-21,8964	6,9	2340	217,44	101,02	135	21	616,99	92	123,95	370	2,22
105313	18,3702	-18,9865	7,5	113	97,31	90,09	40	4	734,05	21	1,33	34	2,41
105327	18,3712	-18,8883	8,4	1130	13,21	104,91	110	14	745,02	65	0,00	14	1,68
105323	18,3712	-18,9405	7,4	4430	200,22	224,87	320	124	569,44	200	664,00	760	-0,06
8139	18,3721	-21,3901	7,4	620	77,28	33,03	15	3	424,33	5	0,00	2	1,31
7575	18,3721	-21,8982	7,6	2150	186,20	91,07	118	15	459,70	61	97,39	430	-0,45
104796	18,3721	-19,3045	7,0	2720	170,19	139,88	142	53	801,11	110	274,45	300	-1,38
1718cb1002	18,3730	-17,7450	8,2	4420	6,01	13,11	1020	8	1155,95	500	8,85	620	-1,11
1818cb1006	18,3733	-18,7208	7,2	1490	114,93	69,94	78	10	390,19	21	37,63	270	0,28
B204/Y3354	18,3740	-19,8000	7,3	970	54,06	80,87	38	1	626,75	6	3,98	8	1,58
104756	18,3740	-19,4297	7,4	1110	101,31	68,00	32	2	574,31	5	56,22	54	0,61
105300	18,3740	-19,1225	7,4	1210	85,29	93,01	44	17	725,51	30	41,17	35	0,32
B215/Y3364	18,3740	-19,6667	7,1	3590	290,32	139,88	164	84	504,81	70	867,62	360	2,03
B227/Y4529	18,3750	-19,5937	7,3	1120	51,26	100,05	49	1	787,70	5	0,44	8	-1,14
8921	18,3760	-21,0865	7,7	520	50,05	31,08	18	2	336,54	10	11,07	5	-1,29
7863	18,3760	-21,7784	7,3	590	67,27	17,00	26	6	314,59	8	19,92	8	1,44
8915	18,3760	-21,1360	7,6	1050	92,10	61,92	66	2	701,13	16	8,85	26	-0,34
104535	18,3760	-19,5027	7,5	1690	95,30	160,03	22	1	582,85	4	199,20	190	1,89
7862	18,3769	-21,8036	7,0	800	115,33	19,91	24	7	438,97	5	14,17	27	1,94
105298	18,3779	-19,0793	7,5	880	74,08	79,89	18	1	619,43	8	3,54	10	1,94
104787	18,3779	-19,3360	7,3	940	93,30	60,95	8		607,24	3	13,28	4	-1,58
105325	18,3779	-18,9550	7,8	2360	109,32	139,88	100	220	965,73	125	203,63	165	1,08
105329	18,3788	-18,9063	8,1	670	45,25	62,90	10	2	481,64	5	0,00	3	-1,02
C370	18,3788	-18,7306	7,8	1500	116,13	82,81	83	12	395,07	27	27,45	328	-0,62
7859	18,3798	-21,7396	7,9	910	54,06	43,95	46	12	278,01	20	44,71	93	1,80
8904	18,3798	-21,2541	7,7	1390	155,37	50,03	41	49	553,59	40	221,33	60	-0,87
8128	18,3808	-21,5153	7,1	660	88,10	25,01	18	4	429,21	4	0,00	5	0,56
1818cb1004	18,3810	-18,5883	7,1	1520	84,09	59,01	157	13	526,76	32	19,92	225	0,77
105299	18,3827	-19,0784	8,4	500	7,21	62,90	10	1	354,83	5	0,00	6	-0,77
9141	18,3837	-21,8622	7,2	1000	69,28	48,08	35	38	392,63	39	110,67	30	0,15
7574	18,3856	-21,9369	6,9	580	84,09	14,08	27	3	346,30	9	29,22	12	-0,50
B748/Y3360	18,3856	-19,7523	7,2	1000	85,29	61,92	30	1	643,82	4	0,44	10	-1,12
C369	18,3856	-18,6685	7,5	1250	74,08	53,43	186	14	554,80	52	26,56	203	0,65
9142	18,3865	-21,8640	7,2	750	60,07	34,97	27	12	331,66	20	54,89	20	0,37
7858	18,3865	-21,7405	7,3	1690	135,35	68,97	66	13	326,79	30	168,21	240	0,55
8884	18,3865	-21,2883	7,4	1970	151,36	97,86	112	5	575,53	66	243,47	190	1,26
105348	18,3865	-18,7928	8,0	3190	10,01	22,10	760	17	1596,13	115	92,96	230	-1,01
9143	18,3875	-21,8703	7,3	2790	167,38	152,99	101	16	292,64	95	708,26	280	-0,68
788	18,3885	-20,0730	7,7	1200	64,07	69,94	106	5	685,28	52	8,85	52	-0,84
C368	18,3885	-18,5973	8,0	1310	78,08	53,43	166	17	548,71	41	15,94	186	1,91
8899	18,3885	-21,2036	7,6	1450	135,35	54,88	84	9	525,54	30	110,67	156	-0,88
787	18,3894	-19,9919	7,1	1250	82,09	50,03	109	19	643,82	5	10,62	94	-0,14
105333	18,3904	-18,8802	8,2	790	35,24	56,10	60	12	536,51	15	5,31	4	-0,07
B204/Y3353	18,3904	-19,8207	7,9	970	40,04	87,91	45	1	649,91	6	0,44	2	1,70
8936	18,3913	-21,1369	7,3	2620	260,28	129,92	151	14	532,86	60	387,33	470	1,86
8140	18,3933	-21,4090	7,2	780	91,30	35,94	24	3	459,70	5	9,30	34	-0,65
7871	18,3942	-21,7333	7,4	790	53,26	28,90	60	13	348,73	30	28,77	28	2,47
105347	18,3942	-18,8279	7,5	790	43,25	76,98	10	9	484,08	5	13,28	25	1,11

Appendix D: Hydrochemical data

Name	Long	Mlat	pH	ec µS/cm	Ca ²⁺ mg/l	Mg ²⁺ mg/l	Na ⁺ mg/l	K ⁺ mg/l	HCO ₃ ⁻ mg/l	SO ₄ ²⁻ mg/l	NO ₃ ⁻ mg/l	Cl ⁻ mg/l	Balance %
7872	18,3942	-21,7279	7,9	1230	28,03	24,04	204	16	477,99	95	30,54	65	2,11
V-5	18,3946	-19,3274	6,7	1619	125,00	108,00	48	11	534,00	31	258,00	119	1,68
104932	18,3962	-19,2342	7,7	880	52,06	52,94	63	3	480,42	16	15,94	45	0,20
7573	18,3971	-21,9748	7,2	670	67,27	26,96	47	6	427,99	14	1,77	5	1,95
8142	18,3971	-21,4378	7,5	700	75,28	34,97	28	3	424,33	12	0,00	20	1,02
8939	18,3971	-21,0946	7,7	770	70,08	50,03	35	5	476,77	18	21,25	15	1,70
8938	18,3971	-21,1009	7,6	840	77,28	51,00	42	3	519,44	15	12,39	22	1,59
104930	18,3971	-19,2108	7,8	1100	65,27	79,89	54	4	557,24	14	28,33	84	0,13
B229/Y4537	18,3971	-19,5306	7,6	1460	28,03	125,06	65	43	546,27	83	44,27	137	1,16
1718cd7	18,3980	-17,8050	8,0	2050	8,41	9,47	612	12	1377,87	47	0,00	138	1,21
9140	18,3990	-21,8333	6,8	630	90,10	10,93	18	6	356,05	10	6,20	7	-0,07
7571	18,3990	-21,8991	7,3	700	50,05	27,93	64	10	427,99	10	8,85	18	-0,24
7860	18,3990	-21,7739	7,0	700	83,29	16,03	31	6	373,12	10	17,71	10	0,62
8926	18,4000	-21,0243	8,1	710	37,24	32,06	60	3	351,17	42	7,53	16	-0,14
1818ab1002	18,4000	-18,0277	8,5	1350	4,81	2,91	330	6	890,13	7	4,43	5	0,14
7572	18,4010	-21,9135	7,2	1170	120,13	57,07	35	17	421,90	20	183,26	74	1,10
B216/Y3347	18,4010	-19,6964	7,5	1390	62,07	113,41	59	2	795,02	12	31,87	59	-1,35
1818ab1003	18,4010	-18,0650	7,9	860	26,03	15,06	158	12	548,71	2	2,21	15	1,17
8903	18,4019	-21,2396	7,7	870	87,29	40,07	40	2	553,59	12	5,75	16	-2,19
8888	18,4029	-21,3288	7,6	830	92,10	41,04	35	5	547,49	12	7,53	11	-0,16
8900	18,4029	-21,1838	7,6	1050	90,10	59,01	54	3	631,62	14	11,07	40	-0,73
7903	18,4038	-21,6477	7,2	580	66,07	11,90	30	3	302,40	8	12,39	16	-1,01
8902	18,4038	-21,2279	7,6	1110	89,30	48,08	66	31	581,63	30	38,51	48	-0,23
105322	18,4038	-18,9883	7,6	1740	104,11	104,91	106	7	490,18	36	128,37	280	-0,36
104757	18,4048	-19,3946	7,6	880	69,28	54,88	38	7	557,24	4	0,00	21	-0,02
B216/Y3348	18,4048	-19,7081	7,8	2260	118,13	113,41	136	90	742,58	10	77,02	350	-0,10
7861	18,4058	-21,8144	6,9	750	106,12	17,97	17	5	402,39	7	34,09	9	0,64
104917	18,4058	-19,0703	7,8	2320	70,08	185,04	142	13	670,64	65	177,07	320	2,04
7900	18,4067	-21,5568	7,2	460	52,06	14,08	16	3	263,38	8	2,66	3	-0,89
104929	18,4067	-19,1874	7,9	800	49,25	76,01	15	4	538,95	6	0,00	14	0,61
104547	18,4067	-19,4649	7,6	1040	92,10	87,91	6	6	741,37	4	0,00	16	-1,77
B989/Y3357	18,4067	-19,7748	7,4	1480	75,28	119,96	84	1	963,29	6	26,56	8	2,19
105297	18,4067	-19,0279	7,5	2000	56,06	135,02	190	55	810,87	79	0,00	220	5,46
1718cd1002	18,4075	-17,8020	7,6	500	14,02	6,07	43	64	202,41	16	4,87	45	-3,01
B203/Y3351	18,4077	-19,8712	7,5	1180	50,05	98,84	53	1	609,68	6	65,96	48	1,68
B989/Y3356	18,4087	-19,7892	8,2	970	55,26	84,99	30	1	649,91	6	0,44	3	0,98
105330	18,4087	-18,9144	7,6	710	42,05	56,10	36	3	469,45	20	0,00	6	0,47
9137	18,4087	-21,8541	7,0	980	70,08	40,07	61	12	351,17	12	101,81	64	1,57
104789	18,4087	-19,3315	7,7	1220	76,08	93,01	32	4	479,21	47	208,05	41	-1,52
8130	18,4096	-21,4505	7,2	710	73,28	20,88	47	4	397,51	22	8,85	9	1,03
9117	18,4096	-21,9018	7,2	770	35,24	40,07	59	14	399,95	17	15,49	20	1,64
B215/Y3363	18,4096	-19,6486	7,3	1690	46,05	56,10	250	1	882,81	50	0,44	94	-0,98
105332	18,4096	-18,8901	7,8	2210	59,26	74,07	350	9	820,62	300	0,00	200	-1,66
105317	18,4106	-18,9441	8,0	1510	39,24	75,04	200	4	730,39	145	1,77	75	-0,58
105331	18,4106	-18,9009	7,8	1600	20,02	25,98	330	10	827,94	130	6,20	52	-0,27
8141	18,4115	-21,4207	7,3	620	73,28	30,11	19	3	364,59	13	5,75	17	1,59
8156	18,4115	-21,3829	7,7	660	77,28	34,00	17	2	453,60	5	2,21	3	-1,41
7873	18,4115	-21,6892	6,9	710	103,31	17,00	17	4	397,51	6	13,28	7	2,39
104788	18,4115	-19,3532	7,4	850	94,10	45,90	10	1	541,39	6	26,56	6	-3,57
104759	18,4135	-19,3622	7,5	900	79,29	59,01	18	2	467,01	30	54,89	18	-0,13
B989/Y3355	18,4135	-19,8189	8,0	1040	55,26	94,95	34	1	702,35	6	0,44	2	1,58
104790	18,4135	-19,3279	7,3	1090	104,11	65,08	12	1	541,39	12	53,12	30	1,25
B216/1/Y3343	18,4144	-19,6775	7,4	1020	73,28	79,89	21	1	620,65	5	23,90	18	0,01

Appendix D: Hydrochemical data

Name	Long	Lat	pH	ec µS/cm	Ca ²⁺ mg/l	Mg ²⁺ mg/l	Na ⁺ mg/l	K ⁺ mg/l	HCO ₃ ⁻ mg/l	SO ₄ ²⁻ mg/l	NO ₃ ⁻ mg/l	Cl ⁻ mg/l	Balance %
8132	18,4154	-21,5216	7,1	500	57,26	16,03	23	4	306,06	5	4,43	4	-0,24
104933	18,4154	-19,2757	7,7	950	88,10	68,00	24	3	659,67	5	0,00	16	-1,13
9136	18,4154	-21,8541	7,2	1080	74,08	48,08	58	12	360,93	10	112,88	86	0,54
7874	18,4173	-21,6775	7,1	680	76,08	18,94	26	17	338,98	5	6,20	33	1,70
8906	18,4173	-21,3135	7,7	870	84,09	39,10	54	3	560,90	24	3,54	8	-0,69
1718ad1	18,4177	-17,3896	7,7	590	60,87	38,37	29	9	445,06	0	0,00	10	0,72
105346	18,4192	-18,8450	8,2	1410	24,03	18,94	300	9	723,08	93	13,72	54	1,60
7898	18,4202	-21,5748	7,5	460	48,05	16,03	19	3	236,55	6	12,84	8	2,05
8905	18,4202	-21,2703	7,8	1010	95,30	50,03	64	3	637,72	32	13,28	23	-1,04
104541	18,4202	-19,4559	7,6	1050	87,29	92,04	4		741,37	7	0,00	8	-1,70
104913	18,4202	-19,1315	7,6	1410	72,08	90,09	47	62	618,21	36	115,09	77	-0,91
7904	18,4212	-21,6216	7,3	500	52,06	15,06	26	3	278,01	9	11,07	12	-2,10
B229/Y4536	18,4212	-19,5541	8,1	920	74,08	76,01	20	1	575,53	43	0,44	26	-1,01
104542	18,4212	-19,4505	7,6	1850	80,09	179,95	20		729,17	15	289,95	120	-1,62
9144	18,4221	-21,8685	7,3	720	45,25	23,07	71	10	395,07	16	0,00	14	2,03
8158	18,4221	-21,3468	7,3	800	98,11	34,97	26	2	519,44	6	0,00	20	-1,36
104931	18,4221	-19,1784	7,3	1930	107,32	119,96	78	74	737,71	73	146,08	190	-1,94
105349	18,4221	-18,7973	7,2	4260	185,40	164,89	410	9	526,76	5	66,40	1080	0,76
7899	18,4260	-21,5306	7,3	700	70,08	25,01	30	6	348,73	6	19,48	22	1,73
7864	18,4260	-21,8045	6,8	1550	188,20	43,95	41	8	443,84	25	128,37	183	-0,10
104912	18,4260	-19,1279	8,1	2210	82,09	114,86	99	160	635,28	87	298,80	205	-1,96
104546	18,4269	-19,4568	7,5	940	90,10	76,01	4	2	674,30	4	0,00	10	-1,97
B230/Y3367	18,4288	-19,6252	8,1	1460	30,03	100,05	142	2	864,52	45	0,44	38	-0,70
7902	18,4288	-21,6198	7,1	1660	200,22	37,88	45	2	329,22	9	265,60	180	0,58
1718cd1020	18,4290	-17,7700	8,1	1560	18,82	17,97	300	7	607,24	125	4,43	147	-3,47
8157	18,4298	-21,3505	7,5	630	72,08	31,08	21	2	382,88	16	15,94	11	-0,39
104758	18,4298	-19,3901	7,7	840	83,29	62,90	16	3	573,10	4	0,00	8	2,04
B203/Y3352	18,4298	-19,8432	7,3	1020	31,23	84,99	68	1	656,01	6	3,98	7	1,76
B218/Y3346	18,4298	-19,7604	7,5	1460	104,11	96,65	61	1	656,01	20	148,29	61	1,76
1718cd1009	18,4300	-17,8750	8,3	990	12,81	8,01	210	10	665,77	1	2,21	2	-1,54
B241/Y4539	18,4308	-19,4901	7,6	990	40,04	76,98	65	1	659,67	8	0,44	18	-1,35
8901	18,4317	-21,2162	7,7	1070	115,33	45,90	59	3	665,77	18	5,75	44	-1,79
<u>1718cd9</u>	18,4323	-17,8880	7,7	950	5,21	5,34	227	6	609,68	27	0,00	10	-0,51
1718cb1006	18,4328	-17,6661	7,7	450	46,05	28,90	6	4	297,52	1	2,21	2	0,50
9118	18,4346	-21,8964	7,2	660	40,04	35,94	38	12	356,05	12	22,58	10	1,35
9119	18,4346	-21,9162	7,1	680	63,27	26,96	23	17	346,30	10	25,67	13	1,09
V-6	18,4355	-19,2785	6,9	978	101,00	55,80	11	6	622,00	8	12,80	13	-3,22
B216/1/Y3344	18,4356	-19,7018	7,7	830	15,22	69,21	50	2	447,50	8	0,44	44	-0,39
B241/Y4538	18,4356	-19,4919	7,8	1210	66,07	119,96	22	1	643,82	15	90,30	53	1,20
105320	18,4365	-18,9910	7,8	5090	42,05	78,92	1180	3	1622,96	790	194,77	400	2,15
8131	18,4375	-21,4982	7,0	640	78,08	19,91	24	4	386,53	6	1,77	9	-0,45
7870	18,4375	-21,7477	7,2	660	61,27	25,01	32	7	365,81	8	10,18	7	1,24
8937	18,4375	-21,1126	7,7	840	61,27	50,03	51	1	420,68	15	56,66	38	1,21
9120	18,4375	-21,9216	6,9	2690	258,28	107,09	70	18	312,15	58	593,17	340	-0,54
104766	18,4385	-19,3351	7,1	900	102,11	54,88	12	1	569,44	4	0,00	20	0,89
C254	18,4394	-17,4081	7,7	590	60,87	38,37	29	9	445,06	0	0,00	10	0,72
8927	18,4394	-21,0018	8,2	790	59,26	34,97	59	4	476,77	24	5,75	14	-1,72
9139	18,4404	-21,8477	6,9	440	59,26	8,99	6	7	221,92	16	0,00	5	0,31
B231/Y3378	18,4404	-19,6532	7,4	920	94,10	42,01	27	1	551,15	5	0,44	19	-1,72
104928	18,4404	-19,1946	7,5	990	76,08	84,99	16	2	677,96	5	13,28	16	-1,46
7869	18,4404	-21,7514	7,1	1530	87,29	28,90	204	9	390,19	285	79,68	62	1,52
C268	18,4404	-17,8054	8,0	2050	8,41	9,47	612	12	1377,87	47	0,00	138	1,21
686	18,4413	-21,9829	7,1	960	82,89	26,96	81	7	365,81	62	74,37	56	-0,04

Appendix D: Hydrochemical data

Name	Long	Mlat	pH	ec µS/cm	Ca ²⁺ mg/l	Mg ²⁺ mg/l	Na ⁺ mg/l	K ⁺ mg/l	HCO ₃ ⁻ mg/l	SO ₄ ²⁻ mg/l	NO ₃ ⁻ mg/l	Cl ⁻ mg/l	Balance %
105334	18,4413	-18,9162	7,9	2320	144,16	139,88	128	7	331,66	175	27,89	560	-1,76
8133	18,4423	-21,5000	7,0	630	82,09	16,03	27	4	386,53	5	1,33	7	0,26
7905	18,4423	-21,6216	6,8	2130	415,65	59,98	94	12	382,88	52	770,24	385	-0,93
1818cb1001	18,4425	-18,7250	8,2	1030	52,06	40,07	113	10	456,04	36	2,21	63	4,88
104914	18,4433	-19,1108	7,3	1370	78,08	90,09	87	6	847,45	5	0,00	62	-1,59
W-1	18,4441	-21,3489	7,4	672	66,80	30,64	20	2	317,20	25	36,20	30	-2,57
7879	18,4442	-21,7135	7,6	710	46,05	16,03	72	13	358,49	10	9,74	21	1,79
104927	18,4452	-19,1613	7,7	970	88,10	68,00	25	7	621,87	15	15,94	26	-1,04
B230/Y3368	18,4462	-19,6108	7,4	1230	78,08	68,97	77	1	666,99	10	22,58	46	0,57
7865	18,4471	-21,7982	7,0	680	84,09	19,91	29	4	387,75	5	11,07	8	2,39
104783	18,4471	-19,2225	7,7	800	53,26	40,07	55	1	458,48	20	0,00	26	-1,71
104780	18,4471	-19,2748	7,2	1000	118,13	54,88	12	4	629,19	4	7,97	14	0,53
C366	18,4481	-18,7342	7,6	780	68,07	40,07	87	8	499,93	28	30,99	48	0,25
104545	18,4481	-19,4414	7,6	920	73,28	74,07	10	2	632,84	4	0,00	9	-2,25
8942	18,4481	-21,1703	7,6	1270	101,31	69,94	73	7	588,95	9	88,53	98	0,47
7901	18,4490	-21,6261	7,4	1040	93,30	30,11	72	4	329,22	21	106,24	98	0,28
105335	18,4490	-18,8505	8,5	1190	15,22	18,94	250	9	723,08	57	1,77	8	0,49
8943	18,4490	-21,1631	6,8	1370	152,17	63,87	40	3	532,86	7	185,92	91	0,76
1818cb1002	18,4492	-18,6650	8,0	1410	26,83	24,04	240	30	712,10	66	8,85	73	-2,43
B230/Y3369	18,4500	-19,5946	7,2	2200	152,17	100,05	162	1	737,71	85	148,29	210	1,61
7876	18,4519	-21,6712	7,5	550	37,24	18,94	49	5	299,96	8	6,64	10	1,84
104784	18,4519	-19,3108	7,4	1110	116,13	71,88	12	1	734,05	4	2,66	10	-0,73
8928	18,4529	-21,0315	7,9	590	48,05	27,93	43	4	343,86	16	8,85	21	-0,26
7894	18,4538	-21,5459	7,4	370	44,05	11,90	16	2	219,48	9	2,21	2	0,61
8166	18,4538	-21,3225	7,1	2180	218,24	93,01	69	3	376,78	45	371,84	290	0,78
7868	18,4548	-21,7477	7,1	790	67,27	32,06	42	9	397,51	35	0,00	16	2,27
104916	18,4548	-19,0946	7,4	1130	100,11	61,92	98	8	686,49	87	0,00	58	-0,48
8963	18,4548	-21,1991	8,3	1290	61,27	59,01	154	4	693,81	61	17,71	76	-1,19
C367	18,4548	-18,6045	8,0	1400	4,00	3,64	400	43	871,84	50	0,89	128	0,12
104762	18,4548	-19,3847	7,1	2030	124,14	144,00	100	43	727,95	88	256,75	160	2,35
7877	18,4548	-21,6667	7,3	5700	505,75	185,04	410	3	370,68	280	1651,14	715	-0,28
1718cb1007	18,4550	-17,6880	6,2	100	4,00	2,91	11	5	29,26	1	2,21	18	0,10
7866	18,4558	-21,7955	7,3	750	95,30	23,07	28	5	431,65	5	10,18	9	2,59
B241/Y4540	18,4567	-19,5171	7,4	1230	62,07	114,86	22	2	653,57	5	115,09	48	-1,70
104915	18,4577	-19,0919	7,6	3200	110,12	90,09	320	176	740,15	185	0,00	430	5,42
7895	18,4587	-21,5279	7,0	460	59,26	15,06	17	3	282,89	5	0,89	2	2,05
8907	18,4587	-21,3027	7,6	1070	116,13	39,10	46	3	448,72	20	146,08	48	-1,73
7878	18,4596	-21,7054	7,5	630	41,24	18,94	59	6	314,59	10	22,13	22	-0,04
9113	18,4596	-21,9541	7,3	920	53,26	25,98	110	11	431,65	72	0,00	32	2,00
104544	18,4596	-19,4360	7,5	990	88,10	82,08	4	2	716,98	4	0,00		-1,97
104782	18,4596	-19,2559	7,4	1000	106,12	60,95	14	2	627,97	5	5,31	18	-0,08
B218/Y3345	18,4596	-19,7153	7,9	1580	92,10	75,04	150	2	696,25	48	51,79	122	1,94
7896	18,4606	-21,5604	7,2	410	37,24	11,90	29	2	236,55	6	3,54	5	-0,60
105339	18,4606	-18,7946	7,3	710	30,03	51,00	37	13	353,61	5	0,00	56	1,05
104761	18,4606	-19,4144	7,2	780	75,28	54,88	14	2	521,88	5	22,13	8	-1,69
104765	18,4615	-19,3450	7,5	1010	107,32	66,05	10		531,64	14	86,32	21	1,07
8941	18,4615	-21,1793	7,6	1060	89,30	53,91	103	2	673,08	44	13,28	50	-0,55
9112	18,4625	-21,9054	7,4	640	39,24	32,06	55	7	392,63	15	20,36	12	-1,69
8155	18,4625	-21,3793	7,5	700	63,27	32,06	42	5	388,97	23	8,41	24	0,54
7867	18,4625	-21,7450	7,3	890	60,07	37,88	65	8	385,32	50	32,31	29	2,53
C273	18,4625	-17,8847	7,7	950	5,21	5,34	227	6	609,68	27	0,00	10	-0,51
B220/Y3350	18,4625	-19,7982	7,2	1740	68,07	139,88	116	2	807,21	99	194,77	78	-1,54
105340	18,4625	-18,8315	7,9	1840	114,12	114,86	73	6	364,59	10	18,59	445	-1,49

Appendix D: Hydrochemical data

Name	Long	Lat	pH	ec µS/cm	Ca ²⁺ mg/l	Mg ²⁺ mg/l	Na ⁺ mg/l	K ⁺ mg/l	HCO ₃ ⁻ mg/l	SO ₄ ²⁻ mg/l	NO ₃ ⁻ mg/l	Cl ⁻ mg/l	Balance %
7909	18,4644	-21,6414	7,8	550	30,03	8,01	66	7	287,77	7	3,54	17	-1,80
9111	18,4644	-21,9207	7,2	1030	82,09	49,05	60	11	379,22	29	121,73	66	1,76
786	18,4644	-19,9883	7,1	2520	125,34	99,08	290	47	1031,57	20	6,20	345	1,93
104763	18,4654	-19,3766	7,7	700	87,29	40,07	2		449,94	5	22,13	4	-1,32
9138	18,4654	-21,8505	7,2	880	56,06	36,91	59	7	324,35	9	115,09	44	-0,12
105337	18,4654	-18,8874	7,8	1130	18,02	30,11	200	9	647,48	26	37,18	28	-0,95
7882	18,4663	-21,6613	7,3	680	60,07	28,90	29	8	321,91	6	57,55	13	1,08
105321	18,4663	-18,9892	7,4	980	67,27	77,95	25	2	574,31	9	27,45	32	-0,16
8940	18,4663	-21,1775	7,5	1030	82,09	51,00	80	2	525,54	36	46,48	56	0,56
B231/Y3379	18,4663	-19,6784	7,6	1480	102,11	62,90	103	1	685,28	35	84,11	76	-2,26
8165	18,4673	-21,3477	7,5	670	69,28	25,98	24	4	317,03	7	56,66	24	-1,40
7880	18,4683	-21,6676	7,4	760	68,07	25,98	52	5	390,19	7	26,56	30	0,70
7906	18,4692	-21,5982	7,4	470	54,06	8,99	24	2	253,63	7	4,43	7	-0,43
V-7	18,4695	-19,2665	6,9	1095	115,00	66,00	29	13	544,00	20	51,30	42	5,99
7896	18,4702	-21,5468	7,3	440	45,25	13,11	24	3	226,80	8	11,07	9	1,62
7881	18,4702	-21,6640	7,3	680	55,26	25,01	55	4	375,56	7	13,28	16	2,41
104760	18,4702	-19,3748	7,3	860	93,30	54,88	14	1	487,74	26	43,82	14	0,88
8962	18,4702	-21,2279	7,7	870	90,10	42,98	62	2	547,49	42	15,49	26	-0,23
8147	18,4712	-21,4153	7,5	960	88,10	37,88	51	5	340,20	28	110,67	67	0,14
8978	18,4731	-21,2847	7,8	690	93,30	25,01	12	4	441,41	5	14,17	7	-2,82
B231/Y3381	18,4731	-19,6360	7,5	950	72,08	58,04	31	1	540,17	10	39,40	17	-2,15
B242/Y3370	18,4731	-19,5730	7,3	1390	100,11	100,05	24	1	620,65	5	95,17	100	-1,15
105336	18,4731	-18,8586	7,5	2360	79,29	75,04	310	16	470,67	85	11,07	530	-1,21
785	18,4731	-19,9009	7,0	2630	98,11	96,89	330	54	1210,82	50	7,53	295	-1,25
7885	18,4740	-21,7135	7,3	910	85,29	33,03	45	5	326,79	7	79,68	72	1,35
103805	18,4750	-19,4288	7,4	740	74,08	51,97	9	3	476,77	5	11,51	10	0,33
B735/Y3805	18,4750	-19,4288	7,4	740	74,08	51,97	9	3	476,77	5	11,51	10	0,33
7886	18,4760	-21,7108	7,3	820	67,27	30,11	54	5	348,73	7	40,73	52	2,01
8146	18,4760	-21,4306	7,5	820	76,08	30,11	48	4	317,03	22	56,22	70	-0,41
8961	18,4760	-21,2270	7,6	1660	122,13	87,91	104	3	420,68	95	265,60	155	1,13
9114	18,4769	-21,9577	7,3	880	80,09	27,93	65	5	443,84	42	5,75	24	1,82
104925	18,4788	-19,1216	7,3	990	85,29	68,97	30	3	595,04	58	0,00	18	-0,68
7908	18,4788	-21,6234	7,0	2340	161,38	77,95	177	8	470,67	25	172,64	400	0,16
9115	18,4788	-21,9631	7,0	2590	176,19	88,88	255	2	443,84	365	72,15	385	0,65
8964	18,4798	-21,1991	8,2	880	60,07	43,95	69	3	413,36	31	73,04	38	0,12
8932	18,4798	-21,1054	7,3	910	64,07	61,92	57	3	581,63	10	20,36	16	1,54
1718ad1001	18,4800	-17,4930	8,4	400	42,05	27,93	4	3	278,01	1	2,21	2	-0,24
8163	18,4808	-21,3072	7,5	590	70,08	19,91	27	2	340,20	12	11,07	13	-0,07
8975	18,4808	-21,2568	7,8	950	71,28	32,06	57	32	379,22	48	88,53	43	-1,87
B220/Y3349	18,4808	-19,8099	7,5	1910	82,09	49,54	265	2	777,95	45	77,91	135	2,60
104579	18,4817	-18,9910	7,7	850	59,26	73,10	28	1	534,08	20	15,94	28	0,00
105319	18,4837	-18,9315	8,4	940	10,01	15,06	200	8	614,55	17	6,20	4	0,02
8164	18,4846	-21,3162	7,4	850	87,29	32,06	33	1	268,26	8	146,08	51	0,58
8931	18,4856	-21,1378	7,6	950	88,10	34,97	60	2	407,26	32	42,05	71	-0,44
8160	18,4865	-21,3568	7,3	1160	93,30	35,94	111	3	399,95	210	20,81	55	-1,17
8162	18,4875	-21,3270	7,0	2700	352,78	84,99	43	36	245,09	80	796,80	305	0,47
103808	18,4885	-19,4099	7,1	810	80,09	60,95	8	1	554,80	5	0,00	4	0,41
104779	18,4885	-19,2721	7,3	1020	79,29	70,91	23	20	645,04	12	3,54	16	-0,12
8930	18,4894	-21,1153	8,0	770	68,07	33,03	44	2	315,81	18	106,24	27	0,34
783	18,4894	-19,6523	7,0	1100	93,30	68,97	19	24	640,16	5	70,83	19	-2,09
7883	18,4904	-21,6586	7,1	790	105,31	20,88	16	3	329,22	6	132,80	14	-1,96
104776	18,4904	-19,2054	7,4	1390	105,31	61,92	43	78	609,68	44	92,96	61	0,31
B233/Y3377	18,4913	-19,7117	7,3	1090	71,28	58,04	67	2	662,11	20	5,31	6	-0,98

Appendix D: Hydrochemical data

Name	Long	Lat	pH	ec µS/cm	Ca ²⁺ mg/l	Mg ²⁺ mg/l	Na ⁺ mg/l	K ⁺ mg/l	HCO ₃ ⁻ mg/l	SO ₄ ²⁻ mg/l	NO ₃ ⁻ mg/l	Cl ⁻ mg/l	Balance %
B242/Y3371	18,4913	-19,5901	7,7	1160	90,10	83,05	30	1	679,18	9	0,44	42	0,60
9110	18,4913	-21,9207	7,3	700	52,06	27,93	65	9	385,32	29	12,39	29	0,11
104921	18,4913	-19,1081	7,4	1130	110,12	75,04	23	7	526,76	195	0,00	14	-0,92
9116	18,4913	-21,9550	7,1	1890	67,27	33,03	304	11	404,82	335	23,46	178	1,48
7907	18,4923	-21,5982	7,0	880	142,15	17,00	11	2	495,06	7	0,00	20	1,12
B231/Y3380	18,4933	-19,6577	7,2	900	67,27	62,90	18	1	580,41	5	0,44	4	-2,07
8148	18,4952	-21,4027	7,5	480	55,26	8,01	34	3	220,70	45	13,72	10	-0,84
8929	18,4962	-21,1135	7,7	970	130,14	24,04	20	1	371,90	6	188,13	15	-1,62
105338	18,4962	-18,8162	7,6	1380	58,06	43,95	186	9	598,70	71	38,95	96	0,71
1818ab1004	18,4967	-18,0371	8,8	710	20,02	11,90	143	7	482,86	1	4,43	3	1,74
8153	18,4971	-21,5135	7,6	400	52,06	16,03	14	2	263,38	5	3,10	1	0,86
8167	18,4971	-21,3216	7,6	770	64,07	33,03	56	2	448,72	28	9,74	18	-1,18
8977	18,4990	-21,2721	7,6	460	55,26	17,00	18	1	273,13	8	7,08	10	-0,74
8976	18,5000	-21,2541	7,7	870	91,30	44,93	25	11	484,08	15	59,76	22	-1,07
7884	18,5000	-21,7270	7,1	910	70,08	30,11	76	4	434,09	41	6,20	36	1,62
V-9	18,5004	-19,2324	6,9	1025	120,00	69,30	28	1	627,00	22	4,50	34	4,67
9122	18,5010	-21,8532	6,9	670	87,29	16,03	33	4	390,19	10	2,21	8	2,48
8145	18,5019	-21,4135	7,3	350	37,24	9,96	24	2	197,53	13	9,30	5	-0,35
7875	18,5019	-21,7432	7,3	800	73,28	27,93	40	12	393,85	20	19,03	24	0,92
8159	18,5029	-21,3595	7,9	590	53,26	23,07	50	4	352,39	24	7,08	8	1,62
5939	18,5038	-21,9802	7,4	1600	128,14	48,08	149	5	403,61	240	75,25	152	-0,45
B251/Y3810	18,5048	-19,4459	7,0	760	84,09	50,03	9	3	508,47	8	2,66	7	0,23
8154	18,5048	-21,4856	7,5	280	45,25	7,04	6	2	179,24	5	3,10	1	0,48
8207	18,5058	-21,4081	7,3	380	37,24	10,93	23	2	203,63	5	8,85	11	-1,11
8161	18,5058	-21,3369	7,4	850	79,29	32,06	59	4	358,49	135	3,54	24	-0,84
105345	18,5058	-18,9009	7,1	5650	200,22	254,98	670	32	732,83	580	0,00	1290	0,38
103807	18,5067	-19,3613	7,1	1220	111,32	79,89	35	2	660,89	9	53,12	52	1,34
105342	18,5077	-18,8360	7,4	850	56,06	51,00	57	13	524,32	22	2,66	21	0,61
814	18,5077	-20,3270	7,6	1090	37,24	23,07	190	21	637,72	20	19,48	36	1,46
7887	18,5087	-21,6874	7,4	1000	53,26	27,93	116	4	309,72	80	16,82	96	1,93
B242/Y3372	18,5087	-19,5739	7,2	890	83,29	59,98	13	1	580,41	7	0,44	1	-0,05
8933	18,5096	-21,1081	7,6	710	70,08	41,04	21	3	413,36	19	25,67	15	-0,90
5938	18,5096	-21,9820	6,9	1470	117,33	51,97	115	5	442,62	183	132,80	70	0,27
B242/Y3375	18,5096	-19,5559	7,7	2260	73,28	135,02	185	1	824,28	35	318,72	148	-1,54
104584	18,5096	-18,9360	7,5	7840	108,12	210,06	1450	29	890,13	1100	56,22	1740	-0,56
8945	18,5106	-21,1676	8,1	730	38,04	27,93	75	4	315,81	28	34,97	55	-2,03
104580	18,5106	-18,9838	7,7	1520	57,26	76,98	176	7	597,48	81	84,11	154	-0,44
W-7	18,5109	-21,4091	7,6	520	56,00	13,60	38	3	217,77	39	29,64	15	3,34
1718dc1007	18,5120	-17,8920	7,7	2950	20,02	17,97	830	11	1507,12	149	6,64	250	5,29
8144	18,5125	-21,4234	7,5	420	51,26	13,11	21	2	251,19	5	11,07	7	0,05
103806	18,5125	-19,4315	7,4	890	73,28	59,01	36	0	448,72	17	123,95	8	0,73
B735/Y3806	18,5125	-19,4315	7,4	890	73,28	59,01	36	0	448,72	17	123,95	8	0,73
8946	18,5125	-21,2000	8,2	1040	70,08	60,95	60	7	532,86	30	16,82	72	-1,56
103809	18,5135	-19,4000	7,4	1760	112,12	129,92	53	9	523,10	62	292,16	134	1,25
8972	18,5144	-21,2342	7,8	800	61,27	53,91	35	8	469,45	23	11,07	25	0,90
104618	18,5154	-19,3072	7,8	910	86,09	62,90	14	27	632,84	7	3,98	10	-0,43
104615	18,5154	-19,2180	7,3	950	87,29	51,97	54	0	579,19	26	13,72	31	-0,67
8152	18,5163	-21,5514	7,4	380	53,26	13,11	12	1	251,19	5	3,54	2	-0,58
8973	18,5163	-21,2649	8,1	670	50,05	34,97	49	3	385,32	32	14,61	15	-0,37
8203	18,5173	-21,3739	7,6	380	45,25	11,90	17	2	235,33	4	4,43	4	-1,18
7891	18,5173	-21,6649	7,1	600	80,09	14,08	18	3	312,15	7	22,58	9	1,14
8935	18,5173	-21,1216	7,8	760	46,05	41,04	65	4	441,41	25	19,48	23	-0,65
8934	18,5173	-21,0892	7,6	1030	30,03	59,98	119	5	476,77	52	47,81	65	1,02

Appendix D: Hydrochemical data

Name	Long	Mlat	pH	ec µS/cm	Ca ²⁺ mg/l	Mg ²⁺ mg/l	Na ⁺ mg/l	K ⁺ mg/l	HCO ₃ ⁻ mg/l	SO ₄ ²⁻ mg/l	NO ₃ ⁻ mg/l	Cl ⁻ mg/l	Balance %
8944	18,5183	-21,1640	7,9	840	75,28	34,00	65	4	399,95	28	57,55	39	1,71
104619	18,5183	-19,3009	7,9	930	73,28	73,10	19	31	635,28	12	3,54	14	0,79
1718da1001	18,5200	-17,5300	7,8	320	36,84	15,06	3	3	192,66	1	2,21	3	-0,21
1718da1	18,5200	-17,5300	7,0	340	43,25	16,27	5	3	225,58	0	0,00	5	-0,61
1818da1005	18,5200	-18,7317	7,5	2050	122,93	78,92	180	16	607,24	64	22,13	370	-2,82
1818da1006	18,5200	-18,6667	7,4	2500	70,08	52,94	390	19	707,22	190	13,28	400	-3,32
8143	18,5202	-21,4514	7,8	370	51,26	10,93	12	2	232,90	5	9,74	4	-1,96
B248/1/Y3815	18,5202	-19,5018	7,1	1280	55,26	92,04	130	2	838,91	37	9,74	26	2,00
8149	18,5212	-21,4928	7,6	380	57,26	10,93	11	2	251,19	5	5,75	2	-0,97
1818da1009	18,5220	-18,5892	7,4	970	54,06	32,06	114	10	451,16	26	22,13	60	2,75
9109	18,5231	-21,9541	7,2	930	72,08	22,10	125	5	448,72	74	13,28	46	2,68
1818da1022	18,5233	-18,5250	7,3	620	56,86	36,91	2	39	404,82	3	2,21	2	1,24
9126	18,5240	-21,8523	6,8	780	107,32	14,08	21	5	375,56	9	39,84	26	-1,06
7890	18,5240	-21,6874	7,2	1050	60,07	31,08	118	5	458,48	51	22,13	48	2,51
104614	18,5240	-19,2189	7,5	1300	79,29	61,92	145	1	715,76	51	49,58	64	-0,04
8202	18,5250	-21,3928	7,8	370	42,05	13,11	20	2	232,90	4	6,20	3	0,17
9127	18,5250	-21,8568	6,9	770	109,32	14,08	27	5	390,19	11	26,56	24	1,20
104923	18,5250	-19,1514	7,8	950	85,29	62,90	26	2	580,41	20	0,00	26	-0,23
B242/Y3374	18,5269	-19,5135	7,1	970	102,11	53,91	13	1	626,75	8	0,44	2	-1,84
5928	18,5269	-21,9676	7,4	1640	105,31	48,08	170	5	420,68	231	22,13	190	-2,01
8150	18,5279	-21,5162	7,6	340	47,25	9,96	12	2	220,70	5	3,54	2	-1,11
8204	18,5279	-21,4027	7,3	360	45,25	8,99	17	2	226,80	4	2,21	1	-0,99
9121	18,5279	-21,8730	7,1	630	78,08	17,97	27	5	365,81	8	4,43	7	1,89
7888	18,5279	-21,6946	7,6	1080	53,26	30,11	136	5	356,05	130	25,23	65	1,81
1718dc1005	18,5280	-17,7670	7,8	510	54,06	33,03	8	5	348,73	1	2,21	2	0,54
W-6	18,5283	-21,3847	7,7	362	43,10	11,10	17	2	225,70	2	2,00	5	-0,81
7889	18,5288	-21,7027	7,6	1070	57,26	31,08	122	5	326,79	105	16,82	91	2,21
8965	18,5298	-21,2405	7,8	440	37,24	16,03	38	2	267,04	11	4,43	8	-0,22
9125	18,5298	-21,8577	7,1	720	96,10	14,08	35	6	390,19	14	3,54	19	2,36
7892	18,5308	-21,6595	7,7	440	49,25	10,93	21	2	246,31	7	4,43	8	-1,79
104613	18,5308	-19,2459	7,3	1210	77,28	114,86	44	1	746,24	5	56,66	49	2,07
817	18,5308	-20,0739	7,8	1650	20,02	17,97	340	28	720,64	93	43,38	103	1,79
C364	18,5308	-18,6793	7,8	1700	56,46	39,83	300	31	681,62	114	5,31	200	1,70
105344	18,5308	-18,9099	7,6	1980	45,25	53,91	340	15	719,42	220	27,45	200	-1,33
B233/Y3376	18,5308	-19,6396	7,5	4860	52,06	59,98	980	3	1219,35	260	887,10	290	2,40
784	18,5317	-19,8081	6,9	2400	133,35	90,09	240	40	1107,17	57	30,10	235	-1,76
B243/Y3382	18,5317	-19,6126	7,4	1000	61,27	69,94	40	1	626,75	12	0,44	9	-0,96
B242/Y3373	18,5317	-19,5414	8,0	1090	54,06	75,04	65	1	725,51	7	0,44	3	-1,69
C365	18,5327	-18,7405	7,2	2200	204,22	114,14	183	17	634,06	46	8,85	585	-0,03
1818dc1003	18,5333	-18,7607	8,5	1800	14,02	56,10	300	21	546,27	130	4,43	260	-0,43
9124	18,5346	-21,8568	6,9	690	85,29	10,93	32	5	360,93	6	2,66	16	1,07
104924	18,5365	-19,1198	7,3	1130	80,09	59,01	64	9	548,71	55	0,00	63	-0,20
104777	18,5365	-19,2045	7,4	1460	79,29	77,95	83	38	613,33	54	123,95	72	-0,84
8174	18,5375	-21,3198	7,3	770	63,27	31,08	59	4	334,10	99	4,43	20	1,28
105341	18,5375	-18,8189	7,7	1340	60,07	42,01	194	13	619,43	80	32,76	100	0,19
9123	18,5385	-21,8559	7,0	620	83,29	10,93	30	4	360,93	5	2,66	9	1,15
8176	18,5385	-21,2739	7,9	700	68,07	31,08	36	3	399,95	22	14,61	13	-0,11
8151	18,5394	-21,5333	7,5	420	49,25	13,11	22	3	245,09	5	4,43	7	2,02
8175	18,5404	-21,2919	7,6	910	74,08	39,10	60	4	496,28	24	11,07	39	-1,46
9909	18,5413	-21,4315	7,5	350	47,25	8,99	17	2	231,68	4	3,10	2	-1,25
8971	18,5423	-21,2252	7,9	360	34,04	16,03	21	2	210,95	10	4,43	9	-0,11
8169	18,5423	-21,3613	7,5	750	88,10	17,00	32	3	245,09	5	141,65	40	-1,82
8172	18,5423	-21,9631	7,2	910	70,08	25,98	81	3	364,59	82	45,59	34	-0,76

Appendix D: Hydrochemical data

Name	Long	Mlat	pH	ec µS/cm	Ca ²⁺ mg/l	Mg ²⁺ mg/l	Na ⁺ mg/l	K ⁺ mg/l	HCO ₃ ⁻ mg/l	SO ₄ ²⁻ mg/l	NO ₃ ⁻ mg/l	Cl ⁻ mg/l	Balance %
8173	18,5423	-21,3279	7.1	2340	182,20	87,91	170	9	388,97	245	376,26	230	-0,17
8168	18,5423	-21,3568	7,6	3840	343,57	79,89	325	6	399,95	140	947,30	420	1,90
W-8	18,5426	-21,2812	7,8	705	76,08	32,00	33	3	348,92	22	33,28	25	3,38
105343	18,5433	-18,8847	7,3	1000	62,07	44,93	90	8	468,23	43	7,08	79	0,01
780	18,5433	-19,6964	7,3	1030	74,08	77,95	31	1	681,62	5	13,72	15	-1,85
B243/Y3383	18,5433	-19,5892	7,4	1740	110,12	119,96	43	8	586,51	33	301,01	100	-1,50
782	18,5433	-19,6829	6,9	3080	57,26	35,94	665	53	1376,65	84	8,41	380	1,31
8950	18,5442	-21,1721	8.2	550	44,05	24,04	39	3	280,45	12	22,58	23	0,77
103811	18,5442	-19,4730	7,2	1080	46,05	100,05	74	0	793,80	33	0,00	16	-1,43
B248/1/Y3811	18,5442	-19,4730	7,2	1080	46,05	100,05	74	0	793,80	33	0,44	16	-1,45
104767	18,5442	-19,3171	7,2	1390	121,33	75,04	50	25	602,36	29	146,08	80	-0,15
781	18,5452	-19,6901	8,3	1340	65,27	73,10	107	10	657,23	16	146,08	48	-2,18
104617	18,5462	-19,2775	7,5	970	106,12	53,91	19	14	521,88	24	69,06	30	-0,44
104550	18,5471	-19,4081	7,4	1050	112,12	48,08	22	0	427,99	24	88,53	73	-2,29
V-10	18,5481	-19,2419	7,0	1068	90,00	95,00	14	1	708,00	6	3,60	36	0,39
8966	18,5490	-21,2432	7,8	770	41,24	16,03	77	49	392,63	21	23,02	31	-0,86
104581	18,5490	-18,9892	8,5	2980	22,02	41,04	680	29	1190,09	325	0,00	265	1,53
W-9	18,5495	-21,3354	8,0	1139	106,00	33,90	74	3	323,30	84	176,00	58	-0,71
104919	18,5500	-19,0883	7,7	1770	112,12	93,01	116	1	536,51	80	0,00	220	4,73
7893	18,5510	-21,6514	7,3	400	47,25	10,93	21	2	214,61	10	4,43	8	2,42
104582	18,5519	-18,9441	7,3	5000	380,41	289,95	500	12	507,25	690	243,47	1300	1,27
8947	18,5529	-21,1694	8	530	45,25	18,94	41	3	301,18	14	10,18	19	-2,16
8171	18,5538	-21,3883	7,4	450	58,06	10,93	20	2	274,35	4	7,97	5	-1,37
104590	18,5558	-18,8225	7,5	2760	73,28	59,01	480	22	752,34	130	16,82	500	0,91
873	18,5567	-21,0450	8,1	500	58,06	15,06	27	3	276,79	9	8,85	13	1,45
B248/1/Y3814	18,5596	-19,4982	7,5	920	95,30	71,88	13	2	624,31	5	13,28	7	2,45
104612	18,5596	-19,2423	7,4	930	72,08	90,09	15	1	697,47	4	0,00	9	-0,34
9154	18,5606	-21,7514	6,8	860	92,10	19,91	40	5	348,73	10	59,76	47	-0,68
5929	18,5606	-21,9820	7,0	1020	57,26	34,00	108	12	493,84	83	0,00	44	-1,85
1818da1010	18,5610	-18,6558	7,8	1750	46,05	37,88	290	19	668,20	100	2,21	204	-0,82
104611	18,5615	-19,1766	7,4	1080	61,27	71,88	92	2	646,26	27	0,00	38	3,17
1718dc1008	18,5620	-17,9070	9,2	900	6,01	8,01	200	8	536,51	12	2,21	31	-0,45
8970	18,5625	-21,2207	8,2	430	50,05	17,00	15	3	224,36	5	24,35	17	-0,30
1818da1013	18,5625	-18,5837	7,4	1420	58,86	40,07	187	28	577,97	46	8,85	164	-0,38
B243/Y3384	18,5625	-19,5577	7,7	1650	30,03	75,04	285	3	1143,75	15	2,21	7	2,17
8189	18,5635	-21,3099	7,7	520	54,06	15,06	27	2	286,55	5	19,92	8	-1,76
779	18,5635	-19,6550	7,3	780	85,29	50,03	11	1	551,15	5	2,66	3	-2,14
104604	18,5635	-19,0964	7,8	7070	54,06	100,05	1500	8	1015,72	1300	0,00	1100	1,09
9155	18,5663	-21,7486	7,0	640	74,08	14,08	29	5	346,30	8	13,28	12	-1,18
104549	18,5663	-19,4288	7,4	940	110,12	39,10	22	20	579,19	10	18,15	18	-1,55
104551	18,5663	-19,4423	7,5	1460	80,09	87,91	104	3	701,13	23	32,76	125	-0,61
1818dc1004	18,5667	-18,7567	7,3	1780	62,87	41,04	270	16	573,10	116	6,64	250	-0,79
8949	18,5673	-21,1901	7.9	370	39,24	14,08	22	3	224,36	7	5,31	10	-0,47
104597	18,5673	-18,9108	7,5	910	52,06	35,94	98	11	452,38	50	17,71	48	0,02
104548	18,5673	-19,4243	7,2	2640	129,34	79,89	300	22	690,15	99	292,16	330	-1,39
8170	18,5683	-21,3649	7,2	400	52,06	9,96	19	3	257,28	4	0,00	2	-0,42
8188	18,5683	-21,3162	7,5	880	91,30	31,08	28	5	274,35	11	159,36	37	0,72
104589	18,5683	-18,7964	8,1	1880	70,08	48,08	315	16	708,44	160	9,74	220	0,61
104605	18,5692	-19,0703	7,4	950	68,07	76,98	38	1	637,72	7	0,00	28	0,10
104778	18,5692	-19,2072	7,3	1000	97,31	66,05	19	1	634,06	4	0,00	17	0,85
1818da1004	18,5703	-18,7343	8,4	1350	18,02	22,10	250	18	563,34	63	90,75	130	-5,46
1818da1021	18,5708	-18,5267	7,4	510	52,86	33,03	2	11	336,54	3	2,21	2	0,47
104595	18,5721	-18,8775	7,5	4640	325,55	210,06	380	15	467,01	140	447,09	1100	1,65

Appendix D: Hydrochemical data

Name	Long	Lat	pH	ec µS/cm	Ca ²⁺ mg/l	Mg ²⁺ mg/l	Na ⁺ mg/l	K ⁺ mg/l	HCO ₃ ⁻ mg/l	SO ₄ ²⁻ mg/l	NO ₃ ⁻ mg/l	Cl ⁻ mg/l	Balance %
104572	18,5740	-19,1378	7,4	990	89,30	74,07	31	1	651,13	9	0,00	32	0,69
104591	18,5740	-18,8252	7,4	1210	109,32	50,03	75	6	495,06	5	24,35	160	-0,52
104596	18,5740	-18,8559	7,7	1710	58,06	33,03	325	10	871,84	93	27,89	95	1,66
8187	18,5740	-21,3198	7,5	3120	300,33	100,05	171	11	426,77	70	920,74	240	1,42
1718dc1009	18,5750	-17,9630	7,7	610	50,05	24,04	51	6	404,82	1	2,21	3	0,53
9148	18,5760	-21,8378	6,8	590	77,28	11,90	26	4	331,66	8	2,21	9	1,48
9877	18,5760	-21,4396	8,1	600	76,08	15,06	32	3	295,08	41	12,39	22	-0,04
9106	18,5769	-21,9640	7,5	810	50,05	33,03	78	7	267,04	78	8,85	83	1,75
9153	18,5779	-21,7892	7,2	500	54,06	13,11	25	3	263,38	10	11,07	12	-1,01
9104	18,5788	-21,9054	7,1	650	89,30	22,10	28	6	427,99	11	3,54	13	-0,14
104575	18,5788	-19,0360	7,5	2650	64,07	100,05	420	27	745,02	335	10,62	345	2,19
8967	18,5798	-21,2766	7,8	740	56,06	30,11	70	5	413,36	42	11,07	19	0,50
104608	18,5798	-19,1973	7,5	1060	88,10	67,02	58	1	641,38	17	0,00	38	2,14
1718dc1003	18,5800	-17,7630	7,7	480	48,05	30,11	7	4	317,03	1	2,21	2	-0,25
8325	18,5817	-21,6658	7,5	390	48,05	15,06	17	2	256,06	4	4,43	7	-1,35
9105	18,5827	-21,9640	7,2	1100	92,10	49,05	78	5	364,59	95	54,01	97	2,50
104609	18,5827	-19,1901	7,8	1520	90,10	78,92	103	43	620,65	87	0,00	106	5,06
104773	18,5827	-19,2883	7,4	1540	77,28	79,89	98	68	749,90	57	0,00	98	0,59
8969	18,5837	-21,2090	7,7	380	45,25	15,06	18	3	252,41	4	3,54	7	-1,33
104603	18,5837	-19,0892	7,6	1300	63,27	65,08	115	66	709,66	68	0,00	54	2,13
B248/1/Y3813	18,5846	-19,5207	8,3	1240	26,03	76,98	174	2	902,32	5	0,44	4	0,80
104576	18,5846	-19,0072	7,5	2100	40,04	59,98	325	20	698,69	155	4,43	265	-1,46
1718dc1002	18,5850	-17,8020	7,8	610	38,04	25,98	63	4	404,82	1	2,21	3	0,76
8327	18,5856	-21,6883	7,7	310	52,06	10,93	17	2	249,97	5	4,43	4	-1,12
9902	18,5856	-21,5450	7,6	320	42,05	8,01	11	1	168,27	4	16,38	9	-1,47
8326	18,5856	-21,6658	7,5	400	47,25	16,03	19	2	256,06	4	6,64	7	-0,33
8182	18,5865	-21,3054	7,5	600	62,07	18,94	34	4	298,74	7	13,28	37	-0,50
8186	18,5875	-21,3252	7,5	960	95,30	22,10	59	5	352,39	11	28,33	109	-1,42
1818da1001	18,5883	-18,7360	7,7	1580	64,07	41,04	210	13	560,90	99	11,51	190	-2,31
9146	18,5894	-21,8793	6,8	580	80,09	9,96	18	4	336,54	6	2,66	6	-1,31
B248/Y3820	18,5894	-19,4928	7,3	810	61,27	69,94	16	1	580,41	5	0,44	1	-0,61
104775	18,5894	-19,2396	7,6	1280	80,09	61,92	103	1	668,20	41	0,00	65	-0,15
B248/1/Y3812	18,5894	-19,5180	7,2	2850	54,06	135,02	440	2	1255,93	90	301,01	154	2,08
9145	18,5904	-21,8757	6,9	560	75,28	11,90	20	4	321,91	9	4,87	7	-0,27
5931	18,5904	-21,9982	7,2	800	59,26	41,04	48	6	470,67	18	6,64	26	-2,02
B248/Y3816	18,5904	-19,4991	7,0	860	70,08	73,10	13	1	592,60	5	0,44	1	1,26
778	18,5904	-19,6270	7,4	1130	68,07	61,92	79	3	643,82	17	27,45	39	-1,81
104573	18,5904	-19,1604	7,4	1240	88,10	66,05	91	7	570,66	61	0,00	98	2,13
8958	18,5913	-21,1649	7,8	520	64,07	17,97	20	3	301,18	9	12,39	16	-1,33
1818da1002	18,5916	-18,7370	7,4	1640	66,07	41,04	220	13	595,04	113	11,07	200	-3,91
9103	18,5923	-21,9099	7,1	470	49,25	20,88	28	6	308,50	14	0,00	12	-1,23
9880	18,5923	-21,4360	7,5	570	82,09	11,90	28	3	329,22	27	12,39	8	-0,10
B246/Y3387	18,5923	-19,5676	7,7	1180	64,07	104,91	44	2	679,18	29	63,74	28	0,89
1818da1017	18,5925	-18,5600	7,4	610	56,86	42,01	7	12	412,14	3	2,21	4	-0,43
1818da1011	18,5925	-18,6540	7,5	1270	32,84	20,88	222	15	502,37	45	4,43	144	0,35
1818da1003	18,5925	-18,7366	7,5	1680	64,07	42,01	230	13	607,24	115	11,07	190	-2,56
8968	18,5933	-21,2342	7,6	400	40,04	18,94	19	4	252,41	9	4,43	6	-0,87
8183	18,5933	-21,2919	7,6	560	47,25	18,94	44	3	298,74	17	13,28	16	-0,07
104571	18,5933	-19,1360	7,4	970	95,30	58,04	41	3	577,97	34	0,00	40	0,37
8190	18,5942	-21,3396	7,5	410	50,05	11,90	21	3	245,09	4	5,31	5	1,60
874	18,5942	-21,1541	7,3	460	54,06	14,08	27	3	276,79	6	7,97	13	-0,47
8298	18,5952	-21,7495	7,3	780	119,33	16,03	21	2	360,93	8	99,60	28	-1,43
1818da1012	18,5962	-18,5850	7,4	1440	64,87	40,07	180	17	463,35	60	11,07	210	-0,49

Appendix D: Hydrochemical data

Name	Long	Mlat	pH	ec µS/cm	Ca ²⁺ mg/l	Mg ²⁺ mg/l	Na ⁺ mg/l	K ⁺ mg/l	HCO ₃ ⁻ mg/l	SO ₄ ²⁻ mg/l	NO ₃ ⁻ mg/l	Cl ⁻ mg/l	Balance %
1718dc2	18,5970	-17,8030	6,9	620	58,06	32,30	30	3	404,82	4	4,43	9	-0,76
1718dc1001	18,5970	-17,8030	7,6	630	56,06	34,00	29	4	417,02	1	4,43	6	-0,97
8297	18,5971	-21,7468	7,3	980	125,34	26,96	38	3	358,49	21	110,67	85	-1,41
103817	18,5981	-19,4703	7,2	980	50,05	90,09	45	3	684,06	13	0,00	4	1,49
B248/Y3817	18,5981	-19,4703	7,2	980	50,05	90,09	45	3	684,06	13	0,44	4	1,46
9882	18,5981	-21,4279	7,3	1140	120,13	23,07	84	6	371,90	82	121,73	64	0,56
9879	18,5990	-21,4631	7,6	370	41,24	10,93	19	2	203,63	7	7,53	10	-0,67
104600	18,5990	-18,9937	8,2	990	17,22	25,98	188	17	665,77	21	0,00	14	-0,57
876	18,6000	-20,9595	8,3	480	37,24	19,91	26	4	193,88	6	43,38	27	-0,35
9149	18,6000	-21,8369	7,3	520	69,28	10,93	18	3	302,40	7	3,10	5	-0,73
8348	18,6010	-21,5811	7,0	340	29,23	8,99	30	2	182,90	8	6,64	15	-1,93
8951	18,6010	-21,1820	7,8	380	40,04	17,97	22	4	238,99	5	5,31	8	2,30
8184	18,6010	-21,2748	7,6	710	65,27	22,10	45	3	317,03	16	26,56	40	0,17
104588	18,6010	-18,8054	7,9	990	28,03	19,91	173	35	570,66	24	18,59	40	0,78
104606	18,6010	-19,0703	7,3	1630	78,08	68,97	200	9	666,99	150	0,00	145	0,98
103819	18,6019	-19,4523	7,1	890	107,32	62,90	3	1	584,07	4	5,31	22	1,55
775	18,6019	-19,5811	7,3	2750	123,33	75,04	390	2	734,05	100	637,44	160	0,75
B248/Y3819	18,6019	-19,4523	7,1	890	107,32	62,90	3	1	584,07	4	5,31	22	1,55
8329	18,6038	-21,7045	7,5	460	59,26	14,08	22	2	280,45	5	8,85	14	-1,10
9883	18,6048	-21,5018	7,8	570	54,06	17,97	39	5	323,13	14	14,61	13	-1,55
9152	18,6058	-21,8090	6,9	530	61,27	9,96	30	3	268,26	9	5,75	15	1,53
8328	18,6058	-21,7054	7,1	1030	125,34	25,01	52	4	371,90	10	161,57	46	2,25
9881	18,6058	-21,4306	7,4	1030	114,12	25,01	54	19	343,86	63	110,67	56	1,32
9889	18,6067	-21,5784	7,9	300	18,02	8,01	32	3	140,23	13	0,00	20	-1,71
104602	18,6067	-18,9523	7,8	1080	37,24	34,97	150	35	595,04	41	48,69	29	-0,22
1718da1002	18,6070	-17,6370	7,5	540	52,86	40,07	3	3	370,68	1	2,21	2	-0,37
1718da2	18,6070	-17,6370	7,5	575	56,86	40,80	4	7	396,29	0	0,00	5	-0,67
8340	18,6077	-21,6036	7,1	390	45,25	13,11	22	3	243,87	4	11,07	8	-1,28
B246/Y3385	18,6077	-19,5405	7,5	1250	25,23	84,02	161	2	853,55	21	1,77	2	2,41
103818	18,6077	-19,4739	7,3	1430	38,04	86,94	166	3	724,29	47	86,76	60	1,27
B248/Y3818	18,6077	-19,4739	7,3	1430	38,04	86,94	166	3	724,29	47	86,76	60	1,27
8296	18,6087	-21,7757	7,6	510	62,07	13,11	32	4	307,28	8	8,85	16	-1,10
C361	18,6087	-18,7477	7,8	650	22,42	56,82	41	6	408,48	14	0,00	29	-0,46
8330	18,6087	-21,7036	7,1	1210	78,08	28,90	99	94	670,64	10	0,00	85	-2,30
C362	18,6087	-18,6640	8,1	1250	39,24	17,48	213	17	499,93	48	5,75	135	0,01
9878	18,6087	-21,4477	7,6	1620	100,11	41,04	137	6	104,86	10	190,35	330	0,63
918	18,6087	-21,9739	7,0	4450	180,20	221,96	520	7	553,59	725	88,53	800	1,93
104774	18,6096	-19,2802	7,4	910	80,09	51,00	28	3	534,08	26	0,00	22	-2,20
816	18,6096	-19,9730	7,8	2610	18,02	16,03	560	38	831,60	380	83,22	172	-0,34
104578	18,6106	-19,0252	7,8	2480	57,26	65,08	450	26	884,03	125	30,54	340	2,30
9147	18,6115	-21,8658	7,2	470	65,27	10,93	16	4	270,70	6	2,21	4	2,53
C363	18,6115	-18,5982	7,9	1300	32,44	22,83	212	23	527,98	74	4,43	104	0,41
8185	18,6125	-21,3225	7,4	370	39,24	10,93	18	2	209,73	5	5,31	3	-0,27
776	18,6125	-19,5802	8,3	2580	158,17	102,96	218	4	467,01	97	814,50	130	-1,00
104601	18,6125	-18,9874	8,0	4640	170,19	189,90	620	18	429,21	650	7,08	1030	1,79
8334	18,6135	-21,6207	7,2	450	48,05	17,00	23	3	195,10	5	39,84	26	2,06
C269	18,6135	-17,7793	7,6	490	53,66	29,38	18	3	359,71	0	0,00	5	-0,67
9107	18,6135	-21,9757	7,1	7740	141,35	284,85	1180	5	673,08	1220	110,67	1420	2,30
104577	18,6144	-18,9991	7,6	840	49,25	57,07	13	65	577,97	3	0,00		-0,81
8177	18,6154	-21,2964	7,8	680	63,27	19,91	41	4	310,93	15	50,02	26	-1,96
1718da3	18,6163	-17,6259	7,5	330	33,64	23,31	18	4	256,06	8	0,00	8	-1,18
8952	18,6163	-21,2009	8,3	460	56,06	15,06	26	3	301,18	5	5,31	10	-1,54
104598	18,6163	-18,9297	7,7	770	55,26	37,88	73	7	465,79	48	0,00	22	-0,13

Appendix D: Hydrochemical data

Name	Long	Mlat	pH	ec µS/cm	Ca ²⁺ mg/l	Mg ²⁺ mg/l	Na ⁺ mg/l	K ⁺ mg/l	HCO ₃ ⁻ mg/l	SO ₄ ²⁻ mg/l	NO ₃ ⁻ mg/l	Cl ⁻ mg/l	Balance %
104599	18,6163	-18,9685	8,3	850	28,03	25,01	87	87	543,83	7	4,87	16	-0,64
1718da16	18,6167	-17,6268	8,1	420	34,04	24,28	28	2	254,84	12	17,71	4	1,44
1718da15	18,6172	-17,6277	7,8	380	40,04	21,37	23	2	264,60	11	0,00	2	1,98
1718da15	18,6172	-17,6277	7,9	430	34,04	21,37	30	2	265,82	12	0,00	2	1,59
9857	18,6183	-21,3874	7,5	360	47,25	8,99	20	2	231,68	5	7,97	2	-0,83
9869	18,6183	-21,4748	7,2	500	49,25	11,90	40	3	267,04	25	8,85	13	-1,43
1818da1020	18,6183	-18,5125	7,3	580	66,07	35,94	3	8	387,75	3	2,21	5	-0,03
9901	18,6192	-21,5523	7,3	460	49,25	9,96	28	2	252,41	8	0,00	15	-1,94
9102	18,6202	-21,9198	7,1	600	74,08	19,91	31	4	357,27	15	3,10	24	-0,79
104593	18,6202	-18,8333	7,9	1130	8,01	3,89	270	22	669,42	49	11,95	31	-0,12
8333	18,6212	-21,6586	7,5	390	51,26	9,96	20	3	249,97	5	4,43	6	-1,34
1818dc1001	18,6217	-18,7000	7,4	2090	78,89	49,05	310	18	599,92	80	2,21	350	1,18
8953	18,6221	-21,2198	7,9	470	57,26	17,00	23	3	273,13	10	20,36	12	-0,17
104585	18,6221	-18,9126	7,7	780	84,09	32,06	42	5	426,77	8	16,82	57	-1,41
8347	18,6221	-21,5847	7,4	1210	91,30	51,97	112	6	573,10	60	17,71	118	-1,42
103824	18,6221	-19,4054	7,5	1760	152,17	94,95	78	1	514,57	28	234,61	180	2,58
9876	18,6231	-21,4252	7,8	760	77,28	17,00	60	5	343,86	40	30,99	39	-0,47
103825	18,6231	-19,4351	7,0	980	98,11	71,88	10	3	637,72	10	15,94	16	-0,20
8957	18,6250	-21,1622	8	440	52,06	10,93	21	3	238,99	5	4,43	15	-0,31
9450	18,6250	-21,8315	8,3	450	30,03	8,99	52	11	224,36	19	0,00	18	2,15
8332	18,6260	-21,6595	7,5	360	43,25	11,90	21	3	231,68	7	4,43	7	-1,01
9870	18,6260	-21,4622	7,4	440	58,06	10,93	19	3	259,72	8	9,30	11	-1,91
C257	18,6260	-17,6180	7,5	580	56,86	40,80	4	7	396,29	0	0,00	5	-0,67
103821	18,6269	-19,4568	7,2	930	43,25	74,07	68	3	620,65	30	3,54	8	0,93
B248/Y3821	18,6269	-19,4568	7,2	930	43,25	74,07	68	3	620,65	30	3,54	8	0,93
9884	18,6279	-21,5279	7,8	230	20,02	8,01	16	3	126,81	6	6,20	8	-1,97
8295	18,6279	-21,7622	7,6	450	65,27	8,01	23	3	297,52	6	4,43	4	-1,88
104587	18,6279	-18,8739	7,9	930	38,04	59,01	76	47	664,55	5	13,28	3	-0,14
8955	18,6279	-21,2333	7,8	2520	138,15	68,97	305	5	364,59	180	486,93	270	1,51
9151	18,6288	-21,8180	8,7	630	14,02	7,04	112	14	287,77	40	11,07	35	-1,56
103823	18,6288	-19,4027	7,1	940	93,30	54,88	32	2	506,03	18	39,84	40	0,84
104586	18,6288	-18,8919	7,8	1020	120,13	48,08	26	3	362,15	5	163,79	98	-1,26
104592	18,6288	-18,8135	8,3	2150	19,22	16,03	500	32	1297,39	91	7,53	60	-0,25
777	18,6298	-19,6396	7,5	1530	47,25	50,03	251	5	809,65	73	36,30	62	1,15
1718da1003	18,6300	-17,6460	7,6	720	64,87	50,03	4	3	382,88	1	2,21	57	-2,15
8331	18,6317	-21,6973	7,8	480	64,07	14,08	23	3	268,26	5	4,43	34	-0,89
8954	18,6317	-21,2207	8	850	72,08	30,11	55	5	267,04	35	99,60	76	-1,49
103822	18,6317	-19,3649	7,3	920	36,04	31,08	116	35	534,08	11	8,85	34	1,05
104772	18,6317	-19,3171	7,6	1130	105,31	63,87	27	4	513,35	18	0,00	64	5,34
8178	18,6346	-21,2640	7,7	540	54,06	11,90	39	2	274,35	8	28,77	18	-1,90
9888	18,6365	-21,5090	7,4	390	48,05	8,99	22	2	238,99	5	5,75	6	-1,63
9900	18,6365	-21,5595	7,0	710	55,26	23,07	28	9	70,72	4	168,21	80	-0,87
104574	18,6375	-19,0505	8,0	1410	59,26	52,94	189	11	618,21	115	8,85	116	-0,39
9858	18,6394	-21,3577	7,1	440	46,05	10,93	37	4	273,13	7	6,64	7	-0,18
8299	18,6394	-21,7423	7,4	640	82,09	15,06	35	2	346,30	11	33,20	22	-1,08
C256	18,6404	-17,6378	7,5	330	33,64	23,31	18	4	256,06	8	0,00	8	-1,18
9868	18,6413	-21,4865	8,6	300	17,22	13,11	33	3	175,59	10	0,00	13	-0,03
104594	18,6423	-18,7901	7,4	1370	113,32	34,97	142	6	538,95	35	8,85	205	-2,06
V-8	18,6429	-19,0966	7,0	1285	81,30	103,00	71	27	758,00	38	22,50	59	3,34
8300	18,6433	-21,7441	7,7	520	59,26	16,03	40	4	328,01	13	6,64	10	0,68
8959	18,6433	-21,1883	8,2	620	83,29	19,91	20	3	351,17	12	11,07	30	-2,09
8960	18,6433	-21,1910	7,8	650	86,09	22,10	21	3	351,17	7	11,07	34	0,47
B987/Y3388	18,6442	-19,5910	7,5	940	46,05	69,94	64	1	586,51	50	0,44	6	0,15

Appendix D: Hydrochemical data

Name	Long	Lat	pH	ec µS/cm	Ca ²⁺ mg/l	Mg ²⁺ mg/l	Na ⁺ mg/l	K ⁺ mg/l	HCO ₃ ⁻ mg/l	SO ₄ ²⁻ mg/l	NO ₃ ⁻ mg/l	Cl ⁻ mg/l	Balance %
B246/Y3386	18,6462	-19,5144	8,1	1440	34,04	85,97	200	1	864,52	71	6,64	34	2,29
8181	18,6471	-21,2775	7,8	430	42,05	13,11	28	3	251,19	11	0,00	9	-1,41
9130	18,6471	-21,8973	7,1	510	61,27	10,93	19	7	287,77	7	0,00	8	-1,25
768	18,6471	-19,5649	7,3	4070	66,07	84,02	790	9	1044,98	700	31,87	420	0,84
9131	18,6481	-21,8541	7,2	450	58,06	8,99	20	4	258,50	4	4,43	6	0,53
9101	18,6481	-21,9378	7,5	480	19,22	9,96	75	4	224,36	8	34,09	22	1,27
8345	18,6481	-21,5595	7,2	830	85,29	20,88	59	6	280,45	40	22,13	128	-3,88
B987/Y3390	18,6481	-19,5252	8,4	1200	14,02	80,87	169	3	812,09	32	0,44	10	1,78
9871	18,6490	-21,4369	8,9	270	20,02	9,96	20	6	160,95	7	0,00	4	-0,95
8338	18,6490	-21,6144	7,4	520	66,87	17,00	22	4	246,31	6	26,56	40	0,67
8956	18,6500	-21,2144	8	720	58,06	24,04	73	2	413,36	25	12,39	24	-0,43
B987/Y3391	18,6500	-19,5270	7,4	1370	38,04	93,01	152	2	807,21	39	7,97	49	2,09
815	18,6510	-20,1649	7,4	820	54,06	22,10	98	17	485,30	11	13,28	18	1,71
9132	18,6519	-21,8252	7,3	410	52,06	8,01	16	4	229,24	5	2,66	5	0,13
103826	18,6529	-19,4189	7,2	1290	85,29	79,89	70	23	597,48	24	85,88	72	2,68
B987/Y3389	18,6529	-19,5613	7,3	7420	175,39	179,95	1210	27	592,60	1100	9,74	1520	0,81
8339	18,6538	-21,6802	7,6	410	53,26	11,90	19	4	256,06	4	8,85	12	-2,10
9860	18,6548	-21,3955	7,2	650	64,07	18,94	52	4	295,08	22	50,91	36	-0,07
103833	18,6558	-19,4658	7,1	1760	61,27	100,05	188	5	834,04	140	38,95	90	-0,39
9885	18,6567	-21,5459	7,3	230	16,02	8,99	16	3	91,45	4	6,64	20	1,27
9887	18,6587	-21,5144	7,3	300	38,04	10,93	28	2	189,00	6	4,43	31	-1,23
8346	18,6587	-21,5739	7,8	360	34,04	10,93	28	3	237,77	5	0,00	7	-3,78
875	18,6587	-21,1369	7,7	440	55,26	13,11	20	4	249,97	5	13,28	12	0,58
8179	18,6587	-21,2865	7,6	470	55,26	16,03	16	6	275,57	8	15,94	5	-1,55
104169	18,6587	-18,9550	7,8	1050	18,02	16,76	198	32	674,30	25	3,54	14	-1,33
104565	18,6606	-19,0982	7,4	1280	68,07	110,01	52	26	704,79	29	53,56	72	1,08
104555	18,6615	-19,3387	7,7	960	83,29	75,04	14		643,82	4	0,00	16	-0,66
9861	18,6615	-21,3865	7,1	1850	179,40	50,03	130	5	323,13	78	433,81	165	0,75
1818da1008	18,6625	-18,7388	7,6	1320	74,08	43,95	140	12	451,16	39	8,85	190	0,01
1718da5	18,6629	-17,6824	7,7	460	42,05	21,86	19	5	280,45	5	0,00	3	0,69
9851	18,6644	-21,4162	7,3	530	73,28	17,00	17	3	336,54	6	9,30	4	-0,27
1818da1014	18,6653	-18,6083	7,3	860	48,85	27,93	107	10	487,74	15	6,64	36	1,14
8180	18,6654	-21,2973	7,7	380	45,25	10,44	19	3	214,61	11	11,95	9	-2,10
104568	18,6663	-19,1739	7,5	1440	93,30	77,95	97	23	656,01	33	141,65	88	-1,02
1818da1007	18,6667	-18,6638	7,8	630	50,86	25,98	48	7	390,19	8	11,07	8	-0,16
8335	18,6673	-21,6838	7,8	410	49,25	15,06	20	4	256,06	5	4,43	12	-0,44
8301	18,6673	-21,7541	7,6	420	65,27	15,06	12	2	281,67	6	4,43	7	0,59
9872	18,6673	-21,4595	7,6	500	54,06	11,90	43	3	273,13	30	5,75	13	0,57
881	18,6673	-20,9505	7,9	730	74,08	31,08	34	5	374,34	7	14,17	37	2,00
9838	18,6673	-21,2685	7,4	1190	122,13	37,88	69	5	315,81	53	221,33	85	0,39
8337	18,6692	-21,6523	7,1	340	43,25	10,93	18	2	219,48	5	6,64	6	-1,09
880	18,6692	-21,0144	7,8	650	64,07	25,01	34	5	332,88	24	21,69	16	0,78
1718da1004	18,6700	-17,6800	8,0	215	42,05	13,11	9	3	207,29	1	2,21	2	1,89
1718da4	18,6700	-17,6800	7,0	340	43,25	16,27	5	3	225,58	0	0,00	5	-0,61
1718da4	18,6700	-17,6800	7,3	485	49,65	25,74	7	18	323,13	0	0,00	5	-0,70
9134	18,6712	-21,8604	7,0	540	68,07	13,11	21	4	307,28	5	2,21	7	1,09
9839	18,6721	-21,2721	7,2	500	55,26	14,08	27	12	295,08	9	0,00	18	-1,22
104170	18,6731	-19,0586	7,6	800	43,25	52,21	53	13	510,91	7	13,28	24	-1,72
9129	18,6740	-21,9144	8,0	340	29,23	9,96	25	2	182,90	6	3,98	9	-0,35
8302	18,6740	-21,7703	7,3	370	47,25	9,96	21	2	235,33	5	6,64	6	-1,14
9827	18,6740	-21,2144	7,2	660	54,06	18,94	69	9	385,32	23	12,39	19	-0,28
104134	18,6750	-18,7955	7,6	730	53,26	20,88	84	5	429,21	6	24,35	14	1,31
8192	18,6760	-21,3054	7,7	430	46,85	9,96	25	3	231,68	12	12,39	5	-0,76

Appendix D: Hydrochemical data

Name	Long	Mlat	pH	ec µS/cm	Ca ²⁺ mg/l	Mg ²⁺ mg/l	Na ⁺ mg/l	K ⁺ mg/l	HCO ₃ ⁻ mg/l	SO ₄ ²⁻ mg/l	NO ₃ ⁻ mg/l	Cl ⁻ mg/l	Balance %
9867	18,6760	-21,4829	8,0	1630	156,17	52,94	87	32	301,18	35	309,87	192	2,05
9133	18,6769	-21,8622	7,2	600	76,08	15,06	23	4	312,15	4	7,97	21	1,81
104166	18,6769	-18,9919	7,5	650	56,06	34,00	27	7	429,21	7	0,00		-1,64
104133	18,6769	-18,8396	8,1	680	39,24	27,93	58	31	448,72	6	7,08		-0,14
9826	18,6769	-21,1802	7,1	720	75,28	27,93	41	5	385,32	53	12,39	8	0,77
C360	18,6769	-18,7550	7,5	1170	55,26	30,84	182	11	438,97	197	0,00	49	3,12
8194	18,6779	-21,3207	7,4	340	40,04	9,96	13	3	185,34	5	10,18	4	0,60
8303	18,6779	-21,7802	7,5	410	53,26	9,96	23	2	256,06	5	8,85	5	-0,61
104171	18,6779	-19,0153	7,4	740	53,26	46,38	39	15	510,91	8	4,87	6	-1,34
1718dc1010	18,6780	-17,9000	8,8	3010	24,03	33,03	560	10	356,05	465	11,51	520	-3,12
104138	18,6788	-18,9162	7,6	1440	62,07	52,94	169	27	621,87	22	204,95	41	1,25
1718da6	18,6795	-17,6968	8,2	390	60,07	18,21	13	4	304,84	4	0,00	5	-0,54
9866	18,6798	-21,4874	7,4	420	49,25	8,99	29	5	238,99	10	10,62	16	-1,73
9041	18,6798	-21,9532	7,4	500	62,07	11,90	27	3	295,08	5	12,39	12	-1,40
104137	18,6798	-18,8946	7,5	580	64,07	34,00	2	12	391,41	5	0,00		-1,01
9873	18,6798	-21,4315	8,1	1620	122,13	45,90	176	11	652,35	73	157,15	92	1,33
9874	18,6808	-21,4351	7,6	490	39,24	11,90	36	4	175,59	22	15,05	41	-1,38
9828	18,6808	-21,2423	7,6	730	48,05	19,91	83	4	312,15	50	24,35	55	-2,22
8193	18,6817	-21,3081	7,6	520	57,26	13,11	28	4	232,90	17	34,09	21	-0,53
7915	18,6817	-21,5468	7,4	590	44,05	19,91	50	4	274,35	30	5,31	27	1,21
104237	18,6817	-19,2396	8,1	700	74,48	46,14	0	3	390,19	22	0,00	48	-3,90
9128	18,6827	-21,8829	7,6	470	40,04	8,99	37	4	185,34	38	0,00	27	-1,56
C359	18,6827	-18,6189	7,8	740	24,83	41,53	90	12	462,13	16	0,00	20	2,34
9886	18,6837	-21,5414	7,2	480	50,05	11,90	34	2	252,41	14	11,07	22	-2,15
9823	18,6846	-21,2018	7,2	540	59,26	16,03	36	3	308,50	12	13,28	16	-0,44
104240	18,6846	-19,2063	8,0	1400	74,08	125,06	66	6	504,81	57	0,00	200	5,95
7916	18,6856	-21,5468	7,6	500	34,04	14,08	52	3	268,26	10	4,87	12	1,71
9875	18,6856	-21,4360	7,4	620	65,27	16,03	36	3	252,41	22	35,41	35	0,53
9850	18,6865	-21,4018	7,2	540	64,07	13,11	36	3	336,54	10	13,28	5	-1,33
8191	18,6865	-21,3018	7,9	600	68,07	18,94	32	3	292,64	22	28,33	18	1,63
9859	18,6875	-21,3459	7,4	350	51,26	13,11	17	2	217,04	6	20,81	16	-0,47
104569	18,6875	-19,1306	7,5	1930	76,08	73,10	265	14	642,60	150	11,51	270	0,56
8336	18,6885	-21,6658	7,6	360	49,25	9,96	17	3	237,77	5	4,43	4	-1,11
104168	18,6904	-18,9441	8,2	870	17,22	15,78	138	54	510,91	24	3,54	26	-0,63
104136	18,6904	-18,8748	8,1	880	6,01	5,10	198	24	571,88	16	0,00		1,22
9818	18,6904	-21,2532	7,1	2720	183,40	91,07	265	3	407,26	120	664,00	300	-0,17
104557	18,6913	-19,2811	7,6	830	70,08	68,97	23	1	525,54	9	0,00	14	5,17
103827	18,6913	-19,3982	7,3	2600	131,34	110,01	255	1	569,44	47	314,29	360	2,28
W-12	18,6920	-19,2446	7,8	697	66,00	44,84	14	1	430,66	8	6,12	14	-0,55
104167	18,6923	-18,9604	7,5	700	50,05	39,58	28	21	463,35	5	0,00		-1,24
9819	18,6933	-21,2559	7,2	850	80,09	22,10	67	3	308,50	22	75,25	70	0,59
9840	18,6942	-21,2829	7,3	700	70,08	18,94	55	6	351,17	38	15,49	33	-0,82
104567	18,6952	-19,1162	8,1	1610	44,05	82,08	210	12	613,33	155	0,00	162	1,50
103828	18,6962	-19,4063	7,1	920	100,11	62,90	6		609,68	4	0,00	8	0,63
9042	18,6971	-21,9261	7,5	440	48,05	11,90	27	4	252,41	5	18,59	11	-2,07
9825	18,6971	-21,1730	7	740	74,08	25,01	55	5	392,63	27	14,61	40	-0,51
103829	18,6971	-19,4405	7,0	920	80,09	63,87	27	3	588,95	10	7,97	10	1,12
104566	18,6971	-19,0892	7,9	990	38,04	51,00	115	12	606,02	28	0,00	46	-1,76
8307	18,6971	-21,7838	7,9	3720	302,33	63,14	222	420	1768,06		0,00	430	-0,52
C263	18,6981	-17,6946	7,3	490	49,65	25,74	7	18	323,13	0	0,00	5	-0,70
7917	18,6990	-21,5793	7,5	520	68,07	11,90	17	4	219,48	6	34,53	25	2,29
9849	18,6990	-21,3811	7,3	800	80,09	17,00	73	13	420,68	41	11,95	35	-0,14
103830	18,6990	-19,4523	7,4	1050	53,26	31,08	140	6	408,48	60	24,79	94	2,07

Appendix D: Hydrochemical data

Name	Long	Mlat	pH	ec µS/cm	Ca ²⁺ mg/l	Mg ²⁺ mg/l	Na ⁺ mg/l	K ⁺ mg/l	HCO ₃ ⁻ mg/l	SO ₄ ²⁻ mg/l	NO ₃ ⁻ mg/l	Cl ⁻ mg/l	Balance %
104238	18,7000	-19,2432	8,1	700	52,06	56,58	33	4	385,32	38	0,00	54	0,93
104139	18,7019	-18,8910	7,5	1060	67,27	17,97	122	6	435,31	15	59,32	54	1,83
8306	18,7029	-21,8135	7,5	530	75,28	15,06	18	5	337,76	6	8,85	11	-1,72
104552	18,7029	-19,3631	7,4	820	78,08	58,04	10	1	521,88	9	0,00	14	-0,01
1718dc3	18,7031	-17,8048	7,4	285	39,64	16,03	4	5	164,61	0	35,41	10	0,67
C275	18,7038	-17,9315	7,6	430	54,06	27,93	18	7	310,93	0	26,56	15	0,09
7918	18,7038	-21,5306	7,3	640	56,06	18,94	45	4	268,26	16	5,75	53	0,77
104135	18,7038	-18,8207	7,3	1530	173,39	42,98	70	10	419,46	5	301,01	141	-1,02
9841	18,7048	-21,2892	7,1	220	34,04	6,07	2	1	132,91	6	0,00	1	-0,45
9862	18,7067	-21,4477	8,1	340	30,03	11,90	28	3	189,00	15	7,97	8	0,11
9824	18,7067	-21,2045	7,6	910	76,08	24,04	88	8	392,63	57	38,95	62	-0,96
104241	18,7067	-19,2126	8,1	3000	71,68	240,41	310	26	957,19	163	0,00	523	5,15
9036	18,7077	-21,9865	7,0	440	52,06	13,11	20	5	267,04	5	7,97	8	-1,68
9842	18,7077	-21,2703	7,3	640	53,26	15,06	70	3	351,17	24	11,07	26	-1,05
9852	18,7077	-21,4216	7,0	870	94,10	16,03	78	4	407,26	34	26,56	68	-1,14
9865	18,7087	-21,5153	9,0	230	17,22	9,96	20	2	126,81	4	0,00	14	0,84
9135	18,7087	-21,8757	7,2	380	48,05	8,01	17	2	204,85	8	7,53	6	0,44
9863	18,7096	-21,4604	7,3	520	65,27	13,11	30	5	315,81	10	3,98	16	-1,12
104559	18,7106	-19,2694	7,3	1040	108,12	56,10	35	3	479,21	18	0,00	78	5,36
9848	18,7115	-21,3649	7,1	260	32,03	8,01	14	2	160,95	5	3,54	2	1,09
8305	18,7125	-21,7360	7,8	570	78,08	10,93	28	3	281,67	7	48,69	19	0,06
8304	18,7125	-21,7568	7,6	880	81,29	17,00	39	90	476,77	35	0,00	35	-0,40
8195	18,7135	-21,3009	7,8	530	59,26	15,06	25	4	226,80	10	22,13	36	0,83
9037	18,7135	-21,9667	7,9	730	26,03	13,11	110	5	231,68	60	37,63	52	1,19
9820	18,7173	-21,2342	7,2	670	58,06	25,98	49	5	336,54	42	19,03	23	-0,35
104140	18,7173	-18,9162	7,6	820	63,27	24,04	77	9	442,62	10	0,00	29	2,56
9845	18,7192	-21,3405	7,4	420	56,06	10,93	16	2	231,68	8	11,95	15	-1,50
9854	18,7192	-21,4000	8,0	820	95,30	39,10	32	6	441,41	20	35,41	44	0,29
7920	18,7212	-21,5288	7,7	590	34,04	9,96	78	3	268,26	20	11,07	28	1,75
9822	18,7212	-21,2036	7,2	590	68,07	17,97	33	3	323,13	11	19,92	26	-1,48
104172	18,7212	-19,0198	7,6	680	80,09	38,61	8	5	374,34	4	15,05	50	-1,43
8197	18,7212	-21,2883	7,4	1350	154,17	39,10	35	7	280,45	15	254,53	120	0,85
C265	18,7221	-17,7315	8,2	390	60,07	18,21	13	4	304,84	4	0,00	5	-0,54
104174	18,7221	-19,0658	8,0	1000	34,04	26,96	164	12	565,78	53	4,43	40	-0,95
7921	18,7231	-21,5324	7,9	630	40,04	11,90	86	3	292,64	28	10,18	32	2,64
9855	18,7231	-21,4063	7,3	1090	100,11	30,11	62	65	547,49	40	7,53	74	-0,76
104143	18,7240	-18,8802	7,4	640	76,08	20,64	27	4	387,75	4	4,43	18	-1,78
9038	18,7240	-21,9649	7,8	710	26,03	8,99	109	5	231,68	60	35,41	48	-0,46
104558	18,7240	-19,2802	7,3	1020	110,12	69,94	17	1	682,84	5	0,00	33	-0,87
9040	18,7250	-21,9378	7,2	490	60,07	14,08	20	4	273,13	5	15,49	16	-1,47
8323	18,7260	-21,6342	7,7	330	39,24	11,90	15	3	195,10	5	8,85	8	-0,04
W-13	18,7260	-19,2454	8,0	935	123,80	40,10	24	18	470,92	9	95,70	32	2,99
9864	18,7279	-21,4874	8,4	330	33,24	11,90	21	3	175,59	6	0,00	22	0,07
9853	18,7279	-21,4000	7,4	740	85,29	34,00	35	4	385,32	53	30,10	35	-1,21
769	18,7288	-19,5171	7,1	1220	74,08	45,90	119	16	685,28	18	11,51	64	-2,02
104244	18,7298	-19,1829	8,0	2700	140,95	163,67	221	26	467,01	63	462,14	484	1,17
8308	18,7308	-21,7342	7,3	470	55,26	15,06	25	2	297,52	8	2,21	8	-1,62
9821	18,7308	-21,1847	7	540	59,26	16,03	38	2	315,81	13	11,51	10	0,56
9856	18,7308	-21,4027	7,3	850	98,11	36,91	33	5	399,95	28	72,15	42	0,06
8322	18,7317	-21,6811	7,3	400	47,25	14,08	24	2	260,94	5	4,43	8	-0,71
8201	18,7317	-21,2631	8,3	470	50,05	14,08	25	6	257,28	7	13,28	8	0,99
104130	18,7317	-18,8000	7,7	710	64,07	28,90	45	7	448,72	6	0,00	14	-1,04
8324	18,7317	-21,6315	7,6	720	90,10	17,97	40	9	312,15	30	66,40	26	2,58

Appendix D: Hydrochemical data

Name	Long	Mlat	pH	ec µS/cm	Ca ²⁺ mg/l	Mg ²⁺ mg/l	Na ⁺ mg/l	K ⁺ mg/l	HCO ₃ ⁻ mg/l	SO ₄ ²⁻ mg/l	NO ₃ ⁻ mg/l	Cl ⁻ mg/l	Balance %
882	18,7327	-20,9892	7,8	440	58,06	9,96	19	3	242,65	5	11,95	10	0,70
1818bd1	18,7333	-18,0550	7,6	660	33,24	31,33	75	9	451,16	0	4,43	6	0,61
1818ba1001	18,7333	-18,0550	7,6	800	62,87	33,03	67	10	536,51	1	17,71	3	-0,87
8196	18,7346	-21,3045	7,5	410	50,05	10,93	16	3	226,80	5	15,94	5	-0,59
8309	18,7356	-21,7495	7,3	460	60,07	11,90	20	3	281,67	5	13,28	7	-2,08
9837	18,7356	-21,2396	7,4	540	45,25	16,03	52	3	323,13	15	11,07	10	-1,28
104245	18,7356	-19,1838	7,9	1000	37,24	91,79	69	14	525,54	12	54,01	95	1,42
7914	18,7365	-21,5811	7,5	360	48,05	8,01	16	3	201,19	5	5,31	6	2,32
9039	18,7365	-21,9495	7,2	410	41,24	13,11	22	4	224,36	5	14,61	10	-1,20
8361	18,7375	-21,4270	7,8	470	73,28	17,97	7	4	317,03	5	11,07	4	-0,44
9847	18,7375	-21,3766	7,3	480	59,26	9,96	30	5	287,77	13	9,74	10	-2,03
8310	18,7375	-21,7505	7,2	660	79,29	17,00	25	5	312,15	10	39,84	26	-0,97
104233	18,7375	-19,2486	8,1	1190	108,92	51,48	29	55	378,00	22	228,41	76	-0,57
1818dc1002	18,7383	-18,7513	7,6	660	48,05	42,01	27	24	441,41	3	4,43	4	1,07
1818da1016	18,7383	-18,6667	7,2	700	68,87	41,04	20	11	458,48	3	2,21	10	0,45
104242	18,7385	-19,1477	7,9	680	42,45	64,35	27	10	390,19	49	7,53	43	0,54
104553	18,7394	-19,3532	8,0	900	80,09	59,25	25	2	542,61	19	0,00	27	-0,19
7911	18,7404	-21,5523	7,0	720	86,09	17,00	21	13	390,19	8	0,00	22	-1,71
1718dc4	18,7420	-17,8245	7,5	355	39,64	14,81	14	6	219,48	3	0,00	13	-0,83
879	18,7423	-21,0586	7,3	440	31,23	20,88	25	5	207,29	5	25,67	16	1,42
9165	18,7433	-21,7946	7,5	450	50,05	8,01	28	5	248,75	7	3,10	8	0,06
8200	18,7442	-21,2523	7,8	720	55,26	17,97	74	8	412,14	14	14,17	11	0,49
104165	18,7442	-18,9658	8,2	1370	41,24	32,06	219	14	560,90	40	152,72	78	-0,37
9169	18,7452	-21,8640	6,8	300	35,24	7,04	14	2	156,08	7	4,87	5	1,26
8359	18,7452	-21,4550	7,4	530	62,07	20,88	21	8	341,42	5	8,85	10	-1,58
9170	18,7452	-21,8360	7,2	540	71,28	10,93	21	4	292,64	5	3,10	19	-0,13
C270	18,7462	-17,8270	7,4	290	39,64	16,03	4	5	164,61	0	35,41	10	0,67
104129	18,7462	-18,8342	7,9	570	42,05	25,01	41	11	375,56	6	0,00		-0,47
774	18,7462	-19,6910	7,6	930	76,08	25,98	78	10	367,02	61	95,17	32	-0,72
7910	18,7462	-21,5486	7,3	930	116,13	23,07	21	4	217,04	8	177,07	86	-1,67
1818da1015	18,7467	-18,5967	7,5	630	62,87	34,00	19	7	385,32	1	2,21	20	0,04
8198	18,7471	-21,2694	7,6	480	70,08	10,93	19	3	280,45	5	35,41	8	-1,83
9011	18,7471	-21,9766	7,3	490	60,07	13,11	26	4	273,13	8	16,38	17	-0,72
773	18,7471	-19,6991	7,5	680	50,05	27,93	47	17	380,44	10	20,36	15	0,56
1718da9	18,7478	-17,7250	8,0	260	31,23	8,99	7	2	160,95	0	0,00	1	-0,23
1718da9	18,7478	-17,7250	7,5	270	36,04	12,14	5	1	164,61	9	0,00	3	1,18
9095	18,7490	-21,9144	6,9	440	55,26	11,90	21	6	196,32	6	27,89	30	1,75
104173	18,7490	-19,1036	7,8	760	3,20	2,91	187	5	531,64	4	0,00		-0,77
104144	18,7490	-18,8919	7,4	1000	122,13	34,97	29	5	421,90	4	123,95	65	-2,21
104141	18,7490	-18,9189	7,4	1180	100,11	27,93	81	5	514,57	4	33,64	67	-0,02
9835	18,7500	-21,2036	8,2	520	30,03	23,07	48	4	259,72	42	7,08	18	-1,46
8341	18,7510	-21,6378	8,0	390	47,25	9,96	25	3	243,87	8	8,85	5	-1,20
9836	18,7510	-21,2324	8,0	910	56,06	28,90	104	5	295,08	56	81,89	100	-1,58
7919	18,7519	-21,5162	7,6	550	54,06	13,11	38	3	201,19	10	10,18	56	2,39
9166	18,7529	-21,8198	8,1	290	23,23	9,96	19	4	151,20	10	3,10	6	0,03
9834	18,7548	-21,1955	7,0	470	35,24	13,11	49	5	245,09	25	0,00	13	1,93
9010	18,7548	-21,9730	7,2	480	63,27	10,93	21	4	267,04	5	19,03	16	-1,62
C358	18,7548	-18,6099	7,8	510	18,02	58,04	16	6	334,10	10	0,00	26	0,83
8360	18,7548	-21,4369	8,0	530	55,26	6,07	61	3	323,13	10	4,43	16	-0,33
8362	18,7558	-21,4117	6,9	320	26,03	11,90	24	2	182,90	5	4,43	10	-1,20
9846	18,7558	-21,3928	7,3	940	67,27	15,06	122	8	407,26	88	8,85	58	-0,87
9833	18,7558	-21,2252	7,4	1200	107,32	43,95	78	6	315,81	50	190,35	103	1,32
8321	18,7567	-21,6604	7,6	370	49,25	11,90	12	3	214,61	6	15,49	10	-1,68

Appendix D: Hydrochemical data

Name	Long	Mlat	pH	ec µS/cm	Ca ²⁺ mg/l	Mg ²⁺ mg/l	Na ⁺ mg/l	K ⁺ mg/l	HCO ₃ ⁻ mg/l	SO ₄ ²⁻ mg/l	NO ₃ ⁻ mg/l	Cl ⁻ mg/l	Balance %
8320	18,7567	-21,6640	7,6	380	51,26	11,90	13	3	230,46	5	11,07	7	-0,92
C357	18,7567	-18,6793	8,0	620	30,43	40,31	60	12	437,75	4	0,00	12	1,02
104231	18,7567	-19,3009	8,1	4400	239,86	193,06	454	30	382,88	293	838,41	744	1,56
104230	18,7567	-19,2973	8,4	6500	192,61	222,20	997	18	738,93	752	431,60	1316	-0,09
1718dd1003	18,7570	-17,8750	8,3	3200	28,83	26,96	640	11	743,80	325	6,64	500	-2,14
9009	18,7577	-21,9514	7,3	490	56,06	14,08	25	6	259,72	7	8,85	26	-0,77
C356	18,7587	-18,7649	7,6	620	21,62	60,95	24	26	465,79	4	0,00	5	-0,35
8343	18,7587	-21,6225	7,2	870	120,93	26,96	23	7	380,44	7	79,68	58	0,70
8344	18,7587	-21,6198	7,7	1530	179,40	48,08	56	11	390,19	22	199,20	198	-0,08
104223	18,7596	-19,2523	8,1	4200	54,46	42,98	937	26	473,11	598	25,67	936	0,69
8199	18,7606	-21,2577	7,5	350	44,05	8,99	20	3	209,73	10	4,43	3	1,08
9844	18,7606	-21,3189	7,2	360	46,05	11,90	18	3	224,36	9	0,00	6	1,26
9164	18,7606	-21,8009	6,9	820	103,31	16,03	30	4	297,52	14	88,53	42	0,65
104232	18,7606	-19,3486	8,2	4000	155,77	162,95	592	15	535,30	294	439,57	825	2,23
9093	18,7615	-21,9333	7,2	380	46,05	9,96	22	5	224,36	7	11,51	9	-0,71
104177	18,7615	-19,0396	7,5	630	46,05	35,94	26	22	408,48	3	15,49	6	-1,61
9167	18,7625	-21,8342	7,1	420	59,26	7,04	14	4	248,75	4	5,75	4	-1,36
7912	18,7625	-21,5351	7,4	680	64,07	15,06	48	5	278,01	25	12,39	39	2,11
9094	18,7644	-21,9054	7,2	380	45,25	8,99	22	5	217,04	7	15,49	9	-1,50
8353	18,7654	-21,4946	7,4	530	68,07	16,03	27	3	329,22	7	8,85	16	-1,39
104131	18,7654	-18,9757	7,7	1300	51,26	31,08	194	18	691,37	15	11,07	61	1,71
9016	18,7663	-21,8847	7,4	450	58,06	13,11	17	6	273,13	8	11,07	6	-1,23
104128	18,7673	-18,8207	8,0	920	75,28	44,93	39	7	373,12	5	97,39	45	1,47
1718db1001	18,7680	-17,7460	7,3	490	48,85	30,11	6	2	290,21	1	28,77	1	-0,39
104243	18,7683	-19,1793	7,9	2300	61,67	73,34	376	21	608,46	171	23,90	406	1,24
9017	18,7692	-21,9027	7,1	420	50,05	11,90	18	6	245,09	10	12,39	6	-2,01
104176	18,7692	-19,0829	8,0	760	3,20	2,91	189	8	517,00	9	21,69		-1,04
104142	18,7702	-18,8820	7,5	480	70,08	17,00	3	3	312,15	4	0,00		-0,93
9168	18,7712	-21,8514	6,8	320	33,24	8,01	16	3	160,95	6	8,85	5	0,72
8358	18,7712	-21,4532	7,4	490	64,07	14,08	25	4	317,03	7	6,64	10	-1,64
887	18,7731	-20,8063	7,6	550	74,08	15,06	25	4	325,57	10	3,54	9	2,26
9843	18,7740	-21,3477	7,1	330	46,05	8,99	15	2	203,63	5	5,75	4	1,27
7913	18,7740	-21,5820	7,3	400	49,25	8,99	19	3	201,19	14	5,75	8	2,41
104175	18,7750	-19,0658	7,6	570	84,09	25,01	4	4	360,93	5	8,41	8	1,16
9018	18,7750	-21,9009	7,2	590	80,09	15,06	22	6	336,54	10	22,13	16	-1,44
8354	18,7760	-21,4658	7,3	510	66,07	18,94	27	4	347,52	4	6,64	4	1,10
8342	18,7769	-21,6333	7,2	300	37,24	9,96	10	3	134,13	5	35,41	15	-1,65
8363	18,7769	-21,4162	8,2	470	58,06	13,11	28	3	274,35	8	6,64	20	-0,59
104229	18,7769	-19,3243	8,1	950	74,08	77,22	50	7	577,97	13	0,00	88	0,73
104561	18,7769	-19,1315	7,5	1300	62,07	32,06	195	5	557,24	105	23,90	107	-1,30
9830	18,7769	-21,2243	7,2	1410	160,17	53,91	54	7	343,86	50	234,61	140	1,87
104162	18,7779	-18,9568	7,2	810	103,31	25,98	1	8	381,66	4	4,43	50	-1,81
9832	18,7788	-21,2207	7,2	890	88,10	33,03	51	10	351,17	41	60,65	65	0,88
C276	18,7798	-17,8505	7,5	360	39,64	14,81	14	6	219,48	3	0,00	13	-0,83
9119	18,7798	-21,9216	7,2	410	52,06	10,93	15	6	245,09	7	11,07	5	-2,04
9015	18,7798	-21,8775	7,1	440	58,06	10,93	20	4	273,13	7	10,18	5	-1,63
9829	18,7817	-21,2342	7,3	440	51,26	13,11	19	3	245,09	6	15,49	12	-2,05
104234	18,7817	-19,2396	8,0	650	62,07	57,80	17	7	460,91	0	0,00	32	1,83
8355	18,7827	-21,4964	7,5	410	52,06	11,90	22	2	249,97	5	6,64	10	-0,05
8352	18,7827	-21,5144	7,6	460	55,26	10,93	30	3	262,16	8	0,00	20	0,11
9571	18,7827	-21,3820	7,5	890	97,31	22,10	85	5	384,10	75	6,64	71	2,61
W-11	18,7830	-21,1942	7,9	553	58,12	24,68	23	4	325,74	3	7,72	3	3,30
8349	18,7837	-21,5396	7,6	1150	92,10	20,88	137	4	438,97	51	44,27	124	-0,37

Name	Long	Lat	pH	ec μS/cm	Ca ²⁺ mg/l	Mg ²⁺ mg/l	Na ⁺ mg/l	K ⁺ mg/l	HCO ₃ ⁻ mg/l	SO ₄ ²⁻ mg/l	NO ₃ ⁻ mg/l	Cl ⁻ mg/l	Balance %
8727	18,7846	-21,9486	7.6	490	65,27	17,97	13	3	302,40	4	10,62	7	-0,28
9020	18,7846	-21,8955	7,3	520	69,28	19,91	12	7	329,22	5	12,39	6	-0,62
9831	18,7846	-21,2126	7,4	540	52,06	23,07	30	4	315,81	17	14,17	10	-1,15
8351	18,7846	-21,5324	8.5	600	53,26	13,11	56	4	237,77	30	22,13	54	-1,00
1718dd1002	18,7850	-17,8470	8,8	830	12,81	8,01	176	4	426,77	34	2,21	41	0,90
8730	18,7856	-21,9694	7.7	460	60,07	11,90	19	4	274,35	3	7,53	9	-0,29
8357	18,7856	-21,4441	7,7	580	68,07	11,90	42	3	329,22	10	6,64	30	-2,16
8728	18,7856	-21,9757	7.4	1040	117,33	18,94	67	5	431,65	3	4,43	133	-2,35
8729	18,7875	-21,9712	7.5	450	59,26	13,11	18	4	269,48	3	7,53	9	0,69
8350	18,7875	-21,5387	7.9	830	73,28	17,00	91	3	371,90	30	19,92	66	1,05
1718dd2	18,7892	-17,7691	8,0	320	30,03	12,14	15	2	139,01	7	2,21	26	0,13
9572	18,7894	-21,3486	7.1	280	27,23	7,04	24	3	167,05	6	4,87	7	-1,29
W-25	18,7897	-19,0424	7,9	602	67,92	26,00	25	7	384,30	3	1,60	5	1,86
9014	18,7904	-21,8685	7,2	430	58,06	11,90	20	4	259,72	8	8,85	6	1,19
8356	18,7923	-21,5216	7.7	370	41,24	8,99	26	3	219,48	10	0,00	12	-1,70
9021	18,7923	-21,9153	7,3	470	58,06	13,11	23	5	280,45	12	12,39	7	-1,34
104163	18,7923	-18,9306	7,8	710	86,09	16,03	48	5	438,97	20	6,64	14	-1,77
8376	18,7952	-21,4541	7.6	390	54,06	9,96	16	3	249,97	5	4,43	4	-1,10
8315	18,7952	-21,7063	7,8	840	45,25	19,91	121	4	445,06	49	8,85	35	-0,97
9582	18,7962	-21,2739	7.5	390	56,06	9,96	15	3	243,87	5	5,75	6	-0,19
104227	18,7962	-19,3514	8,1	1300	58,46	69,45	157	12	484,08	116	72,15	142	0,80
8371	18,7971	-21,3883	7.6	290	39,24	8,99	9	3	176,81	4	4,43	6	-0,87
9159	18,7971	-21,8135	7,1	440	59,26	11,90	10	3	224,36	8	15,94	8	1,39
104562	18,7971	-19,1441	7,4	1190	58,06	39,10	154	11	548,71	45	10,62	120	-1,47
104564	18,7971	-19,2054	7,5	1520	74,08	57,07	168	20	506,03	78	43,82	190	0,71
9217	18,7981	-21,5658	7,5	470	51,26	11,90	37	2	268,26	14	8,85	9	1,10
104180	18,7981	-19,0000	7,5	590	72,08	15,06	40	4	402,39	6	3,54		-0,73
886	18,7990	-20,9117	8,2	510	62,07	13,11	34	4	304,84	10	5,31	15	0,39
9573	18,8010	-21,3144	7.7	350	50,05	5,10	21	2	212,17	9	5,75	6	-0,57
104179	18,8010	-19,0189	7,8	1000	6,01	8,01	235	17	687,71	13	0,00		0,32
104563	18,8010	-19,1802	7,5	1210	45,25	38,61	154	20	514,57	39	10,62	132	-1,92
104226	18,8010	-19,3477	8,2	3000	155,77	121,18	311	13	360,93	540	459,49	238	0,51
8364	18,8029	-21,4180	7,1	380	38,04	9,96	28	3	207,29	6	4,43	16	-0,40
9160	18,8038	-21,8405	7,1	410	48,05	8,99	17	3	204,85	18	10,18	7	-1,74
878	18,8038	-21,1793	7,5	740	71,28	31,08	40	6	401,17	10	11,95	28	1,54
104560	18,8038	-19,1072	7,6	930	46,05	48,08	105	11	629,19	6	10,62	18	-0,06
770	18,8038	-19,5252	8,0	1290	34,04	23,07	227	29	754,78	20	12,39	40	0,35
1818db1001	18,8050	-18,5167	7,3	570	70,88	30,11	4	6	356,05	1	4,43	10	1,06
104147	18,8058	-18,9144	8,1	670	56,06	27,93	48	10	456,04	6	0,00		-1,06
1818db1008	18,8067	-18,6700	7,4	640	54,86	33,03	36	11	419,46	3	4,43	6	0,86
104228	18,8067	-19,3369	8,1	970	24,83	31,33	168	10	442,62	82	12,84	70	1,05
104222	18,8077	-19,2495	7,8	900	54,46	46,14	100	18	457,26	42	20,36	87	0,77
1818db1009	18,8083	-18,7483	7,2	1090	60,07	34,00	148	11	599,92	25	8,85	60	1,32
9581	18,8087	-21,2514	7.3	350	40,04	9,96	23	3	207,29	6	3,98	12	-0,39
104216	18,8087	-19,3243	8,1	2390	6,01	5,10	425	140	660,89	135	36,30	310	-0,40
8375	18,8096	-21,4784	7.7	350	24,03	8,99	40	3	189,00	5	0,00	22	-0,89
104161	18,8115	-18,9577	7,7	650	76,08	22,10	25	5	395,07	5	13,72	8	-1,41
9156	18,8125	-21,7982	7,1	720	85,29	16,03	26	4	280,45	8	61,09	40	-0,50
104218	18,8125	-19,3000	8,3	2400	12,01	13,84	425	162	560,90	133	49,58	411	0,03
9158	18,8135	-21,8036	6,8	520	64,07	13,11	16	4	258,50	8	10,18	14	1,12
8311	18,8144	-21,7604	8,0	980	115,33	30,11	31	5	302,40	12	154,93	76	-0,71
9583	18,8154	-21,2856	7.2	210	28,03	5,10	10	2	123,15	6	2,21	6	-0,94
9222	18,8154	-21,6126	7,5	460	59,26	9,96	15	3	243,87	2	5,75	6	2,33

Appendix D: Hydrochemical data

Name	Long	Mlat	pH	ec µS/cm	Ca ²⁺ mg/l	Mg ²⁺ mg/l	Na ⁺ mg/l	K ⁺ mg/l	HCO ₃ ⁻ mg/l	SO ₄ ²⁻ mg/l	NO ₃ ⁻ mg/l	Cl ⁻ mg/l	Balance %
8312	18,8154	-21,7658	7,5	630	70,08	22,10	23	4	309,72	11	53,12	17	-1,71
8373	18,8163	-21,4946	7,3	1150	118,13	36,91	51	2	207,29	15	99,60	198	1,36
8317	18,8163	-21,6532	7,4	1330	141,35	40,07	79	10	563,34	22	77,47	130	-1,97
9157	18,8173	-21,7991	7,1	540	64,07	11,90	18	4	278,01	9	18,15	8	-1,94
104127	18,8183	-18,8225	8,2	780	55,26	31,08	74	9	454,82	5	9,74	33	0,68
104146	18,8192	-18,8586	7,4	600	66,07	31,08	14	4	395,07	5	0,00	7	-1,57
104145	18,8192	-18,8937	7,8	740	62,07	33,03	46	11	459,70	6	18,59	10	-0,88
8377	18,8212	-21,4387	7,3	460	62,07	13,11	17	4	286,55	7	4,43	8	-1,19
9024	18,8221	-21,9135	7,3	500	60,07	15,06	24	4	267,04	10	17,71	18	0,04
9216	18,8221	-21,5748	7,5	580	87,29	14,08	20	5	359,71	6	6,64	6	1,69
883	18,8221	-21,0234	7,8	2710	179,40	69,94	291	10	304,84	480	38,95	460	-1,73
8374	18,8240	-21,4865	6,9	220	22,02	6,07	14	2	115,84	6	4,43	8	-1,35
9025	18,8240	-21,8973	7,4	520	71,28	16,03	17	6	321,91	15	11,07	6	-1,43
C354	18,8240	-18,6820	7,5	580	20,42	66,78	14	13	420,68	4	0,00	5	2,31
9584	18,8240	-21,2946	7,6	820	39,24	11,90	17	2	187,78	7	4,87	9	2,37
8313	18,8250	-21,7658	7,4	780	86,09	25,98	22	12	312,15	7	66,40	58	-1,72
C355	18,8260	-18,7622	7,8	990	20,42	50,75	155	15	616,99	29	7,08	35	2,09
9580	18,8269	-21,2613	7,9	600	74,08	17,00	27	3	231,68	8	30,10	67	0,06
9023	18,8279	-21,9523	7,7	580	74,08	13,11	20	6	280,45	10	38,95	18	-1,20
9218	18,8279	-21,5477	7,4	690	51,26	16,03	84	3	359,71	42	9,30	17	1,39
877	18,8298	-21,1703	7,5	770	69,28	36,91	30	6	374,34	7	19,92	44	0,69
8318	18,8308	-21,6721	7,5	500	63,27	24,04	16	4	337,76	5	6,64	9	-0,56
9577	18,8317	-21,2405	8,1	310	38,04	8,01	20	3	204,85	4	0,00	6	-1,48
8370	18,8317	-21,4153	7,4	690	66,07	17,00	61	4	298,74	14	13,28	66	1,28
9022	18,8327	-21,8766	7,1	480	60,07	15,06	18	5	280,45	10	12,39	10	-1,33
9579	18,8337	-21,3495	7,7	330	28,03	9,96	38	3	176,81	32	4,87	15	-1,47
9162	18,8337	-21,8270	7,2	400	47,25	8,01	18	3	209,73	9	8,85	6	-0,76
9578	18,8346	-21,3459	7,5	350	30,03	6,07	36	3	187,78	9	7,53	14	-1,89
104181	18,8346	-19,0505	7,5	960	40,04	15,06	162	9	571,88	36	5,31	16	-0,68
9215	18,8356	-21,5919	7,2	460	25,23	18,94	46	8	249,97	18	0,00	11	2,46
104221	18,8365	-19,2910	7,9	940	74,48	36,43	100	11	437,75	63	0,00	97	0,55
8316	18,8375	-21,7207	7,9	510	60,07	13,11	40	2	312,15	12	17,71	12	-1,03
9027	18,8404	-21,9009	7,4	640	87,29	17,00	17	6	301,18	8	48,69	26	0,20
1718dd11	18,8429	-17,9964	7,5	730	22,82	62,17	44	19	451,16	10	11,51	2	4,91
1718dd1009	18,8430	-17,9960	8,4	670	22,02	28,90	79	25	443,84	3	2,21	6	0,07
9225	18,8433	-21,6000	7,2	450	53,26	13,11	17	2	256,06	8	7,08	5	-1,00
104194	18,8433	-19,1937	7,3	1000	71,28	48,08	68	41	606,02	12	12,39	27	1,66
9026	18,8452	-21,9072	7,4	490	61,27	13,11	23	5	295,08	8	13,28	8	-1,66
104193	18,8452	-19,1676	7,5	790	70,08	30,11	33	18	395,07	6	66,40	18	-1,92
9570	18,8452	-21,3793	8,2	870	18,02	8,99	175	20	451,16	49	5,75	30	2,14
8372	18,8471	-21,5081	7,3	720	43,25	14,08	98	3	262,16	80	4,43	58	-0,08
9028	18,8481	-21,9000	7,6	900	123,33	24,04	21	6	357,27	10	79,68	68	-0,36
104212	18,8481	-19,3730	9,5	2960	1,20	0,97	635	109	1586,38	71	3,54	103	0,18
9161	18,8490	-21,8441	7,6	340	33,24	11,90	18	3	190,22	9	0,00	6	0,33
9092	18,8490	-21,9847	7	530	81,29	13,11	19	3	343,86	6	12,39	10	-1,66
9219	18,8490	-21,5505	7,5	760	78,08	20,88	43	4	402,39	17	5,31	10	1,82
1718dd1004	18,8500	-17,8020	7,3	240	34,84	6,07	6	4	136,57	1	8,85	4	1,70
9029	18,8500	-21,8901	7,3	580	62,07	16,03	37	8	343,86	10	13,28	10	-0,87
9226	18,8538	-21,5982	7,4	420	56,06	10,93	18	2	256,06	4	4,43	5	0,43
909	18,8538	-21,1649	8,1	700	46,05	24,04	65	6	415,80	9	7,53	14	-1,77
104217	18,8538	-19,2901	8,2	1800	35,24	5,59	327	106	714,54	90	32,31	181	-0,15
9171	18,8548	-21,8081	7,3	740	89,30	18,94	25	4	219,48	19	95,17	60	-0,11
9574	18,8558	-21,2856	7	370	42,05	9,96	22	3	162,17	4	6,64	39	0,04

Appendix D: Hydrochemical data

Name	Long	Mlat	pH	ec μS/cm	Ca ²⁺ mg/l	Mg ²⁺ mg/l	Na ⁺ mg/l	K ⁺ mg/l	HCO ₃ ⁻ mg/l	SO ₄ ²⁻ mg/l	NO ₃ ⁻ mg/l	Cl ⁻ mg/l	Balance %
104182	18,8558	-19,0829	7,7	720	13,21	6,07	153	11	476,77	11	3,54		-0,03
8319	18,8567	-21,6811	7,5	510	55,26	30,11	17	4	351,17	5	4,43	9	-0,88
9091	18,8577	-21,9892	8,5	230	15,22	10,93	20	4	140,23	5	0,00	12	-2,05
9035	18,8577	-21,9162	7,7	510	47,25	13,11	47	3	280,45	14	14,61	14	0,36
9564	18,8596	-21,3135	7,6	440	40,04	15,06	28	3	108,52	8	15,05	82	0,34
9223	18,8596	-21,6568	7,4	610	78,08	24,04	19	4	384,10	1	6,64	6	1,58
104197	18,8596	-19,2613	7,4	860	43,25	31,08	86	25	449,94	22	19,03	37	-0,47
9569	18,8606	-21,3883	7,9	280	37,24	2,91	21	2	164,61	6	3,54	9	-1,14
9034	18,8606	-21,9342	7,3	460	58,06	14,08	19	3	273,13	6	14,61	8	-1,03
9576	18,8606	-21,2505	7,5	810	116,13	22,10	17	4	265,82	5	148,29	61	-0,69
104150	18,8615	-18,9189	8,2	660	53,26	34,00	38	9	449,94	5	0,00		-0,94
9563	18,8635	-21,3514	7,4	360	44,05	7,04	23	3	192,66	11	4,43	18	-1,42
105159	18,8654	-18,9414	7,4	640	75,28	24,04	22	5	418,24	4	3,54		-1,27
B988/Y4215	18,8663	-19,4063	7,4	1030	67,27	40,07	88	10	537,73	32	3,54	52	-1,22
1818db1007	18,8667	-18,6767	7,5	540	56,86	32,06	8	9	353,61	3	4,43	4	0,10
9030	18,8673	-21,8712	7,4	510	65,27	13,11	24	5	295,08	11	12,39	8	0,16
104210	18,8683	-19,3495	7,5	620	49,25	27,93	45	5	408,48	7	2,66		-0,31
104211	18,8683	-19,3568	7,8	1440	9,21	8,01	340	15	799,89	58	6,20	40	2,35
9209	18,8702	-21,7099	7,9	3030	34,04	17,97	625	8	221,92	1120	2,21	145	-0,83
8369	18,8712	-21,4099	6,9	310	31,23	10,93	19	4	176,81	6	4,43	15	-1,89
9568	18,8712	-21,3793	8,2	950	79,29	22,10	120	8	477,99	54	21,25	51	2,10
9567	18,8721	-21,3766	7,9	730	43,25	17,00	103	9	352,39	44	15,49	33	2,45
B988/Y4213	18,8721	-19,3955	7,5	750	65,27	31,08	49	6	442,62	12	8,85	20	-0,68
104190	18,8731	-19,1387	7,4	570	77,28	17,97	21	3	391,41	3	0,00		-1,18
104160	18,8731	-18,9586	7,5	660	61,27	25,98	33	10	418,24	5	3,54	4	-1,72
1818db1006	18,8733	-18,6875	7,3	640	66,87	35,94	16	10	424,33	1	2,21	4	0,85
1718dd3	18,8743	-17,8123	7,7	240	48,85	4,37	5	3	164,61	7	0,00	15	-2,75
1818dd1002	18,8750	-18,7517	7,3	570	60,87	31,08	6	21	363,37	3	6,64	4	1,23
1818db1003	18,8750	-18,6083	7,4	630	52,86	32,06	37	10	414,58	1	2,21	8	0,45
1818db1002	18,8750	-18,6042	7,4	650	70,88	39,10	11	9	436,53	1	2,21	6	0,56
104148	18,8750	-18,8820	7,6	770	46,05	25,01	86	10	507,25	7	0,00		-0,63
8314	18,8760	-21,7676	7,5	530	65,27	16,03	26	5	332,88	7	6,64	9	-1,08
104196	18,8769	-19,2315	7,8	1940	52,06	34,00	305	10	551,15	140	47,37	250	-2,18
8368	18,8779	-21,4441	7,2	650	81,29	17,00	34	5	365,81	20	15,49	25	-2,11
890	18,8779	-20,9604	8,3	670	52,06	23,07	61	6	346,30	29	8,85	19	2,42
9558	18,8788	-21,3486	7,6	550	63,27	10,93	38	3	318,25	17	2,21	14	-1,82
9566	18,8798	-21,3261	7,5	650	67,27	14,08	57	4	303,62	35	5,75	50	-0,77
9565	18,8808	-21,2964	8,1	210	22,02	5,10	20	2	118,28	4	2,66	9	2,55
104184	18,8817	-19,0667	7,7	680	21,22	22,10	109	9	429,21	20	0,00	10	0,75
104192	18,8817	-19,1757	7,8	1050	56,06	22,10	148	5	510,91	17	15,94	85	-0,89
9575	18,8827	-21,2703	7,6	530	67,27	11,90	28	3	268,26	8	24,35	28	-1,01
9220	18,8827	-21,5667	7,6	1210	107,32	34,97	128	4	310,93	340	5,75	40	1,86
9221	18,8837	-21,6054	7,5	510	60,07	19,91	20	3	304,84	1	5,75	9	2,00
104149	18,8856	-18,8982	7,7	640	49,25	27,68	43	9	415,80	5	0,00	4	-1,41
8366	18,8865	-21,4964	7,3	1100	63,27	31,08	116	6	335,32	100	8,85	126	-1,62
1718dd8	18,8873	-17,9010	7,0	4500	56,06	35,21	20	7	371,90	3	0,00	15	1,23
9172	18,8875	-21,8171	7,0	420	55,66	10,93	17	3	234,12	8	9,74	4	2,51
9208	18,8875	-21,6919	7,7	510	41,24	25,01	28	5	295,08	8	4,43	9	1,25
9210	18,8885	-21,7279	7,6	690	69,28	22,10	46	5	412,14	13	6,64	13	-0,64
104195	18,8904	-19,2658	7,5	1030	53,26	28,90	120	19	486,52	49	17,26	46	0,81
104183	18,8904	-19,0910	8,3	3310	107,32	65,08	485	50	664,55	43	21,69	780	-1,56
9090	18,8913	-21,9829	7	340	52,06	6,07	10	2	195,10	5	4,43	4	1,38
104126	18,8913	-18,8243	7,5	680	55,26	31,08	49	8	417,02	5	8,85	10	1,92

Appendix D: Hydrochemical data

Name	Long	Lat	pH	ec µS/cm	Ca ²⁺ mg/l	Mg ²⁺ mg/l	Na ⁺ mg/l	K ⁺ mg/l	HCO ₃ ⁻ mg/l	SO ₄ ²⁻ mg/l	NO ₃ ⁻ mg/l	Cl ⁻ mg/l	Balance %
8365	18,8913	-21,5018	7.4	990	67,27	24,04	116	7	378,00	72	6,64	110	-1,60
1718dd7	18,8930	-17,8650	7,4	345	42,05	21,86	12	5	262,16	2	0,00	10	-0,80
1718dd7	18,8930	-17,8650	7,4	345	42,05	21,86	12	5	262,16	2	0,00	10	-0,80
9562	18,8933	-21,2955	6.9	640	69,28	17,00	28	4	171,93	14	0,00	117	-1,85
9032	18,8942	-21,9162	7,4	480	62,07	17,97	15	3	295,08	5	16,82	4	-0,18
771	18,8952	-19,6405	8,4	1170	39,24	33,03	166	22	442,62	47	32,76	134	-0,33
9031	18,8962	-21,8811	7,3	550	64,07	19,91	28	4	336,54	11	10,18	8	0,18
B988/Y4214	18,8971	-19,3973	7,7	740	44,05	17,00	94	5	396,29	17	11,07	39	-1,97
9033	18,8981	-21,9505	7,3	510	67,27	15,06	16	5	301,18	5	14,61	10	-1,26
9173	18,9000	-21,8441	7,7	450	63,27	14,08	16	3	276,79	7	7,53	5	1,44
104191	18,9000	-19,1432	7,6	540	60,07	33,03	4	5	370,68	3	0,00		-0,99
9559	18,9010	-21,3288	7.1	273	33,24	5,10	19	2	162,17	8	0,00	9	-2,03
9089	18,9010	-21,9982	7.1	470	68,07	9,96	24	4	323,13	5	3,10	5	-2,08
9224	18,9010	-21,6631	7,3	660	73,28	34,00	17	3	390,19	3	16,38	9	2,07
104199	18,9019	-19,2072	7,5	1210	55,26	27,93	169	10	493,84	60	0,00	130	-1,35
1818dd1003	18,9033	-18,7566	7,4	590	42,05	26,96	49	10	387,75	3	4,43	6	0,34
9556	18,9038	-21,4180	7.2	460	56,06	11,90	25	3	263,38	11	3,54	19	-1,96
9561	18,9048	-21,2874	7.8	260	25,23	6,07	22	3	142,66	7	1,33	12	-0,91
9419	18,9048	-21,3703	7.6	440	60,07	9,96	25	4	258,50	8	5,75	10	2,34
9207	18,9048	-21,7036	7,7	950	98,11	48,08	32	3	406,04	54	4,43	92	-0,60
W-26	18,9078	-19,0481	8,0	510	66,20	26,20	11	6	342,21	2	4,36	1	2,72
9555	18,9106	-21,4414	7.7	670	59,26	9,96	79	4	337,76	45	4,43	33	-1,08
884	18,9115	-21,0973	7,3	500	61,27	11,90	22	5	270,70	7	21,25	12	-1,37
104206	18,9115	-19,3486	7,3	570	57,26	26,96	15	7	353,61	5	5,31		-0,66
885	18,9115	-21,0937	7,8	590	68,07	14,08	35	4	312,15	11	30,10	7	1,25
9542	18,9115	-21,6459	7,6	680	80,09	32,06	21	4	338,98	7	5,75	56	1,84
9557	18,9135	-21,4036	7.4	290	40,04	2,91	22	2	174,37	5	0,00	10	0,04
104200	18,9144	-19,2315	7,4	700	65,27	17,97	55	6	385,32	23	8,85	22	-1,86
W-30	18,9153	-20,9935	8,0	787	58,20	39,52	57	7	368,44	81	5,52	24	1,90
9525	18,9154	-21,4721	7.4	800	89,30	17,00	61	5	326,79	37	20,36	79	-0,27
9204	18,9163	-21,6541	7,7	640	70,08	33,03	18	4	406,04	5	6,20	7	0,31
104207	18,9163	-19,3748	7,7	800	48,05	24,04	89	7	456,04	25	4,43	24	-1,84
104158	18,9173	-18,9459	7,5	700	59,26	32,54	37	8	391,41	24	6,20	20	-0,86
1718dd1006	18,9190	-17,8270	7,9	280	18,02	6,07	36	7	185,34	1	2,21	1	0,34
9539	18,9192	-21,5802	8.2	650	77,28	25,98	34	4	375,56	40	5,31	13	0,91
893	18,9192	-20,9144	7,6	1210	119,33	51,00	91	8	318,25	310	4,87	75	1,60
1818bb2	18,9196	-18,0079	7,5	470	56,86	38,37	7	7	347,52	0	0,00	20	1,72
1818bb1001	18,9196	-18,0075	8,0	800	64,07	36,91	44	20	468,23	4	6,64	24	0,69
9526	18,9202	-21,4667	7.5	910	116,13	24,04	45	6	381,66	38	13,72	90	0,40
9560	18,9212	-21,2991	7.6	240	19,22	8,01	21	3	128,03	9	0,00	10	0,79
104203	18,9212	-19,2775	8,4	930	9,21	3,89	186	50	613,33	10	0,00		-0,55
9541	18,9231	-21,6126	7,5	750	70,08	34,97	50	4	326,79	115	8,85	24	0,48
9540	18,9240	-21,6099	7,6	750	84,09	36,91	30	4	431,65	5	15,49	38	0,82
W-27	18,9268	-19,0507	8,0	514	61,20	26,00	9	6	343,43	2	3,72	1	0,05
C272	18,9269	-17,8829	7,4	350	42,05	21,86	12	5	262,16	2	0,00	10	-0,80
C271	18,9308	-17,8378	7,7	450	46,85	12,87	43	8	256,06	43	2,66	15	-0,78
9552	18,9317	-21,4207	8,6	330	23,23	10,93	37	4	171,93	17	0,00	16	1,99
8367	18,9317	-21,4964	7.2	890	88,10	14,08	93	5	432,87	95	4,43	36	-2,16
9067	18,9327	-21,9883	7.3	360	54,06	8,99	17	2	231,68	8	3,10	5	0,87
104157	18,9327	-18,9721	7,7	640	54,06	28,66	28	6	395,07	5	4,43		-1,71
9553	18,9346	-21,3991	7,4	560	65,27	15,06	37	3	295,08	17	7,97	26	1,07
V-11	18,9351	-19,1666	7,1	845	60,00	37,80	52	8	381,00	8	9,60	69	0,30
104151	18,9365	-18,9117	7,9	730	59,26	32,54	51	8	490,18	5	6,20	6	-2,12

Appendix D: Hydrochemical data

Name	Long	Mlat	pH	ec µS/cm	Ca ²⁺ mg/l	Mg ²⁺ mg/l	Na ⁺ mg/l	K ⁺ mg/l	HCO ₃ ⁻ mg/l	SO ₄ ²⁻ mg/l	NO ₃ ⁻ mg/l	Cl ⁻ mg/l	Balance %
104220	18,9365	-19,3270	7,8	1500	61,67	68,97	206	14	448,72	164	23,02	239	0,53
104152	18,9375	-18,9288	8,0	640	51,26	29,87	38	8	425,55	5	3,54		-1,87
9521	18,9394	-21,4685	7,5	500	83,29	13,11	6	5	332,88	5	0,00	2	0,07
104219	18,9423	-19,3117	7,8	580	52,06	26,96	49	6	348,73	21	0,00	29	0,92
9074	18,9442	-21,9477	7,2	480	69,28	11,90	20	3	308,50	5	7,97	6	-0,69
9418	18,9452	-21,3495	7,5	460	45,25	9,96	50	4	264,60	17	6,64	12	2,08
9174	18,9452	-21,8324	7,7	580	62,07	11,90	49	4	326,79	16	10,18	10	1,41
104188	18,9452	-19,1432	7,3	890	78,08	36,91	57	8	469,45	5	18,59	63	-1,32
104185	18,9452	-19,0757	7,7	1090	69,28	28,90	127	8	507,25	16	18,15	110	-2,02
9206	18,9452	-21,7144	8,0	1720	65,27	40,07	238	6	332,88	200	22,13	230	1,78
104187	18,9462	-19,0586	7,9	520	58,06	27,93	11	7	360,93	5	0,00		-1,40
9214	18,9471	-21,7306	7,7	910	47,25	25,01	119	5	298,74	151	19,92	33	2,25
1818dc0	18,9482	-18,5098	8,4	1090	32,03	23,07	194	14	575,53	10	2,21	72	2,44
104186	18,9490	-19,0306	7,6	910	50,05	28,90	102	8	432,87	14	6,64	83	-1,64
9069	18,9500	-22,0081	7,2	460	69,28	9,96	22	4	308,50	8	3,98	6	-1,12
9181	18,9500	-21,8955	8,1	480	41,24	15,06	41	5	276,79	15	0,00	12	0,21
9417	18,9500	-21,3270	7,7	540	57,26	14,08	47	5	258,50	35	3,54	36	1,24
104209	18,9500	-19,3568	7,8	560	29,23	25,01	41	22	340,20	12	3,98	6	-1,64
9205	18,9500	-21,6748	7,6	760	75,28	36,91	33	4	431,65	5	7,97	33	0,57
1818db1004	18,9500	-18,6083	7,3	820	68,87	42,98	47	14	536,51	1	13,28	10	0,36
104189	18,9519	-19,1721	7,4	890	65,27	39,10	67	8	537,73	4	13,28	31	-2,00
9213	18,9519	-21,7279	7,6	2730	164,18	75,04	340	6	310,93	420	30,54	525	0,29
1818dd1001	18,9533	-18,7583	7,3	880	48,05	50,03	43	63	573,10	3	4,43	10	0,95
C277	18,9548	-18,0234	7,5	470	56,86	38,37	7	7	347,52		0,00	20	1,72
9212	18,9548	-21,7649	7,9	510	63,27	10,93	31	3	308,50	7	4,87	7	0,04
9211	18,9577	-21,7964	7,7	710	71,28	17,97	55	11	363,37	20	16,82	28	1,83
104198	18,9587	-19,2027	7,4	880	47,25	20,88	116	10	442,62	35	7,08	50	-0,68
9543	18,9596	-21,6378	7,6	580	65,27	33,03	20	4	381,66	7	7,97	5	2,03
C296	18,9596	-18,8045	7,7	790	32,84	27,44	29	100	451,16	4	0,00	5	0,64
9548	18,9606	-21,3784	8,1	560	66,07	13,11	43	4	338,98	16	5,75	12	0,23
9175	18,9635	-21,8450	7,8	700	54,06	8,01	89	3	381,66	27	4,43	17	-0,43
9072	18,9654	-21,9811	7,1	540	69,28	14,08	34	6	336,54	13	7,53	12	0,02
892	18,9654	-20,9703	8,0	1330	71,28	42,98	146	13	374,34	125	6,20	165	1,05
9551	18,9673	-21,4081	7,7	510	47,25	10,93	58	4	314,59	17	0,00	19	-1,37
1818bb1002	18,9692	-18,0350	8,3	560	50,86	25,01	28	8	326,79	2	44,27	20	-5,17
9070	18,9702	-22,0090	7,1	590	77,28	9,96	50	4	364,59	15	6,64	16	0,78
889	18,9731	-21,0108	7,5	620	84,09	15,06	25	5	346,30	6	6,20	18	1,86
9522	18,9740	-21,4468	7,8	750	53,26	14,08	94	7	288,99	53	0,00	66	2,43
9073	18,9760	-21,9802	6,9	620	83,29	13,11	37	6	385,32	13	11,07	17	-1,72
910	18,9760	-21,1730	7,4	850	67,27	37,88	57	9	512,13	6	8,85	30	-1,73
772	18,9760	-19,7856	7,8	2400	58,06	54,88	366	18	436,53	275	75,25	350	-0,36
906	18,9769	-21,1135	7,7	2760	235,46	84,99	222	10	415,80	430	247,89	360	-2,16
888	18,9779	-21,0099	7,6	680	71,28	15,06	69	4	312,15	84	5,31	23	1,94
V-12	18,9783	-19,1549	7,8	1125	58,10	9,30	194	13	725,00	11	6,90	35	-2,97
9180	18,9788	-21,8946	7,5	610	73,28	14,08	36	6	326,79	13	18,15	19	0,62
1818db1005	18,9792	-18,6850	7,4	780	58,06	42,01	49	12	465,79	1	28,77	16	1,28
104201	18,9798	-19,2369	7,6	620	25,23	14,08	74	34	391,41	11	3,54		-1,47
104102	18,9798	-19,0541	8,3	940	27,23	31,08	132	37	568,22	12	0,00	38	-0,14
104103	18,9808	-19,0180	8,2	540	53,26	27,93	7	27	369,46	6	0,00		-1,89
894	18,9808	-20,9216	8,0	770	67,27	31,08	41	6	387,75	22	14,61	38	-1,68
C388	18,9808	-18,4018	7,5	860	62,07	27,93	74	11	512,13		1,77	10	1,09
9177	18,9817	-21,8550	7,7	610	78,08	25,01	16	5	369,46	10	4,43	14	0,36
9176	18,9827	-21,8486	8,0	690	22,02	23,07	99	6	295,08	70	3,54	28	2,17

Appendix D: Hydrochemical data

Name	Long	Mlat	pH	ec µS/cm	Ca ²⁺ mg/l	Mg ²⁺ mg/l	Na ⁺ mg/l	K ⁺ mg/l	HCO ₃ ⁻ mg/l	SO ₄ ²⁻ mg/l	NO ₃ ⁻ mg/l	Cl ⁻ mg/l	Balance %
W-28	18,9834	-19,0569	8,1	590	66,48	33,68	5	11	395,28	3	1,76	1	0,17
9420	18,9846	-21,3495	7,8	510	49,25	11,90	54	4	288,99	19	7,97	14	2,02
9080	18,9846	-21,9396	7,2	850	91,30	20,88	64	3	364,59	17	84,11	61	-1,46
104768	18,9846	-19,3243	7,3	1460	125,34	84,99	50	10	575,53	27	205,84	80	0,35
9529	18,9856	-21,5396	7,6	590	69,28	28,90	22	5	381,66	6	7,97	10	0,94
8723	18,9865	-22,1108	8,0	470	58,06	13,11	20	3	263,38	4	11,07	17	-1,35
9530	18,9894	-21,4775	7,4	660	91,30	17,00	31	4	381,66	17	8,41	21	0,47
9071	18,9904	-21,9919	7,1	570	83,29	10,93	35	3	371,90	9	3,10	17	-1,17
9202	18,9904	-21,7252	7,8	690	84,09	19,91	41	4	412,14	26	4,43	11	0,28
8704	18,9913	-22,2270	8,0	400	46,05	16,03	15	3	238,99	5	11,07	10	-1,53
9200	18,9923	-21,6964	7,8	630	54,06	32,06	35	5	338,98	11	20,36	23	1,63
9079	18,9923	-21,9414	7,2	910	98,11	23,07	64	4	364,59	16	99,60	69	-0,92
9550	18,9971	-21,3658	7,3	500	45,25	13,11	50	4	264,60	27	2,21	17	1,82
907	18,9971	-21,0405	7,4	4420	166,18	135,02	630	10	574,31	1050	49,58	570	-1,14
9199	18,9981	-21,6649	7,9	690	43,25	24,04	74	5	357,27	20	23,02	30	-0,04
9549	18,9990	-21,4054	7,7	650	64,07	14,08	62	3	320,69	37	15,49	30	0,05
104156	18,9990	-18,9811	7,4	650	55,26	35,45	22	9	429,21	6	0,00		-2,12
104099	19,0000	-19,1640	8,4	1180	10,01	8,01	290	17	790,14	28	0,00		2,44
104205	19,0000	-19,3631	7,2	1370	78,08	44,93	135	11	360,93	115	9,74	176	1,16
104100	19,0019	-19,1198	8,3	520	53,26	27,93	20	7	365,81	5	5,31		-1,48
104202	19,0029	-19,2063	8,0	930	4,00	2,91	217	13	613,33	12	4,43		-0,79
104101	19,0038	-19,0649	8,0	640	69,28	37,88	5	13	442,62	4	0,00		-1,47
9081	19,0048	-22,0649	8,2	440	39,24	19,91	35	5	280,45	5	2,66	20	-0,57
9182	19,0048	-21,9126	7,7	640	73,28	15,06	40	3	326,79	13	1,33	30	1,65
9179	19,0048	-21,8991	7,6	750	74,08	18,94	62	3	381,66	11	3,54	44	1,56
9534	19,0048	-21,6216	7,3	750	84,09	32,06	49	5	504,81	5	3,54	10	2,12
9533	19,0058	-21,6180	7,4	770	85,29	32,06	47	5	498,71	6	7,53	15	1,25
9058	19,0067	-21,9883	7,2	530	72,08	10,93	33	4	342,64	4	6,20	10	-0,39
9547	19,0077	-21,6550	7,6	780	36,04	20,88	120	9	486,52	12	4,87	17	1,05
8685	19,0096	-22,1441	8,0	440	46,05	14,08	21	3	245,09	4	14,61	8	-1,27
9083	19,0115	-22,0459	7,4	440	67,27	14,08	27	4	315,81	5	7,97	16	-0,57
104125	19,0115	-18,8288	8,1	640	47,25	39,10	26	12	432,87	5	0,00		-1,30
8684	19,0125	-22,1829	7,9	400	46,05	15,06	20	2	238,99	5	11,07	10	-0,26
9520	19,0135	-21,4342	7,5	710	74,08	8,01	76	5	345,08	45	4,87	38	0,30
8724	19,0154	-22,1045	6,6	580	71,28	14,08	25	3	252,41	3	62,86	23	0,16
104155	19,0163	-18,9288	8,2	820	42,05	27,93	103	12	497,50	5	11,51	38	-1,77
104153	19,0163	-18,9153	7,6	850	37,24	31,57	102	17	526,76	8	3,54	20	-0,50
9178	19,0173	-21,8946	7,7	650	66,07	17,00	48	6	345,08	22	7,08	14	2,32
8725	19,0173	-22,1018	7,4	830	107,32	17,97	28	4	291,42	5	121,73	57	-1,79
9077	19,0202	-21,9595	7,3	570	72,08	14,08	35	3	364,59	7	6,20	14	-2,01
9198	19,0202	-21,6820	7,2	710	76,08	32,06	41	4	449,94	12	3,54	13	1,67
8726	19,0212	-22,1234	7,8	440	57,26	13,11	19	3	263,38	5	5,75	12	-0,12
9528	19,0221	-21,5432	7,5	670	81,29	22,10	40	5	412,14	9	6,64	16	1,59
9536	19,0231	-21,6045	7,5	720	78,08	26,96	54	5	480,42	7	6,64	8	1,41
104154	19,0231	-18,8892	7,7	1230	23,23	26,96	140	145	769,41	8	3,54	10	0,23
9059	19,0240	-21,9793	7,4	420	59,26	10,93	22	3	280,45	5	2,21	9	-1,01
9082	19,0240	-22,0532	7,3	470	67,27	13,11	22	3	287,77	5	11,95	10	1,62
9057	19,0240	-21,9919	7,1	510	77,28	15,06	21	4	336,54	5	6,64	10	0,85
9078	19,0240	-21,9369	7,2	640	79,29	17,00	40	4	379,22	16	7,53	30	-2,16
9061	19,0240	-22,0081	7,1	680	83,29	17,00	48	7	420,68	14	16,82	20	-1,26
104124	19,0240	-18,8514	7,5	940	46,05	33,03	108	16	512,13	5	7,08	46	1,07
1819ca1008	19,0250	-18,6150	7,3	1070	54,06	43,95	116	21	565,78	3	4,43	84	0,51
9416	19,0260	-21,3577	7,6	490	59,26	11,90	36	4	288,99	14	4,43	12	1,52

Appendix D: Hydrochemical data

Name	Long	Mlat	pH	ec µS/cm	Ca ²⁺ mg/l	Mg ²⁺ mg/l	Na ⁺ mg/l	K ⁺ mg/l	HCO ₃ ⁻ mg/l	SO ₄ ²⁻ mg/l	NO ₃ ⁻ mg/l	Cl ⁻ mg/l	Balance %
9535	19,0260	-21,6018	7,5	730	86,09	30,11	59	5	541,39	5	3,98	9	0,92
9527	19,0269	-21,5468	7,5	660	81,29	20,88	43	5	424,33	7	6,64	14	1,11
8706	19,0279	-22,1063	7,8	550	69,28	14,08	28	3	287,77	4	32,76	20	0,16
9415	19,0308	-21,3595	7,9	490	59,26	11,90	36	4	288,99	14	4,43	12	1,52
8705	19,0317	-22,2225	8,0	370	44,05	13,11	17	3	210,95	4	13,28	11	0,35
9197	19,0317	-21,7081	7,3	10700	756,02	355,03	1250	15	462,13	2100	42,05	2500	-0,32
9196	19,0337	-21,7108	8,1	2220	128,14	51,97	268	6	357,27	310	10,18	320	2,23
8702	19,0346	-22,2180	7,8	340	43,25	11,90	16	2	210,95	4	7,53	8	-0,04
9531	19,0346	-21,5225	7,9	630	78,08	24,04	31	5	393,85	7	5,75	20	0,64
9537	19,0356	-21,5712	7,6	650	60,07	25,01	55	5	381,66	30	5,31	15	1,25
8703	19,0365	-22,2216	7,7	340	42,05	9,96	18	3	203,63	3	7,53	10	-0,34
9532	19,0365	-21,4883	7,8	580	34,04	22,10	69	5	301,18	51	0,00	12	2,39
103866	19,0365	-19,2252	8,9	1970	8,01	7,04	505	50	1207,16	70	0,00	70	2,13
V-13	19,0368	-19,1445	7,2	910	47,50	32,70	80	26	537,00	9	7,00	34	-4,33
9201	19,0375	-21,7820	7,8	510	57,26	13,11	37	3	301,18	9	6,64	11	0,73
8689	19,0375	-22,1297	7,5	540	74,08	18,94	17	3	315,81	14	17,71	8	0,77
905	19,0375	-21,1117	7,4	1040	87,29	26,96	95	6	401,17	120	49,58	33	0,26
8688	19,0385	-22,1342	7,9	610	51,26	25,98	42	10	357,27	10	24,35	10	0,30
9203	19,0385	-21,7189	8,3	1410	87,29	34,00	156	6	282,89	200	11,07	160	2,18
8700	19,0394	-22,2018	7,8	460	51,26	18,94	19	4	280,45	6	11,07	8	-0,79
8686	19,0404	-22,1315	7,9	540	72,08	19,91	15	3	323,13	9	19,48	9	-0,72
9546	19,0423	-21,6486	7,7	710	56,06	32,06	62	5	406,04	28	11,07	19	1,90
912	19,0423	-21,3063	8,1	950	74,08	41,04	75	8	512,13	46	6,20	28	1,44
9183	19,0433	-21,9135	7,7	660	64,07	17,00	52	5	345,08	17	8,85	31	-0,29
W-29	19,0446	-19,0466	8,1	592	60,00	29,60	27	9	396,50	0	4,96	2	1,34
9060	19,0462	-22,0081	7,1	630	85,29	17,97	33	4	371,90	12	23,46	19	0,09
8701	19,0490	-22,2468	8,0	380	43,25	15,06	17	4	231,68	4	6,64	9	-0,03
C274	19,0490	-17,8559	7,9	750	46,85	18,94	127	9	530,42	4	4,43	15	2,01
9538	19,0510	-21,5937	7,6	1240	89,30	49,05	112	8	412,14	77	24,35	154	1,78
891	19,0519	-21,0036	8,4	660	62,07	28,90	32	6	359,71	17	6,20	26	-0,44
C353	19,0519	-18,7054	8,4	870	28,43	32,30	145	31	609,68	0	4,87	52	-1,59
895	19,0548	-20,8613	7,2	490	57,26	14,08	28	4	312,15	7	5,31	6	-1,66
9076	19,0548	-21,9586	7,2	560	68,07	13,11	39	3	357,27	13	5,75	10	-1,97
9075	19,0567	-21,9324	7,1	600	62,07	15,06	51	4	336,54	20	6,64	29	-1,48
9184	19,0567	-21,8865	7,9	830	71,28	20,88	84	5	393,85	21	6,20	62	1,78
103874	19,0567	-19,2090	8,4	1700	43,25	34,00	315	18	707,22	80	8,85	180	1,71
8690	19,0577	-22,1721	8,0	450	50,05	14,08	27	3	252,41	15	8,85	14	-0,79
104105	19,0577	-19,1225	7,5	640	45,25	26,96	56	9	432,87	5	0,00	6	-1,55
8594	19,0587	-22,0847	7,6	750	86,09	24,04	23	4	384,10	6	8,85	18	2,13
104104	19,0587	-19,1063	7,9	790	74,08	35,94	36	9	429,21	4	12,39	50	-1,61
9185	19,0587	-21,8793	7,6	810	68,07	20,88	82	6	412,14	22	5,75	45	1,50
103875	19,0587	-19,1730	7,5	820	68,07	36,91	52	16	459,70	4	9,74	40	1,13
9523	19,0596	-21,4306	7,4	510	76,08	16,03	6	6	332,88	4	0,00	5	-1,34
9084	19,0606	-22,0441	7,5	480	63,27	11,90	26	3	295,08	10	6,20	15	-2,05
8699	19,0606	-22,2144	8,0	570	50,05	37,88	12	9	364,59	5	8,85	9	-0,85
9411	19,0606	-21,3865	7,7	640	70,08	15,06	51	5	301,18	41	22,13	32	0,23
103869	19,0606	-19,2820	8,7	640	13,21	24,04	105	14	425,55	13	0,00	2	1,76
9412	19,0615	-21,3910	7,6	600	68,07	13,11	48	5	308,50	25	6,64	32	0,80
104113	19,0625	-19,0640	7,5	620	56,06	31,08	34	9	438,97	5	0,00		-1,63
9088	19,0625	-22,0243	7,1	770	93,30	19,91	41	7	392,63	18	42,94	39	-2,05
104115	19,0635	-18,9910	7,8	1180	74,08	43,95	85	14	410,92	4	8,85	151	0,66
8596	19,0644	-22,1063	7,4	660	82,09	8,99	28	2	286,55	8	34,09	28	-0,79
103876	19,0644	-19,1505	7,1	3530	270,29	164,89	240	100	626,75	150	641,86	575	0,11

Appendix D: Hydrochemical data

Name	Long	Lat	pH	ec µS/cm	Ca ²⁺ mg/l	Mg ²⁺ mg/l	Na ⁺ mg/l	K ⁺ mg/l	HCO ₃ ⁻ mg/l	SO ₄ ²⁻ mg/l	NO ₃ ⁻ mg/l	Cl ⁻ mg/l	Balance %
104122	19,0654	-18,8721	7,5	1800	50,05	44,93	270	23	814,53	20	9,74	140	1,80
9190	19,0673	-21,7847	7,6	760	80,09	24,04	55	4	332,88	25	8,85	70	2,27
9545	19,0673	-21,6387	7,8	1110	47,25	25,98	191	7	486,52	175	7,08	32	1,36
9193	19,0683	-21,8423	7,6	600	58,06	28,90	17	4	246,31	26	17,71	50	-1,26
8716	19,0683	-21,9613	7,8	710	80,09	22,10	38	5	351,17	18	33,20	36	-0,56
103865	19,0683	-19,2396	7,6	1200	88,10	42,98	115	12	506,03	42	15,05	138	-0,23
8598	19,0702	-22,0991	7,5	630	81,29	8,01	25	2	274,35	3	35,41	21	1,14
8597	19,0702	-22,1036	7,3	700	88,10	9,96	26	2	249,97	5	68,61	30	1,94
103877	19,0702	-19,2991	7,6	1250	44,05	27,93	200	17	626,75	57	4,43	70	0,47
103849	19,0712	-19,3658	8,6	1140	25,23	68,00	102	16	345,08	40	0,00	170	1,81
103879	19,0712	-19,3351	7,3	1460	45,25	34,00	270	16	707,22	40	29,22	134	1,58
104123	19,0721	-18,8243	7,5	880	44,05	42,01	72	32	581,63	5	0,00	11	-1,75
908	19,0721	-21,1532	7,4	2260	165,38	114,86	160	16	353,61	690	2,66	200	-1,51
104114	19,0731	-19,0441	8,2	770	50,05	36,91	65	16	518,22	6	6,20	12	-1,60
9544	19,0731	-21,6414	7,7	1070	49,25	28,90	175	8	535,30	120	11,51	25	1,98
103878	19,0760	-19,3180	7,3	990	76,08	50,03	78	11	620,65	12	4,43	22	2,09
8595	19,0769	-22,0793	7,4	640	75,28	17,97	17	4	310,93	5	22,13	14	1,04
9087	19,0779	-21,9883	7,0	700	85,29	16,03	38	4	323,13	13	5,31	68	-1,61
1819ca01	19,0783	-18,5705	7,9	1250	22,02	27,93	226	18	716,98	24	2,21	66	-1,65
1819ca1009	19,0788	-18,6250	7,3	780	72,08	40,07	36	16	497,50	1	2,21	24	-0,10
9514	19,0788	-21,5117	7,8	740	36,04	17,00	110	5	282,89	110	9,74	31	0,95
9518	19,0798	-21,4973	7,6	900	82,09	41,04	63	5	437,75	71	8,85	40	2,06
9187	19,0798	-21,9135	7,5	1030	99,31	24,04	96	5	388,97	48	5,75	124	1,23
103868	19,0808	-19,2784	8,2	1830	47,25	63,87	270	22	637,72	90	10,62	240	1,67
103867	19,0817	-19,2613	8,5	1770	30,03	34,00	355	44	914,51	89	0,00	106	2,54
8697	19,0837	-22,1892	7,9	520	59,26	27,93	8	3	329,22	4	8,85	7	-1,21
9409	19,0837	-21,4099	7,7	590	79,29	15,06	39	4	351,17	20	4,43	16	2,19
911	19,0837	-21,2360	7,4	810	59,26	30,11	61	7	443,84	7	10,18	33	-1,47
1719cc8	19,0846	-17,8355	7,6	640	38,04	30,36	54	3	347,52	13	13,28	16	1,41
9086	19,0846	-22,0018	7,1	540	75,28	15,06	29	4	351,17	9	10,18	10	-0,23
9519	19,0846	-21,4982	7,5	880	73,28	35,94	86	5	480,42	72	5,75	20	2,21
1719cc9	19,0847	-17,8359	7,7	500	50,05	18,21	29	3	281,67	13	2,21	10	1,23
9371	19,0856	-21,6919	9,0	340	11,21	9,96	50	4	153,64	27	0,00	14	2,54
9512	19,0856	-21,5793	7,5	850	75,28	33,03	73	6	443,84	37	6,64	42	2,44
9195	19,0875	-21,7982	7,7	990	76,08	30,11	94	4	393,85	58	4,87	108	-1,51
9085	19,0885	-22,0261	7,0	690	82,09	13,11	53	4	379,22	21	4,43	40	-1,74
9410	19,0894	-21,4081	7,5	590	78,08	16,03	36	4	351,17	23	4,43	16	0,93
903	19,0894	-20,9901	8,0	910	64,07	40,07	61	6	367,02	87	8,41	41	0,99
9372	19,0933	-21,7072	7,9	670	61,27	19,91	66	5	345,08	62	5,75	22	0,23
8687	19,0942	-22,1595	7,9	460	54,06	13,11	24	3	259,72	8	11,07	13	-0,72
8715	19,0942	-22,0387	7,7	470	58,06	10,93	28	3	280,45	6	8,85	12	-1,08
8698	19,0942	-22,2180	8,0	610	52,06	23,07	50	4	364,59	10	11,95	14	0,02
8593	19,0942	-22,1342	7,5	1400	80,09	30,11	152	12	378,00	58	75,25	155	1,53
1919cc2	19,0958	-19,9439	7,8	610	59,66	26,96	35	18	390,19	14	22,13	15	-1,97
8696	19,0971	-22,1910	8,0	830	92,10	32,06	24	14	399,95	12	63,30	39	-1,65
V-15	19,0978	-19,1671	7,1	1304	48,80	39,00	156	18	645,00	33	8,90	77	-2,63
9513	19,0981	-21,5405	7,6	620	75,28	25,01	24	4	351,17	6	8,85	24	1,91
9194	19,0981	-21,7973	7,6	910	74,08	33,03	78	4	387,75	22	11,95	91	1,73
8711	19,0990	-22,0153	8,1	520	58,06	17,00	34	4	323,13	7	4,43	15	-0,49
8714	19,0990	-22,0441	7,9	960	127,34	23,07	32	3	301,18	10	146,08	85	-0,90
8710	19,1000	-21,9964	8,0	550	66,07	14,08	37	3	329,22	9	4,43	19	-0,39
1819ca1003	19,1000	-18,6900	7,6	690	60,07	40,07	25	14	456,04	1	15,49	7	-1,29
V-14	19,1038	-19,1978	7,0	1729	55,00	30,90	278	15	877,00	71	2,20	108	-3,17

Appendix D: Hydrochemical data

Name	Long	Lat	pH	ec µS/cm	Ca ²⁺ mg/l	Mg ²⁺ mg/l	Na ⁺ mg/l	K ⁺ mg/l	HCO ₃ ⁻ mg/l	SO ₄ ²⁻ mg/l	NO ₃ ⁻ mg/l	Cl ⁻ mg/l	Balance %
9413	19,1067	-21,3712	7,4	520	67,27	13,11	34	4	314,59	17	3,54	10	1,42
9359	19,1067	-21,7090	7,6	690	60,07	14,08	56	30	308,50	56	25,67	26	-0,07
9192	19,1067	-21,8243	8,0	760	33,24	19,91	106	4	301,18	74	19,03	32	2,06
9494	19,1077	-21,6360	7,6	590	51,26	27,93	50	6	393,85	8	6,64	4	2,45
1819ca1007	19,1083	-18,5392	7,2	940	76,88	42,01	55	16	497,50	4	4,43	62	0,19
9495	19,1106	-21,6387	7,7	580	53,26	32,06	27	6	351,17	9	12,39	9	1,74
9191	19,1125	-21,7685	7,7	850	82,09	25,01	75	5	462,13	22	5,31	46	0,68
9360	19,1135	-21,7090	7,4	660	70,08	14,08	59	5	338,98	58	5,31	19	-0,23
8592	19,1154	-22,1252	7,5	770	40,04	17,97	84	10	359,71	16	21,25	21	1,53
9498	19,1154	-21,6117	7,5	830	68,07	32,06	72	5	381,66	70	13,28	36	1,93
104116	19,1154	-18,9946	8,2	990	55,26	35,94	110	12	556,02	5	0,00	58	-0,21
9370	19,1163	-21,7369	7,6	1000	94,10	24,04	103	4	351,17	165	66,40	36	-0,09
8590	19,1173	-22,0937	7,5	510	68,07	8,01	20	1	274,35	5	8,85	7	0,11
8591	19,1173	-22,1198	7,5	1160	68,07	43,95	97	9	426,77	20	37,63	105	2,16
9501	19,1183	-21,5532	7,6	850	80,09	37,88	58	6	443,84	59	7,97	28	1,92
9502	19,1183	-21,5568	7,5	860	81,29	39,10	56	6	431,65	72	5,75	30	1,81
896	19,1192	-20,8838	7,6	540	73,28	10,93	24	4	312,15	6	15,94	9	-0,43
8693	19,1192	-22,1532	8,0	750	73,28	20,88	53	3	351,17	5	11,07	66	-0,91
103871	19,1212	-19,1775	7,6	1300	47,25	41,04	193	20	666,99	34	7,97	90	1,16
9500	19,1221	-21,5586	7,5	800	70,08	35,94	59	6	387,75	62	7,08	36	2,22
9503	19,1231	-21,5505	7,9	890	60,07	33,03	88	6	295,08	153	7,08	42	1,98
103870	19,1240	-19,2153	8,7	2180	5,21	40,07	500	5	1115,71	81	0,00	168	1,44
104108	19,1250	-19,1495	8,2	1410	52,06	43,95	162	56	713,32	5	5,31	117	-1,63
103852	19,1260	-19,3243	7,8	2330	115,33	69,94	265	20	540,17	5	15,94	490	1,10
8712	19,1269	-22,0153	7,5	580	70,08	15,06	34	3	323,13	23	6,64	15	-0,10
104111	19,1269	-19,0622	8,0	1340	22,02	18,94	164	188	865,74	5	0,00	14	-0,30
104110	19,1269	-19,0892	7,6	2340	21,22	23,07	540	29	1118,15	28	10,62	265	1,18
1819aa1001	19,1275	-18,0950	7,4	470	44,05	32,06	7	7	314,59	1	2,21	5	-0,32
9358	19,1279	-21,8333	7,8	640	31,23	25,98	76	6	264,60	4	0,00	91	1,20
104109	19,1279	-19,1162	8,1	1040	40,04	40,07	119	30	631,62	7	0,00	38	-1,45
8713	19,1288	-22,0099	7,2	550	71,28	15,06	34	3	351,17	7	5,75	15	-0,51
904	19,1298	-21,0784	7,7	640	45,25	25,98	52	8	387,75	13	5,75	8	-0,59
8707	19,1298	-22,0477	7,7	700	75,28	15,06	54	3	357,27	28	19,92	30	-1,23
104120	19,1317	-18,9162	8,0	1150	78,08	49,05	98	14	643,82	4	6,64	65	-0,08
103864	19,1317	-19,2973	7,0	2120	97,31	73,10	227	23	546,27	79	27,45	400	-2,27
104121	19,1337	-18,8748	7,8	2060	113,32	77,95	160	20	498,71	5	0,00	430	-2,17
104117	19,1346	-18,9568	7,4	1630	66,07	51,97	193	21	675,52	5	0,00	163	2,27
9357	19,1356	-21,7919	7,7	760	55,26	31,08	70	3	147,54	210	3,54	43	2,28
103863	19,1375	-19,2423	7,5	2410	113,32	69,94	290	17	534,08	75	20,36	510	-1,15
897	19,1394	-20,7685	7,7	410	53,26	8,99	20	4	235,33	9	3,98	5	1,39
8695	19,1394	-22,2081	8,0	740	57,26	31,08	49	5	315,81	9	37,63	60	0,08
9361	19,1394	-21,7045	7,6	2940	67,27	52,94	575	17	523,10	650	59,76	325	1,41
9515	19,1404	-21,4991	7,6	790	77,28	39,10	39	8	431,65	13	11,95	40	1,75
9496	19,1413	-21,6279	7,5	650	78,08	22,10	34	3	369,46	6	7,53	27	1,45
9516	19,1413	-21,4946	7,4	770	72,08	37,88	42	8	424,33	15	14,17	36	1,36
1819ca1002	19,1417	-18,7308	7,4	800	68,07	34,00	52	13	453,60	1	2,21	38	1,31
9497	19,1423	-21,6324	7,8	680	53,26	24,04	72	4	412,14	8	10,62	17	1,93
9517	19,1442	-21,5027	8,0	790	72,08	37,88	49	8	431,65	21	16,38	34	1,77
1819aa1009	19,1466	-18,0416	7,2	410	72,88	35,94	6	7	419,46	1	2,21	4	-0,07
8719	19,1471	-21,9144	7,8	570	79,29	14,08	27	3	351,17	4	17,71	15	-1,40
9504	19,1490	-21,5505	7,5	680	51,26	27,93	70	6	430,43	25	4,43	4	1,87
8709	19,1500	-21,9838	8,0	600	68,07	17,00	41	3	351,17	10	5,31	23	-0,31
8708	19,1519	-22,0270	7,9	550	70,08	16,03	28	3	351,17	8	0,00	15	-1,88

Appendix D: Hydrochemical data

Name	Long	Lat	pH	ec µS/cm	Ca ²⁺ mg/l	Mg ²⁺ mg/l	Na ⁺ mg/l	K ⁺ mg/l	HCO ₃ ⁻ mg/l	SO ₄ ²⁻ mg/l	NO ₃ ⁻ mg/l	Cl ⁻ mg/l	Balance %
9356	19,1529	-21,7910	7,7	980	95,30	40,07	56	4	215,83	220	60,65	68	-1,95
9407	19,1529	-21,4297	7,6	2160	119,33	71,88	265	2	203,63	820	6,64	114	-0,60
1719cc2	19,1530	-17,8408	7,3	660	55,66	18,46	74	5	408,48	41	0,00	20	-2,98
9406	19,1538	-21,4090	7,9	1370	129,34	36,91	110	8	301,18	125	23,46	230	0,27
1719cc1003	19,1540	-17,8370	6,6	150	14,82	5,10	9	3	70,72	2	2,21	11	2,54
1819ca1006	19,1546	-18,5560	8,4	1450	22,02	20,88	270	37	595,04	7	24,35	200	-1,35
1819aa1007	19,1547	-18,1663	8,3	350	28,83	22,10	11	5	219,48	1	2,21	10	-0,92
9408	19,1548	-21,4369	7,6	1960	120,13	68,00	225	2	221,92	740	10,18	106	-1,76
9511	19,1558	-21,5811	7,6	730	68,07	28,90	55	5	393,85	24	11,07	28	2,30
1719cc1001	19,1580	-17,8580	7,7	1270	72,88	23,07	183	6	582,85	87	43,82	63	-0,72
1719cc1	19,1580	-17,8580	7,9	1600	18,02	15,78	386	9	792,58	163	3,98	85	0,98
913	19,1587	-21,3099	7,7	650	45,25	11,90	73	5	235,33	60	17,71	40	0,16
C295	19,1596	-18,5973	8,3	630	43,65	37,88	49	70	524,32	2	4,43	8	1,57
8694	19,1625	-22,2036	8,0	670	59,26	34,00	34	6	407,26	8	2,21	26	-1,49
914	19,1625	-21,2991	7,3	1880	154,17	103,94	60	26	568,22	130	340,85	76	-0,35
8691	19,1644	-22,1550	7,7	710	78,08	25,98	31	6	343,86	12	50,02	29	0,18
W-16?	19,1667	-19,2615	7,9	2828	117,60	87,60	500	29	664,90	580	11,20	482	-1,62
8692	19,1683	-22,1577	7,8	1090	118,13	41,04	34	15	385,32	15	146,08	78	-0,22
916	19,1702	-21,1523	8,0	730	67,27	35,94	28	7	415,80	20	10,18	16	-0,87
9405	19,1702	-21,4676	7,5	840	87,29	44,93	29	8	438,97	5	11,07	62	1,57
9398	19,1712	-21,5171	7,4	820	76,08	39,10	55	7	412,14	29	16,82	56	2,00
104106	19,1740	-19,1468	8,2	1180	31,23	33,03	170	37	536,51	9	5,75	115	1,21
9362	19,1750	-21,6964	7,3	2650	100,11	50,03	470	9	585,29	470	45,15	305	1,84
8291	19,1769	-22,1216	7,0	2560	355,59	84,99	24	12	409,70	28	575,46	350	-0,69
8722	19,1788	-21,9676	7,7	710	66,07	18,94	64	3	414,58	20	5,75	24	-1,68
9399	19,1798	-21,5144	7,8	740	65,27	31,08	59	6	424,33	14	17,71	28	1,27
1819ca03	19,1810	-18,5317	7,9	2840	22,02	45,90	510	47	941,34	18	16,38	475	-2,08
9510	19,1817	-21,6243	7,5	660	70,08	31,08	33	4	399,95	10	11,07	14	1,72
103859	19,1817	-19,3622	8,0	1880	62,07	62,90	227	38	488,96	19	23,02	370	-0,26
103860	19,1817	-19,3315	7,7	2930	170,19	104,91	320	43	459,70	27	39,84	800	1,32
104107	19,1817	-19,1144	7,3	3530	44,05	46,87	700	42	1370,55	55	7,08	440	1,96
8292	19,1827	-22,1144	7,3	1190	170,19	44,93	17	10	584,07	5	154,93	52	-1,70
1819ca1001	19,1833	-18,6177	7,9	810	48,85	25,98	93	16	470,67	3	6,64	33	1,21
8294	19,1837	-22,0820	7,6	600	58,06	25,01	36	4	374,34	15	8,85	10	-1,84
9352	19,1837	-21,8171	7,4	880	101,31	41,04	23	4	431,65	8	33,20	68	-0,83
9353	19,1856	-21,7405	7,5	490	57,26	28,90	23	4	357,27	10	5,75	9	-0,56
W-31	19,1862	-20,8189	7,9	2141	226,00	54,40	244	9	387,35	694	26,80	167	1,28
104118	19,1865	-18,9874	8,5	2470	17,22	27,93	530	115	1513,22	36	0,00	87	2,01
902	19,1875	-20,9559	8,1	810	50,05	30,11	78	8	423,11	22	23,46	18	1,75
103857	19,1885	-19,3793	8,8	1000	15,22	27,93	160	21	385,32	6	0,00	140	0,79
9369	19,1904	-21,7333	7,5	530	60,07	24,04	22	3	338,98	8	4,87	11	-0,84
1819ca1030	19,1917	-18,5092	8,4	2560	50,05	36,91	480	37	748,68	4	13,28	520	0,23
9188	19,1923	-21,8919	7,5	1150	108,12	36,91	86	7	456,04	73	6,64	114	0,15
103862	19,1923	-19,2901	7,2	2710	74,08	59,98	450	33	620,65	80	7,97	570	1,76
104112	19,1933	-19,0595	7,7	1200	55,26	36,91	157	23	612,11	5	15,49	90	1,10
103861	19,1942	-19,2523	7,7	2410	35,24	34,97	465	30	781,60	97	6,20	350	1,64
8718	19,1952	-21,9135	7,9	730	69,28	25,01	54	4	371,90	31	19,92	34	-0,34
9404	19,1962	-21,3793	7,6	740	76,08	17,97	72	5	381,66	46	4,43	34	1,74
103873	19,1962	-19,2180	8,2	1460	41,24	36,91	214	33	580,41	20	4,43	180	0,56
C279	19,1962	-17,8730	7,9	1600	18,02	15,78	386	9	792,58	163	3,98	85	0,98
1719cc1004	19,1970	-17,9480	7,8	530	50,86	31,08	15	6	351,17	2	2,21	3	-0,13
103872	19,1971	-19,1775	7,8	1440	31,23	23,07	265	36	620,65	34	10,62	154	1,63
9505	19,1981	-21,5640	7,7	1090	70,08	37,88	133	6	399,95	190	8,85	48	2,22

Appendix D: Hydrochemical data

Name	Long	Mlat	pH	ec µS/cm	Ca ²⁺ mg/l	Mg ²⁺ mg/l	Na ⁺ mg/l	K ⁺ mg/l	HCO ₃ ⁻ mg/l	SO ₄ ²⁻ mg/l	NO ₃ ⁻ mg/l	Cl ⁻ mg/l	Balance %
104119	19,1990	-19,0099	7,4	1180	36,04	40,07	158	38	713,32	5	0,00	50	-1,01
9400	19,2019	-21,4838	7,6	1340	87,29	51,00	146	8	412,14	260	11,07	78	1,89
8293	19,2029	-22,1171	7,6	1640	192,21	61,92	28	22	476,77	7	276,67	152	-0,73
915	19,2038	-21,2414	7,2	1280	130,14	63,87	22	5	457,26	20	256,75	36	-0,89
9363	19,2048	-21,6937	7,4	1340	113,32	40,07	133	6	437,75	190	110,67	79	-0,84
1819ca1005	19,2050	-18,5733	7,5	4410	42,05	52,94	860	46	897,44	52	6,64	1080	-1,45
C280	19,2058	-17,8712	7,6	420	15,62	9,96	92	3	286,55	5	30,99	15	-0,40
9509	19,2087	-21,6072	7,7	990	35,24	17,97	184	6	480,42	100	5,31	31	2,15
8290	19,2096	-22,1505	7,6	1000	97,31	54,88	37	15	517,00	10	53,12	66	-0,15
8289	19,2096	-22,1721	7,8	1020	91,30	43,95	68	5	486,52	16	13,28	116	-2,32
9354	19,2115	-21,7495	7,7	440	34,04	20,88	30	3	209,73	34	6,64	20	-0,18
9355	19,2115	-21,8180	7,4	490	48,05	26,96	18	6	308,50	18	5,31	4	-0,69
8586	19,2125	-22,0063	7,5	610	54,06	15,06	50	2	262,16	45	14,17	17	1,83
8587	19,2125	-22,0117	8,1	700	63,27	18,94	44	2	298,74	14	46,48	26	0,08
1819ac1004	19,2133	-18,4625	8,5	1270	2,00	0,97	316	16	821,84	10	2,21	12	1,00
9403	19,2135	-21,4477	7,7	790	60,07	27,93	84	5	301,18	110	10,18	46	2,19
8584	19,2144	-22,0505	7,7	660	56,06	17,00	54	4	365,81	11	5,31	9	0,64
898	19,2154	-20,7054	8,0	450	50,05	9,96	29	3	249,97	9	8,85	8	0,03
8720	19,2154	-21,9306	8,0	600	69,28	17,97	37	3	329,22	33	11,07	15	-0,47
9508	19,2173	-21,6189	7,4	520	58,06	23,07	21	5	314,59	5	11,07	10	1,01
9506	19,2183	-21,6045	7,9	2140	48,05	22,10	415	5	369,46	650	3,54	60	2,42
8585	19,2192	-22,0441	7,9	570	42,05	15,06	46	4	280,45	14	0,00	21	-0,36
8414	19,2192	-22,1955	7,6	840	63,27	23,07	98	5	365,81	87	22,13	50	-0,67
8415	19,2202	-22,2243	7,5	750	73,28	28,90	61	4	420,68	33	25,23	31	-0,41
1719cc5	19,2208	-17,8462	7,6	455	34,84	6,80	63	5	280,45	10	6,20	15	-1,54
9507	19,2221	-21,6081	7,9	1090	20,02	9,96	200	4	462,13	90	6,64	21	2,28
8276	19,2240	-22,1099	7,6	860	85,29	42,01	34	17	537,73	6	28,77	22	-2,01
9401	19,2240	-21,4964	7,5	1120	119,33	56,10	45	5	449,94	41	22,13	124	2,32
901	19,2240	-21,0108	7,6	2280	250,27	68,97	183	10	165,83	1000	1,33	64	1,96
9366	19,2250	-21,6477	7,5	570	55,26	19,91	47	4	387,75	8	3,10	6	-1,49
9189	19,2260	-21,8378	7,9	850	53,26	32,06	93	6	468,23	25	5,31	28	2,29
1819aa1003	19,2267	-18,0217	8,1	610	52,06	25,01	47	7	378,00	1	2,21	12	2,15
9351	19,2269	-21,7757	7,6	590	60,07	30,11	30	4	387,75	9	3,54	10	0,01
1919ac1004	19,2275	-19,4350	7,2	810	58,86	13,11	108	11	412,14	40	22,13	28	1,48
1819ac1003	19,2292	-18,4767	9,6	820	6,01	3,89	184	20	509,69	10	2,21	10	1,42
1919ac5	19,2297	-19,2889	6,9	2090	53,66	52,45	253	46	475,55	2	0,00	400	0,15
1819aa1008	19,2300	-18,2367	8,6	270	22,02	9,96	21	6	170,71	1	2,21	4	0,31
8581	19,2308	-22,0577	7,4	800	48,05	14,08	91	23	402,39	18	19,92	21	1,38
1819aa1002	19,2317	-18,0967	8,3	300	38,04	11,90	7	6	185,34	1	4,43	4	1,41
1819ac1006	19,2323	-18,4017	8,0	1440	8,81	8,99	320	32	819,40	17	11,07	66	0,29
8588	19,2327	-21,9892	7,5	690	68,07	20,88	40	2	353,61	8	5,31	22	1,76
1819ac1007	19,2333	-18,3708	7,7	230	18,02	9,96	7	13	136,57	1	2,21	2	0,09
1819ac1008	19,2333	-18,3167	7,2	530	50,05	17,97	38	9	341,42	1	2,21	6	0,33
8582	19,2356	-22,0604	7,9	800	41,24	14,08	100	18	390,19	19	31,87	21	0,82
9365	19,2365	-21,6937	7,3	1080	103,31	45,90	80	6	430,43	125	64,19	52	1,65
9364	19,2365	-21,6874	7,5	1860	184,20	59,98	144	6	406,04	205	292,16	140	2,40
8275	19,2375	-22,0847	7,3	550	65,27	16,03	39	3	358,49	7	8,85	10	-0,76
917	19,2375	-21,1685	8,4	1040	72,08	27,93	103	6	235,33	225	31,87	50	0,30
9402	19,2423	-21,4784	7,4	820	60,07	35,94	84	7	510,91	36	5,75	14	0,91
8277	19,2423	-22,1162	7,7	860	78,08	39,10	48	10	465,79	13	59,76	35	-2,06
9377	19,2442	-21,5991	7,9	790	40,04	19,91	130	6	412,14	80	6,64	18	2,22
1819cc03	19,2449	-18,8748	8,4	310	44,05	6,07	11	9	187,78	1	2,21	3	2,83
9376	19,2452	-21,6045	8,0	940	12,01	7,04	215	4	431,65	120	8,85	16	2,24

Appendix D: Hydrochemical data

Name	Long	Mlat	pH	ec μS/cm	Ca ²⁺ mg/l	Mg ²⁺ mg/l	Na ⁺ mg/l	K ⁺ mg/l	HCO ₃ ⁻ mg/l	SO ₄ ²⁻ mg/l	NO ₃ ⁻ mg/l	Cl ⁻ mg/l	Balance %
1819cc02	19,2458	-18,7961	8,8	760	12,01	10,93	161	18	490,18	14	8,85	13	0,72
1819ca04	19,2465	-18,7154	8,0	360	34,84	16,03	14	11	229,24	13	2,21	2	-2,13
1819cc01	19,2471	-18,9582	8,4	440	44,05	11,90	32	12	236,55	8	2,21	20	2,45
1819ca02	19,2474	-18,6276	7,9	2330	104,11	70,91	256	28	351,17	8	13,28	560	2,12
1919aa1001	19,2475	-19,2350	7,8	840	36,04	22,10	123	19	487,74	9	6,64	32	1,41
C431	19,2481	-19,3072	6,9	2000	53,66	52,45	253	46	475,55	2	0,00	400	0,15
8583	19,2510	-22,0459	7,4	640	72,08	13,11	39	2	341,42	15	5,31	17	-0,38
9394	19,2510	-21,3928	7,5	660	64,07	39,10	29	7	393,85	18	12,39	18	2,06
8580	19,2548	-22,0649	7,9	510	57,26	8,99	37	2	274,35	7	9,74	10	1,70
9396	19,2548	-21,4333	7,5	900	66,07	34,97	98	7	399,95	100	14,61	44	2,43
8721	19,2548	-21,9586	7,6	1240	91,30	24,04	155	4	371,90	225	6,64	91	-0,28
8417	19,2567	-22,1937	7,2	840	98,11	25,98	55	4	420,68	10	34,53	66	0,04
9395	19,2567	-21,4396	7,9	880	64,07	36,91	94	7	424,33	77	15,49	46	1,93
8416	19,2577	-22,2207	7,5	670	97,31	22,10	25	4	402,39	7	14,61	29	0,45
C304	19,2596	-18,4964	8,2	600	8,41	4,61	169	22	481,64	21	0,00	7	1,07
9397	19,2615	-21,4324	7,7	900	69,28	36,91	94	7	431,65	75	17,71	46	2,59
1819ad1012	19,2633	-18,4333	7,4	450	42,85	19,91	16	12	287,77	2	2,21	4	-1,31
1919ad5	19,2633	-19,3675	8,1	720	68,07	13,36	52	24	292,64	54	17,71	35	1,23
C281	19,2635	-17,8694	7,5	710	32,03	12,14	136	5	353,61	74	23,46	45	-1,94
8505	19,2635	-21,9973	7,2	760	68,07	18,94	77	3	382,88	63	8,85	23	0,02
8287	19,2644	-22,1586	7,2	1190	94,10	34,97	126	6	491,40	53	11,07	136	0,14
C303	19,2654	-18,5027	8,0	1600	50,86	29,87	290	15	343,86	470	36,74	98	-2,13
9342	19,2692	-21,8117	7,5	700	64,07	35,94	35	7	443,84	8	7,08	17	-1,12
9390	19,2702	-21,3766	7,8	1120	85,29	40,07	117	8	338,98	230	5,75	66	2,18
8504	19,2721	-22,0018	7,2	750	71,28	19,91	73	3	380,44	56	9,74	23	1,45
1719cd1007	19,2730	-17,9780	8,2	430	58,86	16,03	9	5	275,57	1	2,21	5	0,65
1819ab8	19,2730	-18,9780	7,0	440	60,07	16,27	9	3	271,92		0,00	7	1,59
8274	19,2731	-22,0784	7,4	560	70,08	14,08	37	3	342,64	7	11,07	21	-1,47
C282	19,2740	-17,8703	7,6	460	34,84	6,80	63	5	280,45	10	6,20	15	-1,54
9375	19,2740	-21,6009	7,7	690	51,26	25,98	69	5	345,08	18	8,85	48	1,94
9350	19,2750	-21,7477	7,9	400	29,23	14,08	36	4	197,53	24	10,18	13	0,21
9367	19,2750	-21,6829	7,2	1180	105,31	33,03	119	5	474,33	180	12,39	58	-0,30
1819ab0	19,2755	-18,1962	8,2	500	40,04	32,06	17	9	329,22	10	4,43	7	-2,33
8412	19,2760	-22,2495	7,3	680	87,29	23,07	38	3	457,26	5	16,82	15	-1,89
8286	19,2760	-22,1577	7,2	1150	98,11	22,10	124	6	470,67	61	13,28	122	-1,52
8506	19,2769	-22,0414	7,2	770	84,09	19,91	62	4	396,29	12	18,59	43	2,23
9389	19,2798	-21,4009	7,7	1180	95,30	39,10	118	8	369,46	235	8,85	66	1,36
8413	19,2808	-22,2144	7,5	760	78,08	25,98	55	6	365,81	8	50,02	51	1,02
1919ac4	19,2811	-19,2042	7,6	2283	96,91	66,30	406	83	195,10	54	26,56	825	3,53
1719cd2	19,2816	-17,8841	7,8	310	40,84	18,94	15	5	243,87	0	0,00	15	-0,48
1819ad1010	19,2867	-18,4042	7,7	610	30,83	25,98	54	19	385,32	4	2,21	7	-0,91
900	19,2885	-20,9649	7,5	880	69,28	37,88	62	8	436,53	47	30,99	23	1,04
9378	19,2904	-21,5568	7,5	740	80,09	36,91	37	6	437,75	13	11,07	28	2,23
9386	19,2913	-21,3459	7,5	1340	102,11	59,98	121	9	314,59	440	36,74	34	-1,09
9392	19,2923	-21,3712	7,8	580	60,07	34,97	20	6	381,66	9	4,43	6	1,59
9393	19,2923	-21,3757	7,3	620	64,07	35,94	19	7	418,24	6	0,00	10	-0,70
9339	19,2942	-21,8784	7,8	700	30,03	15,06	123	5	418,24	8	19,92	19	2,10
1819ad4	19,2943	-18,2864	7,8	420	55,26	15,06	10	10	280,45	6	0,00	5	-1,83
1819ad1002	19,2950	-18,2817	7,6	420	42,85	19,91	14	8	278,01	2	2,21	2	-1,07
9387	19,2952	-21,4477	7,5	690	53,26	27,93	68	6	363,37	34	13,28	34	1,45
9388	19,2962	-21,4523	7,7	740	48,05	25,01	89	6	326,79	86	12,39	30	1,73
9347	19,2971	-21,7784	7,7	610	63,27	35,94	19	5	418,24	5	5,31	6	-1,01
1719cd1003	19,2980	-17,8520	7,5	5670	28,03	35,94	1310	8	1336,41	1020	8,41	720	-1,63

Appendix D: Hydrochemical data

Name	Long	Lat	pH	ec µS/cm	Ca ²⁺ mg/l	Mg ²⁺ mg/l	Na ⁺ mg/l	K ⁺ mg/l	HCO ₃ ⁻ mg/l	SO ₄ ²⁻ mg/l	NO ₃ ⁻ mg/l	Cl ⁻ mg/l	Balance %
9343	19,2981	-21,7270	7,5	610	61,27	31,08	38	5	412,14	12	3,10	5	1,37
1919ad1003	19,2983	-19,4683	8,0	1670	44,05	19,91	275	21	287,77	140	227,97	150	2,50
1719cd1	19,2992	-17,8510	7,2	7000	80,09	31,57	1644	10	1713,19	1160	0,00	970	-0,78
1819cb1003	19,3000	-18,5217	8,6	360	14,02	8,99	38	29	221,92	1	2,21	6	-0,38
9391	19,3000	-21,4288	7,6	760	74,48	42,01	39	7	437,75	15	14,61	34	2,08
9374	19,3000	-21,5901	8,2	1240	24,03	9,96	240	5	320,69	260	11,07	60	0,18
8280	19,3019	-22,1009	7,2	630	60,07	16,03	57	6	363,37	14	4,43	28	-1,13
1819ad1011	19,3025	-18,4217	7,5	430	42,85	22,10	4	18	280,45	1	2,21	2	-1,27
9341	19,3029	-21,8378	7,7	530	35,24	16,03	65	5	308,50	9	11,95	18	0,74
8278	19,3029	-22,1081	7,3	700	66,07	23,07	51	4	342,64	15	15,49	56	-1,58
1919cb1	19,3029	-19,5623	8,1	1200	16,82	17,73	256	63	463,35	91	163,79	88	1,46
918	19,3048	-21,0946	7,7	1060	36,04	11,90	188	6	470,67	110	6,20	30	0,72
9335	19,3048	-21,9676	7,4	1200	148,16	26,96	95	4	449,94	135	29,22	103	1,04
9373	19,3058	-21,5730	7,6	680	66,07	34,97	39	6	462,13	8	8,85	6	-0,17
8410	19,3058	-22,1991	7,3	960	75,28	27,93	100	4	390,19	28	10,18	132	-1,68
8284	19,3058	-22,1432	7,3	1090	52,06	44,93	140	13	645,04	31	8,85	56	-0,87
8283	19,3058	-22,1387	7,4	1110	56,06	44,93	135	13	660,89	31	11,07	55	-1,96
8411	19,3067	-22,2505	7,4	680	88,10	25,98	33	4	451,16	7	15,05	18	-1,33
9340	19,3115	-21,8441	7,7	540	34,04	17,00	66	5	308,50	9	13,28	20	0,61
9385	19,3115	-21,3838	7,5	620	68,07	34,00	21	7	387,75	13	7,97	14	0,96
9336	19,3115	-21,9559	7,2	1220	148,16	17,97	114	3	424,33	145	30,54	103	1,97
1819ab1004	19,3117	-18,0917	7,7	600	62,07	34,00	12	10	402,39	1	2,21	3	-0,47
1919ad1002	19,3133	-19,3358	8,3	580	52,06	7,04	74	9	370,68	1	8,85	13	0,16
C291	19,3135	-17,9964	7,8	400	46,05	24,28	3	6	231,68	0	35,41	10	-0,76
8279	19,3144	-22,1036	7,5	680	56,06	18,94	72	4	397,51	15	11,07	29	-1,51
1819ab6	19,3150	-18,2717	7,7	400	72,88	5,59	4	4	268,26	6	0,00	5	-3,21
1819ad1001	19,3150	-18,2717	7,3	400	64,87	8,01	5	3	263,38	1	2,21	3	-3,08
9379	19,3154	-21,5036	7,7	710	77,28	35,94	31	6	393,85	15	6,64	42	1,57
1719cd1008	19,3170	-17,9280	8,0	480	64,87	18,94	8	7	309,72	1	2,21	5	0,47
899	19,3173	-20,7766	8,4	520	55,26	16,03	31	7	304,84	6	6,64	9	1,10
9384	19,3173	-21,3820	7,5	600	66,07	33,03	18	7	381,66	10	7,97	14	-0,07
8408	19,3173	-22,2144	7,3	670	68,07	22,10	55	4	402,39	9	8,85	29	-0,21
8502	19,3183	-22,0090	7,2	710	80,09	17,97	56	4	420,68	14	6,64	23	0,45
9334	19,3183	-21,9622	7,6	860	91,30	17,97	67	3	326,79	69	30,99	72	-1,62
9333	19,3183	-21,9667	7,9	1280	111,32	22,10	162	5	468,23	195	5,31	94	0,27
1819ab7	19,3183	-18,0058	7,5	470	48,05	21,86	44	6	359,71		0,00	15	-0,43
1819ab1006	19,3183	-18,0058	7,7	560	46,85	25,98	35	7	365,81	1	2,21	4	0,11
9344	19,3202	-21,7288	7,4	500	51,26	26,96	22	4	338,98	9	5,75	4	-0,96
8501	19,3202	-22,0432	7,4	720	79,29	16,03	61	4	420,68	10	6,64	40	-1,87
9368	19,3202	-21,6730	7,4	960	91,30	30,11	82	4	399,95	140	21,25	40	-1,10
1819ad3	19,3217	-18,3117	7,7	300	52,46	11,90	7	5	201,19	2	0,00	20	1,59
1919ad3	19,3228	-19,2809	7,1	840	68,07	21,13	109	18	506,03	26	1,77	25	3,86
8273	19,3231	-22,0802	7,6	750	88,10	17,97	51	3	407,26	22	6,64	43	-1,70
1919ad1	19,3246	-19,2876	8,1	480	26,43	10,69	64	17	249,97	6	22,13	20	2,60
W-15	19,3260	-19,2891	7,9	767	99,56	10,00	58	7	439,20	1	31,20	19	1,41
8285	19,3269	-22,1459	7,5	940	61,27	19,91	128	10	517,00	36	8,85	55	-1,85
8409	19,3269	-22,1937	8,2	1110	27,23	31,08	191	15	560,90	44	6,64	101	-1,78
9380	19,3279	-21,5009	7,6	570	33,24	34,00	40	7	301,18	19	0,00	34	0,67
9346	19,3288	-21,7604	7,4	590	83,29	18,94	25	4	387,75	4	4,43	6	1,66
9381	19,3288	-21,4135	7,5	1180	102,11	42,01	121	6	498,71	160	13,28	66	1,41
C444	19,3308	-19,3955	8,0	700	70,08	31,57	29	22	426,77	18	8,85	20	-0,98
1819cd01	19,3308	-18,8745	8,7	880	8,01	18,94	169	39	521,88	3	4,43	40	2,44
1819cb02	19,3320	-18,6289	8,9	1820	6,81	6,07	445	32	1024,26	42	13,28	123	-0,78

Appendix D: Hydrochemical data

Name	Long	Mlat	pH	ec µS/cm	Ca ²⁺ mg/l	Mg ²⁺ mg/l	Na ⁺ mg/l	K ⁺ mg/l	HCO ₃ ⁻ mg/l	SO ₄ ²⁻ mg/l	NO ₃ ⁻ mg/l	Cl ⁻ mg/l	Balance %
1719cd1004	19,3320	-17,8625	7,4	1900	62,87	17,97	360	6	916,95	15	61,97	153	-0,55
C285	19,3327	-17,9090	7,8	310	40,84	18,94	15	5	243,87	0	0,00	15	-0,48
9345	19,3327	-21,7252	7,5	540	54,06	27,93	24	4	363,37	10	5,75	5	-2,04
1819cd03	19,3339	-18,9563	8,7	480	14,02	19,91	51	28	280,45	2	8,85	8	2,59
1819cb01	19,3340	-18,7171	9,0	1690	6,01	19,91	380	25	660,89	75	22,13	195	2,29
1819ad1013	19,3375	-18,4867	7,6	420	56,86	16,03	3	14	270,70	1	2,21	2	1,04
9382	19,3413	-21,4180	7,5	1060	88,10	42,98	98	7	474,33	135	12,39	48	0,97
9337	19,3423	-21,9054	7,6	790	55,26	34,97	75	5	363,37	94	11,95	29	0,57
9383	19,3423	-21,4144	7,7	1120	87,29	42,98	116	7	462,13	160	11,07	54	1,99
C394	19,3433	-18,2856	7,8	420	55,26	15,06	10	10	280,45	6	0,00	5	-1,83
9349	19,3452	-21,7874	7,9	570	33,24	27,93	54	6	332,88	7	16,38	19	0,45
9338	19,3462	-21,8721	7,5	640	51,26	26,96	58	5	406,04	5	8,85	11	1,47
8489	19,3519	-22,0658	7,2	670	74,08	15,06	51	3	401,17	10	4,43	22	-1,66
919	19,3519	-21,2586	7,6	1880	145,36	42,98	203	7	540,17	360	7,53	122	-0,28
C408	19,3529	-19,3000	7,9	4250	10,01	7,77	955	9	509,69	495	172,64	699	2,08
8247	19,3548	-22,2135	7,3	400	80,09	27,93	52	6	493,84	8	6,20	20	-1,21
1819ab5	19,3583	-18,0133	7,2	11000	460,50	267,13	2485	62	548,71	4900	495,78	1350	-0,78
C283	19,3587	-18,0324	7,5	470	48,05	21,86	44	6	359,71	0	0,00	15	-0,43
1719cd5	19,3588	-17,8572	7,8	950	39,24	13,11	240	4	648,69	46	3,10	50	1,99
1719cd5	19,3588	-17,8572	7,8	1010	32,03	12,14	200	3	523,10	48	4,43	47	1,81
1719cd6	19,3591	-17,8577	8,0	1130	32,03	12,14	232	3	597,48	36	13,28	55	1,83
C302	19,3596	-18,4036	8,5	800	12,01	5,59	175	18	468,23	44	7,97	20	-0,82
C292	19,3615	-18,3342	7,7	300	52,46	11,90	7	5	201,19	2	0,00	20	1,59
1819ad1006	19,3633	-18,3367	7,5	400	62,87	8,99	3	5	253,63	1	2,21	4	-2,26
934	19,3635	-21,6279	8,4	940	59,26	23,07	127	8	312,15	195	8,85	28	2,30
1719cd1005	19,3650	-17,8680	7,3	500	72,08	16,03	12	5	317,03	1	2,21	10	0,28
8272	19,3654	-22,0883	7,4	630	75,28	15,06	43	3	381,66	9	6,64	24	-2,00
8549	19,3654	-21,7495	7,4	640	60,07	32,06	28	4	406,04	5	6,64	9	-1,17
8548	19,3663	-21,7297	7,5	520	45,25	25,01	30	4	328,01	12	6,64	4	-1,05
920	19,3663	-21,2910	7,7	550	48,05	22,10	28	6	291,42	15	12,39	15	-1,09
1819ab1002	19,3667	-18,1967	6,9	260	36,84	7,04	4	5	168,27	2	2,21	3	-3,54
8270	19,3683	-22,1559	7,3	710	84,09	20,88	45	6	430,43	9	6,64	35	-1,90
922	19,3721	-21,2973	7,8	670	61,27	36,91	17	7	415,80	5	8,41	8	-1,87
8271	19,3750	-22,1297	7,6	650	74,08	23,07	38	5	393,85	12	6,64	27	-1,32
8492	19,3750	-22,0441	7,2	790	102,11	23,07	37	4	386,53	7	5,75	70	0,91
8495	19,3760	-22,0063	7,2	730	74,08	17,00	68	4	445,06	10	3,10	20	0,24
8244	19,3760	-22,1856	7,4	840	77,28	33,03	65	10	506,03	13	17,71	41	-1,77
8269	19,3769	-22,1550	7,8	690	79,29	22,10	44	5	419,46	9	6,64	34	-1,95
921	19,3769	-21,2901	7,9	700	71,28	37,88	12	6	415,80	5	31,43	8	-2,01
929	19,3788	-21,5964	8,0	530	74,08	14,08	23	4	318,25	5	14,61	16	-0,40
8552	19,3788	-21,7694	7,4	770	46,05	25,98	74	6	313,37	87	11,51	30	-1,08
8245	19,3808	-22,1856	7,4	1040	46,05	18,94	172	14	563,34	33	18,15	70	-2,05
8243	19,3846	-22,2252	7,5	1100	99,31	44,93	75	13	526,76	11	81,89	90	-1,90
925	19,3856	-21,3459	7,7	550	63,27	15,06	31	3	304,84	6	10,62	17	0,43
8490	19,3865	-22,0694	7,4	640	72,08	20,88	37	4	373,12	8	3,54	23	0,28
8246	19,3865	-22,1856	7,3	1000	47,25	17,97	167	17	577,97	34	0,44	65	-2,06
8550	19,3875	-21,7288	7,3	710	68,07	33,03	31	4	424,33	10	5,31	21	-1,79
8494	19,3894	-21,9910	7,1	750	89,30	17,00	51	4	343,86	56	6,64	42	0,51
8498	19,3913	-22,0180	7,4	690	76,08	22,10	52	4	415,80	8	6,64	25	1,18
8556	19,3923	-21,8414	7,6	1770	62,07	42,01	275	8	341,42	500	11,07	90	0,00
8282	19,3933	-22,0874	8,0	680	76,08	22,10	40	4	393,85	6	4,43	36	-1,38
8499	19,3933	-22,0135	7,3	1010	75,28	19,91	114	4	334,10	170	8,85	60	-1,85
8554	19,3942	-21,7766	7,5	860	46,05	34,00	74	6	299,96	120	11,95	55	-3,92

Appendix D: Hydrochemical data

Name	Long	Mlat	pH	ec µS/cm	Ca ²⁺ mg/l	Mg ²⁺ mg/l	Na ⁺ mg/l	K ⁺ mg/l	HCO ₃ ⁻ mg/l	SO ₄ ²⁻ mg/l	NO ₃ ⁻ mg/l	Cl ⁻ mg/l	Balance %
8555	19,3990	-21,7324	7,3	970	84,09	42,01	52	6	381,66	27	11,95	111	-0,36
8500	19,4000	-22,0216	7,2	720	69,28	27,93	55	4	435,31	7	6,64	25	0,96
1919ad2	19,4030	-19,3028	7,2	415	76,08	2,43	24	6	298,74	3	0,00	10	-0,45
1819cd04	19,4033	-18,8752	8,1	700	38,84	19,91	80	22	414,58	11	10,62	21	-1,09
8253	19,4115	-22,1820	7,6	1230	33,24	15,06	242	21	631,62	61	17,71	90	-1,71
8560	19,4125	-21,7955	7,7	600	39,24	20,88	62	4	359,71	5	11,07	17	-1,38
1819ad1003	19,4133	-18,2680	7,4	430	58,86	14,08	8	5	280,45	1	2,21	2	-1,47
1819cb04	19,4149	-18,6293	8,5	440	20,82	31,08	18	21	265,82	1	8,85	7	2,07
8559	19,4154	-21,8000	7,8	630	36,04	19,91	77	4	378,00	6	13,28	20	-1,50
8267	19,4154	-22,1279	7,8	920	87,29	40,07	41	6	323,13	6	15,49	148	-1,31
923	19,4163	-21,2631	7,9	570	55,26	22,10	31	4	318,25	9	8,41	17	0,07
8557	19,4173	-21,8802	8,0	2010	129,34	44,93	270	4	457,26	610	8,85	79	-1,27
1819cd02	19,4178	-18,8004	8,5	1870	12,81	23,07	350	34	707,22	20	14,61	255	-2,11
1819cd06	19,4178	-18,8004	8,5	1870	12,81	23,07	350	34	707,22	20	14,61	255	-2,11
8281	19,4192	-22,0847	7,7	700	8,01	2,91	139	4	235,33	68	4,43	57	-1,19
8547	19,4192	-21,7135	7,4	860	58,06	34,97	74	6	408,48	46	48,69	29	-0,59
1819cb03	19,4195	-18,7183	8,8	870	12,81	8,99	185	25	543,83	15	11,07	14	1,34
1719cd3	19,4200	-17,9320	7,4	470	54,46	18,46	10	3	280,45	5	0,00	10	-2,41
1719cd1006	19,4200	-17,9320	7,9	510	62,87	23,07	14	6	321,91	1	6,64	5	2,23
8496	19,4212	-22,0225	7,3	770	83,29	16,03	66	4	430,43	8	3,10	39	0,46
8491	19,4231	-22,0468	7,4	650	84,09	18,94	26	4	320,69	7	7,53	48	0,80
8551	19,4240	-21,7225	7,6	730	55,26	32,06	57	6	429,21	25	6,20	18	-0,83
8251	19,4250	-22,2126	7,5	940	61,27	17,97	128	8	512,13	29	14,17	46	-1,03
8553	19,4279	-21,7703	7,7	930	69,28	40,07	62	6	306,06	146	8,85	64	-2,04
928	19,4298	-21,5856	7,4	850	75,28	36,91	53	7	401,17	95	12,84	27	-1,29
8252	19,4298	-22,2126	7,3	910	61,27	20,88	125	6	548,71	25	7,08	38	-1,58
8264	19,4298	-22,2297	7,4	1040	59,26	22,10	160	9	499,93	39	8,85	106	-0,71
927	19,4317	-21,5775	7,4	1410	100,11	52,94	112	7	332,88	245	14,61	130	-0,19
8558	19,4327	-21,8198	7,8	770	35,24	20,88	104	3	280,45	105	13,28	40	-0,29
926	19,4346	-21,5126	7,5	730	62,07	34,00	32	7	387,75	6	19,48	34	-1,89
8268	19,4346	-22,1568	7,5	1110	95,30	27,93	101	7	420,68	50	13,28	141	-2,11
1919ab1001	19,4350	-19,2016	8,0	520	36,04	3,89	79	7	295,08	9	8,85	14	1,53
8497	19,4365	-22,0216	7,2	700	77,28	22,10	49	4	401,17	8	5,75	32	1,10
1819ab1	19,4373	-18,0672	7,5	640	54,86	27,44	72	5	426,77	5	13,28	25	1,46
8493	19,4385	-22,0027	7,1	1050	90,10	17,97	125	3	430,43	105	6,20	67	1,14
1819ab1003	19,4392	-18,0667	7,3	410	58,06	13,11	6	5	256,06	1	2,21	4	-0,01
8579	19,4394	-21,9586	7,9	880	23,23	10,93	125	44	329,22	111	0,00	34	-0,26
8266	19,4404	-22,0694	7,4	840	82,09	22,10	74	4	376,78	14	11,07	100	-1,23
8545	19,4413	-21,6973	7,5	630	47,25	25,01	54	5	335,32	36	7,97	18	0,08
8578	19,4442	-21,9135	7,7	1490	111,32	33,03	168	4	152,42	510	13,28	74	0,85
1919ab2	19,4448	-19,2059	7,9	545	30,83	12,87	67	15	243,87	46	17,71	25	-0,42
8263	19,4462	-22,1802	8,2	1130	34,04	17,97	219	16	614,55	50	11,07	68	-0,37
C301	19,4587	-18,3063	7,8	720	28,43	26,47	109	28	486,52	24	12,39	15	-0,23
8546	19,4606	-21,7036	7,7	800	37,24	28,90	97	11	362,15	83	6,20	23	1,90
8562	19,4615	-21,7910	7,8	780	53,26	32,06	76	5	323,13	105	8,85	34	0,84
8564	19,4625	-21,7946	7,8	740	53,26	27,93	63	4	310,93	87	6,64	34	-1,11
8544	19,4635	-21,7613	7,8	830	52,06	33,03	77	6	357,27	103	12,39	32	-1,58
924	19,4654	-21,2631	7,2	680	68,07	24,04	29	5	263,38	7	28,33	66	-0,12
8563	19,4663	-21,8333	7,7	3920	44,05	45,90	770	7	646,26	1200	4,43	165	-0,82
C443	19,4721	-19,2306	7,9	550	30,83	12,87	67	15	243,87	46	17,71	25	-0,42
8261	19,4731	-22,1315	7,9	2560	165,38	54,88	325	8	435,31	245	35,41	480	1,43
8262	19,4750	-22,1622	7,6	1250	42,05	13,11	246	10	604,80	56	19,92	102	-0,50
8406	19,4760	-22,0604	7,4	640	85,29	17,00	37	3	356,05	6	9,74	55	-2,18

Appendix D: Hydrochemical data

Name	Long	Mlat	pH	ec µS/cm	Ca ²⁺ mg/l	Mg ²⁺ mg/l	Na ⁺ mg/l	K ⁺ mg/l	HCO ₃ ⁻ mg/l	SO ₄ ²⁻ mg/l	NO ₃ ⁻ mg/l	Cl ⁻ mg/l	Balance %
8265	19,4788	-22,2207	8,4	1040	22,02	9,96	227	12	598,70	29	8,85	65	-1,20
8488	19,4808	-22,0009	7,5	970	120,13	23,07	45	5	391,41	10	14,61	114	-0,48
1819ab1001	19,4823	-18,2000	6,9	420	60,87	9,96	10	5	263,38	2	2,21	3	-0,66
930	19,4865	-21,5027	8,4	420	50,05	11,90	17	4	213,39	5	15,05	14	0,93
1819da1058	19,4867	-18,6021	7,3	430	66,87	8,01	12	4	268,26	2	4,43	2	0,60
1919ad7	19,4869	-19,3668	8,0	340	23,63	14,81	37	2	237,77		8,41	5	-1,40
C286	19,4875	-18,0892	7,5	640	54,86	27,44	72	5	426,77	5	13,28	25	1,46
1819cd05	19,4883	-18,8828	7,1	320	44,05	6,07	11	8	190,22	1	2,21	3	1,84
8402	19,4885	-22,0721	7,5	520	65,27	17,97	30	3	323,13	9	14,61	24	-2,22
8258	19,4885	-22,1811	7,7	1150	50,05	22,10	194	14	579,19	61	15,49	88	-1,43
8404	19,4904	-22,0838	7,4	690	85,29	17,00	50	4	362,15	23	15,05	58	-2,22
8487	19,4913	-22,0036	7,3	780	100,11	18,94	40	4	401,17	10	5,75	55	-0,18
8405	19,4923	-22,0495	7,5	590	62,07	19,91	43	4	297,52	6	14,61	60	-1,62
8485	19,4942	-22,0216	7,2	690	76,08	17,00	45	4	378,00	8	5,75	32	-0,70
8577	19,4942	-21,8748	7,2	820	79,29	46,87	28	3	463,35	36	13,28	11	1,34
8403	19,4971	-22,0721	7,5	500	65,27	16,03	28	3	291,42	6	15,05	35	-2,17
8543	19,4971	-21,7387	7,6	720	58,06	30,11	54	7	365,81	32	19,92	28	0,84
1919ad1009	19,4975	-19,3317	7,4	500	78,08	3,89	25	7	304,84	3	11,07	6	0,70
8259	19,4990	-22,1712	7,8	1310	43,25	18,94	246	14	604,80	77	17,71	112	-0,62
1719dc7	19,5000	-17,8830	7,0	400	56,06	12,14	11	8	262,16	0	0,00	15	-2,61
8260	19,5000	-22,1153	7,3	3990	310,34	135,02	370	10	281,67	260	177,07	1000	2,21
941	19,5029	-21,5550	8,3	560	46,05	24,04	45	6	280,45	36	12,39	20	2,22
1819ba1006	19,5047	-18,0583	7,6	470	54,06	19,91	16	6	299,96	1	4,43	2	1,18
1819dc0	19,5063	-18,7939	7,8	630	40,04	34,00	32	31	409,70	18	2,21	10	-2,96
8407	19,5087	-22,0468	7,5	600	71,28	15,06	36	4	304,84	6	9,30	48	-1,23
8257	19,5087	-22,2198	7,9	1520	60,07	30,11	243	16	588,95	76	15,49	185	-0,75
931	19,5096	-21,4703	7,5	670	68,07	33,03	24	6	380,44	6	20,36	24	-0,36
8486	19,5096	-22,0126	7,2	740	84,09	17,00	57	4	430,43	10	4,43	30	-0,02
932	19,5106	-21,4775	7,5	550	59,26	25,01	22	4	332,88	11	13,28	11	-1,09
C416	19,5163	-19,3955	7,7	480	70,08	3,64	27	12	286,55	6	13,28	15	-1,68
1719dc1007	19,5270	-17,9980	7,9	740	80,09	45,90	7	13	417,02	81	2,21	4	-1,52
940	19,5279	-21,5432	7,6	1000	72,08	27,93	108	6	346,30	135	40,73	39	2,40
8535	19,5317	-21,6874	7,3	990	65,27	32,06	96	6	401,17	122	8,85	48	-1,86
8538	19,5394	-21,7288	7,3	820	60,07	34,97	66	7	414,58	46	25,23	29	-0,29
8537	19,5404	-21,7234	7,6	930	59,26	34,00	97	8	421,90	100	13,28	34	0,05
8401	19,5442	-22,0333	9,0	690	5,21	13,11	107	40	353,61	24	15,49	24	-1,44
8254	19,5452	-22,2000	7,4	3890	211,43	167,07	350	44	404,82	185	309,87	880	0,42
8399	19,5471	-22,0757	7,3	780	49,25	26,96	77	5	347,52	47	19,92	50	-1,52
8064	19,5471	-22,2595	7,2	1590	74,08	45,90	215	10	418,24	155	86,32	190	0,73
8063	19,5490	-22,2559	7,3	1460	79,29	43,95	168	8	407,26	100	91,63	165	0,66
1819da1057	19,5500	-18,6150	7,7	310	34,84	10,93	30	7	224,36	1	2,21	3	3,82
8576	19,5529	-21,8748	7,5	890	57,26	20,88	103	4	263,38	230	3,54	14	-2,13
8255	19,5529	-22,2072	7,5	2050	45,25	48,08	360	19	788,92	135	30,99	250	-2,04
8698	19,5548	-22,0991	7,3	950	52,06	34,97	113	7	402,39	82	19,92	60	1,22
1719dc1006	19,5580	-17,8700	7,5	420	56,86	8,99	18	4	207,29	1	37,63	9	2,10
8480	19,5587	-21,9595	7,8	730	89,30	18,94	55	4	286,55	82	10,18	74	-0,85
8482	19,5654	-21,9459	7,7	750	101,31	16,03	30	4	310,93	5	12,39	86	-0,28
1719dc8	19,5656	-17,8742	8,8	83	11,61	1,70	2	2	51,21	1	0,00	2	-3,33
1719dc1020	19,5700	-17,9640	7,7	680	60,87	18,94	58	6	346,30	3	2,21	49	0,81
8574	19,5712	-21,8694	7,8	1140	66,07	15,06	175	4	286,55	290	0,00	39	1,73
8481	19,5721	-21,9541	7,2	730	100,11	17,00	42	4	331,66	27	14,17	84	-1,61
8575	19,5721	-21,8640	7,5	990	49,25	25,98	138	4	390,19	160	8,85	28	0,20
8564	19,5731	-21,7739	7,6	490	26,03	11,90	73	3	317,03	5	8,85	4	-0,23

Appendix D: Hydrochemical data

Name	Long	Mlat	pH	ec µS/cm	Ca ²⁺ mg/l	Mg ²⁺ mg/l	Na ⁺ mg/l	K ⁺ mg/l	HCO ₃ ⁻ mg/l	SO ₄ ²⁻ mg/l	NO ₃ ⁻ mg/l	Cl ⁻ mg/l	Balance %
C305	19,5740	-18,1793	7,5	330	62,07	8,99	4	5	241,43	10	0,00	5	-1,98
8256	19,5788	-22,2099	7,6	2000	45,25	44,93	360	18	773,07	130	28,77	250	-1,82
8565	19,5798	-21,8378	8,3	1080	6,01	0,97	250	3	396,29	175	0,00	36	0,79
C287	19,5865	-17,9117	7,0	400	56,06	12,14	12	8	262,16	0	0,00	15	-2,12
8536	19,5885	-21,6928	7,4	610	53,26	26,96	37	6	357,27	20	5,75	7	0,58
933	19,5913	-21,4595	7,4	670	70,08	32,06	27	6	426,77	6	9,74	10	-0,64
8213	19,5971	-22,2288	7,3	1440	124,14	65,08	100	6	349,95	37	84,11	295	-0,40
8570	19,5981	-21,8523	7,4	620	55,26	35,94	25	4	396,29	10	4,43	10	-1,09
1819ba0	19,5992	-18,0738	6,9	330	56,86	6,07	6	5	202,41	1	13,28	5	0,44
8381	19,6000	-22,0838	7,2	1270	47,25	27,93	186	6	195,10	280	0,00	130	0,81
8569	19,6010	-21,8279	7,8	840	60,07	28,90	74	4	225,58	170	4,43	59	-1,56
8380	19,6029	-22,0505	7,5	810	63,27	13,11	91	4	292,64	68	26,56	62	-0,55
939	19,6029	-21,6225	8,2	1120	58,06	27,93	158	6	346,30	180	22,13	69	2,07
1819da1056	19,6033	-18,6167	7,8	320	36,84	16,03	6	7	207,29	2	2,21	1	1,33
1919bc1	19,6042	-19,3708		650	22,82	6,56	123	19	324,35	7	27,45	33	4,74
C300	19,6048	-18,1450	7,5	300	55,66	6,80	4	3	209,73	6	0,00	6	-1,96
8483	19,6058	-21,9946	7,7	560	31,23	8,01	75	3	214,61	29	15,49	45	-0,74
8250	19,6058	-22,1847	7,4	1300	68,07	40,07	119	7	170,71	31	19,92	310	-1,87
8378	19,6087	-22,0631	7,5	770	53,26	25,01	83	4	292,64	69	17,71	56	2,00
8379	19,6087	-22,0577	7,4	830	59,26	17,97	97	4	304,84	84	19,92	62	-0,32
1819ba1004	19,6150	-18,0633	6,9	190	26,03	5,10	2	3	114,62	1	2,21	5	-4,90
8249	19,6154	-22,1901	6,9	1500	74,08	45,90	138	7	163,39	55	30,54	355	-2,41
8477	19,6192	-21,8775	7,5	910	51,26	23,07	115	4	301,18	210	3,10	14	-1,00
8540	19,6212	-21,6937	7,5	630	59,26	26,96	25	5	325,57	15	12,39	27	-1,68
8478	19,6212	-21,8928	7,3	730	80,09	17,00	60	4	358,49	85	3,54	13	0,24
8248	19,6250	-22,1865	7,3	1630	77,28	40,07	175	7	145,10	74	32,31	390	-1,63
1719dc19	19,6268	-17,8640	8,0	1450	38,04	14,08	380	6	613,33	190	46,04	150	1,96
1719dc19	19,6268	-17,8640	7,9	2150	31,63	8,74	595	87	877,93	368	22,13	235	2,30
1719dc19	19,6268	-17,8640	7,8	2350	66,07	16,27	460	4	857,20	200	19,92	200	1,17
8382	19,6269	-22,0928	7,1	1680	113,32	34,00	188	6	365,81	205	30,99	225	-0,96
1719dc20	19,6277	-17,8628	8,2	1600	34,04	15,30	400	4	626,75	226	46,48	180	-0,84
1719dc20	19,6277	-17,8628	7,7	2610	54,06	20,16	620	4	902,32	210	0,00	420	0,67
C409	19,6292	-19,3973		650	22,82	6,56	120	19	335,32	7	27,45	35	2,17
8539	19,6308	-21,6640	7,4	590	67,27	34,97	3	5	386,53	5	2,66	2	-0,35
8484	19,6327	-21,9919	7,2	690	39,24	14,08	88	5	276,79	59	15,49	42	-0,88
8567	19,6346	-21,8180	7,6	1210	61,27	23,07	185	4	219,48	400	0,00	29	1,40
8566	19,6346	-21,7829	8,6	1870	2,00	0,97	420	2	469,45	380	13,28	75	1,55
8541	19,6365	-21,7198	7,6	810	33,24	20,88	115	6	381,66	77	8,85	20	-0,19
1919bc3	19,6367	-19,5033	7,9	460	55,26	6,56	31	14	268,26	5	3,98	10	1,59
1919da1002	19,6367	-19,5033	7,2	550	76,08	8,01	32	9	343,86	1	6,64	8	0,74
1919da1003	19,6370	-19,5042	7,6	550	76,08	8,01	32	8	346,30	1	6,64	8	0,20
8534	19,6567	-21,6640	7,4	560	55,26	31,08	16	6	357,27	8	9,30	3	-0,74
1819ba3	19,6583	-18,0292	8,0	325	50,86	11,66	2	1	213,39	5	0,00	5	-1,81
1819ba1002	19,6583	-18,0292	7,4	370	62,87	5,10	4	3	224,36	2	2,21	5	-1,14
8475	19,6596	-21,8586	7,5	720	69,28	25,98	50	5	334,10	110	3,98	11	-1,51
1919ba1001	19,6600	-19,0333	7,3	460	76,08	8,01	9	7	287,77	1	2,21	2	2,00
1819ba1003	19,6617	-18,0683	7,5	370	48,85	7,04	19	4	231,68	2	2,21	3	-0,16
8387	19,6663	-21,9180	7,1	1630	95,30	87,91	119	8	219,48	580	4,43	82	-1,94
8388	19,6673	-21,9423	7,3	990	59,26	11,90	135	5	170,71	260	4,43	68	-1,31
8384	19,6692	-22,0847	7,2	1210	75,28	34,97	145	5	463,35	95	88,53	62	1,24
1819da1050	19,6733	-18,7233	6,6	100	4,00	7,04	2	4	48,77	2	13,28	1	-5,59
8473	19,6740	-21,8748	7,4	1340	150,16	20,88	133	4	281,67	400	57,55	34	0,90
1919ba1002	19,6750	-19,0600	7,7	1050	48,05	13,11	162	10	399,95	120	2,21	65	-0,66

Appendix D: Hydrochemical data

Name	Long	Lat	pH	ec µS/cm	Ca ²⁺ mg/l	Mg ²⁺ mg/l	Na ⁺ mg/l	K ⁺ mg/l	HCO ₃ ⁻ mg/l	SO ₄ ²⁻ mg/l	NO ₃ ⁻ mg/l	Cl ⁻ mg/l	Balance %
8386	19,6769	-22,0505	7,6	670	33,24	24,04	91	6	353,61	52	4,43	20	1,54
8472	19,6769	-21,8712	7,4	1580	150,16	26,96	174	4	198,75	590	22,13	44	0,71
1719dc1005	19,6770	-17,9170	8,8	1480	6,81	3,89	330	4	531,64	146	42,05	112	-1,54
1719dc15	19,6770	-17,9170	7,4	8300	20,02	7,29	206	5	420,68	88	17,71	75	-2,02
8389	19,6779	-21,9387	7,2	710	84,09	10,93	52	3	262,16	72	15,49	50	-0,14
8242	19,6779	-22,1721	7,2	830	101,31	23,07	33	4	307,28	3	55,33	100	-1,85
8392	19,6808	-21,9586	7,2	590	61,27	18,94	41	3	286,55	26	15,49	42	-1,49
8212	19,6808	-22,2315	7,1	1900	185,40	48,08	161	5	286,55	315	39,84	305	-0,39
1719dc16	19,6810	-17,9180	8,5	125	10,41	4,61	2	1	54,87	0	0,00	5	-1,39
1719dc1004	19,6810	-17,9180	8,0	830	22,82	8,99	158	5	375,56	53	19,92	41	0,81
8568	19,6817	-21,8252	8,1	900	31,23	8,99	154	4	195,10	220	0,00	46	0,13
8241	19,6817	-22,1405	7,2	940	88,10	34,97	41	4	230,46	5	63,30	164	-1,97
1819da1055	19,6833	-18,6100	7,4	470	58,06	18,94	12	8	297,52	2	2,21	3	1,42
C288	19,6837	-17,8946	7,2	180	33,64	4,13	7	2	128,03	3	0,00	5	1,54
1819bc1001	19,6900	-18,4697	6,6	170	16,02	3,89	9	7	36,58	10	2,21	32	-1,64
8391	19,6904	-21,9541	7,4	600	61,27	14,08	46	3	243,87	39	15,49	44	-0,05
8390	19,6913	-21,9793	7,1	950	95,30	42,01	50	4	469,45	31	79,68	32	-0,17
1819dc1008	19,6917	-18,7833	7,6	240	36,04	8,01	3	5	153,64	1	2,21	2	1,60
8385	19,6923	-22,0243	7,1	810	90,10	34,00	41	4	536,51	11	6,64	16	-2,14
8474	19,6923	-21,8712	7,4	1480	150,16	27,93	166	4	203,63	560	22,13	55	0,62
8533	19,6942	-21,6414	7,2	990	74,08	42,01	77	9	463,35	67	11,07	60	-0,58
8383	19,6981	-22,0919	7,4	910	62,07	17,97	97	4	164,61	130	17,71	124	-1,60
8532	19,7000	-21,6459	7,3	710	68,07	35,94	29	6	434,09	15	6,64	11	-0,48
1719dc1003	19,7050	-17,9050	7,1	500	14,02	3,89	111	6	158,52	47	48,69	45	3,18
937	19,7077	-21,5018	7,6	790	80,09	35,94	38	6	457,26	7	29,66	33	-1,62
1819da1060	19,7117	-18,5650	7,3	260	28,03	13,11	6	6	153,64	11	2,21	2	0,93
8571	19,7125	-21,8225	7,5	880	56,06	25,01	95	5	213,39	200	4,43	50	-0,15
1819da1059	19,7166	-18,5825	7,4	490	62,87	17,00	9	9	258,50	55	8,85	7	-5,18
1819da1061	19,7193	-18,5536	7,4	510	44,05	18,94	35	8	248,75	55	2,21	5	0,78
1919da2	19,7217	-19,5350	8,0	320	37,24	15,06	17	11	195,10	8	4,43	15	3,26
1819dc1009	19,7217	-18,9252	7,7	640	22,02	10,93	107	10	334,10	46	2,21	11	0,94
1819da1062	19,7250	-18,5350	7,0	350	32,03	17,97	7	8	114,62	73	15,49	7	-3,49
W-32	19,7256	-20,6667	7,8	2399	215,20	28,00	143	8	184,22	711	16,40	47	0,12
8393	19,7269	-21,9595	7,4	750	86,09	28,90	36	3	432,87	26	24,35	18	-1,30
1919da1005	19,7283	-19,5183	7,3	540	78,89	11,90	11	11	297,52	1	33,20	10	-0,34
938	19,7288	-21,5568	7,6	940	73,28	27,93	99	6	367,02	120	17,26	50	1,03
1719dc17	19,7300	-17,9120	8,6	1245	8,41	4,61	348	29	597,48	187	0,00	83	1,99
1719dc1002	19,7300	-17,9120	8,3	1690	8,01	2,91	390	4	636,50	215	4,43	88	0,70
1719dc1	19,7325	-17,9588	8,3	520	40,04	15,30	70	3	292,64	26	4,87	20	3,23
1719dc1	19,7325	-17,9588	8,2	640	34,04	12,14	80	3	301,18	30	2,21	18	1,22
1719dc2	19,7330	-17,9573	8,5	320	24,43	16,76	17	7	201,19	8	0,00	5	-1,24
1719dc2	19,7330	-17,9573	8,2	610	38,04	14,08	86	3	297,52	34	6,64	39	0,61
8395	19,7337	-21,9414	7,6	620	67,27	10,93	58	3	353,61	30	11,07	16	-1,39
W-17	19,7342	-19,5194	8,0	505	80,00	12,80	12	8	294,02	0	20,96	6	3,93
C445	19,7346	-19,5505	8,3	390	74,08	12,14	3	6	249,97	9	17,71	20	-1,52
8394	19,7346	-21,9586	7,3	680	77,28	23,07	39	3	408,48	25	13,28	14	-1,93
8573	19,7375	-21,8360	7,8	610	53,26	19,91	52	4	298,74	51	4,43	14	1,81
8470	19,7375	-21,8739	7,7	660	65,27	15,06	59	3	315,81	65	3,98	19	0,07
8572	19,7394	-21,8297	7,6	750	46,05	8,99	114	2	280,45	135	0,00	12	1,91
1819da1002	19,7400	-18,5042	7,4	480	62,07	15,06	16	1	241,43	56	2,21	5	-2,33
1919da1	19,7417	-19,5200	8,3	394	74,08	12,14	3	6	249,97	9	17,71	20	-1,52
8471	19,7423	-21,8757	7,4	680	59,26	8,99	79	3	291,42	110	0,00	14	-1,71
C417	19,7423	-19,4613	7,5	750	76,08	23,07	14	10	286,55	15	20,81	40	0,67

Appendix D: Hydrochemical data

Name	Long	Lat	pH	ec µS/cm	Ca ²⁺ mg/l	Mg ²⁺ mg/l	Na ⁺ mg/l	K ⁺ mg/l	HCO ₃ ⁻ mg/l	SO ₄ ²⁻ mg/l	NO ₃ ⁻ mg/l	Cl ⁻ mg/l	Balance %
8530	19,7423	-21,6441	7,4	1210	58,06	37,88	163	9	507,25	213	4,43	35	-1,74
8531	19,7423	-21,6243	7,2	1640	73,28	54,88	203	10	448,72	375	9,74	96	-2,18
8215	19,7442	-22,2045	7,1	1090	126,14	33,03	62	4	486,52	22	62,42	102	-2,09
1719dc1001	19,7455	-17,9923	8,2	530	24,03	8,01	90	4	299,96	24	22,13	5	-0,32
1719dc14	19,7455	-17,9923	7,9	540	12,01	3,64	141	3	347,52	62	0,00	10	-1,11
1819da1052	19,7467	-18,6867	6,7	130	8,81	5,10	9	6	60,97	1	2,21	9	3,49
1819da1001	19,7472	-18,5325	7,3	370	58,86	9,96	4	5	219,48	16	2,21	2	0,45
1819dc1010	19,7483	-18,9500	6,8	90	6,01	2,91	3	3	23,17	2	4,43	7	3,94
1819da1051	19,7500	-18,6942	7,0	320	42,85	8,99	8	4	192,66	1	17,71	6	-4,39
8214	19,7519	-22,2036	7,3	1120	133,35	33,03	66	4	486,52	20	61,09	120	-1,65
C289	19,7529	-17,9477	8,5	130	10,41	4,61	2	1	54,87	0	0,00	5	-1,39
8218	19,7538	-22,1523	7,1	1130	134,15	34,97	45	5	230,46	5	73,92	215	2,28
1819bb1008	19,7567	-18,0433	7,3	630	72,08	17,00	23	13	202,41	90	2,21	15	5,67
8396	19,7577	-21,9153	7,2	1150	126,14	17,00	97	4	323,13	245	8,85	72	-2,26
8216	19,7577	-22,2342	7,2	2070	162,18	50,03	207	8	449,94	125	141,65	345	-1,32
8217	19,7587	-22,1514	7,1	840	72,08	32,06	44	5	204,85	5	22,13	142	2,81
8529	19,7587	-21,6207	7,6	1330	31,23	41,04	188	12	145,10	350	0,00	111	2,38
1819bb1007	19,7600	-18,0717	7,6	310	54,06	6,07	3	4	148,76	36	2,21	4	1,39
1819bd1003	19,7633	-18,4417	6,4	180	8,81	8,01	11	9	56,09	38	2,21	3	-0,63
1819bb1006	19,7650	-18,1088	6,2	110	14,82	2,91	2	3	51,21	13	4,43	3	-5,11
8397	19,7673	-21,8811	7,3	910	53,26	15,06	122	3	195,10	250	0,00	30	0,17
1819bb1003	19,7675	-18,1433	6,7	180	28,83	5,10	4	2	114,62	1	2,21	3	1,56
1819bd1004	19,7767	-18,4200	7,5	370	58,06	8,01	7	7	207,29	29	2,21	4	-1,33
1819bd1005	19,7883	-18,4042	7,5	360	56,06	8,99	5	4	236,55	1	2,21	2	-1,70
935	19,7923	-21,3892	7,4	870	70,08	37,88	84	8	464,57	51	23,46	40	1,41
8237	19,7942	-22,0811	7,4	350	38,04	9,96	25	2	191,44	9	13,28	13	-0,64
8220	19,7962	-22,2243	7,2	2830	228,25	51,00	305	9	440,19	265	50,91	590	-1,87
C393	19,7990	-18,5162	8,6	230	28,03	13,36	5	8	152,42	0	0,00	10	2,45
8463	19,8000	-21,8820	7,3	1530	204,22	51,97	95	4	328,01	560	0,00	36	1,77
8222	19,8010	-22,1468	7,1	630	53,26	30,11	41	5	340,20	5	15,94	45	-1,12
8526	19,8029	-21,6523	7,3	830	65,27	42,01	55	10	473,11	62	7,97	8	-0,19
1919dd2	19,8046	-19,8462	7,1	1000	32,44	14,33	158	29	292,64	23	110,67	100	2,62
1719dd1001	19,8050	-17,8950	8,0	6860	10,81	30,11	1700	2	2499,67	380	2,21	1010	-0,25
8462	19,8058	-21,8838	7,0	890	87,29	41,04	46	5	473,11	65	0,00	33	-0,88
8528	19,8058	-21,6360	7,4	1580	72,08	62,90	176	10	453,60	350	0,00	84	-1,20
C299	19,8087	-18,0198	7,9	540	12,01	3,64	141	3	347,52	62	0,00	10	-1,11
1819bd2	19,8090	-18,4979	7,6	290	44,05	7,29	7	4	189,00	5	0,00	5	-2,11
8527	19,8096	-21,6640	7,6	2210	75,28	50,03	320	10	318,25	700	5,31	108	-1,94
1819bd1006	19,8100	-18,4192	7,3	620	88,10	16,03	24	5	409,70	2	2,21	11	-1,54
1719dd9	19,8130	-17,9070	7,8	460	42,05	14,57	46	3	298,74	15	0,00	10	-1,06
8461	19,8192	-21,8883	7,0	830	84,09	33,03	47	3	363,37	130	3,10	26	-2,22
8223	19,8202	-22,1604	7,3	720	100,11	32,06	19	4	508,47	5	15,49	9	-2,16
8239	19,8212	-22,0396	8,0	480	34,04	11,90	54	3	189,00	65	2,66	25	-0,93
8219	19,8221	-22,2270	7,1	2180	200,22	37,88	217	6	460,91	205	56,22	390	-2,21
C297	19,8250	-17,9369	8,0	1150	18,82	6,80	241	4	310,93	205	4,43	88	0,69
1819bd1007	19,8250	-18,4133	8,0	1170	179,80	14,08	62	4	424,33	240	2,21	40	-0,71
8240	19,8260	-22,0667	7,4	610	68,07	13,11	41	2	198,75	28	13,28	86	-1,33
8464	19,8260	-21,8946	7,3	620	72,08	13,11	45	3	301,18	59	3,10	20	-0,51
8221	19,8260	-22,1396	7,3	910	46,05	23,07	130	4	368,24	130	7,08	44	-0,72
1719dd17	19,8278	-17,9948	7,6	100	16,02	2,43	8	1	79,26	0	0,00	0	2,76
1719dd10	19,8284	-17,8910	7,3	465	68,07	24,28	15	4	353,61	2	0,00	10	0,25
C293	19,8288	-17,9468	8,1	1200	16,02	13,36	273	2	420,68	180	0,00	95	1,85
8468	19,8308	-21,8108	7,5	830	54,06	33,03	70	6	219,48	225	3,10	21	-1,77

Appendix D: Hydrochemical data

Name	Long	Mlat	pH	ec µS/cm	Ca ²⁺ mg/l	Mg ²⁺ mg/l	Na ⁺ mg/l	K ⁺ mg/l	HCO ₃ ⁻ mg/l	SO ₄ ²⁻ mg/l	NO ₃ ⁻ mg/l	Cl ⁻ mg/l	Balance %
C298	19,8308	-17,9369	8,3	1250	22,02	6,07	278	3	414,58	205	6,20	95	-0,27
1819bd4	19,8317	-18,3675	7,9	400	62,07	12,14	14	6	302,40	4	3,10	5	-3,68
1719dd1004	19,8320	-17,9970	8,1	1190	28,83	34,97	190	21	802,33	2	22,13	6	-2,23
8238	19,8327	-21,9802	7,2	960	95,30	16,03	91	3	184,12	290	3,98	42	-0,95
8519	19,8346	-21,7586	7,2	1140	41,24	32,06	180	6	231,68	330	3,54	48	2,43
8518	19,8346	-21,7270	7,5	1850	44,05	56,10	298	11	260,94	600	11,95	78	2,29
1719dd1002	19,8350	-17,9150	7,5	760	36,84	16,03	115	4	363,37	56	13,28	30	0,49
W-18	19,8426	-19,4577	7,9	463	65,72	8,00	17	8	278,77	0	4,92	7	-0,01
1919bd2	19,8431	-19,4575	7,4	1330	112,52	15,54	170	26	384,10	23	15,49	282	-0,08
W-33	19,8432	-20,6441	7,7	3300	429,60	56,00	286	9	157,38	1300	9,00	311	0,18
1819bd1008	19,8492	-18,3567	7,1	320	46,05	6,07	11	4	199,97	3	2,21	2	-0,79
8454	19,8538	-21,9631	7,5	400	35,24	7,04	39	3	180,46	35	11,07	12	-1,11
8232	19,8587	-22,0775	7,4	440	36,04	14,08	38	3	225,58	26	15,05	10	-0,80
8467	19,8587	-21,8072	7,6	670	37,24	19,91	58	44	336,54	25	12,39	6	5,46
8226	19,8635	-22,2090	7,4	3800	144,16	28,90	645	9	191,44	740	95,17	670	-1,46
1819bb2	19,8641	-18,0455	7,4	2300	56,06	34,00	372	9	426,77	260	13,28	330	0,17
8453	19,8644	-21,8829	7,1	670	107,32	14,08	23	4	443,84	5	3,10	6	0,13
8230	19,8663	-22,0964	7,3	1150	98,11	27,93	122	4	363,37	175	20,36	100	-0,57
8228	19,8683	-22,1162	8,0	1220	21,22	13,11	226	7	342,64	140	64,19	110	-2,10
1819bb1004	19,8692	-18,2016	7,5	320	56,86	3,89	8	2	199,97	1	2,21	3	1,98
C426	19,8692	-19,4928	8,3	440	64,07	6,07	13	9	256,06	3	6,20	10	-1,63
8452	19,8702	-21,8811	7,2	680	106,12	15,06	27	4	415,80	7	12,84	12	1,99
8233	19,8702	-22,0432	7,3	1000	81,29	20,88	109	3	156,08	315	4,43	38	1,60
1919dd3	19,8728	-19,9068	7,8	1800	26,83	12,87	431	39	249,97	370	159,36	225	3,33
1819bd3	19,8733	-18,4050	7,8	560	83,69	16,76	18	4	378,00	3	4,43	10	-1,31
8224	19,8760	-22,1423	8,0	1460	43,25	17,00	272	7	460,91	250	11,51	108	-1,34
8231	19,8760	-22,1027	7,2	1660	95,30	22,10	252	5	296,30	335	5,75	200	0,28
W-34	19,8774	-20,6282	7,8	3330	349,60	42,40	400	13	157,38	1200	25,40	309	2,61
1919db3	19,8776	-19,7308	8,3	2020	24,43	17,97	512	60	621,87	486	70,83	170	0,48
1919db1	19,8790	-19,6198	7,7	570	71,28	11,66	47	10	323,13	5	20,81	23	3,27
1719dd11	19,8797	-17,8874	7,6	800	14,42	7,04	193	3	408,48	97	0,00	35	0,36
8525	19,8817	-21,6514	7,4	1540	43,25	33,03	290	8	632,84	220	15,49	57	2,57
1919dd1	19,8846	-19,7885	8,8	3135	35,24	22,34	788	112	463,35	841	199,20	425	0,54
8225	19,8875	-22,1721	7,3	1460	127,34	22,10	165	5	480,42	120	32,76	186	-2,11
8520	19,8875	-21,7252	7,3	2160	66,07	82,08	285	12	295,08	770	9,74	92	-1,86
C309	19,8894	-18,3964	7,9	400	63,67	13,11	14	6	302,40	4	3,10	5	-2,06
8227	19,8904	-22,1243	7,4	670	94,10	26,96	14	3	414,58	5	39,40	7	-0,86
1719dd1006	19,8920	-17,9530	7,5	420	48,05	17,00	17	4	275,57	1	2,21	3	-0,20
8521	19,8923	-21,6387	7,4	1450	45,25	32,06	262	9	601,14	200	15,05	52	2,47
8234	19,8952	-22,0640	7,1	1550	164,18	34,97	115	5	419,46	120	265,60	113	-1,95
C448	19,8962	-19,9315	7,8	1800	26,83	12,87	428	39	249,97	370	159,36	225	3,03
8469	19,8981	-21,8261	7,6	560	41,24	15,06	62	3	291,42	49	15,94	5	-1,01
1819bd1010	19,9000	-18,3658	7,8	1200	110,12	50,03	42	16	212,17	430	13,28	16	-5,00
1719dd1010	19,9000	-17,8930	8,1	10130	2,00	6,07	2650	9	3370,29	2000	154,93	900	-3,60
1919dd4	19,9001	-19,9020	7,8	1370	38,04	21,37	220	17	249,97	115	216,91	135	-0,49
C414	19,9058	-19,6333	7,7	570	71,28	11,66	47	10	335,32	5	20,81	23	1,73
C446	19,9077	-19,8126	8,5	3350	37,24	29,63	900	112	414,58	1015	208,05	495	1,16
1819bb1005	19,9167	-18,1725	7,3	560	68,07	20,88	21	7	370,68	1	2,21	6	-0,74
C415	19,9192	-19,9279	7,8	1370	38,04	21,37	220	17	249,97	115	216,91	135	-0,49
C310	19,9298	-18,0586	7,6	100	16,02	2,43	7	1	79,26	0	0,00		1,15
8456	19,9298	-21,9396	7,4	500	42,05	6,07	65	3	243,87	57	0,00	11	0,07
C306	19,9298	-18,4405	7,8	560	83,69	16,76	18	4	378,00	3	4,43	10	-1,31
8458	19,9308	-21,8649	7,2	780	65,27	34,97	64	4	415,80	63	3,54	20	1,54

Appendix D: Hydrochemical data

Name	Long	Lat	pH	ec µS/cm	Ca ²⁺ mg/l	Mg ²⁺ mg/l	Na ⁺ mg/l	K ⁺ mg/l	HCO ₃ ⁻ mg/l	SO ₄ ²⁻ mg/l	NO ₃ ⁻ mg/l	Cl ⁻ mg/l	Balance %
8236	19,9317	-22,0829	7,6	590	71,28	23,07	33	2	363,37	21	17,71	13	-0,73
8460	19,9356	-21,8928	7,3	780	71,28	23,07	68	4	378,00	81	4,43	25	-0,83
8235	19,9385	-22,0685	7,4	770	109,32	20,88	27	3	429,21	7	76,58	10	-1,59
936	19,9413	-21,4162	8,4	630	64,07	30,11	29	8	415,80	4	16,82	8	-1,74
1719dd13	19,9420	-17,9210	7,6	560	3,20	1,70	147	3	189,00	19	0,00	120	-0,79
1719dd1009	19,9420	-17,9210	8,6	720	4,81	0,97	176	3	395,07	50	2,21	19	-0,22
8229	19,9442	-22,1874	7,2	1690	190,21	22,10	137	5	460,91	115	39,84	270	-2,27
8459	19,9519	-21,8631	7,5	610	41,24	20,88	69	3	296,30	62	3,10	16	1,53
1819bb1	19,9525	-18,0458	7,0	520	72,08	21,86	17	4	332,88	9	6,64	20	-0,61
8515	19,9538	-21,7450	7,4	1120	52,06	41,04	138	5	226,80	380	0,00	24	-0,82
8516	19,9538	-21,7486	7,7	1130	26,03	24,04	185	3	212,17	375	0,00	20	-1,93
8523	19,9538	-21,6153	8,5	1600	2,00	0,97	390	3	798,68	130	0,00	55	-0,37
C312	19,9548	-17,9162	7,6	800	14,42	7,04	193	3	408,48	97	0,00	35	0,36
8517	19,9567	-21,7054	7,6	1600	38,04	39,10	257	7	212,17	530	0,00	54	1,35
1819dd0	19,9577	-18,7568	6,6	1420	166,98	27,93	95	12	799,89	16	2,21	71	-1,34
1819bd1012	19,9583	-18,3583	7,3	520	86,89	14,08	9	4	356,05	2	2,21	1	0,40
8466	19,9606	-21,7838	8,0	370	13,21	11,90	50	5	217,04	18	0,00	5	-1,64
8524	19,9606	-21,6117	8,9	1810	0,00	1,94	440	2	584,07	312	0,00	83	2,49
8514	19,9644	-21,7477	7,7	1080	45,25	31,08	145	5	212,17	370	0,00	21	-2,27
8455	19,9663	-21,9108	7,3	660	65,27	22,10	52	3	363,37	35	5,75	23	-0,08
8457	19,9683	-21,8910	7,2	690	88,10	26,96	28	4	468,23	9	0,00	8	-0,95
W-19	19,9691	-19,4585	7,9	1572	135,60	22,30	182	19	389,18	3	14,20	356	0,87
1919bd1001	19,9717	-19,4590	7,4	1550	116,13	19,91	169	21	390,19	3	6,64	300	0,97
1719dd14	19,9740	-17,9440	8,5	830	19,62	3,89	184	2	408,48	67	6,20	34	1,11
1719dd1007	19,9740	-17,9440	9,0	1200	6,01	1,94	275	2	504,81	165	2,21	50	-2,66
8565	19,9740	-21,8234	7,5	500	49,25	20,88	29	5	304,84	10	8,85	7	0,19
1919dd5	19,9870	-19,9436	7,7	3025	76,48	49,54	561	85	280,45	705	420,53	255	1,80
1719dd1008	19,9900	-17,9180	8,1	480	8,81	3,89	107	3	278,01	19	2,21	8	2,59
8522	19,9904	-21,6135	8,8	2160	2,00	3,89	535	3	685,28	400	0,00	106	2,63
C264	19,9913	-17,9270	7,6	560	3,20	1,70	147	3	189,00	19	0,00	120	-0,79
9414	20,0067	-21,3901	7,5	560	61,27	13,11	48	4	314,59	32	5,75	16	-0,31
1721cc1001	20,0080	-17,9700	6,7	4970	72,08	129,92	800	7	160,95	1650	51,79	510	-2,90
1820aa1007	20,0083	-18,0500	7,6	710	30,83	25,98	93	15	463,35	4	68,61	6	-4,97
1820ac01	20,0157	-18,3425	8,5	810	120,93	27,93	29	11	307,28	61	2,21	110	2,23
1721cc1002	20,0180	-17,9830	7,6	500	58,86	18,94	21	5	278,01	20	2,21	13	1,49
C311	20,0192	-18,0721	7,0	520	72,08	21,86	22	4	353,61	9	6,64	20	-1,52
C389	20,0202	-18,0198	7,9	560	74,08	19,43	15	7	341,42	2	0,00	10	1,72
1820ac1003	20,0223	-18,4453	7,4	640	74,88	13,11	52	5	395,07	6	11,07	16	-0,16
1820ac1004	20,0223	-18,3443	7,5	840	80,89	41,04	45	12	524,32	4	19,92	26	-0,27
1820aa1006	20,0267	-18,2000	7,4	850	76,08	48,08	42	15	568,22	1	2,21	15	0,87
3747	20,0279	-22,0081	7,7	1080	91,30	8,01	136	3	235,33	297	15,94	38	-0,71
3749	20,0279	-21,9721	8,0	1820	118,13	50,03	215	7	114,62	825	0,00	40	-1,61
1720cc17	20,0319	-17,9071	8,2	340	52,06	16,27	20	4	258,50	8	8,85	7	1,71
1820ac02	20,0365	-18,3740	7,5	920	156,17	17,97	29	8	585,29	9	2,21	15	2,38
3745	20,0375	-21,8595	7,4	730	71,28	36,91	29	4	459,70	8	0,00	7	0,38
1820aa1004	20,0558	-18,1800	8,3	3490	16,82	22,10	820	30	1594,91	210	4,43	320	-0,65
1820aa1009	20,0566	-18,0667	7,6	360	40,04	18,94	12	4	246,31	1	2,21	2	0,38
3748	20,0567	-21,9937	7,4	740	85,29	14,08	56	3	351,17	89	5,75	10	-0,35
1721cc1003	20,0600	-17,9620	6,7	1630	108,92	37,88	151	6	124,37	280	2,21	295	-3,02
1820aa1008	20,0617	-18,1083	8,2	1380	8,01	8,01	320	15	870,62	46	2,21	24	-1,84
1820ac1001	20,0767	-18,2667	7,4	660	48,85	25,98	60	8	434,09	2	30,99	4	-2,49
1721cc8	20,0790	-17,9750	7,2	420	63,27	15,06	8	2	274,35	7	0,00	10	-1,33
1721cc1004	20,0800	-17,9710	7,4	540	62,07	17,97	27	4	346,30	7	2,21	5	-1,22

Appendix D: Hydrochemical data

Name	Long	Lat	pH	ec µS/cm	Ca ²⁺ mg/l	Mg ²⁺ mg/l	Na ⁺ mg/l	K ⁺ mg/l	HCO ₃ ⁻ mg/l	SO ₄ ²⁻ mg/l	NO ₃ ⁻ mg/l	Cl ⁻ mg/l	Balance %
1920ca1002	20,0817	-19,5150	7,5	500	52,86	8,99	31	12	214,61	2	33,20	34	-0,21
1720cc1001	20,0870	-17,9730	8,1	490	22,02	13,11	75	5	309,72	10	2,21	4	1,23
1920cc6	20,0898	-19,8586	7,9	770	16,42	16,76	147	39	432,87	29	8,85	50	1,80
3746	20,0904	-21,9739	7,2	1040	102,11	25,01	87	4	408,48	172	21,69	29	-1,79
1720cc3	20,0915	-17,9099	7,4	425	31,63	18,46	49	4	225,58	29	48,69	15	-1,64
3744	20,0962	-21,9108	7,2	1520	150,16	32,06	133	6	448,72	205	22,13	152	-0,61
1920ac1003	20,0967	-19,3480	7,5	220	14,02	1,94	15	5	87,79	1	2,21	4	0,97
1820aa0	20,0992	-18,2372	7,6	2110	166,98	42,98	268	13	773,07	180	8,85	245	0,82
1920ac5	20,1067	-19,4483	8,0	450	53,66	2,67	64	10	298,74	9	8,85	25	0,05
3742	20,1067	-21,7973	7,8	540	35,24	17,97	56	4	287,77	31	13,72	4	0,69
1920ac4	20,1100	-19,4450	8,1	310	32,84	9,23	17	9	182,90	6	0,00	10	-0,55
1720cc5	20,1357	-17,9062	9,1	1600	6,01	0,00	442	6	834,04	160	9,30	60	2,17
1720cc4	20,1380	-17,9050	8,1	785	64,07	48,57	50	5	530,42	6	7,53	20	-0,04
3741	20,1394	-21,8315	7,5	480	39,24	24,04	26	3	287,77	14	0,00	9	-1,13
3743	20,1394	-21,9486	7,8	1370	106,12	18,94	177	6	252,41	430	17,71	70	-2,14
W-35	20,1432	-20,6802	7,9	3030	228,40	90,00	368	10	195,20	1000	18,10	391	-0,37
C451	20,1500	-19,4784	8,0	500	53,66	2,67	64	10	298,74	9	8,85	25	0,05
C322	20,1519	-18,0072	7,7	270	8,81	3,16	50	4	152,42	3	13,28	6	0,55
3740	20,1529	-21,8541	8,5	780	22,02	8,99	128	8	171,93	170	23,02	32	-0,13
1720cc11	20,1639	-17,8929	7,5	800	32,03	24,28	109	5	420,68	44	0,00	35	-1,92
1720cc9	20,1692	-17,8874	7,3	365	26,03	23,07	43	3	298,74	4	0,00	10	-1,12
C449	20,1692	-19,8901	8,4	550	12,41	10,69	97	16	329,22	11	4,43	15	0,07
1720cc8	20,1699	-17,8860	7,3	390	54,06	14,57	35	3	323,13	4	0,00	10	-1,48
1720cc12	20,1748	-17,8886	9,2	1750	2,00	1,21	425	6	774,29	163	0,00	78	1,50
C316	20,1875	-17,9577	9,1	1600	6,01	0,00	442	6	834,04	160	9,30	60	2,17
C315	20,1904	-17,9486	8,1	790	64,07	48,57	50	5	530,42	6	7,53	20	-0,04
1720cc1002	20,1930	-17,9730	8,3	260	6,01	1,94	53	4	153,64	1	2,21	2	4,30
1720cc2	20,1930	-17,9730	7,7	270	8,81	3,16	50	4	152,42	3	13,28	6	0,55
V-18	20,1931	-19,0897	7,3	1147	119,00	20,70	106	5	580,00	16	3,40	105	-1,92
1920aa3	20,1950	-19,0892	7,5	615	58,86	18,94	43	4	256,06	62	0,00	30	1,06
1820ba1015	20,1967	-18,1950	7,8	450	38,04	25,98	20	4	295,08	5	2,21	4	-0,79
C308	20,1990	-18,2225	8,3	350	53,26	10,20	7	2	219,48	3	0,00	5	0,68
1920ca3	20,2040	-19,5433	7,5	1010	55,26	22,34	128	25	415,80	45	2,66	118	-1,46
C317	20,2058	-17,9450	7,5	800	32,03	24,28	109	5	420,68	44	0,00	35	-1,92
C351	20,2087	-19,1243	7,5	620	58,86	18,94	43	4	256,06	62	0,00	30	1,06
1720cc13	20,2117	-17,8971	9,1	1530	4,00	1,21	406	5	798,68	161	2,66	58	-0,09
3737	20,2125	-21,7703	8,1	540	25,23	15,06	68	4	238,99	54	17,71	14	-1,45
C318	20,2173	-17,9243	7,5	500	100,11	18,21	6	3	408,48		0,00	5	-0,03
3739	20,2173	-21,8757	7,1	880	125,34	20,88	27	3	448,72	14	46,04	32	-0,36
3738	20,2192	-21,7144	8,1	600	44,05	25,98	49	5	338,98	31	13,72	7	-0,18
C320	20,2212	-17,9288	7,6	450	48,05	32,78	21	3	359,71		0,00	5	0,41
C319	20,2240	-17,9234	7,6	590	51,66	36,67	13	3	371,90	0	0,00	5	0,01
C411	20,2279	-19,5811	7,2	420	39,24	10,20	31	16	225,58		1,77	30	-0,18
1820aa1001	20,2333	-18,2000	7,3	860	76,88	37,88	51	11	451,16	4	4,43	57	1,60
C313	20,2346	-17,9396	9,2	1750	2,00	1,21	425	6	774,29	163	0,00	78	1,50
V-16	20,2368	-19,2348	6,7	1895	315,00	29,70	95	8	468,00	528	1,60	95	2,57
1720cc1003	20,2450	-17,8970	7,8	330	26,83	17,00	21	3	219,48	1	2,21	5	-0,89
1720cc15	20,2450	-17,8970	8,3	413	24,83	37,15	17	12	249,97	21	0,00	30	-0,35
W-46	20,2506	-21,7788	7,8	1583	102,00	54,80	215	8	525,82	195	7,50	180	3,46
C450	20,2577	-19,5820	7,9	650	50,05	16,51	84	8	285,33	13	0,00	86	2,27
1720cd1	20,2580	-17,8907	7,1	420	34,04	18,21	16	4	164,61		0,00	50	-1,39
3736	20,2654	-21,7784	7,6	480	45,25	16,03	30	4	241,43	23	14,17	10	0,38
C314	20,2663	-17,9532	9,1	1530	4,00	1,21	406	5	798,68	161	2,66	58	-0,09

Appendix D: Hydrochemical data

Name	Long	Mlat	pH	ec µS/cm	Ca ²⁺ mg/l	Mg ²⁺ mg/l	Na ⁺ mg/l	K ⁺ mg/l	HCO ₃ ⁻ mg/l	SO ₄ ²⁻ mg/l	NO ₃ ⁻ mg/l	Cl ⁻ mg/l	Balance %
C429	20,2750	-19,2775	7,4	2000	216,64	44,68	147	12	463,35	513	0,00	123	-1,29
3735	20,2769	-21,8396	7,9	1690	118,13	18,94	265	6	167,05	750	7,08	45	-1,55
1920ad4	20,2850	-19,3367	8,6	340	41,24	13,84	11	8	152,42	44	0,89	10	2,24
1820cb0	20,2888	-18,6915	7,4	1700	8,81	3,89	455	13	1138,87	35	2,21	52	-0,03
1820ab1002	20,3000	-18,1433	7,4	490	64,07	20,88	12	4	319,47	2	2,21	4	1,04
V-17	20,3053	-19,2290	7,4	453	58,00	10,20	14	8	244,00	8	8,00	11	-0,66
1920ab1001	20,3177	-19,2283	7,5	400	52,86	9,96	17	8	238,99	2	2,21	10	1,44
1920cb1008	20,3183	-19,5208	8,1	410	44,05	8,01	30	6	224,36	5	6,64	14	0,38
1720cc7	20,3184	-17,8855	7,4	470	59,66	12,87	11	3	268,26	7	0,00	8	-1,88
C321	20,3192	-17,9324	7,1	420	34,04	18,21	16	4	164,61	0	0,00	50	-1,39
1820ab1001	20,3247	-18,2133	8,4	630	2,80	0,00	148	3	302,40	13	66,40	35	-4,52
1720cd1001	20,3250	-17,8870	7,6	560	54,06	37,88	8	4	346,30	1	8,85	2	3,04
1820ab1003	20,3433	-18,1357	7,0	490	76,88	15,06	8	5	287,77	17	2,21	7	2,29
1820ab1008	20,3483	-18,0033	7,7	390	38,84	17,97	17	4	258,50	1	2,21	2	-1,05
3733	20,3548	-21,9523	8,0	510	13,21	2,91	94	2	160,95	71	0,00	31	0,49
3734	20,3577	-21,8892	7,5	1500	112,12	17,00	195	6	103,64	625	0,00	52	-1,72
W-20	20,3597	-19,5717	7,8	6490	394,00	76,00	1056	18	201,30	1200	800,00	1093	0,21
1820ab1007	20,3625	-18,0450	7,6	400	48,05	23,07	6	3	265,82	1	2,21	2	1,81
1720cd2	20,3680	-17,9080	7,3	450	35,64	35,45	22	5	329,22	6	0,00	5	1,04
1720cd1002	20,3680	-17,9080	7,5	520	42,05	31,08	26	5	343,86	5	2,21	6	-0,25
1820ab4	20,3697	-18,1333	8,8	690	8,41	13,11	174	16	359,71	78	27,00	50	0,59
1720cd1003	20,3700	-17,9020	7,8	1980	24,83	25,98	410	5	692,59	240	110,67	148	-2,22
1820ab1005	20,3792	-18,1317	7,6	470	40,84	19,91	35	3	297,52	5	2,21	4	1,42
3732	20,3827	-21,7775	7,4	680	44,05	16,03	75	5	207,29	125	23,02	26	-1,41
1720cd3	20,3830	-17,9000	8,9	2580	3,20	1,70	746	17	829,16	705	0,00	175	-0,03
1820ab1006	20,3850	-18,1000	7,1	400	40,84	23,07	0	5	202,41	40	5,75	3	-3,13
1920cb7	20,4046	-19,5796	7,8	1250	26,83	10,44	299	14	652,35	129	3,10	75	0,06
C418	20,4048	-19,6153	7,8	1250	26,83	10,44	299	14	652,35	129	3,10	75	0,06
1920cd1003	20,4167	-19,8217	7,9	970	74,88	36,91	53	26	363,37	8	2,21	130	-0,41
1920cd1002	20,4167	-19,8308	8,2	1410	54,06	23,07	205	50	521,88	34	2,21	200	-0,49
3731	20,4183	-21,8505	7,5	1090	72,08	23,07	137	8	241,43	328	19,48	21	-0,14
1920cb4	20,4219	-19,5346	8,0	2225	28,43	9,47	612	36	1207,16	147	11,95	180	2,81
1920cb5	20,4224	-19,5371	7,7	1400	14,42	11,90	332	46	798,68	106	13,28	45	1,57
1720cd4	20,4259	-17,9415	7,7	2000	80,09	65,57	244	18	670,64	162	39,84	205	-0,78
1920ad3	20,4342	-19,3808	7,7	900	57,26	32,06	87	14	506,03	14	17,71	15	1,82
1920cb1002	20,4367	-19,6500	8,0	960	66,87	42,98	73	13	441,41	16	4,43	88	1,27
W-36	20,4482	-20,6012	8,1	1017	78,00	45,00	95	7	442,86	44	53,90	64	4,56
3730	20,4538	-21,8829	7,3	900	53,26	24,04	97	7	207,29	203	12,84	44	-0,21
C323	20,4567	-17,9423	7,3	450	35,64	35,45	22	5	329,22	6	0,00	5	1,04
C453	20,4567	-19,5712	7,7	1400	14,42	11,90	332	46	798,68	106	13,28	45	1,57
1920cb1005	20,4625	-19,6185	8,3	680	34,84	40,07	50	8	324,35	24	2,21	50	1,05
C439	20,4644	-19,4117	7,7	900	57,26	32,06	87	14	506,03	14	17,71	15	1,82
1720cd5	20,4690	-17,9530	7,8	660	58,06	36,43	22	3	298,74	0	70,83	35	-0,69
1920ad1001	20,4703	-19,3883	7,4	820	88,10	37,88	41	6	497,50	5	17,71	18	2,16
1920cb6	20,4783	-19,5818	7,3	750	80,49	31,33	27	8	445,06	9	8,85	20	-1,33
1920ad1	20,4783	-19,2683	7,7	2400	224,64	81,84	213	17	438,97	172	4,43	575	1,06
1920ad2	20,4803	-19,2784	7,6	750	69,28	25,98	52	12	402,39	38	13,28	30	-1,70
C325	20,4865	-17,9919	7,7	2000	80,09	65,57	244	18	670,64	162	39,84	205	-0,78
1920da3	20,5004	-19,5967	8,0	1500	112,12	12,14	264	9	573,10	19	6,64	240	4,70
1920da1008	20,5007	-19,5954	7,5	780	100,91	17,97	38	10	421,90	12	4,43	40	0,35
1920da5	20,5007	-19,5954	8,1	800	95,70	19,67	56	12	426,77	4	17,71	45	2,84
1920da1	20,5028	-19,6069	7,8	2200	56,06	28,41	403	22	445,06	131	0,00	462	0,38
1920bc6	20,5033	-19,3950	7,7	2050	28,83	27,44	544	16	1103,51	79	0,00	290	-0,25

Appendix D: Hydrochemical data

Name	Long	Mlat	pH	ec µS/cm	Ca ²⁺ mg/l	Mg ²⁺ mg/l	Na ⁺ mg/l	K ⁺ mg/l	HCO ₃ ⁻ mg/l	SO ₄ ²⁻ mg/l	NO ₃ ⁻ mg/l	Cl ⁻ mg/l	Balance %
1920da1009	20,5033	-19,5967	7,8	3740	82,89	28,90	680	38	409,70	220	6,64	900	0,37
1920da6	20,5050	-19,5947	7,1	630	110,92	18,94	43	10	432,87	16	17,71	25	4,55
W-21	20,5060	-19,5958	7,8	1514	103,20	32,60	236	10	480,07	76	8,40	266	3,58
1720dc1	20,5081	-17,9639	7,4	425	36,04	19,91	18	5	219,48	4	8,85	10	2,87
C434	20,5087	-19,6126	8,4	560	46,85	40,80	33	9	353,61	60	0,00	15	-0,72
1820ba1005	20,5100	-18,0383	7,8	430	34,84	22,10	27	4	278,01	6	17,71	3	-2,20
C430	20,5163	-19,3144	7,6	750	69,28	25,98	52	12	402,39	38	13,28	30	-1,70
1920bc1001	20,5200	-19,4367	8,0	950	64,87	48,08	83	8	590,17	15	2,21	26	1,17
W-45	20,5203	-21,3547	7,8	787	79,20	45,80	19	6	381,25	9	94,00	11	2,51
1820ba1006	20,5208	-18,1613	6,9	270	34,04	13,11	1	2	173,15	1	2,21	1	-0,87
1920bc2	20,5239	-19,4217	7,8	960	75,68	39,10	83	18	573,10	26	0,00	55	-1,86
C324	20,5298	-17,9964	7,8	660	58,06	36,43	22	3	298,74	0	70,83	35	-0,69
1720dc2	20,5377	-17,9819	7,4	380	32,03	9,71	56	4	280,45	14	0,00	10	-2,31
C435	20,5385	-19,6360	7,1	630	110,92	18,94	43	10	487,74	16	17,71	25	-0,52
C412	20,5413	-19,6459	7,8	1600	51,66	30,60	282	10	487,74	92	8,85	250	1,48
C413	20,5433	-19,6414	8,0	1300	112,12	12,14	250	9	585,29	19	6,64	250	1,59
1820ba1003	20,5600	-18,1633	6,5	120	10,01	7,04	2	2	75,60	1	2,21	1	-4,19
1820ba1007	20,5625	-18,0183	8,0	450	10,81	5,10	89	3	268,26	12	2,21	6	0,57
1920ba1003	20,5667	-19,1067	7,5	2130	130,14	65,08	205	22	260,94	500	33,20	184	2,20
V-24	20,5699	-20,8630	7,1	4110	275,00	96,20	574	16	403,00	1860	22,00	90	-1,26
1820ba2	20,5752	-18,0890	8,3	400	44,05	20,16	18	2	246,31		0,00	25	-0,54
1920dc9	20,5762	-19,8012	8,0	7100	156,17	92,28	1445	216	268,26	188	26,56	2700	-0,67
1920bc1004	20,5808	-19,3850	7,5	770	74,88	56,10	10	4	531,64	2	2,21	4	-0,07
1920dc1003	20,5850	-19,8025	7,9	1660	136,15	44,93	134	10	285,33	116	73,04	320	-2,13
1920dc1010	20,5917	-19,9550	8,0	2290	46,85	23,07	465	8	863,30	140	26,56	230	1,41
C326	20,5933	-18,0405	7,4	380	32,03	9,71	58	4	280,45	14	0,00	10	-1,44
1920bc4	20,5960	-19,4184	8,2	42500	41,24	11,41	13950	496	890,13	2144	48,69	20850	-2,02
C428	20,5990	-19,8423	8,0	7100	156,17	92,28	1445	216	268,26	188	30,54	2700	-0,71
3728	20,6038	-21,8369	7,5	1320	101,31	34,00	138	7	292,64	396	15,05	42	-1,52
3724	20,6058	-22,0360	7,1	2280	240,26	104,91	53	7	379,22	26	641,86	190	1,40
1820ba1001	20,6067	-18,1633	7,4	300	40,04	14,08	2	2	192,66	1	2,21	1	0,81
3729	20,6096	-21,8243	8,1	1570	120,13	58,04	173	9	201,19	700	15,05	40	-1,90
3725	20,6115	-21,9973	7,7	970	29,23	23,07	168	6	506,03	51	18,15	22	2,61
1720dc3	20,6133	-18,0017	8,2	210	24,83	6,80	6	4	73,16	5	0,00	35	-2,89
1820ba9	20,6145	-18,0172	7,2	525	12,01	2,43	135	4	335,32	5	23,46	20	1,74
1820ba8	20,6189	-18,0111	7,9	410	34,04	18,21	56	3	304,84	22	0,00	10	-0,23
1820bc01	20,6207	-18,2810	6,7	1400	76,08	26,96	146	7	556,02	1	2,21	133	-1,48
1820bc03	20,6207	-18,2810	7,0	2440	142,15	40,07	385	8	1121,80	35	2,21	300	-0,49
1820bc1001	20,6208	-18,3242	6,7	490	16,02	5,10	70	27	136,57	42	5,31	75	-3,50
1820bc1	20,6217	-18,3267	7,9	2500	14,82	4,37	698	18	658,45	580	0,00	295	1,16
1920da11	20,6253	-19,6833	8,1	585	83,69	16,03	17	5	365,81	7	4,43	10	-1,02
1920da1007	20,6283	-19,5558	7,6	790	90,90	17,97	56	7	441,41	10	4,43	38	0,26
W-44	20,6436	-21,2292	8,1	711	61,72	30,20	60	4	386,74	31	31,60	9	3,29
3726	20,6529	-21,9541	8,2	1390	99,31	90,09	35	9	431,65	13	265,60	97	-0,85
3727	20,6538	-21,9595	7,7	680	56,06	44,93	26	7	436,53	11	11,07	6	0,47
1820ba4	20,6542	-18,1633	7,7	460	49,65	18,46	13	4	286,55	2	0,00	5	-2,25
3719	20,6644	-21,8252	7,7	640	53,26	27,93	44	5	385,32	23	0,00	10	-0,56
C438	20,6654	-19,7000	8,1	590	83,69	16,03	17	5	365,81	7	4,43	10	-1,02
1920da1006	20,6692	-19,5692	7,7	750	82,89	25,98	51	2	487,74	2	6,64	10	0,71
1920dc2	20,6715	-19,9421	8,0	1300	40,04	31,57	112	11	378,00	41	0,00	95	0,11
W-37	20,6763	-20,5759	8,1	1277	116,10	43,70	104	7	366,00	187	61,50	87	2,66
1820bc02	20,6768	-18,4427	7,7	5730	160,98	110,01	1000	21	621,87	1080	2,21	1115	-2,43
1820bc04	20,6768	-18,4427	7,0	5850	156,17	110,01	980	21	595,04	1020	2,21	1119	-2,10

Appendix D: Hydrochemical data

Name	Long	Mlat	pH	ec µS/cm	Ca ²⁺ mg/l	Mg ²⁺ mg/l	Na ⁺ mg/l	K ⁺ mg/l	HCO ₃ ⁻ mg/l	SO ₄ ²⁻ mg/l	NO ₃ ⁻ mg/l	Cl ⁻ mg/l	Balance %
1920dc7	20,6769	-19,9198	8,2	2400	34,04	43,71	630	8	506,03	347	0,00	595	0,92
1820ba12	20,6778	-18,0003	8,0	460	41,24	22,34	27	4	307,28	8	0,00	2	-0,82
3723	20,6788	-22,0360	7,4	1940	215,43	56,10	84	5	385,32	12	531,20	168	-1,85
1820ba6	20,6797	-18,0010	7,4	300	36,04	18,21	15		189,00	44	8,85	5	-4,22
3722	20,6798	-21,9730	7,1	2170	240,26	125,06	15	9	368,24	8	796,80	143	0,17
1920dc1008	20,6808	-19,9042	7,8	690	82,09	41,04	12	2	458,48	2	2,21	6	1,81
C328	20,6817	-18,0793	7,2	530	12,01	2,43	135	4	335,32	5	23,46	20	1,74
3718	20,6856	-21,8450	7,4	1710	160,17	63,87	110	5	482,86	20	247,89	200	0,53
1820da1002	20,6867	-18,5792	7,4	730	96,91	14,08	50	6	436,53	28	2,21	18	0,26
C329	20,6875	-18,0523	7,9	410	34,04	18,21	56	3	304,84	22	0,00	10	-0,23
C424	20,6971	-19,9811	8,2	1030	59,66	39,10	74	10	451,16	22	0,00	65	-0,08
1920da8	20,6980	-19,5964	7,2	610	84,09	12,14	38	3	323,13	5	60,65	17	0,49
3720	20,7000	-21,9243	7,7	820	106,12	34,00	31	4	402,39	13	118,63	29	-0,28
1920dc1007	20,7017	-19,9833	7,8	760	44,05	25,98	96	5	504,81	2	2,21	6	0,70
3721	20,7019	-21,9297	7,4	670	80,09	26,96	19	3	385,32	10	31,43	10	-1,35
1820ba10	20,7033	-18,0367	8,0	310	48,05	10,93	10	4	225,58		0,00	5	-0,05
1820ba1012	20,7033	-18,0367	7,0	420	36,84	19,91	14	5	168,27	16	2,21	43	-1,47
1920dc6	20,7090	-19,9067	7,4	650	65,27	49,05	5	1	451,16	5	2,66	5	-0,95
1920dc1	20,7132	-19,9121	8,3	650	30,03	26,71	92	5	420,68	14	0,00	20	0,49
1920da1004	20,7140	-19,6590	7,9	930	48,05	34,00	103	20	548,71	1	33,20	16	0,93
1920ba1	20,7150	-19,0533	7,2	1375	173,39	52,70	112	6	524,32	181	22,13	200	-0,95
1920da9	20,7158	-19,6589	8,0	1700	10,41	5,83	468	13	1054,74	109	4,43	85	-0,77
1920dc4	20,7180	-19,9259	7,6	680	88,10	43,71	24	4	524,32	16	0,00	15	-1,14
1820bc1003	20,7200	-18,2817	8,3	450	10,01	2,91	96	6	265,82	17	2,21	3	2,40
1920dc3	20,7200	-19,9168	7,8	620	56,06	35,21	43	4	445,06	14	15,49	5	-1,97
1920dc5	20,7217	-19,9375	7,6	1500	44,05	32,78	315	31	585,29	85	9,30	315	-2,53
1920dc1004	20,7225	-19,9167	7,6	750	76,88	36,91	44	3	509,69	3	2,21	10	0,75
V-19	20,7226	-19,9107	6,7	735	77,50	33,30	41	2	487,00	10	3,10	4	0,62
1820ba3	20,7226	-18,1848	8,0	365	66,07	4,86	5	2	243,87		0,00	5	-2,13
C335	20,7240	-18,1901	7,7	410	49,65	18,46	13	4	280,45	2	0,00	5	-1,21
1920dc1001	20,7250	-19,7650	7,8	750	56,06	42,01	41	5	419,46	6	46,48	14	0,14
1920dc10	20,7250	-19,7650	8,1	775	55,66	37,88	29	5	384,10	9	44,27	10	-1,31
1820ba1013	20,7267	-18,0158	7,6	1110	50,05	33,03	142	7	368,24	166	2,21	90	-2,09
W-22	20,7317	-19,8307	8,1	885	116,72	63,52	6	1	617,32	3	13,20	6	3,45
V-20	20,7317	-19,8307	6,7	904	126,00	55,80	5	1	643,00	3	10,80	5	0,94
1920bc1	20,7317	-19,3500	7,9	550	77,68	13,60	18	6	359,71	6	0,00	5	-1,89
3717	20,7327	-21,8685	7,4	700	90,10	18,94	32	6	436,53	10	0,00	10	-0,29
C421	20,7327	-19,9811	7,6	1500	44,05	32,78	315	31	560,90	85	9,30	315	-1,54
C420	20,7346	-19,6396	7,2	610	84,09	12,14	38	3	323,13	5	60,65	17	0,49
C422	20,7356	-19,9568	7,8	620	56,06	35,21	43	4	445,06	14	15,49	5	-1,97
3713	20,7365	-22,0297	7,5	920	56,06	35,94	106	7	499,93	30	25,67	29	2,40
1920da1005	20,7367	-19,5917	7,6	800	88,10	20,88	49	3	443,84	9	13,28	34	-1,84
C437	20,7394	-19,6982	8,1	950	120,53	9,47	67	12	463,35	34	26,56	55	-1,31
1920bc1006	20,7400	-19,2883	8,0	1210	48,05	44,93	176	3	734,05	1	2,21	56	0,58
C327	20,7413	-18,0423	7,4	300	36,04	18,21	20	0	189,00	44	8,85	5	-1,54
1820ba1014	20,7417	-18,1558	6,7	160	20,82	2,91	2	4	92,67	1	2,21	2	-5,27
C423	20,7452	-19,9541	7,6	680	88,10	43,71	24	4	524,32	16	0,00	15	-1,14
C427	20,7462	-19,9459	8,3	650	30,03	26,71	92	5	420,68	14	0,00	20	0,49
3716	20,7471	-21,8667	7,4	750	61,27	22,10	75	4	448,72	14	6,20	11	1,13
1820bc2	20,7489	-18,2844	7,8	3300	51,66	20,88	825	11	375,56	1049	4,43	400	1,40
W-43	20,7513	-21,1946	7,9	651	72,80	36,80	15	4	413,58	4	16,80	7	0,44
3715	20,7529	-21,9333	7,3	1320	150,16	42,01	49	4	425,55	10	256,75	77	-1,17
C454	20,7577	-19,8108	8,1	780	55,66	37,88	29	5	384,10	9	44,27	10	-1,31

Appendix D: Hydrochemical data

Name	Long	Lat	pH	ec µS/cm	Ca ²⁺ mg/l	Mg ²⁺ mg/l	Na ⁺ mg/l	K ⁺ mg/l	HCO ₃ ⁻ mg/l	SO ₄ ²⁻ mg/l	NO ₃ ⁻ mg/l	Cl ⁻ mg/l	Balance %
1820db1020	20,7583	-18,6867	7,4	500	80,09	8,99	21	4	326,79	1	2,21	6	1,50
1820bb1001	20,7617	-18,0583	7,9	380	34,84	14,08	29	4	243,87	1	2,21	3	1,47
C330	20,7625	-18,0937	7,5	320	40,04	20,64	7	3	243,87	4	0,00	5	-1,72
3690	20,7625	-21,8649	7,2	920	69,28	27,93	120	4	499,93	43	27,89	38	2,15
V-21	20,7642	-20,6613	7,5	273	33,00	7,30	18	3	150,00	10	3,90	3	4,66
C391	20,7663	-19,1036	7,2	1380	173,39	52,70	112	6	524,32	181	2,21	200	-0,07
3714	20,7663	-22,0045	7,2	2960	300,33	129,92	117	7	332,88	20	1106,66	300	-1,96
3712	20,7692	-22,0387	8,2	890	43,25	37,88	99	13	493,84	17	21,25	31	1,28
W-42	20,7693	-21,1249	7,9	847	85,20	40,00	37	6	391,01	16	96,80	28	1,09
1820da1001	20,7727	-18,5017	7,8	210	18,82	2,91	24	2	126,81	2	2,21	2	1,38
3699	20,7769	-21,8640	7,2	770	108,12	26,96	23	2	465,79	6	46,92	8	-0,44
1820bb1007	20,7783	-18,2000	7,5	1170	64,87	26,96	144	5	265,82	235	4,43	87	0,31
1820bb4	20,7796	-18,0242	8,4	460	24,43	20,40	60	8	292,64	18	4,43	15	0,41
1820dd1002	20,7800	-18,8400	7,3	690	78,08	28,90	37	4	436,53	17	4,43	10	0,79
1820bb6	20,7870	-18,0275	7,6	570	11,21	4,13	117	3	235,33	67	0,00	24	1,14
1820bb7	20,7882	-18,0283	8,1	460	25,23	9,23	66	2	218,26	44	0,00	17	-0,33
1820bb13	20,7920	-18,0316	7,7	510	14,02	4,13	95	1	248,75	33	0,00	15	0,10
3708	20,8019	-21,9234	7,2	3650	260,28	119,96	325	8	465,79	44	192,56	890	0,60
3710	20,8058	-21,9775	7,4	820	59,26	24,04	96	3	442,62	16	27,45	28	2,05
1820bb8	20,8083	-18,0667	7,7	425	46,45	20,40	8	7	274,35	6	4,43	5	-3,31
1920dd1001	20,8117	-19,8883	7,7	760	94,10	39,10	13	4	492,62	2	4,43	8	0,99
3709	20,8154	-21,9207	7,3	2050	140,15	56,10	211	6	442,62	17	73,92	420	0,71
1920bd1007	20,8200	-19,3516	7,4	820	106,12	49,05	5	3	570,66	1	2,21	6	0,25
3691	20,8269	-21,8523	7,5	1110	111,32	28,90	107	5	465,79	25	38,95	124	1,74
3711	20,8279	-22,0234	7,4	4560	200,22	154,93	650	16	540,17	430	619,73	790	1,32
1820bb10	20,8333	-18,2000	8,7	4550	16,42	8,26	1024	10	1085,22	798	0,00	375	1,45
1920db1001	20,8350	-19,6233	8,5	570	38,84	49,05	13	4	375,56	2	4,43	4	2,01
C386	20,8375	-18,2550	7,9	260	42,85	17,73		5	170,71	22	0,00	10	2,57
1820bb1014	20,8383	-18,2417	5,9	510	54,86	6,07	23	7	14,63	156	2,21	15	5,62
3692	20,8404	-21,8468	7,0	920	71,28	18,94	121	2	534,08	16	30,10	20	1,43
1820bb11	20,8406	-18,2428	8,8	1110	2,80	1,94	253	2	370,68	120	1,77	90	0,96
1820bd1	20,8450	-18,2720	8,1	425	38,04	26,71	12	3	268,26	1	0,00	8	0,56
W-38	20,8463	-20,6122	7,9	1429	165,00	60,90	98	8	292,80	480	21,40	66	2,06
1920bd2	20,8495	-19,4756	7,5	560	60,87	46,87	2	2	420,68	5	4,43	5	-1,25
3693	20,8519	-21,7748	7,9	900	25,23	19,91	169	9	476,77	63	22,13	22	1,83
1820db1002	20,8666	-18,7100	7,0	840	90,10	27,93	64	4	502,37	40	2,21	21	-0,07
1820db1001	20,8683	-18,6006	8,1	430	12,01	0,97	89	4	234,12	5	2,21	22	0,60
1820bb1008	20,8717	-18,2400	7,9	700	16,02	2,91	126	2	129,25	148	2,21	52	-0,99
1920dd1002	20,8780	-19,8700	7,7	970	124,94	45,90	16	3	580,41	40	11,07	13	-0,49
3700	20,8808	-21,8523	7,0	1050	123,33	26,96	85	4	482,86	13	11,51	124	1,27
1820bb2	20,8875	-18,0300	7,9	240	37,24	1,70	17	6	176,81		0,00	5	-2,49
C331	20,8990	-18,2486	7,8	11500	74,88	124,58	2485	26	1286,42	3290	0,00	1300	-1,41
3699	20,9010	-21,8928	7,6	2510	235,46	57,07	169	5	178,03	50	593,17	390	-1,24
3706	20,9058	-21,9315	7,0	1640	170,19	50,03	115	4	373,12	57	216,91	250	-0,39
3707	20,9067	-21,9225	7,4	1210	60,07	22,10	143	4	385,32	34	81,45	83	2,11
1920bd1002	20,9070	-19,3633	7,4	770	102,11	45,90	6	3	538,95	1	2,21	6	0,83
C307	20,9096	-18,3270	8,1	430	38,04	26,71	12	3	268,26	1	0,00	8	0,56
3695	20,9106	-21,8234	6,7	4380	570,62	139,88	154	6	368,24	55	796,80	943	0,22
3694	20,9231	-21,8315	7,1	990	88,10	26,96	102	4	431,65	52	70,83	59	0,86
W-39	20,9244	-20,5847	7,9	1204	105,00	41,70	128	7	281,82	338	16,40	54	3,53
1820bb1005	20,9416	-18,0050	7,7	8740	18,02	27,93	2180	8	477,99	3080	2,21	1000	-0,99
1820bb1009	20,9433	-18,2217	7,8	470	40,84	14,08	44	6	273,13	20	2,21	10	0,52
1820dd1	20,9433	-18,9283	7,4	2200	158,97	77,22	193	8	329,22	399	0,00	320	0,35

Appendix D: Hydrochemical data

Name	Long	Lat	pH	ec µS/cm	Ca ²⁺ mg/l	Mg ²⁺ mg/l	Na ⁺ mg/l	K ⁺ mg/l	HCO ₃ ⁻ mg/l	SO ₄ ²⁻ mg/l	NO ₃ ⁻ mg/l	Cl ⁻ mg/l	Balance %
1920db1002	20,9467	-19,6683	7,9	920	70,88	68,00	33	4	592,60	7	2,21	24	0,47
3704	20,9481	-21,9829	7,1	2630	200,22	66,05	285	10	482,86	135	354,13	460	-2,32
3703	20,9490	-21,9793	7,2	2140	160,17	46,87	230	8	459,70	89	201,41	370	-2,24
3705	20,9548	-21,9369	7,3	1420	119,33	34,00	164	4	493,84	57	32,76	196	2,08
C336	20,9596	-18,0784	7,2	40	6,01	3,64	6	1	36,58	7	0,00	5	-0,01
1820bb3	20,9629	-18,0127	8,0	13000	76,08	58,28	4820	14	731,61	7015	0,00	2150	-0,02
3969	20,9635	-21,7919	7,1	960	137,35	33,03	35	4	488,96	11	110,67	28	1,72
3702	20,9779	-21,9838	7,2	3830	160,17	59,98	675	12	753,56	210	354,13	690	0,83
1820bb1010	20,9783	-18,1433	7,9	430	30,83	11,90	51	6	282,89	1	2,21	1	1,76
1920db2	20,9833	-19,5708	7,1	695	84,49	51,97	14	5	548,71	5	0,00	5	-0,04
W-41	20,9852	-20,8428	7,9	3640	312,00	124,00	480	16	217,77	1400	25,40	440	1,64
V-23	20,9853	-20,8425	7,4	4100	315,00	98,00	349	17	262,00	1486	22,40	180	-1,57
1920bd1	20,9867	-19,3183	7,6	1000	57,66	45,17	97	2	603,58	10	4,43	20	0,60
1820bb1012	20,9917	-18,1833	7,4	760	56,06	27,93	79	6	443,84	46	2,21	18	-0,51
W-40	20,9920	-20,6288	7,9	1108	87,50	30,70	138	7	223,87	345	4,80	35	4,59
1820bb1013	20,9955	-18,0820	7,7	270	32,03	14,08	2	4	151,20	1	2,21	3	5,89
1820ba11	20,9998	-18,6779	8,2	10500	20,02	263,00	2200	22	486,52	3575	345,28	940	1,89
3698	21,0000	-21,8829	7,2	1620	260,28	25,98	21	9	298,74	33	522,34	96	-1,35
3697	21,0019	-21,7874	7,1	1110	105,31	35,94	96	5	459,70	34	154,93	61	0,22
3701	21,0087	-21,9892	7,4	3620	51,26	37,88	790	14	914,51	245	44,27	640	1,95
1721cc1	21,0166	-17,9722	8,1	415	56,06	20,64	15	5	286,55	18	0,00	10	-0,72
1821aa1001	21,0183	-18,1183	7,8	400	54,06	16,03	7	4	258,50	1	2,21	4	0,20
C440	21,0192	-19,6135	7,2	700	84,49	51,97	14	5	548,71	5	0,00	5	-0,04
C432	21,0192	-19,9703	7,3	780	80,49	44,68	5	2	463,35	4	0,00	5	0,91
C433	21,0394	-19,3631	7,6	1000	57,66	45,17	97	2	603,58	10	4,43	20	0,60
C333	21,0596	-18,1568	7,6	1450	24,83	6,80	414	10	615,77	119	13,28	240	1,29
C334	21,0894	-18,2955	8,1	560	41,65	23,31	40	4	262,16	43	0,00	15	1,96
C338	21,0923	-18,0351	8,1	420	56,06	20,64	15	5	286,55	18	0,00	10	-0,72
1821aa1003	21,1013	-18,2425	7,5	4230	50,05	85,97	750	10	643,82	970	8,85	580	-5,35
1821aa1005	21,1183	-18,0547	6,0	60	4,81	1,94	2	2	29,26	1	2,21	2	-4,84
1721cc2	21,1210	-17,9545	7,3	595	63,27	30,84	7	5	335,32		8,85	18	-0,15
1721cc4	21,1630	-17,9540	7,8	400	28,03	30,36	22	5	280,45	10	0,00	10	-1,04
1721cc5	21,1681	-17,9479	7,5	480	46,85	26,23	21	4	298,74	19	0,00	10	-0,56
1821aa1002	21,1700	-18,2350	7,3	700	60,07	43,95	24	9	470,67	6	2,21	3	-0,44
1721cc7	21,1711	-17,9965	7,4	575	74,48	21,61	25	5	353,61	3	0,00	30	0,05
C340	21,1817	-18,0450	7,2	420	63,27	15,06	8	2	274,35	7	0,00	10	-1,33
C339	21,2048	-18,0171	7,3	600	63,27	30,84	7	5	335,32	0	8,85	18	-0,15
1721cc1008	21,2350	-17,9630	7,5	520	64,07	22,10	14	3	341,42	3	2,21	4	-0,91
C342	21,2481	-18,0054	7,5	480	46,85	26,23	21	4	298,74	19	0,00	10	-0,56
C341	21,2490	-17,9973	8,4	450	40,84	21,37	16	5	274,35	8	0,00	5	-1,95
1821ab1020	21,2541	-18,0450	7,8	400	50,86	17,97	4	2	253,63	1	2,21	5	-1,31
1721cd1	21,2800	-17,9720	7,1	345	44,05	17,00	3	3	225,58	3	0,00	10	-3,03
1821ab1011	21,2958	-18,0725	6,9	180	22,02	7,04	4	2	107,30	2	2,21	2	0,30
1721cd2	21,3130	-17,9930	7,2	180	33,64	0,97	7	2	128,03	3	0,00	5	-4,25
1821ab1010	21,3167	-18,1800	7,2	330	34,84	17,97	5	3	195,10	3	2,21	6	0,67
1821ab1009	21,3180	-18,1516	7,4	740	68,87	42,98	18	4	273,13	168	2,21	8	-2,34
1721cd3	21,3215	-17,9930	7,8	550	90,90	17,73	9	7	378,00	5	4,43	5	0,41
C387	21,3221	-18,0180	7,9	1530	155,37	49,05	97	16	304,84	244	0,00	230	-0,44
1821ab1007	21,3483	-18,1575	7,3	510	62,07	23,07	14	4	324,35	5	2,21	6	0,73
1821ab8	21,3626	-18,1740	6,6	470	55,26	22,34	12	3	286,55	6	0,00	8	1,45
1821ab1008	21,3775	-18,1950	6,7	200	22,82	3,89	7	3	53,65	45	2,21	2	-1,82
1821ab1012	21,3783	-18,0550	7,2	6120	400,04	299,91	500	10	631,62	380	101,81	1574	1,79
1821ab1003	21,3833	-18,2370	6,3	100	6,81	2,91	7	4	51,21	1	2,21	4	-1,12

Appendix D: Hydrochemical data

Name	Long	Mlat	pH	ec μS/cm	Ca ²⁺ mg/l	Mg ²⁺ mg/l	Na ⁺ mg/l	K ⁺ mg/l	HCO ₃ ⁻ mg/l	SO ₄ ²⁻ mg/l	NO ₃ ⁻ mg/l	Cl ⁻ mg/l	Balance %
1821ab1002	21,3866	-18,2433	7,3	530	60,07	25,01	8	7	329,22	1	2,21	8	-0,84
1821ab1006	21,3943	-18,1125	7,5	590	60,07	34,00	13	9	368,24	11	4,43	7	0,44
C390	21,4019	-18,1523	8,2	300	41,65	12,63	3	2	182,90	2	0,00	5	1,83
C343	21,4163	-18,0532	7,8	550	90,90	17,73	9	7	378,00	5	4,43	5	0,41
1821ab1	21,4283	-18,0378	7,6	270	45,65	13,60	10	3	213,39		8,85	10	-0,17
1821ab1005	21,4283	-18,1258	7,2	380	58,06	10,93	5	2	241,43	1	2,21	4	-0,74
1821ab1013	21,4283	-18,0378	7,2	820	64,87	22,10	89	3	502,37	10	2,21	22	-0,52
C349	21,4327	-18,2523	7,8	370	55,26	23,56	17	4	317,03	3	0,00	8	0,49
1821ab2	21,4329	-18,0403	6,1	80	8,01	4,86	2	1	48,77		0,00	4	-0,02
1821ab9	21,4417	-18,1933	7,3	350	64,87	9,23	6	4	249,97		0,00	7	0,76
1821ab4	21,4457	-18,0617	7,1	600	77,68	34,24	23	2	408,48	14	0,00	30	-0,55
1821ab3	21,4487	-18,0576	7,3	360	43,25	14,33	23	7	243,87	25	2,21	10	-3,40
C344	21,4519	-18,0730	8,8	80	11,61	1,70	2	2	48,77	1	0,00	2	-1,10
1821ab1001	21,4728	-18,2367	7,2	280	30,83	8,99	3	6	165,83	1	2,21	3	-5,48
C345	21,5000	-18,0955	7,6	270	45,65	13,60	10	3	213,39	0	8,85	10	-0,17
C346	21,5096	-18,1054	6,1	80	8,01	4,86	2	1	48,77	0	0,00	4	-0,02
1821ba10	21,5104	-18,0875	7,3	260	36,04	8,01	8	1	153,64	5	2,21	4	1,09
1821ba12	21,5107	-18,0886	7,6	440	62,07	18,21	13	5	304,84		0,00	8	0,65
C350	21,5192	-18,2559	7,3	350	64,87	9,23	6	4	249,97	0	0,00	7	0,76
C348	21,5240	-18,1324	7,1	600	77,68	34,24	23	2	408,48	14	0,00	30	-0,55
C347	21,5269	-18,1225	7,1	370	49,65	11,17	17	7	219,48	14	0,00	20	-1,56
1821ba13	21,5323	-18,0913	7,4	1375	169,78	48,57	49	13	249,97	102	13,28	295	0,60
1821ba3	21,5950	-18,1500	7,0	280	40,04	4,86	5	1	164,61		0,00	4	-3,11
1821ba1001	21,5958	-18,2167	7,5	250	38,84	7,04	3	3	156,08	1	4,43	4	-0,69
1821ba2	21,6033	-18,1750	8,5	300	38,04	8,01	10	2	182,90		0,00	5	-1,53
1821ba1006	21,6200	-18,1120	7,6	3470	380,01	124,09	210	9	336,54	490	19,92	750	1,78
1821ba1002	21,6375	-18,1417	7,5	250	60,07	16,03	11	4	290,21	1	2,21	3	0,00

	Ca ²⁺ mg/l	Mg ²⁺ mg/l	Na ⁺ mg/l	K ⁺ mg/l	HCO ₃ ²⁻ mg/l	SO ₄ ²⁻ mg/l	NO ₃ ⁻ mg/l	Cl ⁻ mg/l
Rain at Tsumkwe	3,2	0,4	3,4	1,7	25,6	0,3	4,9	0,9
Rain at Tsumkwe	2,7	0,4	3,4	1,8	25	0,3	2,8	0,8
Rain at Tsumkwe	2,1	0,3	2,8	1,3	19	0,4	2	0,5
Rain at Windhoek	9,9	1,1	1,5	4,7	31,7	3,6	<0,1	2,8
Rain at Windhoek	2,7	0,4	0,5	0,2	4,8	1,7	4,3	0,8
Rain at Windhoek	5,1	0,5	0,7	0,5	9,0	1,5	7,3	1,2
Okavango water at Popa Falls	7,0	1,4	1,7	1,4	29,3	0,2	0,1	0,8
Omatako embouchure to the Okavango	5,7	1,6	2,8	1,6	29,3	0,2	0,1	1,8

Rain at	Cl ⁻ content with Merck-Quick-Test
Rooiboklaagte, 4 Dec 2000	< 1 mg/l
Eiseb, 29 Nov 2000	< 1 mg/l